ISSN 1007-9327 (print)
ISSN 2219-2840 (online)

World Journal of *Gastroenterology*

World J Gastroenterol 2024 March 14; 30(10): 1261-1469

Published by Baishideng Publishing Group Inc

World Journal of Gastroenterology

Contents

Weekly Volume 30 Number 10 March 14, 2024

EDITORIAL

REVIEW

ORIGINAL ARTICLE

Retrospective Cohort Study

World Journal of Gastroenterology

Weekly Volume 30 Number 10 March 14, 2024

Contents

Contents

ABOUT COVER

Editorial Board Member of *World Journal of Gastroenterology*, Toru Mizuguchi, MD, PhD, Professor, Surgeon, Department of Nursing, Division of Surgical Science, Sapporo Medical University Postgraduate School of Health Science, Sapporo, Hokkaido 0608556, Japan. tmizu@sapmed.ac.jp

AIMS AND SCOPE

The primary aim of *World Journal of Gastroenterology* (*WJG*, *World J Gastroenterol*) is to provide scholars and readers from various fields of gastroenterology and hepatology with a platform to publish high-quality basic and clinical research articles and communicate their research findings online. *WJG* mainly publishes articles reporting research results and findings obtained in the field of gastroenterology and hepatology and covering a wide range of topics including gastroenterology, hepatology, gastrointestinal endoscopy, gastrointestinal surgery, gastrointestinal oncology, and pediatric gastroenterology.

INDEXING/ABSTRACTING

The *WJG* is now abstracted and indexed in Science Citation Index Expanded (SCIE), MEDLINE, PubMed, PubMed Central, Scopus, Reference Citation Analysis, China Science and Technology Journal Database, and Superstar Journals Database. The 2023 edition of Journal Citation Reports® cites the 2022 impact factor (IF) for *WJG* as 4.3; Quartile category: Q2. The *WJG*'s CiteScore for 2021 is 8.3.

RESPONSIBLE EDITORS FOR THIS ISSUE

NAME OF JOURNAL
World Journal of Gastroenterology

ISSN
ISSN 1007-9327 (print) ISSN 2219-2840 (online)

LAUNCH DATE
October 1, 1995

FREQUENCY
Weekly

PUBLICATION DATE
March 14, 2024

PUBLISHING PARTNER
Shanghai Pancreatic Cancer Institute and Pancreatic Cancer Institute, Fudan University
Biliary Tract Disease Institute, Fudan University

INSTRUCTIONS TO AUTHORS
https://www.wjgnet.com/bpg/gerinfo/204

GUIDELINES FOR ETHICS DOCUMENTS
https://www.wjgnet.com/bpg/GerInfo/287

GUIDELINES FOR NON-NATIVE SPEAKERS OF ENGLISH
https://www.wjgnet.com/bpg/gerinfo/240

PUBLICATION ETHICS
https://www.wjgnet.com/bpg/GerInfo/288

PUBLICATION MISCONDUCT
https://www.wjgnet.com/bpg/gerinfo/208

POLICY OF CO-AUTHORS
https://www.wjgnet.com/bpg/GerInfo/310

ARTICLE PROCESSING CHARGE
https://www.wjgnet.com/bpg/gerinfo/242

STEPS FOR SUBMITTING MANUSCRIPTS
https://www.wjgnet.com/bpg/GerInfo/239

ONLINE SUBMISSION
https://www.f6publishing.com

PUBLISHING PARTNER's OFFICIAL WEBSITE
https://www.shca.org.cn
https://www.zs-hospital.sh.cn

World Journal of Gastroenterology

Submit a Manuscript: https://www.f6publishing.com

World J Gastroenterol 2024 March 14; 30(10): 1261-1265

DOI: 10.3748/wjg.v30.i10.1261

ISSN 1007-9327 (print) ISSN 2219-2840 (online)

EDITORIAL

Bridging the gap: Unveiling the crisis of physical inactivity in inflammatory bowel diseases

Remus Stafie, Ana-Maria Singeap, Adrian Rotaru, Carol Stanciu, Anca Trifan

Specialty type: Gastroenterology and hepatology

Provenance and peer review: Invited article; Externally peer reviewed.

Peer-review model: Single blind

Peer-review report's scientific quality classification

Grade A (Excellent): A
Grade B (Very good): 0
Grade C (Good): 0
Grade D (Fair): 0
Grade E (Poor): 0

P-Reviewer: Tsujinaka S, Japan

Received: November 18, 2023
Peer-review started: November 18, 2023
First decision: January 5, 2024
Revised: January 17, 2024
Accepted: February 20, 2024
Article in press: February 20, 2024
Published online: March 14, 2024

Remus Stafie, Ana-Maria Singeap, Adrian Rotaru, Carol Stanciu, Anca Trifan, Department of Gastroenterology, Faculty of Medicine, "Grigore T. Popa" University of Medicine and Pharmacy, Iasi 700115, Romania

Remus Stafie, Ana-Maria Singeap, Adrian Rotaru, Carol Stanciu, Anca Trifan, Institute of Gastroenterology and Hepatology, "St. Spiridon" University Hospital, Iasi 700111, Romania

Corresponding author: Ana-Maria Singeap, MD, PhD, Associate Professor, Department of Gastroenterology, Faculty of Medicine, "Grigore T. Popa" University of Medicine and Pharmacy, No. 16 Universitatii Street, Iasi 700115, Romania. singeapanamaria@gmail.com

Abstract

In this editorial we comment on the article titled "Inflammatory bowel diseases patients suffer from significant low levels and barriers to physical activity: The BE-FIT-IBD study" published in a recent issue of the *World Journal of Gastroenterology* 2023; 29 (41): 5668-5682. Inflammatory bowel diseases (IBD) are emerging as a significant global health concern as their incidence continues to rise on a global scale, with detrimental impacts on quality of life. While many advances have been made regarding the management of the disease, physical inactivity in these patients represents an underexplored issue that may hold the key for further and better understanding the ramifications of IBD. Chronic pain, fatigue, and fear of exacerbating symptoms promotes physical inactivity among IBD patients, while the lack of clear guidelines on safe exercise regimens contributes to a norm of physical inactivity. Physical activity (PA) is accepted to have a positive effect on disease outcomes and quality of life, while inactivity exacerbates comorbidities like cardiovascular disease and mental health disorders. The "BE-FIT-IBD" study, focusing on PA levels and barriers in IBD patients of Southern Italy, revealed that a significant proportion (42.9%) were physically inactive. This lack of PA is attributed to barriers such as fear of flare-ups and misconceptions about exercise exacerbating the disease. The study also highlighted the need for better communication between healthcare providers and patients regarding the benefits of PA and safe incorporation into lifestyles. Moreover, physical inactivity may also contribute to disability in IBD patients, having a great impact on employment status. Of note is the fact that IBD also comes with an important psychological burden with relevant evidence suggesting that regular PA can improve mood, reduce anxiety, and enhance mental health. The "BE-FIT-IBD" study advocated for the integration of PA into IBD management, emphasizing the bidirectional link between PA and IBD. Regular exercise can influence the course of IBD, potentially

reducing symptom severity and prolonging remission periods. As such, it is mandatory that healthcare providers actively educate patients, dispel misconceptions, and tailor exercise recommendations to improve the quality of life and reduce IBD-related complications.

Key Words: Inflammatory bowel disease; Physical activity; Disability; Psychological burden; Body composition; Quality of life

Core Tip: Physical inactivity is emerging as a widely acknowledged matter among inflammatory bowel disease (IBD) patients. The lack of physical activity (PA) can be attributed to concerns over the potential exacerbation of symptoms and misguided beliefs around the impact of exercise on IBD, thus increasing the susceptibility to comorbidities such as cardiovascular disease and mental health issues. This editorial argues in favor of including PA into the management of IBD, highlighting the reciprocal relationship between PA and the condition as well as the importance of healthcare providers educating patients, correcting misunderstandings, and customizing exercise regimens.

Citation: Stafie R, Singeap AM, Rotaru A, Stanciu C, Trifan A. Bridging the gap: Unveiling the crisis of physical inactivity in inflammatory bowel diseases. *World J Gastroenterol* 2024; 30(10): 1261-1265
URL: https://www.wjgnet.com/1007-9327/full/v30/i10/1261.htm
DOI: https://dx.doi.org/10.3748/wjg.v30.i10.1261

INTRODUCTION

Inflammatory bowel diseases (IBD), including Crohn's disease (CD) and ulcerative colitis (UC), represent a growing global health issue, with their prevalence steadily increasing worldwide. These chronic conditions mainly affect the gastrointestinal tract, but their impact extends beyond simply physical symptoms. They also significantly influence the overall physical, psychosocial, and emotional well-being of individuals. The medical and research communities have made significant progress in developing pharmacological and surgical interventions to manage these diseases effectively. However, there is an aspect of IBD patient care that is often overlooked and largely unaddressed: The issue of physical inactivity[1,2]. Thus, it is mandatory to bring this critical issue to the forefront to have a holistic approach in the management of patients with IBD.

The issue of physical inactivity among individuals with IBD is multifaceted and is influenced by several factors including chronic pain, fatigue, and exacerbation of symptoms[3]. The erratic occurrence of IBD flare-ups and the episodic nature of the disease instills a fear of exercise and presents a challenge in maintaining a regular regimen of physical activity (PA), leading to a cycle of sedentary behavior. This fear is compounded by the lack of clear guidelines on safe exercise regimens for IBD patients, creating an environment where physical inactivity becomes a norm rather than an exception[3,4]. Despite the various obstacles encountered, there is a growing recognition of the significance of PA in the management of IBD. This acknowledgment is supported by research indicating the positive impact of PA on disease outcomes and the overall enhancement of quality of life[5]. The implications of a sedentary lifestyle for IBD patients are profound. Physical inactivity is known to exacerbate comorbidities such as cardiovascular disease, osteoporosis, and mental health disorders, which are already increased in IBD patients[6,7].

The "BE-FIT-IBD" study, published in the *World Journal of Gastroenterology*, delves into the PA levels and barriers faced by patients with IBD in Southern Italy. This cross-sectional observational study aimed to assess PA levels using the International Physical Activity Questionnaire (IPAQ) and identify barriers to regular PA among IBD patients[8]. The findings of this study aligned with the regular pattern observed in relation to PA, indicating that a notable proportion (42.9%) of individuals with IBD were physically inactive. In comparison, just 4.1% of individuals met the criteria for engaging in health-enhancing PA. Gravina *et al*[9] identified several barriers that contributed to this lack of PA, such as the fear of flare-ups and a general distrust in exercise post-diagnosis. These findings are in line with the existing literature that suggests IBD patients often have misconceptions about exercise exacerbating their condition, leading to avoidance of physical exertion[5].

The study also highlighted that a patient's social networks often encourage PA, yet many patients feel uninformed about exercise in the context of IBD. This suggests a gap in communication between healthcare providers and patients about the benefits of PA and how it can be safely incorporated into their lifestyle considering their disease status[9].

SYNERGY AND STRUGGLE: BODY COMPOSITION, IBD, AND PA

IBD often leads to alterations in body composition, characterized by a reduction in muscle mass and an increase in fat mass. This phenomenon, known as sarcopenia, is prevalent among IBD patients and is linked to poor outcomes, including increased disability, lower quality of life, and higher rates of surgery[10]. Sarcopenia in IBD can result from

various factors, including chronic inflammation, malnutrition, and reduced PA. Additionally, IBD patients often experience body composition changes due to the catabolic state induced by the chronic inflammation and the side effects of treatments like corticosteroids[11].

While the direct effects of implementing an exercise regimen in individuals with sarcopenia and IBD remain inconclusive, it is advisable to promote PA among patients. Based on research related to other medical conditions, it is probable that the integration of resistance training and aerobic exercise will result in favorable outcomes. The management of the underlying IBD is anticipated to have a positive impact on muscle health. However, additional research is necessary to have a more comprehensive understanding of this association[12].

There exists a correlation between obesity and a decreased occurrence of clinical remission as well as elevated levels of depression, anxiety, fatigue, and pain in individuals with IBD as compared to non-obese people. Furthermore, it was observed that patients with obesity and IBD experienced a significantly greater annual burden and higher expenses associated with hospitalization when compared to their non-obese counterparts. In addition to general obesity, visceral adiposity has demonstrated a more consistent correlation with poor outcomes in individuals with IBD. Patients with CD who had a high volume of visceral adipose tissue had an increased risk of penetrating or stricturing complications and required a shorter time interval to undergo surgery[13].

Moderate-intensity aerobic exercise, in addition to resistance training, can help reduce fat mass and improve cardiovascular health in IBD patients. This type of exercise is beneficial for managing body weight and reducing the risk of comorbid conditions[14]. Ng *et al*[15] demonstrated that low-intensity exercise improved the quality of life in patients with CD, suggesting that even mild forms of PA can have beneficial effects on body composition and overall well-being of IBD patients.

The "BE-FIT-IBD" study does not specifically detail the intensity of PA in terms of light, moderate, or intense categories. However, it does mention the use of the IPAQ to assess PA levels among IBD patients. The IPAQ classifies PA into different types: Intense activities (like running); moderate activities (such as carrying light weights); and mild activities (like walking for at least 10 min). Of note, it is indicated that patients with UC had a negative correlation between their disease activity and the intense activity scores from the IPAQ. This suggests that patients engaging in more intense activities might have lower disease activity scores, although this relationship was not significant[8].

PHYSICAL INACTIVITY AND DISABILITY: UNDERSTANDING THE COMPLEX INTERACTION

The finding that a large percentage of IBD patients are physically inactive unveils a potential disability aspect in these individuals. Physical inactivity is often both a consequence and a cause of disability. This phenomenon may be caused by a variety of factors in patients with IBD, including pain, fatigue, gastrointestinal symptoms, and psychological distress [3]. These elements can limit a patient's ability to engage in regular PA, leading to a vicious cycle where inactivity further exacerbates disease symptoms and quality of life. The "BE-FIT-IBD" study reports a high unemployment rate among IBD patients especially among patients suffering from CD. It seems that the impact of physical inactivity extends beyond the medical sphere, increased fatigue, and decreased stamina due to lower physical fitness making it challenging for some patients to meet the physical demands of many jobs[8].

Other studies have shown that IBD can significantly impact employment status. A higher rate of unemployment is noted among IBD patients compared to the general population, and those who are employed often report difficulties in fulfilling their job responsibilities[15]. IBD patients often face unique challenges in the workplace due to the unpredictability of their symptoms. Flare-ups can lead to frequent bathroom breaks, fatigue, and pain, which can lower job performance and attendance. These challenges can lead to decreased productivity, absenteeism, and even job loss, contributing to the psychological burden of the disease. The economic implications of IBD-related workplace disability are significant. The costs associated with low productivity and unemployment can be substantial, adding to the costs of care of these patients[16-18].

INTERPLAY BETWEEN PSYCHOLOGICAL BURDEN OF IBD AND PA

IBD is often associated with a considerable psychological burden. Patients frequently experience anxiety, depression, and reduced quality of life due to the chronic and unpredictable nature of the disease. The psychological impact is exacerbated by symptoms such as pain and fatigue, resulting in a negative cycle that affects both mental and physical health. Depression in these patients may be further compounded by the social stigma and isolation associated with the disease[19,20]. Stress and anxiety can also exacerbate IBD symptoms, creating a complex interplay between psychological state and disease activity[21].

Engaging in PA has been recognized as a beneficial coping mechanism for IBD patients. Regular PA leads to improvements in mood, reduces anxiety levels, and enhances overall mental health in IBD patients. This can be attributed to the release of endorphins during exercise, which are natural mood lifters[22].

Group exercises or sports activities not only provide the physical benefits associated with exercise but also offer a crucial social dimension. This social interaction can hold therapeutic effects for IBD patients, who often struggle with feelings of isolation due to the chronic nature of their condition. The social support derived from group activities can significantly enhance the mental health of IBD patients. Participating in group exercises allows individuals to connect with others who may share similar experiences and challenges, fostering a sense of community and belonging. This can be incredibly valuable in reducing feelings of loneliness and isolation that often accompany chronic illnesses like IBD.

Moreover, the shared experiences in group settings can lead to the exchange of coping strategies, tips on disease management, and general emotional support. Such interactions can improve overall mental well-being as they feel understood and supported not just by medical professionals but also by peers who truly empathize with their daily experiences[23,24].

IMPACT OF PA AND IBD: A BIDIRECTIONAL LINK

PA has been recognized for its potential role in influencing the course of IBD. Regular exercise can contribute to a reduction in the severity of symptoms and may even play a role in prolonging periods of remission, particularly in CD. Studies have shown that moderate, consistent PA can lead to a decrease in inflammatory markers commonly associated with IBD, suggesting a potential anti-inflammatory effect of exercise. This reduction may be mediated through several mechanisms, including the downregulation of proinflammatory cytokines and the enhancement of anti-inflammatory mediators[3,5,25]. Regular PA is thought to contribute to a reduction in the frequency of IBD flare-ups. This is particularly significant given the unpredictable nature of these diseases. For CD patients, some studies have indicated that those who engage in consistent moderate exercise experience longer periods of remission and fewer episodes of acute exacerbation [26,27].

The "BE-FIT-IBD" study did not find significant difference in PA levels, as measured by the IPAQ total score, in relation to the PRO-2 measured IBD activity. The data related to the frequency of symptoms in patients with CD and UC exhibited diversity, with no significant alterations seen. It is noteworthy that individuals with CD who were in a state of remission and participated in consistent PA acquired better disease activity scores compared to those who engaged in less PA. However, this observation was not valid in patients with UC. The study also draws attention to how treatments, particularly biologics, influence PA levels. Patients on biologic therapy showed better IPAQ scores in moderate PA. This suggests that effective medical management of IBD can potentially reduce disability by enabling patients to increase their PA levels, thus breaking the cycle of inactivity[8].

CONCLUSION

The "BE-FIT-IBD" study serves as a wake-up call, bringing attention to the complex relationship between PA and IBD, revealing concerning levels of inactivity among these patients that contributes to numerous health conditions. The study's findings underscore the necessity of addressing physical inactivity in IBD management, emphasizing the need for comprehensive care strategies that integrate PA. Healthcare providers should proactively engage in patient education, dispelling misconceptions about exercise and IBD, and tailor exercise recommendations to individual patient needs. This approach can enhance patient well-being, reduce IBD-related complications, and improve overall quality of life. The importance of PA in managing IBD is becoming more and more clear as research is conducted, and the incorporation of PA into standard care practice is becoming mandatory.

FOOTNOTES

Author contributions: Trifan A designed the editorial; Stafie R and Rotaru A wrote the paper; Singeap AM and Stanciu C revised the paper.

Conflict-of-interest statement: The authors declare having no conflicts of interest.

Country/Territory of origin: Romania

ORCID number: Remus Stafie 0000-0003-1460-6559; Ana-Maria Singeap 0000-0001-5621-548X; Adrian Rotaru 0000-0002-6459-6996; Carol Stanciu 0000-0002-6427-4049; Anca Trifan 0000-0001-9144-5520.

S-Editor: Chen YL
L-Editor: A
P-Editor: Yuan YY

REFERENCES

1 **Ananthakrishnan AN**, Kaplan GG, Ng SC. Changing Global Epidemiology of Inflammatory Bowel Diseases: Sustaining Health Care

Delivery Into the 21st Century. *Clin Gastroenterol Hepatol* 2020; **18**: 1252-1260 [PMID: 32007542 DOI: 10.1016/j.cgh.2020.01.028]
2 **Ananthakrishnan AN**. Epidemiology and risk factors for IBD. *Nat Rev Gastroenterol Hepatol* 2015; **12**: 205-217 [PMID: 25732745 DOI: 10.1038/nrgastro.2015.34]
3 **Davis SP**, Crane PB, Bolin LP, Johnson LA. An integrative review of physical activity in adults with inflammatory bowel disease. *Intest Res* 2022; **20**: 43-52 [PMID: 33472342 DOI: 10.5217/ir.2020.00049]
4 **Mareschal J**, Douissard J, Genton L. Physical activity in inflammatory bowel disease: benefits, challenges and perspectives. *Curr Opin Clin Nutr Metab Care* 2022; **25**: 159-166 [PMID: 35238803 DOI: 10.1097/MCO.0000000000000829]
5 **DeFilippis EM**, Tabani S, Warren RU, Christos PJ, Bosworth BP, Scherl EJ. Exercise and Self-Reported Limitations in Patients with Inflammatory Bowel Disease. *Dig Dis Sci* 2016; **61**: 215-220 [PMID: 26254773 DOI: 10.1007/s10620-015-3832-4]
6 **Bilski J**, Brzozowski B, Mazur-Bialy A, Sliwowski Z, Brzozowski T. The role of physical exercise in inflammatory bowel disease. *Biomed Res Int* 2014; **2014**: 429031 [PMID: 24877092 DOI: 10.1155/2014/429031]
7 **García-Mateo S**, Martínez-Domínguez SJ, Gargallo-Puyuelo CJ, Arroyo Villarino MT, Laredo De La Torre V, Gallego B, Alfambra E, Gomollón F. Lifestyle Can Exert a Significant Impact on the Development of Metabolic Complications and Quality Life in Patients with Inflammatory Bowel Disease. *Nutrients* 2023; **15** [PMID: 37764769 DOI: 10.3390/nu15183983]
8 **Sajadinejad MS**, Asgari K, Molavi H, Kalantari M, Adibi P. Psychological issues in inflammatory bowel disease: an overview. *Gastroenterol Res Pract* 2012; **2012**: 106502 [PMID: 22778720 DOI: 10.1155/2012/106502]
9 **Gravina AG**, Pellegrino R, Durante T, Palladino G, D'Onofrio R, Mammone S, Arboretto G, Auletta S, Imperio G, Ventura A, Romeo M, Federico A. Inflammatory bowel diseases patients suffer from significant low levels and barriers to physical activity: The "BE-FIT-IBD" study. *World J Gastroenterol* 2023; **29**: 5668-5682 [PMID: 38077160 DOI: 10.3748/wjg.v29.i41.5668]
10 **Ryan E**, McNicholas D, Creavin B, Kelly ME, Walsh T, Beddy D. Sarcopenia and Inflammatory Bowel Disease: A Systematic Review. *Inflamm Bowel Dis* 2019; **25**: 67-73 [PMID: 29889230 DOI: 10.1093/ibd/izy212]
11 **Beaudart C**, Dawson A, Shaw SC, Harvey NC, Kanis JA, Binkley N, Reginster JY, Chapurlat R, Chan DC, Bruyère O, Rizzoli R, Cooper C, Dennison EM; IOF-ESCEO Sarcopenia Working Group. Nutrition and physical activity in the prevention and treatment of sarcopenia: systematic review. *Osteoporos Int* 2017; **28**: 1817-1833 [PMID: 28251287 DOI: 10.1007/s00198-017-3980-9]
12 **Gold SL**, Raman M, Sands BE, Ungaro R, Sabino J. Review article: Putting some muscle into sarcopenia-the pathogenesis, assessment and clinical impact of muscle loss in patients with inflammatory bowel disease. *Aliment Pharmacol Ther* 2023; **57**: 1216-1230 [PMID: 37051722 DOI: 10.1111/apt.17498]
13 **Rozich JJ**, Holmer A, Singh S. Effect of Lifestyle Factors on Outcomes in Patients With Inflammatory Bowel Diseases. *Am J Gastroenterol* 2020; **115**: 832-840 [PMID: 32224703 DOI: 10.14309/ajg.0000000000000608]
14 **Metsios GS**, Moe RH, Kitas GD. Exercise and inflammation. *Best Pract Res Clin Rheumatol* 2020; **34**: 101504 [PMID: 32249021 DOI: 10.1016/j.berh.2020.101504]
15 **Ng V**, Millard W, Lebrun C, Howard J. Low-intensity exercise improves quality of life in patients with Crohn's disease. *Clin J Sport Med* 2007; **17**: 384-388 [PMID: 17873551 DOI: 10.1097/JSM.0b013e31802b4fda]
16 **Büsch K**, da Silva SA, Holton M, Rabacow FM, Khalili H, Ludvigsson JF. Sick leave and disability pension in inflammatory bowel disease: a systematic review. *J Crohns Colitis* 2014; **8**: 1362-1377 [PMID: 25001582 DOI: 10.1016/j.crohns.2014.06.006]
17 **van der Valk ME**, Mangen MJ, Leenders M, Dijkstra G, van Bodegraven AA, Fidder HH, de Jong DJ, Pierik M, van der Woude CJ, Romberg-Camps MJ, Clemens CH, Jansen JM, Mahmmod N, van de Meeberg PC, van der Meulen-de Jong AE, Ponsioen CY, Bolwerk CJ, Vermeijden JR, Siersema PD, van Oijen MG, Oldenburg B; COIN study group; Dutch Initiative on Crohn and Colitis. Risk factors of work disability in patients with inflammatory bowel disease--a Dutch nationwide web-based survey: work disability in inflammatory bowel disease. *J Crohns Colitis* 2014; **8**: 590-597 [PMID: 24351733 DOI: 10.1016/j.crohns.2013.11.019]
18 **Lönnfors S**, Vermeire S, Greco M, Hommes D, Bell C, Avedano L. IBD and health-related quality of life -- discovering the true impact. *J Crohns Colitis* 2014; **8**: 1281-1286 [PMID: 24662394 DOI: 10.1016/j.crohns.2014.03.005]
19 **Ding Z**, Muser E, Izanec J, Lukanova R, Kershaw J, Roughley A. Work-Related Productivity Loss and Associated Indirect Costs in Patients With Crohn's Disease or Ulcerative Colitis in the United States. *Crohns Colitis 360* 2022; **4**: otac023 [PMID: 36777416 DOI: 10.1093/crocol/otac023]
20 **Byrne G**, Rosenfeld G, Leung Y, Qian H, Raudzus J, Nunez C, Bressler B. Prevalence of Anxiety and Depression in Patients with Inflammatory Bowel Disease. *Can J Gastroenterol Hepatol* 2017; **2017**: 6496727 [PMID: 29181373 DOI: 10.1155/2017/6496727]
21 **Eugenicos MP**, Ferreira NB. Psychological factors associated with inflammatory bowel disease. *Br Med Bull* 2021; **138**: 16-28 [PMID: 34057462 DOI: 10.1093/bmb/ldab010]
22 **Mawdsley JE**, Rampton DS. Psychological stress in IBD: new insights into pathogenic and therapeutic implications. *Gut* 2005; **54**: 1481-1491 [PMID: 16162953 DOI: 10.1136/gut.2005.064261]
23 **Mikkelsen K**, Stojanovska L, Polenakovic M, Bosevski M, Apostolopoulos V. Exercise and mental health. *Maturitas* 2017; **106**: 48-56 [PMID: 29150166 DOI: 10.1016/j.maturitas.2017.09.003]
24 **Sebastião E**, Mirda D. Group-based physical activity as a means to reduce social isolation and loneliness among older adults. *Aging Clin Exp Res* 2021; **33**: 2003-2006 [PMID: 33387363 DOI: 10.1007/s40520-020-01722-w]
25 **Mählmann L**, Gerber M, Furlano RI, Legeret C, Kalak N, Holsboer-Trachsler E, Brand S. Psychological wellbeing and physical activity in children and adolescents with inflammatory bowel disease compared to healthy controls. *BMC Gastroenterol* 2017; **17**: 160 [PMID: 29233119 DOI: 10.1186/s12876-017-0721-7]
26 **Strober W**, Zhang F, Kitani A, Fuss I, Fichtner-Feigl S. Proinflammatory cytokines underlying the inflammation of Crohn's disease. *Curr Opin Gastroenterol* 2010; **26**: 310-317 [PMID: 20473158 DOI: 10.1097/MOG.0b013e328339d099]
27 **Neal WN**, Jones CD, Pekmezi D, Motl RW. Physical Activity in Adults With Crohn's Disease: A Scoping Review. *Crohns Colitis 360* 2022; **4**: otac022 [PMID: 36777047 DOI: 10.1093/crocol/otac022]

World Journal of Gastroenterology

Submit a Manuscript: https://www.f6publishing.com

World J Gastroenterol 2024 March 14; 30(10): 1266-1269

DOI: 10.3748/wjg.v30.i10.1266

ISSN 1007-9327 (print) ISSN 2219-2840 (online)

EDITORIAL

Double role of depression in gastric cancer: As a causative factor and as consequence

Grigorios Christodoulidis, Koumarelas Konstantinos-Eleftherios, Kouliou Marina-Nektaria

Specialty type: Gastroenterology and hepatology

Provenance and peer review: Invited article; Externally peer reviewed.

Peer-review model: Single blind

Peer-review report's scientific quality classification

Grade A (Excellent): 0
Grade B (Very good): 0
Grade C (Good): 0
Grade D (Fair): D
Grade E (Poor): 0

P-Reviewer: Tan JK, Malaysia

Received: December 16, 2023
Peer-review started: December 16, 2023
First decision: January 4, 2024
Revised: January 13, 2024
Accepted: February 23, 2024
Article in press: February 23, 2024
Published online: March 14, 2024

Grigorios Christodoulidis, Koumarelas Konstantinos-Eleftherios, Kouliou Marina-Nektaria, Department of General Surgery, University Hospital of Larissa, Larissa 41110, Greece

Corresponding author: Grigorios Christodoulidis, MD, PhD, Surgeon, Department of General Surgery, University Hospital of Larissa, Mezourlo, Larissa 41110, Greece. gregsurg@yahoo.gr

Abstract

In this editorial we comment on the article "Hotspots and frontiers of the relationship between gastric cancer and depression: A bibliometric study". Gastric cancer (GC) is a common malignancy in the digestive system with increased mortality and morbidity rates globally. Standard treatments, such as gastrectomy, negatively impact patients' quality of life and beyond the physical strain, GC patients face psychological challenges, including anxiety and depression. The prevalence of depression can be as high as 57%, among gastrointestinal cancer patients. Due to the advancements in treatment effectiveness and increased 5-year overall survival rates, attention has shifted to managing psychological effects. However, the significance of managing the depression doesn't lie solely in the need for a better psychological status. Depression leads to chronic stress activating the sympathetic nervous system and the hypothalamus-pituitary-adrenal axis, leading release of catecholamines inducing tumor proliferation, migration, and metastasis, contributing to GC progression. The dysregulation of neurotransmitters and the involvement of various signaling pathways underscore the complex interplay between depression and GC. Comprehensive strategies are required to address the psychological aspects of GC, including region-specific interventions and increased monitoring for depression. Understanding the intricate relationship between depression and GC progression is essential for developing effective therapeutic strategies and improving overall outcomes for patients facing this complex disease. In this Editorial we delve into double role of depression in the pathogenesis of GC and as a complication of it.

Key Words: Gastric cancer; Depression; Anxiety; Chronic stress; Pathogenesis of gastric cancer

Core Tip: Gastric cancer (GC), a prevalent malignancy in the digestive system, poses a dual challenge with both physical and psychological implications. While standard treatments like gastrectomy impact patients' quality of life, the psychological burden, including anxiety and depression, cannot be overlooked. Depression, reaching prevalence rates of 57%, significantly influences cancer outcomes, affecting mental well-being, treatment adherence, and overall quality of life. Chronic stress and neurotransmitter dysregulation play a pivotal role in GC development, activating pathways that induce tumor progression. Understanding the intricate connection between depression and GC not only highlights the need for comprehensive psychological support but also unveils potential therapeutic targets. Addressing both the physical and psychological aspects of GC is essential for enhancing the overall well-being and outcomes of patients grappling with this complex disease.

Citation: Christodoulidis G, Konstantinos-Eleftherios K, Marina-Nektaria K. Double role of depression in gastric cancer: As a causative factor and as consequence. *World J Gastroenterol* 2024; 30(10): 1266-1269
URL: https://www.wjgnet.com/1007-9327/full/v30/i10/1266.htm
DOI: https://dx.doi.org/10.3748/wjg.v30.i10.1266

INTRODUCTION

Gastric cancer (GC) stands as the most prevalent malignant tumor in the digestive system, holding the record for the third-highest mortality and fifth-highest morbidity rates among all cancers. Global statistics underscore the gravity of the situation, revealing an estimated 1 million new cases and 760000 deaths in 2020 alone[1-4]. The standard treatment for GC, gastrectomy, while common, has detrimental effects on patients' quality of life (QoL) and mental well-being. Total gastrectomy, an aspect of this treatment, triggers substantial weight loss, thereby impacting the nutritional status of individuals with the disease. GC alone, can cause disturbing and disabling nausea, vomiting, diarrhea having a significant impact on the patients' nutritional status[2,3,5]. Beyond the physical strain, patients diagnosed with GC confront some psychological challenges, including anxiety, depression, pain, and fatigue[1,3,5,6]. The prevalence of anxiety and depression can reach as high as 47.2% and 57% of patients with gastrointestinal cancer[6]. The last years, having an increased effectiveness of the treatment options and an increased 5-year overall survival, the attention shifts to managing the psychological effects accompanying the disease and the treatment. These challenges emphasize the urgent need for interventions aimed to enhance the overall QoL of these patients. Depression emerges as a pervasive issue among cancer patients, particularly affecting their mental well-being. Contributing factors include the dysregulation of miRNA expression, abnormalities in receptors, and structural changes in the brain[1,7]. Such emotional distress not only shapes the attitude of cancer patients but also influences treatment adherence, underscoring its critical role in determining overall QoL[1,6]. Psychological distress becomes a notable risk factor for treatment non-compliance, increasing the mortality rates. The repercussions of depression extend further, exerting a negative influence on the prognosis of GC and resulting in poor survival outcomes. Depression in the context of cancer, including GC, is linked to chronic psychological stress. Stress-associated neurotransmitters, particularly catecholamines, emerge as potential influencers of cancer progression[5,8]. Chronic stress, often manifesting as anxiety and depression, can trigger tumor development through pathways involving β2-adrenergic receptors and epithelial–mesenchymal transition (EMT). Despite the acknowledgment of chronic stress and β2-adrenergic receptors in tumor progression, the precise mechanisms of how EMT is regulated by β2-AR remain elusive[4,8]. Consequently, there is a need for a deeper understanding of these mechanisms to guide more effective therapeutic strategies. Recognizing the gravity of depression's impact on cancer outcomes, proper treatment is deemed essential for cancer patients. This treatment aims not only to mitigate adverse effects but also to improve symptoms, ensuring the long-term efficacy of interventions for individuals grappling with the complexities of GC.

ROLE OF DEPRESSION IN GASTRIC CANCER DEVELOPMENT

Under the influence of chronic stress, the sympathetic nervous system is activated as well as the hypothalamus-pituitary-adrenal axis, thereby triggering the release of neurotransmitters such as norepinephrine and epinephrine ($P < 0.005$)[5]. The increased expression of catecholamines within the tumor microenvironment has been revealed to induce the proliferation, migration, and metastasis of many tumors, such as breast, lung, and colon cancer. Catecholamines play a significant role in promoting EMT by utilizing signaling pathways like c-Jun[4,5,8]. Anxiety and depression can accelerate the onset and advancement of GC through multifaceted mechanisms (*e.g.*, influencing reactive oxygen species-activated ABL1) and modulating the hypothalamic–pituitary–adrenal axis (*e.g.*, FK506 binding protein 5 gene polymorphisms), thereby inducing disease deterioration and increasing the possibility of recurrence in GC patients[9,10].

Functioning as neurotransmitters, catecholamines can influence tumor characteristics, including phenotypic transformation, apoptosis, and drug resistance. The acquisition of a neuroendocrine phenotype in cancer cells strongly correlates with neoplasm metastasis, drug resistance, advanced cancer stage, and the increased expression of neuroendocrine markers-synaptophysin (SYP), CD44, and chromogranin A[5]. The binding of catecholamines to the beta-2 adrenergic receptor (β2-AR) upregulates MACC1 expression, leading to neuroendocrine phenotypic transformation, GC invasion, and metastasis. In this process, α-AR does not exhibit any discernible role. MACC1, an oncogene regulated by c-

Jun, controls c-Met transcriptional levels, enhancing EMT. The activation of the hepatocyte growth factor receptor (c-Met) orchestrates neuroendocrine features in advanced prostate cancer, assuming a parallel role in GC development. Reversal of these effects in mouse models and *in vitro* is achieved through treatment with β2-AR antagonists or MACC1 silencing [5]. MACC1 also forms a complex with SYP, a marker of neuroendocrine phenotypic characteristics, utilizing the MACC1/SYP signaling pathway in the neuroendocrine phenotypic transformation triggered by catecholamine. Targeting β2-AR mitigates depression-induced neuroendocrine phenotypic transformation and lung metastasis of GC, providing potential therapeutic targets for enhancing outcomes in GC patients with concurrent depression. β2-AR stimulation may additionally induce EMT, migration, and invasion by ERK (Extracellular-signal-regulated kinase) phosphorylation[8]. Lu *et al*[8] observed that salbutamol, a β2-AR agonist, heightened the expression of the mesenchymal marker N-cadherin and reduced the epithelial marker E-cadherin in transplanted tumor tissue, thereby inducing further EMT[8]. They also supported the idea that the β2-AR agonist isoproterenol promotes EMT of GC cells through the STAT3-CD44 pathway, shedding light on the association of depression with GC[11]. The β2-AR-HIF-1α-Snail signaling pathway influences the EMT of GC cells, promoting the invasion and migration of GC[12]. Last but not least, Liu *et al*[4] observed that the activation of β2-AR increases the expression of PlexinA1, activates JAK-STAT3 signaling, and further promotes EMT in human GC cells. Consequently, chronic stress is intricately linked with the pathogenesis of GC[4].

T helper (Th) cells modulate the stress response, oxidative stress, and neuroinflammation, potentially participating in the pathogenesis of anxiety, depression, and cognitive impairment. Th1 (P = 0.017) and Th17 (P = 0.049) levels were found to be elevated in patients with depression compared to those without depression[13].

When depression is quantified by the Patient Health Questionnaire-9 score, a positive correlation is observed with serum levels of epinephrine, noradrenaline, MACC1, as well as tumor-node-metastasis (TNM) stage, supporting the association of depression with GC pathogenesis[5].

DEPRESSION AS A RESULT OF GASTRIC CANCER

GC patients face many psychological challenges, including anxiety, depression, pain, and fatigue, underscoring the need to prioritize their QoL. The prevalence of depression among these patients is often underestimated, despite its effects on prognosis and QoL[2]. Notably, depression has been linked to increased suicidal thoughts, anxiety, distress, and fatigue in cancer patients, with studies emphasizing in the need of increased monitoring for this condition[14]. The impact of depression is particularly significant among GC patients, while they are already at risk for malnutrition, lower body mass index, reduced physical activity, and social isolation, exacerbating their susceptibility to depression[2].

The comorbidities accompanying GC and its treatment introduces additional challenges, as gastrectomy, a commonly employed strategy for curative resection, profoundly affects patients' QoL and mental well-being. Total gastrectomy, in particular, results in substantial postoperative malnutrition, with patients experiencing significant weight loss within the first year of surgery[2].

Several studies highlight the prevalence of depression among GC patients, ranging from 4.0% to 68% with a mean of 37% (95%CI). The variability in prevalence underscores the need for comprehensive and region-specific approaches to address this psychological aspect of the disease. A study by Kouhestani *et al*[2] in 2022, drawing data from the National Health Service Sample Cohort, revealed a higher risk of new-onset depression in GC patients, particularly in females aged 60-69 living in metropolitan regions with high income[2].

Kwon *et al*[6] investigate the correlation between depression and stomach cancer further, emphasizing the stressful aspect of cancer diagnosis and therapy, which causes anxiety and depression in a considerable proportion of patients[6].

Patients with recurrent stomach cancer had greater levels of anxiety and sadness than newly diagnosed patients and healthy controls. Age above 60 years, diabetes, TNM stage at diagnosis, shorter duration to recurrence, and distant metastases at recurrence were all risk factors for anxiety. Age above 60 years, diabetes, tumor site upon diagnosis, and shorter time to recurrence were all risk factors for depression[6].

Liu investigates factors associated with anxiety and depression in GC patients, revealing that coping style, type D personality, and neutrophil-to-lymphocyte ratio contribute to preoperative anxiety and depression. Additionally, genetic factors, including polymorphisms in genes related to apoptosis, may play a role in susceptibility to GC and associated psychological distress[3,15].

However, Lou *et al*[15] observed that polymorphisms of BNIP3 and DAPK1 were associated with a protective effect against GC. These two genes are shown to also have a protective effect against depression[15].

CONCLUSION

Considering the global significance of GC as the fifth most frequently diagnosed cancer, efforts to understand and address the psychological impact of the disease, particularly depression and anxiety, are essential. Efforts should involve a multidisciplinary approach, considering both the physical and mental well-being of patients to improve overall outcomes and QoL.

FOOTNOTES

Author contributions: Christodoulidis G, Konstantinos-Eleftherios K and Marina-Nektaria K contributed to this paper; Christodoulidis G designed the overall concept and outline of the manuscript; Christodoulidis G, Konstantinos-Eleftherios K and Marina-Nektaria K contributed to the discussion and design of the manuscript; Christodoulidis G, Konstantinos-Eleftherios K and Marina-Nektaria K contributed to the writing, editing the manuscript, and review of literature.

Conflict-of-interest statement: All the authors report no relevant conflicts of interest for this article.

Country/Territory of origin: Greece

ORCID number: Grigorios Christodoulidis 0000-0003-3413-0666; Koumarelas Konstantinos-Eleftherios 0000-0002-5614-4770; Kouliou Marina-Nektaria 0000-0002-2055-2297.

S-Editor: Li L
L-Editor: A
P-Editor: Zhao YQ

REFERENCES

1 **Liu JY**, Zheng JQ, Yin CL, Tang WP, Zhang JN. Hotspots and frontiers of the relationship between gastric cancer and depression: A bibliometric study. *World J Gastroenterol* 2023; **29**: 6076-6088 [PMID: 38130743 DOI: 10.3748/wjg.v29.i46.6076]
2 **Kouhestani M**, Ahmadi Gharaei H, Fararouei M, Hosienpour Ghahremanloo H, Ghaiasvand R, Dianatinasab M. Global and regional geographical prevalence of depression in gastric cancer: a systematic review and meta-analysis. *BMJ Support Palliat Care* 2022; **12**: e526-e536 [PMID: 32434923 DOI: 10.1136/bmjspcare-2019-002050]
3 **Liu P**, Wang Z. Postoperative anxiety and depression in surgical gastric cancer patients: their longitudinal change, risk factors, and correlation with survival. *Medicine (Baltimore)* 2022; **101** [PMID: 35356898 DOI: 10.1097/MD.0000000000028765]
4 **Liu Y**, Hao Y, Zhao H, Zhang Y, Cheng D, Zhao L, Peng Y, Lu Y, Li Y. PlexinA1 activation induced by β2-AR promotes epithelial-mesenchymal transition through JAK-STAT3 signaling in human gastric cancer cells. *J Cancer* 2022; **13**: 2258-2270 [PMID: 35517411 DOI: 10.7150/jca.70000]
5 **Pan C**, Wu J, Zheng S, Sun H, Fang Y, Huang Z, Shi M, Liang L, Bin J, Liao Y, Chen J, Liao W. Depression accelerates gastric cancer invasion and metastasis by inducing a neuroendocrine phenotype *via* the catecholamine/β(2) -AR/MACC1 axis. *Cancer Commun (Lond)* 2021; **41**: 1049-1070 [PMID: 34288568 DOI: 10.1002/cac2.12198]
6 **Kwon S**, Kim J, Kim T, Jeong W, Park EC. Association between gastric cancer and the risk of depression among South Korean adults. *BMC Psychiatry* 2022; **22**: 207 [PMID: 35313847 DOI: 10.1186/s12888-022-03847-w]
7 **Wang HQ**, Wang ZZ, Chen NH. The receptor hypothesis and the pathogenesis of depression: Genetic bases and biological correlates. *Pharmacol Res* 2021; **167**: 105542 [PMID: 33711432 DOI: 10.1016/j.phrs.2021.105542]
8 **Lu Y**, Zhang Y, Zhao H, Li Q, Liu Y, Zuo Y, Xu Q, Zuo H, Li Y. Chronic stress model simulated by salbutamol promotes tumorigenesis of gastric cancer cells through β2-AR/ERK/EMT pathway. *J Cancer* 2022; **13**: 401-412 [PMID: 35069890 DOI: 10.7150/jca.65403]
9 **Huang T**, Zhou F, Wang-Johanning F, Nan K, Wei Y. Depression accelerates the development of gastric cancer through reactive oxygen species-activated ABL1 (Review). *Oncol Rep* 2016; **36**: 2435-2443 [PMID: 27666407 DOI: 10.3892/or.2016.5127]
10 **Kang JI**, Chung HC, Jeung HC, Kim SJ, An SK, Namkoong K. FKBP5 polymorphisms as vulnerability to anxiety and depression in patients with advanced gastric cancer: a controlled and prospective study. *Psychoneuroendocrinology* 2012; **37**: 1569-1576 [PMID: 22459275 DOI: 10.1016/j.psyneuen.2012.02.017]
11 **Lu YJ**, Geng ZJ, Sun XY, Li YH, Fu XB, Zhao XY, Wei B. Isoprenaline induces epithelial-mesenchymal transition in gastric cancer cells. *Mol Cell Biochem* 2015; **408**: 1-13 [PMID: 26253173 DOI: 10.1007/s11010-015-2477-0]
12 **Shan T**, Cui X, Li W, Lin W, Li Y, Chen X, Wu T. Novel regulatory program for norepinephrine-induced epithelial-mesenchymal transition in gastric adenocarcinoma cell lines. *Cancer Sci* 2014; **105**: 847-856 [PMID: 24815301 DOI: 10.1111/cas.12438]
13 **Zhou Y**, Yu K. Th1, Th2, and Th17 cells and their corresponding cytokines are associated with anxiety, depression, and cognitive impairment in elderly gastric cancer patients. *Front Surg* 2022; **9**: 996680 [PMID: 36386524 DOI: 10.3389/fsurg.2022.996680]
14 **Walker J**, Hansen CH, Martin P, Symeonides S, Ramessur R, Murray G, Sharpe M. Prevalence, associations, and adequacy of treatment of major depression in patients with cancer: a cross-sectional analysis of routinely collected clinical data. *Lancet Psychiatry* 2014; **1**: 343-350 [PMID: 26360998 DOI: 10.1016/S2215-0366(14)70313-X]
15 **Lou X**, Hu D, Li Z, Teng Y, Lou Q, Huang S, Zou Y, Wang F. Associations of BNIP3 and DAPK1 gene polymorphisms with disease susceptibility, clinicopathologic features, anxiety, and depression in gastric cancer patients. *Int J Clin Exp Pathol* 2021; **14**: 633-645 [PMID: 34093949]

World Journal of Gastroenterology

Submit a Manuscript: https://www.f6publishing.com

World J Gastroenterol 2024 March 14; 30(10): 1270-1279

DOI: 10.3748/wjg.v30.i10.1270

ISSN 1007-9327 (print) ISSN 2219-2840 (online)

EDITORIAL

Capsule endoscopy and panendoscopy: A journey to the future of gastrointestinal endoscopy

Bruno Rosa, José Cotter

Specialty type: Gastroenterology and hepatology

Provenance and peer review: Invited article; Externally peer reviewed.

Peer-review model: Single blind

Peer-review report's scientific quality classification
Grade A (Excellent): 0
Grade B (Very good): B
Grade C (Good): 0
Grade D (Fair): 0
Grade E (Poor): 0

P-Reviewer: Serban ED, Romania

Received: December 26, 2023
Peer-review started: December 26, 2023
First decision: January 10, 2024
Revised: January 22, 2024
Accepted: February 21, 2024
Article in press: February 21, 2024
Published online: March 14, 2024

Bruno Rosa, José Cotter, Department of Gastroenterology, Hospital da Senhora da Oliveira, Guimarães 4835-044, Portugal

Bruno Rosa, José Cotter, Life and Health Sciences Research Institute, School of Medicine, University of Minho, Braga 4710-057, Portugal

Bruno Rosa, José Cotter, ICVS/3B's, PT Government Associate Laboratory, Braga 4710-057, Portugal

Corresponding author: Bruno Rosa, MD, Doctor, Department of Gastroenterology, Hospital da Senhora da Oliveira, Rua dos Cutileiros, Creixomil, Guimarães 4835-044, Portugal. bruno.joel.rosa@gmail.com

Abstract

In 2000, the small bowel capsule revolutionized the management of patients with small bowel disorders. Currently, the technological development achieved by the new models of double-headed endoscopic capsules, as miniaturized devices to evaluate the small bowel and colon [pan-intestinal capsule endoscopy (PCE)], makes this non-invasive procedure a disruptive concept for the management of patients with digestive disorders. This technology is expected to identify which patients will require conventional invasive endoscopic procedures (colonoscopy or balloon-assisted enteroscopy), based on the lesions detected by the capsule, *i.e.*, those with an indication for biopsies or endoscopic treatment. The use of PCE in patients with inflammatory bowel diseases, namely Crohn's disease, as well as in patients with iron deficiency anaemia and/or overt gastrointestinal (GI) bleeding, after a non-diagnostic upper endoscopy (esophagogastroduodenoscopy), enables an effective, safe and comfortable way to identify patients with relevant lesions, who should undergo subsequent invasive endoscopic procedures. The recent development of magnetically controlled capsule endoscopy to evaluate the upper GI tract, is a further step towards the possibility of an entirely non-invasive assessment of all the segments of the digestive tract, from mouth-to-anus, meeting the expectations of the early developers of capsule endoscopy.

Key Words: Non-invasive endoscopy; Panendoscopy; Magnetically controlled capsule endoscopy; Crohn's disease; Digestive bleeding

Core Tip: Double-headed capsules are being increasingly used for pan-intestinal endoscopy, assessing the small bowel and the colon in a single non-invasive procedure, mainly to monitor Crohn's disease and to investigate cases of suspected mid to lower gastrointestinal bleeding. Recent developments on artificial intelligence and magnetically controlled capsules have further expanded the scope of non-invasive endoscopy.

Citation: Rosa B, Cotter J. Capsule endoscopy and panendoscopy: A journey to the future of gastrointestinal endoscopy. *World J Gastroenterol* 2024; 30(10): 1270-1279
URL: https://www.wjgnet.com/1007-9327/full/v30/i10/1270.htm
DOI: https://dx.doi.org/10.3748/wjg.v30.i10.1270

INTRODUCTION

Capsule endoscopy emerged at the start of the 21st Century as a disruptive technology, which was destined to change the world of gastrointestinal (GI) endoscopy. It consists of a swallowable pill, featuring a miniaturized imaging device inside a biocompatible resistant external casing. It is composed of an optical dome with a lens and a light source, a complementary metal oxide semiconductor image sensor, two mercury-free silver-oxide batteries and a wireless radio-frequency transmitter and antenna, which allow the transmission of endoscopic images to a receiver (data recorder). The designers of this innovative device foresaw the possibility of acquiring images of the whole digestive tract non-invasively. They named it as *M2A*, standing for the *mouth-to-anus* capsule (Given Diagnostic Imaging, Yokneam, Israel)[1]. The major achievement with these capsules at that time was the possibility to explore the small bowel, which had been until then a largely inaccessible and unexplored segment. It was known as the last frontier of digestive endoscopy. The capsule was soon rebranded as PillCam™ SB. This new endoscopic technique was eagerly accepted and rapidly incorporated in clinical practice, as a safe and effective diagnostic procedure for the investigation of small bowel diseases, mainly in cases of suspected obscure GI bleeding and suspected small bowel Crohn's disease (CD). It was also useful in suspected non-steroidal anti-inflammatory drug (NSAID) enteropathy, polyposis syndromes such as Peutz-Jeghers syndrome, some cases of refractory celiac disease and suspected small bowel neoplasia[2]. Capsules with a single optical dome remain to date the most widely used in clinical practice, with enhanced features such as a higher frame rate acquisition (up to 6 images per second), a wider angle of view, a longer battery lifespan and improved image resolution.

In 2006, the first double-headed capsule was released, called the PillCam™ COLON. In 2009, the PillCam ™ COLON 2 (Given Imaging, Medtronic) was released. At 11.6 mm × 32.3 mm, it was slightly larger than the original SB capsule (11 mm × 26mm), with an increased frame rate for image acquisition (up to 35 images per second), an extended battery time and a wider angle of view (172º in each side), to allow for the coverage of the whole colonic surface. These capsules have been mainly used in the case of a contraindication to conventional colonoscopy, cases of incomplete colonoscopy due to fixed angulation or redundant colon with persistent loop formation, or in average risk populations as an alternative for colorectal cancer screening[3,4]. Two other models of double-headed capsules were released in 2017 (PillCam™ Crohn's, Medtronic) and in 2023 (OMOM CC™, Jinshan). Compared to the PillCam™ COLON, the PillCam™ Crohn's and the OMOM CC™ do not have a sleep mode, continuously acquiring images from the start of the examination. This enables the non-invasive examination of the small bowel and colon [pan-intestinal capsule endoscopy (PCE)], in a single procedure, which is safe and well tolerated by patients[5-7]. The OMOM CC™ integrates a new feature for artificial intelligence (AI) assisted diagnosis. If this is properly validated, it might overcome a current limitation of PCE, which is its time-consuming reading, reaching on average up to 120 min[8]. This will allow a faster examination, without compromising diagnostic accuracy. Table 1 summarizes the technical details of the currently available double-headed capsules, which may be used to perform PCE.

PCE PROCEDURE - BOWEL PREPARATION

For PCE, unlike for small bowel capsule endoscopy, which can be carried out without prior intestinal preparation, a demanding preparation protocol is mandatory. Optimized bowel preparation is essential to ensure an effective colon capsule (CC) endoscopy or PCE. It is not possible to irrigate or aspirate debris, insufflate or change the patient's position to improve the quality of visualization during the examination, at the risk of rendering the procedure inconclusive. This potentially poses a significant additional burden both to the patient and the healthcare system. A recently published systematic review and meta-analysis[9] described that key quality outcomes such as adequate cleansing rate (ACR) and complete examination rate (CR) remain sub-optimal for CC or PCE, with an ACR of 72.5% (95%CI 67.8%–77.5%) and a CR of 83.0% (95%CI 78.7%–87.7%). The Leighton-Rex grading scale[10], and more recently the CC CLEansing Assessment and Report (CC-CLEAR)[11,12], were created to allow a systematic description of the quality of bowel preparation in the colon at capsule endoscopy. The CC-CLEAR basically replicates the methodology of the Boston Bowel Preparation Scale [13], with which many gastroenterologists are familiar, as it is already common practice to use it routinely in conventional colonoscopy. The CC-CLEAR scale divides the colon in 3 segments: Right-sided, transverse, and left-sided, and each segment is scored according to an estimation of the proportion of clear mucosa: 0, < 50%; 1, 50%-75%; 2, > 75%; 3, > 90%. The overall cleansing classification is the sum of each segmental score, grading between 8-9, excellent; 6-7, good; and 0-5

Table 1 Technical details of double-headed capsules currently available to perform pan-intestinal capsule endoscopy

	PillCam™ COLON2 (Medtronic, Given Imaging Inc.)	PillCam™ Crohn's (Medtronic, Given Imaging Inc.)	OMOM™ CC (Jinshan)
Dimensions (mm)	11.6 × 32.3	11.6 × 32.3	11.6 × 31.5
Optical domes	2	2	2
Resolution (pixels)	256 × 256	256 × 256	360 × 360
Lens angle (degrees per side)	172	168	172
Frame rate (frames per second)	4-35	4-35	4-35
Sleep mode	Yes	No	No
Battery life (h)	≥ 10	≥ 10	≥ 10

inadequate; with any segment scoring ≤ 1 rendering the overall classification as inadequate. Although currently available data support the use of a low-fibre diet and adjunctive sennosides prior to the purgative ingestion, split dose polyethylene glycol and routine prokinetics before capsule ingestion, with sodium phosphate as the most consistent option as a booster, there is an unmet need for improvement in order to achieve more effective bowel preparation protocols. Table 2 summarizes a proposed bowel preparation protocol for CC and PCE, based on currently available evidence in the literature.

PCE IN CLINICAL PRACTICE

Double-headed capsules have been used in clinical practice as a pan-enteric tool, mainly in the setting of inflammatory bowel diseases (IBDs) and digestive bleeding [suspected small bowel or colon bleeding, *i.e.* mid or lower GI bleeding (MLGIB)]. Table 3 summarizes the current indications and contraindications for PCE.

CD

The use of PCE in patients with CD has been mainly devoted to patients with an established diagnosis of CD who have already been submitted to ileocolonoscopy and cross-sectional imaging such as computed tomography enterography (CTE) or magnetic resonance enterography (MRE), to evaluate the small bowel and exclude stricturing and/or penetrating phenotypes of the disease[14,15]. In this group of patients, the use of PCE seems especially appealing for monitoring disease progression and evaluating mucosal healing in response to therapy in those cases with extensive disease, *i.e.*, those that involve both the small bowel and the colon. It is estimated that approximately 40% of patients with CD have lesions limited to the small bowel, in another 20% the disease is located only in the colon, and in near 35% it involves both the small bowel and the colon[16]. It is also known that in these patients with small bowel and colonic involvement, the burden of the disease is often driven by the type of small bowel lesions, which are usually more severe, extensive and more difficult to heal. Up to 30% of patients will present with stricturing disease at diagnosis or progress to stricturing or penetrating disease over the years[17]. The subset of patients with inflammatory-type small bowel and colonic disease corresponds to approximately one-fourth of all patients with CD. Those are the patients who are good candidates for PCE as the preferred modality for disease assessment over time. The current standard recommends invasive conventional colonoscopy in addition to cross-sectional imaging of the small bowel, such as CTE or MRE. PCE offers the possibility of a one-step examination of both the small bowel and the colon, which is safe and comfortable for the patient, without the need for sedation, radiation exposure or multiple visits to the clinic. This strategy was demonstrated to be at least as effective for assessing the small bowel and the colon, when compared with colonoscopy plus dedicated small bowel cross-sectional imaging. Preliminary data indicate that under certain circumstances PCE may represent a cost-effective approach, leading to increased quality of life and life expectancy, and making it a cost-effective option[18]. Another study evaluated the cost of PCE *vs* colonoscopy, with or without MRE, in IBD patients. Although initial costs were increased due to the use of PCE and earlier introduction of biologics, an economical benefit was observed in the longer term, due to a significant reduction in the need for surgical interventions[19].

A recent systematic review and meta-analysis by Tamilarasan *et al*[20] evaluated the performance of PCE for the detection of CD lesions in the small bowel and the colon. It found a comparable diagnostic yield of PCE compared to MRE plus colonoscopy [pooled OR 1.25 (95%CI: 0.85%-1.86%). Capsule endoscopy is the only non-invasive modality for the small bowel to adequately assess the main treatment outcome, which is mucosal healing, according to the current treat to target concept for the treatment of IBDs[21]. A meta-analysis by Dionísio *et al*[22] found that capsule endoscopy has a significantly higher diagnostic yield in patients with suspected and established small bowel CD. This new approach may have significant clinical implications, as demonstrated in the multicentric study by Tai *et al*[23], where PCE

Table 2 Standard bowel preparation for pan-intestinal capsule endoscopy

	Bowel preparation protocol
Day 2	Low-fibre diet
Day 1	Clear-liquids diet
	7:00 – 9:00 PM 2 L of PEG
Examination day	06:30 – 7:30 AM 1 L of PEG
	08:15 AM 10 mg metoclopramide p.o.
	08:30 AM 100-200 mg simethicone in water for capsule ingestion
	09:30 AM check real time viewer. Additional 10 mg metoclopramide p.o. if capsule still in stomach
	First alert (capsule detected in SB) NaP 30 mL + 1 L water
	Second alert (3h after 1st booster) NaP 15 mL + 0.5 L water
	Third alert (2h after 2nd booster) 10 mg bisacodyl rectal suppository

PEG: Polyethylene glycol; p.o.: Per os; NaP: Sodium phosphate; SB: Small bowel.

Table 3 Indications and contraindications for pan-intestinal capsule endoscopy

Indications	Contraindications
CD Inflammatory-type (non-stricturing, non-penetrating), extensive (affecting small bowel and colon) Scheduled monitoring to evaluate mucosal healing in response to treatment (to justify and guide treatment change) Evaluate disease distribution and severity: stratify patients to low *vs* high risk (prognosis); asymptomatic CD patients with abnormal analysis; exclude active CD or investigation of symptoms unrelated to disease activity Establish diagnosis in patients with IBD-U, suspected CD or atypical ulcerative colitis **Gastrointestinal bleeding** Suspected mid-lower intestinal bleeding (overt or occult)	(1) Known or suspected intestinal strictures and/or fistulae (if patency not proven based on cross sectional imaging and/or patency capsule assessment[14]); (2) Magnetic resonance imaging examination scheduled for same-day or following days (requires prior confirmation of capsule excretion); and (3) Special conditions and relative contraindications: pregnancy; children under 8 yr of age; swallowing disorders; gastric surgery; implanted cardiac electric devices: Pacemakers, defibrillators, ventricular assist devices, telemetry; allergy or contraindications to any of the drugs or products used in the protocol; patients unable to walk for short periods and/or with neurological and/or psychiatric condition potentially favouring protocol deviations

CD: Crohn's disease; IBD-U: Inflammatory bowel disease - type unclassified.

determined a change in disease management in 46,5% of patients with established CD. Another international multicentre prospective study recently evaluated PCE *vs* ileocolonoscopy plus MRE in 158 patients with non-stricturing CD. It found a high performance of PCE for assessing CD mucosal activity and extent as compared to MRE and/or ileocolonoscopy, without the need for multiple tests[24]. MRE, ileocolonoscopy, and PCE reading were performed by blinded central readers using validated scoring systems. The gold-standard was defined by a consensus panel composed of independent experts. Overall sensitivity for active inflammation (PCE *vs* MRE and/or ileocolonoscopy) was 94% *vs* 100% (P = 0.125), and specificity was 74% *vs* 22% (P = 0,001). PCE sensitivity was superior to MRE in the proximal small bowel (97% *vs* 71%, P = 0.021), and similar to MRE and/or ileocolonoscopy in the terminal ileum and colon (P = 0.5-0.625). A study by Yamada *et al*[25], using double balloon enteroscopy as the gold-standard, reported PCE sensitivities for scars, erosions, and ulcers of 83.3%, 93.8%, and 88.5%, respectively, the specificities being 76%, 78,3%, and 81,6%, respectively.

In up to 10%–15% of cases, IBD remains unclassified after conventional colonoscopy[26]. In such cases, PCE may also have an important role in clarifying the diagnosis, by evaluating the small bowel while simultaneously reassessing the colon. In a study which used the PillCam™ COLON or PillCam™ COLON 2 in patients with ulcerative colitis, 7.1% of patients changed the diagnosis from ulcerative colitis to CD due to inflammatory activity observed in the small bowel[27].

The use of validated scoring systems to objectively evaluate small bowel and colonic lesion, such as the Capsule Endoscopy CD Activity Index (CECDAIic) or the novel PillCam Crohn's™ capsule score (Eliakim score), allows for the standardization of reporting, increasing reproducibility and inter-observer agreement of PCE[28-32].

Regarding safety, in a recent meta-analysis the reported capsule retention rate was 2% for all indications, and it was higher in the setting of CD (relative risk = 4%)[33]. A retention rate of 4.63% (95%CI: 3.42-6.25) in patients with established CD, *vs* 2.35% (95%CI: 1.31-4.19) in patients with suspected CD[34]. The risk of capsule retention can be reduced with the use of small bowel imaging modalities such as CTE or MRE, and/or patency capsule, when indicated. When capsule endoscopy is considered in patients with history of obstructive symptoms, known stricture or surgical anastomosis[35-37], a patency capsule is advisable even in cases of unremarkable cross-sectional imaging[14,35]. PCE has been proven safe in most series, and the occurrence of capsule retention has been rarely described and usually resolved conservatively[38,39].

GI BLEEDING

Recently, the use of PCE has been evaluated for suspected small bowel or colon bleeding[6,40], in patients with iron deficiency anaemia, with or without overt bleeding, and with a non-diagnostic esophagogastroduodenoscopy (EGD). Following current standards of practice, patients are initially submitted to conventional colonoscopy, and then proceed to small bowel capsule endoscopy, when the colonoscopy is also non-diagnostic. However, the diagnostic and therapeutic yields of colonoscopy in this setting are quite low[41]. PCE appears as a possible game changer in the clinical management of these patients, giving the opportunity for a non-invasive and adequately timed pan-intestinal evaluation. This may guide subsequent management, depending on the type and location of the potentially haemorrhagic lesions (PHLs) when present, which may contribute to avoiding further unnecessary examinations[40]. The earlier evaluation of the small bowel which is achieved with this PCE-first approach is expected to increase the diagnostic yield in patients with suspected small bowel bleeding, particularly for patients presenting with overt bleeding[42]. Capsule endoscopy has been shown to be able to detect proximal lesions missed by EGD in a non-negligible proportion of patients[43,44].

A fundamental premise in Medicine is to be able to offer all patients, when clinically indicated, the access to diagnostic and therapeutic procedures that are effective, safe and proportionate, with as minimum degree of invasiveness and discomfort possible. This supported by the Hippocratic principle of "*primum non nocere*". Capsule endoscopy falls perfectly within these principles, as a promising and valuable diagnostic tool that is expected to play an increasingly central role in the upcoming paradigm shift in the field of digestive endoscopy. Indeed, clinicians are expected to make rational use of all the diagnostic modalities available to make a correct diagnosis, which is an essential element before planning an adequate therapeutic and follow-up strategy. There is also a principle of minimum invasiveness, *i.e.*, patients should receive the safer and less invasive diagnostic or therapeutic approach, among the available equally effective alternatives. Invasive interventions should be restricted to those cases where they are required, based on the results of preliminary non-invasive studies, with better safety and tolerability profile, as is the case of imaging tests or endoscopic capsules. Such strategies should also be cost-effective before being adopted in clinical practice.

Timely access to capsule endoscopy in patients with iron deficiency anaemia or melena, no suspected lower intestinal bleeding and negative EGD, results in shortened hospital stays, increased diagnostic yield, and a significant two-third reduction of the number of colonoscopies, when compared to those patients who receive the small bowel capsule endoscopy only after negative upper and lower GI endoscopy have been performed[45]. Mussetto *et al*[46] also assessed the use of PCE in patients presenting with melena and non-diagnostic EGD. PCE was safe and allowed for the identification of the bleeding site in 83% of 128 patients included, leading to small bowel therapeutic interventions in 50% of the cases, therefore avoiding unnecessary invasive colonoscopy. In another retrospective investigation which analyzed 100 consecutive patients[6], PHL were observed in 61% of the cases. The capsule was able to detect small bowel lesions in 68% and colonic lesions in 81% of patients, no further invasive procedures being required in approximately 65% of the patients with negative gastroscopy.

A recent prospective study[47] included 100 consecutive patients with suspected small bowel or colonic bleeding also presenting with iron-deficiency anaemia and/or overt bleeding after non-diagnostic EGD. Colonoscopy detected PHL in 23% of the cohort, which means 50% (23/46) of all patients with PHL, while for PCE the overall diagnostic yield was 44%, meaning 95.7% (44/46) of all patients with PHL, $P < 0.001$. Colonoscopy had a sensitivity of 23/46 = 50%, a specificity of 54/54 = 100%, positive predictive value (PPV) 23/23 = 100% and negative predictive value (NPV) 54/77 = 70.1%, while for PCE the sensitivity was 44/46 = 95.7%, specificity 54/54=100%, PPV 44/44 = 100% and NPV 54/56 = 96.4% for PHL. The authors concluded that PCE was safe and more effective than colonoscopy in identifying PHL, both in the small-bowel and colon. Moreover, PCE was negative in more than half of patients with suspected MLGIB, avoiding further invasive endoscopic investigations. These results support the potential use of PCE as a first-line examination in patients with suspected small bowel and/or colonic bleeding.

MAGNETICALLY CONTROLLED CAPSULE ENDOSCOPY

Although conventional EGD remains the gold standard for the endoscopic evaluation of the upper GI tract, it may be limited due to poor tolerability and acceptability, or in patients at increased risk of complications[48]. Recently, the possibility of external magnetic control of the capsule [magnetically controlled capsule endoscopy (MCCE)] for non-invasive assessment of the esophagus and stomach has been available[49-54]. This novel MCCE is a comfortable, highly

acceptable alternative for patients refusing, or unfit for conventional EGD (including sedated EGD), or at a higher risk of adverse events[53]. It has the advantages of non-invasiveness, with an excellent safety profile and patient acceptance. Clinical indications for MCCE may include esophageal diseases such as esophageal varices and Barrett's esophagus[55], screening for gastric cancer[54], detection and surveillance for gastric or duodenal lesions such as ulcers, polyps, varices, erosive and atrophic gastritis, drug-related GI mucosal injury such as NSAIDs, remote gastric examination[56], stable patients with acute upper GI bleeding[57], or surveillance after partial gastrectomy or minimally invasive endoscopic treatment.

The translation of the MCCE concept and technology into a double-headed pan-intestinal capsule may soon make it possible to assess the entire mucosa of the digestive tract, meeting the expectations of the founders of capsule endoscopy, who coined and aimed for the concept of a *mouth-to-anus (M2A)* endoscopic capsule.

MCCE examination is generally safe, with a low rate of adverse events. The risks of capsule retention and aspiration should be addressed for active prevention and appropriate management[14,58]. Contraindications for MCCE include known or suspected significant GI stricture[14], pregnancy, implanted electronic devices (*e.g.*, pacemakers, cochlear device, drug infusion pumps, nerve stimulator except for MRI-compatible devices) or magnetic metal foreign bodies.

A systematic review and meta-analysis, published in 2021, compared MCCE and conventional gastroscopy in the identification of gastric lesions[59]. Seven studies were included, with a total of 916 patients and 745 gastric lesions. The mean capsule endoscopy examination time was 21.92 ± 8.87 min. The pooled overall sensitivity of MCCE was 87% (95%CI: 84%-89%). The sensitivity for identifying gastric ulcers was 82% (95%CI: 71%-89%), gastric polyps 82% (95%CI: 76%-87%), and gastric erosions 95% (95%CI: 86%-98%). MCCE was well tolerated, with minimal adverse events. The authors reported that MCCE was a relatively time-consuming process compared to conventional gastroscopy (21.92 ± 8.87 min *vs* 5.35 ± 3.01 min, respectively). However, when sedation is required during conventional gastroscopy, patients need to stay in a recovery unit after the procedure and may be incapable of following their regular activity for the rest of the day. Conversely, after MCCE they are alert and able to continue their regular activities.

MCCE still has many disadvantages that currently limit its use in clinical practice. The examination of the esophagus is an important part of routine upper GI investigation, therefore the rapid passage of the capsule through the esophagus is a limitation of MCCE. If proven effective and safe, the use of detachable strings[60] or enhanced magnetic fields to decelerate the passage through the esophagus may improve the investigation of the esophagus through MCCE. The cost of MCCE is significantly higher compared with conventional gastroscopy, and cost-effectiveness analysis in real life clinical settings is lacking[49]. The inability to perform biopsies and therapeutic procedures such as haemostasis or polypectomy, among others, may also be perceived as an important limitation for MCCE, as for any other type of capsule endoscopy. The capsule may, as in other segments of the GI tract, be regarded as a filter diagnostic examination, followed by more invasive examinations only when justified by the capsule endoscopic findings. A propensity score matching analysis[61] for large-scale screening of asymptomatic individuals reported that most patients do not require conventional gastroscopy after MCCE, while patients with GI symptoms or focal lesions detected by MCCE were more likely to require further examination with conventional gastroscopy, for biopsy or endoscopic treatment (3.8% *vs* 10%). Lai *et al*[62] reported that only 18.2% of patients needed a biopsy after MCCE. MCCE may therefore be regarded as a screening tool, allowing the identification of patients who require further evaluation with conventional gastroscopy. Regarding the role of biopsies obtained during EGD to check for *Helicobacter pylori* (*H. pylori*) status, some preliminary evidence has shown that the Kyoto classification of gastritis can be adapted to MCCE, to accurately predict *H. pylori* infection status on conventional gastroscopy[63]. In this setting, major specific findings were mucosal swelling and spotty redness for current infection, regular arrangement of collecting venules, streak redness, fundic gland polyp for non-infection, and map-like redness for past infection.

AI IN CE

There has been a huge expansion of AI models in medicine, and particularly in digestive endoscopy[64-67]. The time-consuming reading of capsule endoscopy procedures, as well as the large number of image frames which are generated, have driven the development of convolutional neural networks (CNN) for digital imaging analysis. AI is expected to tackle some of the current limitations of PCE, by reducing reading times and improving the ability to detect all the relevant lesions[68]. To date, this has been mainly tested for the small bowel[69,70], while it remains scarcely explored in the case of double-headed capsules. A few studies of CNN development for CC endoscopy revealed a very high accuracy for detection of colorectal neoplasia or protruding lesions[71-73]. Mascarenhas *et al*[74] recently developed a CNN for automatic detection of colonic blood in CC endoscopy, enabling the differentiation between normal mucosa, blood or hematic residues and pleomorphic mucosal lesions, namely ulcers and erosions, protruding lesions and vascular lesions. CNN revealed a global sensitivity of 96% and specificity of 98%. Ferreira *et al*[75] developed a CNN for automatic detection of panenteric ulcers in PillCam™ Crohn's capsule, with a sensitivity of 98%, specificity of 99% and accuracy of 99%, having a perfect discriminatory capacity for the detection of ulcers and erosions. AI implementation is expected to achieve a significant reduction in the reading times per exam. Moreover, PCE reading technique is challenging and requires specific training, and AI models are expected to contribute to assist training and shortening the learning curve for this technique. The implementation of AI-powered PCE may therefore become a disruptive change towards an effective and minimally invasive evaluation of the entire GI tract. A multicenter prospective study (n = 131)[76], described a substantial reduction in the reading time of PCE with AI in patients with suspected CD. The sensitivity and specificity for detecting CD was 97% and 90%, respectively, with a NPV of 95%, enabling a faster screening with high diagnostic accuracy in cases of suspected CD.

CONCLUSION

The horizons of capsule endoscopy are evolving. PCE is a non-invasive, effective, and safe procedure to evaluate the small bowel and the colon. Its use in CD and more recently in GI bleeding is expanding in routine clinical practice. Conventional endoscopic procedures for the esophagus, stomach and colon remain superior to PCE considering each individual segment, and have the advantage of enabling biopsy sampling and therapeutic procedures as needed. PCE, however, offers the opportunity to evaluate multiple segments of the digestive tract at the same time, in a single non-invasive procedure. Currently, clinical indications for PCE include the assessment of non-stricturing, non-penetrating and extensive CD (affecting the small bowel and colon), mainly for disease monitoring and evaluation of mucosal healing in response to medical therapy. It could also be considered to clarify the diagnosis in patients with IBD - type unclassified or in atypical cases of ulcerative colitis. PCE has been also proven valuable in patients with suspected overt or occult MLGIB, driving subsequent clinical decisions and avoiding the need for additional invasive procedures in a significant proportion of cases. The central questions that seem to be pressing for the future are: Should capsule endoscopy technology be considered a "niche" procedure to be used only in particular patients and settings? Will it remain in the shadows of the dominant gold standard which is invasive upper digestive endoscopy and colonoscopy? Could it represent the archetype of a coming revolution? The capsule is a disruptive device which has been proven to have the potential to find its place in clinical practice, able to act as a non-invasive diagnostic "filter", offering the opportunity to change the diagnostic approach of patients with digestive tract diseases in the near future. We already have the possibility to evaluate all the small bowel and the colon, non-invasively, with a capsule, in a single procedure, which is effective, safe and well tolerated. Therefore, PCE may be the key to answer the question "Who needs an invasive endoscopic procedure?", as opposed to the current practice, where "All these patients will undergo an invasive endoscopy or colonoscopy, and then some (many) will require a small bowel capsule". PCE is a possible game changer, expanding the field for non-invasive endoscopy and limiting the need for invasive procedures such as conventional colonoscopy or device-assisted enteroscopy, which should be restricted to those cases where biopsies or therapeutic procedures are required, based on the results of the PCE.

ACKNOWLEDGEMENTS

The authors acknowledge the editorial assistance of John Yaphe.

FOOTNOTES

Author contributions: Rosa B conceived the work, performed the literature review, and wrote the manuscript; Cotter J critically contributed to the intellectual content and formal structure of the manuscript.

Conflict-of-interest statement: Bruno Rosa has received consultancy fees from Medtronic in the past. José Cotter declares no conflicts of interest regarding this manuscript.

Country/Territory of origin: Portugal

ORCID number: Bruno Rosa 0000-0003-2885-0720; José Cotter 0000-0002-2921-0648.

S-Editor: Lin C
L-Editor: A
P-Editor: Zhao YQ

REFERENCES

1 **Iddan GJ**, Swain CP. History and development of capsule endoscopy. *Gastrointest Endosc Clin N Am* 2004; **14**: 1-9 [PMID: 15062374 DOI: 10.1016/j.giec.2003.10.022]

2 **Pennazio M**, Rondonotti E, Despott EJ, Dray X, Keuchel M, Moreels T, Sanders DS, Spada C, Carretero C, Cortegoso Valdivia P, Elli L, Fuccio L, Gonzalez Suarez B, Koulaouzidis A, Kunovsky L, McNamara D, Neumann H, Perez-Cuadrado-Martinez E, Perez-Cuadrado-Robles E, Piccirelli S, Rosa B, Saurin JC, Sidhu R, Tacheci I, Vlachou E, Triantafyllou K. Small-bowel capsule endoscopy and device-assisted enteroscopy for diagnosis and treatment of small-bowel disorders: European Society of Gastrointestinal Endoscopy (ESGE) Guideline - Update 2022. *Endoscopy* 2023; **55**: 58-95 [PMID: 36423618 DOI: 10.1055/a-1973-3796]

3 **Boal Carvalho P**, Rosa B, Dias de Castro F, Moreira MJ, Cotter J. PillCam COLON 2 in Crohn's disease: A new concept of pan-enteric mucosal healing assessment. *World J Gastroenterol* 2015; **21**: 7233-7241 [PMID: 26109810 DOI: 10.3748/wjg.v21.i23.7233]

4 **Ahmed M**. Video Capsule Endoscopy in Gastroenterology. *Gastroenterology Res* 2022; **15**: 47-55 [PMID: 35572472 DOI: 10.14740/gr1487]

5 **Cortegoso Valdivia P**, Elosua A, Houdeville C, Pennazio M, Fernández-Urién I, Dray X, Toth E, Eliakim R, Koulaouzidis A. Clinical feasibility of panintestinal (or panenteric) capsule endoscopy: a systematic review. *Eur J Gastroenterol Hepatol* 2021; **33**: 949-955 [PMID: 34034282 DOI: 10.1097/MEG.0000000000002200]

6 **Carretero C**, Prieto de Frías C, Angós R, Betés M, Herráiz M, de la Riva S, Zozaya F, Fernández-Calderón M, Rodríguez-Lago I, Muñoz Navas M. Pan-enteric capsule for bleeding high-risk patients. Can we limit endoscopies? *Rev Esp Enferm Dig* 2021; **113**: 580-584 [PMID: 33267588 DOI: 10.17235/reed.2020.7196/2020]

7 **Brodersen JB**, Knudsen T, Kjeldsen J, Juel MA, Rafaelsen SR, Jensen MD. Diagnostic accuracy of pan-enteric capsule endoscopy and magnetic resonance enterocolonography in suspected Crohn's disease. *United European Gastroenterol J* 2022; **10**: 973-982 [PMID: 36069336 DOI: 10.1002/ueg2.12307]

8 **Piccirelli S**, Mussetto A, Bellumat A, Cannizzaro R, Pennazio M, Pezzoli A, Bizzotto A, Fusetti N, Valiante F, Hassan C, Pecere S, Koulaouzidis A, Spada C. New Generation Express View: An Artificial Intelligence Software Effectively Reduces Capsule Endoscopy Reading Times. *Diagnostics (Basel)* 2022; **12** [PMID: 35892494 DOI: 10.3390/diagnostics12081783]

9 **Rosa B**, Donato H, Cúrdia Gonçalves T, Sousa-Pinto B, Cotter J. What Is the Optimal Bowel Preparation for Capsule Colonoscopy and Pan-intestinal Capsule Endoscopy? A Systematic Review and Meta-Analysis. *Dig Dis Sci* 2023; **68**: 4418-4431 [PMID: 37833441 DOI: 10.1007/s10620-023-08133-7]

10 **Leighton JA**, Rex DK. A grading scale to evaluate colon cleansing for the PillCam COLON capsule: a reliability study. *Endoscopy* 2011; **43**: 123-127 [PMID: 21038293 DOI: 10.1055/s-0030-1255916]

11 **de Sousa Magalhães R**, Chálim Rebelo C, Sousa-Pinto B, Pereira J, Boal Carvalho P, Rosa B, Moreira MJ, Duarte MA, Cotter J. CC-CLEAR (Colon Capsule Cleansing Assessment and Report): the novel scale to evaluate the clinical impact of bowel preparation in capsule colonoscopy - a multicentric validation study. *Scand J Gastroenterol* 2022; **57**: 625-632 [PMID: 35068293 DOI: 10.1080/00365521.2022.2026463]

12 **de Sousa Magalhães R**, Arieira C, Boal Carvalho P, Rosa B, Moreira MJ, Cotter J. Colon Capsule CLEansing Assessment and Report (CC-CLEAR): a new approach for evaluation of the quality of bowel preparation in capsule colonoscopy. *Gastrointest Endosc* 2021; **93**: 212-223 [PMID: 32534054 DOI: 10.1016/j.gie.2020.05.062]

13 **Lai EJ**, Calderwood AH, Doros G, Fix OK, Jacobson BC. The Boston bowel preparation scale: a valid and reliable instrument for colonoscopy-oriented research. *Gastrointest Endosc* 2009; **69**: 620-625 [PMID: 19136102 DOI: 10.1016/j.gie.2008.05.057]

14 **Rosa B**, Dray X, Koulaouzidis A. Retention of small bowel capsule endoscopy. *Curr Opin Gastroenterol* 2023; **39**: 227-233 [PMID: 37144540 DOI: 10.1097/MOG.0000000000000921]

15 **Levartovsky A**, Eliakim R. Video Capsule Endoscopy Plays an Important Role in the Management of Crohn's Disease. *Diagnostics (Basel)* 2023; **13** [PMID: 37189607 DOI: 10.3390/diagnostics13081507]

16 **Irwin J**, Ferguson E, Simms LA, Hanigan K, Carbonnel F, Radford-Smith G. A rolling phenotype in Crohn's disease. *PLoS One* 2017; **12**: e0174954 [PMID: 28384331 DOI: 10.1371/journal.pone.0174954]

17 **Magro F**, Rodrigues-Pinto E, Coelho R, Andrade P, Santos-Antunes J, Lopes S, Camila-Dias C, Macedo G. Is it possible to change phenotype progression in Crohn's disease in the era of immunomodulators? Predictive factors of phenotype progression. *Am J Gastroenterol* 2014; **109**: 1026-1036 [PMID: 24796767 DOI: 10.1038/ajg.2014.97]

18 **Saunders R**, Torrejon Torres R, Konsinski L. Evaluating the clinical and economic consequences of using video capsule endoscopy to monitor Crohn's disease. *Clin Exp Gastroenterol* 2019; **12**: 375-384 [PMID: 31496780 DOI: 10.2147/CEG.S198958]

19 **Lobo A**, Torrejon Torres R, McAlindon M, Panter S, Leonard C, van Lent N, Saunders R. Economic analysis of the adoption of capsule endoscopy within the British NHS. *Int J Qual Health Care* 2020; **32**: 332-341 [PMID: 32395758 DOI: 10.1093/intqhc/mzaa039]

20 **Tamilarasan AG**, Tran Y, Paramsothy S, Leong R. The diagnostic yield of pan-enteric capsule endoscopy in inflammatory bowel disease: A systematic review and meta-analysis. *J Gastroenterol Hepatol* 2022; **37**: 2207-2216 [PMID: 36150392 DOI: 10.1111/jgh.16007]

21 **Turner D**, Ricciuto A, Lewis A, D'Amico F, Dhaliwal J, Griffiths AM, Bettenworth D, Sandborn WJ, Sands BE, Reinisch W, Schölmerich J, Bemelman W, Danese S, Mary JY, Rubin D, Colombel JF, Peyrin-Biroulet L, Dotan I, Abreu MT, Dignass A; International Organization for the Study of IBD. STRIDE-II: An Update on the Selecting Therapeutic Targets in Inflammatory Bowel Disease (STRIDE) Initiative of the International Organization for the Study of IBD (IOIBD): Determining Therapeutic Goals for Treat-to-Target strategies in IBD. *Gastroenterology* 2021; **160**: 1570-1583 [PMID: 33359090 DOI: 10.1053/j.gastro.2020.12.031]

22 **Dionisio PM**, Gurudu SR, Leighton JA, Leontiadis GI, Fleischer DE, Hara AK, Heigh RI, Shiff AD, Sharma VK. Capsule endoscopy has a significantly higher diagnostic yield in patients with suspected and established small-bowel Crohn's disease: a meta-analysis. *Am J Gastroenterol* 2010; **105**: 1240-8; quiz 1249 [PMID: 20029412 DOI: 10.1038/ajg.2009.713]

23 **Tai FWD**, Ellul P, Elosua A, Fernandez-Urien I, Tontini GE, Elli L, Eliakim R, Kopylov U, Koo S, Parker C, Panter S, Sidhu R, McAlindon M. Panenteric capsule endoscopy identifies proximal small bowel disease guiding upstaging and treatment intensification in Crohn's disease: A European multicentre observational cohort study. *United European Gastroenterol J* 2021; **9**: 248-255 [PMID: 32741315 DOI: 10.1177/2050640620948664]

24 **Bruining DH**, Oliva S, Fleisher MR, Fischer M, Fletcher JG; BLINK study group. Panenteric capsule endoscopy versus ileocolonoscopy plus magnetic resonance enterography in Crohn's disease: a multicentre, prospective study. *BMJ Open Gastroenterol* 2020; **7** [PMID: 32499275 DOI: 10.1136/bmjgast-2019-000365]

25 **Yamada K**, Nakamura M, Yamamura T, Maeda K, Sawada T, Mizutani Y, Ishikawa E, Ishikawa T, Kakushima N, Furukawa K, Ohno E, Kawashima H, Honda T, Ishigami M, Fujishiro M. Diagnostic yield of colon capsule endoscopy for Crohn's disease lesions in the whole gastrointestinal tract. *BMC Gastroenterol* 2021; **21**: 75 [PMID: 33593297 DOI: 10.1186/s12876-021-01657-0]

26 **Maaser C**, Sturm A, Vavricka SR, Kucharzik T, Fiorino G, Annese V, Calabrese E, Baumgart DC, Bettenworth D, Borralho Nunes P, Burisch J, Castiglione F, Eliakim R, Ellul P, González-Lama Y, Gordon H, Halligan S, Katsanos K, Kopylov U, Kotze PG, Krustinš E, Laghi A, Limdi JK, Rieder F, Rimola J, Taylor SA, Tolan D, van Rheenen P, Verstockt B, Stoker J; European Crohn's and Colitis Organisation [ECCO] and the European Society of Gastrointestinal and Abdominal Radiology [ESGAR]. ECCO-ESGAR Guideline for Diagnostic Assessment in IBD Part 1: Initial diagnosis, monitoring of known IBD, detection of complications. *J Crohns Colitis* 2019; **13**: 144-164 [PMID: 30137275 DOI: 10.1093/ecco-jcc/jjy113]

27 **San Juan-Acosta M**, Caunedo-Álvarez A, Argüelles-Arias F, Castro-Laria L, Gómez-Rodríguez B, Romero-Vázquez J, Belda-Cuesta A, Pellicer-Bautista F, Herrerías-Gutiérrez JM. Colon capsule endoscopy is a safe and useful tool to assess disease parameters in patients with ulcerative colitis. *Eur J Gastroenterol Hepatol* 2014; **26**: 894-901 [PMID: 24987825 DOI: 10.1097/MEG.0000000000000125]

28 **Limdi JK**, Picco M, Farraye FA. A review of endoscopic scoring systems and their importance in a treat-to-target approach in inflammatory bowel disease (with videos). *Gastrointest Endosc* 2020; **91**: 733-745 [PMID: 31786161 DOI: 10.1016/j.gie.2019.11.032]

29 **Niv Y**, Gal E, Gabovitz V, Hershkovitz M, Lichtenstein L, Avni I. Capsule Endoscopy Crohn's Disease Activity Index (CECDAIic or Niv Score) for the Small Bowel and Colon. *J Clin Gastroenterol* 2018; **52**: 45-49 [PMID: 27753700 DOI: 10.1097/MCG.0000000000000720]

30 **Tabone T**, Koulaouzidis A, Ellul P. Scoring Systems for Clinical Colon Capsule Endoscopy-All You Need to Know. *J Clin Med* 2021; **10** [PMID: 34071209 DOI: 10.3390/jcm10112372]

31 **Arieira C**, Magalhães R, Dias de Castro F, Boal Carvalho P, Rosa B, Moreira MJ, Cotter J. CECDAIic - a new useful tool in pan-intestinal evaluation of Crohn's disease patients in the era of mucosal healing. *Scand J Gastroenterol* 2019; **54**: 1326-1330 [PMID: 31646914 DOI: 10.1080/00365521.2019.1681499]

32 **Eliakim R**, Yablecovitch D, Lahat A, Ungar B, Shachar E, Carter D, Selinger L, Neuman S, Ben-Horin S, Kopylov U. A novel PillCam Crohn's capsule score (Eliakim score) for quantification of mucosal inflammation in Crohn's disease. *United European Gastroenterol J* 2020; **8**: 544-551 [PMID: 32213037 DOI: 10.1177/2050640620913368]

33 **Cortegoso Valdivia P**, Skonieczna-Żydecka K, Elosua A, Sciberras M, Piccirelli S, Rullan M, Tabone T, Gawel K, Stachowski A, Lemiński A, Marlicz W, Fernández-Urién I, Ellul P, Spada C, Pennazio M, Toth E, Koulaouzidis A. Indications, Detection, Completion and Retention Rates of Capsule Endoscopy in Two Decades of Use: A Systematic Review and Meta-Analysis. *Diagnostics (Basel)* 2022; **12** [PMID: 35626261 DOI: 10.3390/diagnostics12051105]

34 **Pasha SF**, Pennazio M, Rondonotti E, Wolf D, Buras MR, Albert JG, Cohen SA, Cotter J, D'Haens G, Eliakim R, Rubin DT, Leighton JA. Capsule Retention in Crohn's Disease: A Meta-analysis. *Inflamm Bowel Dis* 2020; **26**: 33-42 [PMID: 31050736 DOI: 10.1093/ibd/izz083]

35 **Rondonotti E**, Soncini M, Girelli CM, Russo A, de Franchis R; collaborators on behalf of AIGO, SIED and SIGE Lombardia. Short article: Negative small-bowel cross-sectional imaging does not exclude capsule retention in high-risk patients. *Eur J Gastroenterol Hepatol* 2016; **28**: 871-875 [PMID: 27362463 DOI: 10.1097/MEG.0000000000000628]

36 **Nemeth A**, Kopylov U, Koulaouzidis A, Wurm Johansson G, Thorlacius H, Amre D, Eliakim R, Seidman EG, Toth E. Use of patency capsule in patients with established Crohn's disease. *Endoscopy* 2016; **48**: 373-379 [PMID: 26561918 DOI: 10.1055/s-0034-1393560]

37 **Silva M**, Cardoso H, Cunha R, Peixoto A, Gaspar R, Gomes S, Santos AL, Lopes S, Macedo G. Evaluation of Small-Bowel Patency in Crohn's Disease: Prospective Study with a Patency Capsule and Computed Tomography. *GE Port J Gastroenterol* 2019; **26**: 396-403 [PMID: 31832494 DOI: 10.1159/000499722]

38 **Toskas A**, Laskaratos FM, Coda S, Banerjee S, Epstein O. Is Panenteric Pillcam(TM) Crohn's Capsule Endoscopy Ready for Widespread Use? A Narrative Review. *Diagnostics (Basel)* 2023; **13** [PMID: 37370927 DOI: 10.3390/diagnostics13122032]

39 **Rosa B**, Andrade P, Lopes S, Gonçalves AR, Serrazina J, Marílio Cardoso P, Silva A, Macedo Silva V, Cotter J, Macedo G, Figueiredo PN, Chagas C. Pan-Enteric Capsule Endoscopy: Current Applications and Future Perspectives. *GE Port J Gastroenterol* 2023; 1-12 [DOI: 10.1159/000533960]

40 **Mussetto A**, Arena R, Fuccio L, Trebbi M, Tina Garribba A, Gasperoni S, Manzi I, Triossi O, Rondonotti E. A new panenteric capsule endoscopy-based strategy in patients with melena and a negative upper gastrointestinal endoscopy: a prospective feasibility study. *Eur J Gastroenterol Hepatol* 2021; **33**: 686-690 [PMID: 33731583 DOI: 10.1097/MEG.0000000000002114]

41 **Etzel JP**, Williams JL, Jiang Z, Lieberman DA, Knigge K, Faigel DO. Diagnostic yield of colonoscopy to evaluate melena after a nondiagnostic EGD. *Gastrointest Endosc* 2012; **75**: 819-826 [PMID: 22301339 DOI: 10.1016/j.gie.2011.11.041]

42 **Estevinho MM**, Pinho R, Fernandes C, Rodrigues A, Ponte A, Gomes AC, Afecto E, Correia J, Carvalho J. Diagnostic and therapeutic yields of early capsule endoscopy and device-assisted enteroscopy in the setting of overt GI bleeding: a systematic review with meta-analysis. *Gastrointest Endosc* 2022; **95**: 610-625.e9 [PMID: 34952093 DOI: 10.1016/j.gie.2021.12.009]

43 **Kitiyakara T**, Selby W. Non-small-bowel lesions detected by capsule endoscopy in patients with obscure GI bleeding. *Gastrointest Endosc* 2005; **62**: 234-238 [PMID: 16046986 DOI: 10.1016/s0016-5107(05)00292-0]

44 **Juanmartiñena Fernández JF**, Fernández-Urien Sainz I, Zabalza Ollo B, Saldaña Dueñas C, Montañés Guimera M, Elosua González A, Vila Costas JJ. Gastroduodenal lesions detected during small bowel capsule endoscopy: incidence, diagnostic and therapeutic impact. *Rev Esp Enferm Dig* 2018; **110**: 102-108 [PMID: 29152990 DOI: 10.17235/reed.2017.5114/2017]

45 **Yung DE**, Koulaouzidis A, Douglas S, Plevris JN. Earlier use of capsule endoscopy in inpatients with melena or severe iron deficiency anemia reduces need for colonoscopy and shortens hospital stay. *Endosc Int Open* 2018; **6**: E1075-E1084 [PMID: 30211295 DOI: 10.1055/a-0640-2956]

46 **Mussetto A**, Arena R, Triossi O. Pan-enteric capsule in patients with melena and a negative upper endoscopy: A pilot study. *Endoscopy* 2019; **51**: S30 [DOI: 10.1055/s-0039-1681257]

47 **Rosa B**, Cúrdia Gonçalves T, Moreira MJ, Castro FD, Sousa-Pinto B, Dinis-Ribeiro M, Cotter J. Pan-intestinal capsule endoscopy as first-line procedure in patients with suspected mid or lower gastrointestinal bleeding. *Endoscopy* 2024 [PMID: 38365215 DOI: 10.1055/a-2270-4601]

48 **Levy I**, Gralnek IM. Complications of diagnostic colonoscopy, upper endoscopy, and enteroscopy. *Best Pract Res Clin Gastroenterol* 2016; **30**: 705-718 [PMID: 27931631 DOI: 10.1016/j.bpg.2016.09.005]

49 **Zou WB**, Hou XH, Xin L, Liu J, Bo LM, Yu GY, Liao Z, Li ZS. Magnetic-controlled capsule endoscopy vs. gastroscopy for gastric diseases: a two-center self-controlled comparative trial. *Endoscopy* 2015; **47**: 525-528 [PMID: 25590177 DOI: 10.1055/s-0034-1391123]

50 **Liao Z**, Zou W, Li ZS. Clinical application of magnetically controlled capsule gastroscopy in gastric disease diagnosis: recent advances. *Sci China Life Sci* 2018; **61**: 1304-1309 [PMID: 30367341 DOI: 10.1007/s11427-018-9353-5]

51 **Jiang B**, Pan J, Qian YY, He C, Xia J, He SX, Sha WH, Feng ZJ, Wan J, Wang SS, Zhong L, Xu SC, Li XL, Huang XJ, Zou DW, Song DD, Zhang J, Ding WQ, Chen JY, Chu Y, Zhang HJ, Yu WF, Xu Y, He XQ, Tang JH, He L, Fan YH, Chen FL, Zhou YB, Zhang YY, Yu Y, Wang HH, Ge KK, Jin GH, Xiao YL, Fang J, Yan XM, Ye J, Yang CM, Li Z, Song Y, Wen MY, Zong Y, Han X, Wu LL, Ma JJ, Xie XP, Yu WH, You Y, Lu XH, Song YL, Ma XQ, Li SD, Zeng B, Gao YJ, Ma RJ, Ni XG, He CH, Liu YP, Wu JS, Liu J, Li AM, Chen BL, Cheng CS, Sun XM, Ge ZZ, Feng Y, Tang YJ, Li ZS, Linghu EQ, Liao Z; Capsule Endoscopy Group of the Chinese Society of Digestive Endoscopy. Clinical guideline on magnetically controlled capsule gastroscopy (2021 edition). *J Dig Dis* 2023; **24**: 70-84 [PMID: 37220999 DOI: 10.1111/1751-2980.13173]

52 **Szalai M**, Helle K, Lovász BD, Finta Á, Rosztóczy A, Oczella L, Madácsy L. First prospective European study for the feasibility and safety of magnetically controlled capsule endoscopy in gastric mucosal abnormalities. *World J Gastroenterol* 2022; **28**: 2227-2242 [PMID: 35721886 DOI: 10.3748/wjg.v28.i20.2227]

53 **Zhou L**, Wang S, Li J, Zhong J, Zhang L, Shen R, Kouken B, Zhou C, Wang Q, Qian Y, Zou D, Chu Y. The Application of Magnetic-Controlled Capsule Gastroscopy in Patients Refusing C-EGD: A Single-Center 5-Year Observational Study. *Gastroenterol Res Pract* 2021;

2021: 6934594 [PMID: 34675973 DOI: 10.1155/2021/6934594]

54 **Li J**, Ren M, Yang J, Zhao Y, Li Y, Zhang D, Wu F, Zhang Z, Lu X, Ren L, He S, Lu G. Screening value for gastrointestinal lesions of magnetic-controlled capsule endoscopy in asymptomatic individuals. *J Gastroenterol Hepatol* 2021; **36**: 1267-1275 [PMID: 33000488 DOI: 10.1111/jgh.15282]

55 **McCarty TR**, Afinogenova Y, Njei B. Use of Wireless Capsule Endoscopy for the Diagnosis and Grading of Esophageal Varices in Patients With Portal Hypertension: A Systematic Review and Meta-Analysis. *J Clin Gastroenterol* 2017; **51**: 174-182 [PMID: 27548729 DOI: 10.1097/MCG.0000000000000589]

56 **Zhang T**, Chen YZ, Jiang X, He C, Pan J, Zhou W, Hu JP, Liao Z, Li ZS. 5G-based remote magnetically controlled capsule endoscopy for examination of the stomach and small bowel. *United European Gastroenterol J* 2023; **11**: 42-50 [PMID: 36416805 DOI: 10.1002/ueg2.12339]

57 **Yu Y**, Liao Z, Jiang X, Pan J, Zhou W, Lau JYW. The use of magnet-controlled capsule endoscopy as the initial diagnostic tool in patients with acute upper gastrointestinal bleeding. *J Gastroenterol Hepatol* 2023; **38**: 2027-2034 [PMID: 37534802 DOI: 10.1111/jgh.16310]

58 **Dan T**, Dandan S, Enqiang L. Aspiration of a Magnetically Controlled Capsule Endoscopy. *Gastroenterology* 2023; **164**: e30-e31 [PMID: 30981792 DOI: 10.1053/j.gastro.2019.04.006]

59 **Geropoulos G**, Aquilina J, Kakos C, Anestiadou E, Giannis D. Magnetically Controlled Capsule Endoscopy Versus Conventional Gastroscopy: A Systematic Review and Meta-Analysis. *J Clin Gastroenterol* 2021; **55**: 577-585 [PMID: 33883514 DOI: 10.1097/MCG.0000000000001540]

60 **Jiang B**, Qian YY, Wang YC, Pan J, Jiang X, Zhu JH, Qiu XO, Zhou W, Li ZS, Liao Z. A novel capsule endoscopy for upper and mid-GI tract: the UMGI capsule. *BMC Gastroenterol* 2023; **23**: 76 [PMID: 36927462 DOI: 10.1186/s12876-023-02696-5]

61 **Wu TT**, Zhang MY, Tan ND, Chen SF, Zhuang QJ, Luo Y, Xiao YL. Patients at risk for further examination with conventional gastroscopy after undergoing magnetically controlled capsule endoscopy. *J Dig Dis* 2023; **24**: 522-529 [PMID: 37681236 DOI: 10.1111/1751-2980.13228]

62 **Lai HS**, Wang XK, Cai JQ, Zhao XM, Han ZL, Zhang J, Chen ZY, Lin ZZ, Zhou PH, Hu B, Li AM, Liu SD. Standing-type magnetically guided capsule endoscopy versus gastroscopy for gastric examination: multicenter blinded comparative trial. *Dig Endosc* 2020; **32**: 557-564 [PMID: 31483889 DOI: 10.1111/den.13520]

63 **Xi S**, Jing L, Lili W, Tingting L, Jun L, Ming W, Zhiqiang W, Peng J. Magnetic controlled capsule endoscope (MCCE)'s diagnostic performance for H. pylori infection status based on the Kyoto classification of gastritis. *BMC Gastroenterol* 2022; **22**: 502 [PMID: 36474169 DOI: 10.1186/s12876-022-02589-z]

64 **Wu X**, Chen D. Convolutional Neural Network in Microsurgery Treatment of Spontaneous Intracerebral Hemorrhage. *Comput Math Methods Med* 2022; **2022**: 9701702 [PMID: 35983522 DOI: 10.1155/2022/9701702]

65 **Khurshid S**, Friedman S, Reeder C, Di Achille P, Diamant N, Singh P, Harrington LX, Wang X, Al-Alusi MA, Sarma G, Foulkes AS, Ellinor PT, Anderson CD, Ho JE, Philippakis AA, Batra P, Lubitz SA. ECG-Based Deep Learning and Clinical Risk Factors to Predict Atrial Fibrillation. *Circulation* 2022; **145**: 122-133 [PMID: 34743566 DOI: 10.1161/CIRCULATIONAHA.121.057480]

66 **Kim JE**, Choi YH, Lee YC, Seong G, Song JH, Kim TJ, Kim ER, Hong SN, Chang DK, Kim YH, Shin SY. Deep learning model for distinguishing Mayo endoscopic subscore 0 and 1 in patients with ulcerative colitis. *Sci Rep* 2023; **13**: 11351 [PMID: 37443370 DOI: 10.1038/s41598-023-38206-6]

67 **Hassan C**, Spadaccini M, Iannone A, Maselli R, Jovani M, Chandrasekar VT, Antonelli G, Yu H, Areia M, Dinis-Ribeiro M, Bhandari P, Sharma P, Rex DK, Rösch T, Wallace M, Repici A. Performance of artificial intelligence in colonoscopy for adenoma and polyp detection: a systematic review and meta-analysis. *Gastrointest Endosc* 2021; **93**: 77-85.e6 [PMID: 32598963 DOI: 10.1016/j.gie.2020.06.059]

68 **Mascarenhas M**, Martins M, Afonso J, Ribeiro T, Cardoso P, Mendes F, Andrade P, Cardoso H, Ferreira J, Macedo G. The Future of Minimally Invasive Capsule Panendoscopy: Robotic Precision, Wireless Imaging and AI-Driven Insights. *Cancers (Basel)* 2023; **15** [PMID: 38136403 DOI: 10.3390/cancers15245861]

69 **Mascarenhas Saraiva MJ**, Afonso J, Ribeiro T, Ferreira J, Cardoso H, Andrade AP, Parente M, Natal R, Mascarenhas Saraiva M, Macedo G. Deep learning and capsule endoscopy: automatic identification and differentiation of small bowel lesions with distinct haemorrhagic potential using a convolutional neural network. *BMJ Open Gastroenterol* 2021; **8** [PMID: 34580155 DOI: 10.1136/bmjgast-2021-000753]

70 **Tsuboi A**, Oka S, Aoyama K, Saito H, Aoki T, Yamada A, Matsuda T, Fujishiro M, Ishihara S, Nakahori M, Koike K, Tanaka S, Tada T. Artificial intelligence using a convolutional neural network for automatic detection of small-bowel angioectasia in capsule endoscopy images. *Dig Endosc* 2020; **32**: 382-390 [PMID: 31392767 DOI: 10.1111/den.13507]

71 **Blanes-Vidal V**, Baatrup G, Nadimi ES. Addressing priority challenges in the detection and assessment of colorectal polyps from capsule endoscopy and colonoscopy in colorectal cancer screening using machine learning. *Acta Oncol* 2019; **58**: S29-S36 [PMID: 30836800 DOI: 10.1080/0284186X.2019.1584404]

72 **Yamada A**, Niikura R, Otani K, Aoki T, Koike K. Automatic detection of colorectal neoplasia in wireless colon capsule endoscopic images using a deep convolutional neural network. *Endoscopy* 2021; **53**: 832-836 [PMID: 32947623 DOI: 10.1055/a-1266-1066]

73 **Mascarenhas M**, Afonso J, Ribeiro T, Cardoso H, Andrade P, Ferreira JPS, Saraiva MM, Macedo G. Performance of a Deep Learning System for Automatic Diagnosis of Protruding Lesions in Colon Capsule Endoscopy. *Diagnostics (Basel)* 2022; **12** [PMID: 35741255 DOI: 10.3390/diagnostics12061445]

74 **Mascarenhas M**, Ribeiro T, Afonso J, Ferreira JPS, Cardoso H, Andrade P, Parente MPL, Jorge RN, Mascarenhas Saraiva M, Macedo G. Deep learning and colon capsule endoscopy: automatic detection of blood and colonic mucosal lesions using a convolutional neural network. *Endosc Int Open* 2022; **10**: E171-E177 [PMID: 35186665 DOI: 10.1055/a-1675-1941]

75 **Ferreira JPS**, de Mascarenhas Saraiva MJDQEC, Afonso JPL, Ribeiro TFC, Cardoso HMC, Ribeiro Andrade AP, de Mascarenhas Saraiva MNG, Parente MPL, Natal Jorge R, Lopes SIO, de Macedo GMG. Identification of Ulcers and Erosions by the Novel Pillcam™ Crohn's Capsule Using a Convolutional Neural Network: A Multicentre Pilot Study. *J Crohns Colitis* 2022; **16**: 169-172 [PMID: 34228113 DOI: 10.1093/ecco-jcc/jjab117]

76 **Brodersen JB**, Jensen MD, Leenhardt R, Kjeldsen J, Histace A, Knudsen T, Dray X. Artificial Intelligence-assisted Analysis of Pan-enteric Capsule Endoscopy in Patients with Suspected Crohn's Disease: A Study on Diagnostic Performance. *J Crohns Colitis* 2024; **18**: 75-81 [PMID: 37527554 DOI: 10.1093/ecco-jcc/jjad131]

World Journal of Gastroenterology

Submit a Manuscript: https://www.f6publishing.com

World J Gastroenterol 2024 March 14; 30(10): 1280-1286

DOI: 10.3748/wjg.v30.i10.1280

ISSN 1007-9327 (print) ISSN 2219-2840 (online)

EDITORIAL

Vonoprazan-amoxicillin dual regimen with *Saccharomyces boulardii* as a rescue therapy for *Helicobacter pylori*: Current perspectives and implications

Valerie Josephine Dirjayanto, Jessica Audrey, Daniel Martin Simadibrata

Specialty type: Gastroenterology and hepatology

Provenance and peer review: Invited article; Externally peer reviewed.

Peer-review model: Single blind

Peer-review report's scientific quality classification

Grade A (Excellent): 0
Grade B (Very good): B
Grade C (Good): 0
Grade D (Fair): 0
Grade E (Poor): 0

P-Reviewer: Oka A, Japan

Received: December 23, 2023
Peer-review started: December 23, 2023
First decision: January 13, 2024
Revised: January 22, 2024
Accepted: February 21, 2024
Article in press: February 21, 2024
Published online: March 14, 2024

Valerie Josephine Dirjayanto, Jessica Audrey, Faculty of Medicine, Universitas Indonesia, Jakarta Pusat 10430, DKI Jakarta, Indonesia

Daniel Martin Simadibrata, Division of Gastroenterology and Hepatology, Mayo Clinic, Rochester, Minnesota 55905, United States

Daniel Martin Simadibrata, Nuffield Department of Population Health, University of Oxford, Oxford OX3 7LF, United Kingdom

Corresponding author: Daniel Martin Simadibrata, MD, MSc, Postdoctoral Fellow, Division of Gastroenterology and Hepatology, Mayo Clinic, 200 First St. SW, Rochester, Minnesota 55905, United States. simadibrata.daniel@mayo.edu

Abstract

Yu *et al*'s study in the *World Journal of Gastroenterology* (2023) introduced a novel regimen of Vonoprazan-amoxicillin dual therapy combined with *Saccharomyces boulardii* (*S. boulardii*) for the rescue therapy against *Helicobacter pylori* (*H. pylori*), a pathogen responsible for peptic ulcers and gastric cancer. Vonoprazan is a potassium-competitive acid blocker renowned for its rapid and long-lasting acid suppression, which is minimally affected by mealtime. Compared to proton pump inhibitors, which bind irreversibly to cysteine residues in the H^+/K^+-ATPase pump, Vonoprazan competes with the K^+ ions, prevents the ions from binding to the pump and blocks acid secretion. Concerns with increasing antibiotic resistance, effects on the gut microbiota, patient compliance, and side effects have led to the advent of a dual regimen for *H. pylori*. Previous studies suggested that *S. boulardii* plays a role in stabilizing the gut barrier which improves *H. pylori* eradication rate. With an acceptable safety profile, the dual-adjunct regimen was effective regardless of prior treatment failure and antibiotic resistance profile, thereby strengthening the applicability in clinical settings. Nonetheless, *S. boulardii* comes in various formulations and dosages, warranting further exploration into the optimal dosage for supplementation in rescue therapy. Additionally, larger, randomized, double-blinded controlled trials are warranted to confirm these promising results.

Key Words: Vonoprazan; *Saccharomyces boulardii*; *Helicobacter pylori*; Rescue therapy; Eradication rate

Core Tip: Vonoprazan-amoxicillin dual therapy with *Saccharomyces boulardii* (*S. boulardii*, VAS regimen) emerges as a novel rescue therapy for eradicating *Helicobacter pylori* (*H. pylori*). Vonoprazan, a potassium-competitive acid blocker, exhibits superior acid suppression compared to proton pump inhibitors. Notably, dual therapy minimizes the use of an additional antibiotic while maintaining efficacy comparable to traditional triple therapy. This paper highlights the role of *S. boulardii*, a probiotic, in enhancing the efficacy of Vonoprazan dual therapy by restoring gut microbiota balance, directly affecting *H. pylori*, and regulating immunomodulation. The VAS regimen emerges as a promising treatment alternative, demonstrating remarkable eradication of *H. pylori*, even in triple-resistant strains.

Citation: Dirjayanto VJ, Audrey J, Simadibrata DM. Vonoprazan-amoxicillin dual regimen with *Saccharomyces boulardii* as a rescue therapy for *Helicobacter pylori*: Current perspectives and implications. *World J Gastroenterol* 2024; 30(10): 1280-1286
URL: https://www.wjgnet.com/1007-9327/full/v30/i10/1280.htm
DOI: https://dx.doi.org/10.3748/wjg.v30.i10.1280

INTRODUCTION

Yu *et al*'s study introduced a novel regimen involving vonoprazan-amoxicillin dual therapy with *Saccharomyces boulardii* (*S. boulardii*) for the rescue therapy against *Helicobacter pylori* (*H. pylori*), a critical pathogen responsible for gastroduodenal diseases including peptic ulcers and gastric cancer[1]. First approved in Japan in 2014, vonoprazan is a potassium-competitive acid blocker renowned for its profound acid suppression, which is minimally affected by mealtime[2]. The target of action for vonoprazan is the H^+/K^+-ATPase, a proton pump that becomes activated when it gets inserted into the canalicular membrane to secrete acid (H^+) from the gastric parietal cells into the lumen[3]. The current first-line treatment regimen for *H. pylori* eradication includes a standard triple therapy with proton pump inhibitors (PPIs) and two antibiotics. PPIs are prodrugs that are activated in an acidic (low pH) environment and work by irreversibly binding to the cysteine residue on the H^+/K^+-ATPase pump. On the other hand, vonoprazan works independently of the pH level and competes with the K^+ ions, preventing the ions from binding to the pump and, therefore, blocking acid (H^+) secretion [4]. Due to the high negative logarithm of the acid dissociation constant (pKa), vonoprazan quickly accumulates in gastric tissue and has delayed clearance once bound to H^+/K^+-ATPase. This property allows vonoprazan to offer a more rapid and longer-lasting gastric acid suppression than the PPIs. In fact, compared to lansoprazole, vonoprazan resulted in a significantly greater 24-hour holding-time ratio for intragastric pH > 4 on days 1 and 7[3]. Therefore, the superior acid suppression properties of vonoprazan, compared to PPIs, highly attract its potential use for treating gastric acid-related disease[5].

VONOPRAZAN DUAL THERAPY REGIMEN: BREAKTHROUGH AND EVIDENCE

Dual therapy against *H. pylori* is a relatively new treatment regimen approach. Previously, the standard triple therapy containing PPIs, Clarithromycin, and Amoxicillin or Metronidazole was the mainstay treatment for *H. pylori* eradication. However, antibiotic resistance has caused the eradication rate to diminish (< 80%)[6]. In fact, resistance to clarithromycin has continuously increased, with reports in Japan describing an increase from 7% to 28.5% over the course of 14 years[7] and in Australia suggesting an increase of 3.7% annually over the past 20 years[8]. In the United States, eradication rates of triple therapy with PPI have declined to less than 80%, attributable to both antibiotic resistance and failure to maintain the intragastric pH required for effective antimicrobial activity[9].

Yu *et al*'s prospective single-arm trial in the *World Journal of Gastroenterology* introduced a novel regimen involving vonoprazan-amoxicillin dual therapy with the addition of *S. boulardii* (VAS regimen) for the rescue therapy against *H. pylori* in patients with a history of treatment failure[1]. In this study, the resistance of *H. pylori* to clarithromycin, metronidazole, and levofloxacin was 91.3%, 100%, and 60.9%, respectively. Overall, the eradication rate of *H. pylori* was 92.6% (63/68). Interestingly, out of the patients with triple-resistant *H. pylori* (60.9%; n = 14/23), a 92.9% eradication rate was achieved with the vonoprazan-based rescue therapy. This suggested that such a regimen was effective and safe regardless of antibiotic resistance.

Previous studies investigating treatment-naïve patients showed promising findings for Vonoprazan dual therapy. In Chey *et al*'s phase 3 randomized controlled trial (RCT), the reported eradication rate for clarithromycin-resistant *H. pylori* with Vonoprazan-Amoxicillin dual therapy was 69.6%, while eradication rates were 65.8% with vonoprazan-amoxicillin-clarithromycin triple therapy and 31.9% with Lansoprazole triple therapy[9]. Despite not reaching values above 90%, the eradication rate was numerically higher in the dual therapy, suggesting that adding Clarithromycin may be unnecessary in treating clarithromycin-resistant strains. Zuberi *et al*'s study reported that the vonoprazan-based regimen was superior to the PPI triple therapy regimen in eradicating *H. pylori* (93.5% *vs* 83.9%)[10]. Similarly, Liu *et al*'s network meta-analysis suggested that vonoprazan-based therapies were significantly more effective in eradicating *H. pylori* than PPI triple therapy, with the best safety profile shown by the vonoprazan dual therapy[11]. Therefore, vonoprazan dual therapy

presents as a lower-cost, simple, yet effective treatment option for *H. pylori* eradication.

As for patients with a history of two treatment failures, vonoprazan-based triple therapy yielded a significantly higher success rate in comparison to esomeprazole-based therapy[12]. Similarly, for third-line therapy, the eradication rate with the vonoprazan-amoxicillin-sitafloxacin regimen was higher than the PPI-based regimen (75.8% *vs* 53.3%), despite no significant difference in the intention-to-treat analyses (P = 0.071)[13]. The duration of therapy might explain the insignificant difference in eradication rates since Sue *et al*[13] had prescribed the treatment regimens for only seven days, whereas Yu *et al*[1] provided the regimen for 14 d. Therefore, although no study has investigated the effect of therapy duration on eradication rates, available data suggest that long-term regimens may be more effective.

SACCHAROMYCES BOULARDII AS AN ADJUNCT THERAPY IN *H. PYLORI* ERADICATION

The use of antibiotics in treatment regimens for eradicating *H. pylori* has been shown to disrupt the balance of gut microbiota and may elicit adverse events. Recent studies have shown that probiotics, including *S. boulardii*, may contribute to mitigating these effects by: (1) Maintaining the balance and integrity of the normal gut microbiota; (2) direct activity against the pathogenesis of *H. pylori*; and (3) immunomodulation (Figure 1)[14]. In the context of therapy, Keikha and Kamali[14] investigated the addition of *S. boulardii* to the standard triple regimen, and the addition of *S. boulardii* was shown to be associated with a lower proportion of anaerobic bacteria, including *Bacteroides* and *Clostridium*, as well as higher proportion of commensal bacteria including *Bifidobacterium* and *Lactobacillus*[14]. Sakarya and Gunay[15] *in vivo* study proved that *S. boulardii* may also directly contribute to the eradication of *H. pylori via* the α2,3-linked sialic acid–selective neuraminidase activity, leading to reduced adhesion to host cells. Additionally, *S. boulardii* may produce proteins that modulate cytokines, contribute to the activation of peroxisome proliferator-activated receptor-gamma, and trigger antibody production, leading to an anti-inflammatory effect that sustains the gastrointestinal system[16].

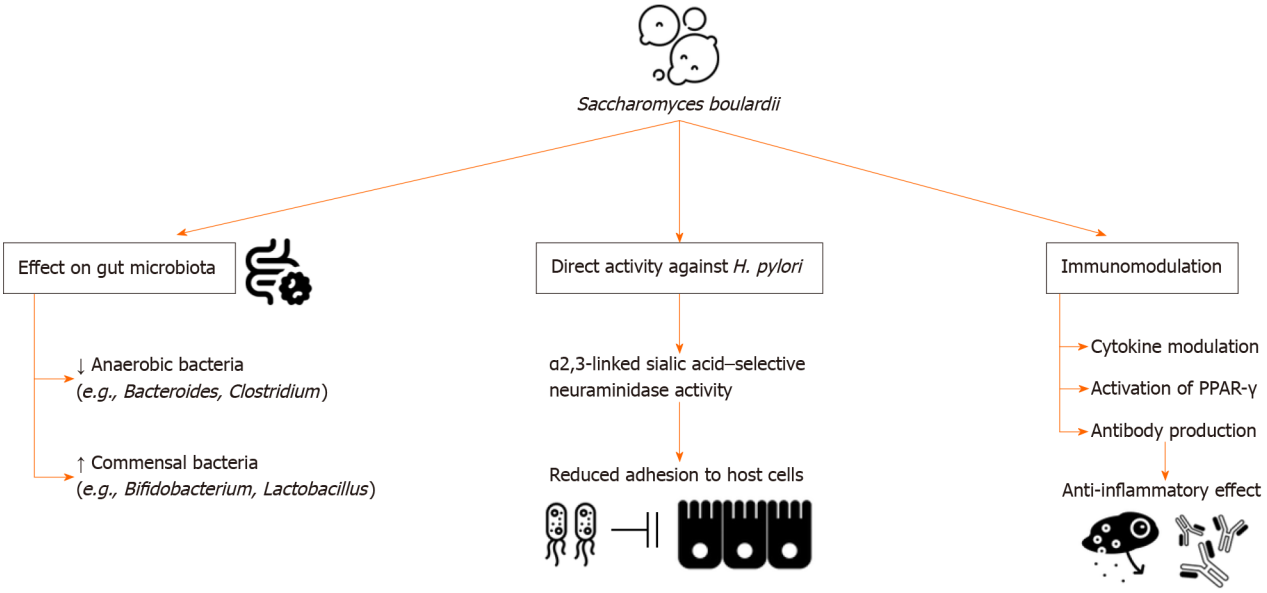

Figure 1 Mechanism of action of *Saccharomyces boulardii* in *Helicobacter pylori* eradication. *H. pylori*: *Helicobacter pylori*.

Yu *et al*[1] were the first to investigate the combination of a vonoprazan dual regimen with *S. boulardii* as an adjunct therapy, providing new insights into its efficacy in rescue therapy. This data builds on previous studies investigating the addition of *S. boulardii* for standard triple or quadruple therapy. Qu *et al*[17] provided a two-stage intervention for rescue therapy, during which the patients were administered *S. boulardii* as monotherapy for two weeks, followed by bismuth quadruple therapy if required. The eradication rates in patients receiving *S. boulardii* were reported to be higher than those who did not receive *S. boulardii*, thus supporting its effectiveness. However, several other studies, including Zojaji *et al*[18], did not show any significant improvement in eradication with the addition of *S. boulardii; however*, it was noted that the side effects, including nausea, bloating, and diarrhea, were lower. In addition, a meta-analysis by Liu *et al*[11] investigating *S. boulardii* in addition to standard triple therapy suggested that it yielded beneficial outcomes in eradication, the occurrence of adverse effects, and symptom reduction. Another meta-analysis of 18 RCTs by Zhou *et al*[19] demonstrated a slight pooled improvement in the eradication rate by 9% while decreasing the adverse effects by half. Therefore, while the effectiveness of adding *S. boulardii* for eradicating *H. pylori* might be modest, the reduction of adverse effects makes it worthwhile for this probiotic to be added to the regimen.

FACTORS AFFECTING TREATMENT FAILURE OF THE VONOPRAZAN-AMOXICILLIN- *S. BOULARDII*

Demographic factors such as age, gender, smoking history, and alcohol consumption were not associated with the VAS treatment regimen failure in Yu *et al*[1] study. Several socio-demographic characteristics, such as gender and areas of residence, have been significantly associated with *H. pylori* eradication failure[20] despite inconsistent results observed across studies[21,22]. This suggests that the impact of socioeconomic and demographic factors on treatment outcomes may vary across different patient populations. Such variations may stem from differences in antibiotic usage patterns, antimicrobial resistance, and medication adherence[23-25].

It is interesting to note that anxiety was identified as a risk factor for treatment failure with the VAS treatment regimen. This finding aligns with previous research linking psychological factors to dyspeptic symptoms. For instance, patients with disorders of the gut-brain interaction were noted to have higher rates of anxiety and depression[26]. This relationship may be correlated to the intricate brain-gut axis, a circuit linking the central, peripheral, and autonomic nervous systems with gastrointestinal functions. Gut microorganisms, including *H. pylori* infection, were hypothesized to interact with this axis, as evident by the observation that stress and emotional disorders negatively impact intestinal flora and digestive function[27]. Further investigations suggest that this relationship may be bidirectional. *H. pylori* infection was associated with altered eating behavior, anxiety and depression-like behaviors, cognitive dysfunction, and lower pain thresholds[27-29]. On the other hand, a study in mice models by Guo *et al*[30] demonstrated that the induction of psychological stress significantly increased *H. pylori* colonization and was associated with more extensive gastric mucosal injury. The underlying mechanisms of altered brain-gut axis potentially involve direct neurotoxic effects, activation of proinflammatory responses, and micronutrient deficiencies, areas which are still highly subject to research[27]. The complex interplay between psychological disorders and *H. pylori* infection underscores the importance of psychological assessments and interventions, such as cognitive behavioral therapy or counseling sessions, to enhance treatment success in *H. pylori* infections[31,32].

Notably, Yu *et al*[1] also showed that the number of previous treatment failures was not associated with treatment failure in this VAS regimen. Eradication rates were consistently high, irrespective of resistance to clarithromycin and levofloxacin. This is in contrast to a prior study that identified any prior exposure to antibiotics as a risk factor for treatment failure with a clarithromycin-containing triple therapy regimen[33]. Clarithromycin resistance was shown to be associated with Metronidazole resistance[34], leading to the prevalence of double-resistant strains, particularly in individuals who had previously failed two eradication treatments[35-38]. Furthermore, sufficient acid inhibition is required for successful *H. pylori* eradication, as it influences the stability and bioavailability of some antibiotics, including amoxicillin. Eradication failure was often observed in patients who are extensive CYP2C19 metabolizers of PPI, as they exhibit rapid PPI inactivation and insufficient acid suppression[39,40]. Vonoprazan exhibits stronger and longer acid suppression than PPI[41], which may explain the significant superiority of a vonoprazan-based regimen over PPI-based therapy regarding *H. pylori* eradication success[42]. This suggests the potential use of the VAS regimen as a rescue therapy for *H. pylori* infections resistant to other essential antibiotics, particularly in the context of increasing global antimicrobial resistance.

SAFETY PROFILE OF VONOPRAZAN-BASED THERAPIES

The impact of adverse events on therapy discontinuation and treatment adherence is a critical aspect of any treatment regimen. In Yu *et al*'s study[1], the VAS regimen exhibited a low rate of adverse events, all of which were reported as mild or moderate. The safety profile of vonoprazan, as reported in numerous clinical studies, consistently demonstrates its superiority or, at the very least, equivalence to that of PPIs. A meta-analysis of RCTs demonstrated a significantly lower rate of adverse events with vonoprazan-based triple therapy (32.7%) compared to PPI-based triple therapy (40.5%) while maintaining a higher efficacy in terms of *H. pylori* eradication rate[43].

Commonly reported adverse events include diarrhea, dysgeusia, loose stool, and skin eruption[44]. While Suzuki *et al*[45] noted a slightly higher incidence of skin rash in vonoprazan-based therapy, it is noteworthy that the vonoprazan-based regimen was generally well-tolerated, and no instances of therapy discontinuation occurred due to the adverse events.

CONCLUSION

The superiority of the vonoprazan-based regimen in terms of both efficacy and safety highlights its potential as an excellent alternative for *H. pylori* treatment and positions it as an effective option for rescue therapy. Notably, the vonoprazan-amoxicillin dual therapy has exhibited acceptable efficacy in *H. pylori* eradication, comparable to the outcomes of vonoprazan-based triple therapy. Given the increasing rates of clarithromycin resistance in various geographical regions, adding clarithromycin to vonoprazan and amoxicillin may only offer a marginal benefit. The dual regimen minimizes the use of an unnecessary additional antibiotic while maintaining efficacy similar to that of triple therapy, a crucial consideration amid the current surge in antibiotic resistance[46]. Additionally, the supplementation of *S. boulardii* as an adjunct therapy to vonoprazan-based regimens has shown positive effects on *H. pylori* eradication and reduced adverse events, possibly attributed to the maintenance of normal gut microbiota.

However, it is essential to acknowledge certain limitations in this study. While this study supported the efficacy of a dual vonoprazan-based regimen with the addition of *S. boulardii* for rescue therapy, it should be noted that the number of study participants is considered small. Additionally, the generalizability of the reduction of adverse events seen with the addition of *S. boulardii* might be limited since different populations possess different gut microbiota, which is affected by geography and dietary habits[47]. Given the various formulations and dosages available, further exploration is needed to determine the optimal dosing of *S. boulardii* supplementation in such rescue therapy. Lastly, as this study employed a single-arm design, direct comparisons of the VAS regimen to currently recommended regimens are lacking. Therefore, randomized double-blinded controlled trials with large sample sizes are required to validate these promising results.

FOOTNOTES

Author contributions: Dirjayanto VJ, Audrey J, and Simadibrata DM reviewed the literature, drafted the original manuscript, and critically revised the manuscript for important intellectual content; all authors have read and approved the final version of the manuscript.

Conflict-of-interest statement: All authors have no conflict of interest to disclose.

Country/Territory of origin: United States

ORCID number: Valerie Josephine Dirjayanto 0000-0003-4170-7742; Jessica Audrey 0000-0003-3329-8651; Daniel Martin Simadibrata 0000-0002-7512-2112.

S-Editor: Lin C
L-Editor: A
P-Editor: Zhao YQ

REFERENCES

1 **Yu J**, Lv YM, Yang P, Jiang YZ, Qin XR, Wang XY. Safety and effectiveness of vonoprazan-based rescue therapy for Helicobacter pylori infection. *World J Gastroenterol* 2023; **29**: 3133-3144 [PMID: 37346155 DOI: 10.3748/wjg.v29.i20.3133]
2 **Garnock-Jones KP**. Vonoprazan: first global approval. *Drugs* 2015; **75**: 439-443 [PMID: 25744862 DOI: 10.1007/s40265-015-0368-z]
3 **Laine L**, Sharma P, Mulford DJ, Hunt B, Leifke E, Smith N, Howden CW. Pharmacodynamics and Pharmacokinetics of the Potassium-Competitive Acid Blocker Vonoprazan and the Proton Pump Inhibitor Lansoprazole in US Subjects. *Am J Gastroenterol* 2022; **117**: 1158-1161 [PMID: 35294415 DOI: 10.14309/ajg.0000000000001735]
4 **Luo HJ**, Deng WQ, Zou K. Protonated form: the potent form of potassium-competitive acid blockers. *PLoS One* 2014; **9**: e97688 [PMID: 24845980 DOI: 10.1371/journal.pone.0097688]
5 **Sugano K**. Vonoprazan fumarate, a novel potassium-competitive acid blocker, in the management of gastroesophageal reflux disease: safety and clinical evidence to date. *Therap Adv Gastroenterol* 2018; **11**: 1756283X17745776 [PMID: 29383028 DOI: 10.1177/1756283X17745776]
6 **Cho JH**, Jin SY. Current guidelines for Helicobacter pylori treatment in East Asia 2022: Differences among China, Japan, and South Korea. *World J Clin Cases* 2022; **10**: 6349-6359 [PMID: 35979311 DOI: 10.12998/wjcc.v10.i19.6349]
7 **Okamura T**, Suga T, Nagaya T, Arakura N, Matsumoto T, Nakayama Y, Tanaka E. Antimicrobial resistance and characteristics of eradication therapy of Helicobacter pylori in Japan: a multi-generational comparison. *Helicobacter* 2014; **19**: 214-220 [PMID: 24758533 DOI: 10.1111/hel.12124]
8 **Schubert JP**, Warner MS, Rayner CK, Roberts-Thomson IC, Mangoni AA, Costello S, Bryant RV. Increasing Helicobacter pylori clarithromycin resistance in Australia over 20 years. *Intern Med J* 2022; **52**: 1554-1560 [PMID: 34865299 DOI: 10.1111/imj.15640]
9 **Chey WD**, Mégraud F, Laine L, López LJ, Hunt BJ, Howden CW. Vonoprazan Triple and Dual Therapy for Helicobacter pylori Infection in the United States and Europe: Randomized Clinical Trial. *Gastroenterology* 2022; **163**: 608-619 [PMID: 35679950 DOI: 10.1053/j.gastro.2022.05.055]
10 **Zuberi BF**, Ali FS, Rasheed T, Bader N, Hussain SM, Saleem A. Comparison of Vonoprazan and Amoxicillin Dual Therapy with Standard Triple Therapy with Proton Pump Inhibitor for Helicobacter Pylori eradication: A Randomized Control Trial. *Pak J Med Sci* 2022; **38**: 965-969 [PMID: 35634610 DOI: 10.12669/pjms.38.4.5436]
11 **Liu L**, Li F, Shi H, Nahata MC. The Efficacy and Safety of Vonoprazan and Amoxicillin Dual Therapy for Helicobacter pylori Infection: A Systematic Review and Network Meta-Analysis. *Antibiotics (Basel)* 2023; **12** [PMID: 36830257 DOI: 10.3390/antibiotics12020346]
12 **Saito Y**, Konno K, Sato M, Nakano M, Kato Y, Saito H, Serizawa H. Vonoprazan-Based Third-Line Therapy Has a Higher Eradication Rate against Sitafloxacin-Resistant Helicobacter pylori. *Cancers (Basel)* 2019; **11** [PMID: 30669474 DOI: 10.3390/cancers11010116]
13 **Sue S**, Shibata W, Sasaki T, Kaneko H, Irie K, Kondo M, Maeda S. Randomized trial of vonoprazan-based *vs* proton-pump inhibitor-based third-line triple therapy with sitafloxacin for Helicobacter pylori. *J Gastroenterol Hepatol* 2019; **34**: 686-692 [PMID: 30151994 DOI: 10.1111/jgh.14456]
14 **Keikha M**, Kamali H. The impact of Saccharomyces boulardii adjuvant supplementation on alternation of gut microbiota after H. pylori

eradication; a metagenomics analysis. *Gene Rep* 2022; **26**: 101499 [DOI: 10.1016/j.genrep.2022.101499]

15 **Sakarya S**, Gunay N. Saccharomyces boulardii expresses neuraminidase activity selective for α2,3-linked sialic acid that decreases Helicobacter pylori adhesion to host cells. *APMIS* 2014; **122**: 941-950 [PMID: 24628732 DOI: 10.1111/apm.12237]

16 **Pothoulakis C**. Review article: anti-inflammatory mechanisms of action of Saccharomyces boulardii. *Aliment Pharmacol Ther* 2009; **30**: 826-833 [PMID: 19706150 DOI: 10.1111/j.1365-2036.2009.04102.x]

17 **Qu P**, Liu X, Xia X, Xie X, Luo J, Cheng S, Chi J, Liu P, Li H, Zhao W, Yang H, Xu C. Saccharomyces boulardii Allows Partial Patients to Avoid Reusing Bismuth Quadruple for Helicobacter pylori Rescue Therapy: A Single-Center Randomized Controlled Study. *Front Cell Infect Microbiol* 2022; **12**: 903002 [PMID: 35880079 DOI: 10.3389/fcimb.2022.903002]

18 **Zojaji H**, Ghobakhlou M, Rajabalinia H, Ataei E, Jahani Sherafat S, Moghimi-Dehkordi B, Bahreiny R. The efficacy and safety of adding the probiotic Saccharomyces boulardiito standard triple therapy for eradication of H.pylori: a randomized controlled trial. *Gastroenterol Hepatol Bed Bench* 2013; **6**: S99-S104 [PMID: 24834296]

19 **Zhou BG**, Chen LX, Li B, Wan LY, Ai YW. Saccharomyces boulardii as an adjuvant therapy for Helicobacter pylori eradication: A systematic review and meta-analysis with trial sequential analysis. *Helicobacter* 2019; **24**: e12651 [PMID: 31414551 DOI: 10.1111/hel.12651]

20 **Peña-Galo E**, Gotor J, Harb Y, Alonso M, Alcedo J. Socioeconomic and demographic factors associated with failure in Helicobacter pylori eradication using the standard triple therapy. *Gastroenterol Hepatol Bed Bench* 2021; **14**: 53-58 [PMID: 33868610]

21 **Smith S**, Jolaiya T, Fowora M, Palamides P, Ngoka F, Bamidele M, Lesi O, Onyekwere C, Ugiagbe R, Agbo I, Ndububa D, Adekanle O, Adedeji A, Adeleye I, Harrison U. Clinical and Socio- Demographic Risk Factors for Acquisition of Helicobacter pylori Infection in Nigeria. *Asian Pac J Cancer Prev* 2018; **19**: 1851-1857 [PMID: 30049197 DOI: 10.22034/APJCP.2018.19.7.1851]

22 **Gebeyehu E**, Nigatu D, Engidawork E. Helicobacter pylori eradication rate of standard triple therapy and factors affecting eradication rate at Bahir Dar city administration, Northwest Ethiopia: A prospective follow up study. *PLoS One* 2019; **14**: e0217645 [PMID: 31163069 DOI: 10.1371/journal.pone.0217645]

23 **Nayar DS**. Current eradication rate of Helicobacter pylori with clarithromycin-based triple therapy in a gastroenterology practice in the New York metropolitan area. *Infect Drug Resist* 2018; **11**: 205-211 [PMID: 29430191 DOI: 10.2147/IDR.S153617]

24 **Lim SG**, Park RW, Shin SJ, Yoon D, Kang JK, Hwang JC, Kim SS, Kim JH, Lee KM. The relationship between the failure to eradicate Helicobacter pylori and previous antibiotics use. *Dig Liver Dis* 2016; **48**: 385-390 [PMID: 26856963 DOI: 10.1016/j.dld.2015.12.001]

25 **Lefebvre M**, Chang HJ, Morse A, van Zanten SV, Goodman KJ; CANHelp Working Group. Adherence and barriers to H. pylori treatment in Arctic Canada. *Int J Circumpolar Health* 2013; **72**: 22791 [PMID: 24416723 DOI: 10.3402/ijch.v72i0.22791]

26 **Xiong RG**, Li J, Cheng J, Zhou DD, Wu SX, Huang SY, Saimaiti A, Yang ZJ, Gan RY, Li HB. The Role of Gut Microbiota in Anxiety, Depression, and Other Mental Disorders as Well as the Protective Effects of Dietary Components. *Nutrients* 2023; **15** [PMID: 37513676 DOI: 10.3390/nu15143258]

27 **Budzyński J**, Kłopocka M. Brain-gut axis in the pathogenesis of Helicobacter pylori infection. *World J Gastroenterol* 2014; **20**: 5212-5225 [PMID: 24833851 DOI: 10.3748/wjg.v20.i18.5212]

28 **Bercik P**, Verdú EF, Foster JA, Lu J, Scharringa A, Kean I, Wang L, Blennerhassett P, Collins SM. Role of gut-brain axis in persistent abnormal feeding behavior in mice following eradication of Helicobacter pylori infection. *Am J Physiol Regul Integr Comp Physiol* 2009; **296**: R587-R594 [PMID: 19129375 DOI: 10.1152/ajpregu.90752.2008]

29 **Gorlé N**, Bauwens E, Haesebrouck F, Smet A, Vandenbroucke RE. Helicobacter and the Potential Role in Neurological Disorders: There Is More Than Helicobacter pylori. *Front Immunol* 2020; **11**: 584165 [PMID: 33633723 DOI: 10.3389/fimmu.2020.584165]

30 **Guo G**, Jia KR, Shi Y, Liu XF, Liu KY, Qi W, Guo Y, Zhang WJ, Wang T, Xiao B, Zou QM. Psychological stress enhances the colonization of the stomach by Helicobacter pylori in the BALB/c mouse. *Stress* 2009; **12**: 478-485 [PMID: 20102319 DOI: 10.3109/10253890802642188]

31 **Kabeer KK**, Ananthakrishnan N, Anand C, Balasundaram S. Prevalence of Helicobacter Pylori Infection and Stress, Anxiety or Depression in Functional Dyspepsia and Outcome after Appropriate Intervention. *J Clin Diagn Res* 2017; **11**: VC11-VC15 [PMID: 28969250 DOI: 10.7860/JCDR/2017/26745.10486]

32 **Haag S**, Senf W, Tagay S, Langkafel M, Braun-Lang U, Pietsch A, Heuft G, Talley NJ, Holtmann G. Is there a benefit from intensified medical and psychological interventions in patients with functional dyspepsia not responding to conventional therapy? *Aliment Pharmacol Ther* 2007; **25**: 973-986 [PMID: 17403002 DOI: 10.1111/j.1365-2036.2007.03277.x]

33 **Guo CG**, Jiang F, Cheung KS, Li B, Ooi PH, Leung WK. Timing of prior exposure to antibiotics and failure of Helicobacter pylori eradication: a population-based study. *J Antimicrob Chemother* 2022; **77**: 517-523 [PMID: 34791274 DOI: 10.1093/jac/dkab415]

34 **Heep M**, Kist M, Strobel S, Beck D, Lehn N. Secondary resistance among 554 isolates of Helicobacter pylori after failure of therapy. *Eur J Clin Microbiol Infect Dis* 2000; **19**: 538-541 [PMID: 10968325 DOI: 10.1007/s100960000288]

35 **Mégraud F**. H pylori antibiotic resistance: prevalence, importance, and advances in testing. *Gut* 2004; **53**: 1374-1384 [PMID: 15306603 DOI: 10.1136/gut.2003.022111]

36 **Gisbert JP**. "Rescue" regimens after Helicobacter pylori treatment failure. *World J Gastroenterol* 2008; **14**: 5385-5402 [PMID: 18803350 DOI: 10.3748/wjg.14.5385]

37 **Cammarota G**, Martino A, Pirozzi G, Cianci R, Branca G, Nista EC, Cazzato A, Cannizzaro O, Miele L, Grieco A, Gasbarrini A, Gasbarrini G. High efficacy of 1-week doxycycline- and amoxicillin-based quadruple regimen in a culture-guided, third-line treatment approach for Helicobacter pylori infection. *Aliment Pharmacol Ther* 2004; **19**: 789-795 [PMID: 15043520 DOI: 10.1111/j.1365-2036.2004.01910.x]

38 **Hwang JY**, Kim C, Kwon YH, Lee JE, Jeon SW, Nam SY, Seo AN, Han MH, Park JH. Dual Clarithromycin and Metronidazole Resistance Is the Main Cause of Failure in Ultimate Helicobacter pylori Eradication. *Dig Dis* 2021; **39**: 451-461 [PMID: 33429397 DOI: 10.1159/000514278]

39 **Kuo CH**, Lu CY, Shih HY, Liu CJ, Wu MC, Hu HM, Hsu WH, Yu FJ, Wu DC, Kuo FC. CYP2C19 polymorphism influences Helicobacter pylori eradication. *World J Gastroenterol* 2014; **20**: 16029-16036 [PMID: 25473155 DOI: 10.3748/wjg.v20.i43.16029]

40 **Zhao X**, Zhang Z, Lu F, Xiong M, Jiang L, Tang K, Fu M, Wu Y, He B. Effects of CYP2C19 genetic polymorphisms on the cure rates of H. pylori in patients treated with the proton pump inhibitors: An updated meta-analysis. *Front Pharmacol* 2022; **13**: 938419 [PMID: 36278195 DOI: 10.3389/fphar.2022.938419]

41 **Kagami T**, Sahara S, Ichikawa H, Uotani T, Yamade M, Sugimoto M, Hamaya Y, Iwaizumi M, Osawa S, Sugimoto K, Miyajima H, Furuta T. Potent acid inhibition by vonoprazan in comparison with esomeprazole, with reference to CYP2C19 genotype. *Aliment Pharmacol Ther* 2016; **43**: 1048-1059 [PMID: 26991399 DOI: 10.1111/apt.13588]

42 **Shinozaki S**, Kobayashi Y, Osawa H, Sakamoto H, Hayashi Y, Lefor AK, Yamamoto H. Effectiveness and Safety of Vonoprazan versus Proton Pump Inhibitors for Second-Line Helicobacter pylori Eradication Therapy: Systematic Review and Meta-Analysis. *Digestion* 2021; **102**:

319-325 [PMID: 31914442 DOI: 10.1159/000504939]

43 **Lyu QJ**, Pu QH, Zhong XF, Zhang J. Efficacy and Safety of Vonoprazan-Based versus Proton Pump Inhibitor-Based Triple Therapy for Helicobacter pylori Eradication: A Meta-Analysis of Randomized Clinical Trials. *Biomed Res Int* 2019; **2019**: 9781212 [PMID: 31211144 DOI: 10.1155/2019/9781212]

44 **Maruyama M**, Tanaka N, Kubota D, Miyajima M, Kimura T, Tokutake K, Imai R, Fujisawa T, Mori H, Matsuda Y, Wada S, Horiuchi A, Kiyosawa K. Vonoprazan-Based Regimen Is More Useful than PPI-Based One as a First-Line Helicobacter pylori Eradication: A Randomized Controlled Trial. *Can J Gastroenterol Hepatol* 2017; **2017**: 4385161 [PMID: 28349044 DOI: 10.1155/2017/4385161]

45 **Suzuki S**, Gotoda T, Kusano C, Iwatsuka K, Moriyama M. The Efficacy and Tolerability of a Triple Therapy Containing a Potassium-Competitive Acid Blocker Compared With a 7-Day PPI-Based Low-Dose Clarithromycin Triple Therapy. *Am J Gastroenterol* 2016; **111**: 949-956 [PMID: 27185079 DOI: 10.1038/ajg.2016.182]

46 **Zhang WL**, Lin BS, Li YY, Ding YM, Han ZX, Ji R. Efficacy and Safety of Vonoprazan and Amoxicillin Dual Therapy for Helicobacter pylori Eradication: A Systematic Review and Meta-Analysis. *Digestion* 2023; **104**: 249-261 [PMID: 37015201 DOI: 10.1159/000529622]

47 **Senghor B**, Sokhna C, Ruimy R, Lagier JC. Gut microbiota diversity according to dietary habits and geographical provenance. *Human Microbiome J* 2018; **7–8**: 1-9 [DOI: 10.1016/j.humic.2018.01.001]

World Journal of Gastroenterology

Submit a Manuscript: https://www.f6publishing.com

World J Gastroenterol 2024 March 14; 30(10): 1287-1290

DOI: 10.3748/wjg.v30.i10.1287

ISSN 1007-9327 (print) ISSN 2219-2840 (online)

EDITORIAL

Women health and microbiota: Different aspects of well-being

Giulia Nannini, Amedeo Amedei

Specialty type: Gastroenterology and hepatology

Provenance and peer review: Invited article; Externally peer reviewed.

Peer-review model: Single blind

Peer-review report's scientific quality classification

Grade A (Excellent): 0
Grade B (Very good): 0
Grade C (Good): C
Grade D (Fair): 0
Grade E (Poor): 0

P-Reviewer: Nooripour R, Iran

Received: December 23, 2023
Peer-review started: December 23, 2023
First decision: January 9, 2024
Revised: January 22, 2024
Accepted: February 25, 2024
Article in press: February 25, 2024
Published online: March 14, 2024

Giulia Nannini, Amedeo Amedei, Department of Experimental and Clinical Medicine, University of Florence, Florence 50134, Italy

Amedeo Amedei, Network of Immunity in Infection, Malignancy and Autoimmunity (NIIMA), Universal Scientific Education and Research Network (USERN), Florence 50134, Italy

Corresponding author: Amedeo Amedei, MSc, Full Professor, Department of Experimental and Clinical Medicine, University of Florence, 3 Largo Brambilla, Florence 50134, Italy. amedeo.amedei@unifi.it

Abstract

In this editorial, we comment on the article by Marano *et al* recently published in the *World Journal of Gastroenterology* 2023; 29 (45): 5945-5952. We focus on the role of gut microbiota (GM) in women's health, highlighting the need to thoroughly comprehend the sex differences in microbiota. Together, the host and GM support the host's health. The microbiota components consist of viruses, bacteria, fungi, and archaea. This complex is an essential part of the host and is involved in neurological development, metabolic control, immune system dynamics, and host dynamic homeostasis. It has been shown that differences in the GM of males and females can contribute to chronic diseases, such as gastrointestinal, metabolic, neurological, cardiovascular, and respiratory illnesses. These differences can also result in some sex-specific changes in immunity. Every day, research on GM reveals new and more expansive frontiers, offering a wealth of innovative opportunities for preventive and precision medicine.

Key Words: Gut microbiota; Women; Immune system; Well-being; Hormones; Sex-differences

Core Tip: The intestinal microbiota, comprising viruses, bacteria, fungi, and archaea, plays a crucial role in neurological development, metabolic control, immune system dynamics, and overall host homeostasis. Differences in gut microbiota between males and females are suggested to contribute to various chronic diseases, including gastrointestinal, metabolic, neurological, cardiovascular, and respiratory illnesses, as well as sex-specific changes in immunity. The editorial highlights the ongoing research in the field, revealing new opportunities for innovative approaches in preventive and precision medicine.

Citation: Nannini G, Amedei A. Women health and microbiota: Different aspects of well-being. *World J Gastroenterol* 2024; 30(10): 1287-1290
URL: https://www.wjgnet.com/1007-9327/full/v30/i10/1287.htm
DOI: https://dx.doi.org/10.3748/wjg.v30.i10.1287

INTRODUCTION

The human body is home to symbiotic bacteria in a variety of sites that support a healthy organism's function. In detail, the gut contains trillions of microorganisms that make up the highly complex and diverse gut microbial kingdom. These microorganisms include bacteria, fungus, viruses, and archaea[1]. As a vital host component, this complex plays a key role in immune system maintenance and dynamics, metabolic regulation, host dynamic homeostasis, and neurological development[2].

The human body and its native microbiota have a strict symbiotic relationship that begins at birth. This interaction is essential to preserving general health and wellbeing. The microbiota is involved in the regulation of metabolic, endocrine, and immune processes and in influencing drug metabolism and absorption[3]. Progesterone, estrogen, and testosterone are examples of sex hormones that have a variety of physiological functions in reproduction, differentiation, cell division, apoptosis, inflammation, metabolism, homeostasis, and brain function. In addition, the sex hormones play a part in communication between microorganisms and their hosts[4]. In essence, hormones generated by commensal bacteria can influence human behavior, immunity, and metabolism through their interactions with microorganisms[5].

In this editorial we comment on the article published by Marano *et al*[6] in the recent issue of the *World Journal of Gastroenterology* 2023. Specifically, the article focused on the emerging role of gut microbiota (GM) in the different women phases of life. Studies on animals have shown that the mother's microbiota during pregnancy affects the development of the fetal brain and the behavior of the postnatal period[7,8]. Predominant opinion holds that the mother's GM, given to the child at birth, regulates the offspring's gut-brain axis, which is developed postnatally and is based on the concept of a sterile womb[9]. However, increasingly a small number of specific bacteria are being discovered in fetuses that could be considered transitional species facilitating the development of an adequate microbiota after birth[10].

Anyway, the human microbial colonization process starts, in part, at birth and lasts for around three years, during which time it develops and changes in species abundance until the microbiota resembles that of an adult. The diversity and richness of gut bacteria continue to react quickly to dietary changes in infants during the first year of life and the introduction of solid foods modifies the gut bacteria's metabolic activity[11]. Sex-dependent differences in the gut microbiome have been reported and the overall composition of the gut microbiomes of men and women is notably different[12,13]. It is well known that differences in the GM of males and females can drive chronic diseases, ranging from gastrointestinal inflammatory and metabolic conditions to neurological, cardiovascular, and respiratory illnesses. These differences can also result in some sex-specific changes in immunity.

Sexes inequalities are becoming more and more relevant in the pathophysiology, epidemiology, and treatment of many diseases, particularly non-communicable diseases[14]. Nonetheless, despite the fact that women make up over half of the population, there has been documented disparity in how the sexes are presented in health research[15]. Although the appropriate definition of a healthy gut microbiome is still unknown, a number of diseases have been linked to gut microbial dysbiosis and the female GM is a subject that deserves further research.

Studies on both animals and humans revealed sex-related changes in GM, albeit the results are contrasting[16-18]. In detail, animals' models, primarily mice, have unequivocally demonstrated sex-specific variations in GM composition. Recently Stapleton *et al*[19] described the variations in sex-related weight gain, plasma lipid profiles, composition of the faecal microbiota, and levels of faecal short chain fatty acids. When given the same high-fat diet, they observed that male mice acquired significantly more weight than female mice. Nevertheless, after receiving antibiotics to deplete the microbiota, sex differences remained.

However, the principal component analysis in a study conducted in 2005 on 91 northern Europeans subjects from France, Denmark, Germany, the Netherlands, and the United Kingdom using fluorescent in situ hybridization with 18 phylogenetic probes, revealed no significant differences in the colonic microbiota between the sexes[20]. Whereas, an additional research, published in 2006 and including four centres in France, Germany, Italy, and Sweden, found that males showed higher amounts of the Bacteroides-Prevotella group[18].

In 2014, researchers who analyzed a 16S rRNA gene sequence data set from the Human Microbiome Project Consortium, simply reported that sex was associated with the community types identified in the stool. In detail, males were three times more likely to have community type D, with fewer *Bacteroides* and higher *Prevotella*[3]. A very recent Japanese study[21] examined sex-related differences and potential causes, analyzing and comparing the GM compositions of males and females throughout a broad age range. The authors did not observed difference between GM relative abundances or alpha diversities between men and women at any age. However, they showed that the GM heterogeneity among women in their 20s was greater than in men.

CONCLUSION

In this scenario, the manuscript of Marano *et al*[6] appears very interesting since gave us lots food for thought to deeply

understand the relationship between women microbiota composition and not only physical but also psychological well-being. Finally, considering the relevance of the microbiota differences in sexes and the linked-consequences such as immune and metabolic disorders, we think that it could be useful deeply analyze the microbiota functional activities, focusing on metabolites such as short-chain fatty acids, amino acids, and lipids, to improve the diagnosis of some diseases and suggest new therapeutic approaches shaping the microbiota composition and function.

FOOTNOTES

Author contributions: Nannini G and Amedei A designed the overall concept and outline of the manuscript; Nannini G and Amedei A contributed to the writing, and editing the manuscript; Nannini G reviewed the literature; Amedei A supervised and revised the manuscript; both authors have read and approve the final manuscript.

Conflict-of-interest statement: The authors declare no conflict of interest to disclose.

Country/Territory of origin: Italy

ORCID number: Giulia Nannini 0000-0002-6481-6864; Amedeo Amedei 0000-0002-6797-9343.

S-Editor: Chen YL
L-Editor: A
P-Editor: Zhao YQ

REFERENCES

1 **Sender R**, Fuchs S, Milo R. Revised Estimates for the Number of Human and Bacteria Cells in the Body. *PLoS Biol* 2016; **14**: e1002533 [PMID: 27541692 DOI: 10.1371/journal.pbio.1002533]
2 **Erny D**, Hrabě de Angelis AL, Jaitin D, Wieghofer P, Staszewski O, David E, Keren-Shaul H, Mahlakoiv T, Jakobshagen K, Buch T, Schwierzeck V, Utermöhlen O, Chun E, Garrett WS, McCoy KD, Diefenbach A, Staeheli P, Stecher B, Amit I, Prinz M. Host microbiota constantly control maturation and function of microglia in the CNS. *Nat Neurosci* 2015; **18**: 965-977 [PMID: 26030851 DOI: 10.1038/nn.4030]
3 **Ding T**, Schloss PD. Dynamics and associations of microbial community types across the human body. *Nature* 2014; **509**: 357-360 [PMID: 24739969 DOI: 10.1038/nature13178]
4 **Edwards DP**. Regulation of signal transduction pathways by estrogen and progesterone. *Annu Rev Physiol* 2005; **67**: 335-376 [PMID: 15709962 DOI: 10.1146/annurev.physiol.67.040403.120151]
5 **Martinelli S**, Nannini G, Cianchi F, Staderini F, Coratti F, Amedei A. Microbiota Transplant and Gynecological Disorders: The Bridge between Present and Future Treatments. *Microorganisms* 2023; **11** [PMID: 37894065 DOI: 10.3390/microorganisms11102407]
6 **Marano G**, Traversi G, Gaetani E, Gasbarrini A, Mazza M. Gut microbiota in women: The secret of psychological and physical well-being. *World J Gastroenterol* 2023; **29**: 5945-5952 [PMID: 38131001 DOI: 10.3748/wjg.v29.i45.5945]
7 **Buffington SA**, Di Prisco GV, Auchtung TA, Ajami NJ, Petrosino JF, Costa-Mattioli M. Microbial Reconstitution Reverses Maternal Diet-Induced Social and Synaptic Deficits in Offspring. *Cell* 2016; **165**: 1762-1775 [PMID: 27315483 DOI: 10.1016/j.cell.2016.06.001]
8 **Kim S**, Kim H, Yim YS, Ha S, Atarashi K, Tan TG, Longman RS, Honda K, Littman DR, Choi GB, Huh JR. Maternal gut bacteria promote neurodevelopmental abnormalities in mouse offspring. *Nature* 2017; **549**: 528-532 [PMID: 28902840 DOI: 10.1038/nature23910]
9 **Escherich T**. The intestinal bacteria of the neonate and breast-fed infant. 1885. *Rev Infect Dis* 1989; **11**: 352-356 [PMID: 2649968 DOI: 10.1093/clinids/11.2.352]
10 **Nyangahu DD**, Jaspan HB. Influence of maternal microbiota during pregnancy on infant immunity. *Clin Exp Immunol* 2019; **198**: 47-56 [PMID: 31121057 DOI: 10.1111/cei.13331]
11 **Bäckhed F**, Roswall J, Peng Y, Feng Q, Jia H, Kovatcheva-Datchary P, Li Y, Xia Y, Xie H, Zhong H, Khan MT, Zhang J, Li J, Xiao L, Al-Aama J, Zhang D, Lee YS, Kotowska D, Colding C, Tremaroli V, Yin Y, Bergman S, Xu X, Madsen L, Kristiansen K, Dahlgren J, Wang J. Dynamics and Stabilization of the Human Gut Microbiome during the First Year of Life. *Cell Host Microbe* 2015; **17**: 690-703 [PMID: 25974306 DOI: 10.1016/j.chom.2015.04.004]
12 **Pugh JN**, Lydon KM, O'Donovan CM, O'Sullivan O, Madigan SM. More than a gut feeling: What is the role of the gastrointestinal tract in female athlete health? *Eur J Sport Sci* 2022; **22**: 755-764 [PMID: 33944684 DOI: 10.1080/17461391.2021.1921853]
13 **Dominianni C**, Sinha R, Goedert JJ, Pei Z, Yang L, Hayes RB, Ahn J. Sex, body mass index, and dietary fiber intake influence the human gut microbiome. *PLoS One* 2015; **10**: e0124599 [PMID: 25874569 DOI: 10.1371/journal.pone.0124599]
14 **Kautzky-Willer A**, Harreiter J, Pacini G. Sex and Gender Differences in Risk, Pathophysiology and Complications of Type 2 Diabetes Mellitus. *Endocr Rev* 2016; **37**: 278-316 [PMID: 27159875 DOI: 10.1210/er.2015-1137]
15 **Friedson-Ridenour S**, Dutcher TV, Calderon C, Brown LD, Olsen CW. Gender Analysis for One Health: Theoretical Perspectives and Recommendations for Practice. *Ecohealth* 2019; **16**: 306-316 [PMID: 31016438 DOI: 10.1007/s10393-019-01410-w]
16 **Yurkovetskiy L**, Burrows M, Khan AA, Graham L, Volchkov P, Becker L, Antonopoulos D, Umesaki Y, Chervonsky AV. Gender bias in autoimmunity is influenced by microbiota. *Immunity* 2013; **39**: 400-412 [PMID: 23973225 DOI: 10.1016/j.immuni.2013.08.013]

17 **Org E**, Mehrabian M, Parks BW, Shipkova P, Liu X, Drake TA, Lusis AJ. Sex differences and hormonal effects on gut microbiota composition in mice. *Gut Microbes* 2016; **7**: 313-322 [PMID: 27355107 DOI: 10.1080/19490976.2016.1203502]

18 **Mueller S**, Saunier K, Hanisch C, Norin E, Alm L, Midtvedt T, Cresci A, Silvi S, Orpianesi C, Verdenelli MC, Clavel T, Koebnick C, Zunft HJ, Doré J, Blaut M. Differences in fecal microbiota in different European study populations in relation to age, gender, and country: a cross-sectional study. *Appl Environ Microbiol* 2006; **72**: 1027-1033 [PMID: 16461645 DOI: 10.1128/AEM.72.2.1027-1033.2006]

19 **Stapleton S**, Welch G, DiBerardo L, Freeman LR. Sex differences in a mouse model of diet-induced obesity: the role of the gut microbiome. *Biol Sex Differ* 2024; **15**: 5 [PMID: 38200579 DOI: 10.1186/s13293-023-00580-1]

20 **Lay C**, Rigottier-Gois L, Holmstrøm K, Rajilic M, Vaughan EE, de Vos WM, Collins MD, Thiel R, Namsolleck P, Blaut M, Doré J. Colonic microbiota signatures across five northern European countries. *Appl Environ Microbiol* 2005; **71**: 4153-4155 [PMID: 16000838 DOI: 10.1128/AEM.71.7.4153-4155.2005]

21 **LE TM**, Nguyen HDT, Lee OE, Lee D, Choi Y, Chong GO, Cho J, Park NJ, Han HS, Seo I. Heterogeneity of gut microbiome compositions in the third decade of life in Japanese women: insights from a comparative analysis. *Biosci Microbiota Food Health* 2024; **43**: 73-80 [PMID: 38188664 DOI: 10.12938/bmfh.2023-043]

World Journal of Gastroenterology

Submit a Manuscript: https://www.f6publishing.com

World J Gastroenterol 2024 March 14; 30(10): 1291-1294

DOI: 10.3748/wjg.v30.i10.1291

ISSN 1007-9327 (print) ISSN 2219-2840 (online)

EDITORIAL

Nomograms and prognosis for superficial esophageal squamous cell carcinoma

Hong Tao Lin, Ahmed Abdelbaki, Somashekar G Krishna

Specialty type: Gastroenterology and hepatology

Provenance and peer review: Invited article; Externally peer reviewed.

Peer-review model: Single blind

Peer-review report's scientific quality classification

Grade A (Excellent): 0
Grade B (Very good): B
Grade C (Good): 0
Grade D (Fair): 0
Grade E (Poor): 0

P-Reviewer: Song T, China

Received: January 2, 2024
Peer-review started: January 2, 2024
First decision: January 19, 2024
Revised: January 28, 2024
Accepted: February 25, 2024
Article in press: February 25, 2024
Published online: March 14, 2024

Hong Tao Lin, Ahmed Abdelbaki, Somashekar G Krishna, Department of Internal Medicine, Division of Gastroenterology, Hepatology and Nutrition, The Ohio State University Wexner Medical Center, Columbus, OH 43210, United States

Corresponding author: Somashekar G Krishna, MD, MPH, FASGE, AGAF, Professor, Department of Internal Medicine, Division of Gastroenterology, Hepatology and Nutrition, The Ohio State University Wexner Medical Center, 395 W 12th Avenue, Suite 262, Columbus, OH 43210, United States. somashekar.krishna@osumc.edu

Abstract

In recent years, endoscopic resection, particularly endoscopic submucosal dissection, has become increasingly popular in treating non-metastatic superficial esophageal squamous cell carcinoma (ESCC). In this evolving paradigm, it is crucial to identify factors that predict higher rates of lymphatic invasion and poorer outcomes. Larger tumor size, deeper invasion, poorer differentiation, more infiltrative growth patterns (INF-c), higher-grade tumor budding, positive lymphovascular invasion, and certain biomarkers have been associated with lymph node metastasis and increased morbidity through retrospective reviews, leading to the construction of comprehensive nomograms for outcome prediction. If validated by future prospective studies, these nomograms would prove highly applicable in guiding the selection of treatment for superficial ESCC.

Key Words: Esophageal cancer; Esophageal squamous cell carcinoma; Esophageal resection; Endoscopic mucosal resection; Endoscopic submucosal dissection; Lymph node metastasis

Core Tip: As endoscopic resection becomes the standard of care for non-metastatic superficial esophageal squamous cell carcinoma (ESCC), it is imperative to identify cases with a high risk of lymphatic invasion. Current retrospective studies suggest an association between lymph node metastasis in superficial ESCC and factors such as larger tumor size, deeper invasion, poorer differentiation, more infiltrative growth patterns (INF-c), higher-grade tumor budding, positive lymphovascular invasion, and specific biomarkers. Future prospective studies are required to validate these findings, isolate other prognostic factors and confounders, and establish a more robust causal relationship.

Citation: Lin HT, Abdelbaki A, Krishna SG. Nomograms and prognosis for superficial esophageal squamous cell carcinoma. *World J Gastroenterol* 2024; 30(10): 1291-1294
URL: https://www.wjgnet.com/1007-9327/full/v30/i10/1291.htm
DOI: https://dx.doi.org/10.3748/wjg.v30.i10.1291

INTRODUCTION

Esophageal cancer ranks as the ninth most prevalent cancer and the sixth leading cause of cancer-related deaths worldwide[1]. Approximately 85% of primary esophageal cancer falls within the esophageal squamous cell carcinoma (ESCC) subtype, with the remainder primarily comprising esophageal adenocarcinoma (EAC)[2]. EAC typically affects the lower third of the esophagus due to gastric reflux, while ESCC predominantly originates from the squamous cells lining the upper and middle esophagus.

The incidence of ESCC is higher in specific regions, including Eastern Asia, Iran, Africa, and South America. It is conversely rare in North America and Europe. Factors such as smoking, alcohol consumption, low socioeconomic status, exposure to polycyclic aromatic hydrocarbons (*e.g.*, from smoked foods and air pollution), and certain dietary habits (*e.g.*, betel nut, hot liquids, pickled foods, and a diet low in fruits and vegetables) are associated with increased rates of ESCC development[3,4]. While the factors above are the most identified etiologies of ESCC, other causes include TP53 gene alterations, chromosomal alterations, genetic syndromes, slow NAT2 (n-acetyltransferase 2) acetylation, and certain variants of *Helicobacter pylori* infection[5].

In general, esophageal cancers are linked to significant mortality and morbidity. The mean 5-year survival rates (combining ESCC and EAC) have been estimated to be less than 20%, with worse outcomes in patients with histories of heavy alcohol and tobacco use. Intervention through surgical resection, with or without chemoradiotherapy, modestly improves mean 5-year survival rates to 35%-40%, depending on tumor characteristics[6].

TREATMENT AND PROGNOSIS

While esophageal cancer has historically been treated with surgical esophagectomy, the use of endoscopic resection (ER) for superficial ESCC has gained popularity in recent years as it is minimally invasive and well-tolerated, while also providing tissue samples for histological analysis. Current guidelines recommend ER for select patients due to its efficacy in removing lesions within the muscularis mucosa and some lesions in the submucosa depending on invasion depth[7,8]. However, ER alone is insufficient for tumors with deeper invasion or tumors with a high risk of lymph node metastasis (LNM) or lymphovascular invasion (LVI), necessitating surgical esophagectomy and neoadjuvant chemoradiotherapy (CRT).

While both endoscopic submucosal dissection (ESD) and endoscopic mucosal resection (EMR) fall under the ER umbrella, ESD is superior to EMR, particularly for larger tumor sizes. A retrospective study by Kawashima *et al*[9] found that for tumors > 15 mm, ESD has a higher *en-bloc* resection rate (100% *vs* 64.3%, $P < 0.001$) and a lower 5-year cumulative local recurrence rate (0% *vs* 8.3%, $P < 0.01$). Despite EMR and ESD, some high-risk patients may require further treatment for complete tumor eradication.

The retrospective study titled "Risk Factors and a Predictive Nomogram for LNM in Superficial Esophageal Squamous Cell Carcinoma", by Wang *et al*[10], aims to assess prognostic factors for LNM in patients specifically diagnosed with the ESCC subtype of esophageal cancer. Investigators enrolled patients with superficial ESCC undergoing esophagectomy and lymph node dissection. They collected detailed pathological information to comprehensively analyze and identify LNM risk factors. Findings indicated that patients with positive LNM were more likely to have larger tumors, deeper invasion, poorer differentiation, more infiltrative growth patterns (INF-c), higher-grade tumor budding, and positive LVI. Multivariate regression analysis confirmed these factors as independent risk factors for LNM.

Based on these findings, a predictive nomogram incorporating tumor size, invasion depth, tumor differentiation, tumor budding, tumor infiltrative growth pattern, and LVI was developed. The nomogram exhibited good predictive performance (AUC 0.789 and 0.827 on the receiver operating characteristics curve for the training and validation sets, respectively), facilitating the assessment of LNM risk and guiding post-ESD treatment decisions.

Despite the paper's advancements, it is crucial to acknowledge the study's limitations. As this is a retrospective study, there is an increased potential for biases in case selection and the inability to collect other relevant measures (*e.g.*, LNM rates after EMR and ESD, changes in outcome with neoadjuvant CRT, *etc.*). Despite multivariate regression analysis, there is still an increased risk for confounders with retrospection as the impact of factors such as age, tumor proximity to blood

and lymphatic vessels, smoking, and alcohol use cannot be ascertained. Additionally, this study excludes cases where fewer than 12 lymph nodes were dissected. Confounders (*e.g.*, from anatomical variation or grossly visible lymphadenopathy due to metastasis) may result in a greater or fewer number of lymph nodes dissected during surgery, and these may influence which cases are selected downstream.

The aims of this study in predicting the outcome of ESCC are not unprecedented. A 2021 retrospective study on 407 ESCC patients demonstrated that a low-performance status [≥ 2 Eastern Cooperative Oncology Group Performance Status (ECOG-PS)] was significantly associated with increased early mortality. Additionally, higher rates of late mortality were associated with male sex, positive smoking history, high ECOG-PS score, high Charlson Comorbidity Index score, low psoas muscle mass index, and low prognostic nutritional index[11]. Moreover, other previous studies have developed similar nomograms for ESCC LNM[12] and evaluated factors like tumor budding and infiltrative growth patterns[13,14]. However, this investigation provides additional data from 474 ESCC patients to determine independent LNM risk factors through multivariate regression analysis, with greater statistical power and significance.

CONCLUSION

The emergent popularity of ESD and EMR provides effective tools in the management of superficial early-stage ESCC. These minimally invasive and cost-effective interventions reduce complications and recovery time compared to traditional esophagectomy. However, esophagectomy, along with lymph node dissection and CRT, may be necessary if there is deeper tissue invasion or a high likelihood of LNM or LVI. Therefore, there is significant clinical and financial value in being able to accurately predict cases where esophagectomy and the addition of CRT may be necessary. Due to the limitations associated with current retrospective studies on predicting LNM and LVI with superficial ESCC, future prospective multicenter studies are required to validate the nomogram's reliability. Prospective study designs would reduce selection bias, permit evaluation of other risk factors and confounders, and present stronger arguments for causation. It would also allow for further exploration of LNM rates with ESD as opposed to EMR, which may influence the selection of specific endoscopic techniques in certain patients and circumstances. A prospective avenue of research could explore molecular biomarkers, given their association with specific outcomes. For instance, the lack of phosphatase and tensin homolog (PTEN), a tumor suppressor, correlates with an elevated rate of locoregional LNM in ESCC at 60.5%, compared to cases with PTEN presence at 36.1%. In contrast, heightened expression of STMN1 (stathmin 1), a cytoskeleton regulator, is linked to a higher 3-year post-surgery LNM rate of 52%, as opposed to cases with low STMN1 expression at 33.8%[15]. Recent studies show potential in predicting locoregional metastasis and poorer outcomes in patients with superficial ESCC. Upon validation in future research, these findings could lead to the development of enhanced guidelines that facilitate improved identification of patients likely to benefit from ESD and EMR procedures.

FOOTNOTES

Author contributions: Lin HT, Abdelbaki A, and Krishna SG wrote the paper; all authors have read and approved the final manuscript.

Conflict-of-interest statement: None of the authors have any relevant conflicts to disclose.

Country/Territory of origin: United States

ORCID number: Hong Tao Lin 0000-0002-1888-2860; Ahmed Abdelbaki 0009-0000-8194-238X; Somashekar G Krishna 0000-0001-5748-7890.

S-Editor: Lin C
L-Editor: A
P-Editor: Zhao YQ

REFERENCES

1 **Mukkamalla SKR**, Recio-Boiles A, Babiker HM. Esophageal Cancer. 2023 Mar 7. In: StatPearls [Internet]. Treasure Island (FL): StatPearls Publishing; 2024 Jan- [PMID: 29083661]
2 **Morgan E**, Soerjomataram I, Rumgay H, Coleman HG, Thrift AP, Vignat J, Laversanne M, Ferlay J, Arnold M. The Global Landscape of Esophageal Squamous Cell Carcinoma and Esophageal Adenocarcinoma Incidence and Mortality in 2020 and Projections to 2040: New Estimates From GLOBOCAN 2020. *Gastroenterology* 2022; **163**: 649-658.e2 [PMID: 35671803 DOI: 10.1053/j.gastro.2022.05.054]
3 **Abnet CC**, Arnold M, Wei WQ. Epidemiology of Esophageal Squamous Cell Carcinoma. *Gastroenterology* 2018; **154**: 360-373 [PMID: 28823862 DOI: 10.1053/j.gastro.2017.08.023]
4 **Sheikh M**, Roshandel G, McCormack V, Malekzadeh R. Current Status and Future Prospects for Esophageal Cancer. *Cancers (Basel)* 2023; **15**

[PMID: 36765722 DOI: 10.3390/cancers15030765]

5 **Tarazi M**, Chidambaram S, Markar SR. Risk Factors of Esophageal Squamous Cell Carcinoma beyond Alcohol and Smoking. *Cancers (Basel)* 2021; **13** [PMID: 33671026 DOI: 10.3390/cancers13051009]

6 **Lundberg E**, Lagergren P, Mattsson F, Lagergren J. Life Expectancy in Survivors of Esophageal Cancer Compared with the Background Population. *Ann Surg Oncol* 2022; **29**: 2805-2811 [PMID: 35190948 DOI: 10.1245/s10434-022-11416-4]

7 **Barret M**, Prat F. Diagnosis and treatment of superficial esophageal cancer. *Ann Gastroenterol* 2018; **31**: 256-265 [PMID: 29720850 DOI: 10.20524/aog.2018.0252]

8 **Park CH**, Yang DH, Kim JW, Kim JH, Min YW, Lee SH, Bae JH, Chung H, Choi KD, Park JC, Lee H, Kwak MS, Kim B, Lee HJ, Lee HS, Choi M, Park DA, Lee JY, Byeon JS, Park CG, Cho JY, Lee ST, Chun HJ. Clinical Practice Guideline for Endoscopic Resection of Early Gastrointestinal Cancer. *Clin Endosc* 2020; **53**: 142-166 [PMID: 32252507 DOI: 10.5946/ce.2020.032]

9 **Kawashima K**, Abe S, Koga M, Nonaka S, Suzuki H, Yoshinaga S, Oda I, Hikichi T, Ohira H, Saito Y. Optimal selection of endoscopic resection in patients with esophageal squamous cell carcinoma: endoscopic mucosal resection *vs* endoscopic submucosal dissection according to lesion size. *Dis Esophagus* 2021; **34** [PMID: 32959874 DOI: 10.1093/dote/doaa096]

10 **Wang J**, Zhang X, Gan T, Rao NN, Deng K, Yang JL. Risk factors and a predictive nomogram for lymph node metastasis in superficial esophageal squamous cell carcinoma. *World J Gastroenterol* 2023; **29**: 6138-6147 [PMID: 38186680 DOI: 10.3748/wjg.v29.i47.6138]

11 **Ogata Y**, Hatta W, Koike T, Saito M, Jin X, Nakagawa K, Kanno T, Uno K, Asano N, Imatani A, Nakamura T, Nakaya N, Masamune A. Predictors of Early and Late Mortality after Endoscopic Resection for Esophageal Squamous Cell Carcinoma. *Tohoku J Exp Med* 2021; **253**: 29-39 [PMID: 33441512 DOI: 10.1620/tjem.253.29]

12 **Shen W**, Shen Y, Tan L, Jin C, Xi Y. A nomogram for predicting lymph node metastasis in surgically resected T1 esophageal squamous cell carcinoma. *J Thorac Dis* 2018; **10**: 4178-4185 [PMID: 30174862 DOI: 10.21037/jtd.2018.06.51]

13 **Li Z**, Liu L, Wang B, Ying J, He J, Xue L. Tumor budding and tumor-infiltrating lymphocytes can predict prognosis in pT1b esophageal squamous cell carcinoma. *Thorac Cancer* 2023; **14**: 2608-2617 [PMID: 37466146 DOI: 10.1111/1759-7714.15043]

14 **Zhao Y**, Xu E, Yang X, Zhang Y, Chen H, Wang Y, Jin M. Tumor infiltrative growth pattern correlates with the immune microenvironment and is an independent factor for lymph node metastasis and prognosis in stage T1 esophageal squamous cell carcinoma. *Virchows Arch* 2020; **477**: 401-408 [PMID: 32232560 DOI: 10.1007/s00428-020-02801-z]

15 **Li J**, Qi Z, Hu YP, Wang YX. Possible biomarkers for predicting lymph node metastasis of esophageal squamous cell carcinoma: a review. *J Int Med Res* 2019; **47**: 544-556 [PMID: 30616477 DOI: 10.1177/0300060518819606]

World Journal of Gastroenterology

Submit a Manuscript: https://www.f6publishing.com

World J Gastroenterol 2024 March 14; 30(10): 1295-1312

DOI: 10.3748/wjg.v30.i10.1295

ISSN 1007-9327 (print) ISSN 2219-2840 (online)

REVIEW

Overview of the immunological mechanisms in hepatitis B virus reactivation: Implications for disease progression and management strategies

Hui Ma, Qing-Zhu Yan, Jing-Ru Ma, Dong-Fu Li, Jun-Ling Yang

Specialty type: Gastroenterology and hepatology

Provenance and peer review: Unsolicited article; Externally peer reviewed.

Peer-review model: Single blind

Peer-review report's scientific quality classification

Grade A (Excellent): 0
Grade B (Very good): B
Grade C (Good): 0
Grade D (Fair): 0
Grade E (Poor): 0

P-Reviewer: Kotlyarov S, Russia

Received: November 17, 2023
Peer-review started: November 17, 2023
First decision: December 14, 2023
Revised: December 25, 2023
Accepted: January 24, 2024
Article in press: January 24, 2024
Published online: March 14, 2024

Hui Ma, Jing-Ru Ma, Department of Clinical Laboratory, The Second Hospital of Jilin University, Changchun 130000, Jilin Province, China

Qing-Zhu Yan, Department of Ultrasound Medicine, The Second Hospital of Jilin University, Changchun 130000, Jilin Province, China

Dong-Fu Li, Digestive Diseases Center, Department of Hepatopancreatobiliary Medicine, The Second Hospital of Jilin University, Changchun 130000, Jilin Province, China

Jun-Ling Yang, Department of Respiratory and Critical Care Medicine, The Second Hospital of Jilin University, Changchun 130000, Jilin Province, China

Corresponding author: Qing-Zhu Yan, MBBS, MD, Associate Professor, Department of Ultrasound Medicine, The Second Hospital of Jilin University. No. 218 Ziqiang Street, Nanguan District, Changchun 130000, Jilin Province, China. yanqingzhu@jlu.edu.cn

Abstract

Hepatitis B virus (HBV) reactivation is a clinically significant challenge in disease management. This review explores the immunological mechanisms underlying HBV reactivation, emphasizing disease progression and management. It delves into host immune responses and reactivation's delicate balance, spanning innate and adaptive immunity. Viral factors' disruption of this balance, as are interactions between viral antigens, immune cells, cytokine networks, and immune checkpoint pathways, are examined. Notably, the roles of T cells, natural killer cells, and antigen-presenting cells are discussed, highlighting their influence on disease progression. HBV reactivation's impact on disease severity, hepatic flares, liver fibrosis progression, and hepatocellular carcinoma is detailed. Management strategies, including anti-viral and immunomodulatory approaches, are critically analyzed. The role of prophylactic anti-viral therapy during immunosuppressive treatments is explored alongside novel immunotherapeutic interventions to restore immune control and prevent reactivation. In conclusion, this comprehensive review furnishes a holistic view of the immunological mechanisms that propel HBV reactivation. With a dedicated focus on understanding its implications for disease progression and the prospects of efficient management strategies, this article contributes significantly to the knowledge base. The more profound insights into the intricate interactions between viral elements and the

immune system will inform evidence-based approaches, ultimately enhancing disease management and elevating patient outcomes. The dynamic landscape of management strategies is critically scrutinized, spanning anti-viral and immunomodulatory approaches. The role of prophylactic anti-viral therapy in preventing reactivation during immunosuppressive treatments and the potential of innovative immunotherapeutic interventions to restore immune control and proactively deter reactivation.

Key Words: Hepatitis B virus reactivation; Immunological mechanisms; Disease progression; Management strategies; Immune response

Core Tip: Hepatitis B virus (HBV) reactivation poses a substantial clinical challenge, demanding a nuanced understanding of immunological mechanisms for effective management. This comprehensive review navigates the intricate landscape of HBV reactivation, spotlighting the delicate balance between host immune responses and viral factors. Emphasis is placed on the roles of T cells, natural killer cells, and antigen-presenting cells in disease progression, alongside the repercussions on severity, hepatic flares, liver fibrosis, and hepatocellular carcinoma. Critical analysis of management strategies, spanning anti-viral and immunomodulatory approaches, informs evidence-based practices. Prophylactic anti-viral therapy's role during immunosuppression and the potential of innovative immunotherapies are explored, contributing significantly to informed disease management and improved patient outcomes.

Citation: Ma H, Yan QZ, Ma JR, Li DF, Yang JL. Overview of the immunological mechanisms in hepatitis B virus reactivation: Implications for disease progression and management strategies. *World J Gastroenterol* 2024; 30(10): 1295-1312
URL: https://www.wjgnet.com/1007-9327/full/v30/i10/1295.htm
DOI: https://dx.doi.org/10.3748/wjg.v30.i10.1295

INTRODUCTION

Hepatitis B virus (HBV) infection is a significant global health challenge, affecting two billion individuals worldwide. It is a major cause of chronic liver diseases, including Cirrhosis and hepatocellular carcinoma, and 820000 individuals succumbed to diseases associated with HBV in 2019. In 2016, it was estimated that over 86 million individuals in China were afflicted with chronic HBV infection, accounting for approximately 6.1% of the total population[1]. HBV is primarily transmitted through contact with infected blood bodily fluids or from mother to child during childbirth. The infection can lead to a broad spectrum of outcomes, ranging from asymptomatic carrier states to acute hepatitis, chronic hepatitis, and even death in severe cases[2]. Chronic HBV infection poses a particularly concerning scenario, as it can lead to long-term complications such as primarily targeting the liver, leading to inflammation, liver fibrosis, cirrhosis, and an increased risk of liver cancer[3]. Developing effective prevention strategies, including vaccination and anti-viral treatments, has significantly contributed to reducing the burden of HBV infection, although challenges remain, especially in regions with high prevalence rates. While advancements in anti-viral therapies have improved outcomes for many patients, the virus can persist in a latent state within the body, posing the risk of reactivation[4,5].

HBV reactivation is characterized by the sudden reappearance or upsurge of HBV DNA in the bloodstream of individuals who had previously had inactive or resolved HBV infection. The reactivation, also known as flare or exacerbation, of hepatitis B is distinguished by a sudden increase in serum alanine aminotransferase (ALT) levels. Typically, the term "it" denotes a sudden elevation in serum ALT levels that surpasses 5-10 times the upper limit of normal or exceeds 3 times the initial baseline level. Mutations in the HBV genome, immunosuppressive therapy, and viral or drug-induced injury are common reactivation causes. The leading factor contributing to acute liver injury in individuals with chronic hepatitis B (CHB) in Eastern areas has been identified. It has been predicted that around 250 million individuals are affected by CHB[6-8]. The leading cause of HBV reactivation is an imbalance between the host's immune response and virus replication. This phenomenon is of particular concern in individuals undergoing immunosuppressive therapies, such as chemotherapy or transplantation, chronic inflammatory diseases, and those with compromised immune systems [9,10].

According to prior research, HBV reactivation after chemotherapy has been shown in multiple studies, with a median of 4 months (range, 1-9 months) separating the start of reactivation from the end of chemotherapy. In patients with chronic HBV who have positive serum hepatitis B surface antigen (HBsAg), the rate of HBV reactivation ranges from 24-88%, while in those with positive HBcAb, it ranges from 3%-22%. There is a 23%-71% mortality rate in cases of HBV reactivation[11,12]. The rate of HBV reactivation in cancer patients with a history of HBV infection following chemotherapy or immunosuppressive medication was found to be 25%, ranging from 4% to 68%. Around 65% of these individuals experienced disease progression, potentially leading to hepatic failure, necessitating either liver transplantation or death[13]. A new research study conducted in Egypt investigated the occurrence of HBV reactivation in patients who were positive for HBsAg and undergoing treatment with direct-acting anti-virals for the hepatitis C virus. The study revealed that 28.6% of the patients experienced HBV reactivation, although only 10.0% exhibited liver hepatitis

[14,15].

Therefore, understanding the immunological mechanisms underlying HBV reactivation is crucial for developing effective management strategies to mitigate its potential impact on disease progression and patient outcomes. The immune system plays a central role in controlling HBV infection and contributing to the potential for reactivation[16]. Dissecting these mechanisms provides insights into the delicate balance between viral suppression and immune responses, which, when disrupted, can lead to HBV reactivation and its associated complications. By unraveling the intricate interplay between viral factors, immune cells, and signaling pathways, researchers and clinicians understand how reactivation occurs and its implications for disease advancement[17]. Furthermore, insights into the immunological underpinnings of HBV reactivation offer opportunities to develop targeted and personalized management strategies. Leveraging this understanding, healthcare professionals can tailor therapeutic interventions to bolster the immune response and prevent reactivation in vulnerable populations[18]. This knowledge can guide the design of prophylactic anti-viral therapies for individuals undergoing immunosuppressive treatments, reducing the risk of HBV reactivation and its potential impact on liver function. Additionally, insights into immunomodulatory mechanisms can inform the exploration of novel therapeutic approaches that restore immune control over HBV, potentially leading to innovative immunotherapies[19]. Thus, comprehending the immunological intricacies of HBV reactivation not only enhances our understanding of disease progression but also empowers the medical community to devise more effective and targeted strategies for its management[20,21].

This review explores the intricate immunological mechanisms underlying HBV reactivation and its profound implications for disease progression and management. With a primary focus on immunological aspects, the review delves into the dynamic interactions between host immune responses and HBV reactivation, shedding light on the intricate processes that govern this phenomenon. By dissecting the roles of various immune cells, cytokine networks, and signaling pathways, the review seeks to elucidate the underlying mechanisms contributing to HBV reactivation, providing a foundation for understanding its impact on disease severity. Moreover, the review highlights the potential of immunomodulatory strategies and anti-viral interventions in effectively managing HBV reactivation, aiming to inform evidence-based approaches that enhance patient care and outcomes.

POSSIBLE IMMUNOLOGICAL MECHANISMS OF HBV REACTIVATION

HBV reactivation is characterized by the sudden return or increase in the concentration of HBV DNA in the serum of individuals who have previously experienced resolved or dormant chronic HBV infection. The administration of either anti-cancer drugs, immunosuppressive medicines, or biological therapy can initiate this occurrence. CD8+ T cell exhaustion resulting from the overexpression of PD-1 is observed in persistent viral infections, such as chronic hepatitis B [22,23] (Figure 1).

HBV reactivation and innate immunological response in the host

The innate immune responses serve as the initial barrier of immunological protection against viral, bacterial, and tumorous pathogens. Soluble factors such as complement components, chemokines, and cytokines constitute integral components of the innate immune system. Granulocytes, dendritic cells (DCs), macrophages, mast cells, and natural killer (NK) cells play crucial roles as effector cells in various biological processes. The initiation of an effective innate immune response typically occurs when pathogen-associated molecular pattern (PAMP) molecules interact with pattern recognition receptors (PRRs)[24,25]. This interaction triggers the production of chemokines and pro-inflammatory cytokines and the activation of innate immune cells. Consequently, this immune response eliminates viral pathogens[26]. Immune system dysfunction plays a pivotal role in HBV reactivation, with impaired host immune responses against HBV-infected cells as a central mechanism.

Interferons type I and HBV reactivation: Interferons type I (IFN-1) plays a crucial role in orchestrating the immune response during the reactivation of HBV. When viral components are recognized by PRRs such as Toll-like receptors (TLRs), retinoic acid-inducible gene I (RIG-I)-like receptors, and melanoma differentiation-associated protein 5, in liver cells known as hepatocytes and hepatic DCs, it leads to a reduced response to PAMPs and a compromised production of IFN-I, which include IFN-alpha and IFN-beta[27,28]. According to a report by Faure-Dupuy and Baumert[29], it has been found that HBV infection leads to an increase in the expression of microRNA-146a (miR-146a) in liver cells. This increase in miR-146a subsequently inhibits the expression of RIG-I-like receptors. According to Faure-Dupuy and Baumert[29], IFN-I production is suppressed.

Furthermore, Wang *et al*[30] revealed that HBsAg, hepatitis B e antigen (HBeAg), hepatitis B x, and HBV virions possess the capability to impede the synthesis of IFN-β, hence reducing mitochondrial anti-viral signaling (MAVS) and disrupt the link between MAVS and RIG-I. The study conducted by Yang *et al*[31] demonstrates that IFN-I can directly reduce HBV infection by activating IFN-stimulated genes upon binding to the IFN receptor. This activation subsequently impedes viral replication. Nevertheless, HBV can substantially impair the signal transduction triggered by IFN-I and attenuate the immunological responses facilitated by IFN-I[31].

Moreover, the work conducted by He *et al*[32] demonstrates that the regulatory effects of IFN-α on HBV covalently closed circular DNA (cccDNA) can be linked to its capacity to disrupt the methylation and succinylation of histone H3 lysine residues, which is mediated by the general control non-depressible (GCN5) enzyme. As mentioned above, the disruption finally results in eradicating HBV cccDNA. The effect of IFN-α on the regulation of HBV cccDNA can be attributed to its ability to disrupt the methylation succinylation process of histone H3 Lysine, which is facilitated by GCN5[32]. According to Wei *et al*[33], the researchers have noticed that MX dynamin-like GTPase 2 exhibits an inhibitory

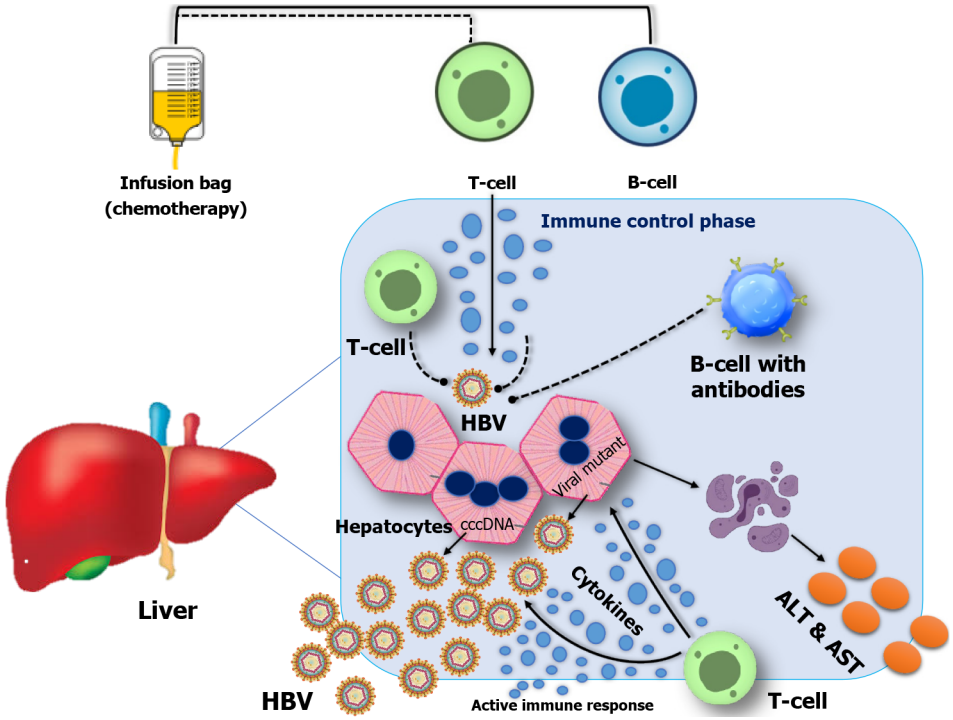

Figure 1 Reactivation mechanism of hepatitis B virus. Immune control phase: B cells produce antibodies against hepatitis B virus (HBV) and prevent the transmission of HBV infection among hepatocytes; HBV covalently closed circular DNA is persistent in hepatocytes; HBV-specific T-cells limit viral replication *via* both cytopathic effects and non-cytopathic cytokine pathways. Immunological suppression phase: HBV DNA replicates again due to treatment-induced loss of immunological control; T-cells and B-cells are suppressed or destroyed by immunosuppressive therapies. HBV mutations cause immunological escape from T cells specific to HBV, and HBV DNA replicates again. When HBV DNA actively amplifies *in vivo*, HBV reactivation takes place. T-cells, the immune system's reconstruction, and the active immunological phase target HBV-DNA and infected hepatocytes. The damaged hepatocytes release aspartate aminotransferase and alanine aminotransferase. cccDNA: Covalently closed circular DNA; HBV: Hepatitis B virus; ALT: Alanine aminotransferase; AST: Aspartate aminotransferase.

effect on converting relaxed circular DNA into cccDNA of the HBV. This inhibitory effect indirectly leads to a decrease in the quantity of cccDNA. Bratulic *et al*[34] demonstrated that IFN-α can induce the synthesis of soluble constituents that can successfully rival HBV in their affinity for heparin glycosaminoglycans, hence hindering the HBV infection process. This finally results in the augmentation of adaptive immune responses. However, chronic HBV infection can result in the impairment of IFN-I signaling. This impairment allows the virus to evade the host's immune defenses and contributes to reactivation.

DCs and HBV reactivation: DCs play a pivotal role in shaping the immune response during HBV reactivation by bridging the gap between innate and adaptive immunity[35]. Previous studies conducted by Soto *et al*[36] have shown compelling evidence suggesting that persons diagnosed with CHB demonstrate a significant reduction in the quantity of peripheral blood DCs in comparison to individuals without the condition. A decline follows the decrease in DCs' functional capacity, directly leading to the impairment of HBV-specific T-cell activity. As professional antigen-presenting cells, DCs are essential for initiating and directing immune responses upon encountering viral antigens[37,38]. During HBV reactivation, infected hepatocytes release viral antigens captured by DCs, which then migrate to secondary lymphoid tissues to present these antigens to T cells. Feola *et al*[39] revealed that DCs activate CD8+ cytotoxic T lymphocytes (CTLs) by presenting HBV-derived peptides in the context of primary histocompatibility complex class I (MHC-I) molecules. This primes CTLs to recognize and eliminate HBV-infected cells, contributing to viral control.

However, DCs can exhibit functional impairment in chronic HBV infection, including reduced antigen presentation capacity and altered cytokine production (Table 1). These deficits can hinder the activation of effective anti-viral T-cell responses, potentially leading to viral persistence and reactivation[40]. Tang *et al*[41] conducted an *in vitro* investigation wherein DCs obtained from healthy individuals were cultivated with HBV DNA. The study revealed decreased functionality of DCs when exposed to HBV DNA. However, the addition of lamivudine resulted in a reduction of HBV DNA levels and a subsequent recovery of DC function. These findings show a direct impact of HBV on the functionality of DCs[41].

Furthermore, the role of DCs in HBV reactivation extends beyond antigen presentation. DCs secrete cytokines and chemokines that modulate the immune response's direction and magnitude. For instance, DCs release interleukin-12 (IL-12) and IL-18, promoting the differentiation of T helper 1 (Th1) cells that enhance anti-viral immune responses[42,43]. However, the immunosuppressive cytokine IL-10 produced by DCs can inhibit immune activation and lead to immune tolerance, facilitating viral persistence. Additionally, DCs can interact with other immune cells, such as NK cells and regulatory T cells (Tregs), influencing their activity and contributing to the delicate balance between immune control and tolerance[44,45]. Further research is necessary to investigate the mechanisms underlying DC impairment resulting from HBV reactivation.

Table 1 Mechanisms of immune cell response in hepatitis B virus reactivation

Immune cells	Mechanism of impairment	Outcomes	Ref.
Innate immune cell responses			
Natural killer cells	Downregulation of activating receptors (NKp30, NKp46, and CD56dim), inhibitory cytokine production (IFN- and TNF-)	Reduced viral clearance, increased reactivation risk	[62, 64]
Dendritic cells	Reduced antigen presentation (CD8+ CTLs), impaired cytokine (IL-12 and IL-18) production	Impaired antiviral response, increased viral persistence	[40, 65]
Macrophages	Dysregulated cytokine secretion (IL-1β, IL-6, and TNF-α)	Altered immune balance, increased inflammation	[49]
Neutrophils	Impaired chemotaxis, reduced phagocytosis	Ineffective pathogen clearance, prolonged viremia	[55]
Adaptive immune cell responses			
CD8+ T cells	Exhaustion (CD8+ T cells), reduced cytotoxic activity	Inadequate viral control, viral persistence	[66]
CD4+ T cells	Decreased help for B and CD8+ T cells	Impaired adaptive immune response	[67]
B cells	Altered antibody production	Reduced neutralizing antibodies, prolonged viremia	[68]
Regulatory T cells	Dysfunction, reduced suppression	Dysregulated immune response, increased inflammation	[69]

IL: Interleukin; CTL: CD8+ cytotoxic T lymphocyte; TNF-α: Tumor necrosis factor-alpha; IFN: Interferons.

Reactivation of HBV in macrophages and monocytes: Macrophages and monocytes, key innate immune system components, play intricate and interrelated roles in HBV reactivation. These versatile phagocytic cells are pivotal in recognizing, engulfing, and eliminating viral particles and infected cells. Monocytes, circulating precursors of macrophages, are recruited to sites of infection, where they differentiate into tissue-resident macrophages specialized in responding to viral threats[46]. Upon encountering HBV antigens, monocytes and macrophages initiate a cascade of immune responses. Macrophages release pro-inflammatory cytokines, such as IL-1 beta (IL-1β), IL-6, and tumor necrosis factor-alpha (TNF-α), creating an inflammatory microenvironment that attracts and activates other immune cells[47,48] (Table 1). Macrophages play a significant role in antigen presentation, wherein they present viral peptides to adaptive immune cells, specifically CD4+ and CD8+ T cells, to elicit targeted immune responses[49].

Macrophages help to contain viral replication and reduce viral load by phagocytosing infected hepatocytes. Monocytes and macrophages are also involved in the phagocytosis and clearance of viral particles and infected hepatocytes, contributing to viral containment. By phagocytosing infected hepatocytes, macrophages help to contain viral replication and reduce viral load[50,51]. The dynamic interplay between macrophages and monocytes in HBV reactivation extends beyond their direct anti-viral functions. HBV has evolved strategies to modulate the polarization and activity of these immune cells. While macrophages exhibit plasticity between M1 (pro-inflammatory) and M2 (anti-inflammatory) phenotypes, chronic HBV infection may promote an immunosuppressive M2-like phenotype, which could contribute to impaired viral clearance and immune evasion[52]. Monocytes and macrophages are also key players in initiating and maintaining inflammation-induced tissue damage. Their interactions with hepatic stellate cells (HSCs) and other liver-resident cells can contribute to fibrosis, a hallmark of chronic HBV infection[53,54].

Neutrophils and HBV reactivation: Neutrophils, prominent members of the innate immune system, play a complex and multifaceted role in HBV reactivation. These rapid-response immune cells are attracted to sites of infection in response to chemotactic signals and are involved in both antimicrobial and inflammatory functions (Table 1). Neutrophils release antimicrobial proteins and reactive oxygen species, killing viral particles and infected hepatocytes[55]. However, excessive neutrophil activation can lead to tissue damage and inflammation, potentially exacerbating liver injury. Neutrophils also contribute to immune surveillance by forming neutrophil extracellular traps (NETs), web-like structures composed of DNA and antimicrobial proteins, which can capture and neutralize pathogens, including HBV[56]. For example, Maronek and Gardlik[57] explained that patients diagnosed with liver cirrhosis demonstrate a reduced capacity of neutrophils to discharge NETs. This impairment concomitates a decline in CD69 and CD80 expression.

Moreover, the study conducted by Sarkar *et al*[58] showed that antigens linked to HBV, namely HBeAg and hepatitis B core antigen (HBcAg), exhibit the ability to diminish the release of NETs through the inhibition of p38 mitogen-activated protein kinase (MAPK) and ERK activation, as well as autophagy. Utilizing this mechanism facilitates the evasion of the immune response by the HBV, therefore enhancing its reproduction and ensuring its prolonged survival[58]. The intricate balance between neutrophils' beneficial anti-viral effects and their potential to induce tissue damage underscores their role in the delicate immune response during HBV reactivation, highlighting the need for a comprehensive understanding to inform potential therapeutic strategies that harness their anti-viral potential while minimizing detrimental effects.

NK cells and HBV reactivation: Impairment of NK cells has been recognized as a significant factor in the reactivation of

HBV infection. NK cells play a crucial role in the body's defense against viral infections and tumors, primarily by identifying and eliminating infected or malignant cells. However, during HBV reactivation, the activity and function of NK cells can be compromised, leading to inadequate immune responses and allowing the virus to replicate and increase. This impairment may result from various factors, including HBV-induced changes in the expression of activating receptors on NK cells and the production of inhibitory cytokines that dampen NK cell function[59,60]. Poor prognosis and survival in individuals with liver cancer have been associated with the persistence of CHB infection and the development of hepatocellular carcinoma (HCC). As Chu *et al*[61] reported, hepatic NK cell activity is reduced, and NK cell receptors are expressed abnormally. According to the findings of Zhang *et al*[62], the levels of activating receptors such as NKp30, NKp46, and NK group 2 member D, as well as cytokines such as IFN- and TNF-, are significantly decreased in those who have been diagnosed with chronic hepatitis B (Table 1)[63-69]. These receptors include NKG2A, IL-10, T cell immunoglobulin, and mucin domain-containing protein 3 (Tim-3)[62,63].

Furthermore, in the context of CHB infection, Marotel *et al*[70] observed a correlation between the poor functionality of NK cells and the reduced expression of CD122. CD122 is the shared β chain of the IL-2 receptor found on CD56dim NK cells. You *et al*[71] explained. The precise effects of circulating antigens associated with HBV, such as Hepatitis B surface antigen (HBsAg) and HBeAg, on suppressing NK cells remain uncertain. Researchers have observed the limitation of NK cell cytotoxicity and cytokine production by HBsAg and HBeAg. This limitation occurs through interference with the activation of STAT1, nuclear factor-kappa B (NF-κB), and p38 MAPK[71]. Cao *et al*[72] showed that the reduction in STAT3 expression induced by HBsAg is associated with degranulation and cytokine production in people diagnosed with HBeAg-negative chronic hepatitis B. Monocytes treated with HBsAg can transform NK cells into regulatory NK cells that produce IL-10. This transformation is facilitated by signals from PD-L1 and MHC class I and E, and it plays a role in the persistence of chronic hepatitis B infection[72]. The study by Kar *et al*[73] revealed that exosomes derived from patients with CHB have a role in the transportation of HBV nucleic acids to NK cells. This process suppresses NK cell activity during HBV infection, achieved through inhibiting several signaling pathways, including RIG-I, NF-κB, and p38 MAPK (Figure 1).

HBV reactivation and adaptive immunological response in the host

T-lymphocytes and HBV reactivation: T-lymphocytes (T cells), central players in adaptive immunity, profoundly influence the dynamics of HBV reactivation through their multifaceted roles in viral clearance and immune regulation. HBV-infected hepatocytes are easily identifiable and eliminated by CD8+ CTLs. CTLs directly induce apoptosis in infected cells by recognizing viral peptides displayed on MHC-I molecules[74,75]. During acute HBV infection and reactivation, robust CTL responses are associated with viral control and recovery. However, chronic HBV infection can lead to T-cell exhaustion and functional impairment (Table 1), allowing the virus to persist[76]. According to Jin and Bi [66], a microarray study shows that HBV significantly increases the expression of Bcl-2-like protein 11 in HBV-specific CD8+ T cells, pointing to a critical mechanism for CD8+ T cell depletion during CHB infection. Inhibitory receptors such as PD-1, CTLA-4, CD244 (2B4), Tim-3, and lymphocyte activation gene 3 are present on exhausted HBV-specific CD8+ T cells, and these receptors closely resemble the transcriptional patterns of CD8+ T cells[66,77].

Furthermore, Tregs, a subset of CD4+ T cells, play a role in maintaining immune tolerance and preventing excessive inflammation. While their role is critical for immune homeostasis, the expansion of Tregs during chronic HBV infection can hinder effective anti-viral immune responses and contribute to viral persistence (Table 1). CD4+ T helper (Th) cells also coordinate immune responses[37,38,78]. Previous research shows that HBV-related antigens, namely HBcAg and HBsAg, can increase CD4+ T cell production of inhibitory molecules. Chuang *et al*[67] found that HBcAg enhanced PD-1 expression on CD4+ T cells, disrupting their function *via* JNK, ERK, and PI3K/AKT signaling pathways[79]. Moreover, the expression of human protein inhibitors of activated STAT1 (dependent on ERK and p38 MAPK signaling pathways) increased in CHB patients, making standard therapies ineffectual. CD4+ T cells develop into Foxp3+ Treg cells, which release inhibitory cytokines IL-10 and TGF-β, leading to a decline in HBV-specific CD8+ T cells[80]. According to Churiso *et al*[69], CD4+ T cells directly influence HBV clearance by regulating CD8+ T cells. IFN- is secreted by Th1 cells to activate macrophages and CTLs, boosting anti-viral activity. Th2 and Th17 cells may promote inflammation (Table 1), contributing to liver damage. Furthermore, the balance between different subsets of T cells shapes the immune response during HBV reactivation.

B-lymphocytes and HBV reactivation: B-lymphocytes (B cells), prominent components of the adaptive immune system, contribute to the complex immunological landscape of HBV reactivation through their roles in antibody production, immune regulation, and memory formation. Upon encountering viral antigens, B cells undergo activation, leading to the differentiation of plasma cells that secrete antibodies specific to HBV components. These antibodies, including anti-HBs and anti-HBc, can neutralize viral particles and contribute to viral clearance[81]. A prior study indicated a decrease in HBsAg-specific B cells in CHB patients. CHB patients also had deficient anti-HB production (Table 1). It was found that HBsAg-specific B cells in CHB patients had a CD21-CD27-atypical memory B cell (atMBC) phenotype with high levels of inhibitory receptors like PD-1, BTLA, and CD22[82,83]. AtMBCs in CHB patients have decreased survival, proliferation, and cytokine production and cannot develop into antibody-producing plasma cells, resulting in reduced humoral immune responses. Vanwolleghem *et al*[68] discovered that HBcAg binding to B cells leads to increased expression of inhibitory receptors FcRL4 and FcRL5, dysfunctional phenotypes, and suppressed B cell proliferation (Table 1) and activation *via* B cell receptor and TLR signaling[68,84].

Furthermore, Ma *et al*[85] revealed that B cells also play a role in immune regulation and memory formation during HBV reactivation. Regulatory B cells (Bregs) have immunosuppressive functions and can modulate immune responses to prevent excessive inflammation. Bregs produce anti-inflammatory cytokines and interact with Tregs, influencing the

balance between pro-inflammatory and anti-inflammatory immune pathways. Likewise, HBeAg can stimulate the activation of B cells by promoting the production of B-cell activating factors through the secretion of IL-6 and IFN-γ. It is indicated that IL-6, in turn, can play a role in fighting against HBV by inducing the decay of cccDNA, reducing HBV transcription, and downregulating the NTPC receptor[86].

Moreover, B cells contribute to the formation of memory responses. Lam *et al*[87] reported that memory B cells generated during acute HBV infection could provide rapid and robust antibody responses upon re-exposure to the virus, contributing to subsequent immune control. However, chronic HBV infection can lead to B cell dysfunction, impaired antibody responses, and immune tolerance.

IMPLICATIONS FOR HBV DISEASE PROGRESSION

Exacerbations in liver inflammation

The escalation of hepatic inflammation is a crucial factor that highlights the possibility of severe consequences, such as fulminant hepatitis (FH). The reactivation of HBV elicits a renewed phase of viral replication and the subsequent release of viral antigens, hence inducing an intensified immune response. The activation of the immune system leads to the migration of immune cells, including macrophages, neutrophils, and T cells, into the liver[88,89]. According to Shi *et al*[90], it was found that liver injury occurring during a spontaneous exacerbation is likely influenced by an increased population of T cells that exhibit reactivity towards HBeAg and HBcAg, which demonstrate cross-reactivity at the T-cell level. These cells then release a wide range of pro-inflammatory cytokines and chemokines. Kawagishi *et al*[91] reported study showed elevated levels of pro-inflammatory cytokines, including TNF-α, IL-1β, and IL-6.

Furthermore, Liu *et al*[93] have shown that chemokines such as CCL2 (MCP-1), CXCL8 (IL-8), and CXCL10 (IP-10) are consistently found in liver inflammation associated with HBV reactivation. These chemokines play crucial roles in attracting immune cells to the liver parenchyma. The resultant inflammatory milieu exacerbates hepatocellular damage and liver inflammation, leading to potentially severe clinical outcomes[92,93].

Moreover, the heightened liver inflammation that occurs after the reactivation of the HBV is of concern due to its correlation with FH. FH is a term used to describe the development of hepatic encephalopathy, which characterizes a severe clinical manifestation of hepatitis, including abrupt onset, rapid progression, complex clinical presentations, and unfavorable prognostic outcomes. It may cause 5%-18% of FH in Europe, 13%-15% in Bangladesh and India, and 22% in Sudan. HBV accounts for approximately 7% of United States FH cases[92]. The study by Kayesh *et al*[94] sheds light on the alarming phenomenon of FH resulting from HBV reactivation. Their research delves into the mechanisms underlying this severe condition, emphasizing the critical role of immune responses in HBV reactivation-related liver damage. Through a comprehensive analysis of clinical cases and molecular studies, Lam *et al*[87] elucidate the intricate interplay between viral factors, host immune responses, and the hepatic microenvironment, contributing to the development of FH. Their findings underscore the urgent need for vigilant monitoring and proactive management strategies in patients at risk of HBV reactivation, particularly those undergoing immunosuppressive treatments or chemotherapy[95]. The early onset of acute liver failure is attributed to the destructive effects of HBV reactivation-induced immunological responses, which are accompanied by the substantial release of inflammatory mediators. This situation can result in hepatic encephalopathy, coagulopathy, and multi-organ failure[96].

Liver fibrosis and cirrhosis

Liver fibrosis and Cirrhosis are complex clinical phenomena that the reactivation of HBV can further aggravate. The reactivation of HBV initiates a cascade of immunological reactions that facilitate the attraction and stimulation of various immune cells, such as macrophages, T cells, and neutrophils, within the milieu of the liver[49,97]. According to Lee *et al*[98], these immune cells release cytokines, chemokines, and profibrotic mediators that cause HSCs to change phenotypically into myofibroblast-like cells. The excessive synthesis and accumulation of extracellular matrix components by the activated HSCs contribute to fibrotic scarring. The chronic activation of the immune system resulting from HBV reactivation leads to the continuous presence of immune cells and the ongoing production of inflammatory mediators, which produce an environment favorable for the sustained development of fibrosis[46,47,99].

Moreover, in their study, Jagdish *et al*[100] discussed the complex immunological mechanisms and intricate feedback loops that contribute to the pathophysiological processes of liver fibrosis and Cirrhosis in the context of HBV reactivation, according to examination by Peiseler *et al*[101], immune cell activation and the subsequent release of cytokines not only promote fibrogenesis but also maintain a state of chronic inflammation. A self-sustaining cascade of inflammation and fibrosis starts due to the persistent immunological responses, which trigger the release of additional pro-inflammatory cytokines and chemokines. Furthermore, as understood by Gherlan *et al*[102], the presence of immune-suppressive components, such as Tregs, can reduce the efficiency of anti-viral immune responses and promote the growth of fibrosis by creating an immunologically tolerable environment. In people with HBV reactivation, the progression of liver fibrosis and cirrhosis is caused by a complex dynamic involving the ongoing interaction of immune activation, fibrogenesis, and immune suppression[102,103]. Comprehending the complex immunological mechanisms involved is of utmost importance to facilitate the formulation of precise therapy strategies that might effectively disrupt these processes and impede the progression of liver fibrosis and Cirrhosis in the context of HBV reactivation[104].

HCC

The pathogenesis of HCC is closely linked to the fundamental involvement of chronic inflammation in oncogenesis. Chronic HBV infection represents a significant risk factor for HCC, a liver cancer. The risk is further exacerbated by HBV

reactivation, which sustains a continuous cycle of persistent inflammation, contributing to the development of HCC. In chronic carriers with HCC receiving chemotherapy, reported rates of HBV reactivation range from 4% to 67%[105]. According to a recent study, the administration of anti-cancer therapy for HCC has been associated with HBV's reactivation. In a study by Midorikawa *et al*[106], 1609 patients who underwent hepatectomy were examined. This study revealed a significant independent association between HBV reactivation and reduced overall and recurrence-free survival. Moreover, Shiri *et al*[107] recommend delaying the planned therapy for HCC until the impaired liver function has been restored in cases of reactivation. Two prospective studies have shown that the reactivation of HCC has resulted in delayed or prematurely terminated treatment regimens.

During the process of HBV reactivation, there has been a significant rise in viral replication, leading to the release of viral antigens. This, in turn, triggers robust immunological responses. However, the continuous activation of the immune system can lead to the release of pro-inflammatory cytokines and chemokines[108]. This creates an environment that is conducive to DNA damage and the transformation of cells. According to Feitelson *et al*[109], prolonged exposure to viral antigens and persistent immune responses create an environment that promotes genetic mutations and epigenetic alterations in hepatocytes. This makes the hepatocytes more vulnerable to malignant transformation.

Furthermore, the significance of chronic inflammation in HCC linked with HBV reactivation is further emphasized by activating pivotal signaling pathways. The study conducted by Sivasudhan *et al*[110] demonstrated that the activation of the NF-κB and MAPKs signaling pathways, frequently observed in chronic inflammation cases, exert a substantial influence on the progression of HCC. The pathways mentioned above influence cell survival, proliferation, and the circumvention of apoptosis, all of which are vital facets of tumor progression. The enduring immunological responses and inflammatory mediators can promote oxidative stress and DNA damage, intensifying carcinogenic potential[111, 112]. In addition, Chekol *et al*[113] have highlighted that the inflammatory response can lead to the production of immunomodulatory substances, including Tregs and anti-inflammatory cytokines. These substances may hinder immune surveillance and promote immunological tolerance. This allows modified hepatocytes to avoid immune detection and subsequent immune response.

MANAGEMENT STRATEGIES FOR HBV REACTIVATION

Anti-viral treatment

The primary objective of existing therapeutic interventions for HBV reactivation is to inhibit viral replication and reinstate immunological regulation. Nucleoside and nucleotide analogs (NAs) are fundamental in treating HBV. The medications mentioned, namely lamivudine, entecavir, tenofovir, and adefovir, act as competitive inhibitors of HBV reverse transcriptase, thereby interfering with the synthesis of viral DNA[114]. NAs demonstrate significant anti-viral properties, resulting in the long-term inhibition of viral activity and decreased HBV DNA levels. The decrease in viral load mitigates hepatic inflammation and contributes to preventing HBV reactivation relapse. It is of utmost significance that the implementation of efficient anti-viral medication has the potential to impede the advancement of liver fibrosis and Cirrhosis, offering a pivotal means of managing individuals who are susceptible to severe liver disease resulting from HBV reactivation[115,116]. In addition to their anti-viral properties, the immunomodulatory capacities of NAs, as revealed by Zheng *et al*[25], are involved in regulating immunological reactions during the reactivation of HBV. Nucleic acid-based therapies have been observed to lower viral load, reducing viral antigen exposure effectively. Consequently, this reduction in viral antigen exposure leads to a subsequent decrease in immune activation triggered by antigens. Therefore, this mitigates the inflammation commonly associated with the reactivation of HBV[117].

Furthermore, nanoparticles (NAs) can augment the functionality of several immune cells, including NK cells, T cells, and DCs, hence facilitating the development of anti-viral immune responses. The simultaneous effect of NAs encompasses inhibiting viral replication and promoting immunological homeostasis restoration[118]. Nevertheless, it is crucial to acknowledge that although NAs exhibit significant efficacy, they generally do not result in a comprehensive eradication of the viral infection. Sustained viral suppression and relapse prevention often need the ongoing administration of these medications over an extended period[119].

Entecavir: Using Entecavir, an NA, has become a key strategy in managing HBV reactivation. The anti-viral actions of this substance are exerted through the inhibition of HBV DNA polymerase, resulting in the efficient suppression of viral replication (Table 2). Entecavir, a potent and specific inhibitor, effectively decreased the amounts of HBV DNA, resulting in enhanced liver function and reduced hepatic inflammation related to HBV reactivation[120]. This treatment option's high genetic barrier to resistance makes it an appealing selection for extended therapeutic interventions, especially in patients susceptible to recurring HBV reactivation[121]. Moreover, the anti-viral effectiveness of Entecavir has a significant role in reducing the advancement of liver fibrosis and decreasing the likelihood of consequences, including Cirrhosis and hepatocellular cancer. Nevertheless, although Entecavir has exhibited significant anti-viral efficacy, its effectiveness can vary depending on specific patient attributes, HBV genotypes, and previous treatment experiences[122, 123]. Like any therapeutic intervention, it is essential to conduct a thorough patient assessment and develop individualized treatment plans to optimize the efficacy of Entecavir in managing HBV reactivation.

Tenofovir: Tenofovir, an NA, has been identified as a fundamental intervention in managing HBV reactivation. The strong inhibitory activity of this compound on the DNA polymerase of the HBV efficiently hampers the reproduction of the virus (Table 2), resulting in a quick decrease in viral load and relief from liver inflammation associated with the infection[124]. According to Mizushima *et al*[125], the efficacy of tenofovir in individuals with HBV reactivation, regardless of their prior treatment history, can be due to its extensive anti-viral activity and strong resistance barrier. In

Table 2 Strategies for the management of hepatitis B virus reactivation

Therapy	Model	Mechanism	Efficacy	Success rate, %	Resistance	Ref.
Anti-viral therapy						
Nucleos(t)ide	Lamivudine	Inhibits viral DNA synthesis	High	80%	Low	[30]
	Entecavir	Potent viral DNA polymerase	High	90%	Rare	[120]
	Adefovir	Inhibits viral DNA polymerase	Moderate	70%-80%	Occasional	[128]
	Tenofovir	Inhibits viral DNA synthesis	High	90%	Rare	[124]
Monoclonal antibodies	Anti-HBV antibodies	Viral neutralization	Moderate	70%	Occasional	[137]
Combination therapy	Tenofovir + emtricitabine	Inhibits viral DNA synthesis	High	95%	Low	[138]
Immune-modulating therapy						
	Toll-like receptor agonists	Immune activation	Moderate	70%	Variable	[139]
	Interferon	Antiviral and immune activation	High	80%	Occasional	[140]
Personalized treatment approaches						
	Tailored	Targeted antiviral therapy based on genomic profile	Variable	75%-90%	Variable	[141]
	Treatment					
Combination therapy	Nucleos(t)ide + immune-modulating therapy	Antiviral + immunomodulation	High	90%-95%	Low	[142]
Monoclonal antibodies	Individualized treatment	Targeted viral neutralization based on antibody profiling	Varies	60%-80%	Occasional	[143]

addition, a study by Hsu *et al*[126] has shown that using tenofovir can effectively reverse liver fibrosis and cirrhosis, leading to persistent viral suppression. This highlights the importance of tenofovir in preventing the development of severe liver diseases. The availability of both oral and injectable forms of medication allows for greater flexibility in tailoring treatment to meet each patient's unique preferences and needs[126].

Nevertheless, it is crucial to consider the potential renal and bone health consequences that may arise from using tenofovir. In a study, Fu *et al*[127] proposed that tenofovir possesses strong anti-viral properties and beneficial resistance characteristics, making it an essential component in treating HBV reactivation. This highlights the significance of tailoring treatment approaches to individual patients to maximize outcomes' effectiveness.

Adefovir: The potential use of adefovir, an NA, as a therapeutic intervention for the reactivation of HBV has been investigated, particularly in situations where alternative treatment options may be impractical or insufficient. The mechanism of action involves the inhibition of HBV DNA polymerase (Table 2), resulting in decreased viral replication and subsequent reduction in viral load[128]. The anti-viral activity of adefovir has demonstrated effectiveness in suppressing HBV reactivation and enhancing liver function. Nevertheless, this treatment has been linked to an elevated susceptibility to resistance in contrast to more contemporary anti-viral medications such as entecavir and tenofovir. The aforementioned highlights the significance of meticulous patient selection, consistent monitoring, and the potential utilization of combination therapy to mitigate resistance development[129]. With more advanced anti-viral drugs emerging, adefovir's potential utility in managing HBV reactivation may be restricted to particular situations, underscoring the importance of tailored treatment strategies to get the best possible results[130].

Lamivudine: Lamivudine's early chain termination-induced HBV replication reduction was discovered in 1995. The medication successfully treated HBV reactivation in a non-Hodgkin's lymphoma patient in 1998. Lamivudine reduces HBV replication within days to weeks of starting treatment, with moderate side effects (Table 2). The conventional treatment for HBV replication is extensively used due to its efficacy, few side effects, high tolerance, and once-daily dosing. While most patients responded well to lamivudine, the treated group had mortality rates of 18% to 40%[131,132]. The study found that non-responders had decompensated liver disease before therapy. The effectiveness of Lamivudine may be diminished in severe hepatic damage. Thus, HBV reactivation, indicated by higher HBV-DNA levels, should be treated immediately. The therapy duration is unclear. Anti-viral drugs reduce reactivation rates. However, a study found a 24% reactivation rate three months after lamivudine cessation[133].

After immunosuppressive therapy, six months of treatment is advised. However, some authors recommend a year-long treatment to prevent HBV reactivation. Drug-resistant mutant strains of HBV constitute a significant concern with extended treatment. Viral resistance is the re-emergence of serum HBV DNA after viremia clearance, even with anti-viral therapy. The incidence of lamivudine-resistant strains with tyrosine-methionine-aspartate (YMDD) mutations increases

with treatment duration[134]. These symptoms usually appear after six months of treatment. The prevalence of these symptoms is 15% in the first year, 38% in the second, 56% in the third, and 65% in the fifth year of treatment. While multiple studies have shown that the YMDD mutant virus does not affect clinical outcomes, one found a greater rate of hepatitis flares and other severe adverse effects in the fifth and sixth years of treatment. Mutations that confer lamivudine resistance caused these outcomes[135,136]. The influence on chronic HBV management is apparent; however, the effects on HBV reactivation therapy are unclear (Table 2)[137-143].

Immune-modulating therapy

The potential efficacy of immune-modulating medications, such as interferon-based therapy, in managing HBV reactivation is encouraging. These therapies can enhance immune surveillance and facilitate viral clearance. Interferons are a class of cytokines that elicit anti-viral responses, augmenting the immune system's capacity to identify and counteract viral infections[140,144]. In the setting of HBV reactivation, therapies based on interferon can elicit immune responses that are both innate and adaptive. The activation of NK cells, DCs, and macrophages is observed, enhancing their ability to identify and eliminate cells infected with HBV[12,145]. In addition, interferons can augment the antigen presentation capability of DCs, promoting T-cell solid responses that specifically target infected hepatocytes. By coordinating a diverse immune response, therapies based on interferon can effectively suppress viral replication (Table 2), impede the advancement of HBV reactivation, and potentially facilitate the resolution of viral infection[146].

Recently, a growing interest has been in utilizing TLR agonists as vaccine adjuvants or immune modulators. This interest stems from their capacity to stimulate the production of IFN, pro-inflammatory cytokines, and chemokines, which can potentially elicit anti-HBV effects. In PHH, TLR1/2 and TLR3 agonists decrease HBV replication (Table 2). Another study found that oral TLR7 agonist GS-9620 (vesatolimod) and nucleos(t)ide analogs increased T cell and NK cell responses and reduced NK cell suppression of T cells in chronically infected patients[139,147].

Personalized treatment approaches

The significance of tailored treatment strategies for persons encountering HBV reactivation cannot be overemphasized, given that the efficacy of therapies can differ considerably depending on patient-specific variables. Individuals' immunological profiles are paramount in assessing and predicting treatment outcomes. Certain patients may exhibit strong immune responses that can be effectively utilized to manage the reactivation of HBV. In contrast, others may necessitate more intensive immune modulation to get the desired effects[148]. Genetic variables additionally influence treatment variability. The presence of genetic differences has the potential to impact drug metabolism, immunological responses, and the likelihood of experiencing adverse effects. As a result, it is crucial to customize treatment approaches to optimize outcomes[149,150].

Moreover, the presence of many genotypes of HBV introduces an additional level of intricacy. Various genotypes display varied levels of virulence and may demonstrate distinct responses to anti-viral or immune-based treatments. Therefore, it is imperative to include the HBV genotype when designing personalized treatment plans to maximize interventions for the individual viral strain[151].

Precision medicine and biomarker research have witnessed significant progress, presenting encouraging prospects for customizing treatment based on specific patient characteristics. Biomarkers, including viral load, liver function tests, and specific immune cell subsets, can offer valuable insights into the patient's response to therapy and facilitate informed decisions regarding treatment modifications[152]. Genetic testing can detect genetic variants that could influence the results of treatment or the metabolism of drugs, thereby facilitating the selection of the most suitable therapies[153]. Furthermore, viral genotyping might provide valuable insights in selecting appropriate anti-viral medicines and forecasting their effectiveness against certain strains of HBV. Incorporating these individualized characteristics into treatment determinations can optimize treatment results, mitigate unfavorable consequences, and increase patients' overall quality of life[110,154]. The progress of personalized medicine can significantly impact the management of HBV reactivation by introducing patient-specific treatment approaches. This advancement can substantially improve clinical outcomes and enhance treatments.

FUTURE DIRECTIONS AND RESEARCH GAPS

Despite considerable progress in elucidating the complex immunological mechanisms behind the reactivation of HBV, specific knowledge gaps hinder a thorough comprehension of its pathophysiology. A significant deficiency exists in the exact coordination of immune responses during the reactivation of HBV and its subsequent implications for the course of the disease. The involvement of immune cells, including T cells, B cells, and innate immune components, has been widely recognized. However, there is ongoing research to determine the precise sequence of events, factors that influence immunological dominance, and the interactions that occur within the intricate hepatic milieu[155]. Furthermore, there is a need for more significant investigation into the mechanisms that govern the shift from regulated viral replication to reactivation and the subsequent effects on immune responses. Examining alternative avenues is necessary to identify specific immunological checkpoints or regulatory pathways that can be altered for therapeutic benefit. Bridging these information gaps is essential in developing precise therapies that aim to avoid the reactivation of HBV and minimize its potentially severe consequences[156].

Moreover, the impact of genetic and epigenetic variables on immune responses and disease course in HBV reactivation has not been thoroughly investigated. Genetic variants among individuals may influence the characteristics and efficacy of immune responses, offering a plausible explanation for the observed variability in patient outcomes. The influence of

epigenetic changes, including DNA methylation and histone acetylation, on immune cell activity and their potential impact on the progression of HBV reactivation is a subject of interest[157]. Furthermore, the influence of comorbidities, such as obesity, diabetes, or co-infections, on immune responses during HBV reactivation has yet to be well investigated. The complete understanding of how these parameters intersect with immune systems can enhance our understanding of the illness spectrum and inform the development of customized treatment methods. The imperative to improve our comprehension of HBV reactivation and its related difficulties becomes increasingly significant as research progresses and novel technologies emerge[158,159].

Future research efforts in HBV reactivation should prioritize numerous prospective avenues to enhance our comprehension and therapeutic approaches. One potential approach involves investigating innovative immune-based treatments that use the complex interaction between immune cells and viral elements in the context of HBV reactivation. The exploration of immune checkpoint inhibitors, adoptive T-cell treatments, and customized immune cells designed to target HBV-infected hepatocytes specifically provide novel strategies for augmenting immune responses and achieving long-term viral suppression[160]. Furthermore, exploring the potential of tailored immunotherapies that leverage patient-specific immune profiles has significant opportunities for enhancing treatment outcomes. To effectively advance the development of innovative therapeutic strategies, it is imperative to conduct comprehensive studies investigating the dynamics of immune cell populations, cytokine profiles, and immunological checkpoint expression during HBV reactivation[161].

Another field of prospective investigation pertains to elucidating the complex intercommunication between the gastrointestinal tract and liver, commonly called the gut-liver axis, within the framework of HBV reactivation. Recent research indicates that increasing evidence supports the notion that the gut microbiota and their metabolic byproducts significantly impact liver immunity and inflammation. Examining the impact of the gut-liver axis on immune responses during HBV reactivation holds promise for shedding fresh light on the etiology of the illness and identifying possible targets for therapeutic intervention[162]. Moreover, gaining insight into the impact of changes in the composition and functioning of gut microbiota on the immunological dysregulation found in HBV reactivation provides opportunities for novel therapies, such as manipulating the gut microbiome to bolster anti-viral immune responses. Adopting a multidisciplinary approach can illuminate aspects of HBV reactivation that have not been thoroughly investigated before and may present innovative therapeutic approaches[163].

Likewise, it is necessary to thoroughly analyze the effects of HBV reactivation on the overall immune system. Although the liver is known to be a primary site for HBV infection and reactivation, there is a lack of comprehensive research on its impact on immune cell distribution, functioning, and memory responses throughout the body[164]. Examining the effects of HBV reactivation on the immunological landscape outside of the liver may yield valuable insights into immune aging and immune exhaustion and potentially inform the formulation of preventive measures against immunosuppression in several scenarios[165]. By incorporating state-of-the-art methodologies like single-cell RNA sequencing and advanced imaging modalities into these inquiries, it is possible to reveal novel understandings regarding the broader consequences of HBV reactivation and establish a foundation for comprehensive treatment interventions[166].

CONCLUSION

In conclusion, this in-depth review article has illuminated the complex immunological mechanisms behind HBV reactivation and their consequences for the disease and treatment approaches. The immunological components examined highlight the complexity of HBV reactivation, particularly the interaction between viral and host immune responses. These mechanisms underscore the need for close monitoring in high-risk populations by contributing to various clinical presentations, from asymptomatic instances to severe liver damage. Furthermore, understanding the immunopathogenesis of HBV reactivation points to effective treatment approaches. Anti-viral treatments that target particular immunological pathways and novel immunomodulatory drugs that may lessen the severity of reactivation and enhance patient outcomes are under development. The information compiled in this review article offers a vital basis for directing clinical practice, improving our comprehension of HBV reactivation dynamics, and encouraging the creation of more efficient management strategies in an era characterized by the development of immunotherapies.

Moreover, the consequences of this review go beyond the field of medicine. They emphasize the significance of treating HBV reactivation holistically, combining immunomodulation techniques with anti-viral treatments. Furthermore, they emphasize the necessity of continued research endeavors to unearth additional complexities in the immunological pathways underlying HBV reactivation. We will be better able to anticipate and stop reactivation occurrences due to this knowledge, which will also help us comprehend the whole picture of viral-host interactions in chronic HBV infection. Conclusively, this review's synthesis of immunological insights and their clinical implications is an essential tool for healthcare professionals, researchers, and clinicians. It will help those at risk of HBV reactivation receive better care and achieve better results.

FOOTNOTES

Author contributions: Ma H contributed to supervision, methodology, formal analysis, and writing-original draft; Yan QZ and Ma JR contributed to validation and data curation; Li DF contributed to resources and writing-review and editing; Yang JL contributed to conceptualization, writing-review, and editing; all authors approved the final submitted version of this manuscript.

Conflict-of-interest statement: The authors declare that there is no conflict of interest.

Country/Territory of origin: China

ORCID number: Qing-Zhu Yan 0009-0000-9369-9647.

S-Editor: Chen YL
L-Editor: A
P-Editor: Zhao YQ

REFERENCES

1 **Zheng P**, Dou Y, Wang Q. Immune response and treatment targets of chronic hepatitis B virus infection: innate and adaptive immunity. *Front Cell Infect Microbiol* 2023; **13**: 1206720 [PMID: 37424786 DOI: 10.3389/fcimb.2023.1206720]
2 **Aliu TB**, Majiyebo AJ, Tsado AN, Ibrahim HA, Berinyuy EB. Biology and molecular pathogenesis of hepatitis B virus infection. *Biomed Natu and App Sci* 2022; **2**: 28-36 [DOI: 10.53858/bnas02022836]
3 **Hsu YC**, Huang DQ, Nguyen MH. Global burden of hepatitis B virus: current status, missed opportunities and a call for action. *Nat Rev Gastroenterol Hepatol* 2023; **20**: 524-537 [PMID: 37024566 DOI: 10.1038/s41575-023-00760-9]
4 **Yuan C**, Peng J, Xia R, He J, Qiu T, Yao Y. Reactivation of Occult Hepatitis B Virus Infection During Long-Term Entecavir Antiviral Therapy. *Front Microbiol* 2022; **13**: 865124 [PMID: 35359734 DOI: 10.3389/fmicb.2022.865124]
5 **Bhat SA**, Hasan SK, Parray ZA, Siddiqui ZI, Ansari S, Anwer A, Khan S, Amir F, Mehmankhah M, Islam A, Minuchehr Z, Kazim SN. Potential antiviral activities of chrysin against hepatitis B virus. *Gut Pathog* 2023; **15**: 11 [PMID: 36895013 DOI: 10.1186/s13099-023-00531-6]
6 **de Almeida Pondé RA**. Detection of the serological markers hepatitis B virus surface antigen (HBsAg) and hepatitis B core IgM antibody (anti-HBcIgM) in the diagnosis of acute hepatitis B virus infection after recent exposure. *Microbiol Immunol* 2022; **66**: 1-9 [PMID: 34528725 DOI: 10.1111/1348-0421.12943]
7 **Rosenberg M**, Poluch M, Thomas C, Sindaco P, Khoo A, Porcu P. Hepatitis B Virus and B-cell lymphoma: evidence, unmet need, clinical impact, and opportunities. *Front Oncol* 2023; **13**: 1275800 [PMID: 37927464 DOI: 10.3389/fonc.2023.1275800]
8 **Benjamin I**, Louis H, Udoikono AD, Agwamba EC, Unimuke TO, Ahuekwe EF. Hydrazineylidene-3-oxopropanal derivatives as antiviral agents for treatment of HBV and HCV: experimental, DFT, and molecular docking studies. *Vietnam J Chem* 2023; **61**: 109-125 [DOI: 10.1002/vjch.202200063]
9 **Chang Y**, Jeong SW, Jang JY. Hepatitis B Virus Reactivation Associated With Therapeutic Interventions. *Front Med (Lausanne)* 2021; **8**: 770124 [PMID: 35096867 DOI: 10.3389/fmed.2021.770124]
10 **Mak JWY**, Law AWH, Law KWT, Ho R, Cheung CKM, Law MF. Prevention and management of hepatitis B virus reactivation in patients with hematological malignancies in the targeted therapy era. *World J Gastroenterol* 2023; **29**: 4942-4961 [PMID: 37731995 DOI: 10.3748/wjg.v29.i33.4942]
11 **Papatheodoridis GV**, Lekakis V, Voulgaris T, Lampertico P, Berg T, Chan HLY, Kao JH, Terrault N, Lok AS, Reddy KR. Hepatitis B virus reactivation associated with new classes of immunosuppressants and immunomodulators: A systematic review, meta-analysis, and expert opinion. *J Hepatol* 2022; **77**: 1670-1689 [PMID: 35850281 DOI: 10.1016/j.jhep.2022.07.003]
12 **Dusheiko G**, Agarwal K, Maini MK. New Approaches to Chronic Hepatitis B. *N Engl J Med* 2023; **388**: 55-69 [PMID: 36599063 DOI: 10.1056/NEJMra2211764]
13 **Zhu Y**, Li H, Wang X, Zheng X, Huang Y, Chen J, Meng Z, Gao Y, Qian Z, Liu F, Lu X, Shi Y, Shang J, Yan H, Zheng Y, Qiao L, Zhang Y, Xiang X, Dan Y, Sun S, Hou Y, Zhang Q, Xiong Y, Li S, Huang Z, Li B, Jiang X, Luo S, Chen Y, Gao N, Liu C, Ji L, Yuan W, Li J, Li T, Zheng R, Zhou X, Ren H, Zhou Y, Xu B, Yu R, Tan W, Deng G. Hepatitis B Virus Reactivation Increased the Risk of Developing Hepatic Failure and Mortality in Cirrhosis With Acute Exacerbation. *Front Microbiol* 2022; **13**: 910549 [PMID: 35875559 DOI: 10.3389/fmicb.2022.910549]
14 **Hassnine AA**, Saber MA, Fouad YM, Sarhan H, Elsayed MM, Zaki ZM, Abdelraheem EM, Abdelhalim SM, Elsayed AM. Clinical study on the efficacy of hepatitis B vaccination in hepatitis C virus related chronic liver diseases in Egypt. *Virus Res* 2023; **323**: 198953 [PMID: 36209916 DOI: 10.1016/j.virusres.2022.198953]
15 **Zhou MJ**, Zhang C, Fu YJ, Wang H, Ji Y, Huang X, Li L, Wang Y, Qing S, Shi Y, Shen L, Wang YY, Li XY, Li YY, Chen SY, Zhen C, Xu R, Shi M, Wang FS, Cheng Y. Cured HCV patients with suboptimal hepatitis B vaccine response exhibit high self-reactive immune signatures. *Hepatol Commun* 2023; **7** [PMID: 37378628 DOI: 10.1097/HC9.0000000000000197]
16 **Liu C**, Shih YF, Liu CJ. Immunopathogenesis of Acute Flare of Chronic Hepatitis B: With Emphasis on the Role of Cytokines and Chemokines. *Int J Mol Sci* 2022; **23** [PMID: 35163330 DOI: 10.3390/ijms23031407]
17 **Cacoub P**, Asselah T. Hepatitis B Virus Infection and Extra-Hepatic Manifestations: A Systemic Disease. *Am J Gastroenterol* 2022; **117**: 253-263 [PMID: 34913875 DOI: 10.14309/ajg.0000000000001575]
18 **Scott D**, Singer DS. Harnessing the Power of Discovery. *Cancer Discov* 2023; **13**: 819-823 [PMID: 36884310 DOI: 10.1158/2159-8290.CD-23-0231]
19 **Kim SW**, Yoon JS, Lee M, Cho Y. Toward a complete cure for chronic hepatitis B: Novel therapeutic targets for hepatitis B virus. *Clin Mol Hepatol* 2022; **28**: 17-30 [PMID: 34281294 DOI: 10.3350/cmh.2021.0093]
20 **Gramantieri L**, Fornari F, Giovannini C, Trerè D. MicroRNAs at the Crossroad between Immunoediting and Oncogenic Drivers in

Hepatocellular Carcinoma. *Biomolecules* 2022; **12** [PMID: 35883486 DOI: 10.3390/biom12070930]

21 **Su Y**, Lu Y, An H, Liu J, Ye F, Shen J, Ni Z, Huang B, Lin J. MicroRNA-204-5p Inhibits Hepatocellular Carcinoma by Targeting the Regulator of G Protein Signaling 20. *ACS Pharmacol Transl Sci* 2023; **6**: 1817-1828 [PMID: 38093845 DOI: 10.1021/acsptsci.3c00114]

22 **Muto S**, Matsubara T, Inoue T, Kitamura H, Yamamoto K, Ishii T, Yazawa M, Yamamoto R, Okada N, Mori K, Yamada H, Kuwabara T, Yonezawa A, Fujimaru T, Kawano H, Yokoi H, Doi K, Hoshino J, Yanagita M. Chapter 1: Evaluation of kidney function in patients undergoing anticancer drug therapy, from clinical practice guidelines for the management of kidney injury during anticancer drug therapy 2022. *Int J Clin Oncol* 2023; **28**: 1259-1297 [PMID: 37382749 DOI: 10.1007/s10147-023-02372-4]

23 **Ando Y**, Nishiyama H, Shimodaira H, Takano N, Sakaida E, Matsumoto K, Nakanishi K, Sakai H, Tsukamoto S, Komine K, Yasuda Y, Kato T, Fujiwara Y, Koyama T, Kitamura H, Kuwabara T, Yonezawa A, Okumura Y, Yakushijin K, Nozawa K, Goto H, Matsubara T, Hoshino J, Yanagita M; Committee of Clinical Practice Guidelines for the Management of Kidney Disease During Anticancer Drug Therapy 2022. Chapter 3: Management of kidney injury caused by cancer drug therapy, from clinical practice guidelines for the management of kidney injury during anticancer drug therapy 2022. *Int J Clin Oncol* 2023; **28**: 1315-1332 [PMID: 37453935 DOI: 10.1007/s10147-023-02382-2]

24 **Zhao HJ**, Hu YF, Han QJ, Zhang J. Innate and adaptive immune escape mechanisms of hepatitis B virus. *World J Gastroenterol* 2022; **28**: 881-896 [PMID: 35317051 DOI: 10.3748/wjg.v28.i9.881]

25 **Zheng JR**, Wang ZL, Feng B. Hepatitis B functional cure and immune response. *Front Immunol* 2022; **13**: 1075916 [PMID: 36466821 DOI: 10.3389/fimmu.2022.1075916]

26 **Santos Apolonio J**, Lima de Souza Gonçalves V, Cordeiro Santos ML, Silva Luz M, Silva Souza JV, Rocha Pinheiro SL, de Souza WR, Sande Loureiro M, de Melo FF. Oncolytic virus therapy in cancer: A current review. *World J Virol* 2021; **10**: 229-255 [PMID: 34631474 DOI: 10.5501/wjv.v10.i5.229]

27 **Maqsood Q**, Sumrin A, Iqbal M, Younas S, Hussain N, Mahnoor M, Wajid A. Hepatitis C virus/Hepatitis B virus coinfection: Current prospectives. *Antivir Ther* 2023; **28**: 13596535231189643 [PMID: 37489502 DOI: 10.1177/13596535231189643]

28 **Medina C**, García AH, Crespo FI, Toro FI, Mayora SJ, De Sanctis JB. A Synopsis of Hepatitis C Virus Treatments and Future Perspectives. *Curr Issues Mol Biol* 2023; **45**: 8255-8276 [PMID: 37886964 DOI: 10.3390/cimb45100521]

29 **Faure-Dupuy S**, Baumert TF. Targeting immuno-metabolism and anti-viral immune responses in chronic hepatitis B. *Hepatol Int* 2023; **17**: 1075-1078 [PMID: 37369910 DOI: 10.1007/s12072-023-10546-5]

30 **Wang L**, Sun Y, Song X, Wang Z, Zhang Y, Zhao Y, Peng X, Zhang X, Li C, Gao C, Li N, Gao L, Liang X, Wu Z, Ma C. Hepatitis B virus evades immune recognition *via* RNA adenosine deaminase ADAR1-mediated viral RNA editing in hepatocytes. *Cell Mol Immunol* 2021; **18**: 1871-1882 [PMID: 34253859 DOI: 10.1038/s41423-021-00729-1]

31 **Yang Z**, Sun B, Xiang J, Wu H, Kan S, Hao M, Chang L, Liu H, Wang D, Liu W. Role of epigenetic modification in interferon treatment of hepatitis B virus infection. *Front Immunol* 2022; **13**: 1018053 [PMID: 36325353 DOI: 10.3389/fimmu.2022.1018053]

32 **He P**, Zhang P, Fang Y, Han N, Yang W, Xia Z, Zhu Y, Zhang Z, Shen J. The role of HBV cccDNA in occult hepatitis B virus infection. *Mol Cell Biochem* 2023; **478**: 2297-2307 [PMID: 36735210 DOI: 10.1007/s11010-023-04660-z]

33 **Wei L**, Cafiero TR, Tseng A, Gertje HP, Berneshawi A, Crossland NA, Ploss A. Conversion of hepatitis B virus relaxed circular to covalently closed circular DNA is supported in murine cells. *JHEP Rep* 2022; **4**: 100534 [PMID: 36035363 DOI: 10.1016/j.jhepr.2022.100534]

34 **Bratulic S**, Limeta A, Dabestani S, Birgisson H, Enblad G, Stålberg K, Hesselager G, Häggman M, Höglund M, Simonson OE, Stålberg P, Lindman H, Bång-Rudenstam A, Ekstrand M, Kumar G, Cavarretta I, Alfano M, Pellegrino F, Mandel-Clausen T, Salanti A, Maccari F, Galeotti F, Volpi N, Daugaard M, Belting M, Lundstam S, Stierner U, Nyman J, Bergman B, Edqvist PH, Levin M, Salonia A, Kjölhede H, Jonasch E, Nielsen J, Gatto F. Noninvasive detection of any-stage cancer using free glycosaminoglycans. *Proc Natl Acad Sci U S A* 2022; **119**: e2115328119 [PMID: 36469776 DOI: 10.1073/pnas.2115328119]

35 **Klein J**, Wood J, Jaycox JR, Dhodapkar RM, Lu P, Gehlhausen JR, Tabachnikova A, Greene K, Tabacof L, Malik AA, Silva Monteiro V, Silva J, Kamath K, Zhang M, Dhal A, Ott IM, Valle G, Peña-Hernández M, Mao T, Bhattacharjee B, Takahashi T, Lucas C, Song E, McCarthy D, Breyman E, Tosto-Mancuso J, Dai Y, Perotti E, Akduman K, Tzeng TJ, Xu L, Geraghty AC, Monje M, Yildirim I, Shon J, Medzhitov R, Lutchmansingh D, Possick JD, Kaminski N, Omer SB, Krumholz HM, Guan L, Dela Cruz CS, van Dijk D, Ring AM, Putrino D, Iwasaki A. Distinguishing features of long COVID identified through immune profiling. *Nature* 2023; **623**: 139-148 [PMID: 37748514 DOI: 10.1038/s41586-023-06651-y]

36 **Soto JA**, Gálvez NMS, Andrade CA, Pacheco GA, Bohmwald K, Berrios RV, Bueno SM, Kalergis AM. The Role of Dendritic Cells During Infections Caused by Highly Prevalent Viruses. *Front Immunol* 2020; **11**: 1513 [PMID: 32765522 DOI: 10.3389/fimmu.2020.01513]

37 **Fisicaro P**, Barili V, Rossi M, Montali I, Vecchi A, Acerbi G, Laccabue D, Zecca A, Penna A, Missale G, Ferrari C, Boni C. Pathogenetic Mechanisms of T Cell Dysfunction in Chronic HBV Infection and Related Therapeutic Approaches. *Front Immunol* 2020; **11**: 849 [PMID: 32477347 DOI: 10.3389/fimmu.2020.00849]

38 **Iannacone M**, Guidotti LG. Immunobiology and pathogenesis of hepatitis B virus infection. *Nat Rev Immunol* 2022; **22**: 19-32 [PMID: 34002067 DOI: 10.1038/s41577-021-00549-4]

39 **Feola S**, Chiaro J, Cerullo V. Integrating immunopeptidome analysis for the design and development of cancer vaccines. *Semin Immunol* 2023; **67**: 101750 [PMID: 37003057 DOI: 10.1016/j.smim.2023.101750]

40 **De Pasquale C**, Campana S, Barberi C, Sidoti Migliore G, Oliveri D, Lanza M, Musolino C, Raimondo G, Ferrone S, Pollicino T, Ferlazzo G. Human Hepatitis B Virus Negatively Impacts the Protective Immune Crosstalk Between Natural Killer and Dendritic Cells. *Hepatology* 2021; **74**: 550-565 [PMID: 33482027 DOI: 10.1002/hep.31725]

41 **Tang L**, Kottilil S, Wilson E. Strategies to eliminate HBV infection: an update. *Futr Virol* 2020; **15**: 35-51 [DOI: 10.2217/fvl-2019-0133]

42 **Ciardi MR**, Iannetta M, Zingaropoli MA, Salpini R, Aragri M, Annecca R, Pontecorvo S, Altieri M, Russo G, Svicher V, Mastroianni CM, Vullo V. Reactivation of Hepatitis B Virus With Immune-Escape Mutations After Ocrelizumab Treatment for Multiple Sclerosis. *Open Forum Infect Dis* 2019; **6**: ofy356 [PMID: 30697576 DOI: 10.1093/ofid/ofy356]

43 **Korsukewitz C**, Reddel SW, Bar-Or A, Wiendl H. Neurological immunotherapy in the era of COVID-19 - looking for consensus in the literature. *Nat Rev Neurol* 2020; **16**: 493-505 [PMID: 32641860 DOI: 10.1038/s41582-020-0385-8]

44 **Yaseen MM**, Abuharfeil NM, Darmani H, Daoud A. Mechanisms of immune suppression by myeloid-derived suppressor cells: the role of interleukin-10 as a key immunoregulatory cytokine. *Open Biol* 2020; **10**: 200111 [PMID: 32931721 DOI: 10.1098/rsob.200111]

45 **Ding L**, Wang N, Wang Q, Fan X, Xin Y, Wang S. Midkine inhibition enhances anti-PD-1 immunotherapy in sorafenib-treated hepatocellular carcinoma *via* preventing immunosuppressive MDSCs infiltration. *Cell Death Discov* 2023; **9**: 92 [PMID: 36906597 DOI: 10.1038/s41420-023-01392-3]

46 **Khanam A**, Chua JV, Kottilil S. Immunopathology of Chronic Hepatitis B Infection: Role of Innate and Adaptive Immune Response in Disease Progression. *Int J Mol Sci* 2021; **22** [PMID: 34071064 DOI: 10.3390/ijms22115497]

47 **Raje N**, Anderson K, Einsele H, Efebera Y, Gay F, Hammond SP, Lesokhin AM, Lonial S, Ludwig H, Moreau P, Patel K, Ramasamy K, Mateos MV. Monitoring, prophylaxis, and treatment of infections in patients with MM receiving bispecific antibody therapy: consensus recommendations from an expert panel. *Blood Cancer J* 2023; **13**: 116 [PMID: 37528088 DOI: 10.1038/s41408-023-00879-7]

48 **Jiang P**, Jia H, Qian X, Tang T, Han Y, Zhang Z, Jiang L, Yu Z, Zheng L, Yu G, Cai H, Zhang S, Zhang X, Gu J, Ye C, Yang L, Lu Y, Liu H, Lu X, Jin C, Ren Y, Lu M, Xu L, Yu J, Jin X, Yang Y, Qian P. Single-cell RNA sequencing reveals the immunoregulatory roles of PegIFN-α in patients with chronic hepatitis B. *Hepatology* 2024; **79**: 167-182 [PMID: 37368993 DOI: 10.1097/HEP.0000000000000524]

49 **Binatti E**, Gerussi A, Barisani D, Invernizzi P. The Role of Macrophages in Liver Fibrosis: New Therapeutic Opportunities. *Int J Mol Sci* 2022; **23** [PMID: 35743092 DOI: 10.3390/ijms23126649]

50 **Tsounis EP**, Tourkochristou E, Mouzaki A, Triantos C. Toward a new era of hepatitis B virus therapeutics: The pursuit of a functional cure. *World J Gastroenterol* 2021; **27**: 2727-2757 [PMID: 34135551 DOI: 10.3748/wjg.v27.i21.2727]

51 **Bassit L**, Amblard F, Patel D, Biteau N, Chen Z, Kasthuri M, Zhou S, Schinazi RF. The premise of capsid assembly modulators towards eliminating HBV persistence. *Expert Opin Drug Discov* 2023; **18**: 1031-1041 [PMID: 37477111 DOI: 10.1080/17460441.2023.2239701]

52 **Bao Z**, Chen X, Li Y, Jiang W, Pan D, Ma L, Wu Y, Chen Y, Chen C, Wang L, Zhao S, Wang T, Lu WY, Ma C, Wang S. The hepatic GABAergic system promotes liver macrophage M2 polarization and mediates HBV replication in mice. *Antiviral Res* 2023; **217**: 105680 [PMID: 37494980 DOI: 10.1016/j.antiviral.2023.105680]

53 **Koda Y**, Teratani T, Chu PS, Hagihara Y, Mikami Y, Harada Y, Tsujikawa H, Miyamoto K, Suzuki T, Taniki N, Sujino T, Sakamoto M, Kanai T, Nakamoto N. CD8(+) tissue-resident memory T cells promote liver fibrosis resolution by inducing apoptosis of hepatic stellate cells. *Nat Commun* 2021; **12**: 4474 [PMID: 34294714 DOI: 10.1038/s41467-021-24734-0]

54 **Hammerich L**, Tacke F. Hepatic inflammatory responses in liver fibrosis. *Nat Rev Gastroenterol Hepatol* 2023; **20**: 633-646 [PMID: 37400694 DOI: 10.1038/s41575-023-00807-x]

55 **Liu K**, Wang FS, Xu R. Neutrophils in liver diseases: pathogenesis and therapeutic targets. *Cell Mol Immunol* 2021; **18**: 38-44 [PMID: 33159158 DOI: 10.1038/s41423-020-00560-0]

56 **Sadeghi M**, Dehnavi S, Jamialahmadi T, Johnston TP, Sahebkar A. Neutrophil extracellular trap: A key player in the pathogenesis of autoimmune diseases. *Int Immunopharmacol* 2023; **116**: 109843 [PMID: 36764274 DOI: 10.1016/j.intimp.2023.109843]

57 **Maronek M**, Gardlik R. The Citrullination-Neutrophil Extracellular Trap Axis in Chronic Diseases. *J Innate Immun* 2022; **14**: 393-417 [PMID: 35263752 DOI: 10.1159/000522331]

58 **Sarkar T**, Sharma K, Ramakrishnan A. A comprehensive review of factors that enhance the readiness level of the immune system and also those that impair immunity. 2022. [cited 22 December 2023]. Available from: https://www.researchgate.net/publication/361424318_A_comprehensive_review_of_factors_that_enhance_the_readiness_level_of_the_immune_system_and_also_those_that_impair_immunity

59 **Björkström NK**, Strunz B, Ljunggren HG. Natural killer cells in antiviral immunity. *Nat Rev Immunol* 2022; **22**: 112-123 [PMID: 34117484 DOI: 10.1038/s41577-021-00558-3]

60 **Li H**, Huang QZ, Zhang H, Liu ZX, Chen XH, Ye LL, Luo Y. The land-scape of immune response to monkeypox virus. *EBioMedicine* 2023; **87**: 104424 [PMID: 36584594 DOI: 10.1016/j.ebiom.2022.104424]

61 **Chu J**, Gao F, Yan M, Zhao S, Yan Z, Shi B, Liu Y. Natural killer cells: a promising immunotherapy for cancer. *J Transl Med* 2022; **20**: 240 [PMID: 35606854 DOI: 10.1186/s12967-022-03437-0]

62 **Zhang C**, Wang XM, Li SR, Twelkmeyer T, Wang WH, Zhang SY, Wang SF, Chen JZ, Jin X, Wu YZ, Chen XW, Wang SD, Niu JQ, Chen HR, Tang H. NKG2A is a NK cell exhaustion checkpoint for HCV persistence. *Nat Commun* 2019; **10**: 1507 [PMID: 30944315 DOI: 10.1038/s41467-019-09212-y]

63 **Gong L**, Kwong DL, Dai W, Wu P, Li S, Yan Q, Zhang Y, Zhang B, Fang X, Liu L, Luo M, Liu B, Chow LK, Chen Q, Huang J, Lee VH, Lam KO, Lo AW, Chen Z, Wang Y, Lee AW, Guan XY. Comprehensive single-cell sequencing reveals the stromal dynamics and tumor-specific characteristics in the microenvironment of nasopharyngeal carcinoma. *Nat Commun* 2021; **12**: 1540 [PMID: 33750785 DOI: 10.1038/s41467-021-21795-z]

64 **Lee J**, Park SS, Kim TY, Lee DG, Kim DW. Lymphopenia as a Biological Predictor of Outcomes in COVID-19 Patients: A Nationwide Cohort Study. *Cancers (Basel)* 2021; **13** [PMID: 33530509 DOI: 10.3390/cancers13030471]

65 **Li M**, Gao Y, Yang L, Lin Y, Deng W, Jiang T, Bi X, Lu Y, Zhang L, Shen G, Liu R, Wu S, Chang M, Xu M, Hu L, Song R, Jiang Y, Yi W, Xie Y. Dynamic changes of cytokine profiles and virological markers during 48 weeks of entecavir treatment for HBeAg-positive chronic hepatitis B. *Front Immunol* 2022; **13**: 1024333 [PMID: 36203581 DOI: 10.3389/fimmu.2022.1024333]

66 **Jin X**, Bi J. Prospects for NK-based immunotherapy of chronic HBV infection. *Front Immunol* 2022; **13**: 1084109 [PMID: 36591230 DOI: 10.3389/fimmu.2022.1084109]

67 **Chuang YC**, Tsai KN, Ou JJ. Pathogenicity and virulence of Hepatitis B virus. *Virulence* 2022; **13**: 258-296 [PMID: 35100095 DOI: 10.1080/21505594.2022.2028483]

68 **Vanwolleghem T**, Adomati T, Van Hees S, Janssen HLA. Humoral immunity in hepatitis B virus infection: Rehabilitating the B in HBV. *JHEP Rep* 2022; **4**: 100398 [PMID: 35059620 DOI: 10.1016/j.jhepr.2021.100398]

69 **Churiso G**, Husen G, Bulbula D, Abebe L. Immunity Cell Responses to RSV and the Role of Antiviral Inhibitors: A Systematic Review. *Infect Drug Resist* 2022; **15**: 7413-7430 [PMID: 36540102 DOI: 10.2147/IDR.S387479]

70 **Marotel M**, Villard M, Drouillard A, Tout I, Besson L, Allatif O, Pujol M, Rocca Y, Ainouze M, Roblot G, Viel S, Gomez M, Loustaud V, Alain S, Durantel D, Walzer T, Hasan U, Marçais A. Peripheral natural killer cells in chronic hepatitis B patients display multiple molecular features of T cell exhaustion. *Elife* 2021; **10** [PMID: 33507150 DOI: 10.7554/eLife.60095]

71 **You H**, Qin S, Zhang F, Hu W, Li X, Liu D, Kong F, Pan X, Zheng K, Tang R. Regulation of Pattern-Recognition Receptor Signaling by HBX During Hepatitis B Virus Infection. *Front Immunol* 2022; **13**: 829923 [PMID: 35251017 DOI: 10.3389/fimmu.2022.829923]

72 **Cao W**, Lu H, Zhang L, Wang S, Deng W, Jiang T, Lin Y, Yang L, Bi X, Lu Y, Shen G, Liu R, Chang M, Wu S, Gao Y, Hao H, Xu M, Chen X, Hu L, Xie Y, Li M. Functional molecular expression of nature killer cells correlated to HBsAg clearance in HBeAg-positive chronic hepatitis B patients during PEG-IFN α-2a therapy. *Front Immunol* 2022; **13**: 1067362 [PMID: 36479104 DOI: 10.3389/fimmu.2022.1067362]

73 **Kar A**, Samanta A, Mukherjee S, Barik S, Biswas A. The HBV web: An insight into molecular interactomes between the hepatitis B virus and its host en route to hepatocellular carcinoma. *J Med Virol* 2023; **95**: e28436 [PMID: 36573429 DOI: 10.1002/jmv.28436]

74 **Ganesan M**, Mathews S, Makarov E, Petrosyan A, Kharbanda KK, Kidambi S, Poluektova LY, Casey CA, Osna NA. Acetaldehyde suppresses

HBV-MHC class I complex presentation on hepatocytes *via* induction of ER stress and Golgi fragmentation. *Am J Physiol Gastrointest Liver Physiol* 2020; **319**: G432-G442 [PMID: 32755306 DOI: 10.1152/ajpgi.00109.2020]

75 **Bybee G**, Moeun Y, Wang W, Kharbanda KK, Poluektova LY, Kidambi S, Osna NA, Ganesan M. Increased liver stiffness promotes hepatitis B progression by impairing innate immunity in CCl4-induced fibrotic HBV(+) transgenic mice. *Front Immunol* 2023; **14**: 1166171 [PMID: 37600826 DOI: 10.3389/fimmu.2023.1166171]

76 **McLane LM**, Abdel-Hakeem MS, Wherry EJ. CD8 T Cell Exhaustion During Chronic Viral Infection and Cancer. *Annu Rev Immunol* 2019; **37**: 457-495 [PMID: 30676822 DOI: 10.1146/annurev-immunol-041015-055318]

77 **Zhang YX**, Ou MY, Yang ZH, Sun Y, Li QF, Zhou SB. Adipose tissue aging is regulated by an altered immune system. *Front Immunol* 2023; **14**: 1125395 [PMID: 36875140 DOI: 10.3389/fimmu.2023.1125395]

78 **Kramvis A**, Chang KM, Dandri M, Farci P, Glebe D, Hu J, Janssen HLA, Lau DTY, Penicaud C, Pollicino T, Testoni B, Van Bömmel F, Andrisani O, Beumont-Mauviel M, Block TM, Chan HLY, Cloherty GA, Delaney WE, Geretti AM, Gehring A, Jackson K, Lenz O, Maini MK, Miller V, Protzer U, Yang JC, Yuen MF, Zoulim F, Revill PA. A roadmap for serum biomarkers for hepatitis B virus: current status and future outlook. *Nat Rev Gastroenterol Hepatol* 2022; **19**: 727-745 [PMID: 35859026 DOI: 10.1038/s41575-022-00649-z]

79 **Prange R**. Hepatitis B virus movement through the hepatocyte: An update. *Biol Cell* 2022; **114**: 325-348 [PMID: 35984727 DOI: 10.1111/boc.202200060]

80 **Wan Z**, Zhou Z, Liu Y, Lai Y, Luo Y, Peng X, Zou W. Regulatory T cells and T helper 17 cells in viral infection. *Scand J Immunol* 2020; **91**: e12873 [PMID: 32090360 DOI: 10.1111/sji.12873]

81 **Mancuso S**, Mattana M, Carlisi M, Santoro M, Siragusa S. Effects of B-Cell Lymphoma on the Immune System and Immune Recovery after Treatment: The Paradigm of Targeted Therapy. *Int J Mol Sci* 2022; **23** [PMID: 35328789 DOI: 10.3390/ijms23063368]

82 **Wu W**, Sun S, Wang Y, Zhao R, Ren H, Li Z, Zhao H, Zhang Y, Sheng J, Chen Z, Shi Y. Circulating Neutrophil Dysfunction in HBV-Related Acute-on-Chronic Liver Failure. *Front Immunol* 2021; **12**: 620365 [PMID: 33717119 DOI: 10.3389/fimmu.2021.620365]

83 **You H**, Zhang N, Yu T, Ma L, Li Q, Wang X, Yuan D, Kong D, Liu X, Hu W, Liu D, Kong F, Zheng K, Tang R. Hepatitis B virus X protein promotes MAN1B1 expression by enhancing stability of GRP78 *via* TRIM25 to facilitate hepatocarcinogenesis. *Br J Cancer* 2023; **128**: 992-1004 [PMID: 36635499 DOI: 10.1038/s41416-022-02115-8]

84 **Suresh M**, Menne S. Recent Drug Development in the Woodchuck Model of Chronic Hepatitis B. *Viruses* 2022; **14** [PMID: 36016334 DOI: 10.3390/v14081711]

85 **Ma L**, Sun X, Kong X, Gao Y. B cell dysfunction in chronic hepatitis B virus infection. *Liver Res* 2021; **5**: 11-15 [DOI: 10.1016/j.livres.2020.09.004]

86 **Mori T**, Yoshio S, Yoshikawa S, Tsustui Y, Sakata T, Yoshida Y, Sakamoto Y, Kawai H, Osawa Y, Yamazoe T, Aoki Y, Fletcher SP, Kanto T. Toll-like receptor 7 agonist, GS-986, is an immune-stimulant inducing follicular helper T cells and expanding HBs antigen-specific B cells in vitro. *Liver Int* 2023; **43**: 1213-1224 [PMID: 37029645 DOI: 10.1111/liv.15568]

87 **Lam JH**, Smith FL, Baumgarth N. B Cell Activation and Response Regulation During Viral Infections. *Viral Immunol* 2020; **33**: 294-306 [PMID: 32326852 DOI: 10.1089/vim.2019.0207]

88 **Meng Z**, Chen Y, Lu M. Advances in Targeting the Innate and Adaptive Immune Systems to Cure Chronic Hepatitis B Virus Infection. *Front Immunol* 2019; **10**: 3127 [PMID: 32117201 DOI: 10.3389/fimmu.2019.03127]

89 **Zhao H**, Yu Y, Wang Y, Zhao L, Yang A, Hu Y, Pan Z, Wang Z, Yang J, Han Q, Tian Z, Zhang J. Cholesterol accumulation on dendritic cells reverses chronic hepatitis B virus infection-induced dysfunction. *Cell Mol Immunol* 2022; **19**: 1347-1360 [PMID: 36369367 DOI: 10.1038/s41423-022-00939-1]

90 **Shi Y**, Wang Z, Ge S, Xia N, Yuan Q. Hepatitis B Core Antibody Level: A Surrogate Marker for Host Antiviral Immunity in Chronic Hepatitis B Virus Infections. *Viruses* 2023; **15** [PMID: 37243197 DOI: 10.3390/v15051111]

91 **Kawagishi N**, Suda G, Sakamori R, Matsui T, Onozawa M, Yang Z, Yoshida S, Ohara M, Kimura M, Kubo A, Maehara O, Fu Q, Hosoda S, Tokuchi Y, Suzuki K, Nakai M, Sho T, Morikawa K, Natsuizaka M, Ogawa K, Sakai H, Ohnishi S, Baba M, Takehara T, Sakamoto N. Serum IL-1β predicts de novo hepatitis B virus reactivation during direct-acting antiviral therapy for hepatitis C, not during anti-cancer/immunosuppressive therapy. *Sci Rep* 2022; **12**: 16800 [PMID: 36207368 DOI: 10.1038/s41598-022-21315-z]

92 **Al-Shimari FH**, Rencken CA, Kirkwood CD, Kumar R, Vannice KS, Stewart BT. Systematic review of global hepatitis E outbreaks to inform response and coordination initiatives. *BMC Public Health* 2023; **23**: 1120 [PMID: 37308896 DOI: 10.1186/s12889-023-15792-8]

93 **Liu J**, Lo CM, Man K. Role of intrahepatic regional immunity in post-transplant cancer recurrence. *Engineering* 2022; **10**: 57-64 [DOI: 10.1016/j.eng.2021.11.012]

94 **Kayesh MEH**, Hashem MA, Kohara M, Tsukiyama-Kohara K. In vivo Delivery Tools for Clustered Regularly Interspaced Short Palindromic Repeat/Associated Protein 9-Mediated Inhibition of Hepatitis B Virus Infection: An Update. *Front Microbiol* 2022; **13**: 953218 [PMID: 35847068 DOI: 10.3389/fmicb.2022.953218]

95 **Datfar T**, Doulberis M, Papaefthymiou A, Hines IN, Manzini G. Viral Hepatitis and Hepatocellular Carcinoma: State of the Art. *Pathogens* 2021; **10** [PMID: 34832522 DOI: 10.3390/pathogens10111366]

96 **Hernandez N**, Bessone F. Hepatotoxicity Induced by Biological Agents: Clinical Features and Current Controversies. *J Clin Transl Hepatol* 2022; **10**: 486-495 [PMID: 35836762 DOI: 10.14218/JCTH.2021.00243]

97 **Antar SA**, Ashour NA, Marawan ME, Al-Karmalawy AA. Fibrosis: Types, Effects, Markers, Mechanisms for Disease Progression, and Its Relation with Oxidative Stress, Immunity, and Inflammation. *Int J Mol Sci* 2023; **24** [PMID: 36835428 DOI: 10.3390/ijms24044004]

98 **Lee C**, Kim M, Han J, Yoon M, Jung Y. Mesenchymal Stem Cells Influence Activation of Hepatic Stellate Cells, and Constitute a Promising Therapy for Liver Fibrosis. *Biomedicines* 2021; **9** [PMID: 34829827 DOI: 10.3390/biomedicines9111598]

99 **Han F**, Cao D, Zhu X, Shen L, Wu J, Chen Y, Xu Y, Xu L, Cheng X, Zhang Y. Construction and validation of a prognostic model for hepatocellular carcinoma: Inflammatory ferroptosis and mitochondrial metabolism indicate a poor prognosis. *Front Oncol* 2022; **12**: 972434 [PMID: 36686830 DOI: 10.3389/fonc.2022.972434]

100 **Jagdish RK**, Roy A, Kumar K, Premkumar M, Sharma M, Rao PN, Reddy DN, Kulkarni AV. Pathophysiology and management of liver cirrhosis: from portal hypertension to acute-on-chronic liver failure. *Front Med (Lausanne)* 2023; **10**: 1060073 [PMID: 37396918 DOI: 10.3389/fmed.2023.1060073]

101 **Peiseler M**, Schwabe R, Hampe J, Kubes P, Heikenwälder M, Tacke F. Immune mechanisms linking metabolic injury to inflammation and fibrosis in fatty liver disease - novel insights into cellular communication circuits. *J Hepatol* 2022; **77**: 1136-1160 [PMID: 35750137 DOI: 10.1016/j.jhep.2022.06.012]

102 **Gherlan GS**. Occult hepatitis B - the result of the host immune response interaction with different genomic expressions of the virus. *World J*

Clin Cases 2022; **10**: 5518-5530 [PMID: 35979101 DOI: 10.12998/wjcc.v10.i17.5518]

103 **Zaltron S**, Cambianica A, Di Gregorio M, Colangelo C, Storti S, Tiecco G, Castelli F, Quiros-Roldan E. Case report: An occult hepatitis B virus infection reactivation in an HIV/HCV coinfected patient during an immune reconstitution inflammatory syndrome. *Front Cell Infect Microbiol* 2023; **13**: 1143346 [PMID: 37124041 DOI: 10.3389/fcimb.2023.1143346]

104 **Iacob DG**, Luminos M, Benea OE, Tudor AM, Olariu CM, Iacob SA, Ruta S. Liver fibrosis progression in a cohort of young HIV and HIV/HBV co-infected patients: A longitudinal study using non-invasive APRI and Fib-4 scores. *Front Med (Lausanne)* 2022; **9**: 888050 [PMID: 35966860 DOI: 10.3389/fmed.2022.888050]

105 **Zhou Q**, Zhang Q, Wang K, Huang T, Deng S, Wang Y, Cheng C. Anti-rheumatic drug-induced hepatitis B virus reactivation and preventive strategies for hepatocellular carcinoma. *Pharmacol Res* 2022; **178**: 106181 [PMID: 35301112 DOI: 10.1016/j.phrs.2022.106181]

106 **Midorikawa Y**, Takayama T, Moriguchi M, Yagi R, Yamagishi S, Nakayama H, Aramaki O, Yamazaki S, Tsuji S, Higaki T. Liver Resection Versus Embolization for Recurrent Hepatocellular Carcinoma. *World J Surg* 2020; **44**: 232-240 [PMID: 31605170 DOI: 10.1007/s00268-019-05225-2]

107 **Shiri Aghbash P**, Ebrahimzadeh Leylabadlo H, Fathi H, Bahmani M, Chegini R, Bannazadeh Baghi H. Hepatic Disorders and COVID-19: From Pathophysiology to Treatment Strategy. *Can J Gastroenterol Hepatol* 2022; **2022**: 4291758 [PMID: 36531832 DOI: 10.1155/2022/4291758]

108 **Zaki MYW**, Fathi AM, Samir S, Eldafashi N, William KY, Nazmy MH, Fathy M, Gill US, Shetty S. Innate and Adaptive Immunopathogeneses in Viral Hepatitis; Crucial Determinants of Hepatocellular Carcinoma. *Cancers (Basel)* 2022; **14** [PMID: 35267563 DOI: 10.3390/cancers14051255]

109 **Feitelson MA**, Arzumanyan A, Spector I, Medhat A. Hepatitis B x (HBx) as a Component of a Functional Cure for Chronic Hepatitis B. *Biomedicines* 2022; **10** [PMID: 36140311 DOI: 10.3390/biomedicines10092210]

110 **Sivasudhan E**, Blake N, Lu Z, Meng J, Rong R. Hepatitis B Viral Protein HBx and the Molecular Mechanisms Modulating the Hallmarks of Hepatocellular Carcinoma: A Comprehensive Review. *Cells* 2022; **11** [PMID: 35203390 DOI: 10.3390/cells11040741]

111 **Du G**, Yang R, Qiu J, Xia J. Multifaceted Influence of Histone Deacetylases on DNA Damage Repair: Implications for Hepatocellular Carcinoma. *J Clin Transl Hepatol* 2023; **11**: 231-243 [PMID: 36406320 DOI: 10.14218/JCTH.2022.00079]

112 **MacDonald CA**, Qian H, Pundir P, Kulka M. Sodium butyrate supresses malignant human mast cell proliferation, downregulates expression of KIT and promotes differentiation. *Front Allergy* 2023; **4**: 1109717 [PMID: 36970068 DOI: 10.3389/falgy.2023.1109717]

113 **Chekol Abebe E**, Asmamaw Dejenie T, Mengie Ayele T, Dagnew Baye N, Agegnehu Teshome A, Tilahun Muche Z. The Role of Regulatory B Cells in Health and Diseases: A Systemic Review. *J Inflamm Res* 2021; **14**: 75-84 [PMID: 33469337 DOI: 10.2147/JIR.S286426]

114 **Ogunnaike M**, Das S, Raut SS, Sultana A, Nayan MU, Ganesan M, Edagwa BJ, Osna NA, Poluektova LY. Chronic Hepatitis B Infection: New Approaches towards Cure. *Biomolecules* 2023; **13** [PMID: 37627273 DOI: 10.3390/biom13081208]

115 **Umemura M**, Ogawa K, Morikawa K, Kubo A, Tokuchi Y, Yamada R, Kitagataya T, Shigesawa T, Shimazaki T, Kimura M, Suzuki K, Nakamura A, Ohara M, Kawagishi N, Izumi T, Nakai M, Sho T, Suda G, Natsuizaka M, Ono K, Murata K, Sugiyama M, Mizokami M, Sakamoto N. Effects of nucleos(t)ide analogs on hepatitis B surface antigen reduction with interferon-lambda 3 induction in chronic hepatitis B patients. *Hepatol Res* 2022; **52**: 586-596 [PMID: 35352445 DOI: 10.1111/hepr.13768]

116 **Yip TCF**, Lai JCT, Liang LY, Hui VWK, Wong VWS, Wong GLH. Risk of HCC in Patients with HBV, Role of Antiviral Treatment. *Curr Hepatology Rep* 2022; **21**: 76-86 [DOI: 10.1007/s11901-022-00588-y]

117 **Osmani Z**, Boonstra A. Recent Insights into the Role of B Cells in Chronic Hepatitis B and C Infections. *Pathogens* 2023; **12** [PMID: 37375505 DOI: 10.3390/pathogens12060815]

118 **Pishavar E**, Oroojalian F, Salmasi Z, Hashemi E, Hashemi M. Recent advances of dendrimer in targeted delivery of drugs and genes to stem cells as cellular vehicles. *Biotechnol Prog* 2021; **37**: e3174 [PMID: 33987965 DOI: 10.1002/btpr.3174]

119 **Hui RWH**, Mak LY, Cheung KS, Fung J, Seto WK, Yuen MF. Novel Combination Strategies With Investigational Agents for Functional Cure of Chronic Hepatitis B Infection. *Curr Hepatology Rep* 2022; **21**: 59-67 [DOI: 10.1007/s11901-022-00590-4]

120 **Degasperi E**, Anolli MP, Lampertico P. Towards a Functional Cure for Hepatitis B Virus: A 2022 Update on New Antiviral Strategies. *Viruses* 2022; **14** [PMID: 36366502 DOI: 10.3390/v14112404]

121 **Zi J**, Gao X, Du J, Xu H, Niu J, Chi X. Multiple Regions Drive Hepatitis Delta Virus Proliferation and Are Therapeutic Targets. *Front Microbiol* 2022; **13**: 838382 [PMID: 35464929 DOI: 10.3389/fmicb.2022.838382]

122 **Oh H**, Lee HY, Kim J, Kim YJ. Systematic Review with Meta-Analysis: Comparison of the Risk of Hepatocellular Carcinoma in Antiviral-Naive Chronic Hepatitis B Patients Treated with Entecavir versus Tenofovir: The Devil in the Detail. *Cancers (Basel)* 2022; **14** [PMID: 35681596 DOI: 10.3390/cancers14112617]

123 **Shahini E**, Donghia R, Facciorusso A. The power of prevention: how tenofovir and entecavir are changing the game in hepatocellular carcinoma. *Hepatobiliary Surg Nutr* 2023; **12**: 936-940 [PMID: 38115931 DOI: 10.21037/hbsn-23-528]

124 **Suda G**, Baba M, Yamamoto Y, Sho T, Ogawa K, Kimura M, Hosoda S, Yoshida S, Kubo A, Fu Q, Yang Z, Tokuchi Y, Kitagataya T, Maehara O, Ohnishi S, Yamada R, Ohara M, Kawagishi N, Natsuizaka M, Nakai M, Morikawa K, Furuya K, Suzuki K, Izumi T, Meguro T, Terashita K, Ito J, Kobayashi T, Tsunematsu I, Sakamoto N. Prophylactic tenofovir alafenamide for hepatitis B virus reactivation and reactivation-related hepatitis. *J Med Virol* 2023; **95**: e28452 [PMID: 36597900 DOI: 10.1002/jmv.28452]

125 **Mizushima D**, Takano M, Aoki T, Ando N, Uemura H, Yanagawa Y, Watanabe K, Gatanaga H, Kikuchi Y, Oka S. Effect of tenofovir-based HIV pre-exposure prophylaxis against HBV infection in men who have sex with men. *Hepatology* 2023; **77**: 2084-2092 [PMID: 36960800 DOI: 10.1097/HEP.0000000000000384]

126 **Hsu CW**, Chen SC, Wang PN, Wang HM, Chen YC, Yeh CT. Preventing viral relapse with prophylactic tenofovir in hepatitis B carriers receiving chemotherapy: A phase IV randomized study in Taiwan. 2023. [cited 22 December 2023]. Available from: https://www.researchsquare.com/article/rs-3013457/v1

127 **Fu S**, Zhang Q, Jing R, Zu C, Ni F, Lv Y, Cui J, Zheng H, Zhang Y, Zhang M, Wei G, Cen Z, Chang AH, Hu Y, Huang H. HBV reactivation in patients with chronic or resolved HBV infection following BCMA-targeted CAR-T cell therapy. *Bone Marrow Transplant* 2023; **58**: 701-709 [PMID: 37002410 DOI: 10.1038/s41409-023-01960-2]

128 **Ding ZN**, Meng GX, Xue JS, Yan LJ, Liu H, Yan YC, Chen ZQ, Hong JG, Wang DX, Dong ZR, Li T. Hepatitis B virus reactivation in patients undergoing immune checkpoint inhibition: systematic review with meta-analysis. *J Cancer Res Clin Oncol* 2023; **149**: 1993-2008 [PMID: 35767193 DOI: 10.1007/s00432-022-04133-8]

129 **Di Stefano M**, Faleo G, Leitner T, Zheng W, Zhang Y, Hassan A, Alwazzeh MJ, Fiore JR, Ismail M, Santantonio TA. Molecular and Genetic

Characterization of Hepatitis B Virus (HBV) among Saudi Chronically HBV-Infected Individuals. *Viruses* 2023; **15** [PMID: 36851671 DOI: 10.3390/v15020458]

130 **Deng M**, Tong M, Fu F, Wei D. Comparative untargeted metabolomics analysis of serum metabolic alterations in patients infected with hepatitis B virus genotypes B and C. *Arab J Chem* 2023; **16**: 105155 [DOI: 10.1016/j.arabjc.2023.105155]

131 **Wang X**, Liu X, Wang P, Yu L, Yan F, Yan H, Zhou D, Yang Z. Antiviral Therapy Reduces Mortality in Hepatocellular Carcinoma Patients with Low-Level Hepatitis B Viremia. *J Hepatocell Carcinoma* 2021; **8**: 1253-1267 [PMID: 34708007 DOI: 10.2147/JHC.S330301]

132 **Block TM**, Chang KM, Guo JT. Prospects for the Global Elimination of Hepatitis B. *Annu Rev Virol* 2021; **8**: 437-458 [PMID: 34586871 DOI: 10.1146/annurev-virology-091919-062728]

133 **Korean Liver Cancer Association**; National Cancer Center. 2018 Korean Liver Cancer Association-National Cancer Center Korea Practice Guidelines for the Management of Hepatocellular Carcinoma. *Gut Liver* 2019; **13**: 227-299 [PMID: 31060120 DOI: 10.5009/gnl19024]

134 **Abdelaal MA**. Lamivudine: An antiviral drug with high risk factor for selection of resistance in HBV patients. *Rec of Pharm and Bio Sci* 2021; **5**: 81-84 [DOI: 10.21608/rpbs.2021.83271.1106]

135 **Mokaya J**, McNaughton AL, Bester PA, Goedhals D, Barnes E, Marsden BD, Matthews PC. Hepatitis B virus resistance to tenofovir: fact or fiction? A systematic literature review and structural analysis of drug resistance mechanisms. *Wellcome Open Res* 2020; **5**: 151 [PMID: 33869791 DOI: 10.12688/wellcomeopenres.15992.1]

136 **Pley C**, Lourenço J, McNaughton AL, Matthews PC. Spacer Domain in Hepatitis B Virus Polymerase: Plugging a Hole or Performing a Role? *J Virol* 2022; **96**: e0005122 [PMID: 35412348 DOI: 10.1128/jvi.00051-22]

137 **Su YT**, Chang ML, Chien RN, Liaw YF. Hepatitis C Virus Reactivation in Anti-HCV Antibody-Positive Patients with Chronic Hepatitis B Following Anti-HBV Therapies. *Viruses* 2022; **14** [PMID: 36146665 DOI: 10.3390/v14091858]

138 **Mican R**, Busca Arenzana C, Vasquez J, Daroca G, Perez-Valero I, Martin-Carbonero L. Hepatitis B reactivation after tenofovir withdrawal in an HIV-infected patient with history of cured hepatitis B virus infection and poor immunological status. *AIDS* 2021; **35**: 1707-1708 [PMID: 34270493 DOI: 10.1097/QAD.0000000000002941]

139 **Kayesh MEH**, Kohara M, Tsukiyama-Kohara K. Toll-Like Receptor Response to Hepatitis B Virus Infection and Potential of TLR Agonists as Immunomodulators for Treating Chronic Hepatitis B: An Overview. *Int J Mol Sci* 2021; **22** [PMID: 34638802 DOI: 10.3390/ijms221910462]

140 **Shen J**, Wang X, Wang N, Wen S, Yang G, Li L, Fu J, Pan X. HBV reactivation and its effect on survival in HBV-related hepatocarcinoma patients undergoing transarterial chemoembolization combined with tyrosine kinase inhibitors plus immune checkpoint inhibitors. *Front Cell Infect Microbiol* 2023; **13**: 1179689 [PMID: 37197205 DOI: 10.3389/fcimb.2023.1179689]

141 **Watanabe T**, Inoue T, Tanaka Y. Hepatitis B Core-Related Antigen and New Therapies for Hepatitis B. *Microorganisms* 2021; **9** [PMID: 34683404 DOI: 10.3390/microorganisms9102083]

142 **Xu H**, Locarnini S, Wong D, Hammond R, Colledge D, Soppe S, Huynh T, Shaw T, Thompson AJ, Revill PA, Hogarth PM, Wines BD, Walsh R, Warner N. Role of anti-HBs in functional cure of HBeAg+ chronic hepatitis B patients infected with HBV genotype A. *J Hepatol* 2022; **76**: 34-45 [PMID: 34371070 DOI: 10.1016/j.jhep.2021.07.031]

143 **Huang SC**, Yang HC, Kao JH. Hepatitis B reactivation: diagnosis and management. *Expert Rev Gastroenterol Hepatol* 2020; **14**: 565-578 [PMID: 32448008 DOI: 10.1080/17474124.2020.1774364]

144 **Herr KJ**, Shen SP, Liu Y, Yang CC, Tang CH. The growing burden of generalized myasthenia gravis: a population-based retrospective cohort study in Taiwan. *Front Neurol* 2023; **14**: 1203679 [PMID: 37426446 DOI: 10.3389/fneur.2023.1203679]

145 **Feld JJ**, Lok AS, Zoulim F. New Perspectives on Development of Curative Strategies for Chronic Hepatitis B. *Clin Gastroenterol Hepatol* 2023; **21**: 2040-2050 [PMID: 37080262 DOI: 10.1016/j.cgh.2023.02.032]

146 **Buschow SI**, Jansen DTSL. CD4(+) T Cells in Chronic Hepatitis B and T Cell-Directed Immunotherapy. *Cells* 2021; **10** [PMID: 34066322 DOI: 10.3390/cells10051114]

147 **Hui RW**, Mak LY, Seto WK, Yuen MF. RNA interference as a novel treatment strategy for chronic hepatitis B infection. *Clin Mol Hepatol* 2022; **28**: 408-424 [PMID: 35172540 DOI: 10.3350/cmh.2022.0012]

148 **Colombatto P**, Coco B, Bonino F, Brunetto MR. Management and Treatment of Patients with Chronic Hepatitis B: Towards Personalized Medicine. *Viruses* 2022; **14** [PMID: 35458431 DOI: 10.3390/v14040701]

149 **Hudu SA**, Jimoh AO, Ibrahim KG, Alshrari AS. Hepatitis B Therapeutic Vaccine: A Patent Review. *Pharmaceuticals (Basel)* 2022; **15** [PMID: 36558991 DOI: 10.3390/ph15121542]

150 **Ruzzi F**, Semprini MS, Scalambra L, Palladini A, Angelicola S, Cappello C, Pittino OM, Nanni P, Lollini PL. Virus-like Particle (VLP) Vaccines for Cancer Immunotherapy. *Int J Mol Sci* 2023; **24** [PMID: 37629147 DOI: 10.3390/ijms241612963]

151 **Chan SL**, Wong N, Lam WKJ, Kuang M. Personalized treatment for hepatocellular carcinoma: Current status and future perspectives. *J Gastroenterol Hepatol* 2022; **37**: 1197-1206 [PMID: 35570200 DOI: 10.1111/jgh.15889]

152 **Salpini R**, D'Anna S, Benedetti L, Piermatteo L, Gill U, Svicher V, Kennedy PTF. Hepatitis B virus DNA integration as a novel biomarker of hepatitis B virus-mediated pathogenetic properties and a barrier to the current strategies for hepatitis B virus cure. *Front Microbiol* 2022; **13**: 972687 [PMID: 36118192 DOI: 10.3389/fmicb.2022.972687]

153 **Shang D**, Wang P, Tang W, Mo R, Lai R, Lu J, Li Z, Wang X, Cai W, Wang H, Zhao G, Xie Q, Xiang X. Genetic Variations of ALDH (rs671) Are Associated With the Persistence of HBV Infection Among the Chinese Han Population. *Front Med (Lausanne)* 2022; **9**: 811639 [PMID: 35237626 DOI: 10.3389/fmed.2022.811639]

154 **Rajendren S**, Karijolich J. The impact of RNA modifications on the biology of DNA virus infection. *Eur J Cell Biol* 2022; **101**: 151239 [PMID: 35623231 DOI: 10.1016/j.ejcb.2022.151239]

155 **Salama II**, Sami SM, Salama SI, Abdel-Latif GA, Shaaban FA, Fouad WA, Abdelmohsen AM, Raslan HM. Current and novel modalities for management of chronic hepatitis B infection. *World J Hepatol* 2023; **15**: 585-608 [PMID: 37305370 DOI: 10.4254/wjh.v15.i5.585]

156 **Manea M**, Apostol D, Constantinescu I. The Connection between MiR-122 and Lymphocytes in Patients Receiving Treatment for Chronic Hepatitis B Virus Infection. *Microorganisms* 2023; **11** [PMID: 38004743 DOI: 10.3390/microorganisms11112731]

157 **Viswanathan U**, Mani N, Hu Z, Ban H, Du Y, Hu J, Chang J, Guo JT. Targeting the multifunctional HBV core protein as a potential cure for chronic hepatitis B. *Antiviral Res* 2020; **182**: 104917 [PMID: 32818519 DOI: 10.1016/j.antiviral.2020.104917]

158 **Stroffolini T**, Ciancio A, Furlan C, Vinci M, Niro GA, Russello M, Colloredo G, Morisco F, Coppola N, Babudieri S, Ferrigno L, Sagnelli C, Sagnelli E; Collaborating group. Chronic hepatitis B virus infection in Italy during the twenty-first century: an updated survey in 2019. *Eur J Clin Microbiol Infect Dis* 2021; **40**: 607-614 [PMID: 33029767 DOI: 10.1007/s10096-020-04065-6]

159 **Rizzo GEM**, Cabibbo G, Craxì A. Hepatitis B Virus-Associated Hepatocellular Carcinoma. *Viruses* 2022; **14** [PMID: 35632728 DOI:

10.3390/v14050986]
160 **Raimondo G**, Locarnini S, Pollicino T, Levrero M, Zoulim F, Lok AS; Taormina Workshop on Occult HBV Infection Faculty Members. Update of the statements on biology and clinical impact of occult hepatitis B virus infection. *J Hepatol* 2019; **71**: 397-408 [PMID: 31004683 DOI: 10.1016/j.jhep.2019.03.034]
161 **Gehring AJ**, Mendez P, Richter K, Ertl H, Donaldson EF, Mishra P, Maini M, Boonstra A, Lauer G, de Creus A, Whitaker K, Martinez SF, Weber J, Gainor E, Miller V. Immunological biomarker discovery in cure regimens for chronic hepatitis B virus infection. *J Hepatol* 2022; **77**: 525-538 [PMID: 35259469 DOI: 10.1016/j.jhep.2022.02.020]
162 **Gallage S**, García-Beccaria M, Szydlowska M, Rahbari M, Mohr R, Tacke F, Heikenwalder M. The therapeutic landscape of hepatocellular carcinoma. *Med* 2021; **2**: 505-552 [PMID: 35590232 DOI: 10.1016/j.medj.2021.03.002]
163 **Yang M**, Yang Y, He Q, Zhu P, Liu M, Xu J, Zhao M. Intestinal Microbiota-A Promising Target for Antiviral Therapy? *Front Immunol* 2021; **12**: 676232 [PMID: 34054866 DOI: 10.3389/fimmu.2021.676232]
164 **Wirusanti NI**, Baldridge MT, Harris VC. Microbiota regulation of viral infections through interferon signaling. *Trends Microbiol* 2022; **30**: 778-792 [PMID: 35135717 DOI: 10.1016/j.tim.2022.01.007]
165 **Milardi G**, Lleo A. Tumor-Infiltrating B Lymphocytes: Promising Immunotherapeutic Targets for Primary Liver Cancer Treatment. *Cancers (Basel)* 2023; **15** [PMID: 37046842 DOI: 10.3390/cancers15072182]
166 **Wen L**, Li G, Huang T, Geng W, Pei H, Yang J, Zhu M, Zhang P, Hou R, Tian G, Su W, Chen J, Zhang D, Zhu P, Zhang W, Zhang X, Zhang N, Zhao Y, Cao X, Peng G, Ren X, Jiang N, Tian C, Chen ZJ. Single-cell technologies: From research to application. *Innovation (Camb)* 2022; **3**: 100342 [PMID: 36353677 DOI: 10.1016/j.xinn.2022.100342]

World Journal of Gastroenterology

Submit a Manuscript: https://www.f6publishing.com

World J Gastroenterol 2024 March 14; 30(10): 1313-1328

DOI: 10.3748/wjg.v30.i10.1313

ISSN 1007-9327 (print) ISSN 2219-2840 (online)

REVIEW

Optimizing nutrition in hepatic cirrhosis: A comprehensive assessment and care approach

Osvely Mendez-Guerrero, Anaisa Carranza-Carrasco, Luis Alberto Chi-Cervera, Aldo Torre, Nalu Navarro-Alvarez

Specialty type: Gastroenterology and hepatology

Provenance and peer review: Invited article; Externally peer reviewed.

Peer-review model: Single blind

Peer-review report's scientific quality classification

Grade A (Excellent): 0
Grade B (Very good): B, B
Grade C (Good): 0
Grade D (Fair): 0
Grade E (Poor): 0

P-Reviewer: Khayyat YM, Saudi Arabia; Malnick SDH, Israel

Received: November 28, 2023
Peer-review started: November 28, 2023
First decision: January 5, 2024
Revised: January 23, 2024
Accepted: February 25, 2024
Article in press: February 25, 2024
Published online: March 14, 2024

Osvely Mendez-Guerrero, Anaisa Carranza-Carrasco, Aldo Torre, Nalu Navarro-Alvarez, Department of Gastroenterology, Instituto Nacional de Ciencias Médicas y Nutrición Salvador Zubirán, Mexico City 14080, Mexico

Luis Alberto Chi-Cervera, Clínica de Especialidades Gastrointestinales y Hepáticas, Hospital Star Medica, Merida 97133, Yucatan, Mexico

Nalu Navarro-Alvarez, Molecular Biology, Universidad Panamericana School of Medicine, Campus México, Mexico City 03920, Mexico

Nalu Navarro-Alvarez, Department of Surgery, University of Colorado Anschutz Medical Campus, Denver, CO 80045, United States

Corresponding author: Nalu Navarro-Alvarez, MD, PhD, Assistant Professor, Department of Gastroenterology, Instituto Nacional de Ciencias Médicas y Nutrición Salvador Zubirán, 15 Vasco de Quiroga, Mexico City 14080, Mexico. nalu.navarroa@incmnsz.mx

Abstract

Cirrhosis is considered a growing cause of morbidity and mortality, which represents a significant public health problem. Currently, there is no effective treatment to reverse cirrhosis. Treatment primarily centers on addressing the underlying liver condition, monitoring, and managing portal hypertension-related complications, and evaluating the potential for liver transplantation in cases of decompensated cirrhosis, marked by rapid progression and the emergence of complications like variceal bleeding, hepatic encephalopathy, ascites, malnutrition, and more. Malnutrition, a prevalent complication across all disease stages, is often underdiagnosed in cirrhosis due to the complexities of nutritional assessment in patients with fluid retention and/or obesity, despite its crucial impact on prognosis. Increasing emphasis has been placed on the collaboration of nutritionists within hepatology and Liver transplant teams to deliver comprehensive care, a practice that has shown to improve outcomes. This review covers appropriate screening and assessment methods for evaluating the nutritional status of this population, diagnostic approaches for malnutrition, and context-specific nutrition treatments. It also discusses evidence-based recommendations for supplementation and physical exercise, both essential elements of the standard care provided to cirrhotic patients.

Key Words: Cirrhosis; Nutritional diagnosis; Treatment; Diet; Guidelines

Core Tip: Currently, there is a wealth of information on the ideal nutritional treatment for cirrhosis. Yet, a critical gap persists: The absence of a concise clinical document encompassing the entire nutritional care process. The significance of nutritional management is increasing, given its profound influence on both patient prognosis and quality of life. We here strongly emphasize the need to offer a practical foundation for managing nutrition in cirrhosis, grounded in scientific evidence.

Citation: Mendez-Guerrero O, Carranza-Carrasco A, Chi-Cervera LA, Torre A, Navarro-Alvarez N. Optimizing nutrition in hepatic cirrhosis: A comprehensive assessment and care approach. *World J Gastroenterol* 2024; 30(10): 1313-1328
URL: https://www.wjgnet.com/1007-9327/full/v30/i10/1313.htm
DOI: https://dx.doi.org/10.3748/wjg.v30.i10.1313

INTRODUCTION

Cirrhosis is a globally highly prevalent disease associated with significantly high morbidity and mortality. It is the 14th cause of death worldwide accounting for 1.03 million deaths/year[1]. This chronic disease is a result of the progression of many forms of necro-inflammatory liver diseases leading to fibrosis, vascular remodeling, development of portal hypertension along with its complications, and ultimately liver failure[2]. The disease's natural progression involves an asymptomatic phase known as "compensated cirrhosis", followed by "decompensated cirrhosis", marked by rapid progression and the emergence of symptoms including portal hypertension, bleeding, hepatic encephalopathy (HE), ascites, malnutrition, among others[3].

Cirrhosis is a condition with a longstanding propensity for the development of malnutrition, sarcopenia, and fragility.

Malnutrition in this population is attributed to the interaction of different factors, including: Metabolic alterations[4], inadequate dietary intake, increased energy requirements as a result of hypermetabolism and systemic inflammation[5], deficiencies of micronutrients, and anorexia due to hormonal imbalances, among others[6]. Malnutrition is not simply an accompanying condition but has a significant impact on the progression of the disease that further worsens the patient prognosis. Its direct impact on patient outcomes and complications is widely acknowledged[7].

Diagnosing malnutrition can be challenging due to its complex evaluation and the potential influence of factors like fluid overload, HE, and obesity, which can mask its effects[7-9].

As one of the few modifiable factors within cirrhosis, early diagnosis and timely treatment offer the potential to influence positively patient outcomes.

In this review we aim to describe the impact of malnutrition in cirrhosis, the adequate strategies for a thorough nutritional status assessment using validated screening tools. We also discuss evidence-based recommendations of nutritional and exercise intervention that can be used to improve outcomes for patients with liver cirrhosis.

DIAGNOSIS AND TREATMENT

The most useful scores to determine the severity of the disease include the Child-Pugh and model for end-stage liver disease (MELD) scores. The Child-Pugh score incorporates biochemical and clinical factors such as total bilirubin, albumin, international normalized ratio (INR), ascites, and HE. However, limitations arise due to the variability in assessing clinical variables like ascites and HE[10]. Therefore, the MELD score was developed, offering a more objective approach. It relies on a mathematical model involving biochemical parameters like creatinine, total bilirubin, and INR. The MELD score is widely used as a measurement to evaluate and prioritize the organ allocation for transplantation, since it accurately predicts short-term survival (3 months). The cut-off value of 15 is widely used to prioritize candidates to receive a liver transplantation[11].

Currently, preventing cirrhosis lacks an effective treatment approach. As a result, the present emphasis is on managing liver diseases and their related complications. This involves meticulous assessment of individuals with decompensated disease for potential liver transplantation[12].

Despite liver transplantation being considered a curative treatment, is not always available to everyone, and in some cases, there is a high incidence of recurrence of the liver disease. In a retrospective cohort evaluating risk factors and outcomes associated with recurrent autoimmune hepatitis (AIH) after liver transplantation, AIH recurrence was found in 20% of patients after 5 years and 31% after 10 years. The authors concluded that AIH recurrence after transplantation is common and is associated with younger age at liver transplant (LT), post-LT use of mycophenolate mofetil, gender mismatch, and elevated pre-transplant IgG levels. They demonstrated an association between disease recurrence and graft impairment and overall survival in patients with AIH, highlighting the importance of continued efforts to better

characterize, prevent, and treat recurrent AIH[12]. The LT community continues to be challenged by limitations in organ supply, allocation, and quality. As the need for transplantation expands, innovations to safely use and potentially salvage all donor organs are being explored and tested. Many groups are attempting to overcome these obstacles by gradually developing novel techniques and using sound translational science[13].

IMPACT OF MALNUTRITION AND SARCOPENIA IN CIRRHOSIS

Malnutrition is defined as inadequate nutrient intake, nutrient imbalance, or altered utilization[14]. The prevalence of malnutrition varies depending on the assessment method, disease etiology, and patient stage. It is higher (40%-70%) in decompensated cirrhosis often accompanied by disease-related complications such as HE, ascites, and esophageal varices (Child-Pugh B-C). In compensated or asymptomatic phases (Child-Pugh A), the prevalence ranges from 10% to 40%[14-16].

The pathophysiology of malnutrition and sarcopenia is complex and is attributed to the interaction of factors including metabolic alterations caused by a decrease in hepatic glycogen reserves, increased lipid catabolism, and increased proteolysis due to an increased gluconeogenesis[4,5]. These metabolic changes lead to a 15%-30% increase in energy requirements[15], which if coupled with the insufficient dietary intake arising from cirrhosis-related complications such as ascites, HE, and dysgeusia, are a significant malnutrition-contributing factor.

Ascites in patients delays gastric emptying, resulting in postprandial satiety and reduced appetite[17]. Cognitive impairment in HE leads to decreased food consumption[18]. Protein intake is often restricted as part of routine clinical management, leading to reduced calorie intake, despite a lack of evidence supporting improvement in HE[19].

Cirrhotic patients often experience dysgeusia, which is linked to deficiency in micronutrients like zinc[20] and other minerals that decrease due to both the drugs used for treating the disease and associated comorbidities, including diuretics[21], and a decreased consumption by the patients.

Following variceal gastrointestinal bleeding, patients may be kept fasting for prolonged periods. Additionally, endoscopic procedures like variceal ligation can induce temporary dysphagia, potentially leading to reduced protein and energy intake[14,15].

Sarcopenia, another facet of malnutrition, involves muscle mass and strength loss alongside reduced physical performance[14,22]. This condition contributes to fragility, marked by reduced physiological reserve and increased stress factors[23].

Furthermore, there is a decline in muscle fiber formation which is attributed to satellite cell differentiation inhibition [24] and an increased in mTOR signaling pathway activity[25], promoting proteolysis. This phenomenon is linked to elevated myostatin activity[26], a member of the TGF-β cytokine family, which is proven to be enhanced in cirrhosis and closely related to disease severity[27].

Sarcopenia, regardless of hepatic function, has been shown to be an important predictor of pre and posttransplant complications[28], including higher risk of infections[29], HE[30], longer hospital stay[31], low quality of life[32] and survival (Figure 1)[33].

A weak correlation between muscle mass and liver function has prompted the consideration of sarcopenia as a significant addition to the MELD score. The presence of sarcopenia in a patient is equivalent to adding 10 points to the MELD score[33]. Therefore, prioritizing these patients and implementing a controlled nutritional plan before transplantation becomes crucial to enhance post-transplant outcomes.

NUTRITIONAL CONTROL AND SCREENING

According to Global Leadership Initiative on Malnutrition criteria, a proper diagnosis requires combining etiological and phenotypic patient characteristics (Table 1)[34].

Implementing the nutritional control protocol outlined by Clinical Practice Guidelines is strongly advised as a fundamental aspect of standard cirrhosis patient management (Figure 2). This comprehensive plan encompasses nutritional assessment, nutritional diagnosis, a personalized nutritional intervention, and monitoring as recommended by the European Association for the Study of the Liver[35] (Figure 3). Assessing nutritional status, interpreting parameters, and clinically evaluating patients with cirrhosis possesses challenges influenced by numerous non-nutritional factors, therefore, this should be a collaborative endeavor, where nutritionists and hepatologists work together to provide holistic treatment, ensuring optimal outcomes for the patients.

Nutritional screening evaluates characteristics related to nutritional concerns, pinpointing patients who need thorough nutritional status assessment. These screenings should occur within 24 h of hospitalization or within the initial 14 d of long-term care facility admission[36]. The tools used must be easy to apply, reproducible, capable of detecting changes over time, and validated for the population in which they are being used[37].

In patients with cirrhosis, the validated screening tools are the Royal Free Hospital Global Assessment (RFH-GA) and the RFH-Nutritional Prioritizing Tool (RFH-NPT)[19].

RFH-GA

This tool evaluates mortality risk in mild/moderate and severe malnutrition stages. It considers objective and subjective factors, incorporating body mass index (BMI). For patients with fluid overload, it considers dry weight, often calculated from post-paracentesis weight or pre-fluid retention weight, or subtracts a percentage based on ascites severity (5% for

Table 1 Global leadership initiative on malnutrition criteria for the diagnosis of malnutrition

Phenotypic criteria			Etiological criteria	
Unintentional weight loss	Low body mass index	Reduction of muscle mass	Decreased intake or assimilation of foods	Inflammatory load
> 5% in the last 6 months or > 10% in more than 6 months	< 20 in < 70 yr or < 22 in > 70 yr	Evaluated by validated body composition techniques	≤ 50% > 1 wk or ≤ 100% > 2 wk or any chronic condition that alters food assimilation	Acute injury/inflammation; chronic inflammatory pathology

Diagnosis requires at least 1 phenotypic criterion and 1 etiological criterion.

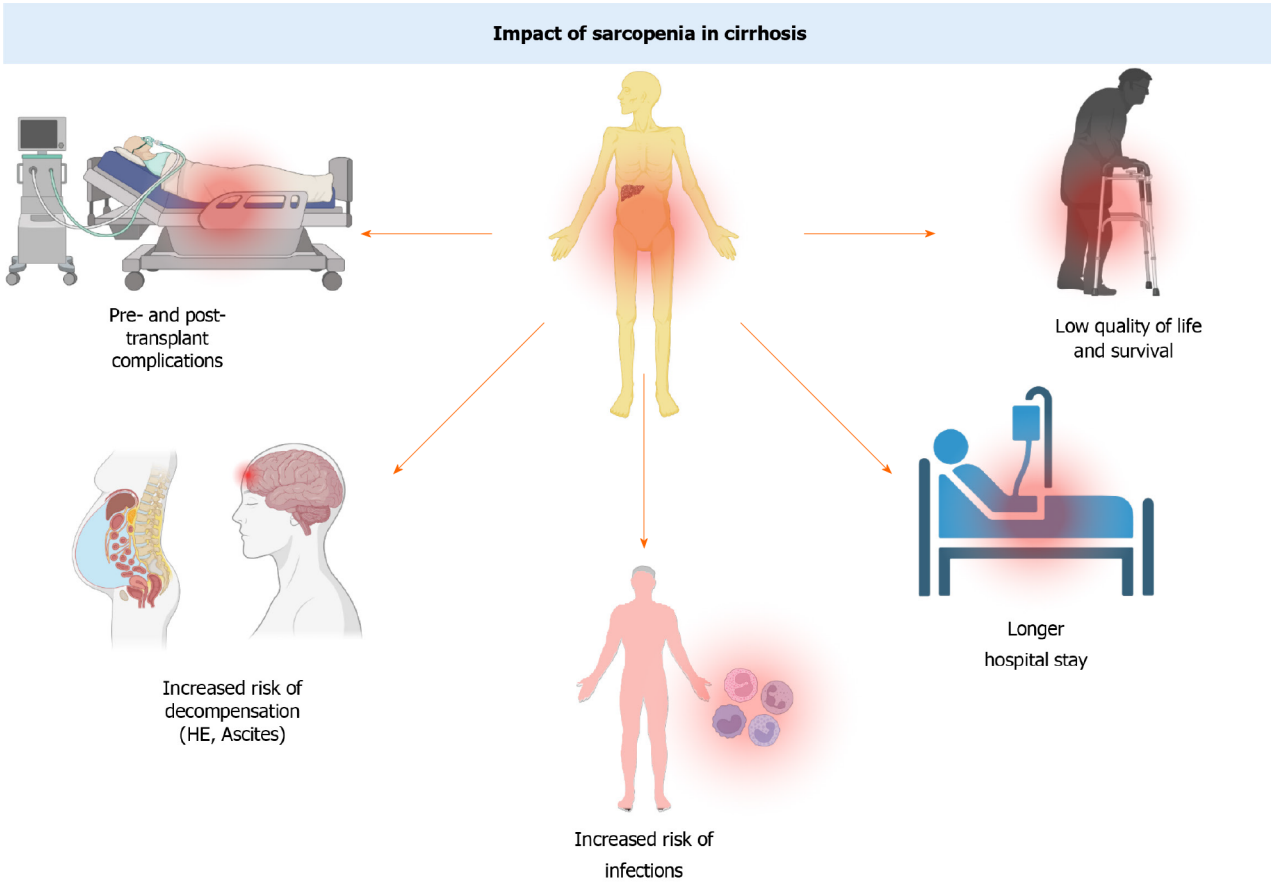

Figure 1 Impact of sarcopenia in cirrhosis. The presence of sarcopenia has been shown to be associated with reduced quality of life and survival. It is a predictor of pre and posttransplant complications, including higher risk of infections, ascites, hepatic encephalopathy, and longer hospital stay. HE: Hepatic encephalopathy. Citation: The authors have obtained the permission for figure using from the BioRender.com (Supplementary material)[112].

mild, 10% for moderate, and 15% for severe), plus an extra 5% for bilateral edema[38]. In this scheme, the corrected mid-arm muscle area (cAMA) is also used along with dietary intake details in a semi-structured algorithmic construction. The RFH-GA exhibits excellent intra- and inter-observer reproducibility and has been validated against a multicomponent model of body composition[39,40].

RFH-NPT

Currently there is international consensus to utilize this tool due to its demonstrated clinical correlation with disease severity and efficient application[41,42]. Taking under 3 minutes to complete, this screening tool is suitable for non-specialized personnel. It boasts remarkable intra- and inter-observer reproducibility and substantial external validity when compared to RFH-GA[40].

The process involves three key steps: (1) Individuals with alcoholic hepatitis or on tube feeding are promptly identified as high risk without further steps; (2) those without alcoholic hepatitis and not on tube feeding are assessed for fluid overload's effect on food intake and weight loss; and (3) individuals without fluid overload are evaluated for nutritional status (BMI, unplanned weight loss, daily dietary intake). Patients are categorized as low risk (score 0), moderate risk (score 1), or high risk (score 2 to 7)[42].

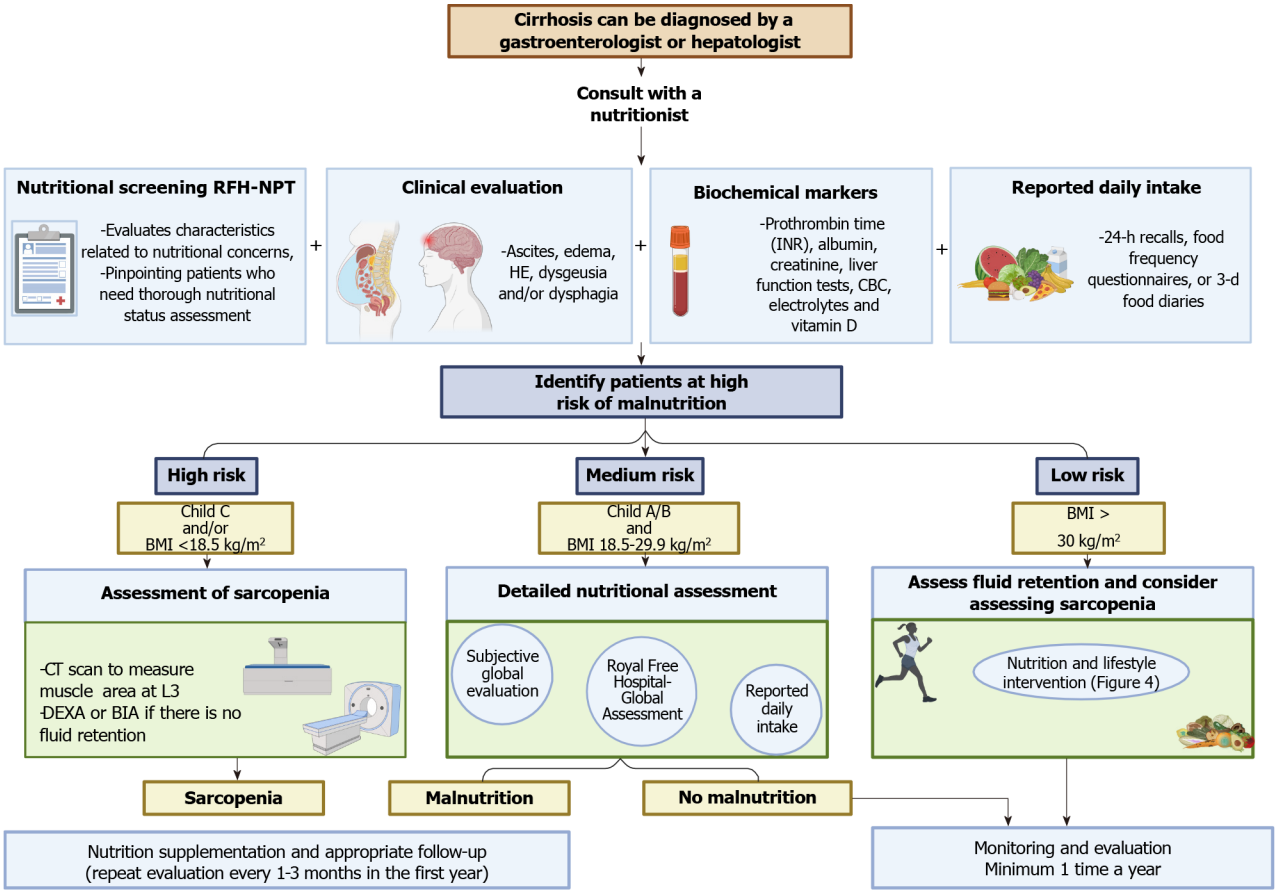

Figure 2 Assessment in patients with cirrhosis. Implementing the nutritional control protocol outlined by Clinical Practice Guidelines is strongly advised as a fundamental aspect of standard cirrhosis patient management. HE: Hepatic encephalopathy; INR: International normalized ratio; CBC: Complete blood count; CT: Computed tomography; DEXA: Dual energy X-ray absorptiometry; BIA: Bioelectrical impedance analysis; BMI: Body mass index; RFH-NPT: Royal Free Hospital Nutritional Prioritizing Tool. The consent was adapted by Clinical Practice Guidelines[41]. Citation: The authors have obtained the permission for figure using from the BioRender.com (Supplementary material)[112].

NUTRITIONAL STATUS ASSESSMENT

Body composition assessment methods vary in their characteristics, benefits, and drawbacks. Their diagnostic effectiveness hinges on the patient's disease-related complications during assessment. Fluid retention can distort measurements due to physical changes in body compartments. The following outlines the key measurements for assessing body composition, including their respective advantages and disadvantages.

Anthropometry

Anthropometric assessment measures physical dimensions and body composition. It's highly accessible but demands evaluator training and intra-observer evaluations for measurement consistency[43,44].

The most used anthropometric measures, in addition to weight and height, are mid-arm circumference (MAC) and triceps skinfold thickness (TSF). These measurements are taken as follows.

MAC: When measuring MAC, the subject should be standing upright with arms by their sides and palms facing inward. The measuring area should be uncovered. To find the midpoint of the arm, the person's arm is flexed at a 90-degree angle with the palm upward. The person taking the measurement stands behind and locates the lateral tip of the acromion, palpating along the upper surface of the scapula's spine. The distance between the acromion (end of the clavicle) and the olecranon (end of the humerus) is measured, marking the midpoint between them. After identifying the midpoint, the arm is relaxed, and the measurement is taken in centimeters (cm)[43].

TSF: To assess TSF, locate the skinfold site on the back of the arm, directly over the triceps muscle. For accurate measurement, have the subject's arm hang to one side to establish the posterior midline. Mark the skinfold site along the posterior midline of the arm, aligning it with the MAC. The person performing the measurement should stand behind the subject, using their left hand to hold the skinfold 1 cm proximal to the marked site. Position the caliper tips 1 cm below the thumb and index finger, maintaining them perpendicular to the skinfold's longitudinal axis. Take three measurements and record the average in millimeters (mm)[45,46].

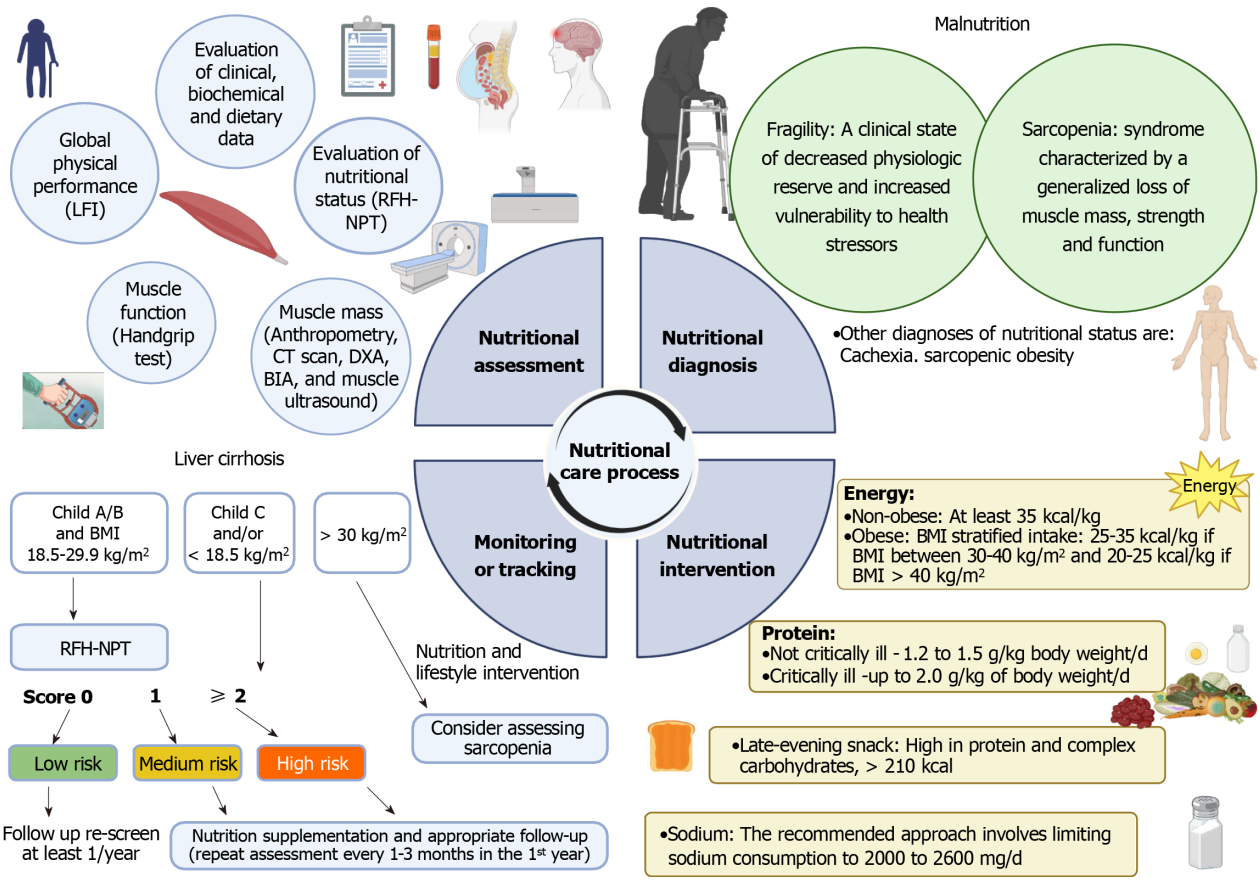

Figure 3 The nutritional care process includes the following steps. (1) Nutritional assessment; (2) nutritional diagnosis; (3) nutritional intervention; and (4) monitoring. LFI: Liver frailty index; RFH-NPT: Royal Free Hospital Nutritional Prioritizing Tool; CT: Computed tomography; DEXA: Dual energy X-ray absorptiometry; BIA: Bioelectrical impedance analysis; BMI: Body mass index. Citation: The authors have obtained the permission for figure using from the BioRender.com (Supplementary material)[112].

cAMA: The cAMA is calculated using the values obtained from measurements of the MAC and TSF with the following formula:

Men cAMA: $[MAC\ cm - (\pi \times PCT\ cm)]^2/4\pi - 10$

Women cAMA: $[MAC\ cm - (\pi \times PCT\ cm)]^2/4\pi - 6.5$

cAMA measurements below the 5th percentile, as indicated by reference tables for sex and age by Frisancho, suggest malnutrition resulting from low muscle mass[45,46]. However, these measurements have limitations in patients with fluid retention, as they can lead to overestimation during assessments and show reduced sensitivity to sudden changes. Consequently, their use is advised in the early stages of the disease[47].

Imaging methods

Radiological imaging analysis is now used to diagnose muscle mass in cirrhosis. These techniques have gained substantial attention primarily due to their diagnostic capability in determining muscle mass and its connection to disease prognosis. Imaging methods are considered objective and reproducible approaches to evaluate skeletal muscle mass, utilizing indices calculated from cross-sectional images obtained *via* computed tomography (CT) or magnetic resonance imaging (MRI)[16,48]. These approaches are predominantly employed for hepatocellular carcinoma screening or during LT protocols. However, they are not specifically recommended for muscle mass assessment due to their high costs, exposure to radiation, and a shortage of trained personnel for image analysis.

CT: A tomographic scan is taken at the L3 lumbar vertebra level, and specialized software is employed to delineate tissues based on hounsfield unit thresholds. Muscles within the L3 region encompass the psoas, erector spinae, quadratus lumborum, transversus abdominis, external and internal obliques, and rectus abdominis. Cross-sectional areas (cm^2) are automatically computed by summing tissue pixels and multiplying by pixel surface area[30,49].

The resulting muscle and adipose tissue cross-sectional areas are then adjusted for height (cm^2/m^2), yielding the L3 Skeletal Muscle Index (L3 SMI)[50].

Recent years have seen the development of specific cutoff values for cirrhosis. Presently, it is advised to utilize the cutoff values established by the North American expert consensus, which are validated and interpreted according to gender: L3 SMI < 39 cm^2/m^2 for women and < 50 cm^2/m^2 for men[51]. This method offers the advantage of maintaining diagnostic accuracy even in the presence of ascites. However, its practical application is restricted due to factors such as

radiation exposure, costs, and the necessity for standardized personnel to conduct measurements and interpretation.

MRI: This method utilizes an L3 vertebral level image, outlining areas expressed in pixels that are then converted into an area measurement (cm^2). This measurement is adjusted for the patient's height and shares the same interpretation as the L3 SMI since it uses the same cutoff points[51].

Similar to CT scans, it remains unaffected by ascites and offers the advantage of avoiding ionizing radiation, while also assisting in quantifying intrahepatic fat. However, limitations include its limited availability, cost, and the requirement for standardized personnel to analyze the images, rendering it less practical for routine monitoring.

Dual-energy X-ray absorptiometry: This method evaluates fat mass, lean mass, and bone mineral content. Using this data, muscle mass in the upper and lower limbs is calculated to eliminate the influence of ascites. After adjusting for height, the Appendicular SMI (ASMI) is derived[52]. A value below two standard deviations from the mean indicates muscle mass loss. Limitations involve potential overestimation of lean mass and inaccuracies due to edema. Nonetheless, the method's advantage is assessing bone mineral density, aiding in tailoring the dietary plan if osteopenia or osteoporosis is detected in the patient[49,53].

Other methods

Bioelectrical impedance analysis: Bioelectrical impedance analysis (BIA) is a common method for assessing body composition, including lean mass, fat mass, and body fluids. It works by measuring the resistance of body tissues to alternating current. However, the equations used in this method are derived from healthy populations and can be affected by fluid retention. Consequently, its use is not recommended due to its tendency to underestimate lean mass[39].

Vector analysis of bioelectrical impedance: This analysis was developed to enhance the diagnostic capabilities of conventional impedance. It utilizes direct data from BIA and standardizes them based on the patient's height. The process involves using software created by Piccoli *et al*[54], which graphically represents the data as a vector. Unlike predicting body composition, this analysis visually represents it as a bivariate vector, assessing both body composition and hydration status. The correlations between these variables lead to an elliptical distribution known as the RXc graph. This graph's normal distribution is derived from a healthy population, yielding three reference percentiles or tolerance ellipses at 50%, 75%, and 95%, specific to each gender. Values beyond the 95th percentile are considered abnormal. Hence, in clinical practice, the 50% and 75% ellipses are used as ranges of normality. Within the graph, there are quadrants with distinct values that offer qualitative insights. These values can be depicted as vectors and interpreted as follows: Hydration variations (edema or dehydration) without tissue structure changes align with the major axis of the tolerance ellipses. Changes in soft tissue quantity (lean and adipose) correspond to vector shifts along the minor axis of the ellipses. The method's advantage lies in its ability to simultaneously assess fluid presence and malnutrition, facilitating nutritional monitoring and diuretic treatment evaluation. It also enables comparisons of a patient's visits to the nutritionist and aims to position the patient within the ellipses of normality[55,56].

Phase angle: The phase angle (PA), derived from bioelectrical impedance measurements, relies on the body's conductivity properties, specifically the resistance and reactance. This metric mirrors the integrity of cell membranes and their ability to resist impedance currents. It is considered a useful tool that indicates the balance between cellular hydration and body mass, ultimately translating into tissue homeostasis and nutritional status. Low levels of the PA have been associated with inflammation and loss of muscle and fat mass in patients with conditions like cancer[57], human immunodeficiency virus[58] among others[59]. It has been validated in patients with cirrhosis from the Mexican population, where a PA of ≤ 4.9 has been observed to be associated with worse clinical outcomes[60,61].

Dynamometry: Dynamometry is a nutritional assessment method that measures muscle function by measuring grip strength with a dynamometer, often using a hand dynamometer. This approach has been verified across diverse populations, as weak grip strength has been linked to functional constraints, diminished quality of life, and heightened morbidity and mortality[62-64]. Grip strength reflects changes occurring in prominent muscle groups, even during the early phases of malnutrition, and likely isn't directly influenced by liver disease. There are specific cutoff points for men and women in different populations[65], where measurements below the mean are indicative of malnutrition or reduced functionality[64,66]. However, in individuals with cirrhosis, its reliability is hindered, particularly in patients with HE, even in mild forms, or those undergoing benzodiazepine therapy, due to cognitive and motor impairments that may skew the outcome[64].

Liver frailty index: To assess frailty, the Liver Frailty Index (LFI) is utilized, previously validated in the population with hepatic cirrhosis[23,67,68]. This index takes into account the following assessments: (1) Grip strength: It considers the average of three measurements taken on the subject's dominant hand using a hand dynamometer[65,66]; (2) Timed chair stands: Measured as the number of seconds it takes to perform five chair stands with the subject's arms crossed over their chest[23]; and (3) Balance test: It is evaluated by counting the number of seconds the subject can balance in three positions (feet placed side by side, semi-tandem, and tandem) for a maximum of 10 s each[23].

The results of each test are incorporated into the following formula (calculator available at http://Liverfrailtyindex.ucsf.edu): (-0.330 × gender - adjusted grip strength) + (-2.529 × number of chair stands per second) + (-0.040 × balance time) + 6. A patient is considered frail when they score > 4.5.

BIOCHEMICAL MARKERS

Biochemical markers play a crucial role in the clinical assessment of cirrhosis, including parameters like prothrombin time (INR), albumin, creatinine, and more[69]. However, the usefulness of these markers in nutritional evaluation is limited. The compromised hepatic synthesis in cirrhosis leads to reduced levels of serum albumin, prealbumin, transferrin, and prolonged INR, potentially leading to an overestimation of malnutrition prevalence. Moreover, creatinine, commonly used as a measure of malnutrition, can be inaccurate due to its sensitivity to renal function changes often present in these patients[70]. Additionally, the lymphocyte count is influenced by the disease, with lymphopenia often caused by hypersplenism due to portal hypertension in cirrhosis, making it an unreliable indicator of the patient's nutritional status.

CLINICAL EVALUATION

In the context of the nutritional care process, it is necessary to assess the presence of complications of cirrhosis, such as ascites and HE, as they can lead to deteriorated nutritional status. Timely identification of these complications allows for necessary adjustments in nutritional treatment.

Ascites

Ascites occurs due to disruptions in renal sodium excretion, resulting in a positive sodium balance, and subsequent fluid retention. This accumulation of fluids leads to an increase in extracellular volume. Decreased sodium excretion is primarily attributed to arterial vasodilation triggered by portal hypertension. This, in turn, activates the renin-angiotensin-aldosterone system and the sympathetic nervous system, causing renal vasoconstriction and sodium retention. Consequently, ascites and edema develop as a consequence of these physiological responses[71].

Ascites is classified into the following grades: Grade I: Mild, detectable only through ultrasound; Grade II: Moderate, evident by symmetrical abdominal distension; and Grade III: Severe and marked abdominal distension.

The cornerstone of ascites treatment is dietary sodium restriction in combination with loop diuretics and aldosterone antagonist diuretics, aiming to create a negative sodium balance that enhances urinary sodium excretion beyond dietary sodium intake[72]. However, dietary sodium restriction is effective in only around 14% of patients due to the poor adherence associated with such diets.

HE

HE is a condition characterized by brain dysfunction due to hepatic insufficiency or portosystemic shunting. It manifests as a wide range of neurological and psychiatric abnormalities, spanning from subtle or minimal presentations to a coma state. The West Haven Criteria serve as the standard for categorizing HE. The overt form encompasses minimal HE and West Haven grade I, whereas West Haven grades II to IV fall under the overt or clinically evident HE category[73]. In the minimal form of HE, observable signs and symptoms are absent, prompting the need for various psychometric and electrophysiological tests for diagnosis. These psychometric tests are straightforward to conduct, and a nutritionist with training in this domain can periodically administer them during consultations to identify the complication when it's not readily apparent. This facilitates necessary adjustments in nutritional treatment. While inadequate diet, low muscle mass, dehydration, and constipation play roles in HE development, early detection is crucial. However, it's important to note that many other unspecified nutritional factors can also contribute to the manifestation of this complication[74,75].

Other complications of cirrhosis

Additional important complications arise during the evaluation of patients with cirrhosis. Dysgeusia and/or dysphagia are frequently encountered in cirrhosis, influencing the patient's dietary intake and demanding consideration during nutritional interventions. For cases of dysgeusia, investigating deficiencies in zinc and B complex vitamins, which could contribute to this issue, is crucial. If deficiencies are identified, supplementing these micronutrients is advisable. Moreover, assessing the diet's palatability is essential, as stringent restrictions on seasonings and salt can affect consumption.

Following endoscopic variceal ligation, patients often experience recurring dysphagia. In such instances, a recommended approach involves softening, chopping, or pureeing solid foods to facilitate safe oral consumption while the patient recovers from dysphagia. Commercial thickeners can provide a valuable alternative by altering food texture and augmenting nutritional content, thus offering a solution for managing complex cases of dysphagia[76].

ASSESSING DIETARY INTAKE, FOR APPROPRIATE NUTRIONAL INTERVENTION

Assessing dietary intake is crucial for determining the quantity of energy and nutrients a patient regularly consumes, as well as for identifying early signs of inadequate intake. Properly identifying the specific needs of each patient and tailoring follow-up according to the disease stage will yield better outcomes. Various methods can be employed for dietary evaluation, including the use of 24-h recalls, food frequency questionnaires, or 3-d food diaries. The information gathered from these assessments serves to pinpoint potential obstacles to proper dietary consumption, personalize meal schedules, and implement strategies to ensure adherence to the prescribed diet plan. In general, opting for a 3-d food diary is preferred over a single 24-h recall or food frequency questionnaire, as it yields more comprehensive and less

biased information that can be both quantitatively and qualitatively assessed. These tools allow for the estimation of the patient's energy and protein intake, while also facilitating the monitoring of sodium, fluid, and micronutrient consumption[77].

Nutritional intervention must be individualized, addressing not only the primary liver disease but also any concurrent health issues (Figure 4). Patients with liver disease often have additional conditions like diabetes, chronic kidney disease, and dyslipidemia. Therefore, a comprehensive nutritional strategy should consider these factors. Following global guidelines and current scientific evidence for treating chronic hepatitis, the following recommendations are proposed:

Energy

The energy intake recommendations set forth by prominent international societies suggest a range of 30 to 40 kcal/kg/d [78]. However, the importance of tailoring this intake to the specific clinical context cannot be overstated. For patients without malnutrition, an appropriate range is 30 to 35 kcal/kg/d, while malnourished individuals may require 35 to 40 kcal/kg/d. In critically ill patients, the preferred method for determining energy expenditure is indirect calorimetry. In cases where this is not feasible, a minimum intake of 35 kcal/kg/d is advised. In instances of obesity and liver cirrhosis, an energy deficit of 500 to 800 kcal/d has been linked to weight loss[72].

When calculating nutritional requirements, the current weight is used for patients not experiencing fluid retention. However, in the presence of ascites or edema, the ideal or dry weight is considered. The dry weight corresponds to the weight after paracentesis, or the weight documented before fluid retention occurred. In cases where this data is unavailable, a percentage of weight is subtracted based on the severity of ascites (mild, 5%; moderate, 10%; and severe, 15%). An additional 5% reduction is applied if bilateral lower limb edema is present[78].

Macronutrients

Protein: The controversy surrounding protein intake is prominent in macronutrient recommendations. Current evidence suggests that protein restriction is not necessary, even in the presence of HE. Protein intake is determined at 1.0 to 1.5 g/kg/d, varying based on the level of malnutrition. For mild malnutrition, the suggestion is 1.0 to 1.2 g/kg/d, 1.3 to 1.4 g/kg/d for moderate malnutrition, and 1.5 g/kg/d for severe malnutrition. To enhance tolerance, it is recommended that 60% to 70% of the protein comes from plant sources[78,79].

Carbohydrates y lipids: In terms of carbohydrate recommendations, it is advised that they make up 45% to 65% of daily caloric intake. The remaining calories are suggested to be supplied by lipids[78,79].

Micronutrients

Micronutrient deficiencies are prevalent in cirrhosis. Nevertheless, it's advisable to provide vitamin and mineral supplementation solely to patients with either clinical suspicion or confirmed deficiency[21]. The goal is to restore normal serum levels.

Sodium: Managing sodium intake is crucial for patients with ascites or edema. The recommended approach involves limiting sodium consumption to 2000 to 2600 mg/d, which corresponds to 5.0 to 6.5 g/d of sodium chloride (NaCl)[80]. However, stricter limitations are not recommended due to the unpalatable nature of such diets, potentially leading to reduced calorie and protein intake and an increased risk of malnutrition[81]. Reducing sodium intake can lead to a 10%-20% reduction in fluid retention, particularly in patients experiencing initial episodes of fluid overload with adequate sodium excretion[17]. It's important to exercise caution when using salt substitutes, as they are high in potassium and could result in hyperkalemia. Offering proper nutritional guidance to patients and their families, including information about salt-to-sodium equivalencies, is essential. Additionally, identifying and limiting the consumption of high-sodium foods is crucial for effective management[82].

Zinc: Zinc deficiency in patients with cirrhosis has been linked to the development of HE due to its role in ammonia detoxification within the urea cycle. Moreover, inadequate zinc levels have been linked to weakened immune responses during bacterial infections and sepsis episodes[6,83,84]. Potential causes of zinc deficiency in cirrhosis include disrupted absorption in the digestive tract and heightened urinary excretion, often caused by diuretic usage that elevates urine output and lactulose contributing to gastrointestinal losses[85].

Vitamina D: Serum vitamin D levels decline with disease progression, and levels below 20 ng/mL are linked to an increased risk of hepatocellular carcinoma, disease decompensation, and increased mortality[86].

Therefore, regular monitoring of serum 25-hydroxyvitamin D levels is recommended. In cases of deficiency, supplementation is necessary to attain levels exceeding 30 ng/mL. For this purpose, a recommended dosage is 600 to 4000 IU/d of cholecalciferol (vitamin D3)[86]. Patients with a T-score lower than -1.5 standard deviations are advised to begin supplementation with calcium (1000 to 1500 mg/d) and vitamin D (400 to 800 IU/d)[87].

Others: Strategies have been devised to counteract fasting periods, and one such strategy involves incorporating a snack into the diet[88]. This approach not only enhances nutritional metabolism but also improves glucose tolerance and nutritional status[89]. By reducing fasting periods and minimizing the extent of gluconeogenesis, this strategy enhances the utilization of substrates for energy production. One of the supplementation methods employed is the use of formulas containing branched-chain amino acids (BCAAs), which have demonstrated remarkable effectiveness in improving both nutritional status and the management of associated complications. While a unanimous agreement on dosage does not yet exist, tested doses for BCAAs typically range from 0.15 g to 0.25 g per kilogram of body weight, which corresponds to 8 g to 20 g per day[90].

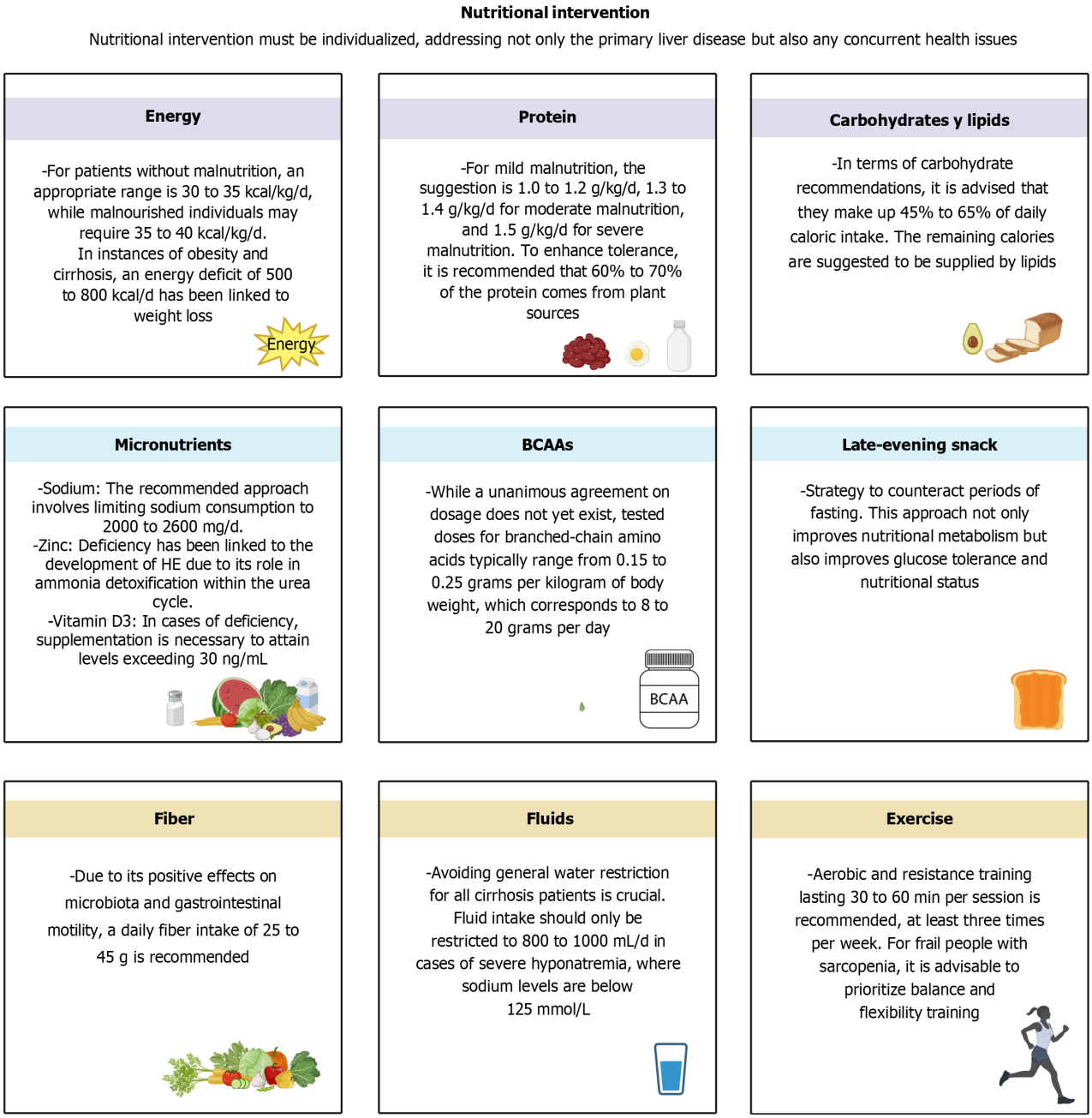

Figure 4 General recommendations for nutritional intervention in patients with cirrhosis. BCAAs: Branched-chain amino acids. Citation: The authors have obtained the permission for figure using from the BioRender.com (Supplementary material)[112].

Fiber

Due to its positive effects on microbiota and gastrointestinal motility, a daily fiber intake of 25 g to 45 g is recommended [19].

Fluids

Avoiding general water restriction for all cirrhosis patients is crucial. Fluid intake should only be restricted to 800 to 1000 mL/d in cases of severe hyponatremia, where sodium levels are below 125 mmol/L. Imposing fluid limitations on patients undergoing diuretic therapy can elevate the risk of dehydration[81].

Exercise

Physical exercise is a key component in clinical practice due to its widely recognized benefits in improving the prognosis of various chronic degenerative diseases. Initially, evidence discouraged exercise recommendation for cirrhotic patients due to its potential elevation of portal pressure. However, these findings were observed in a limited patient group and only during exercise routines; this effect normalized afterward, posing no elevated risk of complications linked to portal hypertension. Presently, clinical trials offer compelling evidence of exercise's positive impact, showing a reduction in portal pressure of around -2.5 mmHg[91,92]. Exercise guidelines for cirrhosis patients encompass a blend of aerobic and

resistance training lasting 30 min to 60 min per session, at least thrice weekly[93]. For frail individuals with sarcopenia, prioritizing balance and flexibility training is advisable, concentrating on bolstering postural muscles and expanding range of motion before delving into aerobic and resistance training[87]. Physiotherapists, especially those specializing in geriatrics, should be integrated into multidisciplinary teams to ensure comprehensive care for this patient population.

ALCOHOL-RELATED LIVER DISEASE

Alcohol-related liver disease (ALD), or alcoholic liver disease, encompasses a range of conditions starting with fatty liver and progressing to alcoholic hepatitis and cirrhosis. Patients with ALD exhibit a higher incidence of malnutrition, reported in at least 50% of both outpatients and hospitalized patients[94]. The compromised nutritional status can be attributed to various factors, including altered olfactory and taste perception[95], changes in appetite-related hormonal [96], lower absorption of nutrients[97] and alterations in intestinal microbiota[98].

Moreover, individuals with ALD commonly experience malnutrition, characterized by protein-energy malnutrition and deficiencies in specific nutrients[99].

One of the key contributors to the development of protein-calorie malnutrition is accelerated catabolism, primarily induced by patients who reduce their energy intake from food while relying on the caloric value of alcohol to meet their basal metabolic expenditure, thereby limiting the contribution of essential macronutrients and micronutrients[100].

Another significant factor is the loss of appetite, linked to the upregulation of inflammatory cytokines (IL-1b, IL-6, and IL-8), tumor necrosis factor (TNF-α), and leptin levels. This upregulation leads to decreased appetite and early satiety, playing a crucial role in the cachexia observed in various acute and chronic diseases[95]. TNF-α further influences metabolism by directly impacting the central nervous system, altering the release of neurotransmitters. This modulation slows intestinal motility and gastric emptying, influencing the patients' food choices[101].

Alcohol interferes with the absorption, storage, metabolism, and activation of certain water-soluble vitamins (thiamine, riboflavin, pyridoxine, ascorbic acid, and folic acid)[102]. Additionally, individuals with alcohol-related issues frequently exhibit zinc deficiency, a consistent biochemical/nutritional manifestation resulting from poor intestinal absorption[103]. In alcohol-related cirrhosis, along with reduced enteric absorption and increased urinary excretion of zinc, patients often adhere to diets lacking in protein and zinc. Zinc deficiency is a common cause of dysgeusia[104].

The consequences of zinc deficiency can manifest as acrodermatitis, anorexia, hypogonadism, impaired immune function, poor wound healing, night vision problems, diarrhea, issues with mental function, and an increased incidence of HE[20,105].

Wernicke encephalopathy can develop in patients with depleted thiamine stores, and clinically, it presents as confusion, oculomotor dysfunction, and ataxia. If left untreated, patients may develop Korsakoff syndrome, which is permanent and results in marked memory deficits[106,107]. Additionally, deficiencies in vitamin B12 and folic acid are prevalent and can lead to macrocytic anemia[108]. Moreover, chronic alcohol consumption disrupts vitamin A metabolism as it relies on the same pathways as alcohol metabolism. This alteration in metabolism results in the depletion of retinoid-binding proteins and increased excretion of retinoids into the bile, ultimately causing vitamin A deficiency [109].

For the management of ALD patients, it is crucial to advise and provide guidance on lifestyle habits such as diet and the cessation of alcohol consumption[99]. Routine nutritional assessments, dietitian involvement, and supplementation are recommended to enhance clinical outcomes in these patients[110]. Additionally, vitamins and trace elements should be consumed at least in the recommended daily amounts. Nutritional support has been demonstrated to improve nutritional status and abnormal liver tests[111].

In summary, nutritional therapy plays a vital role in addressing the complex nutritional needs of individuals with alcoholic liver disease, with the goal of improving clinical outcomes and addressing the challenges associated with this condition.

CONCLUSION

Patients with cirrhosis are at high risk of malnutrition, these patients should have adequate and timely nutritional evaluation, diagnosis, intervention, and monitoring. Dietary management of liver cirrhosis is complex and may require a multipronged approach to address issues of protein-energy malnutrition, muscle wasting, complications of fluid retention, and HE along with other symptoms that can impact nutritional intake. Currently the limited data support patients with liver cirrhosis receiving early nutritional intervention that is high in energy, protein, and carbohydrates, and incorporation of frequent meals, particularly with an additional late evening nutrient-dense snack. Unnecessary dietary restrictions in these patients should be minimized as much as possible. In addition, nutritionist involvement earlier on in the treatment algorithm is an important step to provide aggressive nutritional intervention and ameliorating the high rates of malnutrition in this patient population. Finally, there is an urgent need to bridge the evidence gap between dietary intervention trials and clinical practice, with a bigger focus on the manipulation of whole diets.

FOOTNOTES

Author contributions: Mendez-Guerrero O, Carranza-Carrasco A, Chi-Cervera LA, and Torre A performed the literature revision, collected the data, and wrote the manuscript; Navarro-Alvarez N wrote, reviewed, and edited the manuscript.

Conflict-of-interest statement: The authors declare that they have no conflict of interest.

Country/Territory of origin: Mexico

ORCID number: Osvely Mendez-Guerrero 0000-0002-9308-9352; Luis Alberto Chi-Cervera 0000-0002-3335-8178; Aldo Torre 0000-0002-9299-3075; Nalu Navarro-Alvarez 0000-0003-0118-4676.

S-Editor: Chen YL
L-Editor: A
P-Editor: Zheng XM

REFERENCES

1 **Liu YB**, Chen MK. Epidemiology of liver cirrhosis and associated complications: Current knowledge and future directions. *World J Gastroenterol* 2022; **28**: 5910-5930 [PMID: 36405106 DOI: 10.3748/wjg.v28.i41.5910]
2 **Ginès P**, Krag A, Abraldes JG, Solà E, Fabrellas N, Kamath PS. Liver cirrhosis. *Lancet* 2021; **398**: 1359-1376 [PMID: 34543610 DOI: 10.1016/S0140-6736(21)01374-X]
3 **D'Amico G**, Garcia-Tsao G, Pagliaro L. Natural history and prognostic indicators of survival in cirrhosis: a systematic review of 118 studies. *J Hepatol* 2006; **44**: 217-231 [PMID: 16298014 DOI: 10.1016/j.jhep.2005.10.013]
4 **Glass C**, Hipskind P, Tsien C, Malin SK, Kasumov T, Shah SN, Kirwan JP, Dasarathy S. Sarcopenia and a physiologically low respiratory quotient in patients with cirrhosis: a prospective controlled study. *J Appl Physiol (1985)* 2013; **114**: 559-565 [PMID: 23288550 DOI: 10.1152/japplphysiol.01042.2012]
5 **Müller MJ**, Böttcher J, Selberg O, Weselmann S, Böker KH, Schwarze M, von zur Mühlen A, Manns MP. Hypermetabolism in clinically stable patients with liver cirrhosis. *Am J Clin Nutr* 1999; **69**: 1194-1201 [PMID: 10357739 DOI: 10.1093/ajcn/69.6.1194]
6 **Marchesini G**, Fabbri A, Bianchi G, Brizi M, Zoli M. Zinc supplementation and amino acid-nitrogen metabolism in patients with advanced cirrhosis. *Hepatology* 1996; **23**: 1084-1092 [PMID: 8621138 DOI: 10.1053/jhep.1996.v23.pm0008621138]
7 **Tandon P**, Montano-Loza AJ, Lai JC, Dasarathy S, Merli M. Sarcopenia and frailty in decompensated cirrhosis. *J Hepatol* 2021; **75** Suppl 1: S147-S162 [PMID: 34039486 DOI: 10.1016/j.jhep.2021.01.025]
8 **Göktürk HS**, Selçuk H. Importance of malnutrition in patients with cirrhosis. *Turk J Gastroenterol* 2015; **26**: 291-296 [PMID: 26038997 DOI: 10.5152/tjg.2015.0224]
9 **Maharshi S**, Sharma BC, Srivastava S. Malnutrition in cirrhosis increases morbidity and mortality. *J Gastroenterol Hepatol* 2015; **30**: 1507-1513 [PMID: 25974421 DOI: 10.1111/jgh.12999]
10 **Papatheodoridis GV**, Cholongitas E, Dimitriadou E, Touloumi G, Sevastianos V, Archimandritis AJ. MELD vs Child-Pugh and creatinine-modified Child-Pugh score for predicting survival in patients with decompensated cirrhosis. *World J Gastroenterol* 2005; **11**: 3099-3104 [PMID: 15918197 DOI: 10.3748/wjg.v11.i20.3099]
11 **Wiesner R**, Edwards E, Freeman R, Harper A, Kim R, Kamath P, Kremers W, Lake J, Howard T, Merion RM, Wolfe RA, Krom R; United Network for Organ Sharing Liver Disease Severity Score Committee. Model for end-stage liver disease (MELD) and allocation of donor livers. *Gastroenterology* 2003; **124**: 91-96 [PMID: 12512033 DOI: 10.1053/gast.2003.50016]
12 **Montano-Loza AJ**, Ronca V, Ebadi M, Hansen BE, Hirschfield G, Elwir S, Alsaed M, Milkiewicz P, Janik MK, Marschall HU, Burza MA, Efe C, Calışkan AR, Harputluoglu M, Kabaçam G, Terrabuio D, de Quadros Onofrio F, Selzner N, Bonder A, Parés A, Llovet L, Akyıldız M, Arikan C, Manns MP, Taubert R, Weber AL, Schiano TD, Haydel B, Czubkowski P, Socha P, Ołdak N, Akamatsu N, Tanaka A, Levy C, Martin EF, Goel A, Sedki M, Jankowska I, Ikegami T, Rodriguez M, Sterneck M, Weiler-Normann C, Schramm C, Donato MF, Lohse A, Andrade RJ, Patwardhan VR, van Hoek B, Biewenga M, Kremer AE, Ueda Y, Deneau M, Pedersen M, Mayo MJ, Floreani A, Burra P, Secchi MF, Beretta-Piccoli BT, Sciveres M, Maggiore G, Jafri SM, Debray D, Girard M, Lacaille F, Lytvyak E, Mason AL, Heneghan M, Oo YH; International Autoimmune Hepatitis Group (IAIHG). Risk factors and outcomes associated with recurrent autoimmune hepatitis following liver transplantation. *J Hepatol* 2022; **77**: 84-97 [PMID: 35143897 DOI: 10.1016/j.jhep.2022.01.022]
13 **Bodzin AS**, Baker TB. Liver Transplantation Today: Where We Are Now and Where We Are Going. *Liver Transpl* 2018; **24**: 1470-1475 [PMID: 30080954 DOI: 10.1002/lt.25320]
14 **Lai JC**, Tandon P, Bernal W, Tapper EB, Ekong U, Dasarathy S, Carey EJ. Malnutrition, Frailty, and Sarcopenia in Patients With Cirrhosis: 2021 Practice Guidance by the American Association for the Study of Liver Diseases. *Hepatology* 2021; **74**: 1611-1644 [PMID: 34233031 DOI: 10.1002/hep.32049]
15 **Periyalwar P**, Dasarathy S. Malnutrition in cirrhosis: contribution and consequences of sarcopenia on metabolic and clinical responses. *Clin Liver Dis* 2012; **16**: 95-131 [PMID: 22321468 DOI: 10.1016/j.cld.2011.12.009]
16 **Montano-Loza AJ**, Meza-Junco J, Prado CM, Lieffers JR, Baracos VE, Bain VG, Sawyer MB. Muscle wasting is associated with mortality in patients with cirrhosis. *Clin Gastroenterol Hepatol* 2012; **10**: 166-173, 173.e1 [PMID: 21893129 DOI: 10.1016/j.cgh.2011.08.028]
17 **Biggins SW**, Angeli P, Garcia-Tsao G, Ginès P, Ling SC, Nadim MK, Wong F, Kim WR. Diagnosis, Evaluation, and Management of Ascites,

Spontaneous Bacterial Peritonitis and Hepatorenal Syndrome: 2021 Practice Guidance by the American Association for the Study of Liver Diseases. *Hepatology* 2021; **74**: 1014-1048 [PMID: 33942342 DOI: 10.1002/hep.31884]

18 **Bajaj JS**, O'Leary JG, Tandon P, Wong F, Garcia-Tsao G, Kamath PS, Maliakkal B, Biggins SW, Thuluvath PJ, Fallon MB, Subramanian RM, Vargas HE, Lai J, Thacker LR, Reddy KR. Hepatic Encephalopathy Is Associated With Mortality in Patients With Cirrhosis Independent of Other Extrahepatic Organ Failures. *Clin Gastroenterol Hepatol* 2017; **15**: 565-574.e4 [PMID: 27720916 DOI: 10.1016/j.cgh.2016.09.157]

19 **Amodio P**, Bemeur C, Butterworth R, Cordoba J, Kato A, Montagnese S, Uribe M, Vilstrup H, Morgan MY. The nutritional management of hepatic encephalopathy in patients with cirrhosis: International Society for Hepatic Encephalopathy and Nitrogen Metabolism Consensus. *Hepatology* 2013; **58**: 325-336 [PMID: 23471642 DOI: 10.1002/hep.26370]

20 **Nishikawa H**, Enomoto H, Yoh K, Iwata Y, Sakai Y, Kishino K, Ikeda N, Takashima T, Aizawa N, Takata R, Hasegawa K, Ishii N, Yuri Y, Nishimura T, Iijima H, Nishiguchi S. Serum Zinc Concentration and Sarcopenia: A Close Linkage in Chronic Liver Diseases. *J Clin Med* 2019; **8** [PMID: 30862022 DOI: 10.3390/jcm8030336]

21 **Stirnimann J**, Stirnimann G. Nutritional Challenges in Patients with Advanced Liver Cirrhosis. *J Clin Med* 2019; **8** [PMID: 31717529 DOI: 10.3390/jcm8111926]

22 **Cruz-Jentoft AJ**, Bahat G, Bauer J, Boirie Y, Bruyère O, Cederholm T, Cooper C, Landi F, Rolland Y, Sayer AA, Schneider SM, Sieber CC, Topinkova E, Vandewoude M, Visser M, Zamboni M; Writing Group for the European Working Group on Sarcopenia in Older People 2 (EWGSOP2), and the Extended Group for EWGSOP2. Sarcopenia: revised European consensus on definition and diagnosis. *Age Ageing* 2019; **48**: 16-31 [PMID: 30312372 DOI: 10.1093/ageing/afy169]

23 **Lai JC**, Covinsky KE, Dodge JL, Boscardin WJ, Segev DL, Roberts JP, Feng S. Development of a novel frailty index to predict mortality in patients with end-stage liver disease. *Hepatology* 2017; **66**: 564-574 [PMID: 28422306 DOI: 10.1002/hep.29219]

24 **McPherron AC**, Lawler AM, Lee SJ. Regulation of skeletal muscle mass in mice by a new TGF-beta superfamily member. *Nature* 1997; **387**: 83-90 [PMID: 9139826 DOI: 10.1038/387083a0]

25 **Nardelli S**, Lattanzi B, Merli M, Farcomeni A, Gioia S, Ridola L, Riggio O. Muscle Alterations Are Associated With Minimal and Overt Hepatic Encephalopathy in Patients With Liver Cirrhosis. *Hepatology* 2019; **70**: 1704-1713 [PMID: 31038758 DOI: 10.1002/hep.30692]

26 **Wallner C**, Wagner JM, Dittfeld S, Drysch M, Lehnhardt M, Behr B. Myostatin serum concentration as an indicator for deviated muscle metabolism in severe burn injuries. *Scand J Surg* 2019; **108**: 297-304 [PMID: 30474468 DOI: 10.1177/1457496918812230]

27 **Merli M**. Nutrition in cirrhosis: Dos and Don'ts. *J Hepatol* 2020; **73**: 1563-1565 [PMID: 32891430 DOI: 10.1016/j.jhep.2020.07.019]

28 **Masuda T**, Shirabe K, Ikegami T, Harimoto N, Yoshizumi T, Soejima Y, Uchiyama H, Ikeda T, Baba H, Maehara Y. Sarcopenia is a prognostic factor in living donor liver transplantation. *Liver Transpl* 2014; **20**: 401-407 [PMID: 24357065 DOI: 10.1002/lt.23811]

29 **Krell RW**, Kaul DR, Martin AR, Englesbe MJ, Sonnenday CJ, Cai S, Malani PN. Association between sarcopenia and the risk of serious infection among adults undergoing liver transplantation. *Liver Transpl* 2013; **19**: 1396-1402 [PMID: 24151041 DOI: 10.1002/lt.23752]

30 **Bhanji RA**, Moctezuma-Velazquez C, Duarte-Rojo A, Ebadi M, Ghosh S, Rose C, Montano-Loza AJ. Myosteatosis and sarcopenia are associated with hepatic encephalopathy in patients with cirrhosis. *Hepatol Int* 2018; **12**: 377-386 [PMID: 29881992 DOI: 10.1007/s12072-018-9875-9]

31 **Montano-Loza AJ**, Meza-Junco J, Baracos VE, Prado CM, Ma M, Meeberg G, Beaumont C, Tandon P, Esfandiari N, Sawyer MB, Kneteman N. Severe muscle depletion predicts postoperative length of stay but is not associated with survival after liver transplantation. *Liver Transpl* 2014; **20**: 640-648 [PMID: 24678005 DOI: 10.1002/lt.23863]

32 **Norman K**, Kirchner H, Lochs H, Pirlich M. Malnutrition affects quality of life in gastroenterology patients. *World J Gastroenterol* 2006; **12**: 3380-3385 [PMID: 16733855 DOI: 10.3748/wjg.v12.i21.3385]

33 **Montano-Loza AJ**, Duarte-Rojo A, Meza-Junco J, Baracos VE, Sawyer MB, Pang JX, Beaumont C, Esfandiari N, Myers RP. Inclusion of Sarcopenia Within MELD (MELD-Sarcopenia) and the Prediction of Mortality in Patients With Cirrhosis. *Clin Transl Gastroenterol* 2015; **6**: e102 [PMID: 26181291 DOI: 10.1038/ctg.2015.31]

34 **Cederholm T**, Jensen GL, Correia MITD, Gonzalez MC, Fukushima R, Higashiguchi T, Baptista G, Barazzoni R, Blaauw R, Coats A, Crivelli A, Evans DC, Gramlich L, Fuchs-Tarlovsky V, Keller H, Llido L, Malone A, Mogensen KM, Morley JE, Muscaritoli M, Nyulasi I, Pirlich M, Pisprasert V, de van der Schueren MAE, Siltharm S, Singer P, Tappenden K, Velasco N, Waitzberg D, Yamwong P, Yu J, Van Gossum A, Compher C; GLIM Core Leadership Committee; GLIM Working Group. GLIM criteria for the diagnosis of malnutrition - A consensus report from the global clinical nutrition community. *Clin Nutr* 2019; **38**: 1-9 [PMID: 30181091 DOI: 10.1016/j.clnu.2018.08.002]

35 **European Association for the Study of the Liver**. EASL Clinical Practice Guidelines on nutrition in chronic liver disease. *J Hepatol* 2019; **70**: 172-193 [PMID: 30144956 DOI: 10.1016/j.jhep.2018.06.024]

36 **Charney P**. Nutrition screening vs nutrition assessment: how do they differ? *Nutr Clin Pract* 2008; **23**: 366-372 [PMID: 18682587 DOI: 10.1177/0884533608321131]

37 **Skipper A**, Ferguson M, Thompson K, Castellanos VH, Porcari J. Nutrition screening tools: an analysis of the evidence. *JPEN J Parenter Enteral Nutr* 2012; **36**: 292-298 [PMID: 22045723 DOI: 10.1177/0148607111414023]

38 **Morgan MY**, Madden AM, Soulsby CT, Morris RW. Derivation and validation of a new global method for assessing nutritional status in patients with cirrhosis. *Hepatology* 2006; **44**: 823-835 [PMID: 17006918 DOI: 10.1002/hep.21358]

39 **Morgan MY**, Madden AM, Jennings G, Elia M, Fuller NJ. Two-component models are of limited value for the assessment of body composition in patients with cirrhosis. *Am J Clin Nutr* 2006; **84**: 1151-1162 [PMID: 17093169 DOI: 10.1093/ajcn/84.5.1151]

40 **Georgiou A**, Papatheodoridis GV, Alexopoulou A, Deutsch M, Vlachogiannakos I, Ioannidou P, Papageorgiou MV, Papadopoulos N, Tsibouris P, Prapa A, Yannakoulia M, Kontogianni MD. Evaluation of the effectiveness of eight screening tools in detecting risk of malnutrition in cirrhotic patients: the KIRRHOS study. *Br J Nutr* 2019; **122**: 1368-1376 [PMID: 31735186 DOI: 10.1017/S0007114519002277]

41 **Plauth M**, Bernal W, Dasarathy S, Merli M, Plank LD, Schütz T, Bischoff SC. ESPEN guideline on clinical nutrition in liver disease. *Clin Nutr* 2019; **38**: 485-521 [PMID: 30712783 DOI: 10.1016/j.clnu.2018.12.022]

42 **Wu Y**, Zhu Y, Feng Y, Wang R, Yao N, Zhang M, Liu X, Liu H, Shi L, Zhu L, Yang N, Chen H, Liu J, Zhao Y, Yang Y. Royal Free Hospital-Nutritional Prioritizing Tool improves the prediction of malnutrition risk outcomes in liver cirrhosis patients compared with Nutritional Risk Screening 2002. *Br J Nutr* 2020; **124**: 1293-1302 [PMID: 32600494 DOI: 10.1017/S0007114520002366]

43 **Grant JP**, Custer PB, Thurlow J. Current techniques of nutritional assessment. *Surg Clin North Am* 1981; **61**: 437-463 [PMID: 7020129 DOI: 10.1016/s0039-6109(16)42430-8]

44 **Osuna I**. Soporte Nutricional de Bolsillo. 2019. [cited 20 January 2024]. Available from: http://www.institutoisabellacatolica.com/materiales/

Soporte%20nutricional%20de%20bolsillo.pdf
45 **Frisancho AR**. New norms of upper limb fat and muscle areas for assessment of nutritional status. *Am J Clin Nutr* 1981; **34**: 2540-2545 [PMID: 6975564 DOI: 10.1093/ajcn/34.11.2540]
46 **Frisancho AR**. New standards of weight and body composition by frame size and height for assessment of nutritional status of adults and the elderly. *Am J Clin Nutr* 1984; **40**: 808-819 [PMID: 6486088 DOI: 10.1093/ajcn/40.4.808]
47 **Vieira PM**, De-Souza DA, Oliveira LCM. Evaluación nutricional en cirrosis hepática; los parámetros clínicos, antropométricos, bioquímicos y hematológicos. *Nutr Hosp* 2013; **28**: 1615-1621 [DOI: 10.3305/nh.2013.28.5.6563]
48 **Heymsfield SB**. Development of imaging methods to assess adiposity and metabolism. *Int J Obes (Lond)* 2008; **32** Suppl 7: S76-S82 [PMID: 19136995 DOI: 10.1038/ijo.2008.242]
49 **Mourtzakis M**, Prado CM, Lieffers JR, Reiman T, McCargar LJ, Baracos VE. A practical and precise approach to quantification of body composition in cancer patients using computed tomography images acquired during routine care. *Appl Physiol Nutr Metab* 2008; **33**: 997-1006 [PMID: 18923576 DOI: 10.1139/H08-075]
50 **Ebadi M**, Wang CW, Lai JC, Dasarathy S, Kappus MR, Dunn MA, Carey EJ, Montano-Loza AJ; From the Fitness, Life Enhancement, and Exercise in Liver Transplantation (FLEXIT) Consortium. Poor performance of psoas muscle index for identification of patients with higher waitlist mortality risk in cirrhosis. *J Cachexia Sarcopenia Muscle* 2018; **9**: 1053-1062 [PMID: 30269421 DOI: 10.1002/jcsm.12349]
51 **Carey EJ**, Lai JC, Sonnenday C, Tapper EB, Tandon P, Duarte-Rojo A, Dunn MA, Tsien C, Kallwitz ER, Ng V, Dasarathy S, Kappus M, Bashir MR, Montano-Loza AJ. A North American Expert Opinion Statement on Sarcopenia in Liver Transplantation. *Hepatology* 2019; **70**: 1816-1829 [PMID: 31220351 DOI: 10.1002/hep.30828]
52 **Belarmino G**, Gonzalez MC, Sala P, Torrinhas RS, Andraus W, D'Albuquerque LAC, Pereira RMR, Caparbo VF, Ferrioli E, Pfrimer K, Damiani L, Heymsfield SB, Waitzberg DL. Diagnosing Sarcopenia in Male Patients With Cirrhosis by Dual-Energy X-Ray Absorptiometry Estimates of Appendicular Skeletal Muscle Mass. *JPEN J Parenter Enteral Nutr* 2018; **42**: 24-36 [PMID: 28402708 DOI: 10.1177/0148607117701400]
53 **Giusto M**, Lattanzi B, Albanese C, Galtieri A, Farcomeni A, Giannelli V, Lucidi C, Di Martino M, Catalano C, Merli M. Sarcopenia in liver cirrhosis: the role of computed tomography scan for the assessment of muscle mass compared with dual-energy X-ray absorptiometry and anthropometry. *Eur J Gastroenterol Hepatol* 2015; **27**: 328-334 [PMID: 25569567 DOI: 10.1097/MEG.0000000000000274]
54 **Piccoli A**, Rossi B, Pillon L, Bucciante G. A new method for monitoring body fluid variation by bioimpedance analysis: the RXc graph. *Kidney Int* 1994; **46**: 534-539 [PMID: 7967368 DOI: 10.1038/ki.1994.305]
55 **Espinosa-Cuevas MDLÁ**, Rivas-Rodríguez L, González-Medina EC, Atilano-Carsi X, Miranda-Alatriste P, Correa-Rotter R. Vectores de impedancia bioeléctrica para la composición corporal en población mexicana. *Rev Invest Clin* 2007; **59**: 15-24
56 **Ruiz-Margáin A**, Macías-Rodríguez RU, Duarte-Rojo A, Ríos-Torres SL, Espinosa-Cuevas Á, Torre A. Malnutrition assessed through phase angle and its relation to prognosis in patients with compensated liver cirrhosis: a prospective cohort study. *Dig Liver Dis* 2015; **47**: 309-314 [PMID: 25618555 DOI: 10.1016/j.dld.2014.12.015]
57 **Mohamed Sad L**, Elsaka AM, Abdelmonem Zamzam Y, Gharib Khairallah F. Phase angle, body mass index and KRAS status of metastatic colorectal cancer in response to chemotherapy with and without target therapy: clinical impact and survival. *J BUON* 2020; **25**: 914-926 [PMID: 32521886]
58 **Llames L**, Baldomero V, Iglesias ML, Rodota LP. Values of the phase angle by bioelectrical impedance: nutritional status and prognostic value. *Nutr Hosp* 2013; **28**: 286-295 [DOI: 10.3305/nh.2013.28.2.6306]
59 **Osuna-Padilla IA**, Rodríguez-Moguel NC, Rodríguez-Llamazares S, Aguilar-Vargas A, Casas-Aparicio GA, Ríos-Ayala MA, Hernández-Cardenas CM. Low phase angle is associated with 60-day mortality in critically ill patients with COVID-19. *JPEN J Parenter Enteral Nutr* 2022; **46**: 828-835 [PMID: 34291834 DOI: 10.1002/jpen.2236]
60 **Ruiz-Margáin A**, Macías-Rodríguez RU, Ampuero J, Cubero FJ, Chi-Cervera L, Ríos-Torres SL, Duarte-Rojo A, Espinosa-Cuevas Á, Romero-Gómez M, Torre A. Low phase angle is associated with the development of hepatic encephalopathy in patients with cirrhosis. *World J Gastroenterol* 2016; **22**: 10064-10070 [PMID: 28018114 DOI: 10.3748/wjg.v22.i45.10064]
61 **Barbosa-Silva MC**, Barros AJ, Wang J, Heymsfield SB, Pierson RN Jr. Bioelectrical impedance analysis: population reference values for phase angle by age and sex. *Am J Clin Nutr* 2005; **82**: 49-52 [PMID: 16002799 DOI: 10.1093/ajcn.82.1.49]
62 **Luong R**, Kim M, Lee A, Carey S. Assessing nutritional status in a cohort of liver cirrhosis outpatients: A prospective cross-sectional study. *Nutr Health* 2020; **26**: 19-25 [PMID: 31779515 DOI: 10.1177/0260106019888362]
63 **Hanai T**, Shiraki M, Imai K, Suetsugu A, Takai K, Moriwaki H, Shimizu M. Reduced handgrip strength is predictive of poor survival among patients with liver cirrhosis: A sex-stratified analysis. *Hepatol Res* 2019; **49**: 1414-1426 [PMID: 31408558 DOI: 10.1111/hepr.13420]
64 **Alvares-da-Silva MR**, Reverbel da Silveira T. Comparison between handgrip strength, subjective global assessment, and prognostic nutritional index in assessing malnutrition and predicting clinical outcome in cirrhotic outpatients. *Nutrition* 2005; **21**: 113-117 [PMID: 15723736 DOI: 10.1016/j.nut.2004.02.002]
65 **Rodríguez-García WD**, García-Castañeda L, Orea-Tejeda A, Mendoza-Núñez V, González-Islas D, Santillán-Díaz C, Castillo-Martínez L. Handgrip strength: Reference values and its relationship with bioimpedance and anthropometric variables. *Clin Nutr ESPEN* 2017; **19**: 54-58 [DOI: 10.1016/j.clnesp.2017.01.010]
66 **Budziareck MB**, Pureza Duarte RR, Barbosa-Silva MC. Reference values and determinants for handgrip strength in healthy subjects. *Clin Nutr* 2008; **27**: 357-362 [PMID: 18455840 DOI: 10.1016/j.clnu.2008.03.008]
67 **Lai JC**, Dodge JL, Kappus MR, Dunn MA, Volk ML, Duarte-Rojo A, Ganger DR, Rahimi RS, McCulloch CE, Haugen CE, McAdams-DeMarco M, Ladner DP, Segev DL, Verna EC; Multi-Center Functional Assessment in Liver Transplantation (FrAILT) Study. Changes in frailty are associated with waitlist mortality in patients with cirrhosis. *J Hepatol* 2020; **73**: 575-581 [PMID: 32240717 DOI: 10.1016/j.jhep.2020.03.029]
68 **Lai JC**, Rahimi RS, Verna EC, Kappus MR, Dunn MA, McAdams-DeMarco M, Haugen CE, Volk ML, Duarte-Rojo A, Ganger DR, O'Leary JG, Dodge JL, Ladner D, Segev DL. Frailty Associated With Waitlist Mortality Independent of Ascites and Hepatic Encephalopathy in a Multicenter Study. *Gastroenterology* 2019; **156**: 1675-1682 [PMID: 30668935 DOI: 10.1053/j.gastro.2019.01.028]
69 **Francoz C**, Prié D, Abdelrazek W, Moreau R, Mandot A, Belghiti J, Valla D, Durand F. Inaccuracies of creatinine and creatinine-based equations in candidates for liver transplantation with low creatinine: impact on the model for end-stage liver disease score. *Liver Transpl* 2010; **16**: 1169-1177 [PMID: 20879015 DOI: 10.1002/lt.22128]
70 **Moore KP**, Wong F, Gines P, Bernardi M, Ochs A, Salerno F, Angeli P, Porayko M, Moreau R, Garcia-Tsao G, Jimenez W, Planas R, Arroyo

V. The management of ascites in cirrhosis: report on the consensus conference of the International Ascites Club. *Hepatology* 2003; **38**: 258-266 [PMID: 12830009 DOI: 10.1053/jhep.2003.50315]

71 **European Association for the Study of the Liver**. EASL clinical practice guidelines on the management of ascites, spontaneous bacterial peritonitis, and hepatorenal syndrome in cirrhosis. *J Hepatol* 2010; **53**: 397-417 [PMID: 20633946 DOI: 10.1016/j.jhep.2010.05.004]

72 **European Association for the Study of the Liver**. EASL Clinical Practice Guidelines for the management of patients with decompensated cirrhosis. *J Hepatol* 2018; **69**: 406-460 [PMID: 29653741 DOI: 10.1016/j.jhep.2018.03.024]

73 **Vilstrup H**, Amodio P, Bajaj J, Cordoba J, Ferenci P, Mullen KD, Weissenborn K, Wong P. Hepatic encephalopathy in chronic liver disease: 2014 Practice Guideline by the American Association for the Study of Liver Diseases and the European Association for the Study of the Liver. *Hepatology* 2014; **60**: 715-735 [PMID: 25042402 DOI: 10.1002/hep.27210]

74 **Duarte-Rojo A**, Estradas J, Hernández-Ramos R, Ponce-de-León S, Córdoba J, Torre A. Validation of the psychometric hepatic encephalopathy score (PHES) for identifying patients with minimal hepatic encephalopathy. *Dig Dis Sci* 2011; **56**: 3014-3023 [PMID: 21461913 DOI: 10.1007/s10620-011-1684-0]

75 **Luo M**, Ma P, Li L, Cao WK. Advances in psychometric tests for screening minimal hepatic encephalopathy: From paper-and-pencil to computer-aided assessment. *Turk J Gastroenterol* 2019; **30**: 398-407 [PMID: 31060994 DOI: 10.5152/tjg.2019.18226]

76 **Rofes L**, Arreola V, Almirall J, Cabré M, Campins L, García-Peris P, Speyer R, Clavé P. Diagnosis and management of oropharyngeal Dysphagia and its nutritional and respiratory complications in the elderly. *Gastroenterol Res Pract* 2011; **2011** [PMID: 20811545 DOI: 10.1155/2011/818979]

77 Dietary Reference Intakes for Vitamin A, Vitamin K, Arsenic, Boron, Chromium, Copper, Iodine, Iron, Manganese, Molybdenum, Nickel, Silicon, Vanadium, and Zinc. Washington (DC): National Academies Press (US); 2001– [PMID: 25057538 DOI: 10.17226/10026]

78 **Bischoff SC**, Bernal W, Dasarathy S, Merli M, Plank LD, Schütz T, Plauth M, Burgos Peláez R, Rivera Irigoin R. [ESPEN Practical Guideline: clinical nutrition in liver disease]. *Nutr Hosp* 2022; **39**: 434-472 [PMID: 35014850 DOI: 10.20960/nh.03856]

79 **Bischoff SC**, Bernal W, Dasarathy S, Merli M, Plank LD, Schütz T, Plauth M. ESPEN practical guideline: Clinical nutrition in liver disease. *Clin Nutr* 2020; **39**: 3533-3562 [PMID: 33213977 DOI: 10.1016/j.clnu.2020.09.001]

80 **Kumar R**, Marrapu S. Dietary salt in liver cirrhosis: With a pinch of salt! *World J Hepatol* 2023; **15**: 1084-1090 [PMID: 37970619 DOI: 10.4254/wjh.v15.i10.1084]

81 **Runyon BA**; AASLD. Introduction to the revised American Association for the Study of Liver Diseases Practice Guideline management of adult patients with ascites due to cirrhosis 2012. *Hepatology* 2013; **57**: 1651-1653 [PMID: 23463403 DOI: 10.1002/hep.26359]

82 **Wong F**. Management of ascites in cirrhosis. *J Gastroenterol Hepatol* 2012; **27**: 11-20 [PMID: 21916992 DOI: 10.1111/j.1440-1746.2011.06925.x]

83 **Dhanda A**, Atkinson S, Vergis N, Enki D, Fisher A, Clough R, Cramp M, Thursz M. Trace element deficiency is highly prevalent and associated with infection and mortality in patients with alcoholic hepatitis. *Aliment Pharmacol Ther* 2020; **52**: 537-544 [PMID: 32573823 DOI: 10.1111/apt.15880]

84 **Katayama K**. Zinc and protein metabolism in chronic liver diseases. *Nutr Res* 2020; **74**: 1-9 [PMID: 31891865 DOI: 10.1016/j.nutres.2019.11.009]

85 **Reding P**, Duchateau J, Bataille C. Oral zinc supplementation improves hepatic encephalopathy. Results of a randomised controlled trial. *Lancet* 1984; **2**: 493-495 [PMID: 6147551 DOI: 10.1016/s0140-6736(84)92567-4]

86 **Vieth R**, Kimball S, Hu A, Walfish PG. Randomized comparison of the effects of the vitamin D3 adequate intake versus 100 mcg (4000 IU) per day on biochemical responses and the wellbeing of patients. *Nutr J* 2004; **3**: 8 [PMID: 15260882 DOI: 10.1186/1475-2891-3-8]

87 **Juakiem W**, Torres DM, Harrison SA. Nutrition in cirrhosis and chronic liver disease. *Clin Liver Dis* 2014; **18**: 179-190 [PMID: 24274873 DOI: 10.1016/j.cld.2013.09.004]

88 **Hanai T**, Shiraki M, Imai K, Suetsugu A, Takai K, Shimizu M. Late Evening Snack with Branched-Chain Amino Acids Supplementation Improves Survival in Patients with Cirrhosis. *J Clin Med* 2020; **9** [PMID: 32260139 DOI: 10.3390/jcm9041013]

89 **Leoni L**, Valoriani F, Barbieri R, Pambianco M, Vinciguerra M, Sicuro C, Colecchia A, Menozzi R, Ravaioli F. Unlocking the Power of Late-Evening Snacks: Practical Ready-to-Prescribe Chart Menu for Patients with Cirrhosis. *Nutrients* 2023; **15** [PMID: 37571408 DOI: 10.3390/nu15153471]

90 **Ruiz-Margáin A**, Macías-Rodríguez RU, Ríos-Torres SL, Román-Calleja BM, Méndez-Guerrero O, Rodríguez-Córdova P, Torre A. Effect of a high-protein, high-fiber diet plus supplementation with branched-chain amino acids on the nutritional status of patients with cirrhosis. *Rev Gastroenterol Mex (Engl Ed)* 2018; **83**: 9-15 [PMID: 28408059 DOI: 10.1016/j.rgmx.2017.02.005]

91 **Macías-Rodríguez RU**, Ilarraza-Lomelí H, Ruiz-Margáin A, Ponce-de-León-Rosales S, Vargas-Vorácková F, García-Flores O, Torre A, Duarte-Rojo A. Changes in Hepatic Venous Pressure Gradient Induced by Physical Exercise in Cirrhosis: Results of a Pilot Randomized Open Clinical Trial. *Clin Transl Gastroenterol* 2016; **7**: e180 [PMID: 27415618 DOI: 10.1038/ctg.2016.38]

92 **Berzigotti A**, Saran U, Dufour JF. Physical activity and liver diseases. *Hepatology* 2016; **63**: 1026-1040 [PMID: 26313307 DOI: 10.1002/hep.28132]

93 **Duarte-Rojo A**, Ruiz-Margáin A, Montaño-Loza AJ, Macías-Rodríguez RU, Ferrando A, Kim WR. Exercise and physical activity for patients with end-stage liver disease: Improving functional status and sarcopenia while on the transplant waiting list. *Liver Transpl* 2018; **24**: 122-139 [PMID: 29024353 DOI: 10.1002/lt.24958]

94 **Singal AK**, Charlton MR. Nutrition in alcoholic liver disease. *Clin Liver Dis* 2012; **16**: 805-826 [PMID: 23101983 DOI: 10.1016/j.cld.2012.08.009]

95 **Langhans W**, Hrupka B. Interleukins and tumor necrosis factor as inhibitors of food intake. *Neuropeptides* 1999; **33**: 415-424 [PMID: 10657519 DOI: 10.1054/npep.1999.0048]

96 **Nicolás JM**, Fernández-Solà J, Fatjó F, Casamitjana R, Bataller R, Sacanella E, Tobías E, Badía E, Estruch R. Increased circulating leptin levels in chronic alcoholism. *Alcohol Clin Exp Res* 2001; **25**: 83-88 [PMID: 11198718]

97 **Styskel B**, Natarajan Y, Kanwal F. Nutrition in Alcoholic Liver Disease: An Update. *Clin Liver Dis* 2019; **23**: 99-114 [PMID: 30454836 DOI: 10.1016/j.cld.2018.09.012]

98 **Parlesak A**, Schäfer C, Schütz T, Bode JC, Bode C. Increased intestinal permeability to macromolecules and endotoxemia in patients with chronic alcohol abuse in different stages of alcohol-induced liver disease. *J Hepatol* 2000; **32**: 742-747 [PMID: 10845660 DOI: 10.1016/s0168-8278(00)80242-1]

99 **Rossi RE**, Conte D, Massironi S. Diagnosis and treatment of nutritional deficiencies in alcoholic liver disease: Overview of available evidence and open issues. *Dig Liver Dis* 2015; **47**: 819-825 [PMID: 26164399 DOI: 10.1016/j.dld.2015.05.021]

100 **Parker R**, Neuberger JM. Alcohol, Diet and Drug Use Preceding Alcoholic Hepatitis. *Dig Dis* 2018; **36**: 298-305 [PMID: 29852499 DOI: 10.1159/000487392]

101 **Grossberg AJ**, Scarlett JM, Marks DL. Hypothalamic mechanisms in cachexia. *Physiol Behav* 2010; **100**: 478-489 [PMID: 20346963 DOI: 10.1016/j.physbeh.2010.03.011]

102 **McClain CJ**, Barve SS, Barve A, Marsano L. Alcoholic liver disease and malnutrition. *Alcohol Clin Exp Res* 2011; **35**: 815-820 [PMID: 21284673 DOI: 10.1111/j.1530-0277.2010.01405.x]

103 **Kang X**, Zhong W, Liu J, Song Z, McClain CJ, Kang YJ, Zhou Z. Zinc supplementation reverses alcohol-induced steatosis in mice through reactivating hepatocyte nuclear factor-4alpha and peroxisome proliferator-activated receptor-alpha. *Hepatology* 2009; **50**: 1241-1250 [PMID: 19637192 DOI: 10.1002/hep.23090]

104 **Zhong W**, McClain CJ, Cave M, Kang YJ, Zhou Z. The role of zinc deficiency in alcohol-induced intestinal barrier dysfunction. *Am J Physiol Gastrointest Liver Physiol* 2010; **298**: G625-G633 [PMID: 20167873 DOI: 10.1152/ajpgi.00350.2009]

105 **Prasad AS**. Clinical manifestations of zinc deficiency. *Annu Rev Nutr* 1985; **5**: 341-363 [PMID: 3896271 DOI: 10.1146/annurev.nu.05.070185.002013]

106 **Ota Y**, Capizzano AA, Moritani T, Naganawa S, Kurokawa R, Srinivasan A. Comprehensive review of Wernicke encephalopathy: pathophysiology, clinical symptoms and imaging findings. *Jpn J Radiol* 2020; **38**: 809-820 [PMID: 32390125 DOI: 10.1007/s11604-020-00989-3]

107 **Latt N**, Dore G. Thiamine in the treatment of Wernicke encephalopathy in patients with alcohol use disorders. *Intern Med J* 2014; **44**: 911-915 [PMID: 25201422 DOI: 10.1111/imj.12522]

108 **Medici V**, Halsted CH. Folate, alcohol, and liver disease. *Mol Nutr Food Res* 2013; **57**: 596-606 [PMID: 23136133 DOI: 10.1002/mnfr.201200077]

109 **Leo MA**, Lieber CS. Hepatic vitamin A depletion in alcoholic liver injury. *N Engl J Med* 1982; **307**: 597-601 [PMID: 7202119 DOI: 10.1056/NEJM198209023071006]

110 **Bhavsar-Burke I**, Jansson-Knodell CL, Gilmore AC, Crabb DW. Review article: the role of nutrition in alcohol-associated liver disease. *Aliment Pharmacol Ther* 2021; **53**: 1268-1276 [PMID: 33896017 DOI: 10.1111/apt.16380]

111 **Tome S**, Lucey MR. Review article: current management of alcoholic liver disease. *Aliment Pharmacol Ther* 2004; **19**: 707-714 [PMID: 15043511 DOI: 10.1111/j.1365-2036.2004.01881.x]

112 **BioRender**. [cited 2 February 2024]. Available from: https://www.biorender.com/

World Journal of Gastroenterology

Submit a Manuscript: https://www.f6publishing.com

World J Gastroenterol 2024 March 14; 30(10): 1329-1345

DOI: 10.3748/wjg.v30.i10.1329

ISSN 1007-9327 (print) ISSN 2219-2840 (online)

REVIEW

Optimizing prediction models for pancreatic fistula after pancreatectomy: Current status and future perspectives

Feng Yang, John A Windsor, De-Liang Fu

Specialty type: Gastroenterology and hepatology

Provenance and peer review: Invited article; Externally peer reviewed.

Peer-review model: Single blind

Peer-review report's scientific quality classification
Grade A (Excellent): 0
Grade B (Very good): B
Grade C (Good): 0
Grade D (Fair): 0
Grade E (Poor): 0

P-Reviewer: Kelemen D, Hungary

Received: December 5, 2023
Peer-review started: December 5, 2023
First decision: January 4, 2024
Revised: January 15, 2024
Accepted: February 25, 2024
Article in press: February 25, 2024
Published online: March 14, 2024

Feng Yang, De-Liang Fu, Department of Pancreatic Surgery, Huashan Hospital, Shanghai Medical College, Fudan University, Shanghai 200040, China

John A Windsor, Surgical and Translational Research Centre, Faculty of Medical and Health Sciences, University of Auckland, Auckland 1142, New Zealand

Corresponding author: Feng Yang, MD, PhD, Doctor, Surgeon, Department of Pancreatic Surgery, Huashan Hospital, Shanghai Medical College, Fudan University, No. 12 Central Urumqi Road, Shanghai 200040, China. yffudan98@126.com

Abstract

Postoperative pancreatic fistula (POPF) is a frequent complication after pancreatectomy, leading to increased morbidity and mortality. Optimizing prediction models for POPF has emerged as a critical focus in surgical research. Although over sixty models following pancreaticoduodenectomy, predominantly reliant on a variety of clinical, surgical, and radiological parameters, have been documented, their predictive accuracy remains suboptimal in external validation and across diverse populations. As models after distal pancreatectomy continue to be progressively reported, their external validation is eagerly anticipated. Conversely, POPF prediction after central pancreatectomy is in its nascent stage, warranting urgent need for further development and validation. The potential of machine learning and big data analytics offers promising prospects for enhancing the accuracy of prediction models by incorporating an extensive array of variables and optimizing algorithm performance. Moreover, there is potential for the development of personalized prediction models based on patient- or pancreas-specific factors and postoperative serum or drain fluid biomarkers to improve accuracy in identifying individuals at risk of POPF. In the future, prospective multicenter studies and the integration of novel imaging technologies, such as artificial intelligence-based radiomics, may further refine predictive models. Addressing these issues is anticipated to revolutionize risk stratification, clinical decision-making, and postoperative management in patients undergoing pancreatectomy.

Key Words: Pancreatic fistula; Pancreaticoduodenectomy; Distal pancreatectomy; Central pancreatectomy; Prediction model; Machine learning; Artificial intelligence

Core Tip: Postoperative pancreatic fistula (POPF) is a common complication following pancreatectomy, associated with increased morbidity and mortality. Optimizing prediction models for POPF is a critical focus in surgical research. Although over sixty models following pancreaticoduodenectomy have been documented, their predictive accuracy remains suboptimal across diverse populations. The validation of models after distal pancreatectomy is anticipated, while POPF prediction after central pancreatectomy requires further development and validation. Machine learning and big data analytics offer promising prospects for enhancing prediction model accuracy. Personalized prediction models and novel imaging technologies, such as AI-based radiomics, may further refine predictive models.

Citation: Yang F, Windsor JA, Fu DL. Optimizing prediction models for pancreatic fistula after pancreatectomy: Current status and future perspectives. *World J Gastroenterol* 2024; 30(10): 1329-1345
URL: https://www.wjgnet.com/1007-9327/full/v30/i10/1329.htm
DOI: https://dx.doi.org/10.3748/wjg.v30.i10.1329

INTRODUCTION

With the ongoing development of surgical techniques and technologies, the outcomes of pancreatectomy has significantly improved. Although the mortality rate after pancreatectomy has decreased to less than 5%, the occurrence of morbidity remains high, ranging from 15% to 65%[1,2]. One frequent complication that arises after pancreatectomy is postoperative pancreatic fistula (POPF), which varies in incidence depending on many factors including the definition of POPF and type of pancreatic anastomosis employed. The rate of POPF has not shown significant changes over time. Recent reports indicate that the incidence of POPF after pancreaticoduodenectomy (PD) is about 15%-20%[3], and after distal pancreatectomy (DP) 20%-30%[4]. Central pancreatectomy (CP) has the highest incidence of POPF, exceeding 30%[5]. The consequences of POPF include secondary complications of intra-abdominal abscess, sepsis, and life-threatening massive hemorrhage, which combine to further extend hospital stay and increase healthcare costs.

While accurate prediction of patients at high risk of POPF is a high priority, it remains a challenge. Predictive models serve as useful tools for risk stratification and resource allocation, with a focus on patients who stand to benefit the most. By efficiently identifying patients at a higher risk of POPF, these models allow healthcare providers to tailor their management approach based on an individual patient's risk profile. With the ability to pinpoint high-risk patients, predictive models empower providers to proactively implement preventive strategies, including appropriate anastomotic technique, octreotide administration, prophylactic drains, and Wirsung's duct stenting, while also initiating closer postoperative monitoring. Furthermore, predictive models offer valuable information for shared decision-making between healthcare providers and patients. This ensures that patients are well-informed about their risk of developing POPF, along with the potential benefits and risks associated with various prevention and management strategies. As a result, patients can actively participate in decisions regarding their treatment and care. These models utilize a range of risk factors, including clinical parameters, to determine the likelihood of POPF in individual patients, thereby improving surgical outcomes and reducing healthcare burden. Future iterations of these models hold the potential to further enhance their accuracy and effectiveness by incorporating valid risk factors and improving predictive algorithms. The aim of this paper is to provide a reference for surgeons to select suitable models in their clinical practice, and to propose strategies for optimizing these models.

LITERATURE SEARCH

A comprehensive literature search was conducted in the PubMed database to identify relevant studies on prediction models for POPF after pancreatectomy. The search strategy included the terms "pancreatic fistula" AND "predictive model" or "score" AND "pancreaticoduodenectomy " or "pancreatic resection". Only studies published in English between January 2005 and October 2023 were included in the screening process.

GRADING OF POPF

The definition (drain fluid amylase level from postoperative day 3 exceeds 3 times the serum amylase activity) and grading system of POPF was first published in 2005[6] and later revised by the International Study Group of Pancreatic Surgery (ISGPS) in 2016[7]. This system is now widely accepted and utilized, grading POPF on the basis of its severity. Grade A refers to a 'biochemical leak' that is characterized by an elevated drain fluid amylase level. However, it does not result in adverse clinical consequences and is no longer considered a true POPF. Grade B affects postoperative recovery and requires intervention, although it does not lead to severe consequences. This grade is clinically relevant as it can interfere with the management and impact clinical outcome. Within Grade B, there are three subtypes: B1, B2, and B3, each increasing in severity[8]. B1 is the least prevalent subtype and is characterized by persistent abdominal drainage for more than three weeks. Although it does not require specific treatment, it still requires monitoring. B2 is the most

common subtype and necessitates medical therapy, including antibiotics, enteral or parenteral nutrition, somatostatin and analogues, and transfusions, regardless of the need for extended catheter drainage. B3 is the most severe subtype, which demands interventional procedures under general anesthesia. Grade C is the most severe form of POPF and is associated with significant clinical implications, including organ failure and death. This grade requires immediate attention and intervention. Clinically relevant POPF (CR-POPF, B+C grades only) is accompanied by clinically relevant developments or conditions directly related to the POPF. By using this grading system, healthcare professionals can effectively grade and manage POPF based on its severity, helping to ensure appropriate treatment.

In recent study, it has been observed that patients who experienced postoperative pancreatitis (POAP) had an increased likelihood of developing CR-POPF[9]. Although the exact mechanism by which POAP leads to CR-POPF formation is yet to be determined, the association between them suggests a potential link. Postoperative hyperamylasemia, which is considered a biochemical marker of pancreatic tissue irritation, can be likened to a biochemical leak. Its significance in terms of clinical outcomes is not well understood. Additional research is required to clarify the clinical implications of postoperative hyperamylasemia and its relationship with the development of POPF[10].

RISK FACTORS OF POPF

Risk factors in the models for PD

Numerous risk factors have been identified in association with POPF (Table 1), leading to the development of several prediction models based on these factors. The risk factors can be described in three groups: preoperative, intraoperative, and postoperative factors[11]. It's important to note that the risk factors of POPF may vary depending on the type of pancreatic resection being performed[12].

Preoperative risk factors for POPF in patients undergoing PD include demographic characteristics such as gender, age, and body mass index (BMI)[13-15]. Comorbidities such as diabetes and pancreatitis, as well as imaging findings including pancreatic density, main pancreatic duct (MPD) diameter, visceral adipose tissue and radiomics score, are also risk factors [13,15-19]. Furthermore, biochemical markers like preoperative bilirubin and albumin levels, as well as preoperative biliary drainage and neoadjuvant chemotherapy, also contribute to the risk.

Intraoperative risk factors for POPF include pancreas-specific characteristics, such as soft pancreas and small MPD diameter. The surgical approach utilized (open, laparoscopic, and robotic) and type of anastomosis are also important. Other intraoperative risk factors include extended operating time, massive blood loss, combined venous resection, and extended lymphadenectomy[20-23].

Postoperative risk factors for POPF include high drain amylase levels, hyperamylasemia, hyperlipasemia, hypoalbuminemia, elevated C-reactive protein (CRP) level, and increased neutrophil count. Delayed gastric emptying is also a risk factor[24]. The pathology report may describe risk factors for POPF such as pancreatosteatosis and the absence of pancreatic fibrosis. Many prediction models for POPF after PD have been developed, and the reported predictors for these models are detailed in Table 1.

Risk factors in the models for DP

Numerous studies have examined the risk factors associated with POPF following DP. However, compared with PD, there are fewer reported risk factors. These predictors can also be grouped as preoperative, intraoperative, and postoperative factors.

Preoperative risk factors for DP include young age, high BMI, the presence of preoperative comorbidities such as diabetes and coronary artery disease, hypoalbuminemia and certain pancreas-specific characteristics[25-27]. For instance, large MPD diameter and thick pancreas have been identified as potential risk factors.

Intraoperative risk factors include extended operating time, massive blood loss, soft pancreas, transection at pancreatic neck, and vascular resection.

Postoperative risk factors include surgical drain characteristics such as high amylase levels, elevated CRP, and the presence of high-risk pathology. Interestingly, there is a reversed predictive effect of MPD diameter between DP and PD. While a wider diameter is considered a risk factor for DP, it is reported as having a protective effect in PD[28]. Several models for predicting POPF following DP have been developed, with their reported predictors summarized in Table 2. Further research is needed to expand the understanding risk factors for POPF after DP, as well as to identify additional indicators that may contribute to more accurate prediction models. By considering a broader range of factors and conducting larger-scale studies, researchers can gain a more comprehensive understanding of POPF risk and develop effective strategies for its prevention and management.

Risk factors in the models for CP

Only a limited number of risk factors for POPF after CP have been reported, and of potential value for establishing prediction models. These risk factors include sex, BMI, diabetes, MPD diameter, pancreatic thickness and texture, operating time, transection site, technique of pancreatic anastomosis, and pathology (Table 3). As research in this field progresses, it is expected that additional risk factors will be identified to enhance our understanding of POPF risk after CP.

Table 1 Reported risk factors for postoperative pancreatic fistula after pancreaticoduodenectomy

Stage	Factors
Preoperative	(1) Sex, (2) age, (3) BMI, (4) weight, (5) weight loss, (6) smoking history, (7) hypertension, (8) diabetes mellitus, (9) history of acute pancreatitis, (10) history of abdominal surgery, (11) chronic steroid use, (12) ASA score, (13) preoperative biliary drainage, (14) preoperative chemotherapy, (15) albumin, (16) bilirubin, (17) alanine transaminase, (18) creatine, (19) tumor site, (20) MPD diameter, (21) MPD index[1], (22) pancreatic thickness, (23) pancreatic density, (24) pancreatic texture, (25) relation with PV on CT, (26) pancreatic density index, (27) intra-abdominal fat thickness, (28) visceral adipose tissue, (29) total adipose tissue, (30) sarcopenic obesity, (31) L3 subcutaneous fat area, (32) pancreatic remnant volume, (33) stump area, (34) fat score, (35) atrophy score, (36) A/L ratio, (37) subcutaneous fat index, (38) radiomics score, (39) combined radiomics score, (40) liver density, (41) muscle attenuation, (42) PS SIratio, (43) PM SIratio, (44) fat mass at BIVA, (45) SWV value of pancreas, (46) MIPD experience, (47) preoperative diagnosis
Intraoperative	(A) MPD diameter, (B) pancreatic texture, (C) operating time, (D) estimated blood loss, (E) transfusion, (F) intraoperative colloid infusion, (G) surgical approach, (H) minimally invasive approach, (I) open conversion, (J) pancreatic anastomosis, (K) gastrojejunostomy, (L) extended lymphadenectomy, (M) venous resection, (N) nasojejunal feeding tube
Postoperative	(a) Postoperative DFA, (b) change of postoperative DFA, (c) WBC on POD1, (d) change of postoperative WBC, (e) neutrophil on POD3, (f) postoperative CRP, (g) temperature on POD3, (h) postoperative albumin, (i) albumin difference[2], (j) postoperative CRP/albumin, (k) serum creatinine on POD1, (l) hyperamylasemia on POD1-2, (m) serum lipase on POD1, (n) DFL on POD1, (o) pathology, (p) PV invasion, (q) pancreatic fibrosis, (r) pancreatic steatosis, (s) deep surgical site infection, (t) DGE

[1]Main pancreatic duct index indicates the ratio of main pancreatic duct diameter to pancreatic thickness at the transection site.
[2]Albumin difference indicates the difference of albumin level between preoperative and postoperative day 1.
A/L ratio: Arterial/late phase pancreas computed tomography attenuation value ratio; ASA: American Society of Anesthesiologists; BIVA: Bioimpedance vector analysis; BMI: Body mass index; CRP: C-reactive protein; CT: Computed tomography; DFA: Drain fluid amylase; DFL: Drain fluid lipase; DGE: Delayed gastric emptying; L3: The third lumbar vertebra; MIPD: Minimally invasive pancreaticoduodenectomy; MPD: Main pancreatic duct; POD: Postoperative day; PV: Portal vein; SWV: Shear wave velocity; PM SIratio: Signal intensity ratio of pancreas to muscle; PS SIratio: Signal intensity ratio of pancreas to spleen; WBC: White blood cell.

Table 2 Reported risk factors for postoperative pancreatic fistula after distal pancreatectomy

Preoperative	Intraoperative	Postoperative
(1) Age	(A) Epidural use	(a) CRP on POD1
(2) BMI	(B) Operating time	(b) DFA on POD1
(3) Diabetes mellitus	(C) Estimated blood loss	(c) DFA on POD3
(4) Coronary artery disease	(D) Transfusion	(d) Change of postoperative DFA
(5) ASA score	(E) Pancreatic texture	(e) Pathology
(6) Albumin	(F) Transection site	
(7) MPD diameter	(G) Splenectomy	
(8) Pancreatic thickness	(H) Vascular resection	
(9) Pancreatic neck major diameter		
(10) Pancreatic neck minor diameter		
(11) Predicted pancreatic neck area		

ASA: American Society of Anesthesiologists; BMI: Body mass index; CRP: C-reactive protein; DFA: Drain fluid amylase; MPD: Main pancreatic duct; POD: Postoperative day.

DEVELOPING PREDICTION MODELS

A range of statistical methods are used to develop POPF prediction models. These models can take the form of scores, calculation formulas, or nomograms, providing clinicians with a tool to assess individual patient risk. It is important to note that certain risk factor can be evaluated at different stages of the patient's journey. For example, the MPD diameter can be measured preoperatively using enhanced CT/MRI scans or during the surgical procedure itself. Although both measurements may introduce some degree of error, MPD diameter measured through preoperative imaging is generally considered accurate[29]. Similarly, while pathology is typically assessed postoperative, a preoperative diagnosis by radiological imaging or biopsy serves as a reliable proxy. Furthermore, advancements in imaging technology have enabled evaluation of pancreatic texture not only during surgery but also with preoperative imaging by CT/MRI scans, and elastography[30]. This expanded imaging capability provides additional insights into the identification of risk factors such as pancreatic fibrosis or inflammation.

Table 3 Reported risk factors for postoperative pancreatic fistula after central pancreatectomy

Preoperative	Intraoperative	Postoperative
(1) Sex	(A) Operating time	(a) Pathology
(2) BMI	(B) Pancreatic texture	
(3) Diabetes mellitus	(C) Transection site	
(4) Cephalic MPD diameter	(D) Pancreatic anastomosis	
(5) Distal MPD diameter		
(6) Pancreatic thickness		

BMI: Body mass index; MPD: Main pancreatic duct.

PREDICTION MODELS FOR POPF AFTER PD

In the past decade, over sixty prediction models for POPF after PD have demonstrated potential value in clinical practice. Among these models, one of the earliest reported prediction scores, originating from a single-center prospective study conducted in 2010, categorized patients into four subgroups based on the presence of three risk factors: BMI, pancreatic steatosis and fibrosis[31]. This model shed light on the impact of pancreatic fat infiltration and fibrosis on the potential for POPF and showed high accuracy in predicting grade B and C POPF. However, the reliance on histological analysis for determining the scores of pancreatic steatosis and fibrosis is only available after surgery and cannot be used for surgical strategies, limiting the applicability of this model for instituting steps to prevent or reduce the risk of POPF. Subsequently, Wellner *et al*[13] and Yamamoto *et al*[14] proposed models that utilized preoperative indicators to predict the occurrence of POPF. However, these models did not gain widespread acceptance possibly due to the challenges associated with evaluating certain variables, including the MPD index and the distance from the portal vein. Furthermore, subsequent external validations revealed suboptimal performance of these models[32,33], further limiting their adoption into clinical practice.

Despite the limitations of early prediction models, continued research efforts have led to more models. These new models take into consideration a broader range of variables and aim to improve accuracy and clinical applicability. In 2013, a prospective study introduced the fistula risk score (FRS) to predict the risk of POPF[34]. The FRS is based on four variables: pancreatic texture, MPD diameter, intraoperative blood loss, and pathology. This scoring system was developed to address the limitations of preoperative assessments and has been validated by several studies, demonstrating its acceptable predictive performance with a c-statistic of over 0.7[35,36]. One of the areas of debated with this model is the relationship between blood loss and the occurrence of POPF[37]. It has been observed that minimally invasive surgery, which results in lower blood loss compared to open surgery, is not consistently associated with a reduced incidence of POPF. In light of this, Mungroop *et al*[37] proposed an alternative FRS (a-FRS), which removes the variables of intraoperative blood loss and pathological diagnosis. Instead, it includes the BMI as an additional variable. Subsequently, an updated alternative FRS (ua-FRS) was introduced, which incorporates the gender variable specifically for patients undergoing minimally invasive PD (MIPD)[38]. These modified scoring systems have shown improved convenience and enhanced predictive performance compared to the original FRS in subsequent external validations[39].

Preoperative prediction

Preoperative prediction models may have the potential to help in enabling preventive measures and guiding surgical decision-making compared to intraoperative and postoperative prediction models. One such preoperative predictive score was developed by Roberts *et al*[15], utilizing only BMI and MPD diameter, and it showed a significant increase with increasing severity of POPF ($P < 0.001$) in a subsequent multicenter study[40]. Building on this, Perri *et al*[41] established a more simplified risk-tree using the same two parameters. This risk-tree effectively categorized patients into three distinct risk groups with significantly different rates of POPF. However, it is worth noting that the area under the curve (AUC) for this risk-tree in the validation cohort was 0.65, indicating only moderate predictive accuracy. This would mean that 35% of patients are misclassified, which is not sufficiently accurate for application to individual patients.

With the advancements in medical imaging technology, imaging parameters have gained prominence in POPF prediction, and many preoperative prediction models now rely on these parameters (Table 4)[13-15,17,19,41-53]. However, certain imaging parameters require external software for preoperative evaluation, which poses challenges in terms of accessibility, standardization, and compatibility with different imaging systems, as well as external validation for these models. Additionally, the past three years have witnessed the development of over 10 POPF prediction models based on machine learning algorithms (Table 5)[22,48,54-64]. While these models are often considered superior to traditional regression models, it is important to highlight that a recent study revealed machine learning did not outperform logistic regression in predicting POPF after PD[22]. Furthermore, the predictive models developed using nationwide population data exhibited lower AUC values compared to models developed in single- and multicenter studies[22,60,62,63]. This discrepancy implies that the generalisability of the latter two models may be compromised in terms of their predictive value.

Table 4 Preoperative prediction models of postoperative pancreatic fistula after pancreaticoduodenectomy

Ref.	Year	Country	Center	Study period	Design cohort	CR-POPF (%)	Variables[5]	C-index/AUC (95%CI)	Validation
Wellner *et al*[13]	2010	Germany	Single	2006-2008	62	30.6[4]	(2)(5)(6)(9)(47)		Internal
Yamamoto *et al*[14]	2011	Japan	Single	2004-2007	279	36.9	(1)(21)(25)(27)(47)	0.808 (0.757-0.860)	Internal
Roberts *et al*[15]	2014	United Kingdom	Single[1]	2007-2012	217	22.1[4]	(3)(20)	0.832 (0.768-0.897)	Internal
Casadei *et al*[42]	2015	Italy	Single	2008-2012	208[2]	20.2	(3)(20)(47)		
Zhang *et al*[43]	2018	China	Single		80	42.5[4]	(38)	0.825 (0.736-0.913)	Internal
Shi *et al*[44]	2020	China	Multi	2009-2019	718	15.6	(20)(32)(33)(34)(35)	0.729 (0.678-0.775)	External
Yu *et al*[17]	2021	China	Single	2016-2018	124	25.8	(21)(23)	0.775 (0.687-0.862)	Internal
Lin *et al*[19]	2021	China	Single	2013-2019	175	21.1	(38)	0.801 (0.719-0.884)	Internal
							(39)	0.871 (0.816-0.926)	
Tang *et al*[45]	2021	China	Single	2013-2019	239	19.7	(3)(20)(36)	0.823 (0.769-0.877)	
Lapshyn *et al*[46]	2021	Germany	Single[1]	2012-2018	120	19[3]	(1)(20)(22)	0.808 (0.726-0.874)	Internal
Perri *et al*[41]	2021	Italy	Multi	2017-2019	566	20	(3)(20)	0.70 (0.63-0.77)	External
Savin *et al*[47]	2021	Romania	Single	2015-2020	78	28.2	(20)(23)(32)	0.846 (0.694-0.941)	
							(20)(32)(40)	0.774 (0.599-0.850)	
Skawran *et al*[48]	2021	Switzerland	Single	2008-2018	62	27.4	(43)	0.75 (0.63-0.84)	
Box *et al*[49]	2021	United States	Single	2013-2018	220	15.9[4]	(3)(20)(37)	0.822	
							(3)(20)(26)	0.757	
							(3)(20)(26)(37)	0.844	
Kolbinger *et al*[50]	2022	Germany	Single	2012-2021	195	28.7	(20)(24)(47)	0.82	Internal
							(20)(24)(32)(47)	0.83	
Maqueda González *et al*[51]	2022	Spain	Single	2010-2019	103	30.1	(20)(29)	0.78 (0.68-0.87)	
Zou *et al*[52]	2023	China	Single	2015-2021	125	17.6	(20)(28)(42)	0.903	Internal
Tian *et al*[53]	2023	China	Single[1]	2020-2021	143[2]	36	(20)(45)	0.866	Internal

[1]Indicates prospective studies, others are retrospective studies.
[2]Surgical procedures included pancreaticoduodenectomy and distal pancreatectomy.
[3]The data is the CR-POPF rate of total cohort.
[4]The data includes biochemical leak.
[5]From Table 1.
AUC: Area under the curve; CI: Confidence interval; CR-POPF: Clinically relevant postoperative pancreatic fistula.

Intraoperative prediction

The simplest intraoperative prediction model for POPF is known as the ISGPS risk classification. This classification categorizes patients into four risk groups based on intraoperative measurements of MPD diameter and pancreatic texture [65]. Interestingly, a nationwide validation study of this classification revealed no significant difference between the two intermediate risk categories, leading to the proposal of a simplified three-tier system[66]. The current literature indicates that a-FRS[37] and ua-FRS[38] have been validated by numerous external studies with acceptable accuracy and are two recommended models. However, the surgeon's determination of pancreatic texture by intraoperative palpation is subjective and prone to bias. Specific details regarding more intraoperative POPF prediction model are shown in Table 6 [16,18,21,22,37,38,50,61,65,67-71].

Postoperative prediction

Recent studies have made significant advances in identifying early postoperative variables that are closely associated with POPF, including high drain fluid amylase (DFA), hyperamylasemia, and high-risk pathology, among others. These variables, combined with postoperative clinical data, biochemical indicators, and histopathological analysis, contribute to the development of dynamic POPF prediction models (Table 7)[20,23,24,31,34,72-88]. One particularly intriguing model is the "90-1000" score, which demonstrates superior performance in predicting POPF after PD compared to intraoperative

Table 5 Machine learning prediction models of postoperative pancreatic fistula after pancreaticoduodenectomy

Ref.	Year	Country	Center	Study period	Design cohort	CR-POPF (%)	C-index/AUC (95%CI)	Validation
Mu *et al*[54]	2020	China	Multi	2006-2019	359	15.6	0.85 (0.80-0.90)	Internal-external
Han *et al*[55]	2020	Korea	Single	2007-2016	1769	12.5	0.74	
Skawran *et al*[48]	2021	Switzerland	Single	2008-2018	62	27.4	0.82 (0.74-0.89), 0.74 (0.63-0.89), 0.90 (0.84-0.95)	Internal
Giovinazzo *et al*[56]	2021	Multinational	Multi		1638	27	0.962 (0.940-0.984)	
Shen *et al*[57]	2022	China	Single	2010-2021	2421	17.5	0.79-0.81	Internal
Long *et al*[58]	2022	China	Multi	2012-2021	618	18.1	0.897 (0.370-1.424)	Internal
Capretti *et al*[59]	2022	Italy	Single[1]	2011-2019	100	20	0.807, 0.749	Internal
Chen *et al*[60]	2022	United States	Nationwide	2014-2019	13940	14.4	0.746 (0.733-0.760)	Internal-external
Zheng *et al*[61]	2023	China	Single	2013-2021	257[2]	21.8	0.977	Internal
Ingwersen *et al*[22]	2023	Netherlands	Nationwide	2014-2020	4912	16.3	0.74 (0.73-0.74)	
Verma *et al*[62]	2023	United States	Nationwide	2014-2018	8597	11	0.74 (0.72-0.76)	Internal-external
Ashraf Ganjouei *et al*[63]	2023	United States	Nationwide	2014-2019	8666	13	0.67-0.72	Internal
Ingwersen *et al*[64]	2023	Multinational	Multi	2013-2018	118	42.4	0.9 (0.71-0.99), 0.86, 0.81, 0.8	Internal-external

[1]Indicates prospective studies, others are retrospective studies.
[2]Surgical procedures included open and laparoscopic pancreaticoduodenectomy.
AUC: Area under the curve; CI: Confidence interval; CR-POPF: Clinically relevant postoperative pancreatic fistula.

pancreatic parenchymal features[79]. This model relies on the measurement of DFA and serum CRP levels on the first postoperative day. Its simplicity makes it particularly suitable for clinical practice; however, further validation is needed to establish its reliability, accuracy and applicability.

Many postoperative prediction models incorporate a combination of preoperative and intraoperative parameters. This approach holds the potential to enhance the clinical risk stratification of POPF and may offer a window of opportunity for pre-emptive interventions before the actual occurrence of POPF.

PREDICTION MODELS FOR POPF AFTER DP

Compared to PD, there have been fewer studies of prediction models for POPF after DP. Efforts in developing reliable models after DP are relatively limited. Although DP involves fewer anastomoses, it is appears to be associated with a higher incidence of POPF[2]. A retrospective study conducted on 2026 patients from 10 institutions identified several risk factors for CR-POPF after DP[25]. These risk factors included age below 60 years, obesity, low levels of albumin, absence of epidural use, high-risk pathology such as neuroendocrine and benign tumors, combined splenectomy, and vascular resection. However, the model constructed using these factors exhibited relatively poor accuracy in predicting POPF, with a c-statistic of 0.654 [95% confidence interval (CI): 0.620-0.688].

Recently, De Pastena *et al*[27] developed two DP fistula risk score (D-FRS) models. The preoperative model included two factors (pancreatic thickness and MPD diameter) and showed good predictive performance with an AUC of 0.83 (95%CI: 0.78-0.88) and 0.73 (95%CI: 0.70-0.76) for internal and external validation, respectively. In addition to pancreatic thickness and MPD diameter, the intraoperative D-FRS model included BMI, pancreatic texture, and operating time as factors and this achieved an AUC of 0.80 (95%CI: 0.74-0.85) without external validation. The DISPAIR model, developed by Bonsdorff *et al*[89] in the same year, incorporated three parameters: transection at pancreatic neck, pancreatic thickness, and diabetes. The model's internal and external validation resulted in notable AUC values of 0.904 (95%CI: 0.855-0.949) and 0.798 (95%CI: 0.748-0.848), respectively. While these models offer valuable insights, it is vital to consider their limitations, one of which is the need for external validation across diverse populations. To address this, Xu *et al*[28] conducted a validation study on the D-FRS and DISPAIR models using 653 Chinese patients who underwent DP. The study demonstrated acceptable discrimination for both models, with no significant differences between them. The AUC values were as follows: preoperative D-FRS 0.723 (95%CI: 0.687-0.757), intraoperative D-FRS 0.737 (95%CI: 0.701-0.770), and DISPAIR model 0.721 (95%CI: 0.685-0.755). The preoperative D-FRS is the most recommended model due to its

Table 6 Intraoperative prediction models of postoperative pancreatic fistula after pancreaticoduodenectomy

Ref.	Year	Country	Center	Study period	Design cohort	CR-POPF (%)	Variables[5]	C-index/AUC (95%CI)	Validation
Kim *et al*[67]	2013	Korea	Single	2003-2008	100	41[4]	(A)(B)(M)	0.728 (0.630-0.812)	Internal
Chen *et al*[68]	2015	China	Single	2008-2013	921	9.7	(3)(A)(B)(D)(E)	0.812 (0.766-0.858)	
Kantor *et al*[69]	2017	United States	Nationwide	2011-2012	1731	18.3	(1)(3)(16)(A)(B)	0.70 (0.65-0.74)	Internal-external
Li *et al*[70]	2019	China	Single	2011-2014	189	20.1	(15)(A)(B)(D)	0.821 (0.736-0.905)	Internal
Mungroop *et al*[37]	2019	Multinational	Multi	2007-2016	1924	12[4]	(3)(20)(B)	0.75 (0.71-0.78)	Internal-external
Angrisani *et al*[21]	2020	Italy	Multi[1]	2016-2018	148	19.6	(44)(A)(B)(D)	0.774 (0.683-0.866)	
							(44)(A)(B)	0.784 (0.680-0.888)	
Zhang *et al*[16]	2021	China	Single	2012-2020	232	7.8	(7)(8)(10)(B)(K)	0.916	
Mungroop *et al*[38]	2021	Multinational	Multi	2007-2017	952[2]	21	(1)(3)(20)(B)	0.75 (0.71-0.79)	External
Kolbinger *et al*[50]	2022	Germany	Single	2012-2021	195	28.7	(47)(A)(B)	0.82	Internal
Lucassen *et al*[18]	2022	Netherlands	Single	2009-2018	329	16.7	(20)(41)(B)	0.73 (0.68-0.79)	
							(20)(28)(B)	0.81 (0.75-0.86)	
							(20)(28)(41)(B)	0.81 (0.75-0.86)	
Zheng *et al*[61]	2023	China	Single	2013-2021	257	21.8	(3)(20)(B)	0.743	Internal
Hayashi *et al*[71]	2023	Japan	Single	2010-2021	169	22.5	(30)(31)(B)	0.832	
Ingwersen *et al*[22]	2023	Netherlands	Nationwide	2014-2020	4912	16.3	(1)(3)(5)(13)(16)(19)(A)(B)(G)(J)(M)(N)	0.73	
Schuh *et al*[65]	2023	Multinational	Multi	2004-2019	5533[3]	15.7	(A)(B)		External

[1]Indicates prospective studies, others are retrospective studies.
[2]The surgical procedure was minimally invasive pancreaticoduodenectomy.
[3]The cohort is for validation.
[4]The data includes biochemical leak.
[5]From Table 1.
AUC: Area under the curve; CI: Confidence interval; CR-POPF: Clinically relevant postoperative pancreatic fistula.

practicality and ease of use, as it relies on easily measurable radiographic images to assess pancreatic thickness and MPD diameter for preoperative risk stratification. Despite these positive outcomes, there is still room for improvement in the performance of the predictive models. Standardizing classification thresholds may help to enhance their accuracy. There has been the emergence of additional prediction models for POPF after DP, and these are summarized in Table 8[26,79,90-92].

PREDICTION MODELS FOR POPF AFTER CP

There is a trend toward offering CP more frequently in clinical practice because it allows for preservation of more pancreatic endocrine and exocrine function by resecting less normal pancreatic tissue. However, it appears to have a higher risk of POPF compared with PD and DP because of the presence of two pancreatic stumps[93]. While previous studies have primarily focused on the safety of CP and risk factors for POPF, the exploration of prediction models for POPF after CP has been relatively recent (Table 9). In a study by Ouyang *et al*[94], involving 194 CP patients, independent

Table 7 Postoperative prediction models of postoperative pancreatic fistula after pancreaticoduodenectomy

Ref.	Year	Country	Center	Study period	Design cohort	CR-POPF (%)	Variables[6]	C-index/AUC (95%CI)	Validation
Gaujoux *et al*[31]	2010	France	Single[1]	2004-2005	100	24	(3)(q)(r)	0.82	
Callery *et al*[34]	2013	United States	Single[1]	2002-2007	233	13	(A)(B)(D)(o)	0.942	Internal
Xia *et al*[23]	2018	China	Single	2009-2017	225	17.8	(A)(B)(L)(h)	0.813 (0.737-0.889)	Internal
Xingjun *et al*[72]	2019	China	Multi	2014-2017	457	12.6[5]	(A)(q)(r)	0.868	External
You *et al*[73]	2019	Korea	Single	2007-2016	1771	12.5	(1)(3)(12)(15)(A)(o)	0.709	Internal
Guo *et al*[74]	2020	China	Single	2012-2016	220	22.7	(A)(B)(o)(p)	0.793 (0.731-0.855)	Internal
Li *et al*[75]	2021	China	Single	2018-2020	176	21.1	(a)(e)(f)(g)(k)	0.814 (0.736-0.892)	
Shen *et al*[76]	2021	China	Single	2016-2020	302	16.6	(3)(B)(a)(i)	0.87 (0.81-0.94)	Internal
Liu *et al*[77]	2021	China	Single	2016-2019	251[4]	7.6	(15)(18)(a)(j)	0.866 (0.737-0.996)	
							(15)(18)(a)(j)	0.896 (0.814-0.978)	
							(15)(18)(a)(j)	0.888 (0.806-0.971)	
Huang *et al*[78]	2021	China	Multi	2010-2018	762	11.4	(3)(A)(a)	0.934 (0.914-0.950)	External
Guilbaud *et al*[79]	2021	France	Multi[1]	2017-2019	182[3]	21.2	(a)(f)	0.834 (0.769-0.900)	
Honselmann *et al*[20]	2021	Germany	Single	2012-2017	182	16	(12)(A)(C)(c)(m)	0.903	Internal
							(12)(B)(c)(d)(m)	0.891	
Suzuki *et al*[80]	2021	Japan	Single	2007-2012	349	17.5	(20)(B)(b)(n)		
Al Abbas *et al*[81]	2021	United Sates	Nationwide	2014-2016	9867	13.9	(1)(2)(3)(7)(8)(A)(B)(o)	0.70 (0.69-0.71)	Internal
Yin *et al*[82]	2022	China	Single	2012-2016	662	16.3	(17)(A)(F)(M)(o)	0.667	Internal
							(A)(F)(a)(e)	0.809	
Gu *et al*[24]	2023	China	Nationwide	2014-2017	3609[2]	16.7	(4)(20)(B)(o)(s)(t)	0.855 (0.702-0.853)	External
Bannone *et al*[83]	2023	Italy	Single[1]	2016-2021	905	20.2	(A)(B)(D)(a)(o)	0.85 (0.82-0.87)	
							(A)(B)(D)(a)(l)(o)	0.87 (0.84-0.89)	
							(A)(B)(D)(a)(f)(l)(o)	0.90 (0.87-0.91)	
Choi *et al*[84]	2023	Korea	Multi	2012-2020	429[4]	12.4	(12)(20)(46)(B)(E)(H)(I)(o)	0.739 (0.668-0.800)	Internal
van Dongen *et al*[85]	2023	Netherlands	Nationwide	2014-2018	3271	14.6	(1)(3)(8)(20)(o)	0.73	External
Raza *et al*[86]	2023	United Kingdom	Multi	2009-2019	187	12.8	(1)(a)(f)(h)	0.78	External
Mohamed *et al*[87]	2023	United Sates	Nationwide	2015-2018	5975	17	(1)(3)(14)(A)(B)(o)	0.72 (0.704-0.737)	
Ahmad *et al*[88]	2023	United States	Nationwide	2014-2017	2417	12.6	(3)(11)(B)(C)(a)	0.720 (0.687-0.752)	Internal
							(3)(11)(B)(C)(a)(b)	0.758 (0.726-0.789)	

[1]Indicates prospective studies, others are retrospective studies.

[2]The study population was from the American College of Surgeons-National Surgical Quality Improvement Program database in the United States.

[3]Surgical procedures included pancreaticoduodenectomy and distal pancreatectomy.
[4]The surgical procedure was minimally invasive pancreaticoduodenectomy.
[5]The data is the clinically relevant postoperative pancreatic fistula rate of total cohort.
[6]From Table 1.
AUC: Area under the curve; CI: Confidence interval; CR-POPF: Clinically relevant postoperative pancreatic fistula.

Table 8 Postoperative pancreatic fistula prediction models after distal pancreatectomy

Ref.	Year	Country	Center	Design cohort	Study period	CR-POPF (%)	Variables[3]	AUC (95%CI)	Validation
Ecker *et al*[25]	2019	Multinational	Multi	2026	2001-2016	15.1	(1)(2)(6)(A)(G)(H)(e)	0.654 (0.620-0.688)	
Guilbaud *et al*[79]	2021	France	Multi[1]	92[2]	2017-2019	21.2	(a)(b)	0.762 (0.640-0.885)	
Rollin *et al*[90]	2022	France	Single	103	2015-2019	32	(2)(8)(B)(c)	0.83 (0.75-0.92)	
Nassour *et al*[91]	2022	USA	Nationwide	692	2014-2018	15.9	(1)(B)(D)(b)	0.731 (0.685-0.796)	Internal
							(1)(B)(b)(d)	0.791 (0.742-0.836)	
Bonsdorff *et al*[89]	2022	Multinational	Multi	266	2013-2021	19.5	(3)(8)(F)	0.904 (0.855-0.949)	Internal-external
He *et al*[92]	2023	China	Single	115	2005-2020	33	(2)(6)(8)(E)	0.842 (0.762-0.921)	
Pecorelli *et al*[26]	2023	Italy	Single	220	2016-2019	33.6	(2)(3)(4)(5)	0.651 (0.58-0.73)	Internal
							(2)(9)(10)(C)	0.725 (0.66-0.79)	
							(5)(11)(C)	0.733 (0.64-0.80)	
De Pastena *et al*[27]	2023	Multinational	Multi[1]	339	2014-2016	23	(7)(8)	0.731 (0.70-0.76)	Internal-external
							(2)(7)(8)(B)(E)	0.851 (0.80-0.90)	Internal

[1]Indicates prospective studies, others are retrospective studies.
[2]Including patients underwent pancreaticoduodenectomy.
[3]From Table 2.
AUC: Area under the curve; CI: Confidence interval; CR-POPF: Clinically relevant postoperative pancreatic fistula.

risk factors for POPF were identified as obesity and pancreatic anastomosis technique. They constructed a nomogram based on these variables, which demonstrated a modest AUC of 0.678. However, this study overlooked certain pancreas-specific features such as pancreatic texture, MPD diameters on both sides of the transection, and pancreatic thickness, despite its large sample size.

In light of these omissions, Yang *et al*[95] conducted a study that identified additional risk factors for POPF after CP. They found that BMI, pancreatic thickness, and MPD diameters at both ends of the lesion were independent predictors. Building upon the probability (P) of the union of two events [formula: $P(PD \cup DP) = P(PD) + P(DP) - P(PD \cap DP)$], they innovatively combined the existing FRS for PD and DP to develop specific FRS for CP (Figure 1). Consequently, they obtained a total of 12 central FRS (C-FRS) models. The predictive performance of these C-FRS models was generally acceptable, with AUC values ranging from 0.748 to 0.847. Particularly, the Preop-D-Roberts-FRS model emerged as a preoperative prediction model composed of four parameters: BMI, MPD diameters at both ends of the lesion, and pancreatic thickness. This model exhibited an AUC of 0.832 (95%CI, 0.751-0.895). Using this model, patients were categorized into three risk groups: low risk (< 25%), intermediate risk (25%-45%), and high risk (> 45%). The corresponding incidence of POPF in these risk groups was 0%, 30%, and 66.7%, respectively. Due to its ease of use and accurate preoperative prediction, the Preop-D-Roberts-FRS is recommended for clinical practice.

It is worth noting, however, that despite the promising predictive efficacy of these models, they were both derived from single-center retrospective studies in China and lacked valid external validation. Therefore, further prospective studies involving multiple centers and diverse populations are required for external validation and generalizability of the C-FRS models.

Table 9 Postoperative pancreatic fistula prediction models after central pancreatectomy

Ref.	Year	Design cohort	Study period	CR-POPF (%)	Variables[1]	AUC (95%CI)
Ouyang *et al*[94]	2022	194	2009-2020	45.9	(2)(D)	0.678
Yang *et al*[95]	2023	115	2010-2022	30.4	(2)(4)(5)(6)	0.832 (0.751-0.895)
					(2)(4)(5)(6)(B)	0.827 (0.745-0.891)
					(1)(2)(4)(5)(6)(B)	0.828 (0.746-0.892)
					(1)(2)(3)(4)(5)(6)(a)	0.826 (0.744-0.890)
					(2)(4)(5)(6)(A)(B)	0.845 (0.766-0.906)
					(2)(4)(5)(6)(A)(B)	0.847 (0.768-0.907)
					(1)(2)(4)(5)(6)(A)(B)	0.823 (0.741-0.888)
					(1)(2)(3)(4)(5)(6)(A)(B)(a)	0.840 (0.760-0.902)
					(2)(3)(5)(6)(C)	0.758 (0.669-0.833)
					(2)(3)(5)(6)(B)(C)	0.748 (0.659-0.824)
					(1)(2)(3)(5)(6)(B)(C)	0.784 (0.698-0.855)
					(1)(2)(3)(5)(6)(C)(a)	0.750 (0.661-0.826)

[1]From Table 3.
AUC: Area under the curve; CI: Confidence interval; CR-POPF: Clinically relevant postoperative pancreatic fistula.

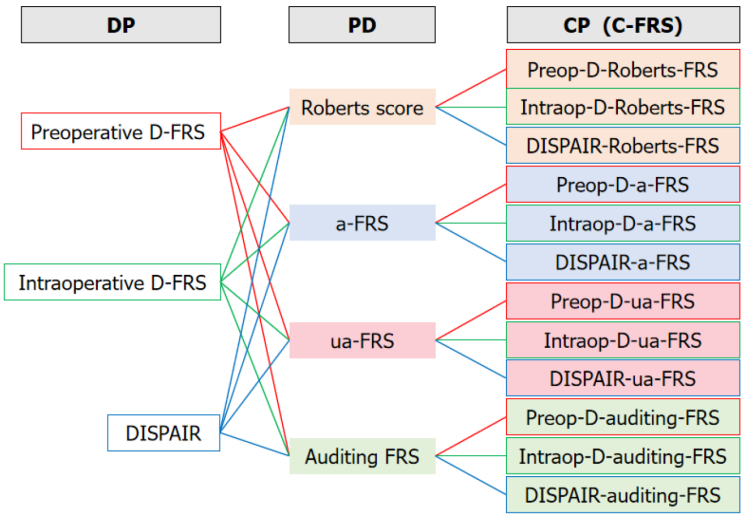

Figure 1 Central fistula risk score models for central pancreatectomy based on the fistula risk score for pancreaticoduodenectomy and distal pancreatectomy. C-FRS: Central fistula risk score; CP: Central pancreatectomy; D-FRS: Distal fistula risk score; DP: Distal pancreatectomy; FRS: Fistula risk score; PD: Pancreaticoduodenectomy.

CURRENT STATUS AND LIMITATIONS

Due to the influence of multiple risk factors (pre, intra and postoperative) and the inherent complexity of pancreatectomy, there is still room to improve the accuracy of predicting POPF. It is unlikely that a single model will be possible for all circumstances. The pathophysiological mechanisms relevant to POPF are not fully understood, and with time other factors might be identified. Moreover, the lack of consensus on diagnostic thresholds, judging criteria, non-blinded assessment of predictors, different statistical methods and potential interactions among various risk factors contribute to inferior performance of prediction models. A comprehensive review of 52 prediction models revealed that the average adherence rate to the Transparent Reporting of a multivariable prediction model for Individual Prognosis Or Diagnosis (TRIPOD) guidelines for POPF prediction models after PD was 65%[33]. Only 13 models surpassed this average TRIPOD adherence rate, indicating the importance of improving reporting standards and ensuring transparency in model development and evaluation.

Despite the development of many POPF prediction models, including some that are based on multicenter or nationwide cohort studies, over 80% of them lack external validation or demonstrate modest performance during subsequent validation[96], with AUCs ranging from 0.62 to 0.70[97]. One of the main reasons is their reliance on retrospective data, which may not encompass all the relevant factors contributing to POPF. Additionally, different models may incorporate varying variables and scoring systems, creating challenges when it comes to comparing and validating their performance. The lack of standardized and objective variables and scoring systems further hampers the universal applicability and reliability of these models. Another significant factor that has been overlooked in most models is the impact of individual surgeon experience and skill on the occurrence of POPF[98]. The surgical technique employed, decision-making process during operation, and proficiency of the surgeon can all have a substantial influence on the development of postoperative complications, including POPF. Ignoring these important aspects in the prediction models may contribute to their modest performance and decrease the translation of POPF prediction models into clinical practice.

Notably, while existing POPF prediction models show good performance in sample populations, their ability to predict and generalize may be limited when applied to ethnically diverse populations. Blunck *et al*[99] conducted an external validation study and found that although some models performed well for the overall population, their predictive value was limited for Black patients. Kang *et al*[100] validated three prediction models in a Korean population, yielding AUCs of 0.61-0.64, which were significantly lower than the original reports[15,34,37]. It is important to recognize that models developed in Western countries may not be directly applicable to Asian populations. In recent years, numerous prediction models have been developed in Asian countries such as China, Japan, and Korea. However, most of these models are from single-center retrospective studies and lack external validation. Consequently, there is a pressing need for large-scale prospective studies that integrate various factors to establish prediction models specifically suitable for respective populations.

FUTURE PERSPECTIVES

The risk of POPF following pancreatectomy remains high, highlighting the need for a thorough understanding of pathophysiology and risk factors in order to reduce the risk where possible and improve surgical outcomes. Continuous improvement and refinement of POPF prediction models is necessary for better clinical utility. This iterative process allows for development of personalized treatment strategies to optimize patient outcomes. To overcome the limitations and challenges faced by current models, future efforts should consider collecting comprehensive and standardized data. Ongoing research is directed towards developing robust models that account for the multifactorial nature of POPF. By predicting the risk of POPF based on preoperative factors, clinicians will be able to adequately prepare patients before surgery, choose appropriate surgical procedure, and make timely decisions regarding whether the patient should be transferred to a specialized surgical center for further treatment. In addition to static variables, efforts should also be focused on developing models that incorporate dynamic variables. Intraoperative findings and early postoperative markers, which can provide valuable real-time information, could be integrated into the prediction models. By including these factors, the models can better adapt to individual patient characteristics and enhance their predictive power. The dynamic monitoring models can guide surgeons in determining the best course of postoperative treatment for patients affected by POPF.

CONCLUSION

Prospective studies involving large cohorts and multiple centers are of utmost importance to establish reliable prediction models. Advancements in imaging techniques hold great promise in refining prediction models. High-resolution imaging modalities can provide detailed information about pancreatic and abdominal features and help identify important predictive factors. The integration of machine learning algorithms and artificial intelligence systems are likely to enhance the predictive capabilities of these models. By continuously learning from real-time data and adapting to new information, it is anticipated these systems will provide more accurate predictions of POPF. Nevertheless, it is crucial to validate the developed models externally to ensure their generalizability across different clinical settings and patient populations.

FOOTNOTES

Author contributions: Yang F collected the materials, discussed the topic, wrote the manuscript, and supervised this publication; Windsor JA and Fu DL discussed the topic and revised the manuscript.

Conflict-of-interest statement: We declare no conflicts of interest.

Country/Territory of origin: China

ORCID number: Feng Yang 0000-0001-8790-6072; John A Windsor 0000-0001-5995-5432; De-Liang Fu 0000-0003-4060-8101.

S-Editor: Yan JP
L-Editor: A
P-Editor: Zhao YQ

REFERENCES

1 **Yang F**, Jin C, Hao S, Fu D. Drain Contamination after Distal Pancreatectomy: Incidence, Risk Factors, and Association with Postoperative Pancreatic Fistula. *J Gastrointest Surg* 2019; **23**: 2449-2458 [PMID: 30815778 DOI: 10.1007/s11605-019-04155-7]
2 **McMillan MT**, Christein JD, Callery MP, Behrman SW, Drebin JA, Hollis RH, Kent TS, Miller BC, Sprys MH, Watkins AA, Strasberg SM, Vollmer CM Jr. Comparing the burden of pancreatic fistulas after pancreatoduodenectomy and distal pancreatectomy. *Surgery* 2016; **159**: 1013-1022 [PMID: 26670325 DOI: 10.1016/j.surg.2015.10.028]
3 **Yang F**, Jin C, Li J, Di Y, Zhang J, Fu D. Clinical significance of drain fluid culture after pancreaticoduodenectomy. *J Hepatobiliary Pancreat Sci* 2018; **25**: 508-517 [PMID: 30328297 DOI: 10.1002/jhbp.589]
4 **Chong E**, Ratnayake B, Lee S, French JJ, Wilson C, Roberts KJ, Loveday BPT, Manas D, Windsor J, White S, Pandanaboyana S. Systematic review and meta-analysis of risk factors of postoperative pancreatic fistula after distal pancreatectomy in the era of 2016 International Study Group pancreatic fistula definition. *HPB (Oxford)* 2021; **23**: 1139-1151 [PMID: 33820687 DOI: 10.1016/j.hpb.2021.02.015]
5 **Iacono C**, Verlato G, Ruzzenente A, Campagnaro T, Bacchelli C, Valdegamberi A, Bortolasi L, Guglielmi A. Systematic review of central pancreatectomy and meta-analysis of central versus distal pancreatectomy. *Br J Surg* 2013; **100**: 873-885 [PMID: 23640664 DOI: 10.1002/bjs.9136]
6 **Bassi C**, Dervenis C, Butturini G, Fingerhut A, Yeo C, Izbicki J, Neoptolemos J, Sarr M, Traverso W, Buchler M; International Study Group on Pancreatic Fistula Definition. Postoperative pancreatic fistula: an international study group (ISGPF) definition. *Surgery* 2005; **138**: 8-13 [PMID: 16003309 DOI: 10.1016/j.surg.2005.05.001]
7 **Bassi C**, Marchegiani G, Dervenis C, Sarr M, Abu Hilal M, Adham M, Allen P, Andersson R, Asbun HJ, Besselink MG, Conlon K, Del Chiaro M, Falconi M, Fernandez-Cruz L, Fernandez-Del Castillo C, Fingerhut A, Friess H, Gouma DJ, Hackert T, Izbicki J, Lillemoe KD, Neoptolemos JP, Olah A, Schulick R, Shrikhande SV, Takada T, Takaori K, Traverso W, Vollmer CR, Wolfgang CL, Yeo CJ, Salvia R, Buchler M; International Study Group on Pancreatic Surgery (ISGPS). The 2016 update of the International Study Group (ISGPS) definition and grading of postoperative pancreatic fistula: 11 Years After. *Surgery* 2017; **161**: 584-591 [PMID: 28040257 DOI: 10.1016/j.surg.2016.11.014]
8 **Maggino L**, Malleo G, Bassi C, Allegrini V, McMillan MT, Borin A, Chen B, Drebin JA, Ecker BL, Fraker DL, Lee MK, Paiella S, Roses RE, Salvia R, Vollmer CM Jr. Decoding Grade B Pancreatic Fistula: A Clinical and Economical Analysis and Subclassification Proposal. *Ann Surg* 2019; **269**: 1146-1153 [PMID: 31082914 DOI: 10.1097/SLA.0000000000002673]
9 **Bonsdorff A**, Helanterä I, Tarvainen T, Sirén J, Kokkola A, Sallinen V. Prediction and consequences of postoperative pancreatitis after pancreaticoduodenectomy. *BJS Open* 2022; **6** [PMID: 35470380 DOI: 10.1093/bjsopen/zrac012]
10 **Chui JN**, Yang AJ, Nahm CB, Connor S, Gill AJ, Samra JS, Mittal A. Clinical validation of the international study group of pancreatic surgery (ISGPS) definition for post-pancreatectomy acute pancreatitis. *HPB (Oxford)* 2023; **25**: 704-710 [PMID: 36934027 DOI: 10.1016/j.hpb.2023.01.014]
11 **Bonsdorff A**, Sallinen V. Prediction of postoperative pancreatic fistula and pancreatitis after pancreatoduodenectomy or distal pancreatectomy: A review. *Scand J Surg* 2023; **112**: 126-134 [PMID: 37083016 DOI: 10.1177/14574969231167781]
12 **Yang F**, Jin C, Fu D. Pasireotide for postoperative pancreatic fistula. *N Engl J Med* 2014; **371**: 875 [PMID: 25162895 DOI: 10.1056/NEJMc1407470]
13 **Wellner UF**, Kayser G, Lapshyn H, Sick O, Makowiec F, Höppner J, Hopt UT, Keck T. A simple scoring system based on clinical factors related to pancreatic texture predicts postoperative pancreatic fistula preoperatively. *HPB (Oxford)* 2010; **12**: 696-702 [PMID: 21083795 DOI: 10.1111/j.1477-2574.2010.00239.x]
14 **Yamamoto Y**, Sakamoto Y, Nara S, Esaki M, Shimada K, Kosuge T. A preoperative predictive scoring system for postoperative pancreatic fistula after pancreaticoduodenectomy. *World J Surg* 2011; **35**: 2747-2755 [PMID: 21913138 DOI: 10.1007/s00268-011-1253-x]
15 **Roberts KJ**, Hodson J, Mehrzad H, Marudanayagam R, Sutcliffe RP, Muiesan P, Isaac J, Bramhall SR, Mirza DF. A preoperative predictive score of pancreatic fistula following pancreatoduodenectomy. *HPB (Oxford)* 2014; **16**: 620-628 [PMID: 24246089 DOI: 10.1111/hpb.12186]
16 **Zhang JY**, Huang J, Zhao SY, Liu X, Xiong ZC, Yang ZY. Risk Factors and a New Prediction Model for Pancreatic Fistula After Pancreaticoduodenectomy. *Risk Manag Healthc Policy* 2021; **14**: 1897-1906 [PMID: 34007227 DOI: 10.2147/RMHP.S305332]
17 **Yu J**, Ren CY, Wang J, Cui W, Zhang JJ, Wang YJ. Establishment of risk prediction model of postoperative pancreatic fistula after pancreatoduodenectomy: 2016 edition of definition and grading system of pancreatic fistula: a single center experience with 223 cases. *World J Surg Oncol* 2021; **19**: 257 [PMID: 34461923 DOI: 10.1186/s12957-021-02372-6]
18 **Lucassen CJ**, Groen JV, Aziz MH, Bastiaannet E, Bonsing BA, Leistra E, Shahbazi Feshtali S, Vahrmeijer AL, Droop A, Mieog JSD. Visceral adipose tissue is a better predictor than BMI in the alternative Fistula Risk Score in patients undergoing pancreatoduodenectomy. *HPB (Oxford)* 2022; **24**: 1679-1687 [PMID: 35527105 DOI: 10.1016/j.hpb.2022.03.004]
19 **Lin Z**, Tang B, Cai J, Wang X, Li C, Tian X, Yang Y. Preoperative prediction of clinically relevant postoperative pancreatic fistula after pancreaticoduodenectomy. *Eur J Radiol* 2021; **139**: 109693 [PMID: 33857829 DOI: 10.1016/j.ejrad.2021.109693]
20 **Honselmann KC**, Antoine C, Frohneberg L, Deichmann S, Bolm L, Braun R, Lapshyn H, Petrova E, Keck T, Wellner U, Bausch D. A simple nomogram for early postoperative risk prediction of clinically relevant pancreatic fistula after pancreatoduodenectomy. *Langenbecks Arch Surg* 2021; **406**: 2343-2355 [PMID: 34009458 DOI: 10.1007/s00423-021-02184-y]
21 **Angrisani M**, Sandini M, Cereda M, Paiella S, Capretti G, Nappo G, Roccamatisi L, Casciani F, Caccialanza R, Bassi C, Zerbi A, Gianotti L. Preoperative adiposity at bioimpedance vector analysis improves the ability of Fistula Risk Score (FRS) in predicting pancreatic fistula after

pancreatoduodenectomy. *Pancreatology* 2020; **20**: 545-550 [PMID: 31980350 DOI: 10.1016/j.pan.2020.01.008]

22 **Ingwersen EW**, Stam WT, Meijs BJV, Roor J, Besselink MG, Groot Koerkamp B, de Hingh IHJT, van Santvoort HC, Stommel MWJ, Daams F; Dutch Pancreatic Cancer Group. Machine learning versus logistic regression for the prediction of complications after pancreatoduodenectomy. *Surgery* 2023; **174**: 435-440 [PMID: 37150712 DOI: 10.1016/j.surg.2023.03.012]

23 **Xia W**, Zhou Y, Lin Y, Yu M, Yin Z, Lu X, Hou B, Jian Z. A Predictive Risk Scoring System for Clinically Relevant Pancreatic Fistula After Pancreaticoduodenectomy. *Med Sci Monit* 2018; **24**: 5719-5728 [PMID: 30113999 DOI: 10.12659/MSM.911499]

24 **Gu Z**, Du Y, Wang P, Zheng X, He J, Wang C, Zhang J. Development and validation of a novel nomogram to predict postoperative pancreatic fistula after pancreatoduodenectomy using lasso-logistic regression: an international multi-institutional observational study. *Int J Surg* 2023; **109**: 4027-4040 [PMID: 37678279 DOI: 10.1097/JS9.0000000000000695]

25 **Ecker BL**, McMillan MT, Allegrini V, Bassi C, Beane JD, Beckman RM, Behrman SW, Dickson EJ, Callery MP, Christein JD, Drebin JA, Hollis RH, House MG, Jamieson NB, Javed AA, Kent TS, Kluger MD, Kowalsky SJ, Maggino L, Malleo G, Valero V 3rd, Velu LKP, Watkins AA, Wolfgang CL, Zureikat AH, Vollmer CM Jr. Risk Factors and Mitigation Strategies for Pancreatic Fistula After Distal Pancreatectomy: Analysis of 2026 Resections From the International, Multi-institutional Distal Pancreatectomy Study Group. *Ann Surg* 2019; **269**: 143-149 [PMID: 28857813 DOI: 10.1097/SLA.0000000000002491]

26 **Pecorelli N**, Palumbo D, Guarneri G, Gritti C, Prato F, Schiavo Lena M, Vallorani A, Partelli S, Crippa S, Doglioni C, De Cobelli F, Falconi M. Preoperative CT image analysis to improve risk stratification for clinically relevant pancreatic fistula after distal pancreatectomy. *Br J Surg* 2023; **110**: 891-895 [PMID: 36308335 DOI: 10.1093/bjs/znac348]

27 **De Pastena M**, van Bodegraven EA, Mungroop TH, Vissers FL, Jones LR, Marchegiani G, Balduzzi A, Klompmaker S, Paiella S, Tavakoli Rad S, Groot Koerkamp B, van Eijck C, Busch OR, de Hingh I, Luyer M, Barnhill C, Seykora T, Maxwell T T, de Rooij T, Tuveri M, Malleo G, Esposito A, Landoni L, Casetti L, Alseidi A, Salvia R, Steyerberg EW, Abu Hilal M, Vollmer CM, Besselink MG, Bassi C. Distal Pancreatectomy Fistula Risk Score (D-FRS): Development and International Validation. *Ann Surg* 2023; **277**: e1099-e1105 [PMID: 35797608 DOI: 10.1097/SLA.0000000000005497]

28 **Xu Y**, Jin C, Fu D, Yang F. External validation of fistula risk scores for postoperative pancreatic fistula after distal pancreatectomy. *Surgery* 2023; **174**: 1416-1421 [PMID: 37827899 DOI: 10.1016/j.surg.2023.09.007]

29 **Roberts KJ**, Storey R, Hodson J, Smith AM, Morris-Stiff G. Pre-operative prediction of pancreatic fistula: is it possible? *Pancreatology* 2013; **13**: 423-428 [PMID: 23890142 DOI: 10.1016/j.pan.2013.04.322]

30 **Kalayarasan R**, Himaja M, Ramesh A, Kokila K. Radiological parameters to predict pancreatic texture: Current evidence and future perspectives. *World J Radiol* 2023; **15**: 170-181 [PMID: 37424737 DOI: 10.4329/wjr.v15.i6.170]

31 **Gaujoux S**, Cortes A, Couvelard A, Noullet S, Clavel L, Rebours V, Lévy P, Sauvanet A, Ruszniewski P, Belghiti J. Fatty pancreas and increased body mass index are risk factors of pancreatic fistula after pancreaticoduodenectomy. *Surgery* 2010; **148**: 15-23 [PMID: 20138325 DOI: 10.1016/j.surg.2009.12.005]

32 **Adamu M**, Plodeck V, Adam C, Roehnert A, Welsch T, Weitz J, Distler M. Predicting postoperative pancreatic fistula in pancreatic head resections: which score fits all? *Langenbecks Arch Surg* 2022; **407**: 175-188 [PMID: 34370113 DOI: 10.1007/s00423-021-02290-x]

33 **Alhulaili ZM**, Linnemann RJ, Dascau L, Pleijhuis RG, Klaase JM. A Transparent Reporting of a multivariable prediction model for Individual Prognosis Or Diagnosis analysis to evaluate the quality of reporting of postoperative pancreatic fistula prediction models after pancreatoduodenectomy: A systematic review. *Surgery* 2023; **174**: 684-691 [PMID: 37296054 DOI: 10.1016/j.surg.2023.04.058]

34 **Callery MP**, Pratt WB, Kent TS, Chaikof EL, Vollmer CM Jr. A prospectively validated clinical risk score accurately predicts pancreatic fistula after pancreatoduodenectomy. *J Am Coll Surg* 2013; **216**: 1-14 [PMID: 23122535 DOI: 10.1016/j.jamcollsurg.2012.09.002]

35 **Miller BC**, Christein JD, Behrman SW, Drebin JA, Pratt WB, Callery MP, Vollmer CM Jr. A multi-institutional external validation of the fistula risk score for pancreatoduodenectomy. *J Gastrointest Surg* 2014; **18**: 172-79; discussion 179 [PMID: 24002771 DOI: 10.1007/s11605-013-2337-8]

36 **Shubert CR**, Wagie AE, Farnell MB, Nagorney DM, Que FG, Reid Lombardo KM, Truty MJ, Smoot RL, Kendrick ML. Clinical Risk Score to Predict Pancreatic Fistula after Pancreatoduodenectomy: Independent External Validation for Open and Laparoscopic Approaches. *J Am Coll Surg* 2015; **221**: 689-698 [PMID: 26296680 DOI: 10.1016/j.jamcollsurg.2015.05.011]

37 **Mungroop TH**, van Rijssen LB, van Klaveren D, Smits FJ, van Woerden V, Linnemann RJ, de Pastena M, Klompmaker S, Marchegiani G, Ecker BL, van Dieren S, Bonsing B, Busch OR, van Dam RM, Erdmann J, van Eijck CH, Gerhards MF, van Goor H, van der Harst E, de Hingh IH, de Jong KP, Kazemier G, Luyer M, Shamali A, Barbaro S, Armstrong T, Takhar A, Hamady Z, Klaase J, Lips DJ, Molenaar IQ, Nieuwenhuijs VB, Rupert C, van Santvoort HC, Scheepers JJ, van der Schelling GP, Bassi C, Vollmer CM, Steyerberg EW, Abu Hilal M, Groot Koerkamp B, Besselink MG; Dutch Pancreatic Cancer Group. Alternative Fistula Risk Score for Pancreatoduodenectomy (a-FRS): Design and International External Validation. *Ann Surg* 2019; **269**: 937-943 [PMID: 29240007 DOI: 10.1097/SLA.0000000000002620]

38 **Mungroop TH**, Klompmaker S, Wellner UF, Steyerberg EW, Coratti A, D'Hondt M, de Pastena M, Dokmak S, Khatkov I, Saint-Marc O, Wittel U, Abu Hilal M, Fuks D, Poves I, Keck T, Boggi U, Besselink MG; European Consortium on Minimally Invasive Pancreatic Surgery (E-MIPS). Updated Alternative Fistula Risk Score (ua-FRS) to Include Minimally Invasive Pancreatoduodenectomy: Pan-European Validation. *Ann Surg* 2021; **273**: 334-340 [PMID: 30829699 DOI: 10.1097/SLA.0000000000003234]

39 **Shinde RS**, Acharya R, Chaudhari VA, Bhandare MS, Mungroop TH, Klompmaker S, Besselink MG, Shrikhande SV. External validation and comparison of the original, alternative and updated-alternative fistula risk scores for the prediction of postoperative pancreatic fistula after pancreatoduodenectomy. *Pancreatology* 2020; **20**: 751-756 [PMID: 32340876 DOI: 10.1016/j.pan.2020.04.006]

40 **Roberts KJ**, Sutcliffe RP, Marudanayagam R, Hodson J, Isaac J, Muiesan P, Navarro A, Patel K, Jah A, Napetti S, Adair A, Lazaridis S, Prachalias A, Shingler G, Al-Sarireh B, Storey R, Smith AM, Shah N, Fusai G, Ahmed J, Abu Hilal M, Mirza DF. Scoring System to Predict Pancreatic Fistula After Pancreaticoduodenectomy: A UK Multicenter Study. *Ann Surg* 2015; **261**: 1191-1197 [PMID: 25371115 DOI: 10.1097/SLA.0000000000000997]

41 **Perri G**, Marchegiani G, Partelli S, Crippa S, Bianchi B, Cinelli L, Esposito A, Pecorelli N, Falconi M, Bassi C, Salvia R. Preoperative risk stratification of postoperative pancreatic fistula: A risk-tree predictive model for pancreatoduodenectomy. *Surgery* 2021; **170**: 1596-1601 [PMID: 34315629 DOI: 10.1016/j.surg.2021.06.046]

42 **Casadei R**, Ricci C, Taffurelli G, D'Ambra M, Pacilio CA, Ingaldi C, Minni F. Are there preoperative factors related to a "soft pancreas" and are they predictive of pancreatic fistulas after pancreatic resection? *Surg Today* 2015; **45**: 708-714 [PMID: 25331230 DOI: 10.1007/s00595-014-1045-7]

43 **Zhang W**, Cai W, He B, Xiang N, Fang C, Jia F. A radiomics-based formula for the preoperative prediction of postoperative pancreatic fistula in patients with pancreaticoduodenectomy. *Cancer Manag Res* 2018; **10**: 6469-6478 [PMID: 30568506 DOI: 10.2147/CMAR.S185865]

44 **Shi Y**, Gao F, Qi Y, Lu H, Ai F, Hou Y, Liu C, Xu Y, Zhang X, Cai X. Computed tomography-adjusted fistula risk score for predicting clinically relevant postoperative pancreatic fistula after pancreatoduodenectomy: Training and external validation of model upgrade. *EBioMedicine* 2020; **62**: 103096 [PMID: 33161232 DOI: 10.1016/j.ebiom.2020.103096]

45 **Tang B**, Lin Z, Ma Y, Zhang A, Liu W, Zhang J, Wang X, Tian X, Yang Y. A modified alternative fistula risk score (a-FRS) obtained from the computed tomography enhancement pattern of the pancreatic parenchyma predicts pancreatic fistula after pancreatoduodenectomy. *HPB (Oxford)* 2021; **23**: 1759-1766 [PMID: 33975799 DOI: 10.1016/j.hpb.2021.04.015]

46 **Lapshyn H**, Petruch N, Thomaschewski M, Sondermann S, May K, Frohneberg L, Petrova E, Zemskov S, Honselmann KC, Braun R, Keck T, Wellner UF, Bolm L. A simple preoperative stratification tool predicting the risk of postoperative pancreatic fistula after pancreatoduodenectomy. *Pancreatology* 2021; **21**: 957-964 [PMID: 33775565 DOI: 10.1016/j.pan.2021.03.009]

47 **Savin ML**, Mihai F, Gheorghe L, Lupascu Ursulescu C, Negru D, Trofin AM, Zabara M, Nutu V, Cadar R, Blaj M, Lovin O, Crumpei F, Lupascu C. Proposal of a Preoperative CT-Based Score to Predict the Risk of Clinically Relevant Pancreatic Fistula after Cephalic Pancreatoduodenectomy. *Medicina (Kaunas)* 2021; **57** [PMID: 34202601 DOI: 10.3390/medicina57070650]

48 **Skawran SM**, Kambakamba P, Baessler B, von Spiczak J, Kupka M, Müller PC, Moeckli B, Linecker M, Petrowsky H, Reiner CS. Can magnetic resonance imaging radiomics of the pancreas predict postoperative pancreatic fistula? *Eur J Radiol* 2021; **140**: 109733 [PMID: 33945924 DOI: 10.1016/j.ejrad.2021.109733]

49 **Box EW**, Deng L, Morgan DE, Xie R, Kirklin JK, Wang TN, Heslin MJ, Reddy S, Vickers S, Dudeia V, Rose JB. Preoperative anthropomorphic radiographic measurements can predict postoperative pancreatic fistula formation following pancreatoduodenectomy. *Am J Surg* 2021; **222**: 133-138 [PMID: 33390246 DOI: 10.1016/j.amjsurg.2020.10.023]

50 **Kolbinger FR**, Lambrecht J, Leger S, Ittermann T, Speidel S, Weitz J, Hoffmann RT, Distler M, Kühn JP. The image-based preoperative fistula risk score (preFRS) predicts postoperative pancreatic fistula in patients undergoing pancreatic head resection. *Sci Rep* 2022; **12**: 4064 [PMID: 35260701 DOI: 10.1038/s41598-022-07970-2]

51 **Maqueda González R**, Di Martino M, Galán González I, Rodríguez Carnero P, Martín-Pérez E. Development of a prediction model of pancreatic fistula after duodenopancreatectomy and soft pancreas by assessing the preoperative image. *Langenbecks Arch Surg* 2022; **407**: 2363-2372 [PMID: 35643803 DOI: 10.1007/s00423-022-02564-y]

52 **Zou J**, Xue X, Qin L. Development of a Nomogram to Predict Clinically Relevant Postoperative Pancreatic Fistula After Pancreaticoduodenectomy on the Basis of Visceral Fat Area and Magnetic Resonance Imaging. *Ann Surg Oncol* 2023; **30**: 7712-7719 [PMID: 37530992 DOI: 10.1245/s10434-023-13943-0]

53 **Tian XF**, Zhang L, Lou WH, Qiu YJ, Zuo D, Wang WP, Dong Y. Application of ultrasound shear wave elastography in pre-operative and quantitative prediction of clinically relevant post-operative pancreatic fistula after pancreatectomy: a prospective study for the investigation of risk evaluation model. *Eur Radiol* 2023; **33**: 7866-7876 [PMID: 37368114 DOI: 10.1007/s00330-023-09859-8]

54 **Mu W**, Liu C, Gao F, Qi Y, Lu H, Liu Z, Zhang X, Cai X, Ji RY, Hou Y, Tian J, Shi Y. Prediction of clinically relevant Pancreatico-enteric Anastomotic Fistulas after Pancreatoduodenectomy using deep learning of Preoperative Computed Tomography. *Theranostics* 2020; **10**: 9779-9788 [PMID: 32863959 DOI: 10.7150/thno.49671]

55 **Han IW**, Cho K, Ryu Y, Shin SH, Heo JS, Choi DW, Chung MJ, Kwon OC, Cho BH. Risk prediction platform for pancreatic fistula after pancreatoduodenectomy using artificial intelligence. *World J Gastroenterol* 2020; **26**: 4453-4464 [PMID: 32874057 DOI: 10.3748/wjg.v26.i30.4453]

56 **Giovinazzo F**, Linneman R, Riva GVD, Greener D, Morano C, Patijn GA, Besselink MGH, Nieuwenhuijs VB, Abu Hilal M; Artificial Intelligence Pancreatic Fistula Group, de Hingh IH, Kazemier G, Festen S, de Jong KP, van Eijck CHJ, Scheepers JJG, van der Kolk M, den Dulk M, Bosscha K, Boerma D, van der Harst E, Armstrong T, Takhar A, Hamady Z. Clinical relevant pancreatic fistula after pancreatoduodenectomy: when negative amylase levels tell the truth. *Updates Surg* 2021; **73**: 1391-1397 [PMID: 33770412 DOI: 10.1007/s13304-021-01020-8]

57 **Shen Z**, Chen H, Wang W, Xu W, Zhou Y, Weng Y, Xu Z, Deng X, Peng C, Lu X, Shen B. Machine learning algorithms as early diagnostic tools for pancreatic fistula following pancreaticoduodenectomy and guide drain removal: A retrospective cohort study. *Int J Surg* 2022; **102**: 106638 [PMID: 35500881 DOI: 10.1016/j.ijsu.2022.106638]

58 **Long ZD**, Lu C, Xia XG, Chen B, Xing ZX, Bie L, Zhou P, Ma ZL, Wang R. Personal predictive model based on systemic inflammation markers for estimation of postoperative pancreatic fistula following pancreaticoduodenectomy. *World J Gastrointest Surg* 2022; **14**: 963-975 [PMID: 36185559 DOI: 10.4240/wjgs.v14.i9.963]

59 **Capretti G**, Bonifacio C, De Palma C, Nebbia M, Giannitto C, Cancian P, Laino ME, Balzarini L, Papanikolaou N, Savevski V, Zerbi A. A machine learning risk model based on preoperative computed tomography scan to predict postoperative outcomes after pancreatoduodenectomy. *Updates Surg* 2022; **74**: 235-243 [PMID: 34596836 DOI: 10.1007/s13304-021-01174-5]

60 **Chen KA**, Berginski ME, Desai CS, Guillem JG, Stem J, Gomez SM, Kapadia MR. Differential Performance of Machine Learning Models in Prediction of Procedure-Specific Outcomes. *J Gastrointest Surg* 2022; **26**: 1732-1742 [PMID: 35508684 DOI: 10.1007/s11605-022-05332-x]

61 **Zheng J**, Lv X, Jiang L, Liu H, Zhao X. Development of a Pancreatic Fistula Prediction Model After Pancreaticoduodenectomy Based on a Decision Tree and Random Forest Algorithm. *Am Surg* 2023; 31348231158692 [PMID: 36803027 DOI: 10.1177/00031348231158692]

62 **Verma A**, Balian J, Hadaya J, Premji A, Shimizu T, Donahue T, Benharash P. Machine Learning Based Prediction of Postoperative Pancreatic Fistula Following Pancreaticoduodenectomy. *Ann Surg* 2023 [PMID: 37947154 DOI: 10.1097/SLA.0000000000006123]

63 **Ashraf Ganjouei A**, Romero-Hernandez F, Wang JJ, Casey M, Frye W, Hoffman D, Hirose K, Nakakura E, Corvera C, Maker AV, Kirkwood KS, Alseidi A, Adam MA. A Machine Learning Approach to Predict Postoperative Pancreatic Fistula After Pancreaticoduodenectomy Using Only Preoperatively Known Data. *Ann Surg Oncol* 2023; **30**: 7738-7747 [PMID: 37550449 DOI: 10.1245/s10434-023-14041-x]

64 **Ingwersen EW**, Bereska JI, Balduzzi A, Janssen BV, Besselink MG, Kazemier G, Marchegiani G, Malleo G, Marquering HA, Nio CY, de Robertis R, Salvia R, Steyerberg EW, Stoker J, Struik F, Verpalen IM, Daams F; Pancreatobiliary and Hepatic Artificial Intelligence Research (PHAIR) consortium. Radiomics preoperative-Fistula Risk Score (RAD-FRS) for pancreatoduodenectomy: development and external validation. *BJS Open* 2023; **7**: zrad100 [PMID: 37811791 DOI: 10.1093/bjsopen/zrad100]

65 **Schuh F**, Mihaljevic AL, Probst P, Trudeau MT, Müller PC, Marchegiani G, Besselink MG, Uzunoglu F, Izbicki JR, Falconi M, Castillo CF, Adham M, Z'graggen K, Friess H, Werner J, Weitz J, Strobel O, Hackert T, Radenkovic D, Kelemen D, Wolfgang C, Miao YI, Shrikhande SV, Lillemoe KD, Dervenis C, Bassi C, Neoptolemos JP, Diener MK, Vollmer CM Jr, Büchler MW. A Simple Classification of Pancreatic Duct Size and Texture Predicts Postoperative Pancreatic Fistula: A classification of the International Study Group of Pancreatic Surgery. *Ann Surg* 2023; **277**: e597-e608 [PMID: 33914473 DOI: 10.1097/SLA.0000000000004855]

66 **Suurmeijer JA**, Emmen AM, Bonsing BA, Busch OR, Daams F, van Eijck CH, van Dieren S, de Hingh IH, Mackay TM, Mieog JS, Molenaar IQ, Stommel MW, de Meijer VE, van Santvoort HC, Groot Koerkamp B, Besselink MG; Dutch Pancreatic Cancer Group. Nationwide validation of the ISGPS risk classification for postoperative pancreatic fistula after pancreatoduodenectomy: "Less is more". *Surgery* 2023; **173**: 1248-1253 [PMID: 36858874 DOI: 10.1016/j.surg.2023.01.004]

67 **Kim JY**, Park JS, Kim JK, Yoon DS. A model for predicting pancreatic leakage after pancreaticoduodenectomy based on the international study group of pancreatic surgery classification. *Korean J Hepatobiliary Pancreat Surg* 2013; **17**: 166-170 [PMID: 26155234 DOI: 10.14701/kjhbps.2013.17.4.166]

68 **Chen JY**, Feng J, Wang XQ, Cai SW, Dong JH, Chen YL. Risk scoring system and predictor for clinically relevant pancreatic fistula after pancreaticoduodenectomy. *World J Gastroenterol* 2015; **21**: 5926-5933 [PMID: 26019457 DOI: 10.3748/wjg.v21.i19.5926]

69 **Kantor O**, Talamonti MS, Pitt HA, Vollmer CM, Riall TS, Hall BL, Wang CH, Baker MS. Using the NSQIP Pancreatic Demonstration Project to Derive a Modified Fistula Risk Score for Preoperative Risk Stratification in Patients Undergoing Pancreaticoduodenectomy. *J Am Coll Surg* 2017; **224**: 816-825 [PMID: 28408176 DOI: 10.1016/j.jamcollsurg.2017.01.054]

70 **Li Y**, Zhou F, Zhu DM, Zhang ZX, Yang J, Yao J, Wei YJ, Xu YL, Li DC, Zhou J. Novel risk scoring system for prediction of pancreatic fistula after pancreaticoduodenectomy. *World J Gastroenterol* 2019; **25**: 2650-2664 [PMID: 31210716 DOI: 10.3748/wjg.v25.i21.2650]

71 **Hayashi H**, Shimizu A, Kubota K, Notake T, Masuo H, Yoshizawa T, Hosoda K, Sakai H, Ikehara T, Soejima Y. A new fistula risk score using sarcopenic obesity and subcutaneous fat area for predicting postoperative pancreatic fistula after pancreaticoduodenectomy. *J Hepatobiliary Pancreat Sci* 2023; **30**: 792-801 [PMID: 36448256 DOI: 10.1002/jhbp.1283]

72 **Xingjun G**, Feng Z, Meiwen Y, Jianxin J, Zheng H, Jun G, Tao H, Rui Z, Leida Z, Min W, Renyi Q; FACS. A score model based on pancreatic steatosis and fibrosis and pancreatic duct diameter to predict postoperative pancreatic fistula after Pancreatoduodenectomy. *BMC Surg* 2019; **19**: 75 [PMID: 31269932 DOI: 10.1186/s12893-019-0534-4]

73 **You Y**, Han IW, Choi DW, Heo JS, Ryu Y, Park DJ, Choi SH, Han S. Nomogram for predicting postoperative pancreatic fistula. *HPB (Oxford)* 2019; **21**: 1436-1445 [PMID: 30982739 DOI: 10.1016/j.hpb.2019.03.351]

74 **Guo CX**, Shen YN, Zhang Q, Zhang XZ, Wang JL, Gao SL, Lou JY, Que RS, Ma T, Liang TB, Bai XL. Prediction of postoperative pancreatic fistula using a nomogram based on the updated definition. *Ann Surg Treat Res* 2020; **98**: 72-81 [PMID: 32051815 DOI: 10.4174/astr.2020.98.2.72]

75 **Li B**, Pu N, Chen Q, Mei Y, Wang D, Jin D, Wu W, Zhang L, Lou W. Comprehensive Diagnostic Nomogram for Predicting Clinically Relevant Postoperative Pancreatic Fistula After Pancreatoduodenectomy. *Front Oncol* 2021; **11**: 717087 [PMID: 34277458 DOI: 10.3389/fonc.2021.717087]

76 **Shen J**, Guo F, Sun Y, Zhao J, Hu J, Ke Z, Zhang Y, Jin X, Wu H. Predictive nomogram for postoperative pancreatic fistula following pancreaticoduodenectomy: a retrospective study. *BMC Cancer* 2021; **21**: 550 [PMID: 33992090 DOI: 10.1186/s12885-021-08201-z]

77 **Liu R**, Cai Y, Cai H, Lan Y, Meng L, Li Y, Peng B. Dynamic prediction for clinically relevant pancreatic fistula: a novel prediction model for laparoscopic pancreaticoduodenectomy. *BMC Surg* 2021; **21**: 7 [PMID: 33397337 DOI: 10.1186/s12893-020-00968-5]

78 **Huang XT**, Huang CS, Liu C, Chen W, Cai JP, Cheng H, Jiang XX, Liang LJ, Yu XJ, Yin XY. Development and Validation of a New Nomogram for Predicting Clinically Relevant Postoperative Pancreatic Fistula After Pancreatoduodenectomy. *World J Surg* 2021; **45**: 261-269 [PMID: 32901325 DOI: 10.1007/s00268-020-05773-y]

79 **Guilbaud T**, Garnier J, Girard E, Ewald J, Risse O, Moutardier V, Chirica M, Birnbaum DJ, Turrini O. Postoperative day 1 combination of serum C-reactive protein and drain amylase values predicts risks of clinically relevant pancreatic fistula. The "90-1000" score. *Surgery* 2021; **170**: 1508-1516 [PMID: 34092376 DOI: 10.1016/j.surg.2021.04.033]

80 **Suzuki S**, Shimoda M, Shimazaki J, Oshiro Y, Nishida K, Shiihara M, Izumo W, Yamamoto M. Drain Lipase Levels and Decreased Rate of Drain Amylase Levels as Independent Predictors of Pancreatic Fistula with Nomogram After Pancreaticoduodenectomy. *World J Surg* 2021; **45**: 1921-1928 [PMID: 33721069 DOI: 10.1007/s00268-021-06038-y]

81 **Al Abbas AI**, Borrebach JD, Pitt HA, Bellon J, Hogg ME, Zeh HJ 3rd, Zureikat AH. Development of a Novel Pancreatoduodenectomy-Specific Risk Calculator: an Analysis of 10,000 Patients. *J Gastrointest Surg* 2021; **25**: 1503-1511 [PMID: 32671801 DOI: 10.1007/s11605-020-04725-0]

82 **Yin J**, Zhu Q, Zhang K, Gao W, Wu J, Lu Z, Jiang K, Miao Y. Development and validation of risk prediction nomogram for pancreatic fistula and risk-stratified strategy for drainage management after pancreaticoduodenectomy. *Gland Surg* 2022; **11**: 42-55 [PMID: 35242668 DOI: 10.21037/gs-21-550]

83 **Bannone E**, Marchegiani G, Vollmer C, Perri G, Procida G, Corvino G, Peressotti S, Vacca PG, Salvia R, Bassi C. Postoperative Serum Hyperamylasemia Adds Sequential Value to the Fistula Risk Score in Predicting Pancreatic Fistula after Pancreatoduodenectomy. *Ann Surg* 2023; **278**: e293-e301 [PMID: 35876366 DOI: 10.1097/SLA.0000000000005629]

84 **Choi M**, Lee JH, Roh YH, Kim H, Jang JY, Choi SH, Kang CM. Multidimensional Nomogram to Predict Postoperative Pancreatic Fistula after Minimally Invasive Pancreaticoduodenectomy. *Ann Surg Oncol* 2023; **30**: 5083-5090 [PMID: 37195514 DOI: 10.1245/s10434-023-13360-3]

85 **van Dongen JC**, van Dam JL, Besselink MG, Bonsing BA, Bosscha K, Busch OR, van Dam RM, Festen S, van der Harst E, de Hingh IH, Kazemier G, Liem MSL, de Meijer VE, Mieog JSD, Molenaar IQ, Patijn GA, van Santvoort HC, Wijsman JH, Stommel MWJ, Wit F, De Wilde RF, van Eijck CHJ, Groot Koerkamp B; Dutch Pancreatic Cancer Group. Fistula Risk Score for Auditing Pancreatoduodenectomy: The Auditing-FRS. *Ann Surg* 2023; **278**: e272-e277 [PMID: 35837978 DOI: 10.1097/SLA.0000000000005532]

86 **Raza SS**, Nutu A, Powell-Brett S, Marchetti A, Perri G, Carvalheiro Boteon A, Hodson J, Chatzizacharias N, Dasari BV, Isaac J, Abradelo M, Marudanayagam R, Mirza DF, Roberts JK, Marchegiani G, Salvia R, Sutcliffe RP. Early postoperative risk stratification in patients with pancreatic fistula after pancreaticoduodenectomy. *Surgery* 2023; **173**: 492-500 [PMID: 37530481 DOI: 10.1016/j.surg.2022.09.008]

87 **Mohamed A**, Nicolais L, Fitzgerald TL. Revisiting the Pancreatic Fistula Risk Score: Clinical Nomogram Accurately Assesses Risk. *Am Surg* 2023; **89**: 837-843 [PMID: 34633224 DOI: 10.1177/00031348211047471]

88 **Ahmad SB**, Hodges JC, Nassour I, Casciani F, Lee KK, Paniccia A, Vollmer CM Jr, Zureikat AH. The risk of clinically-relevant pancreatic fistula after pancreaticoduodenectomy is better predicted by a postoperative trend in drain fluid amylase compared to day 1 values in isolation. *Surgery* 2023; **174**: 916-923 [PMID: 37468367 DOI: 10.1016/j.surg.2023.06.009]

89 **Bonsdorff A**, Ghorbani P, Helanterä I, Tarvainen T, Kontio T, Belfrage H, Sirén J, Kokkola A, Sparrelid E, Sallinen V. Development and external validation of DISPAIR fistula risk score for clinically relevant postoperative pancreatic fistula risk after distal pancreatectomy. *Br J Surg* 2022; **109**: 1131-1139 [PMID: 35983583 DOI: 10.1093/bjs/znac266]

90 **Rollin N**, Cassese G, Pineton DE Chambrun G, Serrand C, Navarro F, Blanc P, Panaro F, Valats JC. An easy-to-use score to predict clinically relevant postoperative pancreatic fistula after distal pancreatectomy. *Minerva Surg* 2022; **77**: 354-359 [PMID: 34693675 DOI:

10.23736/S2724-5691.21.09001-8]

91 **Nassour I**, AlMasri S, Hodges JC, Hughes SJ, Zureikat A, Paniccia A. Novel Calculator to Estimate the Risk of Clinically Relevant Postoperative Pancreatic Fistula Following Distal Pancreatectomy. *J Gastrointest Surg* 2022; **26**: 1436-1444 [PMID: 35352209 DOI: 10.1007/s11605-022-05275-3]

92 **He C**, Zhang Y, Li L, Zhao M, Wang C, Tang Y. Risk factor analysis and prediction of postoperative clinically relevant pancreatic fistula after distal pancreatectomy. *BMC Surg* 2023; **23**: 5 [PMID: 36631791 DOI: 10.1186/s12893-023-01907-w]

93 **Yang F**, Jin C, Di Y, He H, Hao S, Yao L, Li J, Fu D. Central pancreatectomy with external drainage of monolayer pancreaticojejunostomy for prevention of postoperative pancreatic fistula: A retrospective cohort study. *Int J Surg* 2018; **51**: 104-108 [PMID: 29367037 DOI: 10.1016/j.ijsu.2018.01.009]

94 **Ouyang L**, Liu RD, Ren YW, Nie G, He TL, Li G, Zhou YQ, Huang ZP, Zhang YJ, Hu XG, Jin G. Nomogram predicts CR-POPF in open central pancreatectomy patients with benign or low-grade malignant pancreatic neoplasms. *Front Oncol* 2022; **12**: 1030080 [PMID: 36591477 DOI: 10.3389/fonc.2022.1030080]

95 **Yang F**, Xu Y, Jin C, Windsor JA, Fu D. Predicting pancreatic fistula after central pancreatectomy using current fistula risk scores for pancreaticoduodenectomy and distal pancreatectomy. *Pancreatology* 2023; **23**: 843-851 [PMID: 37739874 DOI: 10.1016/j.pan.2023.09.079]

96 **PARANOIA Study Group**; Writing committee, Pande R, Halle-Smith JM, Phelan L, Thorne T, Panikkar M, Hodson J, Roberts KJ; Steering committee, Arshad A, Connor S, Conlon KC, Dickson EJ, Giovinazzo F, Harrison E, de Liguori Carino N, Hore T, Knight SR, Loveday B, Magill L, Mirza D, Pandanaboyana S, Perry RJ, Pinkney T, Siriwardena AK, Satoi S, Skipworth J, Stättner S, Sutcliffe RP, Tingstedt B. External validation of postoperative pancreatic fistula prediction scores in pancreatoduodenectomy: a systematic review and meta-analysis. *HPB (Oxford)* 2022; **24**: 287-298 [PMID: 34810093 DOI: 10.1016/j.hpb.2021.10.006]

97 **Schouten TJ**, Henry AC, Smits FJ, Besselink MG, Bonsing BA, Bosscha K, Busch OR, van Dam RM, van Eijck CH, Festen S, Groot Koerkamp B, van der Harst E, de Hingh IHJT, Kazemier G, Liem MSL, de Meijer VE, Patijn GA, Roos D, Schreinemakers JMJ, Stommel MWJ, Wit F, Daamen LA, Molenaar IQ, van Santvoort HC; Dutch Pancreatic Cancer Group. Risk Models for Developing Pancreatic Fistula After Pancreatoduodenectomy: Validation in a Nationwide Prospective Cohort. *Ann Surg* 2023; **278**: 1001-1008 [PMID: 36804843 DOI: 10.1097/SLA.0000000000005824]

98 **Casciani F**, Trudeau MT, Asbun HJ, Ball CG, Bassi C, Behrman SW, Berger AC, Bloomston MP, Callery MP, Christein JD, Falconi M, Fernandez-Del Castillo C, Dillhoff ME, Dickson EJ, Dixon E, Fisher WE, House MG, Hughes SJ, Kent TS, Malleo G, Partelli S, Salem RR, Stauffer JA, Wolfgang CL, Zureikat AH, Vollmer CM Jr; Pancreas Fistula Study Group. Surgeon experience contributes to improved outcomes in pancreatoduodenectomies at high risk for fistula development. *Surgery* 2021; **169**: 708-720 [PMID: 33386129 DOI: 10.1016/j.surg.2020.11.022]

99 **Blunck CK**, Vickers SM, Wang TN, Dudeja V, Reddy S, Rose JB. External validation of four Pancreatic Fistula Risk Score models in the Deep South US: Do racial disparities affect pancreatic fistula prediction? *Am J Surg* 2022; **224**: 557-561 [PMID: 35219491 DOI: 10.1016/j.amjsurg.2022.02.042]

100 **Kang JS**, Park T, Han Y, Lee S, Kim JR, Kim H, Kwon W, Kim SW, Heo JS, Choi SH, Choi DW, Kim SC, Hong TH, Yoon DS, Park JS, Park SJ, Han SS, Choi SB, Kim JS, Lim CS, Jang JY. Clinical validation of scoring systems of postoperative pancreatic fistula after pancreatoduodenectomy: applicability to Eastern cohorts? *Hepatobiliary Surg Nutr* 2019; **8**: 211-218 [PMID: 31245401 DOI: 10.21037/hbsn.2019.03.17]

World Journal of Gastroenterology

Submit a Manuscript: https://www.f6publishing.com

World J Gastroenterol 2024 March 14; 30(10): 1346-1357

DOI: 10.3748/wjg.v30.i10.1346

ISSN 1007-9327 (print) ISSN 2219-2840 (online)

ORIGINAL ARTICLE

Retrospective Cohort Study

Cumulative effects of excess high-normal alanine aminotransferase levels in relation to new-onset metabolic dysfunction-associated fatty liver disease in China

Jing-Feng Chen, Zhuo-Qing Wu, Hao-Shuang Liu, Su Yan, You-Xiang Wang, Miao Xing, Xiao-Qin Song, Su-Ying Ding

Specialty type: Gastroenterology and hepatology

Provenance and peer review: Unsolicited article; Externally peer reviewed.

Peer-review model: Single blind

Peer-review report's scientific quality classification

Grade A (Excellent): 0
Grade B (Very good): B
Grade C (Good): 0
Grade D (Fair): 0
Grade E (Poor): 0

P-Reviewer: Gorrell MD, Australia

Received: November 7, 2023
Peer-review started: November 7, 2023
First decision: December 27, 2023
Revised: January 12, 2024
Accepted: February 18, 2024
Article in press: February 18, 2024
Published online: March 14, 2024

Jing-Feng Chen, Hao-Shuang Liu, Su Yan, Xiao-Qin Song, Su-Ying Ding, Health Management Center, The First Affiliated Hospital of Zhengzhou University, Zhengzhou 450052, Henan Province, China

Zhuo-Qing Wu, Institute of Systems Engineering, Dalian University of Technology, Dalian 116024, Liaoning Province, China

You-Xiang Wang, College of Public Health, Zhengzhou University, Zhengzhou 450001, Henan Province, China

Miao Xing, School of Basic Medicine and Forensic Medicine, Henan University of Science and Technology, Luoyang 471003, Henan Province, China

Corresponding author: Su-Ying Ding, MD, Director, Doctor, Health Management Center, The First Affiliated Hospital of Zhengzhou University, No. 1 Longhu Middle Ring Road, Jinshui District, Zhengzhou 450052, Henan Province, China. fccdingsy@zzu.edu.cn

Abstract

BACKGROUND

Within the normal range, elevated alanine aminotransferase (ALT) levels are associated with an increased risk of metabolic dysfunction-associated fatty liver disease (MAFLD).

AIM

To investigate the associations between repeated high-normal ALT measurements and the risk of new-onset MAFLD prospectively.

METHODS

A cohort of 3553 participants followed for four consecutive health examinations over 4 years was selected. The incidence rate, cumulative times, and equally and unequally weighted cumulative effects of excess high-normal ALT levels (ehALT) were measured. Cox proportional hazards regression was used to analyse the association between the cumulative effects of ehALT and the risk of new-onset MAFLD.

RESULTS
A total of 83.13% of participants with MAFLD had normal ALT levels. The incidence rate of MAFLD showed a linear increasing trend in the cumulative ehALT group. Compared with those in the low-normal ALT group, the multivariate adjusted hazard ratios of the equally and unequally weighted cumulative effects of ehALT were 1.651 [95% confidence interval (CI): 1.199-2.273] and 1.535 (95%CI: 1.119-2.106) in the third quartile and 1.616 (95%CI: 1.162-2.246) and 1.580 (95%CI: 1.155-2.162) in the fourth quartile, respectively.

CONCLUSION
Most participants with MAFLD had normal ALT levels. Long-term high-normal ALT levels were associated with a cumulative increased risk of new-onset MAFLD.

Key Words: Metabolic dysfunction-associated fatty liver disease; High-normal alanine aminotransferase level; Cumulative effect; Cox proportional hazards regression; Cohort study

Core Tip: Limited evidence exists regarding the association between persistently elevated high-normal alanine transaminase (ALT) levels and the risk of new-onset metabolic dysfunction-associated fatty liver disease (MAFLD). This cohort study analysed 3553 participants followed for four consecutive health examinations between 2017 and 2020 and measured the cumulative effects of excess high-normal ALT (ehALT). Among the participants, the incidence rate of MAFLD showed a linear increasing trend for the cumulative ehALT group. The hazard ratios of new-onset MAFLD were significantly increased in the third and fourth quartiles of the equally and unequally weighted cumulative effects of ehALT. Among Chinese adults, long-term high-normal ALT levels were related to a cumulative increased risk of new-onset MAFLD.

Citation: Chen JF, Wu ZQ, Liu HS, Yan S, Wang YX, Xing M, Song XQ, Ding SY. Cumulative effects of excess high-normal alanine aminotransferase levels in relation to new-onset metabolic dysfunction-associated fatty liver disease in China. *World J Gastroenterol* 2024; 30(10): 1346-1357
URL: https://www.wjgnet.com/1007-9327/full/v30/i10/1346.htm
DOI: https://dx.doi.org/10.3748/wjg.v30.i10.1346

INTRODUCTION

Metabolic dysfunction-associated fatty liver disease (MAFLD) is defined as the combination of nonalcoholic fatty liver disease (NAFLD) and metabolic dysfunction and includes overweight/obesity, type 2 diabetes, or other metabolic disorders, as indicated by liver biopsy or imaging examination or even blood biomarker tests suggesting the presence of fatty liver[1,2]. MAFLD has become a growing public health problem, affecting up to a third of the global population, and its burden has grown in parallel with rising rates of type 2 diabetes mellitus and obesity[3,4]. The prevalence of MAFLD is reportedly 25.0% among adults worldwide[5], 29.2% in China[6], and 33.9% in Korea after sex and age standardization [7], with an increasing incidence each year. MAFLD is a multisystemic disease beyond the liver that can increase the risk of heart failure, obstructive sleep apnoea, and malignancy and can result in an increase in cancer-related and cardiovascular disease mortality[8]. Given the high harm and enormous disease burden of MAFLD, a comprehensive analysis of risk factors is essential[9].

Alanine aminotransferase (ALT) has been recognized globally as a reliable indicator reflecting the degree of liver cell damage, such as the damage associated with NAFLD, chronic hepatitis, and cirrhosis[10]. Many studies have suggested that liver damage can occur in the presence of normal ALT levels[11]. Recently, a growing body of evidence has indicated that an ALT level that is within the normal range is an important biomarker for predicting NAFLD; additionally, nonalcoholic steatohepatitis (NASH) or advanced fibrosis is diagnosed in up to 37.5%-59% of patients with NAFLD who have normal ALT levels[12,13]. Our previous work also indicated that an ALT trajectory at a normal level is associated with the risk of new-onset MAFLD based on a cohort study[14]. Thus, we hypothesized that a specific ALT level, particularly a long-term high-normal ALT level, is associated with the risk of new-onset MAFLD.

Some evidence has suggested that the Youden index, a popular summary statistic for receiver-operating characteristic (ROC) curves, provides the optimal cut-off point for a biomarker to distinguish diseased and healthy individuals[15]. In a study of adolescents with obesity, the optimal ALT cut-off points for diagnosing NAFLD were 36 U/L for males and 33 U/L for females[16]. However, limited evidence exists on the determination of optimal ALT cut-off points for diagnosing MAFLD and on the associations between repeated high-normal ALT measurements and both the incidence of MAFLD and risk of new-onset MAFLD. In light of the public health burden of MAFLD in China, we investigated the association between repeated ALT levels that are high-normal and new-onset MAFLD using an ambispective cohort from a health examination population.

MATERIALS AND METHODS

Data sources and recruitment

This retrospective and prospective population-based cohort study was based on data from an ambispective cohort from a health examination population in Henan Province. All eligible participants were interviewed by uniformly trained medical staff to gather information about common chronic diseases and factors influencing health. Participants aged ≥ 18 years who underwent a health examination at the First Affiliated Hospital of Zhengzhou University over a period of 3 consecutive years from January 2017 to December 2019 were retrospectively selected. We identified a total of 7817 participants (4975 male and 2842 female individuals); 4521 had no diagnosis of MAFLD according to three consecutive health examinations and were followed up at their fourth health examination in 2020. During the follow-up period, 738 participants did not participate in the health examination for various reasons or had missing information on some of the studied factors; we also excluded 230 participants with viral hepatitis, alcoholic hepatitis, autoimmune hepatitis, severe cardiovascular and cerebrovascular diseases, or malignant tumours. Finally, 3553 eligible participants (1741 male and 1812 female individuals) were selected from the pool of 7817 participants.

Data collection

The data collected included physical measurements, laboratory test results, abdominal colour Doppler ultrasound results, and diagnostic criteria for MAFLD, as described below: (1) Physical measurements. Participants' body mass index (BMI), systolic blood pressure (SBP), diastolic blood pressure (DBP), and waist circumference (WC) were measured by clinicians using a uniform measurement instrument; (2) Laboratory tests. An automatic biochemical analyser was used to measure fasting plasma glucose (FPG), glycated haemoglobin (HbA1c), total cholesterol, triglyceride (TG), high-density lipoprotein cholesterol (HDL-C), low-density lipoprotein cholesterol (LDL-C), serum uric acid (SUA), and ALT levels[15]; (3) Abdominal colour Doppler ultrasound. Ultrasound was used to determine the presence of diffuse echogenic changes in the liver; and (4) Diagnostic criteria for MAFLD. These findings included diffuse echogenic changes in the liver as revealed by abdominal colour Doppler ultrasonography and were accompanied by at least one of the following conditions: (1) Overweight/obese (BMI > 23 kg/m^2); (2) Type 2 diabetes; and (3) Metabolic dysfunction, defined as the presence of at least two of the following conditions: (1) WC ≥ 90 cm for men and WC ≥ 80 cm for women; (2) Hypertension or use of blood pressure-lowering medication or SBP ≥ 130 mmHg and/or DBP ≥ 85 mmHg; (3) FPG ≥ 5.6 mmol/L or 2-h postprandial glucose ≥ 7.8 mmol/L or HbA1c ≥ 5.7%; (4) TG ≥ 1.7 mmol/L or use of lipid-lowering drugs; and (5) HDL-C < 1.0 mmol/L in men and HDL-C < 1.3 mmol/L in women or use of lipid-lowering medication[16].

Study design and measurements

In total, 7817 participants with three consecutive health examinations from 2017 to 2019 were analysed to determine the optimal ALT cut-off points for the diagnosis of MAFLD, with ALT within the normal range (0-40 U/L). The participants were divided into three groups: Those with a low-normal ALT (lALT) level, those with a high ALT (hALT) level, and those with an abnormal ALT (aALT) level. A follow-up cohort of 3553 participants who completed their fourth health examination in 2020 was subsequently analysed to calculate the cumulative effects of excess hALT (ehALT) and explore its association with the risk of new-onset MAFLD. In this study, the cumulative effects of ehALT were classified into the following three categories: (1) Cumulative number of ehALT occurrences; (2) Equally weighted cumulative effects of ehALT; and (3) Unequally weighted cumulative effects of ehALT[17]. Finally, a single ehALT occurrence (noncumulative ehALT) was also included as a control for the cumulative effects of ehALT. The study design is shown in Figure 1, and some terms are defined in Table 1.

Statistical analyses

The ROC curve with the maximum value of the Youden index (sensitivity + specificity-1) was used to determine the ALT cut-off points for the diagnosis of MAFLD using ALT in 7817 participants from 2017 to 2019. Normally distributed continuous data are presented as the means (SD); comparisons among groups were performed using one-way analysis of variance (ANOVA) along with pairwise comparisons, the least significant difference test for homogeneous variance, and Dunnett's T3 test for nonhomogeneous variance. Continuous data with a skewed distribution are presented as medians [interquartile ranges (IQRs)], and comparisons were performed using nonparametric tests. Categorical data are described as counts (percentages), and comparisons of rates were performed using Pearson's χ^2 test.

A total of 3553 participants who were followed up in 2020 were used to analyse the association between the cumulative effects of ehALT and new-onset MAFLD *via* a Cox proportional hazards regression model. MAFLD and follow-up time were regarded as dependent variables, and the cumulative number of ehALT occurrences (four groups: 0, 1, 2, 3 occurrences, with 0 occurrences regarded as the reference group), equally weighted cumulative effect, unequally weighted cumulative effect, and single ehALT occurrence [continuous variable, analysed with the per-SD increase after Z score standardization; discrete variable, five groups, a cumulative effect of 0 as the reference group; more than 0 was divided into four quartile groups (Q_1, Q_2, Q_3, Q_4)] were the independent variables. Hazard ratios (HRs) and 95% confidence intervals (CIs) were calculated, and trend tests were also conducted. Furthermore, we used restricted cubic splines with five knots at the 5th, 35th, 65th, and 95th percentiles to flexibly model the associations of the equally or unequally weighted effects of ehALT with new-onset MAFLD and adopted variance analysis to verify whether there was a nonlinear correlation (12). All the data management and statistical analyses were performed using the statistical software R version 4.2.0 (The R Project for Statistical Computing, Vienna, Austria). $P < 0.05$ was considered to indicate statistical significance.

Table 1 Definitions of some specific terms

Term	Definition
lALT group	ALT ≤ optimal ALT cut-off points (U/L)
hALT group	Optimal ALT cut-off point < ALT ≤ 40 (U/L)
aALT group	ALT > 40 (U/L)
ehALT	ALT-optimal ALT cut-off point, if ehALT < 0, redefine ehALT = 0
Cumulative occurrences of ehALT	Sum of times that ehALT > 0 in 2017-2019, time = {0, 1, 2, 3}
Equally weighted cumulative effects of ehALT	Sum of ehALT levels with a weight of 1 in 2017-2019, *i.e.*, $ehALT_{2017}$ + $ehALT_{2018}$ + $ehALT_{2019}$
Unequally weighted cumulative effects of ehALT	Sum of ehALT levels with an increasing weight in 2017-2019, *i.e.*, 1 × $ehALT_{2017}$ + 2 × $ehALT_{2018}$ + 3 × $ehALT_{2019}$
Single ehALT occurrence	$ehALT_{2019}$ along with $ehALT_{2017}$ = 0 and $ehALT_{2018}$ = 0

ALT: Alanine aminotransferase; lALT: Low-normal alanine aminotransferase; hALT: High-normal alanine aminotransferase; aALT: Abnormal alanine aminotransferase; ehALT: Excess high-normal alanine aminotransferase.

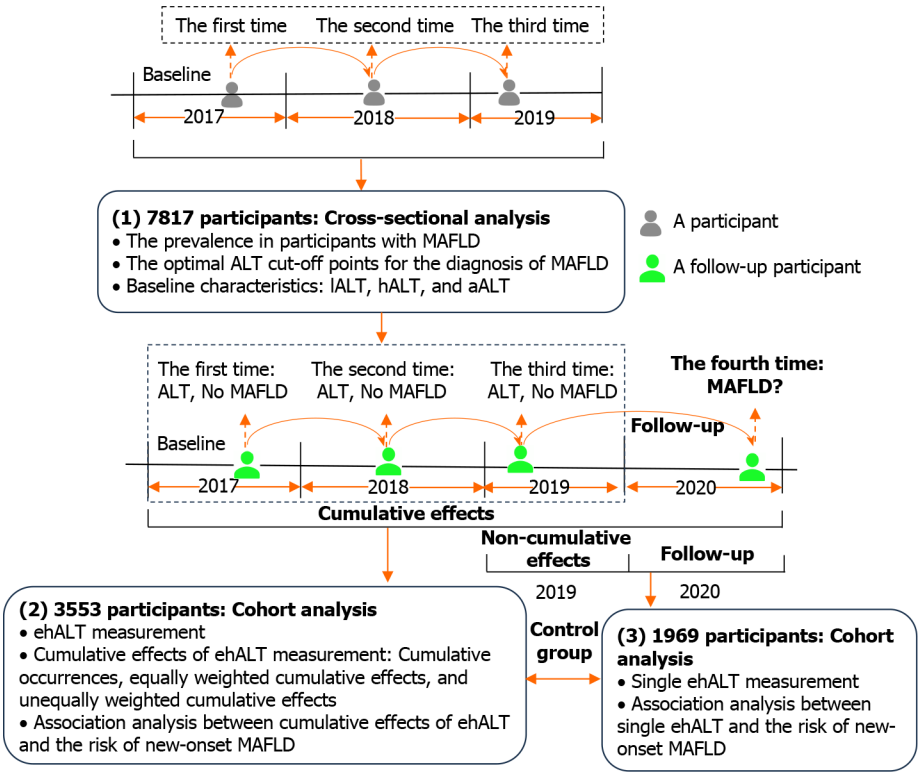

Figure 1 Schematic description of the study design. 7817 participants with three consecutive health examinations from 2017 to 2019 were analysed to determine the optimal alanine aminotransferase (ALT) cut-off points for the diagnosis of metabolic dysfunction-associated fatty liver disease (MAFLD). A follow-up cohort of 3553 participants who completed their fourth health examination in 2020 was subsequently analysed to calculate the cumulative effects of excess high-normal ALT and explore its association with the risk of new-onset MAFLD. ALT: Alanine aminotransferase; MAFLD: Metabolic dysfunction-associated fatty liver disease; lALT: Low-normal alanine aminotransferase; hALT: High-normal alanine aminotransferase; aALT: Abnormal alanine aminotransferase; ehALT: Excess high-normal alanine aminotransferase.

RESULTS

Prevalence of MAFLD in participants

The results of 7817 participants at baseline in 2017 showed that the prevalence of MAFLD was 34.27% (2679/7817), and 83.13% (36.36% + 46.77%) of participants with MAFLD had normal ALT levels (≤ 40 U/L) (Figure 2A). Analysis of differences based on nonparametric tests indicated that ALT levels were significantly greater in MAFLD patients than in healthy individuals (P < 0.001), with median (IQR) ALT levels of 24 (18, 35) U/L and 17 (13, 23) U/L (Figure 2B).

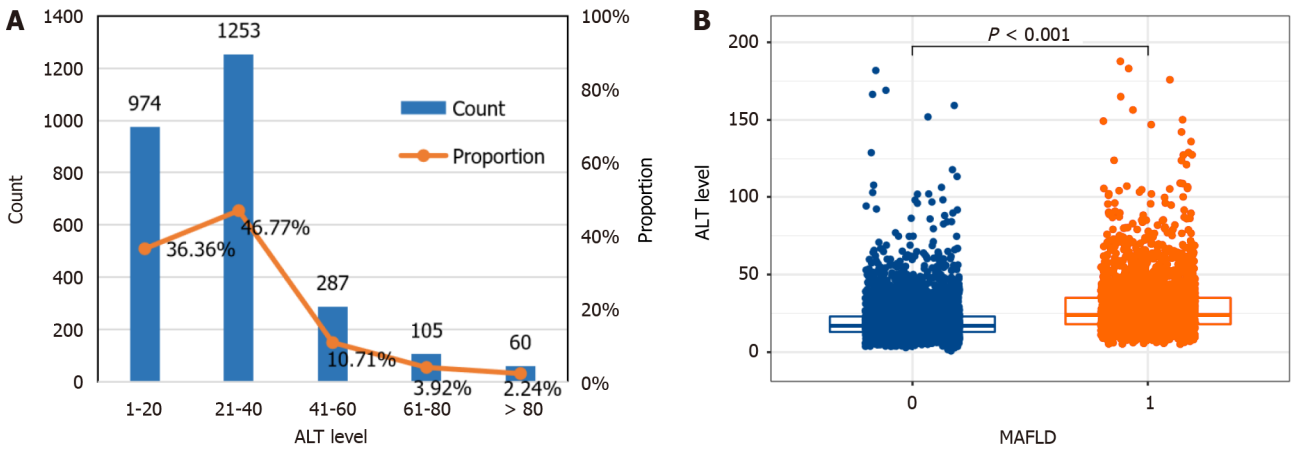

Figure 2 The prevalence of metabolic dysfunction-associated fatty liver disease in a large-scale, longitudinal population-based cohort. A: Distribution of alanine aminotransferase (ALT) levels in participants with metabolic dysfunction-associated fatty liver disease (MAFLD); B: Differential analysis of ALT levels between healthy participants and those with MAFLD. The prevalence of MAFLD was 34.27%, and 83.13% of participants with MAFLD had normal ALT levels. ALT levels were significantly greater in MAFLD patients than in healthy individuals. ALT: Alanine aminotransferase; MAFLD: Metabolic dysfunction-associated fatty liver disease.

The optimal ALT cut-off points for the diagnosis of MAFLD

The ROC curve was obtained for the annual and 3-year health examination data of the 7817 participants from 2017 to 2019. The optimal ALT cut-off points and corresponding sensitivity and specificity for diagnosing MAFLD were determined according to the maximum Youden index. The results showed that the optimal ALT cut-off points were 18.5 U/L in 2017, 18.5 U/L in 2018, 17.5 U/L in 2019, and 18.5 U/L in 2017-2019, as shown in Figure 3. Therefore, the optimal ALT cut-off point was 18.5 U/L based on ROC curve and Youden index, and the cut-off point for hALT was 18.6-40 U/L.

Baseline characteristics of follow-up participants

According to the definition of hALT (18.6-40 U/L), 3553 participants who were eligible for follow-up were included in the baseline analysis in 2017; their mean age was 48.39 (15.13) years, and 49% were male. The baseline characteristics of the 3553 participants according to hALT level are shown in Table 2. Compared with those in the lALT group, participants in the hALT and aALT groups were significantly more likely to have a higher DBP, BMI, SUA, and TG and lower HDL-C levels ($P < 0.001$). Compared with those in the hALT group, participants in the aALT group were more likely to be younger and to have lower FPG and HbA1c values.

Incidence rate of MAFLD under the cumulative effects of ehALT

Taking the date of the participants' health examinations in 2019 as the starting point of follow-up and the occurrence of MAFLD (no = 0, yes = 1) in the health examinations of participants in 2020 as the outcome, we calculated the incidence rate of MAFLD under the cumulative effects of ehALT in different groups and analysed the linear associations, as shown in Figure 4. For the cumulative number of ehALT occurrences of 0, 1, 2, and 3 times before the end of follow-up (by 2020), the incidence rates of MAFLD were 5.81%, 9.64%, 13.67%, and 18.36%, respectively. For the equally weighted cumulative effects of ehALT, the incidence rates of MAFLD in group 0 (reference), Q_1, Q_2, Q_3, and Q_4 were 5.81%, 8.47%, 11.11%, 14.91%, and 17.62%, respectively. For the unequally weighted cumulative effects of ehALT, the incidence rates of MAFLD in group 0 (reference), Q_1, Q_2, Q_3, and Q_4 were 5.81%, 9.85%, 10.67%, 13.47%, and 17.84%, respectively. Furthermore, $P < 0.001$ for both the χ^2 test and linear association test of the abovementioned cumulative effects, indicating that the incidence rates of MAFLD in the different groups were significantly different, with a linear increasing trend. For a single ehALT occurrence (control group), the incidence rates of MAFLD in group 0 (reference), Q_1, Q_2, Q_3, and Q_4 were 5.81%, 4.11%, 3.92%, 7.27%, and 9.62%, respectively. The χ^2 test and linear association test showed $P = 0.682$ and $P = 0.434$, respectively, indicating that no significant difference existed in the incidence rate of MAFLD among the five groups and that no linear increasing trend was shown.

Cox regression analysis of the cumulative effects of ehALT and risk of new-onset MAFLD

Taking the cumulative effects of ehALT in different groups and confounders such as age, sex, and WC as independent variables and new-onset MAFLD (no = 0, yes = 1) in the health examinations of participants in 2020 as the outcome, we used a Cox proportional hazards regression model to analyse the association between the cumulative effects of ehALT in different groups and the risk of new-onset MAFLD. The univariate Cox proportional hazards regression model revealed that sex, WC, SBP, DBP, BMI, SUA, TG, LDL-C, FPG, and HbA1c were risk factors for new-onset MAFLD, with an HR > 1 ($P < 0.05$). HDL-C was a protective factor against new-onset MAFLD, with an HR < 1 ($P < 0.05$).

The results of a multivariate Cox proportional hazards regression model showed the following: (1) Cumulative number of ehALT occurrences: After adjustment for relevant confounding factors, the risk of new-onset MAFLD in the group of patients with 2 and 3 cumulative episodes of ehALT was 1.443 (95%CI: 1.050-1.982) and 1.551 (95%CI: 1.135-2.119), respectively, higher than that in the group with 0.82% ehALT. Furthermore, the trend test indicated that the risk of new-

Table 2 Baseline characteristics of 3553 participants on follow-up

Variables	Total (3553)	lALT group (2409)	hALT group (1046)	aALT group (98)	*F*/χ^2/*H*	*P* value
Sex, *n* (%)					264.16	< 0.001
Male	1741 (49.00)	955 (39.64)	712 (68.07)	74 (75.51)		
Female	1812 (51.00)	1454 (60.36)	334 (31.93)[a]	24 (24.49)[a]		
Age (yr), mean (SD)	48.39 (15.13)	47.82 (15.39)	50.17 (14.54)[a]	43.51 (12.59)[a,b]	14.11	< 0.001
WC (cm), mean (SD)	85.81 (1.81)	85.79 (1.67)	85.85 (1.94)	85.85 (3.11)	0.44	0.643
SBP (mmHg), mean (SD)	120.33 (16.66)	119.18 (16.64)	122.93 (16.70)[a]	121.08 (13.41)	18.77	< 0.001
DBP (mmHg), mean (SD)	72.68 (10.27)	71.70 (10.03)	74.81 (10.60)[a]	74.07 (8.92)[a]	35.09	< 0.001
BMI (kg/m^2), mean (SD)	22.80 (2.41)	22.46 (2.39)	23.46 (2.32)[a]	23.94 (2.21)[a]	76.76	< 0.001
SUA (μmol/L), mean (SD)	290.53 (72.07)	280.17 (69.87)	311.33 (71.51)[a]	323.01 (74.16)[a]	82.00	< 0.001
TC (mmol/L), mean (SD)	4.53 (0.84)	4.51 (0.82)	4.58 (0.88)[a]	4.55 (0.84)	2.72	0.066
TG (mmol/L), median (IQR)	0.97 (0.72, 1.29)	0.93 (0.70, 1.26)	1.06 (0.79, 1.40)[a]	1.09 (0.82, 1.52)[a]	79.73	< 0.001
HDL-C (mmol/L), mean (SD)	1.47 (0.34)	1.50 (0.34)	1.42 (0.34)[a]	1.39 (0.39)[a]	18.51	< 0.001
LDL-C (mmol/L), mean (SD)	2.77 (0.75)	2.74 (0.73)	2.85 (0.78)[a]	2.83 (0.72)	7.76	< 0.001
FPG (mmol/L), median (IQR)	4.96 (4.68, 5.25)	4.95 (4.67, 5.21)	5.00 (4.71, 5.30)[a]	4.94 (4.65, 5.27)[b]	10.65	0.005
HbA1c (%), median (IQR)	5.70 (5.50, 5.70)	5.70 (5.50, 5.70)	5.70 (5.40, 5.70)	5.70 (5.40, 5.70)[a,b]	10.69	0.005

[a]*P* < 0.05, compared with the low-normal alanine aminotransferase level group.
[b]*P* < 0.05, compared with the high-normal alanine aminotransferase level group.
lALT: Low-normal alanine aminotransferase; hALT: High-normal alanine aminotransferase; aALT: Abnormal alanine aminotransferase; WC: Waist circumference; SBP: Systolic blood pressure; DBP: Diastolic blood pressure; BMI: Body mass index; TC: Total cholesterol; FPG: Fasting plasma glucose; HbA1c: Glycated haemoglobin; TG: Triglycerides; HDL-C: High-density lipoprotein cholesterol; LDL-C: Low-density lipoprotein cholesterol; SUA: Serum uric acid; IQR: Interquartile range.

onset MAFLD showed an increasing trend; (2) Equal and unequally weighted cumulative effects of ehALT: After adjustment for the relevant confounding factors, the risk of new-onset MAFLD increased by 8.8% (95%CI: 0.3%-17.9%) and 9.8% (95%CI: 1.7%-18.5%), respectively, per SD increase in the cumulative effect. For the five grouping variables, compared with those in group 0 (reference), the HRs of new-onset MAFLD in the Q_3 and Q_4 groups for the equally weighted cumulative effects of ehALT were 1.651 (95%CI: 1.199-2.273) and 1.535 (95%CI: 1.119-2.106), respectively. For the unequally weighted cumulative effects of ehALT, the HRs of new-onset MAFLD in the Q_3 and Q_4 groups were 1.616 (95%CI: 1.162-2.246) and 1.580 (95%CI: 1.155-2.162), respectively; Q_1 and Q_2 were not significantly different from those in the reference group. Additionally, the trend test indicated that the risk of new-onset MAFLD showed an increasing trend for all cumulative occurrences of ehALT; and (3) Single ehALT (control group): Compared with those of the reference group, the univariate and multivariate models did not differ significantly for the continuous or categorical variable of a single ehALT occurrence. Additionally, the trend test showed that the risk of new-onset MAFLD did not increase (Table 3).

Figure 5 shows the dose-response relationship between the cumulative effects of ehALT and the risk of new-onset MAFLD using restricted cubic splines. After adjustment for sex, WC, SBP, DBP, BMI, SUA, TG, HDL-C, LDL-C, FPG, and HbA1c, the equally and unequally weighted cumulative effects of ehALT had a positive nonlinear relationship with the risk of new-onset MAFLD in approximately 95% of the enrolled participants (*i.e.*, total association *P* = 0.005 and nonlinearity *P* = 0.011; total association *P* = 0.006 and nonlinearity *P* = 0.029). Specifically, for the equally weighted cumulative effects of ehALT (Figure 5A), the HR increased rapidly to 1.5 with a cumulative effect of 10 U/L and then maintained a steady value thereafter, to a cumulative effect of 38.5 U/L. For the unequally weighted cumulative effects of ehALT (Figure 5B), the HR increased rapidly to 1.5 with a cumulative effect of 20 U/L and then maintained a steady value thereafter, with a cumulative effect of 82.0 U/L.

DISCUSSION

In this study, a large-scale, longitudinal population-based cohort of 7817 participants in China had a prevalence of MAFLD of 34.27%, and 83.13% of participants with MAFLD had normal ALT levels. The optimal ALT cut-off point for

Table 3 Risks of new-onset metabolic dysfunction-associated fatty liver disease stratified by different categories of cumulative effects of excess high-normal alanine aminotransferase level

Categories	Univariate, HR (95%CI)	*P* value	Sex-, WC-, SBP-, DBP- and BMI-adjusted[1], HR (95%CI)	*P* value	Multivariate-adjusted[2]	*P* value
Cumulative occurrences of ehALT (*n* = 3553)						
0 (101/1738)	1.000		1.000		1.000	
1 (82/851)	1.672 (1.249-2.237)	0.001	1.312 (0.975-1.765)	0.073	1.261 (0.935-1.699)	0.128
2 (70/512)	2.325 (1.714-3.154)	< 0.001	1.495 (1.091-2.049)	0.012	1.443 (1.050-1.982)	0.024
3 (83/452)	2.963 (2.215-3.962)	< 0.001	1.559 (1.142-2.128)	0.005	1.551 (1.135-2.119)	0.006
P value for trend[3]	< 0.001		0.005		0.005	
Equally weighted cumulative effects of ehALT (*n* = 3553)						
Increase per SD[4]	1.227 (1.149-1.310)	< 0.001	1.090 (1.006-1.182)	0.036	1.088 (1.003-1.179)	0.041
0 (reference)	1.000		1.000		1.000	
Q_1 (0.01-3.00 U/L)	1.541 (1.069-2.225)	0.020	1.139 (0.785-1.652)	0.493	1.083 (0.744-1.575)	0.678
Q_2 (3.01-8.50 U/L)	1.770 (1.261-2.485)	0.001	1.329 (0.941-1.876)	0.106	1.297 (0.916-1.837)	0.916
Q_3 (8.51-20.50 U/L)	2.620 (1.926-3.564)	< 0.001	1.671 (1.214-2.300)	0.002	1.651 (1.199-2.273)	0.002
Q_4 (≥ 20.51 U/L)	2.852 (2.120-3.838)	< 0.001	1.578 (1.151-2.162)	0.005	1.535 (1.119-2.106)	0.008
P value for trend[3]	< 0.001		0.005		0.007	
Unequally weighted cumulative effects of ehALT (*n* = 3553)						
Increase per SD[4]	1.231 (1.154-1.312)	< 0.001	1.102 (1.020-1.191)	0.014	1.098 (1.017-1.185)	0.016
0 (reference)	1.000		1.000		1.000	
Q_1 (0.01-5.00 U/L)	1.709 (1.209-2.416)	0.002	1.190 (0.835-1.697)	0.336	1.114 (0.779-1.591)	0.555
Q_2 (5.01-15.00 U/L)	1.749 (1.234-2.478)	0.002	1.283 (0.900-1.830)	0.168	1.278 (0.895-1.826)	0.177
Q_3 (15.01-40.50 U/L)	2.319 (1.688-3.187)	< 0.001	1.636 (1.178-2.273)	0.003	1.616 (1.162-2.246)	0.004
Q_4 (≥ 40.51 U/L)	2.996 (2.236-4.015)	< 0.001	1.626 (1.191-2.220)	0.002	1.580 (1.155-2.162)	0.004
P value for trend[3]	< 0.001		0.003		0.004	
Single ehALT occurrence (control group, *n* = 1969)						
Increase per SD[4]	1.055 (0.866-1.286)	0.594	1.010 (0.819-1.245)	0.929	1.012 (0.811-1.262)	0.917
0 (reference)	1.000		1.000		1.000	
Q_1 (0.01-1.50 U/L)	0.688 (0.218-2.171)	0.524	0.497 (0.150-1.528)	0.214	0.557 (0.174-1.783)	0.324
Q_2 (1.51-3.50 U/L)	0.612 (0.151-2.485)	0.492	0.462 (0.113-1.886)	0.282	0.352 (0.085-1.462)	0.151
Q_3 (3.51-8.50 U/L)	1.250 (0.460-3.397)	0.662	1.326 (0.486-3.620)	0.582	1.043 (0.374-2.908)	0.936
Q_4 (≥ 8.51 U/L)	1.990 (0.808-4.898)	0.134	1.688 (0.675-4.221)	0.263	1.828 (0.772-4.593)	0.199
P value for trend[3]	0.142		0.259		0.264	

[1]Adjusted for sex, waist circumference, systolic blood pressure, diastolic blood pressure, and body mass index.

[2]Adjusted for sex, waist circumference, systolic blood pressure, diastolic blood pressure, body mass index, serum uric acid, triglycerides, high-density lipoprotein cholesterol, low-density lipoprotein cholesterol, fasting plasma glucose, and glycated haemoglobin.

[3]For the trend test, Cox proportional hazards regression models were used with group medians in each group instead of grouping variables (*e.g.*, 0, Q_1, Q_2, Q_3, and Q_4). The cumulative excess high-normal alanine aminotransferase (ehALT) level concentrations were 12 U/L, 15 U/L, 20 U/L, and 26 U/L in the four groups, and the equally weighted cumulative effects of ehALT were 0, 1.5 U/L, 5.5 U/L, 13 U/L, and 33.5 U/L in the five groups. The unequally weighted cumulative effects of ehALT were 0, 2.5 U/L, 10.5 U/L, 24.5 U/L, and 69 U/L in the five groups, and the single ehALT occurrence (control group) were 0, 0.5 U/L, 2.5 U/L, 5.5 U/L, and 17.5 U/L in the five groups.

[4]The SD of the equally weighted cumulative effects of excess high-normal alanine aminotransferase (ehALT) level was 15.93, the SD of the unequally weighted cumulative effects of ehALT was 32.73, and the SD of a single ehALT occurrence (control group, only 2019 ALT > 18.5 U/L) was 3.76.

WC: Waist circumference; SBP: Systolic blood pressure; DBP: Diastolic blood pressure; BMI: Body mass index; ehALT: Excess high-normal alanine

aminotransferase; HR: Hazard ratio; CI: Confidence interval.

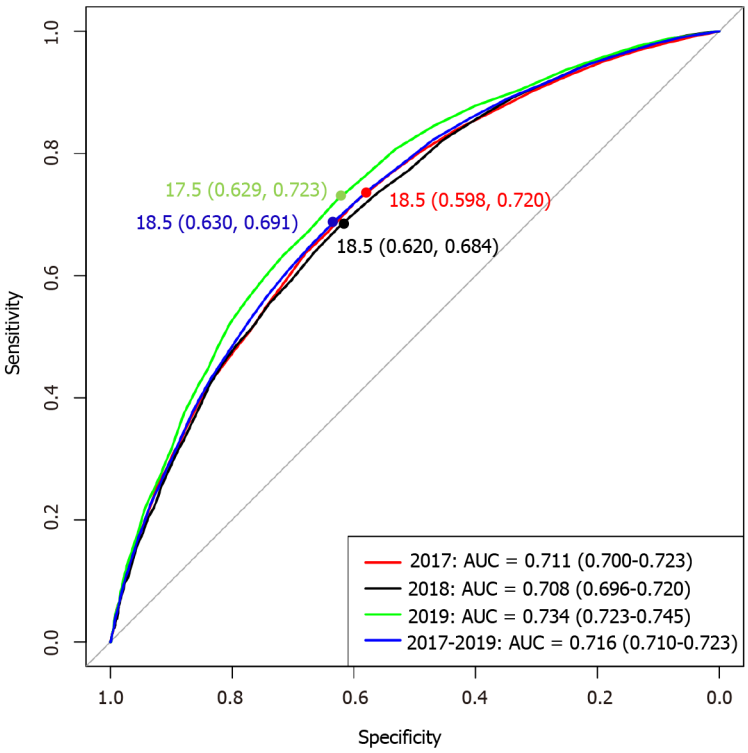

Figure 3 Optimal alanine aminotransferase cut-off points for the diagnosis of metabolic dysfunction-associated fatty liver disease. The optimal alanine aminotransfer (ALT) cut-off point was 18.5 U/L based on receiver-operating characteristic curve and Youden index, and the cut-off point for high-normal ALT was 18.6-40 U/L. AUC: Area under the curve.

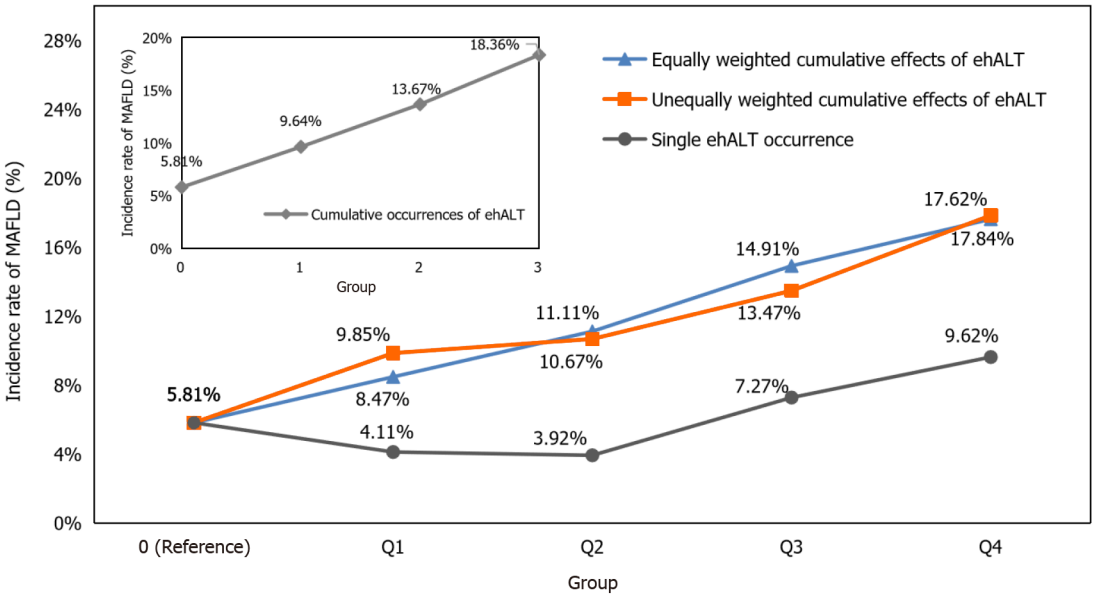

Figure 4 Incidence rate of metabolic dysfunction-associated fatty liver disease under the cumulative effects of excess high-normal alanine aminotransferase levels and a single excess high-normal alanine aminotransferase level occurrence in different groups. The incidence rate of metabolic dysfunction-associated fatty liver disease showed a linear increasing trend in the cumulative excess high-normal alanine aminotransferase (ehALT) levels groups, while a single ehALT occurrence did not show a linear increasing trend in different groups. MAFLD: Metabolic dysfunction-associated fatty liver disease; ehALT: Excess high-normal alanine aminotransferase.

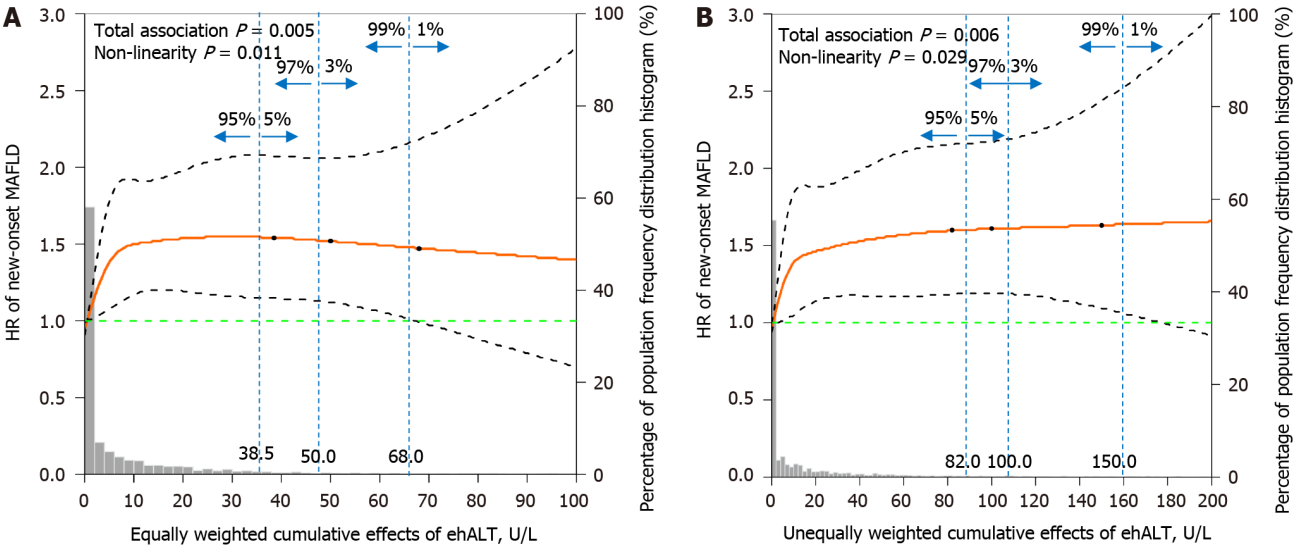

Figure 5 Dose-response relationship between the cumulative effects of excess high-normal alanine aminotransferase levels and the risk of new-onset metabolic dysfunction-associated fatty liver disease. A: Equally weighted cumulative effects of excess high-normal alanine aminotransferase (ehALT) levels; B: Unequally weighted cumulative effects of ehALT. The equally and unequally weighted cumulative effects of ehALT had a positive nonlinear relationship with the risk of new-onset metabolic dysfunction-associated fatty liver disease in approximately 95% of the enrolled participants. Gray histogram: The probability distribution of the population corresponding to the accumulation of ehALT. Orange solid line: The restricted cubic splines [hazard ratios (HRs)]. Black dashed curves: The 95% confidence interval of the restricted cubic splines (HRs). Green dashed line: The reference line of the restricted cubic splines (HR = 1). Blue dashed lines: The dividing lines indicating population proportions of less than 5%, 3%, and 1%, respectively. MAFLD: Metabolic dysfunction-associated fatty liver disease; ehALT: Excess high-normal alanine aminotransferase; HR: Hazard ratio.

the diagnosis of MAFLD was 18.5 U/L. Our findings indicate that MAFLD has become one of the most common chronic liver diseases and is a growing public health problem. According to a systematic review and meta-analysis, NAFLD and normal ALT levels are closely related to diabetes, hypertension, and metabolic syndrome[18]. Additionally, the highest ALT cut-off points among 526641 participants without excessive alcohol consumption or known liver disease were 32 U/L, 37 U/L for men; 31 U/L for women; 39 U/L for overweight people; and 36 U/L for patients with diabetes, all of which were lower than the upper limit for ALT (40 U/L)[19]. According to the Liver-Bible-2020 cohort study, the best ALT cut-off for steatosis detection was 35 U/L in males and 22 U/L in females, and the best cut-off for fibrosis detection was 27 U/L in males[20]. Wahlang *et al*[21] reported that elevated ALT within the normal range was a substitute biomarker of NAFLD. However, there is no scientific evidence for whether the long-term, dynamic, or continuous accumulation of ehALT affects new-onset MAFLD (NAFLD accompanied by metabolic disorders).

The incidence rate of MAFLD was significantly different and showed a linear growth trend with the cumulative effects of ehALT in the different groups, whereas there was no such relationship for a single ehALT occurrence (control group). After adjustment for confounding factors, compared with those in the lALT group, the cumulative ehALT level was significantly associated with new-onset MAFLD according to three factors: The cumulative frequency of ehALT and both the equally and unequally weighted cumulative effects of ehALT. Moreover, there was no such relationship for a single ehALT occurrence (control group). This finding suggested that the cumulative effects of ehALT within the long-term normal range will significantly increase the risk of new-onset MAFLD. A prospective study conducted by Gawrieh *et al* [22] revealed that the histological characteristics of NAFLD, advanced fibrosis, and the frequency and severity of NASH gradually increase when ALT levels increase gradually from < 20 U/L to 20-39 U/L, within the normal range. Our previous study showed that, compared with those in the stable low-ALT subgroup (13.10-13.92 U/L for 3 consecutive years), the stable middle-ALT (22.65-24.08 U/L) and stable high-ALT (32.50-39.78 U/L) groups had a significantly increased risk of MAFLD among men and women in the general population[14]. Thus, long-term hALT intake can increase the risk of developing MAFLD and aggravate the severity of NASH and advanced fibrosis. However, in-depth studies are presently lacking regarding the cumulative effects of and dynamic changes in hALT and the risk of new-onset MAFLD.

With lifestyle changes, a growing number of patients with MAFLD (dominated by NAFLD with metabolic disorders) who were physically asymptomatic had fluctuating ALT levels mostly within the normal range, although liver biopsy results revealed marked inflammation or fibrosis in some patients[23]. ALT is an enzyme that exists widely in the cytoplasm of liver cells. Once hepatocyte apoptosis and damage occur, the serum ALT concentration increases significantly. Therefore, ALT is the most sensitive detection indicator reflecting liver function damage and liver inflammation and is an important marker for detecting steatosis, diagnosing NASH, evaluating NASH-related fibrosis stages, and detecting liver cirrhosis[24]. Clinically, most physicians assess the hepatic risk of NAFLD based on changes in ALT levels, which are often overlooked in patients with MAFLD who have long-standing normal ALT levels, leading to aggravation of the degree of hepatic inflammatory response with insulin resistance and multi-hit pathogenesis, and further resulting in NASH, liver fibrosis, and eventually the development of cirrhosis and even hepatocellular carcinoma [25].

This study used a population-based cohort to explore the cumulative effects of ehALT and the risk of new-onset MAFLD. The main strengths of this study were the determination of the optimal ALT cut-off points and the use of different measurement methods for the cumulative effects of ehALT from three perspectives (*i.e.*, cumulative number of ehALT measurements and equally and unequally weighted cumulative effects). In contrast, previous studies have investigated the association between a single ALT measurement or the ALT trajectory and neglected the effects of new-onset MAFLD by considering the quantitative cumulative effects of ALT on long-term dynamic changes *via* a lifespan approach.

This study has several limitations. First, the cohort's follow-up time was short, and the proportion of participants with aALT was low, which led to a decrease in the dose-response relationship and made it difficult to accurately detect a significant difference between the aALT group (> 40 U/L) and the hALT group (18.6-40 U/L) for the cumulative effects on the risk of new-onset MAFLD. Additionally, randomized controlled trials with different lifestyle interventions (including weight loss through diet and physical exercise) will be conducted to explore whether those interventions can improve long-term ALT levels in individuals who are high-normal and ultimately prevent MAFLD.

CONCLUSION

In conclusion, a large-scale population-based study in Henan Province indicated that a high-normal ALT level was 18.6-40 U/L, that a normal ALT level was common in patients with MAFLD, and that a long-term change in the ALT level had cumulative effects on the risk of new-onset MAFLD. We recommend that individuals in this population, especially those in young adulthood, maintain long-term ALT levels within the normal range.

ARTICLE HIGHLIGHTS

Research background

Additional evidence is needed regarding the association between repeated high-normal alanine transaminase (ALT) measurements and metabolic dysfunction-associated fatty liver disease (MAFLD), and only a few cross-sectional studies have shown that ALT trajectory is associated with the risk of MAFLD. In light of the public health burden of MAFLD in China, we investigated the association between persistently elevated high-normal ALT levels and new-onset MAFLD using an ambispective cohort from a health examination population.

Research motivation

MAFLD has become a growing public health problem and affects up to one-third of the global population, with a heavy disease burden. MAFLD can occur in the presence of normal ALT levels, and a trajectory within the normal range can increase the risk of MAFLD. However, the link between repeated high-normal ALT measurements and new-onset MAFLD has not been well studied.

Research objectives

We investigated the optimal ALT cut-off points for diagnosing MAFLD and the association between repeated high-normal ALT measurements and the risk of new-onset MAFLD in a health examination population in China.

Research methods

This study used data from an ambispective cohort of individuals from a health examination population in China. Repeated high-normal ALT measurements were assessed by considering equally and unequally weighted cumulative effects of excess high-normal ALT (ehALT), and participants were categorized into quartile groups. We performed multivariable Cox proportional hazards regression analysis to evaluate the association between cumulative ehALT and the risk of new-onset MAFLD and calculated the hazard ratios (HRs) and 95% confidence intervals.

Research results

A total of 83.13% of participants with MAFLD had normal ALT levels. The HRs of new-onset MAFLD in the group of patients with 2 or 3 cumulative episodes of ehALT (Q_3 and Q_4 for the equally and unequally weighted cumulative effects of ehALT) were greater than those in the group with low-normal ALT levels from 2017 to 2019. Additionally, the dose-response relationship indicated that the equally and unequally weighted cumulative effects of ehALT had positive nonlinear relationships with the risk of new-onset MAFLD.

Research conclusions

A cohort study of the Chinese adult population revealed that persistently elevated high-normal ALT levels were associated with a dose-dependent increase in the risk of new-onset MAFLD in all participants. The identification and management of high-normal ALT levels for several years may play a crucial role in preventing MAFLD.

Research perspectives

Long-term prospective cohort or randomized controlled trials are needed to confirm the relationship between repeated

high-normal ALT measurements and new-onset MAFLD. Future studies should focus on whether a healthy lifestyle can improve ALT levels and prevent MAFLD.

FOOTNOTES

Author contributions: Chen JF and Ding SY designed the study and acquired funding; Chen JF and Wu ZQ were responsible for developing the methodology; Yan S and Wang YX participated in the formal analysis and investigation; Chen JF wrote the original draft; Chen JF, Wu ZQ, Liu HS, Yan S, Wang YX, Xing M, Song XQ, and Ding SY participated in the review and editing.

Supported by National Natural Science Foundation of China, No. 72101236; China Postdoctoral Science Foundation, No. 2022M722900; Collaborative Innovation Project of Zhengzhou City, No. XTCX2023006; and Nursing Team Project of the First Affiliated Hospital of Zhengzhou University, No. HLKY2023005.

Institutional review board statement: The study was reviewed and approved by the Institutional Review Board of the First Affiliated Hospital of Zhengzhou University (Approval No. 2020-KY-381).

Informed consent statement: Signed informed consent was obtained from all participants.

Conflict-of-interest statement: All the authors report no relevant conflicts of interest for this article.

Data sharing statement: No additional data are available.

STROBE statement: The authors have read the STROBE Statement-checklist of items, and the manuscript was prepared and revised according to the STROBE Statement-checklist of items.

Country/Territory of origin: China

ORCID number: Jing-Feng Chen 0009-0005-2898-1490; Zhuo-Qing Wu 0000-0003-2415-5202; Hao-Shuang Liu 0000-0002-3108-7001; Su Yan 0009-0007-3959-2989; You-Xiang Wang 0009-0002-6797-876X; Miao Xing 0009-0003-3440-3430; Xiao-Qin Song 0000-0002-1788-3933; Su-Ying Ding 0000-0002-2649-8332.

S-Editor: Wang JJ
L-Editor: A
P-Editor: Yuan YY

REFERENCES

1 **Lim GEH**, Tang A, Ng CH, Chin YH, Lim WH, Tan DJH, Yong JN, Xiao J, Lee CW, Chan M, Chew NW, Xuan Tan EX, Siddiqui MS, Huang D, Noureddin M, Sanyal AJ, Muthiah MD. An Observational Data Meta-analysis on the Differences in Prevalence and Risk Factors Between MAFLD vs NAFLD. *Clin Gastroenterol Hepatol* 2023; **21**: 619-629.e7 [PMID: 34871813 DOI: 10.1016/j.cgh.2021.11.038]

2 **Eslam M**, Sanyal AJ, George J; International Consensus Panel. MAFLD: A Consensus-Driven Proposed Nomenclature for Metabolic Associated Fatty Liver Disease. *Gastroenterology* 2020; **158**: 1999-2014.e1 [PMID: 32044314 DOI: 10.1053/j.gastro.2019.11.312]

3 **Yang J**, Luo S, Li R, Ju J, Zhang Z, Shen J, Sun M, Fan J, Xia M, Zhu W, Liu Y. Sleep Factors in Relation to Metabolic Dysfunction-Associated Fatty Liver Disease in Middle-Aged and Elderly Chinese. *J Clin Endocrinol Metab* 2022; **107**: 2874-2882 [PMID: 35900115 DOI: 10.1210/clinem/dgac428]

4 **Eslam M**, El-Serag HB, Francque S, Sarin SK, Wei L, Bugianesi E, George J. Metabolic (dysfunction)-associated fatty liver disease in individuals of normal weight. *Nat Rev Gastroenterol Hepatol* 2022; **19**: 638-651 [PMID: 35710982 DOI: 10.1038/s41575-022-00635-5]

5 **Liu J**, Ayada I, Zhang X, Wang L, Li Y, Wen T, Ma Z, Bruno MJ, de Knegt RJ, Cao W, Peppelenbosch MP, Ghanbari M, Li Z, Pan Q. Estimating Global Prevalence of Metabolic Dysfunction-Associated Fatty Liver Disease in Overweight or Obese Adults. *Clin Gastroenterol Hepatol* 2022; **20**: e573-e582 [PMID: 33618024 DOI: 10.1016/j.cgh.2021.02.030]

6 **Huang YP**, Zhang S, Zhang M, Wang Y, Wang WH, Li J, Li C, Lin JN. Gender-specific prevalence of metabolic-associated fatty liver disease among government employees in Tianjin, China: a cross-sectional study. *BMJ Open* 2021; **11**: e056260 [PMID: 34911725 DOI: 10.1136/bmjopen-2021-056260]

7 **Kim M**, Yoon EL, Cho S, Lee CM, Kang BK, Park H, Jun DW, Nah EH. Prevalence of advanced hepatic fibrosis and comorbidity in metabolic dysfunction-associated fatty liver disease in Korea. *Liver Int* 2022; **42**: 1536-1544 [PMID: 35338555 DOI: 10.1111/liv.15259]

8 **Quek J**, Ng CH, Tang ASP, Chew N, Chan M, Khoo CM, Wei CP, Chin YH, Tay P, Lim G, Tan DJH, Lim WH, Chan KE, Teng M, Tan E, Tamaki N, Huang DQ, Siddiqui MS, Young DY, Noureddin M, Muthiah MD. Metabolic Associated Fatty Liver Disease Increases the Risk of Systemic Complications and Mortality. A Meta-Analysis and Systematic Review of 12 620 736 Individuals. *Endocr Pract* 2022; **28**: 667-672 [PMID: 35364328 DOI: 10.1016/j.eprac.2022.03.016]

9 **Lee GB**, Huh Y, Lee SH, Han B, Kim YH, Kim DH, Kim SM, Choi YS, Cho KH, Nam GE. Association of low muscle strength with

metabolic dysfunction-associated fatty liver disease: A nationwide study. *World J Gastroenterol* 2023; **29**: 5962-5973 [PMID: 38131000 DOI: 10.3748/wjg.v29.i45.5962]

10 **Wang M**, Wang M, Zhang R, Zhang L, Ding Y, Tang Z, Fan H, Wang H, Zhang W, Chen Y, Wang J. A combined association of serum uric acid, alanine aminotransferase and waist circumference with non-alcoholic fatty liver disease: a community-based study. *PeerJ* 2022; **10**: e13022 [PMID: 35265397 DOI: 10.7717/peerj.13022]

11 **Kang Y**, Park S, Kim S, Koh H. Normal serum alanine aminotransferase and non-alcoholic fatty liver disease among Korean adolescents: a cross-sectional study using data from KNHANES 2010-2015. *BMC Pediatr* 2018; **18**: 215 [PMID: 29976192 DOI: 10.1186/s12887-018-1202-z]

12 **Seko Y**, Sumida Y, Tanaka S, Mori K, Taketani H, Ishiba H, Hara T, Okajima A, Yamaguchi K, Moriguchi M, Mitsuyoshi H, Kanemasa K, Yasui K, Minami M, Imai S, Itoh Y. Serum alanine aminotransferase predicts the histological course of non-alcoholic steatohepatitis in Japanese patients. *Hepatol Res* 2015; **45**: E53-E61 [PMID: 25429984 DOI: 10.1111/hepr.12456]

13 **Wu Y**, Yang X, Morris HL, Gurka MJ, Shenkman EA, Cusi K, Bril F, Donahoo WT. Noninvasive Diagnosis of Nonalcoholic Steatohepatitis and Advanced Liver Fibrosis Using Machine Learning Methods: Comparative Study With Existing Quantitative Risk Scores. *JMIR Med Inform* 2022; **10**: e36997 [PMID: 35666557 DOI: 10.2196/36997]

14 **Chen JF**, Qin Q, Wu ZQ, Yan S, Song XQ, Ding SY. A cohort study on the correlation between alanine aminotransferase trajectories and new-onset metabolic fatty liver disease. *Zhonghua Liu Xing Bing Xue Za Zhi* 2022; **43**: 234-240 [PMID: 35184490 DOI: 10.3760/cma.j.cn112338-20210809-00621]

15 **Zhang YB**, Yang G, Bu Y, Lei P, Zhang W, Zhang DY. Development of a machine learning-based model for predicting risk of early postoperative recurrence of hepatocellular carcinoma. *World J Gastroenterol* 2023; **29**: 5804-5817 [PMID: 38074914 DOI: 10.3748/wjg.v29.i43.5804]

16 **Rong Y**, Chun-Yan N, Hong-Xin Z, Lu Y, Wen W, Yu T. Association of Adolescent Obesity with Nonalcoholic Fatty Liver Disease and Related Risk Factors in Xi 'an, China. *Ann Hepatol* 2018; **17**: 85-91 [PMID: 29311392 DOI: 10.5604/01.3001.0010.7538]

17 **Li X**, Jansen L, Chang-Claude J, Hoffmeister M, Brenner H. Risk of Colorectal Cancer Associated With Lifetime Excess Weight. *JAMA Oncol* 2022; **8**: 730-737 [PMID: 35297997 DOI: 10.1001/jamaoncol.2022.0064]

18 **Ma X**, Liu S, Zhang J, Dong M, Wang Y, Wang M, Xin Y. Proportion of NAFLD patients with normal ALT value in overall NAFLD patients: a systematic review and meta-analysis. *BMC Gastroenterol* 2020; **20**: 10 [PMID: 31937252 DOI: 10.1186/s12876-020-1165-z]

19 **Huang DQ**, Yeo YH, Tan E, Takahashi H, Yasuda S, Saruwatari J, Tanaka K, Oniki K, Kam LY, Muthiah MD, Hyogo H, Ono M, Barnett SD, Li J, Zou B, Fung J, Lee TY, Wong VW, Yuen MF, Dan YY, Lim SG, Cheung R, Toyoda H, Eguchi Y, Nguyen MH. ALT Levels for Asians With Metabolic Diseases: A Meta-analysis of 86 Studies With Individual Patient Data Validation. *Hepatol Commun* 2020; **4**: 1624-1636 [PMID: 33163833 DOI: 10.1002/hep4.1593]

20 **Valenti L**, Pelusi S, Bianco C, Ceriotti F, Berzuini A, Iogna Prat L, Trotti R, Malvestiti F, D'Ambrosio R, Lampertico P, Colli A, Colombo M, Tsochatzis EA, Fraquelli M, Prati D. Definition of Healthy Ranges for Alanine Aminotransferase Levels: A 2021 Update. *Hepatol Commun* 2021; **5**: 1824-1832 [PMID: 34520121 DOI: 10.1002/hep4.1794]

21 **Wahlang B**, Appana S, Falkner KC, McClain CJ, Brock G, Cave MC. Insecticide and metal exposures are associated with a surrogate biomarker for non-alcoholic fatty liver disease in the National Health and Nutrition Examination Survey 2003-2004. *Environ Sci Pollut Res Int* 2020; **27**: 6476-6487 [PMID: 31873887 DOI: 10.1007/s11356-019-07066-x]

22 **Gawrieh S**, Wilson LA, Cummings OW, Clark JM, Loomba R, Hameed B, Abdelmalek MF, Dasarathy S, Neuschwander-Tetri BA, Kowdley K, Kleiner D, Doo E, Tonascia J, Sanyal A, Chalasani N; NASH Clinical Research Network. Histologic Findings of Advanced Fibrosis and Cirrhosis in Patients With Nonalcoholic Fatty Liver Disease Who Have Normal Aminotransferase Levels. *Am J Gastroenterol* 2019; **114**: 1626-1635 [PMID: 31517638 DOI: 10.14309/ajg.0000000000000388]

23 **Sun DQ**, Zheng KI, Xu G, Ma HL, Zhang HY, Pan XY, Zhu PW, Wang XD, Targher G, Byrne CD, Chen YP, Yuan WJ, Zheng MH. PNPLA3 rs738409 is associated with renal glomerular and tubular injury in NAFLD patients with persistently normal ALT levels. *Liver Int* 2020; **40**: 107-119 [PMID: 31519069 DOI: 10.1111/liv.14251]

24 **Kim WR**, Flamm SL, Di Bisceglie AM, Bodenheimer HC; Public Policy Committee of the American Association for the Study of Liver Disease. Serum activity of alanine aminotransferase (ALT) as an indicator of health and disease. *Hepatology* 2008; **47**: 1363-1370 [PMID: 18366115 DOI: 10.1002/hep.22109]

25 **Shim JJ**, Kim JW, Oh CH, Lee YR, Lee JS, Park SY, Kim BH, Oh IH. Serum alanine aminotransferase level and liver-related mortality in patients with chronic hepatitis B: A large national cohort study. *Liver Int* 2018; **38**: 1751-1759 [PMID: 29377574 DOI: 10.1111/liv.13705]

World Journal of Gastroenterology

Submit a Manuscript: https://www.f6publishing.com

World J Gastroenterol 2024 March 14; 30(10): 1358-1367

DOI: 10.3748/wjg.v30.i10.1358

ISSN 1007-9327 (print) ISSN 2219-2840 (online)

ORIGINAL ARTICLE

Retrospective Cohort Study

Time trends and outcomes of gastrostomy placement in a Swedish national cohort over two decades

Martin Löfling Skogar, Magnus Sundbom

Specialty type: Gastroenterology and hepatology

Provenance and peer review: Unsolicited article; Externally peer reviewed.

Peer-review model: Single blind

Peer-review report's scientific quality classification

Grade A (Excellent): A
Grade B (Very good): B
Grade C (Good): C, C
Grade D (Fair): 0
Grade E (Poor): 0

P-Reviewer: Cabezuelo AS, Spain; Jadallah KA, Jordan; Osatakul S, Thailand

Received: November 15, 2023
Peer-review started: November 15, 2023
First decision: December 14, 2023
Revised: December 27, 2023
Accepted: January 31, 2024
Article in press: January 31, 2024
Published online: March 14, 2024

Martin Löfling Skogar, Magnus Sundbom, Department of Surgical Sciences, Uppsala University, Uppsala 75185, Sweden

Corresponding author: Martin Löfling Skogar, MD, PhD, Doctor, Researcher, Statistical Worker, Surgeon, Department of Surgical Sciences, Uppsala University, Entrance 70, 1 Floor, Uppsala 75185, Sweden. martin.skogar@uu.se

Abstract

BACKGROUND

Percutaneous endoscopic gastrostomy (PEG) and laparoscopically inserted gastrostomy have become the gold standard for adult patients and children, respectively, requiring long-term enteral nutrition support. Procedure-related mortality is a rare event, often reported to be zero in smaller studies. National data on 30-d mortality and long-term survival rates after gastrostomy placement are scarce in the literature.

AIM

To study the use of gastrostomies in Sweden from 1998-2019 and to analyze procedure-related mortality and short-term (< 30 d) and long-term survival.

METHODS

In this retrospective, population-based cohort study, individuals that had received a gastrostomy between 1998-2019 in Sweden were included. Individuals were identified in the Swedish National Patient Register, and survival analysis was possible by cross-referencing the Swedish Death Register. The cohort was divided into three age groups: Children (0-18 years); adults (19-64 years); and elderly (≥ 65 years). Kaplan-Meier with log-rank test and Cox regression were used for survival analysis.

RESULTS

In total 48682 individuals (52% males, average age 60.9 ± 25.3 years) were identified. The cohort consisted of 12.0% children, 29.5% adults, and 58.5% elderly. An increased use of gastrostomies was observed during the study period, from 13.7/100000 to 22.3/100000 individuals ($P < 0.001$). The use of PEG more than doubled (about 800 to 1800/year), with a corresponding decrease in open gastrostomy (about 700 to 340/year). Laparoscopic gastrostomy increased more than ten-fold (about 20 to 240/year). Overall, PEG, open gastrostomy, and laparoscopic gastrostomy constituted 70.0% ($n = 34060$), 23.3% ($n = 11336$), and 4.9% ($n = 2404$),

respectively. Procedure-related mortality was 0.1% (n = 44) overall (PEG: 0.05%, open: 0.24%, laparoscopic: 0.04%). The overall 30-d mortality rate was 10.0% (PEG: 9.8%, open: 12.4%, laparoscopic: 1.7%) and decreased from 11.6% in 1998-2009 *vs* 8.5% in 2010-2019 (P < 0.001). One-year and ten-year survival rates for children, adults, and elderly were 93.7%, 67.5%, and 42.1% and 79.9%, 39.2%, and 6.8%, respectively. The most common causes of death were malignancies and cardiovascular and respiratory diseases.

CONCLUSION

The annual use of gastrostomies in Sweden increased during the study period, with a shift towards more minimally invasive procedures. Although procedure-related death was rare, the overall 30-d mortality rate was high (10%). To overcome this, we believe that patient selection should be improved.

Key Words: Gastrostomy; Percutaneous endoscopic gastrostomy; Dysphagia; Enteral nutrition; Long-term; Survival; Complication

Core Tip: In this large population-based cohort of 48682 individuals, the use of gastrostomies in Sweden increased during the 22-year study period, from 13.7/100000 to 22.3/100000 individuals. Percutaneous endoscopic gastrostomy more than doubled, while a 10-fold increase was seen in laparoscopic gastrostomies. Although the procedure-related mortality was low (0.1%), a 10% 30-d mortality was seen. The latter, however, decreased from 11.6% in 1998-2009 to 8.5% in 2010-2019. One-year and ten-year survival rates for children, adults, and elderly were 93.7%, 67.5%, and 42.1% and 79.9%, 39.2%, and 6.8%, respectively. The most common causes of death were malignancies and cardiovascular and respiratory diseases.

Citation: Skogar ML, Sundbom M. Time trends and outcomes of gastrostomy placement in a Swedish national cohort over two decades. *World J Gastroenterol* 2024; 30(10): 1358-1367
URL: https://www.wjgnet.com/1007-9327/full/v30/i10/1358.htm
DOI: https://dx.doi.org/10.3748/wjg.v30.i10.1358

INTRODUCTION

In modern health care, gastrostomies play a crucial role in the management of patients that require long-term enteral nutrition support[1]. Dysphagia due to stroke, neurodegenerative diseases like Parkinson's or Alzheimer's, and head and neck cancers are among the most common indications[2]. A gastrostomy may also be placed for stomach decompression to resolve persistent nausea and vomiting (*e.g.*, as a palliative procedure in patients with malignant bowel obstruction)[3].

The technique for placing a gastrostomy has evolved significantly over the years with several approaches available today. In 1980, percutaneous endoscopic gastrostomy (PEG) was introduced as a minimally invasive approach[4]. The low complication rates associated with PEG has led to widespread acceptance, making PEG the gold standard for enteral access in patients that require long-term enteral nutrition support[5]. Other available techniques include radiologically inserted gastrostomy and insertion by open surgery or laparoscopic surgery. Radiologically inserted gastrostomy, percutaneously placed under radiological guidance, is a good alternative when endoscopy is contraindicated (*e.g.*, obstructing pharyngeal or esophageal cancer). Today, open surgical gastrostomy is mostly reserved for specific situations where endoscopic or radiological approaches are not feasible or during emergent surgery for stomach decompression. Finally, laparoscopically-inserted gastrostomy has become standard in children at many institutions because of less complications as compared to PEG in children[6,7].

Long-term survival and quality of life outcomes following gastrostomy have been the subject of extensive research. In short, gastrostomy has been associated with improved nutritional status, reduced hospitalizations[8], and enhanced overall quality of life[9] in patients that require long-term enteral nutrition support. Furthermore, studies have shown that timely gastrostomy placement is associated with improved survival rates and fewer complications when compared to delayed placement[10-12]. However, in patients with dementia, there is no evidence that enteral tube feeding improves survival or quality of life[13]. This underlines the importance of choosing the right indication to treat patients who actually benefit from a gastrostomy. In addition, a delayed intervention leads to loss of benefit and greater harm, which is illustrated by higher rates of morbidity and mortality[2].

This paper aimed to provide an overview of the use of gastrostomies in Sweden by studying the trends during the last two decades. In addition, we analyzed data pertaining to procedure-related mortality as well as short-term (< 30 d) and long-term survival after a gastrostomy procedure. The purpose was to assist physicians in the risk-benefit assessment of a gastrostomy procedure in the clinical setting.

MATERIALS AND METHODS

This retrospective population-based cohort study included all patients that had a gastrostomy between January 1, 1998 to December 31, 2019 in Sweden, according to the Swedish National Patient Register (NPR). NPR stores sex, age, name of hospital, admission and discharge dates, and principal and additional diagnoses on all inpatient care and outpatient visits at hospital-based clinics. Diagnoses and surgical procedures[14] are coded according to the Swedish version of the International Statistical Classification of Diseases and Related Health Problems (ICD)[15] with a validity of 85%-95% in general[16]. Data from NPR were cross matched with data from the Swedish Death Register, which added information about date of death and cause of death. All data was anonymized. The study was conducted in accordance with the ethical standards of the Helsinki Declaration.

Population and type of gastrostomy

Individuals were identified in the NPR by the codes for gastrostomy, *i.e.* JDB 00 (gastrostomy inserted by open surgery), JDB 01 (laparoscopically-inserted gastrostomy), and JDB 10 (PEG). Calculation of annual operative volumes per 100000 inhabitants was performed. For analysis of time trends, the cohort was halved into an early group (receiving gastrostomy in 1998-2009) and a late group (receiving gastrostomy in 2010-2019). The cohort was further divided into three age groups: Children (0-18 years); adults (19-64 years); and elderly (≥ 65 years).

Indication

The indication for gastrostomy was based on the principal ICD-10 diagnosis, or if not applicable (*e.g.*, dysphagia-R13), indication was searched in the additional diagnoses at the time of gastrostomy. Indication was then grouped into four main categories: (1) Malignancy; (2) Neurological diseases; (3) Cerebrovascular lesions (CVL); and (4) Non-malignant gastrointestinal conditions (*e.g.*, gastric, duodenal, or other bowel perforations, fixation of large hiatal hernias, bowel obstruction without concomitant gastrointestinal malignancies).

Outcome

Procedure-related mortality was defined as having a surgical complication as the cause of death (ICD10-code: T80-T88) within 30 d. Short-term mortality was defined as death within 30 d, while long-term survival was analyzed until 10 years after the insertion of the gastrostomy.

Statistics

Independent sample t test and χ^2 test were used as univariate analyses for continuous and categorical variables, respectively. Kaplan-Meier with log-rank test was used for survival analyses. Multivariate adjusted survival analyses were performed using Cox regression, adjusting for differences in sex, age group, type of gastrostomy, and time period and presented as hazard ratios (HR) with 95% confidence intervals (CI). All P values were two-sided, and $P < 0.05$ was considered statistically significant. All analyses were done using IBM SPSS Statistics version 28.

RESULTS

In total, 48682 patients had a gastrostomy during the study period, with 23500 (48.3%) in the early time period. The cohort consisted of 52% males, and the average age was 60.9 ± 25.3 years. A population-based increase in the use of gastrostomies during the study period was observed, from 13.7/100000 to 22.3/100000 individuals ($P < 0.001$).

Age distribution

Children constituted 12.0% (n = 5828), adults 29.5% (n = 14340) and elderly 58.5% (n = 28483) of the cohort. In all three groups, the number of gastrostomies increased during the study period, from 6.1/100000 to 16.3/100000, from 7.1/100000 to 10.7/100000, and from 46.5/100000 to 62.5/100000, respectively. The total number of gastrostomies are demonstrated in Figure 1.

Type of gastrostomy

The technique used for placing the gastrostomy was PEG, open gastrostomy, and laparoscopic gastrostomy in 70.0% (n = 34060), 23.3% (n = 11336), and 4.9% (n = 2404), respectively. The remaining 1.8% (n = 882) were not specified in the register. During the study period, the use of PEG more than doubled (about 800 to 1800/year), with a corresponding decrease in open gastrostomy (about 700 to 340/year). Laparoscopic gastrostomy increased more than 10-fold (about 20 to 240/year). All changes were statistically significant ($P < 0.001$) (Figure 2).

PEG was the most commonly used technique in all three age groups, followed by open surgery in adults and elderly. The gradual increase in laparoscopically-inserted gastrostomy made laparoscopic gastrostomy the second most common in children (Figure 3).

Indications

The most common indication for a gastrostomy was various non-malignant gastrointestinal conditions (19.7%), closely followed by CVL (18.9%), malignancies (18.7%), and neurological disorders (16.7%). The two most common individual diagnoses were stroke and neurodegenerative disorders, including amyotrophic lateral sclerosis (Table 1). As

Table 1 Indication for gastrostomy based on the International Statistical Classification of Diseases and Related Health Problems version 10, adapted for use in Sweden

Indication	Subgroup (ICD-10 codes)	*n*	% of total
Malignancy		9103	18.7
	Head and neck cancer (C00-C14)	2670	5.5
	Esophageal cancer (C15)	1784	3.7
	Other gastrointestinal malignancies (C16-C26)	3539	7.3
	Laryngeal cancer (C32-C33)	469	1.0
	Lung cancer (C34)	384	0.8
	Malignant brain tumors (C70-C72)	257	0.5
Neurological diseases		8129	16.7
	Dementia (F00-F03)	1251	2.6
	Meningitis/encephalitis (G00-G07)	147	0.3
	Neurodegenerative disorders (G10-G37)	3185	6.5
	Amyotrophic lateral sclerosis (G12.2)	2276	4.7
	Neuromuscular disorders (G70-G73)	349	0.7
	Cerebral palsy (G80)	921	0.9
Cerebrovascular lesions		9196	18.9
	Hemorrhagic or ischemic stroke (I60-I63)	8263	17.0
	Traumatic brain injury (S06)	933	1.9
Non-malignant gastrointestinal conditions		9588	19.7
	Non-malignant diseases of the esophagus (K22)	1318	2.7
	Peptic ulcer with perforation (K25-K28)	1560	3.2
	Hiatal hernia (K44)	596	1.2
	Bowel obstruction (K56)	1587	3.3
	Other gastrointestinal diseases (*e.g.*, bowel perforations, pancreatitis)	4527	9.3
Other/missing		12666	26.0
Total		48682	100

ICD-10: International Statistical Classification of Diseases and Related Health Problems version 10.

demonstrated in Figure 4, PEG dominated in CVL and neurological diseases, while the opposite was seen in non-malignant gastrointestinal conditions where open gastrostomy placement was predominantly used.

Outcome

30-d mortality: The overall 30-d mortality rate was 10.0% (n = 4863), ranging from 0.3% (n = 17) in children to 6.2% (n = 883) in adults and 13.9% (n = 3962) in elderly. For the three different types of gastrostomies, the 30-d mortality was 9.8%, 12.4%, and 1.7% for PEG, open gastrostomy, and laparoscopic gastrostomy, respectively. The 30-d mortality during the early period was higher than during the late period (11.6% *vs* 8.5%, $P < 0.001$) (Figure 5).

Adjusted analysis (Cox regression) of differences in sex, time period, age group, and type of gastrostomy, identified male sex (HR = 1.11, 95%CI: 1.05-1.18), early time period (HR = 1.33, 95%CI: 1.26-1.41), open gastrostomy (HR = 1.44, 95%CI: 1.35-1.53), and belonging to the adult group (HR = 20.9, 95%CI: 12.7-34.4) or elderly group (HR = 50.2, 95%CI: 30.7-82.3) as risk factors for 30-d mortality (Supplementary Table 1).

Procedure-related mortality: In 44 patients (16 PEG, 27 open, and 1 laparoscopic) the primary cause of death was coded as directly related to a complication of the procedure, giving an overall procedure-related mortality of 0.1% (PEG: 0.05%, open: 0.24%, laparoscopic: 0.04%). The most common procedure-related death was bowel perforation (n = 16), followed by acute cardiovascular event (n = 9), acute respiratory failure (including aspiration and overdose of sedative drugs, n = 8), and gastrointestinal bleeding (n = 1). In the remaining 10 cases septicemia was coded as the secondary cause of death.

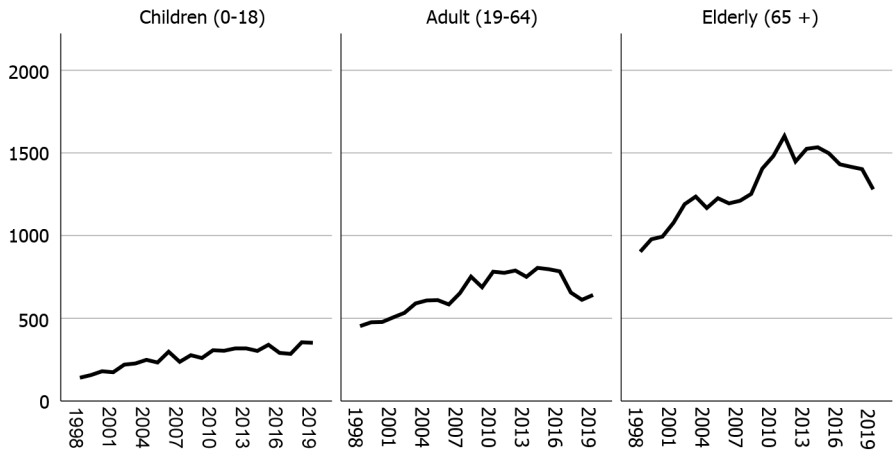

Figure 1 Total number of gastrostomies by year and age group.

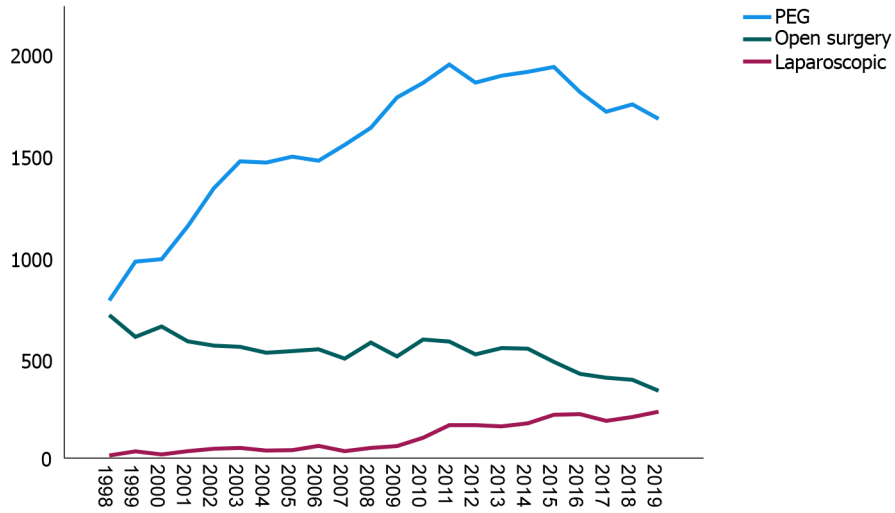

Figure 2 Time trends for different types of gastrostomies (total number by year). PEG: Percutaneous endoscopic gastrostomy.

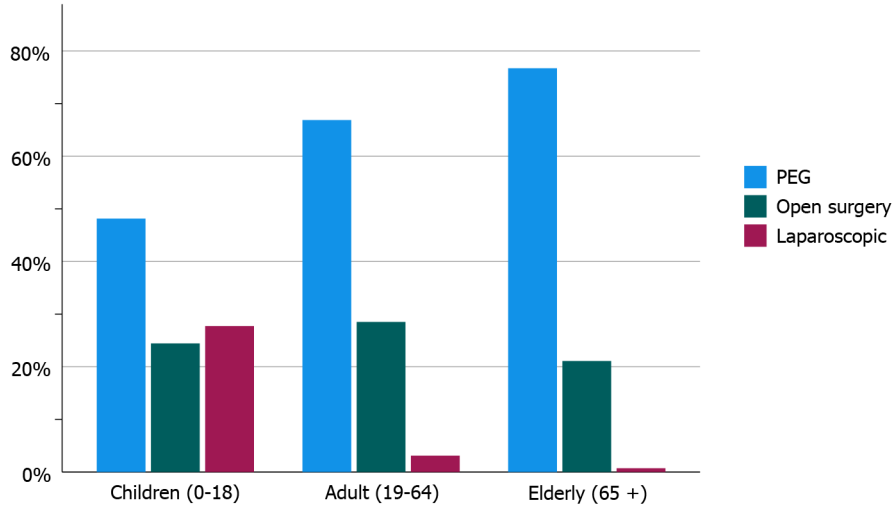

Figure 3 Type of gastrostomy by age group. PEG: Percutaneous endoscopic gastrostomy.

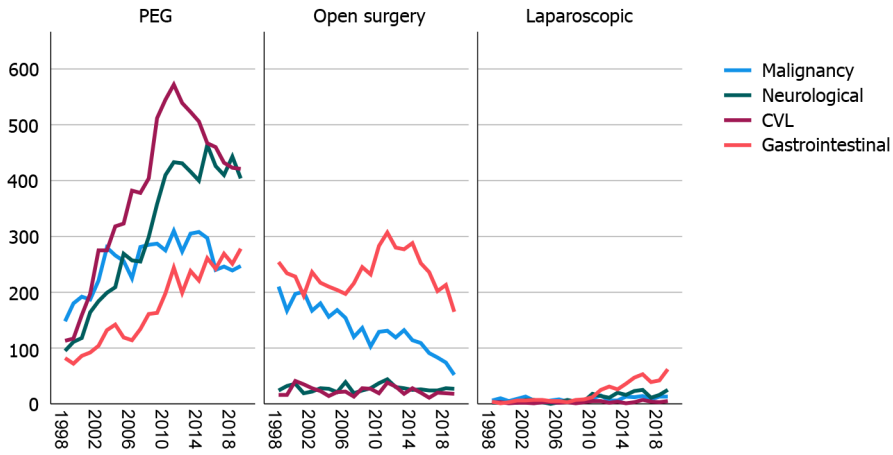

Figure 4 Time trends for different types of gastrostomies (total number by year) by indication. CVL: Cerebrovascular lesions; PEG: Percutaneous endoscopic gastrostomy.

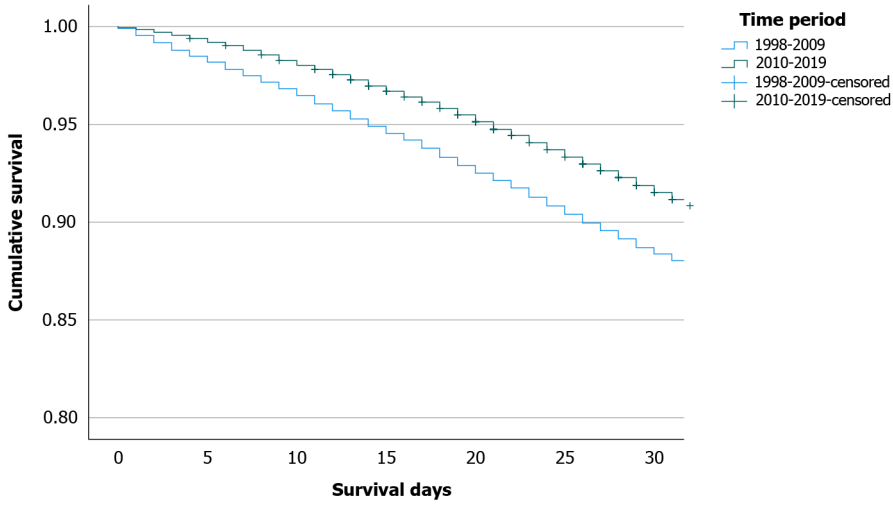

Figure 5 30-d cumulative survival during the early period (1998-2009) and late period (2010-2019).

In an additional 141 patients, a procedure-related complication was judged to have contributed to the cause of death within 30 d. Thus, in 185 patients (0.4%), a procedure-related complication was either the direct cause of death or a contributing factor. This was more common among those that had undergone an open gastrostomy (0.9%, n = 102) compared to PEG (0.2%, n = 74) and laparoscopic gastrostomy (0.2%, n = 6, P < 0.001).

Long-term survival: During the mean observational time of 10.0 ± 6.1 years, 70% (n = 34055) of the patients had died after 21.9 ± 35.6 mo (on average) after receiving the gastrostomy. One-year and ten-year survival rates were 93.7%, 67.5%, and 42.1% and 79.9%, 39.2%, and 6.8% in children, adults, and elderly, respectively (Figure 6). The most common stated causes of death were malignancies (C00-D48, 24.4%), cardiovascular diseases (I00-I99, 23.1%), and respiratory conditions (J00-J99, 20.3%).

DISCUSSION

In this nationwide cohort study of 48682 individuals who received a gastrostomy from 1998-2019 in Sweden, an increased use of gastrostomies was seen, from 13.7/100000 to 22.3/100000 inhabitants. The increase was found in PEG and laparoscopically-inserted gastrostomy, while open gastrostomy was halved. We believe that this mirrors the international shift towards more minimally invasive procedures[17]. Very few studies have examined the number of gastrostomy placements in other countries, but the observed doubling of PEG is similar to the 2.5-fold increase observed in Poland from 2010-2020[18]. The United States experienced an exponential increase in PEG use from 1980-2000, resulting in more than 216000 annual PEGs[19]. Based on a population of about 280 million in 2000, this should correspond to 77/100000 inhabitants. However, the opposite trend has been described in Japan, where a decreased use of PEG has been observed since 2011[20], especially in patients aged 80 years and over. This has resulted in an increased use of total parenteral nutrition in home care. Stated reasons include changes in the health insurance system, reimbursement-related factors, and

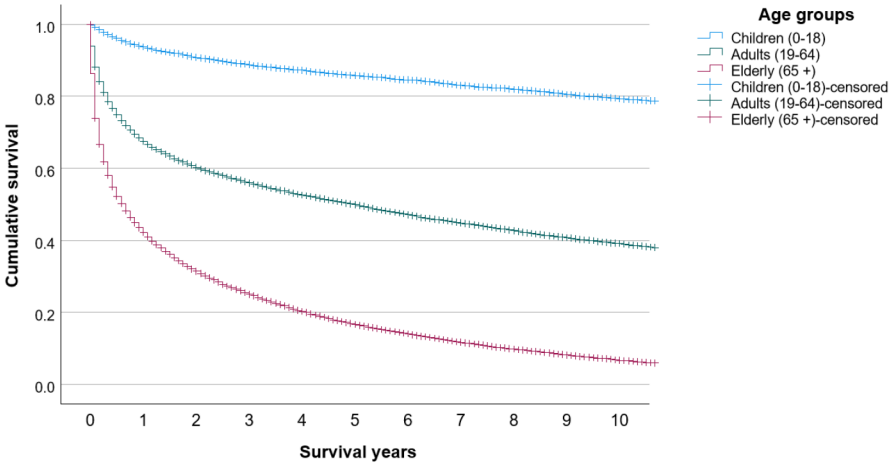

Figure 6 Cumulative overall survival in the three age groups.

emotional and ethical barriers.

The most common indication for gastrostomy in the present study was various non-malignant gastrointestinal conditions (19.7%), closely followed by CVL (18.9%), malignancies (18.7%), and neurological disorders (16.7%). Neurological dysphagia is one of the most common indications for PEG tube insertion, and the incidence among stroke patients has been reported to be as high as 78%[21]. In our study, stroke (ischemic or hemorrhagic) was the most common subgroup (17%). In a prospectively collected case series of 1041 PEG patients in Germany, the most common indication was neurogenic dysphagia (43%), followed by cancer (37%)[22]. In the previously mentioned Polish PEG study[18], where indication was also based on ICD-10 codes, the most common indication was dysphagia and malnutrition (37.2%), which as the author states might have been a consequence of other diseases. The high proportion of non-malignant gastrointestinal conditions in this study was due to perioperative placement of a gastrostomy for stomach decompression in the case of emergency surgery. Examples of such conditions include perforated ulcer, bowel obstruction, or incarcerated hiatal hernia.

Although gastrostomy tube placement, especially PEG, is considered a relatively safe surgical procedure, complications are common, which is likely due to greater frailty given an elderly population with multiple comorbidities. About one-third of PEG insertions result in minor complications, such as local wound infection, tube dislodgement, or peristomal leakage. Major complications, such as bowel or liver injuries, aspiration pneumonia, or major bleedings, are rare, affecting 2%-4% of the patients[23-26]. In this registry-based study, it was unfortunately not possible to explore the incidence of specific complications. However, in 0.1% (PEG: 0.05%, open: 0.24%, laparoscopic: 0.04%) a procedure-related complication was stated as the primary cause of death, and in 0.4% (PEG: 0.2%, open: 0.9%, laparoscopic: 0.2%) of the patients, a procedure-related complication was stated as a contributing factor to death within 30 d. Our large number of patients allowed for the detection of this rare event, which is often reported to be zero in smaller studies[22,26-28]. The fact that the majority of the procedure-related deaths occurred after an open gastrostomy is no surprise and likely explained by other concomitant surgical procedures as previously mentioned.

The 30-d mortality rates are difficult to compare between studies because of differences in indication, age, comorbidities, *etc.* Previous PEG studies reported a 30-d mortality of 3.3% (n = 302, Taiwan)[28], 3.9% (n = 388, Japan)[29], 6.5% (n = 168, Brazil and n = 787, Germany)[26,30], 13.0% (n = 277, Canada)[27], and 23.5% (n = 272, Israel)[31]. Our 30-d mortality rate of 9.8% in PEG patients was similar to these studies. Interestingly, the overall 30-d mortality decreased from 11.6% in the early time period (1998-2009) to 8.5% in the late time period (2010-2019). We hypothesize that the main driving factor was the shift towards the more minimally invasive techniques, PEG and laparoscopic gastrostomy. In addition to time period and open gastrostomy, older age and male sex was associated with an increased 30-d mortality. Due to the registry-based design, we were not able to verify other predictive factors, such as elevated C-reactive protein, anemia, previous intensive care admission, low albumin, high creatinine levels, malignancy, diabetes, heart failure, and low body mass index, found in other studies[23,26,27,29,30].

One of the first publications on laparoscopic gastrostomy in children was published in 1997[32], and the technique has since then been modified by Backman *et al*[33]. In a meta-analysis from 2018[6], it was found that PEG was associated with a significantly higher risk of major complications (odds ratio = 3.86, 95%CI: 1.90-7.81) compared to laparoscopic gastrostomy in a pediatric population. Therefore, it was stated that laparoscopic gastrostomy should be the preferred method in children. The adoption of the new modified technique for laparoscopic gastrostomy is mirrored in this study, where a clear increase was observed from 2010 on. Likely, it explains the 10-fold increase in laparoscopic gastrostomy procedures in Sweden during the study period.

Although procedure-related mortality was a rare event (0.1% overall), an observed 30-d mortality of 10% cannot be ignored. In the cases of patient deaths within 30 d of placement, the gastrostomy hardly benefited the patient. We believe these numbers are important to consider in the risk-benefit analysis when consulting patients before gastrostomy placement, especially in frail patients. However, we acknowledge the difficulties in deciding which patients will benefit from a gastrostomy. Indication, timing of the intervention, and ethical aspects are of importance. A recent Cochrane review found no evidence that enteral tube feeding improved survival or quality of life in patients with dementia[13].

However, in patients with amyotrophic lateral sclerosis, PEG placement was found to prolong survival if performed before the disease had become too advanced[34]. The present 42.1% 1-year survival in the elderly is very similar to the 38% reported from a systematic review of patients (> 65 years) receiving a PEG[35]. Thus, on a national level, our patient selection seems acceptable. In children, however, the situation is completely different, as almost 80% were alive at 10 years in this study.

The cause of death is often related to the underlying diseases[23], which we could confirm when comparing indication for gastrostomy and cause of death, *e.g.*, malignancies (18.7% *vs* 24.4%) and cardiovascular diseases (17.0% stroke *vs* 23.1% overall cardiovascular death). Respiratory conditions were the third most common cause of death (20.3% of the overall mortality), likely because dysphagia (with the concomitant risk of aspiration pneumonia) was one of the main indications for gastrostomy.

Strengths and limitations

The registry-based nature of this study was both a strength and a limiting factor. The registries made it possible to include all gastrostomies in Sweden with a 100% follow-up on survival time and cause of death since it is mandatory for physicians to register these data in the Swedish Death Register. However, the major limiting factor of this study was the impossibility of determining the indication for the gastrostomy since it was based on ICD-10 codes. Many patients had symptomatic diagnoses such as dysphagia (R13) as the principal diagnosis or a principal diagnosis was missing at the index occasion of gastrostomy. Despite efforts to find the indication among secondary diagnosis or at the occasion before gastrostomy, it was not possible to categorize 26% of the patients into one of the four main categories.

CONCLUSION

During the last two decades in Sweden, there has been a significant increase in the number of PEG and laparoscopically-inserted gastrostomies, while open gastrostomy has become less common. Although, procedure-related death was rare, the overall 30-d mortality rate was high (10%). One-year and ten-year survival rates were 93.7%, 67.5%, and 42.1% and 79.9%, 39.2%, and 6.8% in children, adults, and elderly, respectively. This study contributes robust survival data that can assist physicians in a risk-benefit assessment before gastrostomy placement, and we predict that the 30-d mortality should be lowered by selecting patients who actually benefit from a gastrostomy.

ARTICLE HIGHLIGHTS

Research background

Placing a gastrostomy in patients requiring long-term nutritional support is standard care. Since the introduction of percutaneous endoscopic gastrostomy (PEG), there has been a continuous shift towards minimally invasive procedures. However, nationwide population-based data on the use of different techniques and overall outcomes is scarce.

Research motivation

As many patients are frail, the balance between risk and benefit is of particular importance. In the present nationwide population-based cohort, we could evaluate indication, choice of gastrostomy technique, complications, mortality, and time trends over two decades. The dissemination of such findings can lead to improved care.

Research objectives

To study the use of gastrostomies in clinical praxis concerning number and type of procedures (PEG, open gastrostomy, and laparoscopic gastrostomy) as well as indication (malignancy, neurological diseases, cerebrovascular lesions, and non-malignant gastrointestinal conditions). To analyze time trends concerning any shift between the three different methods, procedure-related mortality, and short-term mortality (within 30 d). To explore long-term survival up until 10 years after gastrostomy placement.

Research methods

Data on 48682 individuals who had a gastrostomy between 1998-2019 in Sweden were collected from the mandatory National Patient Register. Indication, type of gastrostomy, and complications were based on registered International Statistical Classification of Diseases and Related Health Problems-diagnoses. Date and cause of death were retrieved by cross-matched data from the Death Register. The cohort was divided into three age groups: Children (0-18 years); adults (19-64 years); and elderly (≥ 65 years). The cohort was also divided by type of gastrostomy: PEG; open gastrostomy; and laparoscopic gastrostomy.

Research results

The annual use of gastrostomies in Sweden increased during the study period, from 13.7/100000 to 22.3/100000 individuals. PEG more than doubled, while a 10-fold increase was seen in laparoscopic gastrostomies. Although the procedure-related mortality was low (0.1%), a 10%-overall 30-d mortality was seen. The latter, however, decreased over time. One-year and ten-year survival rates for children, adults, and elderly were 93.7%, 67.5%, and 42.1% and 79.9%,

39.2%, and 6.8%, respectively. The most common causes of death were malignancies, cardiovascular conditions, and respiratory diseases.

Research conclusions

More and more gastrostomies were placed in Sweden. The increase was due to the number of PEG procedures doubling. Although the 30-d mortality rate decreased during the study period, it was still high (10%). The most common causes of death were consistent with the gastrostomy indication, and as expected long-term survival was mainly dependent on patient age.

Research perspectives

The present nationwide population-based results can be used as a reference in future trials and in quality controls at various levels.

FOOTNOTES

Author contributions: Skogar ML interpretated and analyzed the data and drafted the article; Sundbom M contributed to data acquisition and drafting the article; Skogar ML and Sundbom M contributed equally to conception and design of the study, made critical revisions of the manuscript, and approved the final version of the article to be published.

Institutional review board statement: The study was approved by the Swedish Ethical Review Authority.

Informed consent statement: Since this was a retrospective registry-based study, signed informed consent was not applicable.

Conflict-of-interest statement: All the authors report no relevant conflicts of interest for this article.

Data sharing statement: No additional data are available.

STROBE statement: The authors have read the STROBE Statement-checklist of items, and the manuscript was prepared and revised according to the STROBE Statement-checklist of items.

Country/Territory of origin: Sweden

ORCID number: Martin Löfling Skogar 0000-0002-6840-2749.

S-Editor: Wang JJ
L-Editor: Filipodia
P-Editor: Yuan YY

REFERENCES

1 **Park RH**, Allison MC, Lang J, Spence E, Morris AJ, Danesh BJ, Russell RI, Mills PR. Randomised comparison of percutaneous endoscopic gastrostomy and nasogastric tube feeding in patients with persisting neurological dysphagia. *BMJ* 1992; **304**: 1406-1409 [PMID: 1628013 DOI: 10.1136/bmj.304.6839.1406]
2 **Dietrich CG**, Schoppmeyer K. Percutaneous endoscopic gastrostomy - Too often? *World J Gastroenterol* 2020; **26**: 2464-2471 [PMID: 32523304 DOI: 10.3748/wjg.v26.i20.2464]
3 **Kawata N**, Kakushima N, Tanaka M, Sawai H, Imai K, Hagiwara T, Takao T, Hotta K, Yamaguchi Y, Takizawa K, Matsubayashi H, Ono H. Percutaneous endoscopic gastrostomy for decompression of malignant bowel obstruction. *Dig Endosc* 2014; **26**: 208-213 [PMID: 23772988 DOI: 10.1111/den.12139]
4 **Gauderer MW**, Ponsky JL, Izant RJ Jr. Gastrostomy without laparotomy: a percutaneous endoscopic technique. *J Pediatr Surg* 1980; **15**: 872-875 [PMID: 6780678 DOI: 10.1016/s0022-3468(80)80296-x]
5 **Rahnemai-Azar AA**, Rahnemaiazar AA, Naghshizadian R, Kurtz A, Farkas DT. Percutaneous endoscopic gastrostomy: indications, technique, complications and management. *World J Gastroenterol* 2014; **20**: 7739-7751 [PMID: 24976711 DOI: 10.3748/wjg.v20.i24.7739]
6 **Sandberg F**, Viktorsdóttir MB, Salö M, Stenström P, Arnbjörnsson E. Comparison of major complications in children after laparoscopy-assisted gastrostomy and percutaneous endoscopic gastrostomy placement: a meta-analysis. *Pediatr Surg Int* 2018; **34**: 1321-1327 [PMID: 30291404 DOI: 10.1007/s00383-018-4358-6]
7 **Baker L**, Beres AL, Baird R. A systematic review and meta-analysis of gastrostomy insertion techniques in children. *J Pediatr Surg* 2015; **50**: 718-725 [PMID: 25783383 DOI: 10.1016/j.jpedsurg.2015.02.021]
8 **Rutter CE**, Yovino S, Taylor R, Wolf J, Cullen KJ, Ord R, Athas M, Zimrin A, Strome S, Suntharalingam M. Impact of early percutaneous endoscopic gastrostomy tube placement on nutritional status and hospitalization in patients with head and neck cancer receiving definitive

chemoradiation therapy. *Head Neck* 2011; **33**: 1441-1447 [PMID: 21928416 DOI: 10.1002/hed.21624]
9 **Klose J**, Heldwein W, Rafferzeder M, Sernetz F, Gross M, Loeschke K. Nutritional status and quality of life in patients with percutaneous endoscopic gastrostomy (PEG) in practice: prospective one-year follow-up. *Dig Dis Sci* 2003; **48**: 2057-2063 [PMID: 14627355 DOI: 10.1023/a:1026199110891]
10 **Gavazzi C**, Colatruglio S, Valoriani F, Mazzaferro V, Sabbatini A, Biffi R, Mariani L, Miceli R. Impact of home enteral nutrition in malnourished patients with upper gastrointestinal cancer: A multicentre randomised clinical trial. *Eur J Cancer* 2016; **64**: 107-112 [PMID: 27391922 DOI: 10.1016/j.ejca.2016.05.032]
11 **Dorst J**, Dupuis L, Petri S, Kollewe K, Abdulla S, Wolf J, Weber M, Czell D, Burkhardt C, Hanisch F, Vielhaber S, Meyer T, Frisch G, Kettemann D, Grehl T, Schrank B, Ludolph AC. Percutaneous endoscopic gastrostomy in amyotrophic lateral sclerosis: a prospective observational study. *J Neurol* 2015; **262**: 849-858 [PMID: 25618254 DOI: 10.1007/s00415-015-7646-2]
12 **Suzuki Y**, Urashima M, Izumi M, Ito Y, Uchida N, Okada S, Ono H, Orimo S, Kohri T, Shigoka H, Shintani S, Tanaka Y, Yoshida A, Ijima M, Ito T, Endo T, Okano H, Maruyama M, Iwase T, Kikuchi T, Kudo M, Takahashi M, Goshi S, Mikami T, Yamashita S, Akiyama K, Ogawa T, Ono S, Onozawa S, Kobayashi J, Matsumoto M, Matsumoto T, Jomoto K, Mizuhara A, Nishiguchi Y, Nishiwaki S, Aoki M, Ishizuka I, Kura T, Murakami M, Murakami A, Ohta T, Onishi K, Nakahori M, Tsuji T, Tahara K, Tanaka I, Kitagawa K, Shimazaki M, Fujiki T, Kusakabe T, Iiri T, Kitahara S, Horiuchi A, Suenaga H, Washizawa N, Suzuki M. The Effects of Percutaneous Endoscopic Gastrostomy on Quality of Life in Patients With Dementia. *Gastroenterology Res* 2012; **5**: 10-20 [PMID: 27785173 DOI: 10.4021/gr392w]
13 **Davies N**, Barrado-Martín Y, Vickerstaff V, Rait G, Fukui A, Candy B, Smith CH, Manthorpe J, Moore KJ, Sampson EL. Enteral tube feeding for people with severe dementia. *Cochrane Database Syst Rev* 2021; **8**: CD013503 [PMID: 34387363 DOI: 10.1002/14651858.CD013503.pub2]
14 **Berg L**. NOMESCO Classification of Surgical Procedures. [cited 11 November 2023]. Available from: https://norden.diva-portal.org/smash/get/diva2:970547/FULLTEXT01.pdf
15 **World Health Organization**. International Statistical Classification of Diseases and Related Health Problems 10th Revision. 2019. [cited 11 November 2023]. Available from: https://icd.who.int/browse10/2019/en#!
16 **Ludvigsson JF**, Andersson E, Ekbom A, Feychting M, Kim JL, Reuterwall C, Heurgren M, Olausson PO. External review and validation of the Swedish national inpatient register. *BMC Public Health* 2011; **11**: 450 [PMID: 21658213 DOI: 10.1186/1471-2458-11-450]
17 **Arvanitakis M**, Gkolfakis P, Despott EJ, Ballarin A, Beyna T, Boeykens K, Elbe P, Gisbertz I, Hoyois A, Mosteanu O, Sanders DS, Schmidt PT, Schneider SM, van Hooft JE. Endoscopic management of enteral tubes in adult patients - Part 1: Definitions and indications. European Society of Gastrointestinal Endoscopy (ESGE) Guideline. *Endoscopy* 2021; **53**: 81-92 [PMID: 33260229 DOI: 10.1055/a-1303-7449]
18 **Folwarski M**, Klek S, Brzeziński M, Szlagatys-Sidorkiewicz A, Wyszomirski A, Meyer-Szary J, Skonieczna-Żydecka K. Prevalence and Trends in Percutaneous Endoscopic Gastrostomy Placement: Results From a 10-Year, Nationwide Analysis. *Front Nutr* 2022; **9**: 906409 [PMID: 35707793 DOI: 10.3389/fnut.2022.906409]
19 **Gauderer MW**. Percutaneous endoscopic gastrostomy-20 years later: a historical perspective. *J Pediatr Surg* 2001; **36**: 217-219 [PMID: 11150469 DOI: 10.1053/jpsu.2001.20058]
20 **Komiya K**, Usagawa Y, Kadota JI, Ikegami N. Decreasing Use of Percutaneous Endoscopic Gastrostomy Tube Feeding in Japan. *J Am Geriatr Soc* 2018; **66**: 1388-1391 [PMID: 29799111 DOI: 10.1111/jgs.15386]
21 **Martino R**, Foley N, Bhogal S, Diamant N, Speechley M, Teasell R. Dysphagia after stroke: incidence, diagnosis, and pulmonary complications. *Stroke* 2005; **36**: 2756-2763 [PMID: 16269630 DOI: 10.1161/01.STR.0000190056.76543.eb]
22 **Richter-Schrag HJ**, Richter S, Ruthmann O, Olschewski M, Hopt UT, Fischer A. Risk factors and complications following percutaneous endoscopic gastrostomy: a case series of 1041 patients. *Can J Gastroenterol* 2011; **25**: 201-206 [PMID: 21523261 DOI: 10.1155/2011/609601]
23 **Stenberg K**, Eriksson A, Odensten C, Darehed D. Mortality and complications after percutaneous endoscopic gastrostomy: a retrospective multicentre study. *BMC Gastroenterol* 2022; **22**: 361 [PMID: 35902805 DOI: 10.1186/s12876-022-02429-0]
24 **Blomberg J**, Lagergren J, Martin L, Mattsson F, Lagergren P. Complications after percutaneous endoscopic gastrostomy in a prospective study. *Scand J Gastroenterol* 2012; **47**: 737-742 [PMID: 22471958 DOI: 10.3109/00365521.2012.654404]
25 **Vujasinovic M**, Ingre C, Baldaque Silva F, Frederiksen F, Yu J, Elbe P. Complications and outcome of percutaneous endoscopic gastrostomy in a high-volume centre. *Scand J Gastroenterol* 2019; **54**: 513-518 [PMID: 30905223 DOI: 10.1080/00365521.2019.1594354]
26 **Figueiredo FA**, da Costa MC, Pelosi AD, Martins RN, Machado L, Francioni E. Predicting outcomes and complications of percutaneous endoscopic gastrostomy. *Endoscopy* 2007; **39**: 333-338 [PMID: 17427069 DOI: 10.1055/s-2007-966198]
27 **Lima DL**, Miranda LEC, da Penha MRC, Lima RNCL, Dos Santos DC, Eufrânio MS, Miranda ACG, Pereira LMMB. Factors Associated with 30-Day Mortality in Patients after Percutaneous Endoscopic Gastrostomy. *JSLS* 2021; **25** [PMID: 34456551 DOI: 10.4293/JSLS.2021.00040]
28 **Lee TH**, Shih LN, Lin JT. Clinical experience of percutaneous endoscopic gastrostomy in Taiwanese patients--310 cases in 8 years. *J Formos Med Assoc* 2007; **106**: 685-689 [PMID: 17711805 DOI: 10.1016/S0929-6646(08)60029-7]
29 **Limpias Kamiya KJL**, Hosoe N, Takabayashi K, Hayashi Y, Fukuhara S, Mutaguchi M, Nakamura R, Kawakubo H, Kitagawa Y, Ogata H, Kanai T. Factors predicting major complications, mortality, and recovery in percutaneous endoscopic gastrostomy. *JGH Open* 2021; **5**: 590-598 [PMID: 34013060 DOI: 10.1002/jgh3.12538]
30 **Zopf Y**, Maiss J, Konturek P, Rabe C, Hahn EG, Schwab D. Predictive factors of mortality after PEG insertion: guidance for clinical practice. *JPEN J Parenter Enteral Nutr* 2011; **35**: 50-55 [PMID: 21224433 DOI: 10.1177/0148607110376197]
31 **Sbeit W**, Kadah A, Mari A, Mahamid M, Khoury T. Simple Bedside Predictors of Survival after Percutaneous Gastrostomy Tube Insertion. *Can J Gastroenterol Hepatol* 2019; **2019**: 1532918 [PMID: 31828049 DOI: 10.1155/2019/1532918]
32 **Andersson L**, Mikaelsson C, Arnbjörnsson E, Larsson LT. Laparoscopy aided gastrostomy in children. *Ann Chir Gynaecol* 1997; **86**: 19-22 [PMID: 9181214]
33 **Backman T**, Sjövie H, Kullendorff CM, Arnbjörnsson E. Continuous double U-stitch gastrostomy in children. *Eur J Pediatr Surg* 2010; **20**: 14-17 [PMID: 19830661 DOI: 10.1055/s-0029-1238316]
34 **Castanheira A**, Swash M, De Carvalho M. Percutaneous gastrostomy in amyotrophic lateral sclerosis: a review. *Amyotroph Lateral Scler Frontotemporal Degener* 2022; **23**: 176-189 [PMID: 34196236 DOI: 10.1080/21678421.2021.1946089]
35 **Mitchell SL**, Tetroe JM. Survival after percutaneous endoscopic gastrostomy placement in older persons. *J Gerontol A Biol Sci Med Sci* 2000; **55**: M735-M739 [PMID: 11129395 DOI: 10.1093/gerona/55.12.m735]

World Journal of Gastroenterology

Submit a Manuscript: https://www.f6publishing.com

World J Gastroenterol 2024 March 14; 30(10): 1368-1376

DOI: 10.3748/wjg.v30.i10.1368

ISSN 1007-9327 (print) ISSN 2219-2840 (online)

ORIGINAL ARTICLE

Retrospective Study

Stage at diagnosis of colorectal cancer through diagnostic route: Who should be screened?

Nobukazu Agatsuma, Takahiro Utsumi, Yoshitaka Nishikawa, Takahiro Horimatsu, Takeshi Seta, Yukitaka Yamashita, Yukari Tanaka, Takahiro Inoue, Yuki Nakanishi, Takahiro Shimizu, Mikako Ohno, Akane Fukushima, Takeo Nakayama, Hiroshi Seno

Specialty type: Gastroenterology and hepatology

Provenance and peer review: Invited article; Externally peer reviewed.

Peer-review model: Single blind

Peer-review report's scientific quality classification

Grade A (Excellent): A
Grade B (Very good): 0
Grade C (Good): 0
Grade D (Fair): 0
Grade E (Poor): 0

P-Reviewer: Verma V, United States

Received: December 27, 2023
Peer-review started: December 27, 2023
First decision: January 5, 2024
Revised: January 17, 2024
Accepted: February 20, 2024
Article in press: February 20, 2024
Published online: March 14, 2024

Nobukazu Agatsuma, Takahiro Utsumi, Yukari Tanaka, Takahiro Inoue, Yuki Nakanishi, Takahiro Shimizu, Hiroshi Seno, Department of Gastroenterology and Hepatology, Kyoto University Graduate School of Medicine, Kyoto 606-8507, Japan

Nobukazu Agatsuma, Takeshi Seta, Yukitaka Yamashita, Department of Gastroenterology and Hepatology, Japanese Red Cross Wakayama Medical Center, Wakayama 640-8558, Japan

Yoshitaka Nishikawa, Takeo Nakayama, Department of Health Informatics, Kyoto University School of Public Health, Kyoto 606-8501, Japan

Takahiro Horimatsu, Institute for Advancement of Clinical and Translational Science (iACT), Kyoto University Hospital, Kyoto 606-8507, Japan

Mikako Ohno, Akane Fukushima, Medical Support Section, Medical Affairs Division, Kyoto University Hospital, Kyoto 606-8507, Japan

Corresponding author: Nobukazu Agatsuma, MD, Doctor, Department of Gastroenterology and Hepatology, Kyoto University Graduate School of Medicine, 54 Kawaharacho, Shogoin, Sakyo-ku, Kyoto 606-8507, Japan. agatsuma@kuhp.kyoto-u.ac.jp

Abstract

BACKGROUND

Colorectal cancer (CRC) is a global health concern, with advanced-stage diagnoses contributing to poor prognoses. The efficacy of CRC screening has been well-established; nevertheless, a significant proportion of patients remain unscreened, with > 70% of cases diagnosed outside screening. Although identifying specific subgroups for whom CRC screening should be particularly recommended is crucial owing to limited resources, the association between the diagnostic routes and identification of these subgroups has been less appreciated. In the Japanese cancer registry, the diagnostic routes for groups discovered outside of screening are primarily categorized into those with comorbidities found during hospital visits and those with CRC-related symptoms.

AIM

To clarify the stage at CRC diagnosis based on diagnostic routes.

METHODS
We conducted a retrospective observational study using a cancer registry of patients with CRC between January 2016 and December 2019 at two hospitals. The diagnostic routes were primarily classified into three groups: Cancer screening, follow-up, and symptomatic. The early-stage was defined as Stages 0 or I. Multivariate and univariate logistic regressions were exploited to determine the odds of early-stage diagnosis in the symptomatic and cancer screening groups, referencing the follow-up group. The adjusted covariates were age, sex, and tumor location.

RESULTS
Of the 2083 patients, 715 (34.4%), 1064 (51.1%), and 304 (14.6%) belonged to the follow-up, symptomatic, and cancer screening groups, respectively. Among the 2083 patients, CRCs diagnosed at an early stage were 57.3% (410 of 715), 23.9% (254 of 1064), and 59.5% (181 of 304) in the follow-up, symptomatic, and cancer screening groups, respectively. The symptomatic group exhibited a lower likelihood of early-stage diagnosis than the follow-up group [$P < 0.001$, adjusted odds ratio (aOR), 0.23; 95% confidence interval (95%CI): 0.19-0.29]. The likelihood of diagnosis at an early stage was similar between the follow-up and cancer screening groups ($P = 0.493$, aOR for early-stage diagnosis in the cancer screening group *vs* follow-up group = 1.11; 95%CI = 0.82-1.49).

CONCLUSION
CRCs detected during hospital visits for comorbidities were diagnosed earlier, similar to cancer screening. CRC screening should be recommended, particularly for patients without periodical hospital visits for comorbidities.

Key Words: Colorectal neoplasms; Cancer registry; Diagnostic route; Cancer screening; Stage at diagnosis

Core Tip: Colorectal cancer (CRC) screening reduces CRC deaths, yet several patients remain unscreened. To encourage more individuals to participate in screening, identifying subgroups at high risk is crucial. This study used cancer registries from two Japanese facilities to clarify the stage at diagnosis in three groups: cancer screening, follow-up (patients detected during follow-up for other comorbidities), and symptomatic. The proportion of early-stage diagnoses was higher in the follow-up group than in the symptomatic group and was comparable to that in the cancer screening group. Therefore, CRC screening should be recommended, particularly for patients without periodical hospital visits for comorbidities.

Citation: Agatsuma N, Utsumi T, Nishikawa Y, Horimatsu T, Seta T, Yamashita Y, Tanaka Y, Inoue T, Nakanishi Y, Shimizu T, Ohno M, Fukushima A, Nakayama T, Seno H. Stage at diagnosis of colorectal cancer through diagnostic route: Who should be screened? *World J Gastroenterol* 2024; 30(10): 1368-1376
URL: https://www.wjgnet.com/1007-9327/full/v30/i10/1368.htm
DOI: https://dx.doi.org/10.3748/wjg.v30.i10.1368

INTRODUCTION

Colorectal cancer (CRC) is a commonly diagnosed cancer and is a leading cause of cancer-related deaths worldwide[1]. CRC has a poor prognosis when diagnosed at an advanced stage, and screening can lead to more early-stage diagnoses, potentially improving patient survival[2-5]. Despite evidence showing the effectiveness of CRC screening, some (30%-50%) of the eligible population does not undergo the process, with over 70% of all CRC cases discovered through non-screening routes[6-8]. Although encouraging individuals to participate in CRC screening is essential, there remains insufficient guidance on effectively and efficiently recommending screening for the non-adherent population.

Understanding the individuals for whom screening should be particularly recommended is crucial for its efficient promotion. Screening should be recommended for all eligible individuals; however, personalized messages for all eligible individuals are impractical due to limited human and financial resources[9-13]. Targeted interventions to increase cancer screening are considered cost-effective[14]. Therefore, identifying individuals for whom CRC screening should be particularly recommended based on the subgroup to which the screening-eligible population belongs is beneficial. However, few reports have appreciated the value of the diagnostic route to clarify subgroups of patients that are more likely to be diagnosed at a later stage.

CRC is diagnosed through various routes besides screening, leading to different stages at diagnosis. In Western countries, diagnostic routes for CRC are primarily classified into emergency and non-emergency pathways, with emergency cases typically diagnosed at more advanced stages than those of non-emergency[8,15,16]. Conversely, the Japanese cancer registry categorizes CRC cases other than those in the screening pathway into two primary groups: Those discovered during hospital visits owing to comorbidities and those found through symptom-driven medical consultations[17]. CRC cases detected during hospital visits for comorbidities are those detected during the monitoring or management of other chronic diseases or pre- and post-operative examinations for unrelated benign or malignant diseases or malignant tumors. They may be discovered at an earlier stage compared with those of patients with CRC-

related symptoms. However, there are no reports on the comparison regarding the stages at diagnosis between the two groups to determine which group is more likely to be diagnosed at a later stage.

This study aimed to clarify the stages at diagnosis based on the diagnostic routes of CRC using hospital-based cancer registries from two Japanese facilities. We evaluated the diagnostic stage distribution and compared the proportion of early-stage cases among three groups: (1) Patients detected during hospital visits for other comorbidities; (2) patients detected following presentation with CRC-related symptoms; and (3) patients detected during cancer screening.

MATERIALS AND METHODS

Study population

This retrospective observational study was conducted at Kyoto University Hospital (KU) in Kyoto Prefecture and Japanese Red Cross Wakayama Medical Center (WMC) in Wakayama Prefecture. Both facilities are among the hospitals that have treated the largest CRC cases in each prefecture and are designated cancer care hospitals. KU covers approximately 20% of patients with CRC in Kyoto Prefecture, and WMC covers approximately 40% of these patients in Wakayama Prefecture[18]. All patients with CRC registered in the hospital-based cancer registry at both institutions between January 2016 and December 2019 were included in this study.

Assessments

Data from each registry were extracted from cancer registrars based on medical records according to the standard registry definition. The diagnostic routes were primarily classified into three groups: Cancer screening, follow-up (patients detected during the follow-up of comorbidities), and symptomatic[19]. The two other groups were CRC cases with unknown diagnostic routes and those discovered at autopsy. However, the total number is less than 5% nationwide[18]. The cancer screening group included patients who underwent a population-based or opportunistic screening. In the cancer screening group, almost all patients were estimated to undergo an immunochemical fecal occult blood test (iFOBT) because iFOBT is strongly recommended for population-based and opportunistic screening in the Japanese CRC screening guidelines[20]. The follow-up group comprised patients detected during examinations conducted as part of the follow-up for existing comorbidities (lifestyle-related diseases, such as hypertension and diabetes, heart disease, other organ cancers, and benign digestive disorders). Cases in which CRC was discovered due to CRC-related symptoms during a hospital visit for comorbidity follow-up were classified as the follow-up group. Patients with CRC who presented to the hospital primarily for CRC-related symptoms were classified as "other group" in the cancer registry, distinguished from the patients with CRC detected *via* screening or during hospital visits for comorbidities[17,19]. Stages were recorded according to the tumor-node-metastasis staging system of the Union for International Cancer Control (8th edition). If the patient had undergone surgery, the post-operative stage was used; if the patient had not, the preoperative stage was used. Data on age, sex, diagnostic routes, tumor location, clinical and pathological stages, and pathological findings were obtained from a hospital-based cancer registry. No data were missing. We excluded patients with non-epithelial or neuroendocrine tumors, those whose stage or route of discovery was unknown, and autopsy-detected cases. Patients with multiple CRCs were considered to have advanced-stage disease. Regarding tumor location, we defined right-sided CRC as tumors from the cecum to the splenic flexure, whereas left-sided CRC was defined as tumors from the descending colon to the rectum. For advanced lesions on both sides of the colorectum, left-sided lesions were excluded because previous reports indicated a poorer prognosis in right-sided primary CRC than in left-sided[21]. Localized disease, corresponding to Stages 0 and I, is associated with a 5-year survival rate of over 90%, making its prognosis more favorable than that in the regional or distant stages[2]. Hence, as in previous reports, we categorized Stages 0 and I as early stages in this study[22,23]. The stage distribution and proportion of patients with early-stage CRC were evaluated using the diagnostic routes. We compared the proportion of patients with early-stage CRC between the follow-up, symptomatic, and cancer screening groups.

Statistical analysis

Pearson's Chi-square test was used to compare the proportion of early-stage CRCs in the follow-up group with those in the symptomatic and screening groups. Differences were considered statistically significant at $P < 0.05$. Logistic regression analysis was used to determine the odds of early-stage diagnosis in the symptomatic and cancer screening groups using the follow-up group as a reference. Univariate logistic regression analysis was used to calculate the crude odds ratios of early-stage detection, comparing the follow-up group with the symptomatic and cancer screening groups. Multivariate logistic regression analysis was also used to calculate adjusted odds ratios (aORs), adjusted for age, sex, and tumor location. Statistical results were calculated as point estimates with a 95% confidence interval (95%CI). All statistical analyses were performed using JMP Pro® 16.1.0 (SAS Institute Inc., Cary, NC, United States).

RESULTS

A flowchart of the participants is shown in Figure 1. Of the 2575 lesions and 2435 patients, the study included 2083 patients (879 at KU and 1204 at WMC). Table 1 presents patient characteristics for each discovery route. Among the 2083 patients included in the study, 715 (34.4%), 1064 (51.1%), and 304 (14.6%) belonged to the follow-up, symptomatic, and cancer screening groups, respectively. Patient characteristics at each hospital are presented in Table 2. The stage distri-

Table 1 Characteristics of the patients and colorectal lesions according to diagnostic routes in two hospitals

Variable	Follow-up group (*n* = 715)	Symptomatic group (*n* = 1064)	Cancer screening group (*n* = 304)
Age (median, IQR)	74 (68-79)	71 (62-78)	64 (56-71)
Sex, male, *n* (%)	444 (62.1)	559 (52.5)	172 (56.6)
Right side, *n* (%)	318 (44.5)	302 (28.4)	96 (31.6)

Follow-up group: Patients with cancer detected during follow-up for other comorbidities; symptomatic group: Patients with complaints associated with colorectal cancer-related symptoms; cancer screening group: Patients detected by screening or medical check-up. IQR: Interquartile range; Right side: Tumors from the cecum to the splenic flexure.

Table 2 Characteristics of the patients and colorectal lesions according to diagnostic routes at each hospital

Variable	KU			WMC		
	Follow-up group (*n* = 271)	Symptomatic group (*n* = 480)	Cancer screening group (*n* = 128)	Follow-up group (*n* = 444)	Symptomatic group (*n* = 584)	Cancer screening group (*n* = 176)
Age (median, IQR)	72 (66-79)	69 (59-76)	64 (54-70)	74 (69-79)	72.5 (64.3-80.0)	64.0 (56.3-71.8)
Sex, male, *n* (%)	168 (62.0)	251 (52.3)	71 (55.5)	276 (62.2)	308 (52.7)	101 (57.4)
Right side, *n* (%)	116 (42.8)	125 (26.0)	41 (32.0)	202 (45.5)	177 (30.3)	55 (31.3)

KU: Kyoto University Hospital; WMC: Japanese Red Cross Wakayama Medical Center.

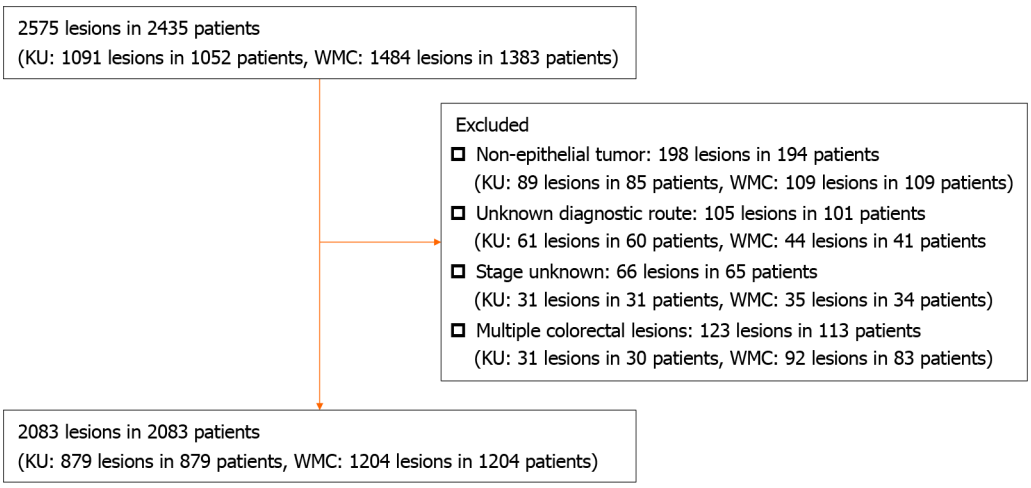

Figure 1 Flow diagram of colorectal lesions and patients from two hospitals. Between January 2016 and December 2019, cancer registries listed 2575 colorectal lesions in 2435 patients. Of these, 198 non-epithelial tumors in 194 patients were excluded. From the remaining 2377 lesions, 105 lesions in 101 patients with unknown diagnostic routes were excluded. Further, 66 lesions in 65 patients with unknown stages were excluded. Of the remaining 2206 lesions, 123 lesions in 113 patients were identified as synchronous colorectal cancers, and after excluding early-stage lesions, 2083 lesions in 2083 patients remained. KU: Kyoto University Hospital; WMC: Japanese Red Cross Wakayama Medical Center.

bution and early-stage diagnosis proportions for each diagnostic route are presented in Table 3. In each hospital, as for the early-stage diagnosed proportion, the follow-up, symptomatic, and cancer screening groups had 55.7%, 21.7%, and 54.7%, respectively, in KU, and 58.3%, 25.7%, and 63.1%, respectively, in WMC, indicating similar trends at both institutions (Table 4). The proportion of patients with CRC diagnosed at an early stage was 57.3% (410 of 715), 23.9% (254 of 1064), and 59.5% (181 of 304) in the follow-up, symptomatic, and cancer screening groups, respectively. The symptomatic group exhibited a lower likelihood of early-stage diagnosis than the follow-up group ($P < 0.001$; aOR: 0.23; 95%CI: 0.19-0.29). The likelihood of being diagnosed at an early stage was similar between the follow-up and cancer screening groups ($P = 0.493$; aOR for early-stage diagnosis in the cancer screening group *vs* the follow-up group = 1.11, 95%CI = 0.82-1.49) (Table 5).

Table 3 Stage distribution of colorectal cancer by diagnostic route in two hospitals, *n* (%)

Tumor stage	Follow-up group (*n* = 715)	Symptomatic group (*n* = 1064)	Cancer screening group (*n* = 304)
Stage 0	216 (30.2)	92 (8.7)	81 (26.6)
Stage I	194 (27.1)	162 (15.2)	100 (32.9)
Stage II	106 (14.8)	240 (22.6)	39 (12.8)
Stage III	109 (15.2)	297 (27.9)	54 (17.8)
Stage IV	90 (12.6)	273 (25.7)	30 (9.9)
Early-stage	410 (57.3)	254 (23.9)	181 (59.5)

Follow-up group: Patients with cancer detected during follow-up for other comorbidities; symptomatic group: Patients with complaints associated with colorectal cancer-related symptoms; cancer screening group: Patients detected by screening or medical check-up. Early stages: 0 and I.

Table 4 Stage distribution according to diagnostic routes at each hospital, *n* (%)

Tumor stage	KU			WMC		
	Follow-up group (*n* = 271)	Symptomatic group (*n* = 480)	Cancer screening group (*n* = 128)	Follow-up group (*n* = 444)	Symptomatic group (*n* = 584)	Cancer screening group (*n* = 176)
Stage 0	62 (22.9)	22 (4.6)	20 (15.6)	154 (34.7)	70 (12.0)	61 (34.7)
Stage I	89 (32.8)	82 (17.1)	50 (39.1)	105 (23.7)	80 (13.7)	50 (28.4)
Stage II	39 (14.4)	113 (23.5)	14 (10.9)	67 (15.1)	127 (21.8)	25 (14.2)
Stage III	43 (15.9)	120 (25.0)	23 (18.0)	66 (14.9)	177 (30.3)	31 (17.6)
Stage IV	38 (14.0)	143 (29.8)	21 (16.4)	52 (11.7)	130 (22.3)	9 (5.1)
Early-stage	151 (55.7)	104 (21.7)	70 (54.7)	259 (58.3)	150 (25.7)	111 (63.1)

KU: Kyoto University Hospital; WMC: Japanese Red Cross Wakayama Medical Center.

Table 5 Univariate and multivariate analyses of early-stage detection rate comparing follow-up group *vs* symptomatic group and cancer screening group

Variable	Early-stage detection rate (%)	Univariate		Multivariate	
		cOR (95%CI)	*P* value	aOR (95%CI)	*P* value
Follow-up group	57.3	Reference		Reference	
Symptomatic group	23.9	0.23 (0.19-0.29)	< 0.001	0.23 (0.19-0.29)	< 0.001
Cancer screening group	59.5	1.09 (0.83-1.44)	0.516	1.11 (0.82-1.49)	0.493

Adjusted covariates are age, sex, and tumor location. cOR: Crude odds ratio; CI: Confidence interval; aOR: Adjusted odds ratio.

DISCUSSION

In this study, we conducted a comparative analysis of stages at diagnosis of CRC based on diagnostic routes. This study had two major findings. First, patients with CRC, which was detected during hospital visits for existing comorbidities, exhibited a higher proportion of early-stage diagnoses than those who presented with CRC-related symptoms. Second, the proportion of early-stage CRC diagnoses detected during hospital visits for comorbidities was comparable to that in the cancer screening group.

Patients with CRC detected at a comorbidity visit had a higher rate of early-stage diagnosis than those who presented with CRC-related symptoms. The first potential explanation for this derived from the fact that asymptomatic patients were included among the patients with CRC who were detected during hospital visits for other comorbidities. The frequency of symptomatic early-stage cancer is low, and the proportion of symptomatic cases increases with cancer progression[23]. Follow-up testing for comorbidities would incidentally detect asymptomatic CRC at an earlier stage compared to CRC detected in symptomatic patients. Second, the increased frequency of hospital visits owing to

comorbidities likely results in early-stage cancer diagnosis due to incidental detection (surveillance hypothesis)[24]. Previous studies have shown that certain chronic diseases, such as end-stage kidney disease and high levels of comorbidities, are correlated with the detection of CRCs in earlier stages owing to frequent visits to healthcare providers [25,26]. In our study, patients with comorbidities were more likely to undergo imaging studies and colonoscopies because of abnormal tests and some symptoms, which could lead to an earlier diagnosis. Therefore, CRC detection during hospital visits for comorbidities may have been at an earlier stage than that in symptomatic patients.

We also found that the proportion of early-stage CRCs detected during hospital visits for comorbidities was comparable to that in the cancer screening group. The proportion of early-stage detection was 57.3% in the follow-up group compared with 59.5% in the screening group (P = 0.493). The odds of early detection were similar between groups, with an OR of 1.11 (95%CI: 0.82-1.49) (screening *vs* follow-up), and no significant differences were observed between the two groups. There have been no reports comparing the proportion of early-stage CRC diagnoses detected during hospital visits for comorbidities with those detected through regular screening. Our findings can be attributed to the unique medical context seen in Japan, characterized by unrestricted access to medical facilities facilitated by the universal insurance system[27]. The swift examinations during hospital visits potentially increase the chances of rapid diagnosis and early detection. Extended diagnosis periods are reportedly correlated with later detection stages[28]. Notably, Japan's healthcare infrastructure facilitates easy access to advanced diagnostic technologies, such as colonoscopies and computed tomography, potentially contributing to early detection. Therefore, patients regularly monitored for comorbidities may have an increased early-stage diagnosis rate, which is comparable to that of patients who undergo cancer screening, even if they present with CRC-related symptoms.

Therefore, CRC screening should be recommended, particularly for patients without periodical hospital visits for comorbidities. Our study suggests that, in clinical practice, CRC is detected relatively early when it is found in patients presenting for follow-up for existing comorbidities. To date, no report has demonstrated that CRC detection during the follow-up of comorbidities is at an earlier stage than that after presenting with symptoms and that it occurs as early as that during cancer screening. Previous studies suggest that patients who visit hospitals for comorbidities can be recommended for cancer screening during consultation with their family physician[29,30]. Conversely, individuals without underlying conditions or those who do not undergo CRC screening may harbor undiagnosed CRC owing to a lack of hospital visits. CRC screening should be recommended for all screening-eligible individuals. Tailored message interventions for screening recommendations targeting segmented individuals reportedly increase screening attendance rates[9]. However, the resources required for screening outreach are limited, and colonoscopies for diagnostic testing require financial and human resources[10-13]. CRC detected at late stages contributes to higher medical costs[31]. Therefore, recommending screening would be essential, particularly for populations at a high risk of diagnosis with late-stage cancer, to take advantage of limited resources. Hence, it would be beneficial to develop policies that specifically encourage cancer screening for those who do not regularly visit the hospital due to comorbidities, considering the barriers to acceptance of screening and the causes of lack of access to healthcare facilities in this population. Encouraging populations other than those who regularly visit the hospital for any comorbidities to undergo screening could increase the earlier-stage detection, which would further contribute to an improved prognosis for patients with CRC.

Our study has some limitations in interpreting the results. First, the type and number of comorbidities and frequency of hospital visits in patients with CRC detected during follow-up for other comorbidities in this study have not been considered. Second, whether individuals presenting with CRC-related symptoms include those who undergo regular cancer screening is unclear. However, in Japan, approximately half of the eligible candidates do not undergo screening, and it is presumed that most individuals exist within the symptomatic group who do not undergo regular cancer screening[6]. Third, our study was conducted at two designated cancer care hospitals in Japan and may not apply to other regions or countries. Healthcare systems and classification of CRC routes for diagnosis may differ in other countries; however, there were no significant differences in the proportions and stage distributions of each population between our study population and the Japanese cohort[18]. While our study only had access to cancer registration data from two facilities, using cancer registration data from other facilities or nationwide cancer registration data in Japan would aid in investigating whether the trends observed in this study are universally applicable.

CONCLUSION

This study suggests that CRC detection during hospital visits for comorbidities is likely at earlier stages than those detected *via* the symptomatic route. Furthermore, CRCs detected during hospital visits for comorbidities may be detected as early as those detected through cancer screening. While CRC screening should be recommended for all eligible individuals, particular attention could be directed towards populations without periodical hospital visits for comorbidities as they may not derive early CRC detection benefits due to fewer opportunities for hospital visits.

ARTICLE HIGHLIGHTS

Research background

Colorectal cancer (CRC) screening reduces CRC mortality, yet several patients remain unscreened.

Research motivation
Although identifying specific subgroups at high risk is crucial to encourage more individuals to participate in screening, the association between the diagnostic routes and identification of these subgroups has been less appreciated.

Research objectives
To determine the stage at diagnosis of CRC based on various diagnostic routes.

Research methods
A retrospective observational study was conducted using data from the cancer registry of two hospitals to clarify the stage at diagnosis in three groups: Follow-up (patients detected during follow-up for other comorbidities), symptomatic (patients detected following presentation with CRC-related symptoms), and cancer screening.

Research results
In a study of 2083 patients, early-stage CRCs were diagnosed in 57.3% of the follow-up group, 23.9% of the symptomatic group, and 59.5% of the cancer screening group. The symptomatic group had a lower likelihood of early-stage diagnosis compared to the follow-up group, while the follow-up and cancer screening groups showed similar likelihoods of early-stage diagnosis.

Research conclusions
CRCs detected during hospital visits for comorbidities were diagnosed earlier, similar to cancer screening.

Research perspectives
Encouraging CRC screening in individuals who do not make regular hospital visits for comorbidities could enhance early detection and improve patient prognoses.

ACKNOWLEDGEMENTS

We would like to thank Ms. Hiroko Kimura and Ms. Naoko Nishioka at the Japanese Red Cross Wakayama Medical Center for registering the cancer registry.

FOOTNOTES

Author contributions: Agatsuma N, Utsumi T, Nishikawa Y, and Horimatsu T contributed to conception and design; Agatsuma N, Utsumi T, Nishikawa Y, Horimatsu T, Seta T, Yamashita Y, Tanaka Y, Inoue T, Nakanishi Y, Shimizu T, Ohno M, Fukushima A, Nakayama T, and Seno H contributed to data analysis and interpretation; Agatsuma N, Utsumi T, and Nishikawa Y contributed to manuscript drafting; Horimatsu T, Seta T, Yamashita Y, Tanaka Y, Inoue T, Nakanishi Y, Shimizu T, Ohno M, Fukushima A, Nakayama T, and Seno H contributed to critical article revision for important intellectual content; and all authors have read and agreed to the final version of the manuscript.

Supported by the Foundation for Cancer Research supported by Kyoto Preventive Medical Center and the Japan Society for the Promotion of Science (JSPS) Grants-in-Aid KAKENHI, No. JP 22K21080.

Institutional review board statement: The study protocol was approved by the Institutional Review Boards of Kyoto University Hospital (approval No. R3472), and the Japanese Red Cross Wakayama Medical Center (approval No. 1004).

Informed consent statement: Anonymized data were used in this study. The board approved an opt-out approach for the research use of the data. Information about the study's purpose and data usage was posted on the hospital's website rather than obtaining patient informed consent, ensuring patients' right to withdraw.

Conflict-of-interest statement: Yoshitaka Nishikawa reports a donation from Datack outside the submitted work. Takeo Nakayama reports the following potential conflicts of interest outside the submitted work: Grants from I&H Co., Ltd, Cocokarafine Group Co., Ltd, Konica Minolta, Inc., and NTT DATA.; consulting fees from Ohtsuka Pharmaceutical Co., Takeda Pharmaceutical Co., Johnson & Johnson K.K., and Nippon Zoki Pharmaceutical Co., Ltd.; honoraria from Pfizer Japan Inc., MSD K.K., Chugai Pharmaceutical Co., Takeda Pharmaceutical Co., Janssen Pharmaceutical K.K., Boehringer Ingelheim International GmbH, Eli Lilly Japan K.K., Maruho Co., Ltd, Mitsubishi Tanabe Pharma Co., Novartis Pharma K.K., Allergan Japan K.K., Novo Nordisk Pharma Ltd, Toa Eiyo Ltd, Dentsu Co., Ono Pharmaceutical Co., Ltd, GSK, Alexion Pharmaceuticals, Inc., Canon Medical Systems Co., Kowa Company Ltd, Araya, and AbbVie Inc.; stock option from BonBon Inc.; and donation from CancerScan and YUYAMA Co., Ltd. All the other authors declare no competing interests.

Data sharing statement: No additional data are available.

Country/Territory of origin: Japan

ORCID number: Nobukazu Agatsuma 0000-0002-4605-5985; Yoshitaka Nishikawa 0000-0003-3313-1990; Takahiro Horimatsu 0000-0002-4188-9059; Takeshi Seta 0000-0002-3057-6284; Takahiro Inoue 0000-0001-5470-9718; Yuki Nakanishi 0000-0001-5493-6312; Takahiro Shimizu 0000-0001-8392-2526; Takeo Nakayama 0000-0002-7918-6252; Hiroshi Seno 0000-0002-8509-8128.

S-Editor: Chen YL
L-Editor: A
P-Editor: Yuan YY

REFERENCES

1 **Siegel RL**, Miller KD, Wagle NS, Jemal A. Cancer statistics, 2023. *CA Cancer J Clin* 2023; **73**: 17-48 [PMID: 36633525 DOI: 10.3322/caac.21763]
2 **Siegel RL**, Wagle NS, Cercek A, Smith RA, Jemal A. Colorectal cancer statistics, 2023. *CA Cancer J Clin* 2023; **73**: 233-254 [PMID: 36856579 DOI: 10.3322/caac.21772]
3 **Kubisch CH**, Crispin A, Mansmann U, Göke B, Kolligs FT. Screening for Colorectal Cancer Is Associated With Lower Disease Stage: A Population-Based Study. *Clin Gastroenterol Hepatol* 2016; **14**: 1612-1618.e3 [PMID: 27085763 DOI: 10.1016/j.cgh.2016.04.008]
4 **Friedrich K**, Grüter L, Gotthardt D, Eisenbach C, Stremmel W, Scholl SG, Rex DK, Sieg A. Survival in patients with colorectal cancer diagnosed by screening colonoscopy. *Gastrointest Endosc* 2015; **82**: 133-137 [PMID: 25986151 DOI: 10.1016/j.gie.2014.12.048]
5 **Araghi M**, Arnold M, Rutherford MJ, Guren MG, Cabasag CJ, Bardot A, Ferlay J, Tervonen H, Shack L, Woods RR, Saint-Jacques N, De P, McClure C, Engholm G, Gavin AT, Morgan E, Walsh PM, Jackson C, Porter G, Møller B, Bucher O, Eden M, O'Connell DL, Bray F, Soerjomataram I. Colon and rectal cancer survival in seven high-income countries 2010-2014: variation by age and stage at diagnosis (the ICBP SURVMARK-2 project). *Gut* 2021; **70**: 114-126 [PMID: 32482683 DOI: 10.1136/gutjnl-2020-320625]
6 Ministry of Health, Labour and Welfare. Comprehensive Survey of Living Conditions, 2022. [cited 1 September 2023]. Available from: https://www.mhlw.go.jp/toukei/saikin/hw/k-tyosa/k-tyosa22/index.html
7 **Sabatino SA**, Thompson TD, White MC, Shapiro JA, Clarke TC, Croswell JM, Richardson LC. Cancer Screening Test Use-U.S., 2019. *Am J Prev Med* 2022; **63**: 431-439 [PMID: 35469700 DOI: 10.1016/j.amepre.2022.02.018]
8 **Weller D**, Menon U, Zalounina Falborg A, Jensen H, Barisic A, Knudsen AK, Bergin RJ, Brewster DH, Cairnduff V, Gavin AT, Grunfeld E, Harland E, Lambe M, Law RJ, Lin Y, Malmberg M, Turner D, Neal RD, White V, Harrison S, Reguilon I; ICBP Module 4 Working Group, Vedsted P. Diagnostic routes and time intervals for patients with colorectal cancer in 10 international jurisdictions; findings from a cross-sectional study from the International Cancer Benchmarking Partnership (ICBP). *BMJ Open* 2018; **8**: e023870 [PMID: 30482749 DOI: 10.1136/bmjopen-2018-023870]
9 **Hirai K**, Ishikawa Y, Fukuyoshi J, Yonekura A, Harada K, Shibuya D, Yamamoto S, Mizota Y, Hamashima C, Saito H. Tailored message interventions versus typical messages for increasing participation in colorectal cancer screening among a non-adherent population: A randomized controlled trial. *BMC Public Health* 2016; **16**: 431 [PMID: 27220976 DOI: 10.1186/s12889-016-3069-y]
10 **Kapinos KA**, Halm EA, Murphy CC, Santini NO, Loewen AC, Skinner CS, Singal AG. Cost Effectiveness of Mailed Outreach Programs for Colorectal Cancer Screening: Analysis of a Pragmatic, Randomized Trial. *Clin Gastroenterol Hepatol* 2022; **20**: 2383-2392.e4 [PMID: 35144024 DOI: 10.1016/j.cgh.2022.01.054]
11 **Hamashima C**, Sano H. Association between age factors and strategies for promoting participation in gastric and colorectal cancer screenings. *BMC Cancer* 2018; **18**: 345 [PMID: 29587681 DOI: 10.1186/s12885-018-4244-6]
12 **Sekiguchi M**, Igarashi A, Matsuda T, Matsumoto M, Sakamoto T, Nakajima T, Kakugawa Y, Yamamoto S, Saito H, Saito Y. Optimal use of colonoscopy and fecal immunochemical test for population-based colorectal cancer screening: a cost-effectiveness analysis using Japanese data. *Jpn J Clin Oncol* 2016; **46**: 116-125 [PMID: 26685321 DOI: 10.1093/jjco/hyv186]
13 **Steinwachs D**, Allen JD, Barlow WE, Duncan RP, Egede LE, Friedman LS, Keating NL, Kim P, Lave JR, Laveist TA, Ness RB, Optican RJ, Virnig BA. National Institutes of Health state-of-the-science conference statement: Enhancing use and quality of colorectal cancer screening. *Ann Intern Med* 2010; **152**: 663-667 [PMID: 20388702 DOI: 10.7326/0003-4819-152-10-201005180-00237]
14 **Lairson DR**, DiCarlo M, Myers RE, Wolf T, Cocroft J, Sifri R, Rosenthal M, Vernon SW, Wender R. Cost-effectiveness of targeted and tailored interventions on colorectal cancer screening use. *Cancer* 2008; **112**: 779-788 [PMID: 18098272 DOI: 10.1002/cncr.23232]
15 **Elliss-Brookes L**, McPhail S, Ives A, Greenslade M, Shelton J, Hiom S, Richards M. Routes to diagnosis for cancer - determining the patient journey using multiple routine data sets. *Br J Cancer* 2012; **107**: 1220-1226 [PMID: 22996611 DOI: 10.1038/bjc.2012.408]
16 **Downing A**, Aravani A, Macleod U, Oliver S, Finan PJ, Thomas JD, Quirke P, Wilkinson JR, Morris EJ. Early mortality from colorectal cancer in England: a retrospective observational study of the factors associated with death in the first year after diagnosis. *Br J Cancer* 2013; **108**: 681-685 [PMID: 23287990 DOI: 10.1038/bjc.2012.585]
17 Center for Cancer Control and Information Services, National Cancer Center, Japan. Coding definitions of the hospital-based cancer registry in designated cancer care hospitals. 2023. [cited 1 September 2023]. Available from: https://ganjoho.jp/med_pro/cancer_control/can_reg/hospital/regulation.html
18 Cancer Information Service, National Cancer Center, Japan. Annual report of hospital-based cancer registries. [cited 27 January 2023]. Available from: https://jhcr-cs.ganjoho.jp/hbcrtables/
19 **Kajiwara Saito M**, Morishima T, Ma C, Koyama S, Miyashiro I. Diagnosis and treatment of digestive cancers during COVID-19 in Japan: A Cancer Registry-based Study on the Impact of COVID-19 on Cancer Care in Osaka (CanReCO). *PLoS One* 2022; **17**: e0274918 [PMID: 36126088 DOI: 10.1371/journal.pone.0274918]

20 Center for Cancer Control, National Cancer Center, Japan. Updated Version of Evidence-based Guidelines for Colorectal Cancer Screening. January 9, 2023. [cited 1 September 2023]. Available from: https://canscreen.ncc.go.jp/koukaiforum/2023/G_CRC_2023.pdf

21 **van de Veerdonk W**, Hoeck S, Peeters M, Van Hal G, Francart J, De Brabander I. Occurrence and characteristics of faecal immunochemical screen-detected cancers vs non-screen-detected cancers: Results from a Flemish colorectal cancer screening programme. *United European Gastroenterol J* 2020; **8**: 185-194 [PMID: 32213071 DOI: 10.1177/2050640619882157]

22 **Gornick ME**, Eggers PW, Riley GF. Associations of race, education, and patterns of preventive service use with stage of cancer at time of diagnosis. *Health Serv Res* 2004; **39**: 1403-1427 [PMID: 15333115 DOI: 10.1111/j.1475-6773.2004.00296.x]

23 **Nakabayashi N**, Hirose M, Suzuki R, Suzumiya J, Igawa M. How asymptomatic are early cancer patients of five organs based on registry data in Japan. *Int J Clin Oncol* 2018; **23**: 999-1006 [PMID: 29785620 DOI: 10.1007/s10147-018-1287-2]

24 **Fleming ST**, Pursley HG, Newman B, Pavlov D, Chen K. Comorbidity as a predictor of stage of illness for patients with breast cancer. *Med Care* 2005; **43**: 132-140 [PMID: 15655426 DOI: 10.1097/00005650-200502000-00006]

25 **Zafar SY**, Abernethy AP, Abbott DH, Grambow SC, Marcello JE, Herndon JE 2nd, Rowe KL, Kolimaga JT, Zullig LL, Patwardhan MB, Provenzale DT. Comorbidity, age, race and stage at diagnosis in colorectal cancer: a retrospective, parallel analysis of two health systems. *BMC Cancer* 2008; **8**: 345 [PMID: 19032772 DOI: 10.1186/1471-2407-8-345]

26 **Taneja S**, Mandayam S, Kayani ZZ, Kuo YF, Shahinian VB. Comparison of stage at diagnosis of cancer in patients who are on dialysis versus the general population. *Clin J Am Soc Nephrol* 2007; **2**: 1008-1013 [PMID: 17702737 DOI: 10.2215/CJN.00310107]

27 **Sugiyama K**, Oshio T, Kuwahara S, Kimura H. Association between having a primary care physician and health behavioral intention in Japan: results from a nationwide survey. *BMC Prim Care* 2023; **24**: 280 [PMID: 38114896 DOI: 10.1186/s12875-023-02238-8]

28 **Tørring ML**, Murchie P, Hamilton W, Vedsted P, Esteva M, Lautrup M, Winget M, Rubin G. Evidence of advanced stage colorectal cancer with longer diagnostic intervals: a pooled analysis of seven primary care cohorts comprising 11 720 patients in five countries. *Br J Cancer* 2017; **117**: 888-897 [PMID: 28787432 DOI: 10.1038/bjc.2017.236]

29 **Wang H**, Roy S, Kim J, Farazi PA, Siahpush M, Su D. Barriers of colorectal cancer screening in rural USA: a systematic review. *Rural Remote Health* 2019; **19**: 5181 [PMID: 31394041 DOI: 10.22605/RRH5181]

30 **Swan J**, Breen N, Coates RJ, Rimer BK, Lee NC. Progress in cancer screening practices in the United States: results from the 2000 National Health Interview Survey. *Cancer* 2003; **97**: 1528-1540 [PMID: 12627518 DOI: 10.1002/cncr.11208]

31 **Utsumi T**, Horimatsu T, Nishikawa Y, Hoshino N, Takahashi Y, Goto R, Kashihara S, Fukuyoshi J, Nakayama T, Seno H. Medical costs according to the stages of colorectal cancer: an analysis of health insurance claims in Hachioji, Japan. *J Gastroenterol* 2021; **56**: 903-913 [PMID: 34215929 DOI: 10.1007/s00535-021-01798-9]

World Journal of Gastroenterology

Submit a Manuscript: https://www.f6publishing.com

World J Gastroenterol 2024 March 14; 30(10): 1377-1392

DOI: 10.3748/wjg.v30.i10.1377

ISSN 1007-9327 (print) ISSN 2219-2840 (online)

ORIGINAL ARTICLE

Observational Study

Differential diagnosis of Crohn's disease and intestinal tuberculosis based on ATR-FTIR spectroscopy combined with machine learning

Yuan-Peng Li, Tian-Yu Lu, Fu-Rong Huang, Wei-Min Zhang, Zhen-Qiang Chen, Pei-Wen Guang, Liang-Yu Deng, Xin-Hao Yang

Specialty type: Gastroenterology and hepatology

Provenance and peer review: Unsolicited article; Externally peer reviewed.

Peer-review model: Single blind

Peer-review report's scientific quality classification

Grade A (Excellent): 0
Grade B (Very good): B
Grade C (Good): C
Grade D (Fair): 0
Grade E (Poor): 0

P-Reviewer: Iizuka M, Japan

Received: October 31, 2023
Peer-review started: October 31, 2023
First decision: December 5, 2023
Revised: January 2, 2024
Accepted: February 6, 2024
Article in press: February 6, 2024
Published online: March 14, 2024

Yuan-Peng Li, College of Physical Science and Technology, Guangxi Normal University, Guilin, Guangxi 541004, China

Tian-Yu Lu, Department of Gastroenterology, The Affiliated Hospital of South University of Science and Technology, Shenzhen 518000, Guangdong Province, China

Fu-Rong Huang, Zhen-Qiang Chen, Pei-Wen Guang, Liang-Yu Deng, Xin-Hao Yang, Department of Optoelectronic Engineering, Jinan University, Guangzhou 510632, Guangdong Province, China

Wei-Min Zhang, Department of Gastroenterology, Integrated Hospital of Traditional Chinese Medicine, Southern Medical University, Guangzhou 510632, Guangdong Province, China

Corresponding author: Wei-Min Zhang, PhD, Chief Physician, Director, Department of Gastroenterology, Integrated Hospital of Traditional Chinese Medicine, Southern Medical University, No. 13 Shiliugang Road, Haizhu District, Guangzhou 510632, Guangdong Province, China. weigert@163.com

Abstract

BACKGROUND

Crohn's disease (CD) is often misdiagnosed as intestinal tuberculosis (ITB). However, the treatment and prognosis of these two diseases are dramatically different. Therefore, it is important to develop a method to identify CD and ITB with high accuracy, specificity, and speed.

AIM

To develop a method to identify CD and ITB with high accuracy, specificity, and speed.

METHODS

A total of 72 paraffin wax-embedded tissue sections were pathologically and clinically diagnosed as CD or ITB. Paraffin wax-embedded tissue sections were attached to a metal coating and measured using attenuated total reflectance fourier transform infrared spectroscopy at mid-infrared wavelengths combined with XGBoost for differential diagnosis.

RESULTS

The results showed that the paraffin wax-embedded specimens of CD and ITB

were significantly different in their spectral signals at 1074 cm^{-1} and 1234 cm^{-1} bands, and the differential diagnosis model based on spectral characteristics combined with machine learning showed accuracy, specificity, and sensitivity of 91.84%, 92.59%, and 90.90%, respectively, for the differential diagnosis of CD and ITB.

CONCLUSION

Information on the mid-infrared region can reveal the different histological components of CD and ITB at the molecular level, and spectral analysis combined with machine learning to establish a diagnostic model is expected to become a new method for the differential diagnosis of CD and ITB.

Key Words: Infrared spectroscopy; Machine learning; Intestinal tuberculosis; Crohn's disease; Differential diagnosis; Inflammatory bowel disease

Core Tip: Crohn's disease (CD) is often misdiagnosed as intestinal tuberculosis (ITB). However, the treatment and prognosis of these two diseases are dramatically different. Therefore, it is important to develop a method to identify CD and ITB with high accuracy, specificity, and speed. For the first time the paraffin wax-embedded tissue sections were attached to a metal coating and measured using attenuated total reflectance fourier transform infrared spectroscopy at mid-infrared wavelengths combined with XGBoost for differential diagnosis of CD and ITB. Information on the mid-infrared region can reveal the different histological components of CD and ITB at the molecular level, and spectral analysis combined with machine learning to establish a diagnostic model is expected to become a new method for the differential diagnosis of CD and ITB.

Citation: Li YP, Lu TY, Huang FR, Zhang WM, Chen ZQ, Guang PW, Deng LY, Yang XH. Differential diagnosis of Crohn's disease and intestinal tuberculosis based on ATR-FTIR spectroscopy combined with machine learning. *World J Gastroenterol* 2024; 30(10): 1377-1392

URL: https://www.wjgnet.com/1007-9327/full/v30/i10/1377.htm

DOI: https://dx.doi.org/10.3748/wjg.v30.i10.1377

INTRODUCTION

Crohn's disease (CD) is an inflammatory bowel disease involving interactions between various pathogenic factors of unknown etiology[1,2]. CD has a high prevalence in North America and Europe but has shown an apparent increasing prevalence across the globe in recent years, especially in the Asia-Pacific region (China, India, *etc*.)[3,4]. Intestinal tuberculosis (ITB) is a primary or secondary chronic intestinal infection caused by *Mycobacterium tuberculosis* (*M. tuberculosis*)[5]. Due to economic development, lifestyle, and other reasons, ITB is mostly prevalent in Asia, but its prevalence in developed countries and regions has increased in recent years[6]. CD and ITB are two completely different diseases with similar symptoms, signs, and examination results, but completely different treatment methods, and misdiagnosis and mistreatment may cause serious consequences and even patient death[7]. Therefore, it is important to differentiate between CD and ITB prior to treatment.

Currently, CD and ITB can be diagnosed by many methods, such as observation of clinical manifestations[8], endoscopy[9-13], histopathological examination[14], imaging examination[15,16], and *M. tuberculosis* detection[17-19], but these methods have limitations. Patients with CD and ITB have similar clinical manifestations. On histopathological biopsy examination, the specific manifestation of ITB was caseous necrotizing granuloma, and the specific manifestation of CD was non-caseous granuloma, but the detection rate of each manifestation was not high. Given the many similarities between ITB and CD, high misdiagnosis rates, and likely severe consequences of misdiagnosis and mistreatment, there is an urgent need to develop a new, rapid, and accurate differential diagnostic method.

Infrared spectroscopy is a fast and non-destructive detection technology that works mainly through illumination of the surface of a material with infrared light to induce changes in the molecular vibrations of the material, which are then used to conduct qualitative and quantitative analyses of the material. Regular fourier transform infrared (FTIR) spectrometers equipped with accessories for attenuated total reflectance (ATR) have the advantages of simple specimen preparation, no need for chemical reagents, non-destructiveness, and no special requirements for specimen size and water content. The main component of biological tissues is water, and in addition to water, tissues mainly contain organic compounds, such as proteins, lipids, and sugars, which have strong infrared activity. For example, the characteristic absorption of proteins in the mid-infrared region is mainly attributed to the stretching vibration of the amide carbonyl C = O in the band-1685-1630 cm^{-1}, also known as the amide I band, and the scissoring vibration of NH_2 in R-$CONH_2$ molecules in the band-1640-1600 cm^{-1}, also known as the amide II band[20]. These materials undergo significant changes in structure, conformation, and quantity during the pathological processes of tissues and cells, which may cause a certain degree of difference between diseased and normal tissues in the infrared absorption spectra. Different pathological processes result in different tissue components. Infrared spectroscopy is particularly sensitive to specimen changes, thereby providing a possibility for differential diagnosis of the disease.

Given that infrared spectroscopy may contain abundant characteristic biochemical information, and in view of the complexity of CD and ITB pathology, this study is the first to propose a new differential diagnosis method for CD and ITB based on ATR-FTIR spectroscopy combined with machine learning. Paraffin wax-embedded tissue sections with a confirmed diagnosis of CD or ITB were subjected to ATR-FTIR measurements, and the spectral feature changes in the two types of sections in different spectral regions were analyzed. Next, the spectral features were combined with eXtreme Gradient Boosting of the gradient boosted decision trees (XGBoost) to establish a machine-learning model as a new, fast, and accurate detection method for the differential diagnosis of CD and ITB.

MATERIALS AND METHODS

Experimental instruments

A Bruker Vertex 70 FTIR spectrometer equipped with an ATR specimen measurement accessory was used. The ATR specimen cell was composed of a mixed crystal of diamond and ZnSe. The specimen was illuminated with infrared light at an incident angle of 45° such that total internal reflection occurred three times. Spectra were acquired in the range of 4000-600 cm^{-1} using a deuterated triglycine sulfate detector with a KBr beam splitter. The number of scans was 16, the resolution was 4 cm^{-1}, the experimental temperature was 25 ˚C ± 1 ˚C, and the relative humidity was 46%. During spectral acquisition, paraffin wax-embedded tissue sections of the intestinal mucosa were attached to the ATR accessory to obtain the FTIR absorption spectra. Each specimen was measured in three regions and each measurement was repeated 16 times and averaged.

Experimental specimen preparation

Specimen information: A total of 72 paraffin wax-embedded tissue sections that were pathologically and clinically diagnosed with CD or ITB with typical microscopic pathological features were collected from four hospitals: The Department of Gastroenterology of the 74th Army Group Hospital (formerly the 421 Hospital), Nanfang Hospital of Southern Medical University, Guangzhou Chest Hospital, and General Hospital of Southern Military Command, consisting of 28 CD tissue sections (16 males and 12 females) and 44 ITB tissue sections (36 males and 8 females). All specimens were from the same ethnic group with the same socioeconomic background, and were collected in accordance with the relevant laws and regulations.

Specimen preparation process: (1) Metal-coated slide preparation: Ordinary quartz glass slides were coated with a metal-silver film, as shown in Figure 1. We filed an application for a patent for the invention of our method for coating a metal-coated slide; (2) Conventional paraffin wax embedding: The study objects were paraffin wax-embedded tissue sections; after collection from patients. All fresh tissue specimens were fixed in formalin solution, washed, dehydrated, and embedded according to routine methods; (3) Mounting: Paraffin wax-embedded tissues were sectioned and picked with forceps after being subjected to routine warming treatment, and the selected tissue sections were accurately mounted onto a metal-silver film; and (4) Dewaxing: Dewaxing was carried out using xylene and gradient ethanol in a typical procedure as follows: the specimen was treated with the solvent in the order of xylene (first time, 15 min), xylene (second time, 15 min), 100% ethanol (first time, 3 min), 100% ethanol (second time, 3 min), 95% ethanol (3 min), 83% ethanol (3 min), 70% ethanol (3 min), 50% ethanol (3 min), 30% ethanol (3 min), and distilled water (3 min); after dewaxing, the sections were allowed to stand for more than 30 h and then subjected to spectral measurement.

Optimization of dewaxing durations: To explore the effect of the dewaxing duration on the spectral measurement results, tissue sections attached to the metal slides were dewaxed for different durations and then subjected to spectral measurements: (1) Pre-test: Two paraffin wax-embedded specimens (one CD and the other ITB) were taken and each was sliced into eight sections for dewaxing. Every six hours from the start of the dewaxing, two sections from the same original specimen were removed from the dewaxing process and subjected to spectral measurements in the time order of 0 (not dewaxed), 6 h (waxed; the same hereinafter), 12 h, 18 h, 24 h, 30 h, 36 h, and 42 h for a total of eight time points; and (2) Confirmation test: Two paraffin wax-embedded specimens (one CD and the other ITB) were obtained, and each was sliced into five sections for dewaxing. Two sections were sequentially removed from the dewaxing procedure at 25 h, 26 h, 27 h, 28 h, and 29 h after the start of dewaxing and were subjected to spectral measurements, resulting in five time points.

Principle of the XGBoost method

XGBoost is short for Extreme Gradient Boosting, which works by constructing a set of classification and regression tree (CART) models and summing up the results of multiple CARTs as the final predictive output. The greatest advantage of this method is that during training, classifiers with good classification performance can compensate for those with poor classification performance. The theoretical basis is that the model classification output based on a combination of multiple-base classifiers is better than that based on a single-base classifier[21].

This principle is illustrated in Figure 2. In each iteration of gradient boosting, residuals are used to correct the previous predictor by optimizing a specific loss function. The loss function was significantly improved by including a regularization term to balance the gradient of the objective function and complexity of the model to avoid overfitting[22]. This principle is mathematically expressed by equation (Eq.) 1.

$$J(\Theta) = L(\Theta) + \Omega(\Theta) \quad (1)$$

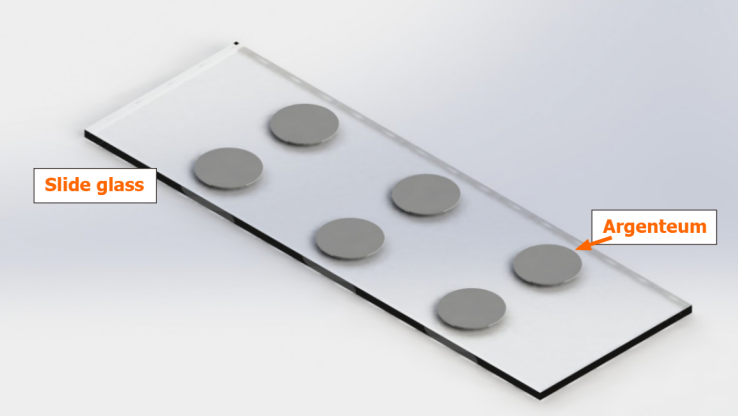

Figure 1 Argentum film on glass slides.

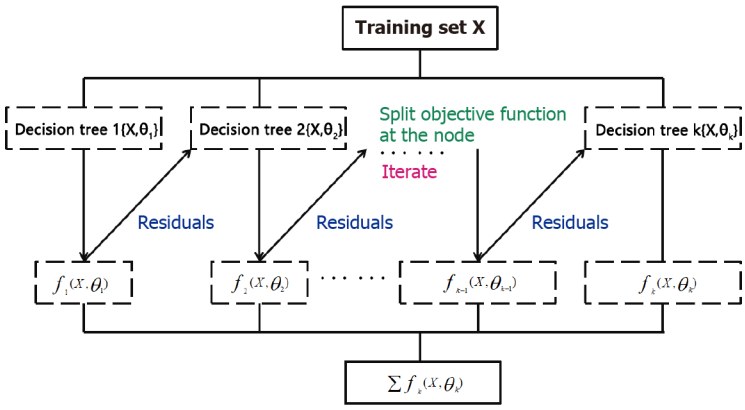

Figure 2 Schematic of XGBoost.

The training parameters for a given data set are denoted as, and "L" is the loss function of the training set, such as square loss or logic loss, which measures the fitness of the model to the training data. is a regularization term, such as an L1-regularization or L2-regularization term, which mainly measures the complexity of the model. The simpler the model, the better its ability to prevent over-fitting. Because the base classifiers are decision trees, the output of the model is obtained by averaging every tree's classification or regression result over the ensemble F of k decision trees.

The objective function after t iterations can be expressed as Eq. 2.

$$J^{(t)} = \sum_{i=1}^{n} L(y_i, \vec{y}_i) + \sum_{k=1}^{t} \Omega(f_k) \quad (2)$$

In Eq. (2), n is the number of predictions, and $\rightarrow$(t)/y_i is expressed by Eq. 3.

$$\vec{y}_i^{(t)} = \sum_{k=1}^{t} f_k(x_i) = \vec{y}_i^{(t-1)} + f_t(x_i) \quad (3)$$

The regularization term Ω (f_k) of the decision tree is defined as Eq. 4.

$$\Omega(f_k) = \gamma T + \frac{1}{2}\lambda \sum_{j=1}^{T} w_j^2 \quad (4)$$

In Eq. 4, γ is the complexity of each leaf, T is the number of child leaf nodes in the decision tree, and λ is the penalty parameter. In the XGBoost method, the loss function is approximated using a second-order Taylor expansion rather than the first-order Taylor expansion, which is adopted for general gradient boosting. Assuming that the loss function is the mean square error (MSE) function, the objective function can be expressed as below.

$$J^{(t)} \approx \sum_{i=1}^{n} [g_i w_{q(x_i)} + \frac{1}{2}(h_i w^2_{q(x_i)})] + \frac{1}{2}\lambda \sum_{j=1}^{T} w_j^2 \quad (5)$$

In Eq. 5, the constant term can be dropped for simplicity, and q (xi) is a function that assigns data points to a corresponding child leaf node, with g_i and h_i representing the first and second derivatives of the MSE loss function, respectively. In Eq. 5, the loss function was determined by the sum of the loss values of each data sample. As each data sample corresponds to only one leaf node, the loss function can also be represented by the sum of the loss values of each leaf node. Accordingly, Eq. 5 can be rewritten as Eq. 6.

$$J^{(t)} \approx \sum_{j=1}^{T}[(\sum_{i\in I_j} g_i)w_j + \frac{1}{2}(\sum_{i\in I_j} h_i + \lambda)w_j^2)] + \gamma T \quad (6)$$

According to Eqs. 3-13, G_i and H_i can be defined as in Eq. 7.

$$G_j = \sum_{i\in I_j} g_i \qquad H_j = \sum_{i\in I_j} h_i \quad (7)$$

Where I_j represents all data samples in leaf node j. Therefore, the optimization of the objective function can be transformed into minimizing the quadratic function.

Regarding the main model parameters, the parameter space of XGBoost is mainly comprised of three types of parameters: general, booster, and learning objective. The general and learning objective parameters are intended to guide the overall functioning and control the metrics for the results of each step, whereas the booster parameters control each boosting step and are the main tuning parameters. The booster parameters include n_estimators, learning_rate, min_child_weight, gamma, subsample, and alpha. The parameter n_estimators is the number of base classifiers. If the number is set to a value that is too small or too large, underfitting or overfitting will occur. Learning_rate represents the weight reduction coefficient of each base classifier, and an incorrect setting of this parameter leads to failure in model fitting. Min_child_weight represents the minimum sum of instance weights required in a child leaf node and is used to improve the generalization of the model. Gamma controls the decrease in the value of the model loss function when a node splits. The subsample mainly controlled the probability of random sampling for each tree, which was typically set in the range of 0.5-1.0. The regularization parameter alpha represents the L1-regularization term of the weight and is used to reduce the complexity of the model.

The machine learning model was mainly run in Python 3.6.1, and scientific computing libraries, such as numpy 1.12.1, and pandas 0.19.2, were used for training and importing. Scikit-learn 0.18.1, and Xgboost 0.6 were used to support the XGBoost-based integrated learning model.

Evaluation parameters

The accuracy, specificity, and sensitivity are important evaluation indicators for XGBoost-based diagnosis models. The greater the accuracy of these indicators, the better the diagnostic performance of the model. The formulas for each parameter are shown in Eqs. 8-10.

$$Accuracy = \frac{n_{correct}}{n_{total}} \quad (8)$$

$$TPR = \frac{TP}{TP + FN} \qquad FPR = \frac{FP}{FP + TN} \quad (9)$$

$$AUC = \frac{\sum_{i\in positiveClass} rank_i - \frac{M(1+M)}{2}}{M \times N} \quad (10)$$

In Eq. 8, "TPR" is the sensitivity, "FPR" is the specificity, "TP" is the number of positive samples in the dataset correctly classified by the model, "FN" is the number of positive samples in the dataset incorrectly classified by the model, "FP" is the number of negative samples in the dataset incorrectly classified by the model, and "TN" is the number of negative samples in the dataset correctly classified by the model. In Eq. 10, "M" and "N" represent the number of positive and negative samples, respectively.

RESULTS

Typical pathological features

Pathological diagnosis was conducted in accordance with the "Chinese Consensus on the Diagnosis and Treatment of Inflammatory Bowel Disease"[23]. The CD biopsy specimens included in this study all had characteristic manifestations, such as focal chronic inflammation, structural abnormalities of the focal crypt, and non-caseous granulomas. In the absence of granulomas, at least three of the following characteristic pathological manifestations must be observed: (1) Segmental or focal lesions; (2) confluent longitudinal linear ulcers; (3) pebble-like appearance and fistula formation; (4) mesenteric fat-enwrapped lesions; and (5) intestinal wall thickening and stenosis. If there were non-caseous granulomas, another characteristic manifestation of CD was observed under an optical microscope, and all specimens with ITB symptoms were excluded. Typical CD specimens are shown in Figure 3A. The characteristic manifestations of CD under an optical microscope include: (1) Transmural inflammation; (2) aggregated distribution of inflammation and transmural lymphoid hyperplasia; (3) submucosal thickening (due to fibrosis and fibromuscular tissue damage, inflammation, and edema); (4) fissures (fissure-like ulcers); (5) non-caseous granulomas (including lymph nodes); (6) abnormalities of the intestinal nervous system (submucosal nerve fiber hyperplasia, ganglion inflammation, and proliferation of intermuscular nerve fibers); and (7) normal maintenance of mucus secretion in the epithelium (the goblet cells are usually normal). ITB specimens underwent typical pathological changes, such as the appearance of caseous granulomas or related cell structures, as shown in Figure 3B. Specimens without the aforementioned significant pathological features were excluded from the study, as shown in Figure 3C and D.

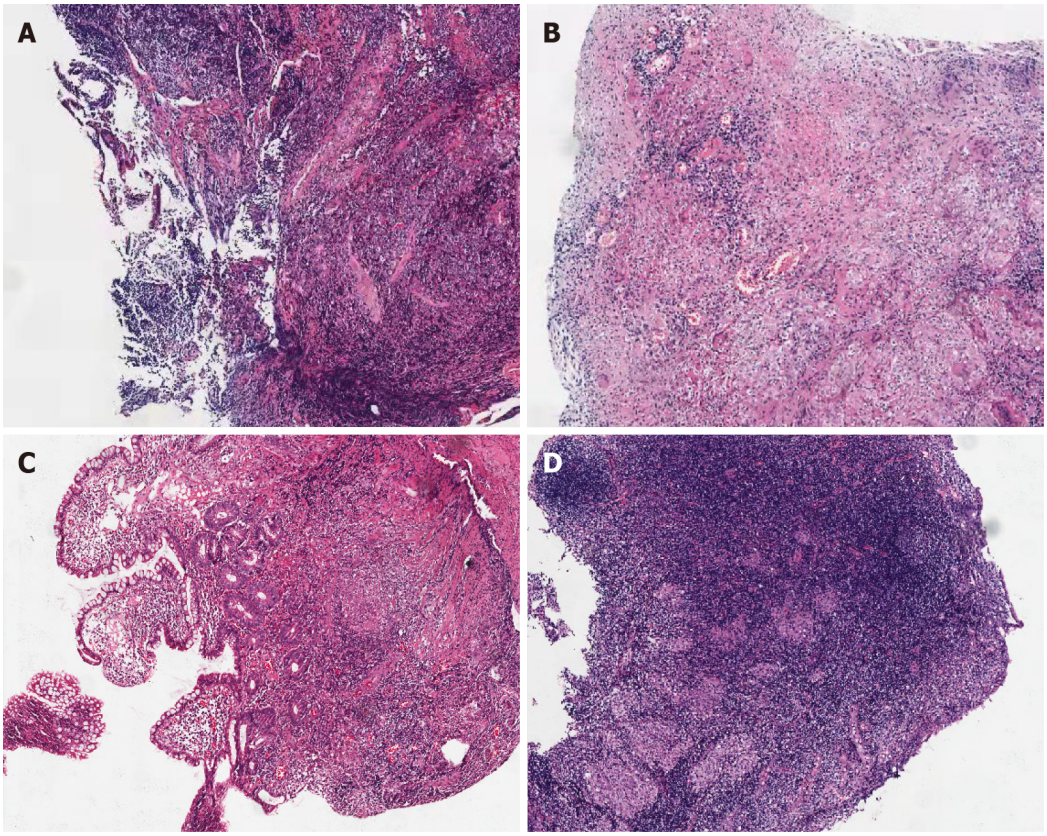

Figure 3 Pathological images of Crohn's disease and intestinal tuberculosis. A: Typical pathological images of Crohn's disease (CD); B: Pathological images of typical intestinal tuberculosis (ITB); C: Atypical pathological images of CD; D: pathological images of atypical ITB.

Spectral analysis

Effects of the background glass and paraffin wax: The effects of the background quartz glass and paraffin wax were investigated. As shown in Figure 4A, the characteristic absorption bands of quartz glass are centered at 785 cm^{-1}, 990 cm^{-1}, and 1145 cm^{-1}, whereas the characteristic absorption bands of paraffin wax are centered at 2956 cm^{-1}, 2916 cm^{-1}, 2848 cm^{-1}, 1461 cm^{-1}, and 719 cm^{-1}, as shown in Figure 4B. The characteristic absorption of proteins, lipids, and carbohydrates in the mid-infrared region occurs mainly in the 1800 cm^{-1}-600 cm^{-1} and 3000 cm^{-1}-2500cm^{-1} bands. Therefore, these bands interfere with the characteristic signals of the tissues.

To remove the interference of the background quartz glass and paraffin wax, a metal-silver film with a diameter of 5 mm was coated on quartz glass to shield the interfering absorption of the quartz glass. Figure 5 presents the shielding performance of the metal-silver in undewaxed sections 1, 2, and 3. The characteristic absorption of quartz glass at 785 cm^{-1}, 990 cm^{-1}, and 1145 cm^{-1} was substantially shielded. In addition, paraffin wax-embedded tissue sections were dewaxed to reduce the interfering absorption of paraffin wax, as depicted in Figure 5. After being subjected to the dewaxing for 6 h, 12 h, and 18 h, the characteristic absorption of paraffin wax at 1461 cm^{-1} and 719 cm^{-1} was essentially eliminated, whereas its characteristic absorption at 2956 cm^{-1}, 2916 cm^{-1}, and 2848 cm^{-1} remained to some extent.

Optimization of dewaxing duration: To further reduce the interfering effects of paraffin wax on the absorption of tissue sections, the duration of dewaxing was optimized. First, the paraffin wax-embedded tissue sections were subjected to the dewaxing process for a time series of 6 h, 12 h, 18 h, 24 h, 30 h, 36 h, and 42 h, followed by observation of the absorption at 3000-2500 cm^{-1} as shown in Figure 6A. An abrupt decrease in absorption occurred from 24 h to 30 h of dewaxing, while the absorption after 30 h showed little variation. Second, further optimization was performed for a dewaxing duration of 24-30 h as shown in Figure 6B; after 26 h, the characteristic absorption of paraffin wax leveled off without further reduction. Therefore, the optimal dewaxing time was determined to be 26 h.

Spectral feature analysis: The infrared spectral features of the biological tissues are outlined in Table 1. In addition to water, the intestinal mucosa mainly contains organic compounds such as lipids, proteins, and sugars, all of which have strong infrared activity. For example, the absorption band at 1800-1700 cm^{-1} is mainly attributed to the stretching vibration of lipid C = O; the absorption band at 1685-1630 cm^{-1} is mainly attributed to the stretching vibration of amide carbonyl C = O, also known as the amide I band; the absorption band at 1640-1600 cm^{-1} is mainly attributed to the scissoring vibration of NH_2 in R-$CONH_2$ molecules, also known as the amide II band; the 1500-800 cm^{-1} absorption band is mainly attributed to the stretching vibration of the P-O bond and the P = O double bond in nucleic acids as well as the stretching vibration of sugar C-OH[24]. The FTIR-ATR spectra of CD and ITB tissues are shown in Figure 7. The water absorption band was centered at approximately 3302 cm^{-1}, and the vibration absorption bands of CH_3 and CH_2 were mainly centered at 2956 cm^{-1}, 2916 cm^{-1}, and 2848 cm^{-1}, whereas the characteristic absorption bands of other tissue

Table 1 Signature fingerprint of infrared spectra

Bands position (cm^{-1})	Assignments of group	Assignments of substance
2925	υas, CH_3	Lipid related
2855	υas, CH_2	Lipid related
1740	υC=O	Lipid
1640	Amide I	Protein
1550	Amide II	Protein
1460	δC-H	Lipid related
1400	δC-H, δC-O-H	Lipid related
1305	δC-H, δC-O-H	Undetermined
1240	υas, PO_2^-	Nucleic acid related
1160	υC-O, δC-O-H, δC-O-C	Carbohydrate related
1120	υC-O, δC-O-H, δC-O-C	Carbohydrate related
1080	υas, PO_2^-	Nucleic acid related

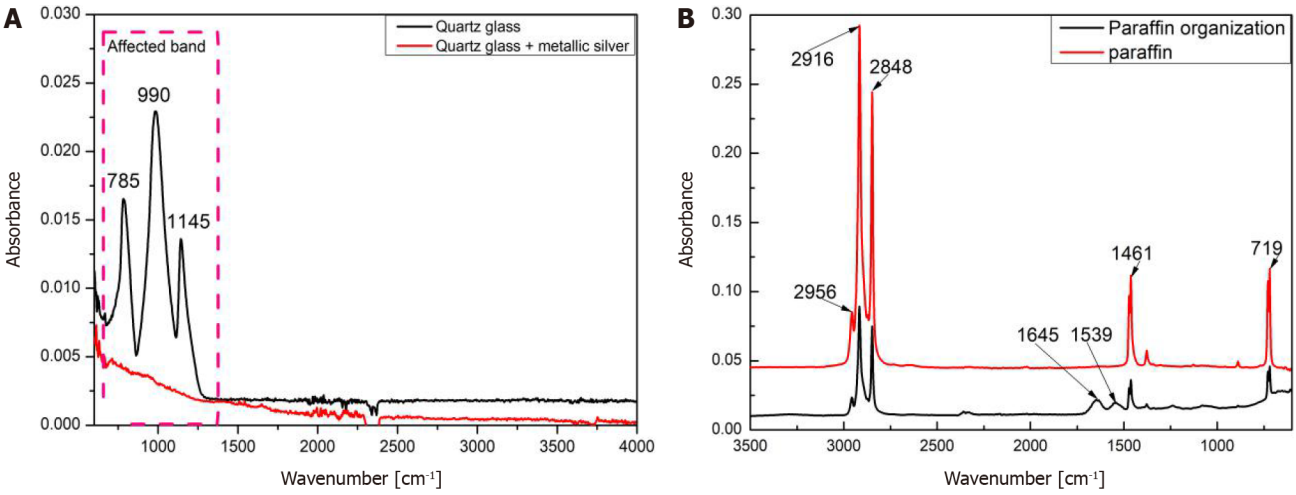

Figure 4 Background absorption spectra of quartz and paraffin. A: Quartz; B: Paraffin.

components mainly appeared at 1645 cm^{-1}, 1539 cm^{-1}, 1456 cm^{-1}, 1394 cm^{-1}, 1234 cm^{-1}, and 1056 cm^{-1} in the mid-infrared fingerprint region (1800-800 cm^{-1}).

Analysis results of the ITB and CD FTIR-ATR spectra are shown in Figure 7. Figure 7B depicts the average spectral intensity of the characteristic absorption bands, with the error bars representing the intrinsic fluctuation of the spectral band intensity. The average spectral intensity of ITB at 3302 cm^{-1}, 2956 cm^{-1}, 2916 cm^{-1}, 2848 cm^{-1}, 1645 cm^{-1}, 1539 cm^{-1}, 1456 cm^{-1}, 1394 cm^{-1}, and 1234 cm^{-1} was slightly higher than that of CD, while CD had slightly higher average spectral intensity at 1056 cm^{-1} than ITB. However, both ITB and CD showed large intrinsic fluctuations in spectral intensity, with a significant overlap of spectral intensity within the error ranges. Therefore, the differential diagnosis of ITB and CD based on the original spectral intensity is subject to large uncertainties and likely leads to misjudgment.

The derivative spectra are shown in Figure 8. Between ITB and CD, the first- and second-derivative spectra differed significantly at 1134 cm^{-1} (carbohydrate C-O bond) and 1074 cm^{-1} (phosphodiester bond P-O), respectively. An intensity comparison of the two characteristic absorption bands is shown in Figure 9, with the error bars representing the intrinsic fluctuations of CD and ITB in the spectral intensity. The average spectral intensity of CD at 1134 cm^{-1} was stronger than that of ITB, with the former fluctuating in a relatively large range and the latter in a relatively small range; however, the two intensities overlapped severely within almost half of the error ranges. The average spectral intensity of CD at 1074 cm^{-1} was stronger than that of ITB, with the former fluctuating in a relatively large range and the latter in a relatively small range; the two intensities overlapped within almost one-third of the error ranges. As shown above, ITB and CD still showed a significant overlap in the intensity distribution of the derivative spectra despite the obvious characteristic absorption bands, which likely led to misdiagnosis. Therefore, it is necessary to employ a machine learning-based classification method to extract the spectral characteristics of the ITB and CD in a more effective manner.

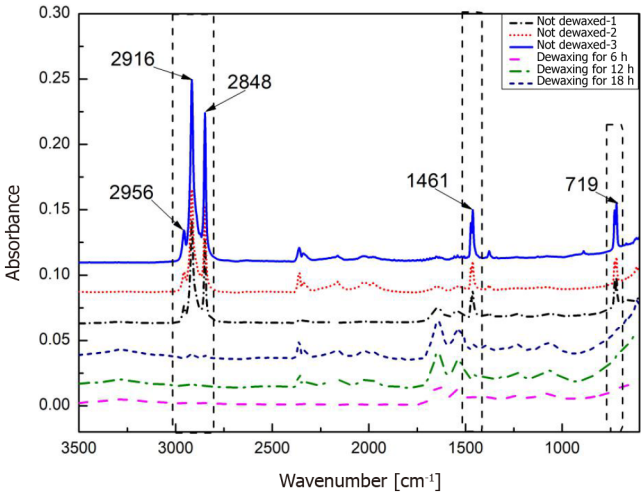

Figure 5 Absorption spectra of dewaxed and unwaxed tissue sections.

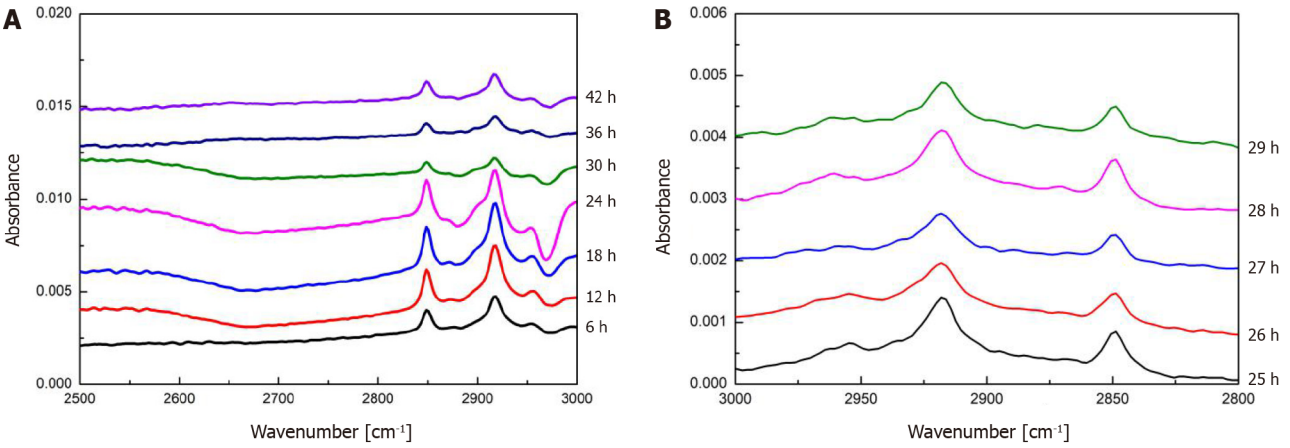

Figure 6 Optimization of dewaxing duration. A: Absorption spectra of tissues during the dewaxing process for 6-42 h; B: Absorption spectra of tissues during the dewaxing process for 24-30 h.

XGBoost model

Sample set partitioning: At present, the methods for selecting data samples mainly include the random sampling (RS) method, the Kenard-Stone (KS) method, the SPXY method (*i.e.*, sample set partitioning based on joint x-y distances), and the duplex method. In the experiment, the RS method was used to partition sample sets. The prediction set samples of an XGBoost model are usually required to be independent; that is, they should not originate from the original calibration set samples. Therefore, for the 72 specimens collected in the study, each was measured in three different regions to generate three average spectra, totaling 194, after excluding spectra with outlying data points. Next, 194 spectra were randomly partitioned at a ratio of 3:1 into a calibration set (n = 145) and an independent prediction set (n = 49), as shown in Table 2.

XGBoost model results: In this study, an XGBoost model was designed in accordance with the characteristics of the ATR-FTIR spectral data and the classification requirements to perform the binary classification of ITB and CD. The entire procedure is shown in Figure 10. The procedure consisted of three steps: Figure 10A and B acquisition of ATR-FTIR spectral datasets; Figure 10C implementation of principal component analysis and independent component analysis to extract the fingerprint spectral features of ITB and CD; and Figure 10C-E the use of a series of XGBoost decision trees as classifiers to classify the extracted fingerprint spectral features to produce the classification information for ITB and CD.

As shown in Table 3, a comparison of different data preprocessing methods revealed that the first-derivative spectra yielded the best results, with 17 ITB specimens and 23 CD specimens correctly identified by the model using original data, 20 ITB specimens and 25 CD specimens correctly identified by the model using first-derivative spectral data, and 16 ITB specimens and 26 CD specimens correctly identified by the model using second-derivative spectral data. As shown above, the preprocessing methods significantly influenced the models, and the number of misdiagnosed cases based on the derivative spectra was smaller than that based on the original spectra. In particular, the first-derivative spectral model exhibited the highest accuracy (91.84%).

In this study, the XGBoost model parameters were optimized using a grid search method. The relevant search ranges were set as follows: Max_depth varied between 1 and 50 with steps of 1; n_estimators varied between 1 and 500 with

Table 2 Sample set divisions of Crohn's disease and intestinal tuberculosis

Sample set	CD	ITB	Total
Training set	79	66	145
Prediction set	22	27	49

CD: Crohn's disease; ITB: Intestinal tuberculosis.

Table 3 Results of the XGBoost model

Group	True value	Predicted value		Accuracy (%)
		ITB	CD	
Original spectral data	ITB	17.0000	5.0000	
	CD	4.0000	23.0000	
	Specificity (%)	0.8519		
	Sensitivity (%)		0.7727	
	Accuracy (%)			0.8163
First derivative spectral data	ITB	20.0000	2.0000	
	CD	2.0000	25.0000	
	Specificity (%)	0.9259		
	Sensitivity (%)		0.9090	
	Accuracy (%)			0.9184
Second derivative spectral data	ITB	16.0000	6.0000	
	CD	1.0000	26.0000	
	Specificity (%)	0.9630		
	Sensitivity (%)		0.7270	
	Accuracy (%)			0.8571

CD: Crohn's disease; ITB: Intestinal tuberculosis.

steps of 10; min_child_weight varied between 1 and 30 with steps of 1; gamma varied between 0 and 15 with steps of 1; subsample varied between 0 and 1.1 with steps of 0.1; alpha varied between 0 and 10 with steps of 0.2; and learning_rate varied between 0 and 0.2 with steps of 0.01. The optimization process of the XGBoost model parameters is illustrated in Figure 10, and the optimal parameters are listed in Table 4.

As shown in Figure 11, the accuracy and area under the curve (AUC) increased gradually with the increase in max_depth, n_estimators, subsample, and learning_rate, eventually approaching a stable value, and decreased with an increase in min_child_weight, gamma, and alpha, eventually approaching a stable value. The AUC was significantly greater than accuracy in all cases. The optimal parameters of the XGBoost model are listed in Table 4: Max_depth = 3, n_estimators = 71, min_child_weight = 4, gamma = 0, subspecimen = 1, alpha = 0.3, and learningrate = 0.1. Finally, all optimal parameters were used to establish an optimal XGBoost model, which led to a sensitivity of 90.90% (20/22), specificity of 92.59% (25/27), and accuracy of 91.84% (45/49) for differential diagnoses, as shown in Table 3.

DISCUSSION

Differential diagnosis of CD and ITB has long been the focus of research worldwide. Daperno *et al*[25] established a diagnostic model for CD and ITB based on endoscopic parameters, with a sensitivity and specificity of 82.9% and 82.0%, respectively. Ramadass *et al*[26] extracted DNA from fecal specimens and conducted a polymerase chain reaction for *M. tuberculosis* (TB-PCR) targeting the IS6110 sequence, achieving a sensitivity of 79% and a specificity of 88% for the differential diagnosis of CD and ITB. Li *et al*[27] of the Department of Gastroenterology, Peking Union Medical College Hospital of the Chinese Academy of Medical Sciences, investigated the usefulness of *in vitro* interferon γ release assay (T-SPOT.TB) in differentiating ITB from CD and determined the sensitivity and specificity of T-SPOT. The prevalence of TB in the diagnosis of CD was 84.2% and 75.4%, respectively. Kedia *et al*[28] used computed tomography of the small

Table 4 Optimal parameters of the XGBoost model based on first-derivative spectral data

Parameters	Step length	Optimal range	AUC (%)		Accuracy (%)	
			Optimal value	Test	Optimal value	Test
Max_depth	1.00	(1, 50.0)	3.0	79.9	4.0.	74.5
N_estimators	10.00	-1500	71.0	80.3	81.0	74.4
Min_child_weight	1.00	(1, 30.0)	4.0	82.1	4.0	76.0
Gamma	1.00	(0, 15.0)	0	82.1	0	76.0
Subsample	0.10	(0, 1.1)	1.0.	82.1	1.0.	76.0
Alpha	0.10	(0, 10.0)	0.3	82.0	2.8	75.9
Learning_rate	0.01	(0, 0.2)	0.1	82.0	0.1	75.2

AUC: Area under the curve.

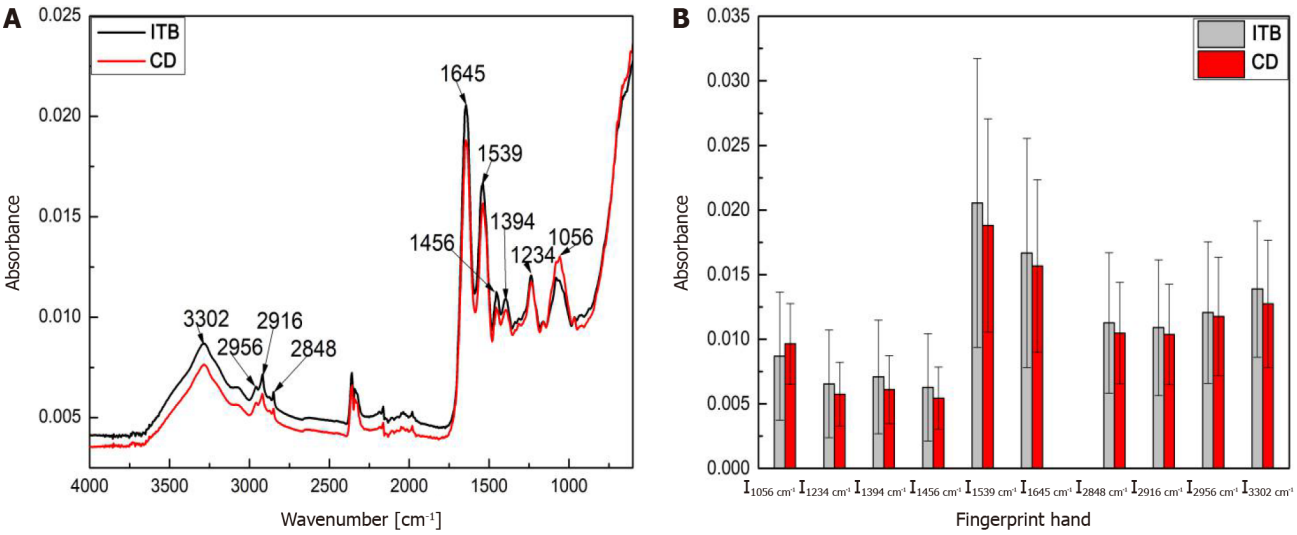

Figure 7 Fourier transform infrared spectrometers equipped with accessories for attenuated total reflectance spectral analysis of intestinal tuberculosis and Crohn's disease. A: Original spectrum; B: Spectral intensity of the characteristic bands. CD: Crohn's disease; ITB: Intestinal tuberculosis.

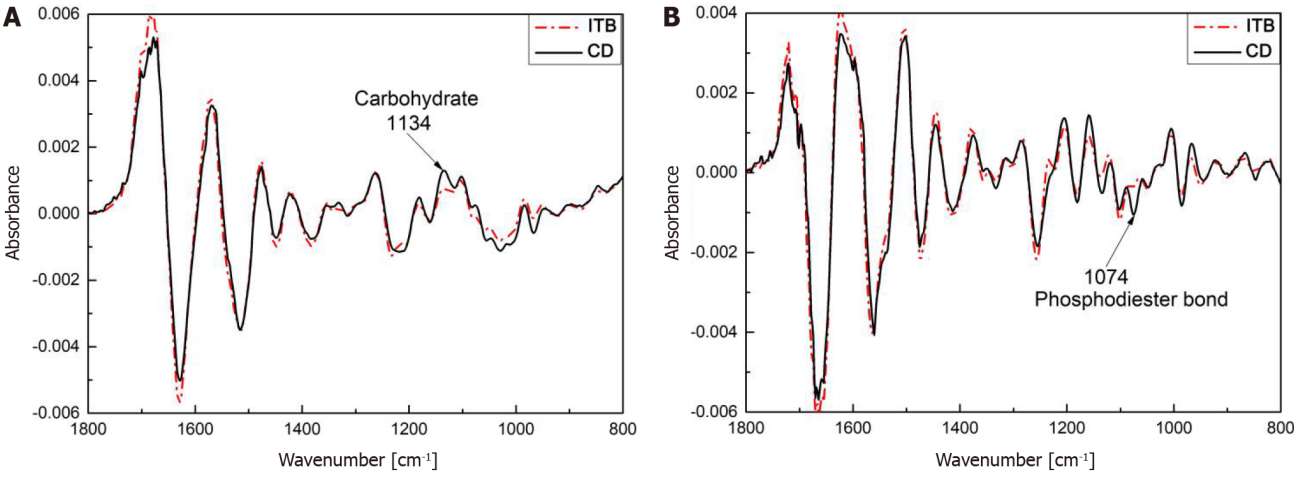

Figure 8 Derivative spectrum. A: First-derivative spectra; B: Second-derivative spectra. CD: Crohn's disease; ITB: Intestinal tuberculosis.

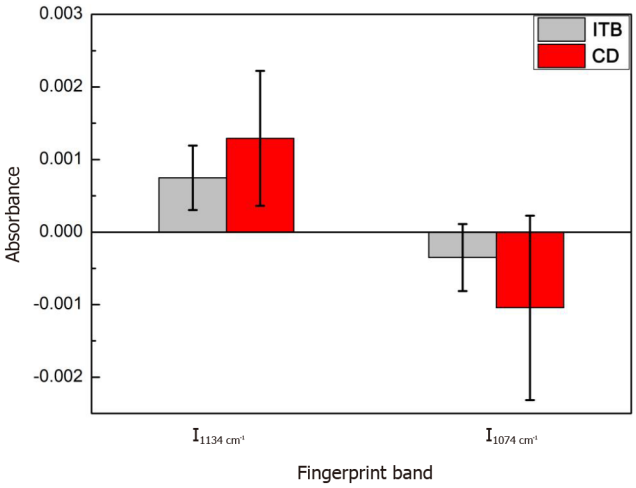

Figure 9 Derivative spectral characteristic intensity analysis. CD: Crohn's disease; ITB: Intestinal tuberculosis.

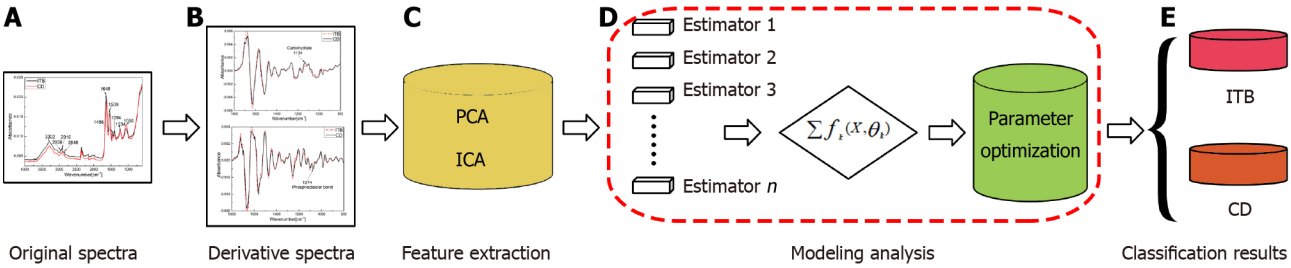

Figure 10 Schematic diagram of XGBoost used to identify intestinal tuberculosis and Crohn's disease. A: Original spectra; B: Derivative spectra; C: Feature extraction; D: Modeling analysis; E: Classification results. CD: Crohn's disease; ITB: Intestinal tuberculosis; PCA: principal component analysis; ICA: Independent component analysis.

intestine to diagnose CD and ITB and achieved a sensitivity of 68% and specificity of 80%. Despite many clinical studies on the differential diagnosis of CD and ITB using clinical features, radiology, endoscopy, histopathology, immunology, *M. tuberculosis* identification, and serum markers, these methods have drawbacks that result in great difficulty in the differential diagnosis of CD and ITB and high misdiagnosis rates.

In order to overcome obstacles to the differential diagnosis of CD and ITB, ATR-FTIR spectroscopy in the mid-infrared region was adopted in this study as a new method for the differential diagnosis of CD and ITB. In recent years, extensive studies have been conducted on the application of ATR-FTIR spectroscopy for the differential diagnosis of diseases[29-34]. However, one drawback of infrared spectroscopy is that groups with infrared activity are subject to a high degree of collinearity, making it difficult to understand disease progression through changes in the groups. As shown in Figures 7B and 9, the pathological differences between tissues and cells were prone to be obscured by the differences between individual specimens and the noise of instrumentation, with a significant overlap in the distribution of the band position and peak intensity of the ATR-FTIR spectroscopy. Therefore, the differential diagnosis of TB and CD based solely on spectral intensities is subject to large errors and is likely to lead to misdiagnosis. Therefore, to reduce the influence of these factors and extract effective discriminative information, this study, for the first time, proposes a differential diagnosis model for CD and ITB based on the combination of spectral information with machine learning.

XGBoost is a type of machine learning algorithm based on multiple classifiers, with the advantages of fast computation speed, good learning performance, and ability to process large-scale complex data[35]. This algorithm has been widely used in biomedicine[36-38]. The results of this study showed that the differential diagnosis model of CD and ITB based on ATR-FTIR spectral information combined with XGBoost achieved an accuracy rate of up to 91.84%, a significant improvement over previous research results. The high diagnostic accuracy of the XGBoost-based method is mainly due to its ability to differentiate subtle differences in the composition and concentration of the intestinal mucosa by differentiating the differences in the position, intensity, and shape of the characteristic absorption bands in ATR-FTIR spectroscopy. Machine learning can be used to determine the best classification function from these spectral feature differences to obtain satisfactory classification results.

In addition, to eliminate the background interference of the glass substrate and paraffin wax, ATR-FTIR spectroscopy was improved in three ways: (1) Quartz glass was used as the substrate. As shown in Figure 4A, compared with ordinary glass, quartz glass is transparent in the infrared region and does not interfere with the spectral signal of paraffin wax-embedded tissues; (2) The paraffin wax-embedded tissue specimens were dewaxed, and the optimal dewaxing duration was determined. According to a recent study, paraffin wax does not affect ATR-FTIR spectroscopy. However, in this study, paraffin wax seriously interfered with the signals of the intestinal tissues. As shown in Figure 4B, the characteristic

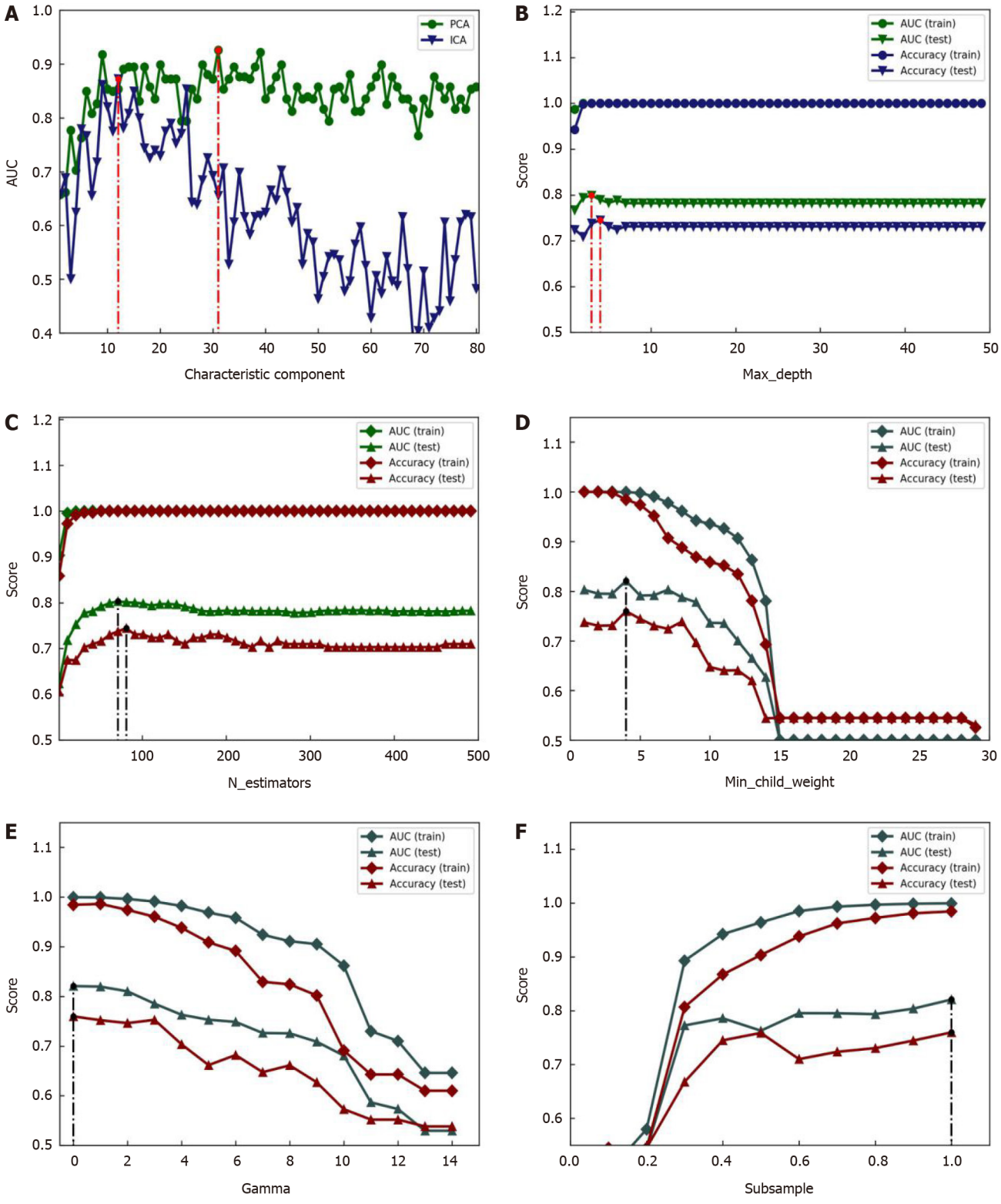
A
AUC
Characteristic component
PCA
ICA
B
Score
Max_depth
AUC (train)
AUC (test)
Accuracy (train)
Accuracy (test)
C
Score
N_estimators
D
Score
Min_child_weight
E
Score
Gamma
F
Score
Subsample

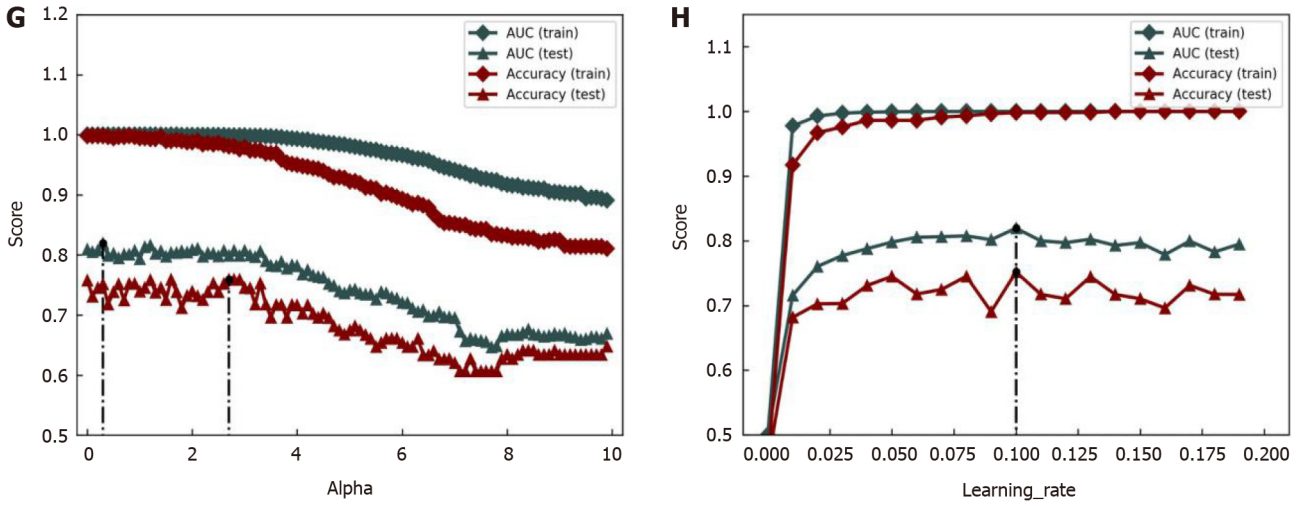

Figure 11 XGBoost model optimization results based on first derivative spectral data. A: Characteristic component; B: Max_depth; C: N_estimators; D: Min_child_weight; E: Gamma; F: Subsample; G: Alpha; H: Learning_rate.

absorption bands of paraffin wax were centered at 2956 cm^{-1}, 2916 cm^{-1}, 2848 cm^{-1}, 1461 cm^{-1}, and 719 cm^{-1}. The characteristic absorption of proteins, lipids, and carbohydrates in the mid-infrared region was mainly at 1800 cm^{-1}-600 cm^{-1} and 3000 cm^{-1}-2500 cm^{-1}. Therefore, the characteristic spectral signals of paraffin wax had a large overlap with the characteristic signals of tissues, causing significant interference in the later spectral analysis. To reduce the spectral signal interference of paraffin wax-embedded tissues, the tissues were subjected to dewaxing treatment, and the dewaxing duration was optimized. These improvements ultimately minimized the influence of paraffin wax (Figures 5 and 6); and (3) The spectra were preprocessed. Converting the original spectra into derivative spectra improved the spectral resolution and reduced noise, thereby increasing the model accuracy from 81.63% to 91.84%.

CONCLUSION

A differential diagnosis model of CD and ITB based on ATR-FTIR spectral information in the mid-infrared region combined with a machine learning algorithm (XGBoost) was established in this study, aimed at exploring the feasibility of applying ATR-FTIR mid-infrared spectra to the differential diagnosis of CD and ITB. The results showed that the derivative spectra of the ATR-FTIR mid-infrared spectra could not only provide spectral features of CD and ITB but also reveal more differential information for the machine learning algorithm to learn, so that the algorithm could use the spectral features of CD and ITB to achieve classification. The XGBoost model based on ATR-FTIR spectral information showed significant improvements in accuracy, specificity, and sensitivity compared to previous models. The results suggest that owing to the advantages of non-destructiveness, high sensitivity, and the ability for real-time diagnosis, ATR-FTIR mid-infrared spectroscopy technology may serve as a new method for the differential diagnosis of CD and ITB.

ARTICLE HIGHLIGHTS

Research background

Crohn's disease (CD) is often misdiagnosed as intestinal tuberculosis (ITB). However, the treatment and prognosis of these two diseases are dramatically different. Therefore, it is important to develop a method to identify CD and ITB with high accuracy, specificity, and speed.

Research motivation

Here we present the application of ATR-FTIR Spectroscopy as an easy-to-use method without chemical reagents and label-free diagnostic tool for the identification of CD and ITB.

Research objectives

To develop a method to identify CD and ITB with high accuracy, specificity, and speed.

Research methods

For the first time the paraffin wax-embedded tissue sections were attached to a metal coating and measured using attenuated total reflectance (ATR) fourier transform infrared (FTIR) spectroscopy at mid-infrared wavelengths combined with XGBoost for differential diagnosis of CD and ITB.

Research results

ATR-FTIR spectroscopy combined with XGBoost methods led to a sensitivity of 90.90% (20/22), specificity of 92.59% (25/27), and accuracy of 91.84% (45/49) for differential diagnoses of CD and ITB.

Research conclusions

ATR-FTIR spectroscopy combined with XGBoost methods can effectively increase the accuracy of differential diagnosis of CD and ITB.

Research perspectives

ATR-FTIR spectroscopy combined with XGBoost methods is expected to become a new method for the differential diagnosis of CD and ITB.

FOOTNOTES

Co-first authors: Yuan-Peng Li and Tian-Yu Lu.

Co-corresponding authors: Fu-Rong Huang and Wei-Min Zhang.

Author contributions: Huang FR and Zhang WM conceived, designed, and refined the study protocol; Chen ZQ, Guang PW, Deng LY, and Yang XH were involved in the data collection; Li YP, Lu TY, and Chen ZQ analyzed the data; Li YP and Lu TY drafted the manuscript; all authors were involved in the critical review of the results and have contributed to, read, and approved the final manuscript. Li YP and Lu TY contributed equally to this work as co-first authors; Huang ER and Zhang WM contributed equally to this work as co-corresponding authors. The reasons for designating Huang ER and Zhang WM as co-corresponding authors are threefold. First, the research was performed as a collaborative effort, and the designation of co-corresponding authorship accurately reflects the distribution of responsibilities and burdens associated with the time and effort required to complete the study and the resultant paper. This also ensures effective communication and management of post-submission matters, ultimately enhancing the paper's quality and reliability. Second, the overall research team encompassed authors with a variety of expertise and skills from different fields, and the designation of co-corresponding authors best reflects this diversity. This also promotes the most comprehensive and in-depth examination of the research topic, ultimately enriching readers' understanding by offering various expert perspectives. Third, Huang FR and Zhang WM contributed efforts of equal substance throughout the research process. The choice of these researchers as co-corresponding authors acknowledges and respects this equal contribution, while recognizing the spirit of teamwork and collaboration of this study. In summary, we believe that designating Huang FR and Zhang WM as co-corresponding authors of is fitting for our manuscript as it accurately reflects our team's collaborative spirit, equal contributions, and diversity.

Supported by the National Natural Science Foundation of China, No. 61975069 and No. 62005056; Natural Science Foundation of Guangxi Province, No. 2021JJB110003; Natural Science Foundation of Guangdong Province, No. 2018A0303131000; Academician Workstation of Guangdong Province, No. 2014B090905001; and Key Project of Scientific and Technological Projects of Guangzhou, No. 201604040007 and No. 201604020168.

Institutional review board statement: The Institutional review board statement has been exempted since we used wax-embedded tissue sections collected over many years from two hospitals.

Informed consent statement: Patients were not required to give informed consent to the study because the patients to whom these wax-embedded tissue sections belonged have been discharged for a long time, or have moved away from the area, and we are unable to contact them.

Conflict-of-interest statement: There are no conflicts of interest to declare.

Data sharing statement: Technical appendix, statistical code, and dataset available from the co-first author at lutianyu1978@163.com.

STROBE statement: The authors have read the STROBE Statement—checklist of items, and the manuscript was prepared and revised according to the STROBE Statement—checklist of items.

Country/Territory of origin: China

ORCID number: Tian-Yu Lu 0009-0001-1215-2664; Wei-Min Zhang 0000-0003-0318-5189.

S-Editor: Chen YL
L-Editor: A
P-Editor: Yuan YY

REFERENCES

1 **Baumgart DC**, Sandborn WJ. Crohn's disease. *Lancet* 2012; **380**: 1590-1605 [PMID: 22914295 DOI: 10.1016/S0140-6736(12)60026-9]

2 **Makharia GK**. Rising incidence and prevalence of Crohn's disease in Asia: is it apparent or real? *J Gastroenterol Hepatol* 2006; **21**: 929-931 [PMID: 16724974 DOI: 10.1111/j.1440-1746.2006.04471.x]

3 **Baumgart DC**, Sandborn WJ. Inflammatory bowel disease: clinical aspects and established and evolving therapies. *Lancet* 2007; **369**: 1641-1657 [PMID: 17499606 DOI: 10.1016/S0140-6736(07)60751-X]

4 **Torres J**, Mehandru S, Colombel JF, Peyrin-Biroulet L. Crohn's disease. *Lancet* 2017; **389**: 1741-1755 [PMID: 27914655 DOI: 10.1016/S0140-6736(16)31711-1]

5 **Donoghue HD**, Holton J. Intestinal tuberculosis. *Curr Opin Infect Dis* 2009; **22**: 490-496 [PMID: 19623062 DOI: 10.1097/QCO.0b013e3283306712]

6 **Almadi MA**, Ghosh S, Aljebreen AM. Differentiating intestinal tuberculosis from Crohn's disease: a diagnostic challenge. *Am J Gastroenterol* 2009; **104**: 1003-1012 [PMID: 19240705 DOI: 10.1038/ajg.2008.162]

7 **Ma JY**, Tong JL, Ran ZH. Intestinal tuberculosis and Crohn's disease: challenging differential diagnosis. *J Dig Dis* 2016; **17**: 155-161 [PMID: 26854750 DOI: 10.1111/1751-2980.12324]

8 **Huang X**, Liao WD, Yu C, Tu Y, Pan XL, Chen YX, Lv NH, Zhu X. Differences in clinical features of Crohn's disease and intestinal tuberculosis. *World J Gastroenterol* 2015; **21**: 3650-3656 [PMID: 25834333 DOI: 10.3748/wjg.v21.i12.3650]

9 **Lee YJ**, Yang SK, Byeon JS, Myung SJ, Chang HS, Hong SS, Kim KJ, Lee GH, Jung HY, Hong WS, Kim JH, Min YI, Chang SJ, Yu CS. Analysis of colonoscopic findings in the differential diagnosis between intestinal tuberculosis and Crohn's disease. *Endoscopy* 2006; **38**: 592-597 [PMID: 16673312 DOI: 10.1055/s-2006-924996]

10 **Makharia GK**, Srivastava S, Das P, Goswami P, Singh U, Tripathi M, Deo V, Aggarwal A, Tiwari RP, Sreenivas V, Gupta SD. Clinical, endoscopic, and histological differentiations between Crohn's disease and intestinal tuberculosis. *Am J Gastroenterol* 2010; **105**: 642-651 [PMID: 20087333 DOI: 10.1038/ajg.2009.585]

11 **Lee JM**, Lee KM. Endoscopic Diagnosis and Differentiation of Inflammatory Bowel Disease. *Clin Endosc* 2016; **49**: 370-375 [PMID: 27484813 DOI: 10.5946/ce.2016.090]

12 **Moka P**, Ahuja V, Makharia GK. Endoscopic features of gastrointestinal tuberculosis and crohn's disease. *J Dig Endosc* 2017; **8**: 1-11 [DOI: 10.4103/jde.jde_48_16]

13 **Pratap Mouli V**, Munot K, Ananthakrishnan A, Kedia S, Addagalla S, Garg SK, Benjamin J, Singla V, Dhingra R, Tiwari V, Bopanna S, Hutfless S, Makharia G, Ahuja V. Endoscopic and clinical responses to anti-tubercular therapy can differentiate intestinal tuberculosis from Crohn's disease. *Aliment Pharmacol Ther* 2017; **45**: 27-36 [PMID: 27813111 DOI: 10.1111/apt.13840]

14 **Magro F**, Langner C, Driessen A, Ensari A, Geboes K, Mantzaris GJ, Villanacci V, Becheanu G, Borralho Nunes P, Cathomas G, Fries W, Jouret-Mourin A, Mescoli C, de Petris G, Rubio CA, Shepherd NA, Vieth M, Eliakim R; European Society of Pathology (ESP); European Crohn's and Colitis Organisation (ECCO). European consensus on the histopathology of inflammatory bowel disease. *J Crohns Colitis* 2013; **7**: 827-851 [PMID: 23870728 DOI: 10.1016/j.crohns.2013.06.001]

15 **Zhao XS**, Wang ZT, Wu ZY, Yin QH, Zhong J, Miao F, Yan FH. Differentiation of Crohn's disease from intestinal tuberculosis by clinical and CT enterographic models. *Inflamm Bowel Dis* 2014; **20**: 916-925 [PMID: 24694791 DOI: 10.1097/MIB.0000000000000025]

16 **Park MJ**, Lim JS. Computed tomography enterography for evaluation of inflammatory bowel disease. *Clin Endosc* 2013; **46**: 327-366 [PMID: 23964329 DOI: 10.5946/ce.2013.46.4.327]

17 **Pulimood AB**, Peter S, Rook GW, Donoghue HD. In situ PCR for Mycobacterium tuberculosis in endoscopic mucosal biopsy specimens of intestinal tuberculosis and Crohn disease. *Am J Clin Pathol* 2008; **129**: 846-851 [PMID: 18479999 DOI: 10.1309/DKKECWQWMG4J23E3]

18 **Zhang T**, Fan R, Wang Z, Hu S, Zhang M, Lin Y, Tang Y, Zhong J. Differential diagnosis between Crohn's disease and intestinal tuberculosis using integrated parameters including clinical manifestations, T-SPOT, endoscopy and CT enterography. *Int J Clin Exp Med* 2015; **8**: 17578-17589 [PMID: 26770348]

19 **Abreu C**, Afonso J, Camila Dias C, Ruas R, Sarmento A, Magro F. Serial Tuberculosis Screening in Inflammatory Bowel Disease Patients Receiving Anti-TNFα Therapy. *J Crohns Colitis* 2017; **11**: 1223-1229 [PMID: 28605520 DOI: 10.1093/ecco-jcc/jjx080]

20 **Rohman A**. The use of infrared spectroscopy in combination with chemometrics for quality control and authentication of edible fats and oils: A review. *Appl Spectrosc Rev* 2017; **52**: 589-604 [DOI: 10.1080/05704928.2016.1266493]

21 **Ding C**, Cao XY, Naess P. Applying gradient boosting decision trees to examine non-linear effects of the built environment on driving distance in Oslo. *Transp Res Part A Policy Pract* 2018; **110**: 107-17 [DOI: 10.1016/j.tra.2018.02.009]

22 **Chen T**. Introduction to boosted trees, University of Washington Computer Science. 2014. [cited 10 January 2024]. Available from: https://web.njit.edu/~usman/courses/cs675_fall16/BoostedTree.pdf

23 **Gionchetti P**, Dignass A, Danese S, Magro Dias FJ, Rogler G, Lakatos PL, Adamina M, Ardizzone S, Buskens CJ, Sebastian S, Laureti S, Sampietro GM, Vucelic B, van der Woude CJ, Barreiro-de Acosta M, Maaser C, Portela F, Vavricka SR, Gomollón F; ECCO. 3rd European Evidence-based Consensus on the Diagnosis and Management of Crohn's Disease 2016: Part 2: Surgical Management and Special Situations. *J Crohns Colitis* 2017; **11**: 135-149 [PMID: 27660342 DOI: 10.1093/ecco-jcc/jjw169]

24 **Hands JR**, Dorling KM, Abel P, Ashton KM, Brodbelt A, Davis C, Dawson T, Jenkinson MD, Lea RW, Walker C, Baker MJ. Attenuated total reflection fourier transform infrared (ATR-FTIR) spectral discrimination of brain tumour severity from serum samples. *J Biophotonics* 2014; **7**: 189-199 [PMID: 24395599 DOI: 10.1002/jbio.201300149]

25 **Daperno M**, D'Haens G, Van Assche G, Baert F, Bulois P, Maunoury V, Sostegni R, Rocca R, Pera A, Gevers A, Mary JY, Colombel JF, Rutgeerts P. Development and validation of a new, simplified endoscopic activity score for Crohn's disease: the SES-CD. *Gastrointest Endosc* 2004; **60**: 505-512 [PMID: 15472670 DOI: 10.1016/s0016-5107(04)01878-4]

26 **Ramadass B**, Chittaranjan S, Subramanian V, Ramakrishna BS. Fecal polymerase chain reaction for Mycobacterium tuberculosis IS6110 to distinguish Crohn's disease from intestinal tuberculosis. *Indian J Gastroenterol* 2010; **29**: 152-156 [PMID: 20577845 DOI: 10.1007/s12664-010-0022-3]

27 **Li Y**, Zhang LF, Liu XQ, Wang L, Wang X, Wang J, Qian JM. The role of in vitro interferonγ-release assay in differentiating intestinal tuberculosis from Crohn's disease in China. *J Crohns Colitis* 2012; **6**: 317-323 [PMID: 22405168 DOI: 10.1016/j.crohns.2011.09.002]

28 **Kedia S**, Sharma R, Nagi B, Mouli VP, Aananthakrishnan A, Dhingra R, Srivastava S, Kurrey L, Ahuja V. Computerized tomography-based predictive model for differentiation of Crohn's disease from intestinal tuberculosis. *Indian J Gastroenterol* 2015; **34**: 135-143 [PMID:

25966870 DOI: 10.1007/s12664-015-0550-y]

29 **Baker MJ**, Hussain SR, Lovergne L, Untereiner V, Hughes C, Lukaszewski RA, Thiéfin G, Sockalingum GD. Developing and understanding biofluid vibrational spectroscopy: a critical review. *Chem Soc Rev* 2016; **45**: 1803-1818 [PMID: 26612430 DOI: 10.1039/c5cs00585j]

30 **Butler HJ**, Smith BR, Fritzsch R, Radhakrishnan P, Palmer DS, Baker MJ. Optimised spectral pre-processing for discrimination of biofluids *via* ATR-FTIR spectroscopy. *Analyst* 2018; **143**: 6121-6134 [PMID: 30484797 DOI: 10.1039/c8an01384e]

31 **Siqueira LFS**, Lima KMG. A decade (2004-2014) of FTIR prostate cancer spectroscopy studies: An overview of recent advancements. *Trac-Trend Anal Chem* 2016; **82**: 208-21 [DOI: 10.1016/j.trac.2016.05.028]

32 **Paraskevaidi M**, Morais CLM, Lima KMG, Snowden JS, Saxon JA, Richardson AMT, Jones M, Mann DMA, Allsop D, Martin-Hirsch PL, Martin FL. Differential diagnosis of Alzheimer's disease using spectrochemical analysis of blood. *Proc Natl Acad Sci U S A* 2017; **114**: E7929-E7938 [PMID: 28874525 DOI: 10.1073/pnas.1701517114]

33 **Paraskevaidi M**, Morais CLM, Lima KMG, Ashton KM, Stringfellow HF, Martin-Hirsch PL, Martin FL. Potential of mid-infrared spectroscopy as a non-invasive diagnostic test in urine for endometrial or ovarian cancer. *Analyst* 2018; **143**: 3156-3163 [PMID: 29878018 DOI: 10.1039/c8an00027a]

34 **De Bruyne S**, Speeckaert R, Boelens J, Hayette MP, Speeckaert M, Delanghe J. Infrared spectroscopy as a novel tool to diagnose onychomycosis. *Br J Dermatol* 2019; **180**: 637-646 [PMID: 30216405 DOI: 10.1111/bjd.17199]

35 **Chen TQ**, Guestrin C. XGBoost: A Scalable Tree Boosting System. *Data Min Knowl Disc* 2016; 785-794 [DOI: 10.1145/2939672.2939785]

36 **Li YY**, Bingham A, Li QJ, Zhuang Y, Umbach DM, Li LP. Using tumor sample gene expression data to infer tumor purity levels with stochastic gradient boosting machines. *Cancer Res* 2018; **78** [DOI: 10.1158/1538-7445.AM2018-2255]

37 **Ogunleye A**, Wang QG. Enhanced XGBoost-Based Automatic Diagnosis System for Chronic Kidney Disease. *ICCA* 2018; 805-810 [DOI: 10.1109/ICCA.2018.8444167]

38 **Torlay L**, Perrone-Bertolotti M, Thomas E, Baciu M. Machine learning-XGBoost analysis of language networks to classify patients with epilepsy. *Brain Inform* 2017; **4**: 159-169 [PMID: 28434153 DOI: 10.1007/s40708-017-0065-7]

World Journal of Gastroenterology

Submit a Manuscript: https://www.f6publishing.com

World J Gastroenterol 2024 March 14; 30(10): 1393-1404

DOI: 10.3748/wjg.v30.i10.1393

ISSN 1007-9327 (print) ISSN 2219-2840 (online)

ORIGINAL ARTICLE

Prospective Study

Establishment and validation of an adherence prediction system for lifestyle interventions in non-alcoholic fatty liver disease

Ming-Hui Zeng, Qi-Yu Shi, Liang Xu, Yu-Qiang Mi

Specialty type: Gastroenterology and hepatology

Provenance and peer review: Unsolicited article; Externally peer reviewed.

Peer-review model: Single blind

Peer-review report's scientific quality classification

Grade A (Excellent): 0
Grade B (Very good): B
Grade C (Good): 0
Grade D (Fair): 0
Grade E (Poor): 0

P-Reviewer: Abbas Z, Pakistan

Received: December 24, 2023
Peer-review started: December 24, 2023
First decision: January 4, 2024
Revised: January 16, 2024
Accepted: February 18, 2024
Article in press: February 18, 2024
Published online: March 14, 2024

Ming-Hui Zeng, Liang Xu, Yu-Qiang Mi, Clinical School of the Second People's Hospital, Tianjin Medical University, Tianjin 300192, China

Qi-Yu Shi, Department of Gastroenterology, Cangzhou People's Hospital, Cangzhou 061000, Hebei Province, China

Liang Xu, Yu-Qiang Mi, Department of Hepatology, Tianjin Second People's Hospital, Tianjin 300192, China

Liang Xu, Yu-Qiang Mi, Tianjin Research Institute of Liver Diseases, Tianjin 300192, China

Corresponding author: Yu-Qiang Mi, MD, Chief Doctor, Professor, Department of Hepatology, Tianjin Second People's Hospital, Clinical School of the Second People's Hospital, Tianjin Medical University, No. 7 Sudi South Road, Nankai District, Tianjin 300192, China.
yuqiangmi68@163.com

Abstract

BACKGROUND

Non-alcoholic fatty liver disease (NAFLD) is the most common liver disease worldwide, affecting about 1/4th of the global population and causing a huge global economic burden. To date, no drugs have been approved for the treatment of NAFLD, making the correction of unhealthy lifestyles the principle method of treatment. Identifying patients with poor adherence to lifestyle correction and attempting to improve their adherence are therefore very important.

AIM

To develop and validate a scale that can rapidly assess the adherence of patients with NAFLD to lifestyle interventions.

METHODS

The Exercise and Diet Adherence Scale (EDAS) was designed based on compilation using the Delphi method, and its reliability was subsequently evaluated. Demographic and laboratory indicators were measured, and patients completed the EDAS questionnaire at baseline and after 6 months. The efficacy of the EDAS was evaluated in the initial cohort. Subsequently, the efficacy of the EDAS was internally verified in a validation cohort.

RESULTS

The EDAS consisted of 33 items in six dimensions, with a total of 165 points. Total EDAS score correlated significantly with daily number of exercise and daily reduction in calorie intake ($P < 0.05$ each), but not with overall weight loss. A total score of 116 was excellent in predicting adherence to daily reduction in calorie intake (> 500 kacl/d), (sensitivity/specificity was 100.0%/75.8%), while patients score below 97 could nearly rule out the possibility of daily exercise (sensitivity/specificity was 89.5%/44.4%). Total EDAS scores ≥ 116, 97-115, and < 97 points were indicative of good, average, and poor adherence, respectively, to diet and exercise recommendations.

CONCLUSION

The EDAS can reliably assess the adherence of patients with NAFLD to lifestyle interventions and have clinical application in this population.

Key Words: Fatty liver; Lifestyle intervention; Behavioral change; Patient adherence; Compliance

Core Tip: This study developed and validated an Exercise and Diet Adherence Scale (EDAS) to rapidly assess adherence to lifestyle interventions in patients with non-alcoholic fatty liver disease (NAFLD). Patients can be grouped based on their EDAS scores and receive personalized treatments accordingly. The EDAS demonstrated reliability and effectiveness in predicting adherence to lifestyle changes and served as a vital tool in the clinical management of patients with NAFLD.

Citation: Zeng MH, Shi QY, Xu L, Mi YQ. Establishment and validation of an adherence prediction system for lifestyle interventions in non-alcoholic fatty liver disease. *World J Gastroenterol* 2024; 30(10): 1393-1404
URL: https://www.wjgnet.com/1007-9327/full/v30/i10/1393.htm
DOI: https://dx.doi.org/10.3748/wjg.v30.i10.1393

INTRODUCTION

The prevalence of non-alcoholic fatty liver disease (NAFLD) has been increasing over the past few decades, with this disease estimated to affect more than 30% of adults worldwide[1]. NAFLD is a progressive disease that can give rise to complications, such as hepatocellular carcinoma (HCC) and cardiovascular disease, which place a burden on the health care system and economy[2]. Additionally, the United Network for Organ Sharing has reported that NAFLD is currently the second leading indication for all liver transplants and will become the primary indication for liver transplantation in patients with HCC[3,4].

To date, no drugs have been approved for the treatment of NAFLD, with correction of unhealthy lifestyles remains a fundamental means of curing it. Therapeutic lifestyle changes can have a direct or significant effect on patients with NAFLD and contribute to a high rate of "placebo response"[5-8]. Because exercises and diets vary greatly, however, it has been difficult to quantify and evaluate patient adherence with these changes. Lifestyle interventions rely on patients' "conscious" adherence to recommendations, with patient "self-reporting" required to evaluate adherence. Thus, patients must be intrinsically motivated to change their lifestyles. Some patients, however, are unable or unwilling to adhere to recommendations about diet and exercise. Approximately 3%-4% of healthy people are diagnosed with NAFLD each year, with lifestyle changes resulting in improvements in only 60% of these patients[9]. Additionally, the high rates of cardiovascular diseases, osteoarthritis and rheumatism in patients with NAFLD make exercise interventions difficult, with other conditions, including depression and anxiety, limiting the persistence of dietary interventions[10]. The adherence to lifestyle interventions for NAFLD remains largely unexplored. A questionnaire assessing adherence with lifestyle interventions is therefore urgently needed. This questionnaire can be used in the clinical and scientific assessment of patients with NAFLD, especially in assessing their responses to lifestyle changes (Figure 1).

MATERIALS AND METHODS

Objects

Data from NAFLD patients aged 18-70 years who were admitted to the Second People's Hospital of Tianjin from August 2013 to January 2014 were used to design the Exercise and Diet Adherence Scale (EDAS). The practice guidelines of the American Gastroenterological Association, the American Association for the Study of Liver Diseases, and the American College of Gastroenterology have defined NAFLD as an imaging or pathological diagnosis of hepatic steatosis in the absence of other known secondary causes of hepatic steatosis[11]. Patients with NAFLD combined with viral hepatitis, autoimmune liver disease and other types of hepatitis, those suspected of having cirrhosis or liver cancer; and men and women who consumed > 140 g and > 70 g, respectively, of alcohol per week were excluded. Also excluded were patients with serum creatinine concentrations > 1.5 times the upper limit of normal, and those with other serious systemic or

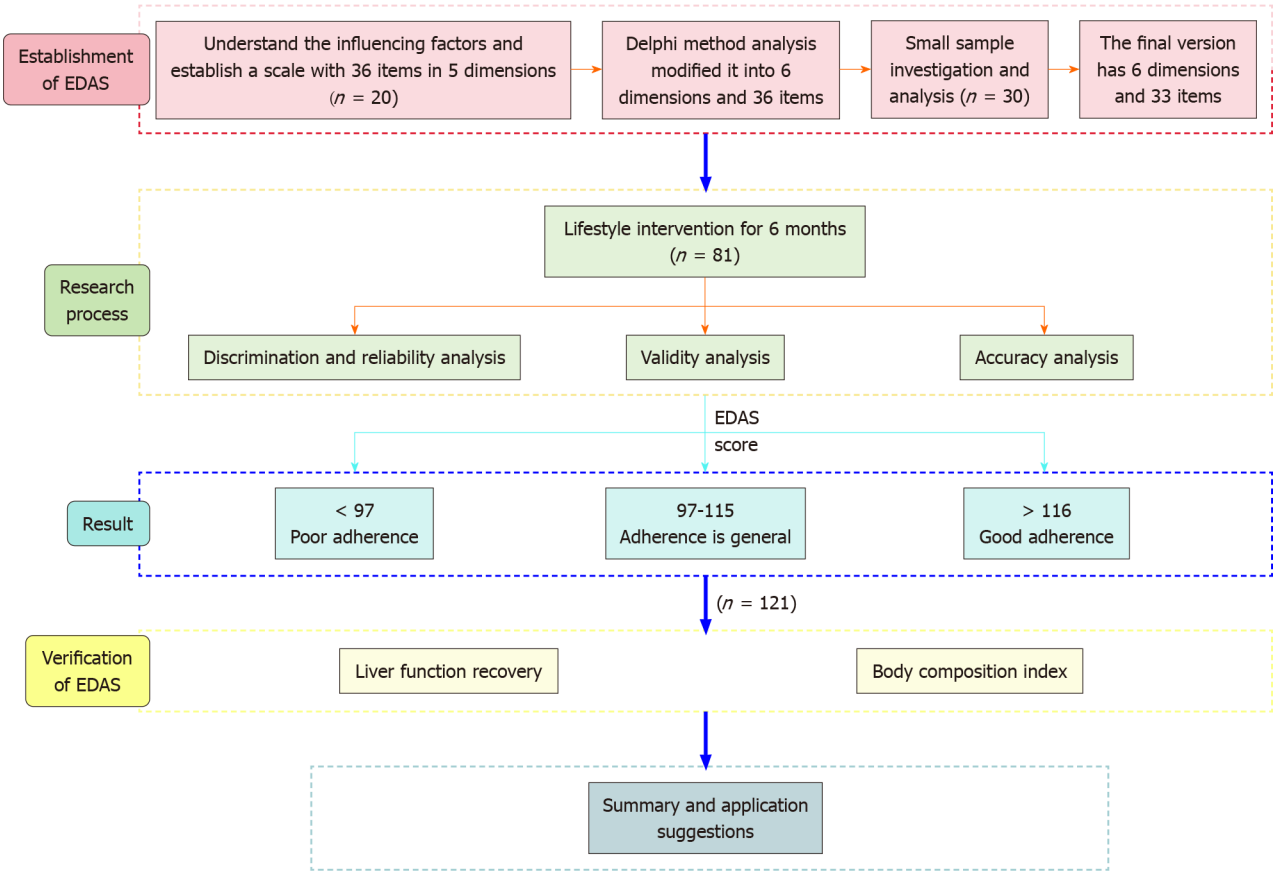

Figure 1 Study flow chart, showing the method used to develop and verify the Exercise and Diet Adherence Scale. EDAS: Exercise and Diet Adherence Scale.

infectious diseases, such as malignant tumors and severe cardiopulmonary diseases. Patients unable to control their diets or perform aerobic exercises due to illness or other reasons were also excluded. The validation cohort consisted of patients with NAFLD who were admitted between October 2022 and June 2023, using the same inclusion and exclusion criteria.

Sample size was calculated using a factor analysis approach, with eight times the number of items in the largest dimension of the EDAS, which has seven items. Based on a 20% dropout rate, the target enrollment was 67 participants. All patients enrolled in this study after providing informed consent.

Establishment of an item pool

Professional medical workers conducted face-to-face conversations with 20 patients with typical NAFLD. The reasons mentioned by the patients that affected their exercise and diet adherence were recorded in detail. Subsequently, the scale was divided into the following five dimensions and 36 items: Understanding and valuing (eight items), belief (six items), self-control (12 items), conditional restrictions (eight items), and mental stress in life and work (two items). To assess the validity of these items, the scale was analyzed using the Delphi method.

Initial screening of items

Five professors with NAFLD as their research field and one professor of psychology were selected for consultation. Some of these experts believed that "mental stress in life and work" should be incorporated into the condition "conditional restriction"; that "self-control" should be divided into "self-control of diet" and "strengthen exercise self-control"; and that "conditional restriction" should be divided into "control dietary conditions", and "strengthen conditions for exercise". After modification, the experts were again consulted and the importance of these items were scored. Each item was rated on a scale of 1-9 points, with higher score indicating greater importance. Feedback was received from all six experts, with the average score of each item being greater than 7; moreover, the coefficients of variation were less than 0.25, and the expert opinions tended to be consistent. The EDAS questionnaire was divided into the following six dimensions and 36 items: understanding and valuing (eight items), belief (six items), self-control of diet (seven items), strengthen exercise self-control (five items), control dietary conditions (three items), and strengthen conditions for exercise (seven items).

Rescreening and modification of the items

Based on the inclusion and exclusion criteria, 30 NAFLD patients were selected. Analysis of their completed questionnaires showed that the item "I believe that taking medicine can control fatty liver" in the dimension of "understanding

and valuing" had a low degree of discrimination, and that, after deleting the items "I will measure my weight" and "I will review it regularly" in the dimension of "belief" improved the internal consistencies of the dimension "belief" and the total scale. Thus, these three items are deleted. Analysis of exploratory factors found six common factors, which can correspond to six dimensions, indicating that the EDAS scale had good construct validity. The final version of the EDAS consisted of 33 items across six dimensions, with 15 items of these items being reverse scored. The lowest score on this scale was 33, and the highest was 165, with higher scores indicating better patient adherence with lifestyle interventions.

Survey of samples

Lifestyle interventions: The enrolled patients were subjected to exercise and dietary interventions for 6 months. Moderate aerobic exercise was generally recommended, consisting of walking quickly more than four times a week for a cumulative total of at least 150-250 min. Patients with a preferred exercise method were allowed to do so, while recording it in detail. The 24-h diet of each patient was reviewed at baseline, including the names of foods and raw materials, the quantity of raw materials, and the time and place of eating. Dietary recommendations included a reduction of 500-1000 kcal per day, consuming a balanced diet with low sugar and low fat, reducing the intake of sugary drinks and saturated fats, and increasing dietary fiber content. Beginning one week from the date of enrollment, the 24-h diet of each patient was reviewed after dinner on one day a week for the next 24 wk.

Demographic characteristics and laboratory indices: Body composition indices of patients were analyzed at baseline and after 3 and 6 months using InBodyS10 (Biospace, Seoul, South Korea). Parameters evaluated included weight, waist circumference, upper arm circumference and abdominal fat area. Laboratory variables, including serum concentrations of alanine aminotransferase (ALT), aspartate aminotransferase (AST), gamma-glutamyl transferase (GGT), alkaline phosphatase (ALP), total bilirubin (TBIL), triglyceride (TG), total cholesterol (TC), fasting blood glucose (FBG), and umbilical artery, were measured by a chemiluminescence method an Hitachi automatic biochemical instrument-7180 and reagents purchased from Guang Co., Ltd. Controlled attenuation parameter (CAP) and liver stiffness measurement (LSM) were determined using a the FibroScan 502 Touch device (Echosens, Paris, France). A pedometer was given to each subject to record the number of days per week of exercise, the type of exercise and the number of steps walked by fast walking patients, and the type and time of daily exercise in non-fast walking patients.

Reliability and validity testing of the EDAS

Reliability was determined by measuring Cronbach's α coefficient and test-retest reliability. Validity analysis included content, criterion, and construct. Content validity was evaluated by experts, criterion validity was assessed to select a recognized criterion to test the correlation between the criterion and the scale. Construct validity was tested by confirmatory factor analysis.

Statistical analysis

Normally distributed continuous data were reported as the mean ± SD and compared by *t*-tests, abnormally distributed continuous data were reported as median and interquartile intervals and compared by rank sum tests, and categorical variables were reported as number (%) and compared by chi-squared tests. Reliability was analyzed by determining internal consistency and test-retest reliability. Internal consistency was expressed as Cronbach's α coefficient, which ranged from 0-1, with values of 0.8-0.9, 0.7-0.8, and 0.6-0.7 indicating very good, good, and minimally acceptable values.

The retest interval was one week, with test-retest reliability determined by analyzing the correlation coefficient of two scores, with a retest reliability > 0.7 considered good. Correlations of normally distributed data were determined using Pearson correlation coefficients, whereas correlations of non-normally distributed data were determined using Spearman correlation coefficients.

Validity analysis included content validity, criterion validity and construct validity. Content validity was evaluated by experts, with the content validity index of each item scored as 1 (irrelevant), 2 (weakly relevant), 3 (strongly relevant), or 4 (very relevant). The proportion of experts providing scores of 3 and 4 was defined as the content validity index of each item. Construct validity was evaluated by confirmatory factor analysis.

The efficacy of the EDAS score in judging exercise steps and reducing calorie intake was evaluated by determining the areas under the receiver operating characteristics curves (AUROC). The optimal critical value for adherence, as well as the sensitivity, specificity, positive predictive value, negative predictive value positive likelihood ratio and negative likelihood ratio, were determined based on the maximum value of the Jordan index. AUROCs of 0.9-1.0, 0.8-0.9, 0.7-0.8, and < 0.7 were indicative of excellent, good, average, and poor effectiveness of judgment, respectively.

Statistical analyses were performed using SPSS 27.0 (SPSS Inc., Chicago, IL, United States) and MedCalc 9.3 (MedCalc Software, Mariakerke, Belgium) software and OriginPro 9.0 (OriginPro, Northampton, United States) was used for mapping. A P value < 0.05 was considered statistically significant.

RESULTS

Characteristics of the enrolled population

This study included a total of 81 patients with NAFLD, with 66 completed the follow-up. The average amount of daily exercise completed was 4519 steps/d, and the caloric intake was reduced to 68 kcal/d. Of the 66 subjects, 37 (56.1%) lost weight. The average weight loss of these 37 subjects was 4.2 kg ± 2.9 kg, with the maximum weight loss being 15 kg (Table 1).

Table 1 Characteristics of enrolled subjects

Variable	Numerical value
Male, *n* (%)	49 (74.2)
Age (yr), mean ± SD	39 ± 12
Fatty liver disease course (month) (M, Q)	36 (9.0)
Smoking, *n* (%)	15 (22.7)
Likes fried food, *n* (%)	20 (30.3)
BMI (kg/m^2), mean ± SD	28.4 ± 3.3
Waist-hip ratio, mean ± SD	0.9 ± 0.0
Abnormal blood pressure, *n* (%)	20 (30.3)
ALT (U/L) (M, Q)	64.5 (60.8)
AST (U/L) (M, Q)	36.0 (25.4)
GGT (U/L) (M, Q)	48.0 (44.0)
ALP (U/L) (M, Q)	78.0 (29.5)
TBIL (μmol/L) (M, Q)	14.7 (7.3)
FBG (mmol/L) (M, Q)	6.0 (0.9)
TG (mmol/L) (M, Q)	2.0 (1.3)
CHO (mmol/L), mean ± SD	5.0 ± 1.1
FINS (μU/L) (M, Q)	13.9 (8.2)
UA (μmol/L) (M, Q)	421.5 (116.5)
CAP (dB/m), mean ± SD	331.4 ± 33.0
LSM (kPa) (M, Q)	6.6 (2.9)
Walking (number of steps) (M, Q)	4519.0 (4564.5)
Reduction in caloric intake (kcal) (M, Q)	68.0 (127.8)

ALT: Alanine aminotransferase; AST: Aspartate aminotransferase; GGT: Gamma-glutamyl transferase; ALP: Alkaline phosphatase; TBIL: Total bilirubin; TG: Triglyceride; TC: Total cholesterol; UA: Umbilical artery; BMI: Body mass index; FBG: Fasting blood glucose; FINS: Fasting insulin; CAP: Controlled attenuation parameter; LSM: Liver stiffness measurement.

Discrimination and reliability analysis of the EDAS

A comparison of the 27% of patients with the highest scores and the 27% of patients with the lowest scores showed that each item differed significantly ($P < 0.05$). The test-retest reliability after one week was 0.82. The internal consistency reliabilities of the seven dimensions were 0.739, 0.747, 0.771, 0.813, 0.791, 0.776, and 0.874, respectively, with each being above 0.7, and the Cronbach's α coefficient of the total scale being 0.874 (Table 2). The inter-dimension correlation of EDAS ranged from 0.050 (understanding and valuing and strengthening conditions for exercise) to 0.624 (controlling diet and exercise conditions). The correlations between pairs of dimensions were not strong, indicating that the contents of these items were less repetitive (Table 3).

Validity analysis of the EDAS

Evaluation by experts showed that the content validity index of the EDAS items was 1, indicating good content validity. The total score of the scale correlated significantly with daily walking or other exercises and daily reduction in calorie intake, but not with weight loss. The number of exercise steps per day correlated significantly with belief ($r = 0.29$, $P = 0.020$), strengthening exercise self-control ($r = 0.40$, $P = 0.001$) and strengthening exercise conditions ($r = 0.33$, $P = 0.007$), whereas reduced daily calorie intake correlated significantly with belief ($r = 0.34$, 0.006), self-control of diet ($r = 0.64$, $P < 0.001$), control of dietary conditions ($r = 0.56$, $P < 0.001$) and strengthening exercise conditions ($r = 0.26$, $P = 0.035$) (Table 4).

Confirmatory factor analysis of the EDAS showed that the KMO coefficient was 0.675 ($P < 0.001$ on the Bartlett spherical test), with the spherical hypothesis being rejected. Variance maximization orthogonal rotation in factor analysis identified six common factors. These six factors explained 66.2% of the total table, with factor 1 accounting for 25.4% of the variation in interpretation. After the second dimensionality reduction of the six dimensions, the KMO coefficient was 0.710 ($P < 0.001$ on the Bartlett spherical test). Two common factors accounted for 64.7% of the total table; the first factor can be explained by external conditions and the second factor by internal motives.

Table 2 Basic information and internal consistency reliability

EDAS	Number of entries	Score	Mean score	Standard deviation	Lowest score	Highest score	Cronbach's α
Understanding and valuing	7	35	24.65	4.64	13	35	0.739
Belief	4	20	16.23	2.39	7	20	0.747
Self-control of diet	7	35	22.39	3.89	10	33	0.771
Strengthen exercise self-control	5	25	15.00	3.65	7	25	0.813
Control dietary conditions	3	15	10.35	2.58	3	15	0.791
Strengthen exercise conditions	7	35	21.80	5.07	9	33	0.776
Total scale	33	165	110.42	14.49	67	149	0.874

EDAS: Exercise and Diet Adherence Scale.

Table 3 Correlations among the six dimensions

EDAS	Understanding and valuing	Belief	Self-control of diet	Strengthen exercise self-control	Control dietary conditions	Strengthen exercise conditions
Understanding and valuing	1.000					
Belief	0.280	1.000				
Self-control of diet	0.056	0.335	1.000			
Strengthen exercise self-control	0.096	0.324	0.455	1.000		
Control dietary conditions	0.057	0.137	0.583	0.398	1.000	
Strengthen exercise conditions	0.050	0.322	0.473	0.494	0.624	1.000

EDAS: Exercise and Diet Adherence Scale.

Table 4 Calibration validity analysis

EDAS	*r* (*P* value)		
	Daily exercise steps	Daily calorie intake reduction (kcal)	Weight loss (kg)
Understanding and valuing	0.03 (0.842)	0.11 (0.373)	0.05 (0.712)
Belief	0.29 (0.020)[a]	0.34 (0.006)[a]	0.24 (0.054)
Self-control of diet	0.23 (0.064)	0.64 (< 0.001)[a]	0.14 (0.262)
Strengthen exercise self-control	0.40 (0.001)[a]	0.17 (0.183)	0.14 (0.279)
Control dietary conditions	0.20 (0.104)	0.56 (< 0.001)[a]	0.26 (0.037)[a]
Strengthen exercise conditions	0.33 (0.007)[a]	0.26 (0.035)[a]	0.19 (0.133)
Total scale	0.37 (0.002)[a]	0.50 (< 0.001)[a]	0.24 (0.056)

[a]$P < 0.05$.

EDAS: Exercise and Diet Adherence Scale.

ROC curve analysis of the exercise and diet compliance of the EDAS

Exercise conditions were divided into five categories: ≤ 3000, 3000-5000, 5000-8000, 8000-10000, and ≥ 10000 steps per day. The EDAS in patients with NAFLD was highly sensitive in determining exercise conditions, but its specificity was low. EDAS scores < 97 were therefore indicative of a lack of daily exercise (Figures 2A and 3).

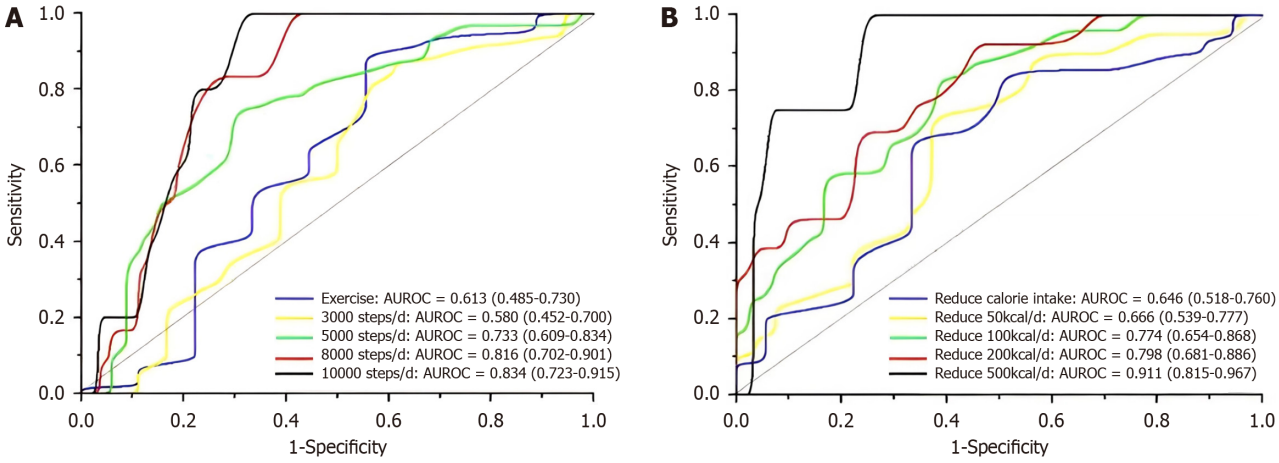

Figure 2 Receiver operating characteristics analysis. A: Receiver operating characteristics (ROC) analysis of the relationship between total Exercise and Diet Adherence Scale (EDAS) score and daily exercise; B: ROC analysis of the relationship between total EDAS score and daily calorie reduction. AUROC: Areas under the receiver operating characteristics curves.

	Daily exercise					Reduce daily calorie intake				
	Exercise	⩾ 3000 steps/d	⩾ 5000 steps/d	⩾ 8000 steps/d	⩾ 10000 steps/d	Reduce calorie intake	50 kcal/d	100 kcal/d	200 kcal/d	500 kcal/d
Area under curve	0.613 (0.485-0.730)	0.580 (0.452-0.700)	0.733 (0.609-0.834)	0.816 (0.702-0.901)	0.834 (0.723-0.915)	0.646 (0.518-0.760)	0.666 (0.539-0.777)	0.774 (0.654-0.868)	0.798 (0.681-0.886)	0.911 (0.815-0.967)
Optimal critical value	97.0	99.0	109.0	109.0	113.0	102.0	107.0	108.0	108.0	116.0
Sensitivity (%)	89.5	87.5	75.0	100.0	100.0	83.3	71.8	83.3	92.3	100.0
Specificity (%)	44.4	38.9	70.6	59.3	68.9	50.0	63.0	61.9	54.7	75.8
Positive predictive value (%)	91.1	79.2	70.6	35.3	20.8	81.7	73.7	55.6	33.3	21.1
Negative predictive value (%)	40.0	53.8	75.0	100.0	100.0	52.9	60.7	86.7	96.7	100.0
Positive likelihood ratio	1.6	1.4	2.6	2.5	3.2	1.7	1.9	2.2	2.0	4.1
Negative likelihood ratio	0.2	0.3	0.4	0.0	0.0	0.3	0.4	0.3	0.1	0.0

Figure 3 Efficacy of total score in judging daily exercise and daily calorie reduction.

The average daily calorie intake of patients was also divided into five categories: reductions of ≤ 50 kcal/d or an increase, and reductions of 50-100 kcal/d, 100-200 kcal/d, 200-500 kcal/d, and ≥ 500 kcal/d. The EDAS was highly sensitive and specific in determining large daily reductions in diet (> 500 kcal/d). EDAS scores > 116 were therefore indicative of a greater control of diet than scores below (Figures 2B and 3).

Verification of the effectiveness of the EDAS

Characteristics of the enrolled population: 121 NAFLD patients admitted to our hospital for fatty liver treatment from January 2022 to June 2023, with 103 of these patients' completing follow-up. After excluding 22 patients who were not at the first visit and 10 who were not followed up after 3 or 6 month, 84 patients were included, including 62 who completed the 3-month follow-up and 57 who completed the 6-month follow-up. The average age of these 84 patients was 38 years. They had a mean ± SD body mass index of 28.19 ± 2.99 kg/m^2, ALT of 87.64 ± 44.80 U/L, AST of 40.2 U/L, GGT of 52.0 U/L, ALP of 72.0 U/L, and TBIL of 14.9 μmol/L. They had a mean ± SD FBG of 5.96 ± 0.76 mmol/L, TG of 1.8 mmol/L, FINS of 18.16 μU/L, CAP of 315.81 ± 35.16 dB/m, and LSM of 6.8 kPa. The EDAS questionnaire survey showed that 26 patients (31.0%) had poor compliance, 37 (44.0%) had moderate compliance, and 21 (25.0%) had good compliance.

Results of verification: NAFLD patients with better adherence had a greater proportion of weight, abdominal circumference, LSM reduction and ALT return to normal, but this difference decreased with the extension of follow-up months (Figure 4). The worse the compliance, the lower the proportion of blood glucose returning to normal in 6 months, indicating that fatty liver will affect the control of blood sugar and make blood sugar fluctuate. Further exploring the effects of exercise and diet intervention on patients in different groups, it was found that ALT, abdominal circumference, arm circumference, CAP, and LSM of patients with high EDAS scores all changed significantly ($P < 0.05$), while TC in the three groups did not change significantly ($P > 0.05$) between 6 months of follow-up (Figure 5).

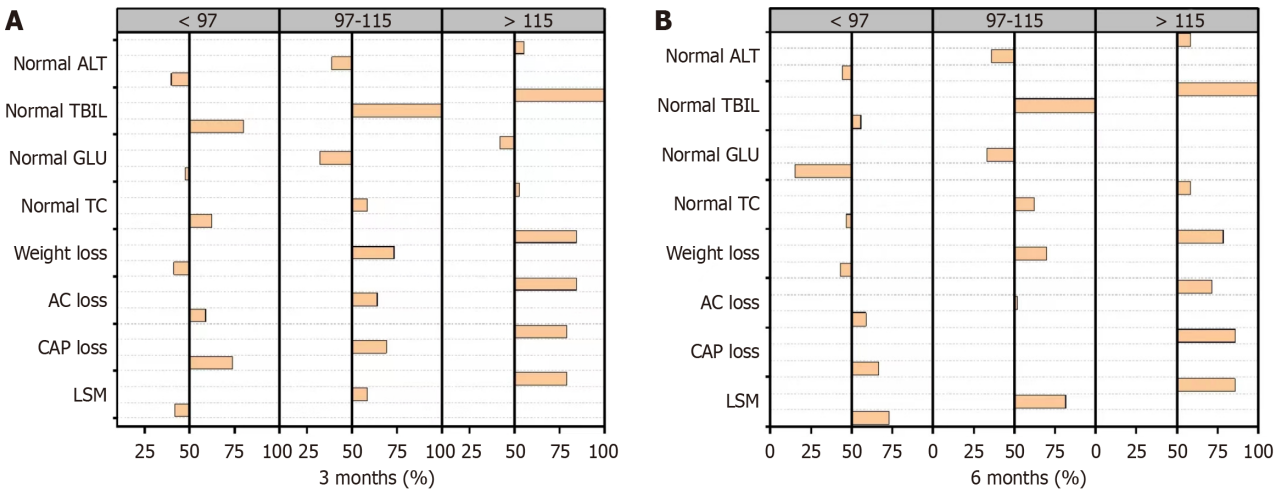

Figure 4 Relationships between Exercise and Diet Adherence Scale grouping and various indicators of non-alcoholic fatty liver disease. A: 3 months; B: 6 months. ALT: Alanine aminotransferase; TBIL: Total bilirubin; GLU: Glucose; TC: Total cholesterol; AC: Abdominal circumference; CAP: Controlled attenuation parameter; LSM: Liver stiffness measurement.

DISCUSSION

Therapeutic changes in patient lifestyle remains the treatment of choice in NAFLD[12]. Because many of these patients are at high risk of cardiovascular disease, a healthy lifestyle can reduce its incidence[13]. Although adherence with therapeutic recommendations is important in managing chronic diseases[14], most patients have difficulty changing their long-standing dietary habits[15]. In addition, regular exercise decreases as patients age, with more than 50% of individuals stopping routine exercise and treatment within 1 year[16-18]. Early identification of patients with poor adherence can result in efforts to improve their adherence[19].

Most assessments of adherence are in relation to medication, but these studies have generally shown poor adherence [20-23]. For example, a retrospective study of initial treatment of patients with type 2 diabetes found that 48% stopped their medication within the first year, with most discontinuations occurring within the first 3 months after starting treatment[24]. Moreover, only about 50% of patients with myocardial infarction show adherence with the long-term use of antihypertensive and lipid-lowering drugs[25]. Fewer studies to date have assessed adherence with lifestyle interventions than those on drugs. with physicians paying no attention to lifestyle modifications. Therefore, patients were less able to recognize the importance of lifestyle interventions.

NAFLD is a progressive liver disease, with histology ranging from steatosis to fibrosis and cirrhosis. NAFLD is the eighth most common cause of death worldwide, being responsible for 1.2 million annual deaths. To date, however, there is currently no comprehensive scale to evaluate adherence with lifestyle interventions for NAFLD at home or abroad. The EDAS scale described in the present study was based on standardized scale preparation requirements and is, to our knowledge, the first scale to measure adherence in patients with NAFLD.

The internal consistency reliability of each dimension of the EDAS was above 0.7, and the Cronbach's α coefficient of the total volume table was 0.874. No strong correlation was observed among the dimensions, indicating that the item content was less repetitive. The test-retest reliability at one-week was 0.820, indicating that the EDAS has high stability, consistency, and reliability. Experts rated each item of the EDAS as level 3 or 4, making the item content validity index of the EDAS 1, indicating that content validity was good.

Daily number of exercise steps was directly proportional to three dimensions on the EDAS: Belief, exercise self-control and strengthen conditions for exercise. In addition, daily calorie intake reduction was proportional to three dimensions: Belief, self-control of diet and control dietary conditions. These findings indicate that the EDAS reflects the actual adherence of NAFLD patients before exercise and diet intervention. Belief was significantly and positively correlated with exercise enhancement and diet control, suggesting that physician encouragement and a good doctor-patient relationship can establish a belief in patients that they can cure or control NAFLD. Strengthening exercise self-control and conditions were related to exercise, whereas dietary self-control and conditions were related to diet, indicating that the EDAS can independently reflect the exercise and diet conditions of patients. In contrast, weight loss was only significantly related to the control of diet, possibly because a controlled diet is more likely to lead to weight loss than exercise.

Confirmatory factor analysis showed that the KMO coefficient was 0.710, with Bartlett's spherical test showing a P value < 0.001. Two common factors were identified, with the most frequent variation being the control of dietary conditions. Thus, the importance of improving diet control conditions should be emphasized in patients with poor adherence.

Clinically, patients with EDAS scores ≥ 116 should be regarded as having good adherence. If abnormalities in the liver function are not evident, lifestyle interventions alone can be administered. Adherence is considered general for patients with EDAS scores ranging from 97 to 115. The importance of lifestyle improvement should be emphasized in these patients, including improved adherence with exercise and diet recommendations, as well as treatment with hepatopro-

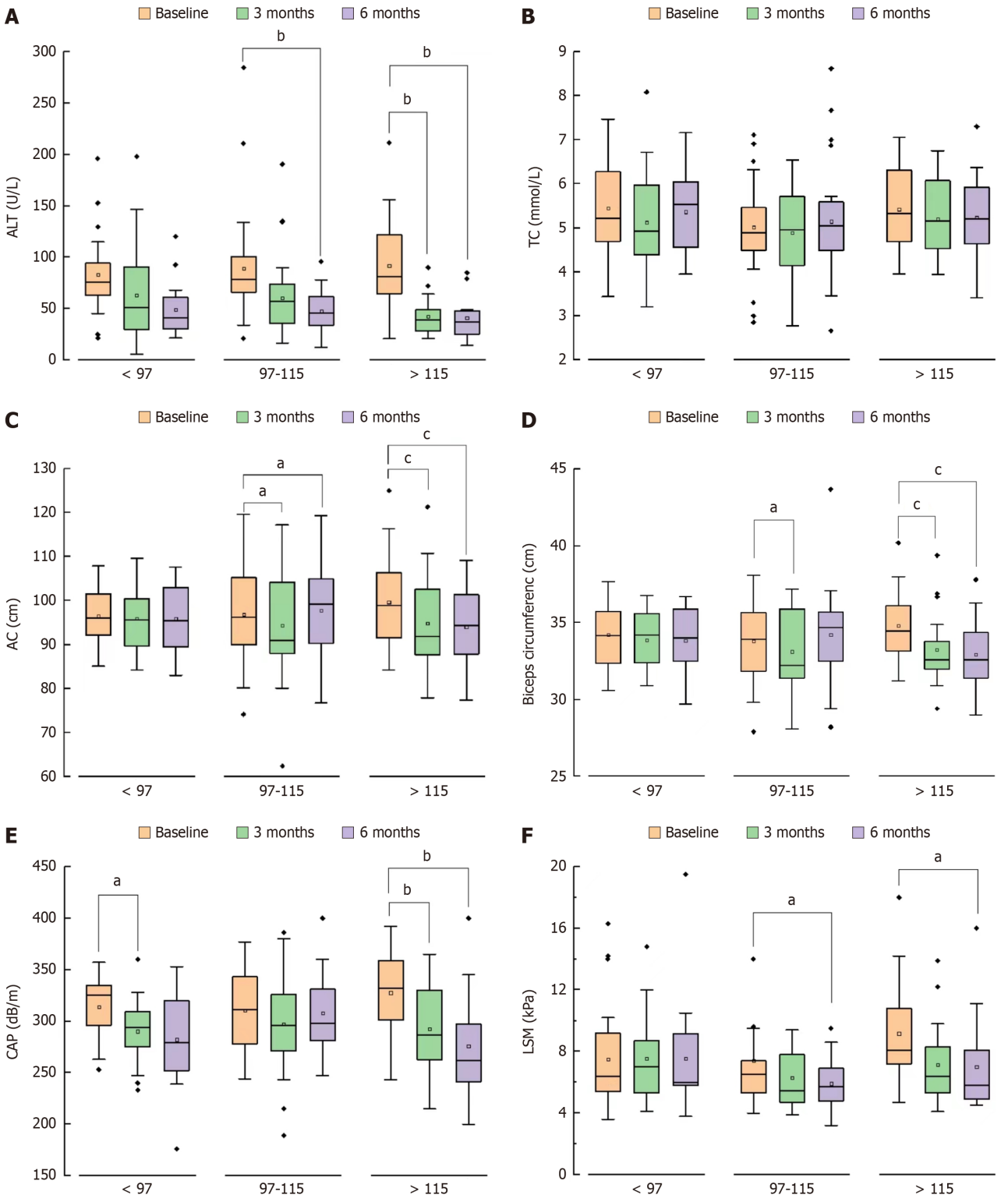

Figure 5 Effects of lifestyle interventions on body composition and biochemical indices of patients grouped by Exercise and Diet Adherence Scale scores. A: Alanine aminotransferase; B: Total cholesterol; C: Abdominal circumference; D: Biceps circumference; E: Controlled attenuation parameter; F: Liver stiffness measurement. ALT: Alanine aminotransferase; TBIL: Total bilirubin; GLU: Glucose; TC: Total cholesterol; CAP: Controlled attenuation parameter; LSM: Liver stiffness measurement.

tective drugs when necessary. Patients with EDAS scores < 97 have poor adherence and should receive early administration of anti-inflammatory agents and psychotherapy (Figure 6).

To the best of our knowledge, this is the first study to use a questionnaire to assess adherence with lifestyle interventions in patients with NAFLD and it has been verified to show the generalizability of its results. This study also had several limitations. First, the follow-up duration was relatively short. NAFLD is a chronic, long-term disease, and short-term evaluations may not fully reveal the actual effects of lifestyle interventions in these patients. Second, a self-report questionnaire about lifestyle changes and patient behavior is likely to be affected by recall, measurement bias and

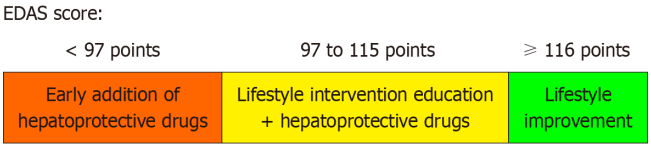

Figure 6 Associations of Exercise and Diet Adherence Scale scores with adherence with lifestyle interventions and associated clinical guidelines. EDAS: Exercise and Diet Adherence Scale.

emotions. Patients may tend to provide answers that meet social expectations, leading to an overly idealized description rather than a reflection of the actual situation. Additionally, these participants go to the hospital for treatment more regularly than the general population of patients with NAFLD, suggesting they may be more strongly interested in being treated intention, which may have introduced sampling errors. This was a single center study, suggesting the possibility of selection bias. Prospective, multicenter studies should be conducted with a longer follow-up large sample size, including verification by physical examination and more stringent sampling methods to ensure the representativeness of samples, and improve the external validity of the study. In addition, prospective studies are needed to assess the correlation between EDAS scores and outcome events, such as liver cirrhosis and liver cancer.

CONCLUSION

Lifestyle intervention adherence scale developed in this study for patients with NAFLD was effective in determining the adherence of these patients with exercise and diet. This scale, which was relatively comprehensive in content, underwent appropriate verification in an independent patient cohort. The EDAS scale can be used as a tool to measure adherence with lifestyle interventions in patients with NAFLD and guide clinical interventions.

ARTICLE HIGHLIGHTS

Research background

Non-alcoholic fatty liver disease (NAFLD) is a progressive disease that can lead to complications such as liver fibrosis, cirrhosis, hepatocellular carcinoma, cardiovascular diseases, and metabolic disorders such as type 2 diabetes. However, to date, no medications have been approved for treating NAFLD, and lifestyle modifications remain the cornerstone of treatment.

Research motivation

Changing an unhealthy lifestyle can be useful for alleviating hepatic steatosis in patients with NAFLD. However, not everyone is able or willing to adhere to the dietary and exercise guidelines. The variety of exercise and dietary controls makes it challenging to quantify and evaluate patient's adherence.

Research objectives

To evaluate adherence effectively and swiftly with the recommendations for lifestyle changes in patients with NAFLD, implementing various intervention strategies based on adherence levels to prevent disease progression is crucial.

Research methods

First, we identified factors affecting exercise and dietary adherence in patients with NAFLD. The Delphi method was used to analyze and modify the Exercise and Diet Adherence Scale (EDAS). After a preliminary small-scale survey and further adjustments, the EDAS was established. Enrolled patients with NAFLD followed exercise and diet interventions, filled the EDAS at the beginning, and were followed up for 6 months. Finally, we evaluated and validated the reliability of the EDAS.

Research results

The EDAS demonstrated good item discrimination; internal consistency reliability; test-retest reliability; and content, construct, and criterion validity. It can reliably measure the adherence of patients with NAFLD to exercise and dietary interventions.

Research conclusions

The EDAS has been established to assess the adherence of patients objectively, directly, and rapidly with NAFLD to changing unhealthy lifestyles. This reliable tool supports early intervention in NAFLD, aims to prevent disease progression, and reduces the healthcare burden.

Research perspectives

EDAS plays an important clinical role in the assessment, treatment, and management of NAFLD. However, its widespread application requires multicenter prospective studies. Additionally, the participants in this study did not undergo a liver biopsy. Thus, future research should explore the impact of EDAS on liver pathology.

ACKNOWLEDGEMENTS

The authors thank You-Fei Zhao and Lin Chen for inputting some of data.

FOOTNOTES

Co-first authors: Ming-Hui Zeng and Qi-Yu Shi.

Co-corresponding authors: Liang Xu and Yu-Qiang Mi.

Author contributions: Zeng MH and Shi QY contributed equally to this work as co-first authors; Mi YQ and Xu L conceptualized and designed the study; Shi QY participated in the acquisition, analysis, interpretation of the data, and drafting of the manuscript; Zeng MH participated in the acquisition and analysis of the data, and editing of the manuscript.

Supported by the Science and Technology Foundation of Tianjin Municipal Health Bureau, No. 12KG119; Tianjin Key Medical Discipline (Specialty) Construction Project, No. TJYXZDXK-059B; Tianjin Health Science and Technology Project key discipline special, No. TJWJ2022XK034; and Research project of Chinese traditional medicine and Chinese traditional medicine combined with Western medicine of Tianjin municipal health and Family Planning Commission, No. 2021022.

Institutional review board statement: This study has been reviewed and approved by the Ethics Committee of Tianjin Second People's Hospital [approved No. (2012)06].

Clinical trial registration statement: This study is registered at (https://www.chictr.org.cn/showproj.html?proj=5809). The registration identification number is (ChiCTR-ONRC-13003751).

Informed consent statement: All study participants provided informed written consent prior to study enrollment.

Conflict-of-interest statement: The authors of this manuscript have no conflicts of interest to disclose.

Data sharing statement: There are no additional data available.

CONSORT 2010 statement: The authors have read the CONSORT 2010 statement, and the manuscript was prepared and revised according to the CONSORT 2010 statement.

Country/Territory of origin: China

ORCID number: Ming-Hui Zeng 0000-0002-1224-0525; Liang Xu 0000-0001-5441-1217; Yu-Qiang Mi 0000-0001-7809-2679.

S-Editor: Chen YL
L-Editor: A
P-Editor: Zheng XM

REFERENCES

1 **Younossi ZM**, Golabi P, Paik JM, Henry A, Van Dongen C, Henry L. The global epidemiology of nonalcoholic fatty liver disease (NAFLD) and nonalcoholic steatohepatitis (NASH): a systematic review. *Hepatology* 2023; **77**: 1335-1347 [PMID: 36626630 DOI: 10.1097/HEP.0000000000000004]

2 **Ekstedt M**, Hagström H, Nasr P, Fredrikson M, Stål P, Kechagias S, Hultcrantz R. Fibrosis stage is the strongest predictor for disease-specific mortality in NAFLD after up to 33 years of follow-up. *Hepatology* 2015; **61**: 1547-1554 [PMID: 25125077 DOI: 10.1002/hep.27368]

3 **Younossi ZM**, Stepanova M, Ong J, Trimble G, AlQahtani S, Younossi I, Ahmed A, Racila A, Henry L. Nonalcoholic Steatohepatitis Is the Most Rapidly Increasing Indication for Liver Transplantation in the United States. *Clin Gastroenterol Hepatol* 2021; **19**: 580-589.e5 [PMID: 32531342 DOI: 10.1016/j.cgh.2020.05.064]

4 **Doycheva I**, Issa D, Watt KD, Lopez R, Rifai G, Alkhouri N. Nonalcoholic Steatohepatitis is the Most Rapidly Increasing Indication for Liver

Transplantation in Young Adults in the United States. *J Clin Gastroenterol* 2018; **52**: 339-346 [PMID: 28961576 DOI: 10.1097/MCG.0000000000000925]

5 **Chalasani N**, Younossi Z, Lavine JE, Charlton M, Cusi K, Rinella M, Harrison SA, Brunt EM, Sanyal AJ. The diagnosis and management of nonalcoholic fatty liver disease: Practice guidance from the American Association for the Study of Liver Diseases. *Hepatology* 2018; **67**: 328-357 [PMID: 28714183 DOI: 10.1002/hep.29367]

6 **Han MAT**, Altayar O, Hamdeh S, Takyar V, Rotman Y, Etzion O, Lefebvre E, Safadi R, Ratziu V, Prokop LJ, Murad MH, Noureddin M. Rates of and Factors Associated With Placebo Response in Trials of Pharmacotherapies for Nonalcoholic Steatohepatitis: Systematic Review and Meta-analysis. *Clin Gastroenterol Hepatol* 2019; **17**: 616-629.e26 [PMID: 29913275 DOI: 10.1016/j.cgh.2018.06.011]

7 **Michel M**, Schattenberg JM. Effectiveness of lifestyle interventions in NAFLD (nonalcoholic fatty liver disease) - how are clinical trials affected? *Expert Opin Investig Drugs* 2020; **29**: 93-97 [PMID: 31933385 DOI: 10.1080/13543784.2020.1716333]

8 **Plauth M**, Bernal W, Dasarathy S, Merli M, Plank LD, Schütz T, Bischoff SC. ESPEN guideline on clinical nutrition in liver disease. *Clin Nutr* 2019; **38**: 485-521 [PMID: 30712783 DOI: 10.1016/j.clnu.2018.12.022]

9 **Fan JG**, Kim SU, Wong VW. New trends on obesity and NAFLD in Asia. *J Hepatol* 2017; **67**: 862-873 [PMID: 28642059 DOI: 10.1016/j.jhep.2017.06.003]

10 **Barritt AS**, Watkins S, Gitlin N, Klein S, Lok AS, Loomba R, Schoen C, Reddy KR, Trinh HN, Mospan AR, Vos MB, Weiss LM, Cusi K, Neuschwander-Tetri BA, Sanyal AJ. Patient Determinants for Histologic Diagnosis of NAFLD in the Real World: A TARGET-NASH Study. *Hepatol Commun* 2021; **5**: 938-946 [PMID: 34141981 DOI: 10.1002/hep4.1689]

11 **Chalasani N**, Younossi Z, Lavine JE, Diehl AM, Brunt EM, Cusi K, Charlton M, Sanyal AJ. The diagnosis and management of non-alcoholic fatty liver disease: practice Guideline by the American Association for the Study of Liver Diseases, American College of Gastroenterology, and the American Gastroenterological Association. *Hepatology* 2012; **55**: 2005-2023 [PMID: 22488764 DOI: 10.1002/hep.25762]

12 **Chen Y**, Feng R, Yang X, Dai J, Huang M, Ji X, Li Y, Okekunle AP, Gao G, Onwuka JU, Pang X, Wang C, Li C, Sun C. Yogurt improves insulin resistance and liver fat in obese women with nonalcoholic fatty liver disease and metabolic syndrome: a randomized controlled trial. *Am J Clin Nutr* 2019; **109**: 1611-1619 [PMID: 31136662 DOI: 10.1093/ajcn/nqy358]

13 **Kasper P**, Martin A, Lang S, Kütting F, Goeser T, Demir M, Steffen HM. NAFLD and cardiovascular diseases: a clinical review. *Clin Res Cardiol* 2021; **110**: 921-937 [PMID: 32696080 DOI: 10.1007/s00392-020-01709-7]

14 **De Geest S**, Sabaté E. Adherence to long-term therapies: evidence for action. *Eur J Cardiovasc Nurs* 2003; **2**: 323 [PMID: 14667488 DOI: 10.1016/S1474-5151(03)00091-4]

15 **Shim JS**, Heo JE, Kim HC. Factors associated with dietary adherence to the guidelines for prevention and treatment of hypertension among Korean adults with and without hypertension. *Clin Hypertens* 2020; **26**: 5 [PMID: 32190348 DOI: 10.1186/s40885-020-00138-y]

16 **Resurrección DM**, Motrico E, Rigabert A, Rubio-Valera M, Conejo-Cerón S, Pastor L, Moreno-Peral P. Barriers for Nonparticipation and Dropout of Women in Cardiac Rehabilitation Programs: A Systematic Review. *J Womens Health (Larchmt)* 2017; **26**: 849-859 [PMID: 28388314 DOI: 10.1089/jwh.2016.6249]

17 **Saida TGRH**, Juul Sørensen T, Langberg H. Long-term exercise adherence after public health training in at-risk adults. *Ann Phys Rehabil Med* 2017; **60**: 237-243 [PMID: 28462861 DOI: 10.1016/j.rehab.2017.02.006]

18 **Lopes S**, Félix G, Mesquita-Bastos J, Figueiredo D, Oliveira J, Ribeiro F. Determinants of exercise adherence and maintenance among patients with hypertension: a narrative review. *Rev Cardiovasc Med* 2021; **22**: 1271-1278 [PMID: 34957769 DOI: 10.31083/j.rcm2204134]

19 **Lee YM**, Kim RB, Lee HJ, Kim K, Shin MH, Park HK, Ahn SK, Kim SY, Lee YH, Kim BG, Lee H, Lee WK, Lee KS, Kim MJ, Park KS. Relationships among medication adherence, lifestyle modification, and health-related quality of life in patients with acute myocardial infarction: a cross-sectional study. *Health Qual Life Outcomes* 2018; **16**: 100 [PMID: 29788961 DOI: 10.1186/s12955-018-0921-z]

20 **Chan AHY**, Horne R, Hankins M, Chisari C. The Medication Adherence Report Scale: A measurement tool for eliciting patients' reports of nonadherence. *Br J Clin Pharmacol* 2020; **86**: 1281-1288 [PMID: 31823381 DOI: 10.1111/bcp.14193]

21 **Hammad M**, Bakry H. Satisfaction and Adherence to Biological Treatment in Patients with Rheumatic Diseases. *Curr Rheumatol Rev* 2022; **18**: 250-256 [PMID: 34967297 DOI: 10.2174/1573397118666211230101451]

22 **Huang Z**, Tan E, Lum E, Sloot P, Boehm BO, Car J. A Smartphone App to Improve Medication Adherence in Patients With Type 2 Diabetes in Asia: Feasibility Randomized Controlled Trial. *JMIR Mhealth Uhealth* 2019; **7**: e14914 [PMID: 31516127 DOI: 10.2196/14914]

23 **Chan AHY**, Vervloet M, Lycett H, Brabers A, van Dijk L, Horne R. Development and validation of a self-report measure of practical barriers to medication adherence: The medication practical barriers to adherence questionnaire (MPRAQ). *Br J Clin Pharmacol* 2021; **87**: 4197-4211 [PMID: 33486802 DOI: 10.1111/bcp.14744]

24 **Horsburgh S**, Sharples K, Barson D, Zeng J, Parkin L. Patterns of metformin monotherapy discontinuation and reinitiation in people with type 2 diabetes mellitus in New Zealand. *PLoS One* 2021; **16**: e0250289 [PMID: 33882106 DOI: 10.1371/journal.pone.0250289]

25 **Choudhry NK**, Avorn J, Glynn RJ, Antman EM, Schneeweiss S, Toscano M, Reisman L, Fernandes J, Spettell C, Lee JL, Levin R, Brennan T, Shrank WH; Post-Myocardial Infarction Free Rx Event and Economic Evaluation (MI FREEE) Trial. Full coverage for preventive medications after myocardial infarction. *N Engl J Med* 2011; **365**: 2088-2097 [PMID: 22080794 DOI: 10.1056/NEJMsa1107913]

World Journal of Gastroenterology

Submit a Manuscript: https://www.f6publishing.com

World J Gastroenterol 2024 March 14; 30(10): 1405-1419

DOI: 10.3748/wjg.v30.i10.1405

ISSN 1007-9327 (print) ISSN 2219-2840 (online)

ORIGINAL ARTICLE

Basic Study

Alkaline sphingomyelinase deficiency impairs intestinal mucosal barrier integrity and reduces antioxidant capacity in dextran sulfate sodium-induced colitis

Ye Tian, Xin Li, Xu Wang, Si-Ting Pei, Hong-Xin Pan, Yu-Qi Cheng, Yi-Chen Li, Wen-Ting Cao, Jin-Dong Ding Petersen, Ping Zhang

Specialty type: Gastroenterology and hepatology

Provenance and peer review: Unsolicited article; Externally peer reviewed.

Peer-review model: Single blind

Peer-review report's scientific quality classification

Grade A (Excellent): 0
Grade B (Very good): B
Grade C (Good): C
Grade D (Fair): 0
Grade E (Poor): 0

P-Reviewer: Diener M, Germany

Received: October 12, 2023
Peer-review started: October 12, 2023
First decision: December 8, 2023
Revised: December 26, 2023
Accepted: January 29, 2024
Article in press: January 29, 2024
Published online: March 14, 2024

Ye Tian, Si-Ting Pei, Hong-Xin Pan, Wen-Ting Cao, Jin-Dong Ding Petersen, Ping Zhang, International School of Public Health and One Health, Hainan Medical University, Haikou 571199, Hainan Province, China

Xin Li, Yu-Qi Cheng, Yi-Chen Li, Medical Laboratory Science and Technology College, Harbin Medical University - Daqing Campus, Daqing 163000, Heilongjiang Province, China

Xu Wang, Department of Laboratory Diagnosis, Qiqihar Tuberculosis Control Center, Qiqihar 161000, Heilongjiang Province, China

Jin-Dong Ding Petersen, Department of Public Health, University of Copenhagen, Copenhagen 1353, Denmark

Jin-Dong Ding Petersen, Department of Public Health, University of Southern Denmark, Odense 5000, Denmark

Corresponding author: Ping Zhang, MD, PhD, Professor, International School of Public Health and One Health, Hainan Medical University, No. 3 Xueyuan Road, Haikou 571199, Hainan Province, China. pingzhang@hainmc.edu.cn

Abstract

BACKGROUND

Ulcerative colitis is a chronic inflammatory disease of the colon with an unknown etiology. Alkaline sphingomyelinase (alk-SMase) is specifically expressed by intestinal epithelial cells, and has been reported to play an anti-inflammatory role. However, the underlying mechanism is still unclear.

AIM

To explore the mechanism of alk-SMase anti-inflammatory effects on intestinal barrier function and oxidative stress in dextran sulfate sodium (DSS)-induced colitis.

METHODS

Mice were administered 3% DSS drinking water, and disease activity index was determined to evaluate the status of colitis. Intestinal permeability was evaluated

by gavage administration of fluorescein isothiocyanate dextran, and bacterial translocation was evaluated by measuring serum lipopolysaccharide. Intestinal epithelial cell ultrastructure was observed by electron microscopy. Western blotting and quantitative real-time reverse transcription-polymerase chain reaction were used to detect the expression of intestinal barrier proteins and mRNA, respectively. Serum oxidant and antioxidant marker levels were analyzed using commercial kits to assess oxidative stress levels.

RESULTS

Compared to wild-type (WT) mice, inflammation and intestinal permeability in alk-SMase knockout (KO) mice were more severe beginning 4 d after DSS induction. The mRNA and protein levels of intestinal barrier proteins, including zonula occludens-1, occludin, claudin-3, claudin-5, claudin-8, mucin 2, and secretory immunoglobulin A, were significantly reduced on 4 d after DSS treatment. Ultrastructural observations revealed progressive damage to the tight junctions of intestinal epithelial cells. Furthermore, by day 4, mitochondria appeared swollen and degenerated. Additionally, compared to WT mice, serum malondialdehyde levels in KO mice were higher, and the antioxidant capacity was significantly lower. The expression of the transcription factor nuclear factor erythroid 2-related factor 2 (Nrf2) in the colonic mucosal tissue of KO mice was significantly decreased after DSS treatment. mRNA levels of Nrf2-regulated downstream antioxidant enzymes were also decreased. Finally, colitis in KO mice could be effectively relieved by the injection of tertiary butylhydroquinone, which is an Nrf2 activator.

CONCLUSION

Alk-SMase regulates the stability of the intestinal mucosal barrier and enhances antioxidant activity through the Nrf2 signaling pathway.

Key Words: Alkaline sphingomyelinase; Intestinal mucosal barrier; Antioxidant capacity; Dextran sulfate sodium-induced colitis; nuclear factor erythroid 2-related factor 2

Core Tip: The protective effect of alkaline sphingomyelinase (alk-SMase) against intestinal inflammation has been demonstrated, but the underlying molecular mechanism remains unclear. In the present study, we found that alk-SMase deficiency exacerbated damage to the intestinal mucosal barrier in dextran sulfate sodium-induced colitis. Additionally, alk-SMase was shown to enhance antioxidant activity, thereby reducing susceptibility to proinflammatory factors in colitis. Furthermore, our findings revealed that alk-SMase may maintain intestinal barrier stability and increase antioxidant capacity through the nuclear factor erythroid 2-related factor 2 signaling pathway.

Citation: Tian Y, Li X, Wang X, Pei ST, Pan HX, Cheng YQ, Li YC, Cao WT, Petersen JDD, Zhang P. Alkaline sphingomyelinase deficiency impairs intestinal mucosal barrier integrity and reduces antioxidant capacity in dextran sulfate sodium-induced colitis. *World J Gastroenterol* 2024; 30(10): 1405-1419
URL: https://www.wjgnet.com/1007-9327/full/v30/i10/1405.htm
DOI: https://dx.doi.org/10.3748/wjg.v30.i10.1405

INTRODUCTION

Ulcerative colitis (UC), which is a kind of inflammatory bowel disease (IBD), is a chronic and recurrent inflammatory disease of the colon that causes destruction and inflammation in the colonic mucosa and a persistent increase in the risk of developing colorectal cancer (CRC)[1,2]. However, the etiology of UC is unclear, and it is believed that UC is related to many factors, such as genetics, the environment, infection and immunomodulatory disorders, and damage to the intestinal mucosal barrier is the core of its pathogenesis[3]. The intestinal mucosal barrier includes the mechanical barrier, immune barrier, microbial barrier and chemical barrier. Any instability in intestinal barrier function leads to the destruction of intestinal mucosal tissue and causes inflammatory disease[4,5]. However, inflammation might be an important risk factor for the development of colitis-associated CRC[6,7].

It is well known that the intestinal mucosa is exposed to immune and inflammatory stimuli triggered by various pathogenic and oxidative factors[8,9]. Currently, most people believe that intestinal inflammation is caused by a weakened intestinal mucosal barrier and increased permeability of the intestinal mucosa, which leads to the passage of intestinal pathogenic bacteria through the barrier[10-12]. Therefore, intestinal barrier integrity and normal immune function are crucial for maintaining cellular homeostasis[13,14].

Alkaline sphingomyelinase (alk-SMase), which is also called nucleotide pyrophosphatase/phosphodiesterase 7 (NPP7), is specifically expressed in the gut in mammals and in the human liver and is the key enzyme for hydrolyzing phospholipids, such as SM, lysophosphatidylcholine (lyso-PC) and platelet activating factor (PAF), in the intestinal lumen [15,16]. In addition, a recent study reported that alk-SMase might play a role in intestinal immune homeostasis through

the regulation of dendritic cell and T-lymphocyte numbers in mesenteric lymph nodes and both the small and large intestines[17]. Therefore, the potential role of alk-SMase in intestinal inflammation has attracted increasing attention. Sjöqvist *et al*[18] reported that chronic colitis was associated with a reduction in mucosal alk-SMase activity, and the authors first suggested the role of alk-SMase in intestinal inflammation. Several studies have confirmed the anti-inflammatory effects of the enzyme on colitis and colitis-associated carcinogenesis[19-21]. Our previous research showed that alk-SMase deficiency increased autotaxin (NPP2) and upregulated the levels of the proinflammatory factor lysophosphatidic acid in a dextran sulfate sodium (DSS)-induced colitis model. Furthermore, the early increase in PAF could trigger DSS-induced inflammation[20]. However, whether alk-SMase affects specific factors related to the stability and permeability of the intestinal mucosa is still unknown.

In this study, we used alk-SMase gene knockout (KO) mice to further investigate the effect of alk-SMase on intestinal barrier function and mucosal permeability in DSS-induced colitis; DSS is a widely used colitis model because of its simplicity and many similarities with human UC[22]. We identified significant changes in several key molecules related to intestinal stability, permeability and antioxidant activity, thus deepening our understanding of the protective roles of these enzymes in the intestinal tract.

MATERIALS AND METHODS

Animals

Duan's group at Lund University, Sweden generously provided alk-SMase$^{-/-}$ mice generated from mice on a C57BL/6 background[23]. The alk-SMase$^{+/+}$ mice and alk-SMase$^{-/-}$ mice used in the experiments were crossbred from alk-SMase$^{+/-}$ mice. The genotypes of the animals were confirmed by polymerase chain reaction (PCR). All mice were kept in the animal facilities under laboratory conditions (23 °C, 12 h/12 h light/dark, 50% humidity, commercial standard pellets and free access to drinking water). The animal protocol was designed to minimize pain or discomfort. All the experimental animals were anesthetized with isoflurane prior to the operation.

Treatment of mice with DSS

Twelve-week-old mice were provided 3% DSS (MW 36000-50000) (MP Biomedicals, Santa Ana, CA, United States) in their daily drinking water for 4 or 6 d and were fed a normal diet during the induction of acute colitis. The disease activity index (DAI) was measured by examining weight loss, stool consistency and blood in the stool during the experiments according to previous methods[20] (Table 1). After DSS was induced, the mice were anesthetized by isoflurane inhalation, and blood was harvested for subsequent analysis. The organs were removed, and the colon length was measured. Colon tissue sections (0.5 mm) were stained with hematoxylin-eosin, and histopathological examinations were performed by microscopy. Colonic mucosal tissues were scraped for subsequent experiments. For the colitis model treated with tertiary butylhydroquinone (t-BHQ) (Sigma-Aldrich, St Louis, MO, United States), KO mice in the t-BHQ group were intraperitoneally injected with 50 mg/kg/d t-BHQ for 6 d and subsequently sacrificed. The experiments were performed as described above.

Detection of intestinal permeability

A fluorescein isothiocyanate dextran (FITC-D) experiment was performed to examine intestinal permeability. Briefly, on days 0, 4 and 6 after 3% DSS treatment, the mice were administered 4 kDa FITC-D (50 mg/100 g body weight) by gavage and sacrificed after 4 h. Serum was obtained by centrifugation at 1000 × *g* for 15 min, after which the fluorescence of FITC-D was measured with a fluorescence microplate reader at excitation and emission wavelengths of 485 nm and 535 nm, respectively. The concentration of FITC-D in serum was calculated based on the standard curve.

Analysis of lipopolysaccharide in serum and secretory immunoglobulin A in mucosal tissue by enzyme-linked immunosorbent assay

Mouse serum lipopolysaccharide (LPS) concentrations were analyzed using an enzyme-linked immunosorbent assay (ELISA) kit (AndyGene Biotechnology, Beijing, China). An anti-mouse LPS antibody was added to the microporous plate. Serum samples and standards were pipetted into separate wells, followed by the addition of a biotin-conjugated LPS antibody. The LPS in the sample or standard was sandwiched between pairs of antibodies. After the wells were thoroughly washed, HRP-conjugated streptavidin was added. The solution turned blue after the addition of the TMB substrate (HRP catalyzes the enzyme-substrate reaction). The LPS concentration of each serum sample was calculated using the standard curve. Intestinal mucosal tissue was homogenized and centrifuged, after which the proteins were extracted. The supernatant was carefully collected. The level of secretory immunoglobulin A (sIgA) in the intestinal mucosa was assessed by an ELISA kit (AndyGene Biotechnology) according to the manufacturer's instructions.

Assessment of intestinal ultrastructural changes by electron microscopy

Colon sections (0.5 cm) were removed and fixed in 2% glutaraldehyde. After fixation, embedding and staining, 60 nm continuous sections were cut. These sections were stained with 1% uranyl acetate for 20 min and lead citrate for 7 min. The microvilli, cell structure, organelles and cell junctions of intestinal mucosal epithelial cells were observed by electron microscopy.

Table 1 Assessment of the disease activity index scores

Score	Weight loss	Stool consistency	Blood in stool
0	None	Normal pellets	Negative
1	1%-5%	Slight loose but still sharp	Hemoccult positive
2	5%-10%	Loose pellet	Visual slightly bleeding
3	10%-15%	Loose feces and no shape	Obvious bleeding but no adhesion around the anus
4	> 15%	Diarrhea	Gross bleeding and blood incrustation around the anus

Protein isolation and western blotting

Colonic mucosal tissues were first lysed in RIPA buffer and subsequently homogenized on ice using a homogenizer. The supernatants of the homogenates were collected after centrifugation at 13500 × rpm at 4°C for 15 min. Total extracted proteins (50 μg) were separated by sodium-dodecyl sulfate gel electrophoresis, transferred to nitrocellulose membranes and blocked with 5% skim milk for 1 h at room temperature. Afterward, the membranes were incubated with primary antibodies overnight at 4°C. The primary antibodies used were claudin-3 (1:800 dilution) (Abcam, Cambridge, United Kingdom), claudin-5 (1:800 dilution) (Abcam), occludin (1:400 dilution) (Abcam), zonula occludens-1 (ZO-1) (1:500 dilution) (Abcam), nuclear factor erythroid 2-related factor 2 (Nrf2) (1:500 dilution) (Santa Cruz Biotechnology, Dallas, TX, United States) and β-actin (1:8000 dilution). The membranes were washed with TBST buffer three times for 10 min each. Then, the membranes were incubated with the appropriate peroxidase-conjugated secondary antibodies (1:20000 dilution), after which chemiluminescence was detected. ImageJ software was used to measure the optical density of the bands. The expression levels of the target proteins relative to β-actin were calculated.

Total RNA isolation and quantitative real-time reverse transcription-PCR

Total RNA was isolated from colonic mucosal tissues using TRIzol reagent (Invitrogen of Thermo Fisher Scientific, Waltham, MA, United States). To remove the inhibitory effect of DSS on qPCR, the RNA was purified using lithium chloride[24]. RNA concentration and purity were determined by using a Nanodrop (Thermo Fisher Scientific), and RNA integrity was verified by 2% agarose gel electrophoresis. Briefly, the RNA was reverse-transcribed into cDNA using ReverTra Ace qPCR RT Master Mix with gDNA Remover (Toyobo, Osaka, Japan). Real-time PCR was performed according to the instructions of the SYBR Green Real-time PCR Master Mix Kit (Toyobo). The primers used are shown in Table 2. The relative expression levels of the target genes were normalized to that of glyceraldehyde-3-phosphate dehydrogenase (GAPDH)[25,26] in each sample by the $2^{-\Delta\Delta Ct}$ method.

Detection of serum oxidant and antioxidant markers

The concentration of malondialdehyde (MDA) and the activities of superoxide dismutase (SOD) and glutathione peroxidase (GSH-Px) were determined using commercially available kits (Nanjing Jiancheng Bioengineering Institute, Nanjing, China) according to the manufacturer's instructions. The assay for SOD activity was based on its ability to inhibit the oxidation of hydroxylamine by $O_2^{\cdot-}$ produced from the xanthine-xanthine oxidase system. One unit of SOD activity was defined as the amount that reduced the absorbance at 550 nm by 50%. GSH-Px activity was assayed by quantifying the rate of oxidation of reduced glutathione to oxidized glutathione by H_2O_2, as catalyzed by GSH-Px. MDA levels were measured according to the thiobarbituric acid (TBA) method (Nanjing Jiancheng Bioengineering Institute). The method was based on spectrophotometric measurements of the color produced during the reaction of TBA with MDA. MDA concentrations were calculated by measuring the absorbance of TBA reactive substances at 532 nm.

Statistical analysis

The data are presented as the mean ± standard error of the mean. Each experiment was performed in triplicate and independently repeated a minimum of three times, and every experiment was performed with a sample size of no less than 3 mice per group. Statistical significance was assessed using an unpaired Student's *t*-test for 2-group comparisons. Multigroup comparisons were performed using one-way analysis of variance (ANOVA), followed by using the Least Significant Difference test. A P value < 0.05 was considered statistically significant. Data analysis was conducted using SPSS 20.0 software (IBM Corp., Armonk, NY, United States), while graphical representations were created using GraphPad Prism software, version 5 (GraphPad Software, Inc., La Jolla, CA, United States).

RESULTS

alk-SMase (NPP7) deficiency exacerbates DSS-induced colitis

In this study, 3% DSS successfully induced acute colitis in both wild-type (WT) and KO mice. As shown in Figure 1A, the body weights of WT and KO mice were slightly decreased on day 4 but were substantially decreased from day 5 to day 6 of DSS treatment. On day 6, the weight of KO mice decreased by 23.1%, whereas that of WT mice decreased by 14.5%. Similarly, the changes in the DAI scores were consistent with the effects on body weight, and the scores were significantly

Table 2 Quantitative real-time reverse transcription-polymerase chain reaction primers for target genes

Gene	Gene ID	Primer
ZO-1 F	21872	AGCTGCCTCGAACCTCTACTCTAC
ZO-1 R		GCCTGGTGGTGGAACTTGCTC
Occludin F	18260	TGCTTCATCGCTTCCTTAGTAA
Occludin R		GGGTTCACTCCCATTATGTACA
Claudin2 F	12738	GGGCAATCGTACCAACTA
Claudin2 R		CAGTCAGGCTGTATGAGTTG
Claudin3 F	12739	GGCGGCTCTGCTCACCTTA
Claudin3 R		CGTACAACCCAGCTCCCATC
Claudin5 F	12741	TGGTGCTGTGTCTGGTAGGATGG
Claudin5 R		GTCACGATGTTGTGGTCCAGGAAG
Claudin8 F	54420	TGTCTGCCTTCATCGAAAGTAA
Claudin8 R		GGCATGCCTCATACAATTCATC
MUC2 F	17831	TGCTGACGAGTGGTTGGTGAATG
MUC2 R		TGATGAGGTGGCAGACAGGAGAC
Nrf2 F	18024	CGAGATATACGCAGGAGAGGTAAGA
Nrf2 R		GCTCGACAATGTTCTCCAGCTT
HO-1 F	15368	ACCGCCTTCCTGCTCAACATTG
HO-1 R		CTCTGACGAAGTGACGCCATCTG
GSH-Px F	14775	AGGGCTGTGCTGATTGAGAATGTG
GSH-Px R		CTCCTGATGTCCGAACTGGTTGC
GCLc F	14629	ATGTGGACACCCGATGCAGTATT
GCLc R		TGTCTTGCTTGTAGTCAGGATGGTTT
SOD2 F	20656	TCCCAGACCTGCCTTACGACTATG
SOD2 R		CTCCTCGGTGGCGTTGAGATTG
GAPDH F	14433	GGTTGTCTCCTGCGACTTCA
GAPDH R		TGGTCCAGGGTTTCTTACTCC

F: Forward; GAPDH: Glyceraldehyde-3-phosphate dehydrogenase; GCLc: Glutamate-cysteine ligase catalytic subunit; GSH-Px: Glutathione peroxidase; HO-1: Heme oxygenase-1; MUC2: Mucin 2; Nrf2: Nuclear factor erythroid 2-related factor 2; R: Reverse; SOD: Superoxide; ZO-1: Zonula occludens-1.

higher in KO mice than in WT mice on day 6 (Figure 1B). Compared with those of WT mice, the colon lengths of KO mice were significantly shorter before DSS treatment or after DSS treatment for 6 d, as shown in Figure 1C. The changes in tumor necrosis factor-alpha and interleukin-6 levels were significantly higher in KO mice than in WT mice after DSS treatment for 4 d (Figure 1D).

Histopathological changes were characterized, and there were different degrees of epithelial damage, inflammatory cell infiltration, goblet cell depletion and crypt damage (Figure 1E). Before DSS induction, the colonic mucosal epithelium of WT and KO mice was intact, and abundant goblet cells were observed, with a clear mucosal structure and no inflammatory cell infiltration. On day 4 after DSS induction, WT mice exhibited relatively minor epithelial cell damage, reduced goblet cells, mild glandular hyperplasia, and infiltrating inflammatory cells. In contrast, KO mice exhibited extensive infiltration of inflammatory cells in the submucosal layer of connective tissue and a small amount of necrosis and desquamation of mucosal epithelial cells. By day 6, WT mice exhibited disorderly arranged glands, with partial necrosis and loss and a significant decrease in goblet cells. KO mice exhibited disruption of the intestinal epithelial layer, marked vascular dilation, abnormal morphology of goblet cells with a large cellular cavity, and widespread inflammation and inflammatory cells extending to blood vessels, the submucosa, and even the muscle layers.

alk-SMase (NPP7) deficiency increases intestinal mucosal permeability in DSS-induced colitis

To explore why the KO mice had more severe colitis than the WT mice, intestinal permeability after DSS administration was examined by measuring changes in the serum concentration of FITC-D. As shown in Figure 2A, the intestinal

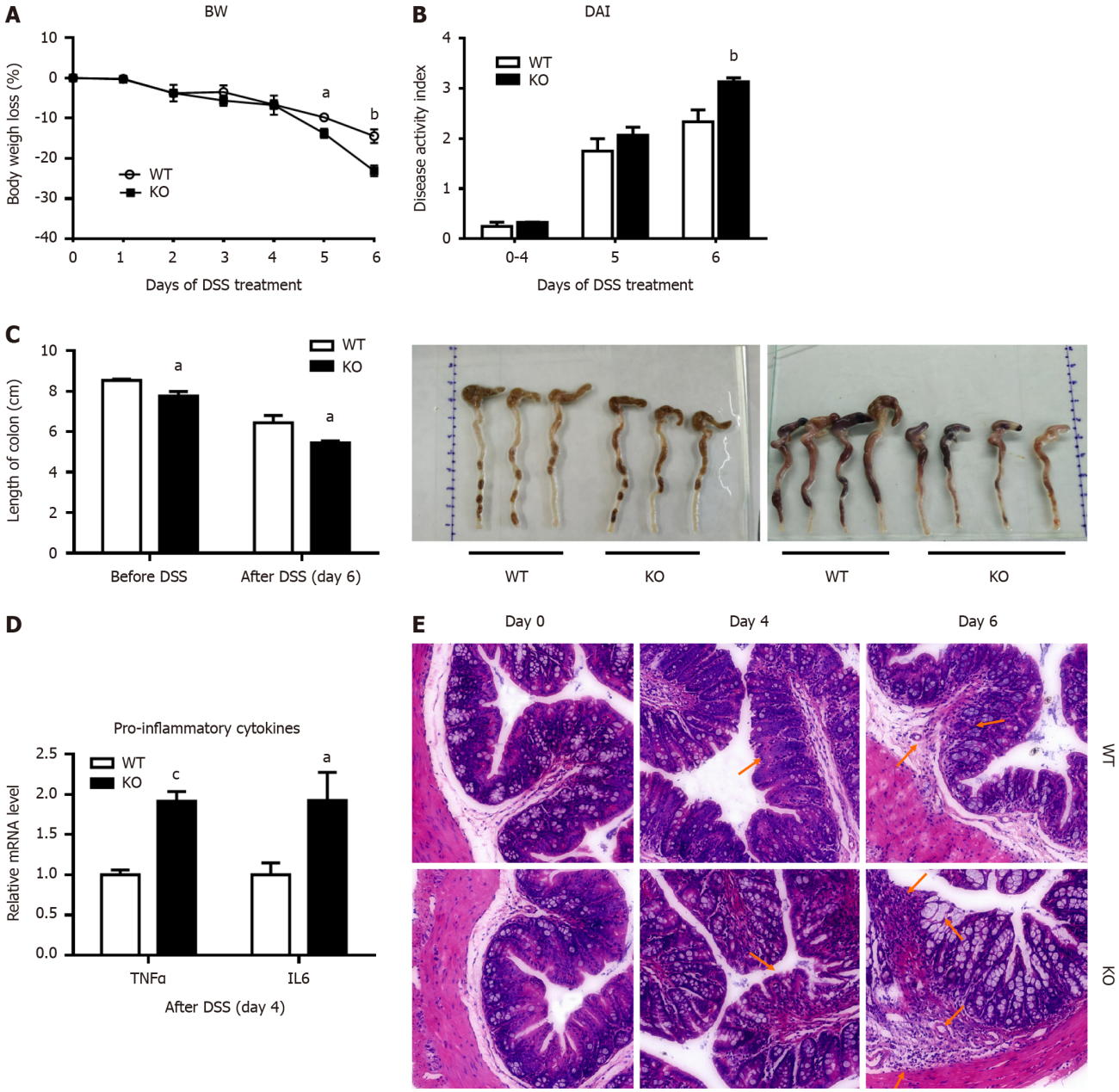

Figure 1 Alkaline sphingomyelinase deficiency exacerbates dextran sulfate sodium-induced colitis in mice. The mice were treated with 3% dextran sulfate sodium (DSS) in drinking water for 6 d. A: Body weight (BW) was measured, and the percentage of BW loss was calculated (n = 6 per group); B: The disease activity index (DAI) was calculated according to the stool bleeding score, BW loss, stool consistency, and disease signs (n = 4 per group); C: After 6 d of DSS treatment, the colon was removed, and the length of the colon was measured (before DSS, n = 3 per group; after DSS, n = 4 per group); D: The mRNA levels of tumor necrosis factor (TNF)-alpha and interleukin (IL)-6 in colonic mucosal tissue were analyzed (n = 4 per group); E: Histopathological characterization of the colon was performed. Arrows: Decreased goblet cells; dysplastic glands; dilated congested blood vessels; destroyed mucosal layer; severe damage to the intestinal epithelium; intensive inflammatory cell infiltration to the submucosa and muscularis. $^{a}P < 0.05$, $^{b}P < 0.01$, $^{c}P < 0.005$ compared with wild-type (WT). KO: Gene knockout.

permeability of WT mice and KO mice did not change before DSS induction. However, on day 4 ($P < 0.005$) and day 6 ($P < 0.05$) after DSS induction, the intestinal permeability of KO mice was significantly higher than that of WT mice. Therefore, we verified that alk-SMase deficiency enhanced intestinal epithelial permeability on day 4 of DSS-induced colitis.

To observe the extent of colonic epithelial cell damage, we compared the levels of the bacterial translocation marker LPS in the serum of WT and KO mice (Figure 2B). We found that the serum concentration of LPS was significantly increased in WT and KO mice after DSS induction, but there was no significant difference between WT and KO mice on day 4, while serum concentrations were significantly higher in KO mice than in WT mice on day 6. The damage to the colonic mucosal epithelial cells in the KO mice had occurred on day 4 and was more severe on day 6.

alk-SMase deficiency changes the expression of intestinal barrier proteins

The expression of ZO-1, occludin, claudin-2, claudin-3, claudin-5 and claudin-8 in mouse colonic mucosal tissues before and after DSS induction was examined. Before DSS treatment (day 0), the mRNA levels of claudin-3 and claudin-8 were

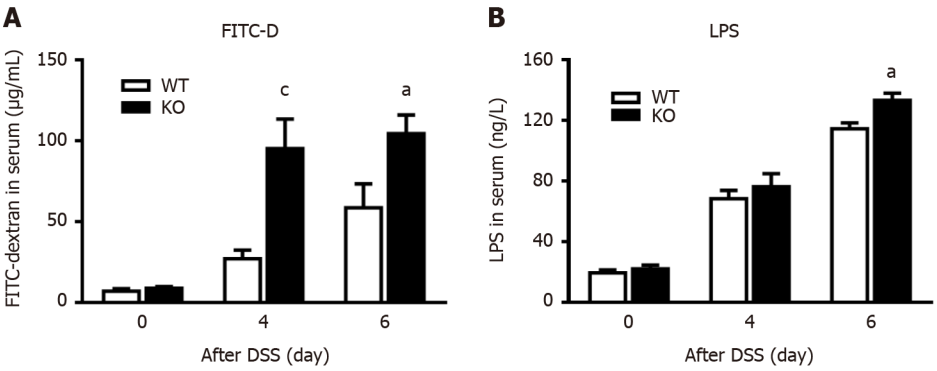

Figure 2 Alkaline sphingomyelinase deficiency increases intestinal permeability in dextran sulfate sodium-induced colitis. The mice were treated with 3% dextran sulfate sodium (DSS) water, and blood was collected on days 0, 4, and 6. A: The mice were administered 4 kDa fluorescein isothiocyanate dextran (FITC-D) by gavage 4 h before blood sampling, after which the fluorescence intensity of FITC-D in serum was measured (n = 5-9 per group); B: Serum lipopolysaccharide (LPS) concentrations were detected on days 0, 4, and 6 after DSS treatment (n = 3 per group). $^{a}P < 0.05$, $^{c}P < 0.005$ compared with wild-type (WT) mice. KO: Gene knockout.

significantly lower in KO mice than in WT mice, but claudin-5 mRNA levels were significantly lower (Figure 3A). However, the mRNA levels in KO mice were significantly lower than those in the WT mice after DSS induction (day 4) (Figure 3B). Western blotting was subsequently performed to detect the protein expression of ZO-1, occludin, claudin-3 and claudin-5. Before DSS treatment (day 0), the expression levels of all the proteins in KO mice were lower than those in WT mice ($P < 0.05$) (Figure 3C). However, after DSS induction for 4 d, the decreases in proteins levels in KO mice were more significant than those in WT mice ($P < 0.01$) (Figure 3D). Furthermore, the level of mucin 2 (MUC2), which is an important secretory protein in the gut, was significantly lower in KO mice than in WT mice on days 0 and 4 after DSS induction. We also examined the levels of the intestinal secretory protein sIgA, which is an important component of the intestinal mucosal immune barrier. On day 4 after DSS induction, sIgA levels were lower in WT and KO mice than before DSS induction, but no significant difference was observed between the two groups. However, on day 6, KO mice exhibited significantly lower levels of sIgA than WT mice, suggesting greater impairment of the intestinal immune barrier in KO mice (Figure 3E and F).

Ultrastructural changes in the colonic epithelial cells of alk-SMase KO mice

As shown in Figure 4, before DSS treatment (day 0), the ultrastructure of colonic mucosal epithelial cells was normal, as shown by electron microscopy. However, there was slight loss of microvilli, swollen mitochondria and impaired tight junctions (TJs) in WT mice and KO mice on day 4 of DSS induction. The damage to the intestinal mechanical barrier in KO mice was more severe than that in WT mice on day 4. Moreover, we found widespread mitochondrial swelling and degeneration in intestinal epithelial cells after DSS induction for 4 d. However, on day 6, compared with WT mice, KO mice exhibited more severe colonic epithelial damage, and the intestinal epithelial cells in KO mice showed abscission of microvilli, widening of intercellular spaces, severe disruption of TJs, nuclear pyknosis, and epithelial ablation, as shown by the arrows in Figure 4.

alk-SMase deficiency decreases antioxidant capacity in vivo

To verify whether mitochondrial damage caused changes in oxidative stress levels, changes in the antioxidant capability of serum were measured after DSS induction for 4 d. There was no difference in the levels of the antioxidant enzymes GSH-Px and SOD before DSS induction, but these levels were significantly lower in KO mice than in WT mice after DSS induction (Figure 5A and B). In contrast, the MOD of KO mice was significantly higher than that of WT mice after DSS induction (Figure 5C).

alk-SMase deficiency attenuates the antioxidant activity of colon tissues

To explore the extent to which antioxidant capacity decreased, changes in the expression of the key transcription factor Nrf2 in colonic mucosal tissues were examined. As shown in Figure 6A and B, the expression of Nrf2 in KO mice was significantly lower than that in WT mice after DSS stimulation for 4 d. Heme oxygenase-1 (HO-1), which is an antioxidant enzyme regulated by Nrf2, was further examined, and the mRNA level in KO mice was significantly lower than that in WT mice. Similarly, on day 4 after DSS treatment, the mRNA levels of GSH-Px, glutamate-cysteine ligase catalytic subunit (GCLc), and SOD in KO mice were significantly lower than those in WT mice (Figure 6C).

Nrf2 activation can rescue the effects of alk-SMase deficiency in colitis

To verify the effect of alk-SMase on the Nrf2 signaling pathway, KO mice were intraperitoneally injected with the Nrf2 activator t-BHQ every day during DSS induction. Body weight loss (Figure 7A), active state, stool consistency and blood in the stool were effectively alleviated by t-BHQ in KO mice. The increased DAI of KO mice after DSS treatment was significantly decreased by t-BHQ-mediated activation of Nrf2 (Figure 7B). Furthermore, the changes in the thymus, spleen, and liver weights caused by the knockout of alk-SMase were significantly reversed to almost the same levels as

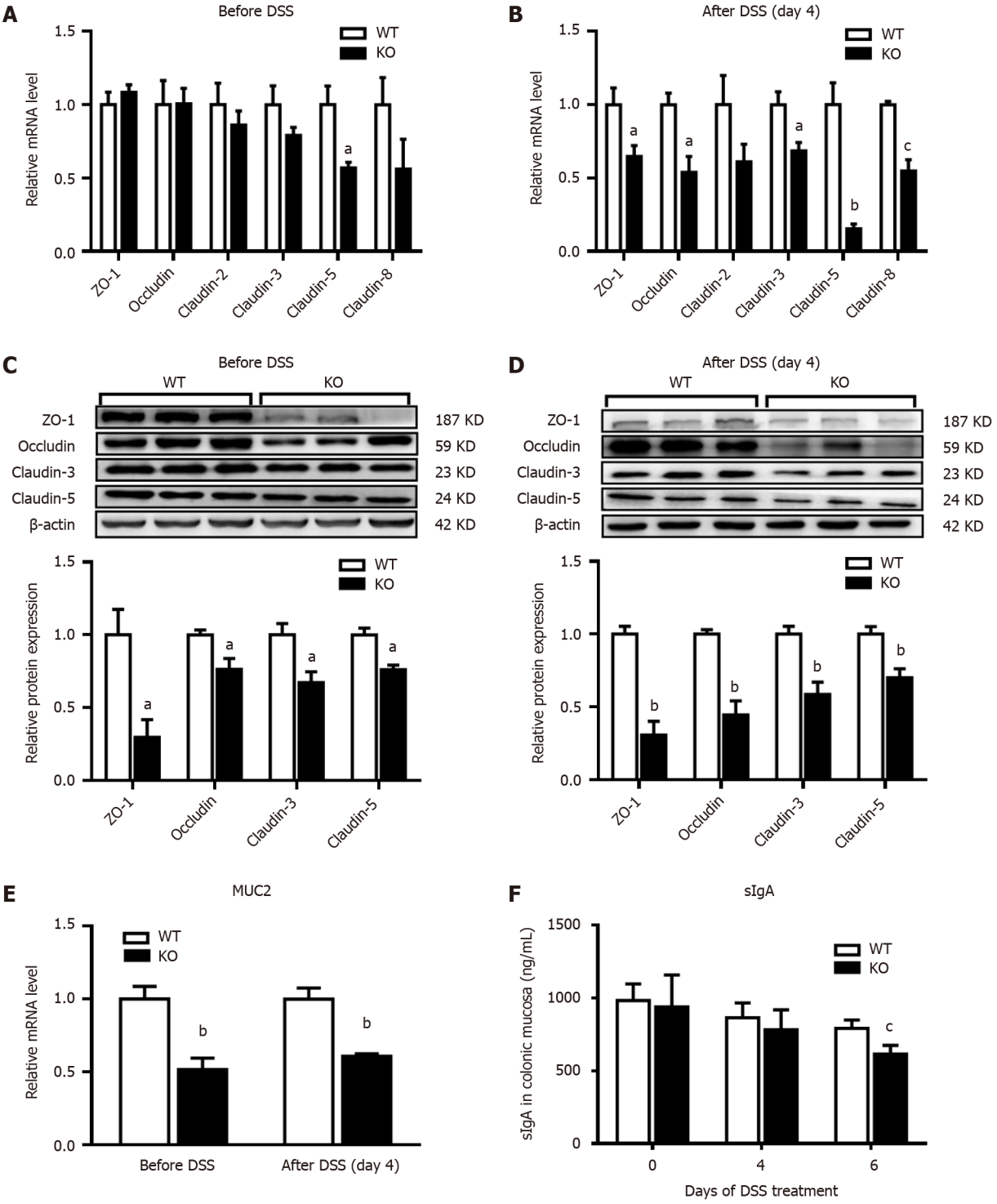

Figure 3 Changes in intestinal mucosal barrier proteins in mice after dextran sulfate sodium induction. The mice were given normal drinking water before dextran sulfate sodium (DSS) treatment, and then the mice were given 3% DSS water for 4 d. Quantitative real-time reverse transcription-polymerase chain reaction and western blot analysis of intestinal barrier proteins were performed on homogenates of colonic mucosa tissues. A and B: The relative mRNA levels were determined relative to those in the wild-type (WT) group; C and D: The densities of the bands were determined relative to those in the WT group; E: Mucin 2 (MUC2) mRNA levels were examined in the homogenates of colonic mucosa tissues; F: The animals were euthanized on days 0, 4, and 6 after receiving DSS water. The levels of secretory immunoglobulin A (sIgA) in the homogenates of colonic mucosa tissues were examined by enzyme-linked immunosorbent assay. n = 3 per group. $^{a}P < 0.05$, $^{b}P < 0.01$, $^{c}P < 0.005$ compared with WT mice. KO: Gene knockout; ZO-1: Zonula occludens-1.

those in WT mice after t-BHQ treatment of experimental colitis (Figure 7C-E). The colons of the KO mice treated with t-BHQ were obviously longer than those of KO mice that were not treated with t-BHQ (Figure 7F).

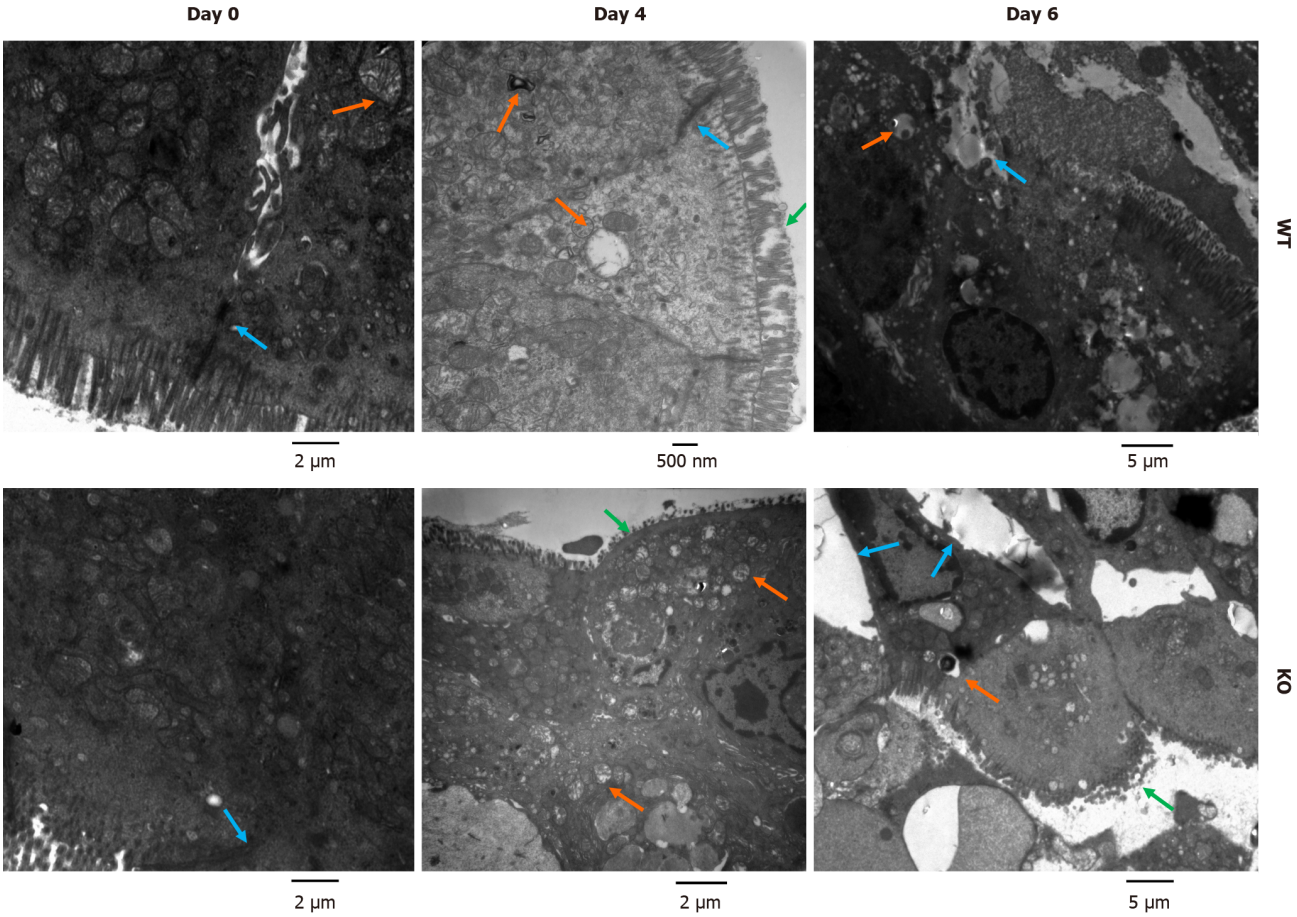

Figure 4 Ultrastructure of colonic mucosal epithelial cells in mice after dextran sulfate sodium induction. Mice were treated with 3% dextran sulfate sodium (DSS) water. Colon sections (0.5 cm) were removed on days 0, 4, and 6 after DSS treatment and fixed in 2% glutaraldehyde. The microvilli, cell structure, organelles and cell junctions of intestinal mucosal epithelial cells were examined by electron microscopy. Before DSS induction, the junctions between epithelial cells in wild-type (WT) and gene knockout (KO) mice were normal. After DSS induction, WT mice exhibited a loss of microvilli, pyknotic nuclei and impaired tight junctions. In KO mice, severe colonic epithelial damage was observed, and the intestinal epithelial cells exhibited damaged microvilli, widening of intercellular spaces, nuclear pyknosis, and mitochondrial swelling and degeneration (green arrows show damaged microvilli, orange arrows show mitochondrial swelling, and blue arrows show the intercellular space).

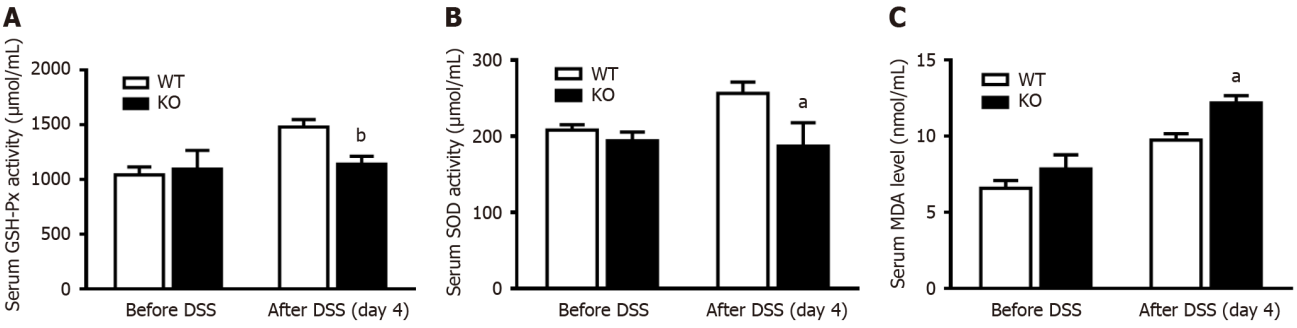

Figure 5 Changes in antioxidant enzyme activity in the serum of mice after dextran sulfate sodium induction. The mice were given normal drinking water before dextran sulfate sodium (DSS) treatment, and the mice were then given 3% DSS water for 4 d. The concentration of malondialdehyde (MDA) and the activities of superoxide (SOD) and glutathione peroxidase (GSH-Px) were determined before and after DSS induction for 4 d. A: Serum MDA levels; B: GSH-Px activity; C: SOD activity. n = 4 per group. $^{a}P < 0.05$, $^{b}P < 0.01$ compared with wild-type (WT) mice. KO: Gene knockout.

DISCUSSION

Alk-SMase is the key enzyme that hydrolyzes SM in the intestinal lumen. It can also hydrolyze many other phospholipids, such as lyso-PC and PAF[15,16]. In this study, alk-SMase KO mice were used to elucidate the pathogenesis of intestinal inflammation in an experimental colitis model and explore the mechanisms underlying the anti-inflammatory effect of alk-SMase. Our results were consistent with those of previous studies, in which weight was lower, the colon was shorter and the DAI was higher in alk-SMase KO mice than in control mice[20]. These findings confirmed that mice with

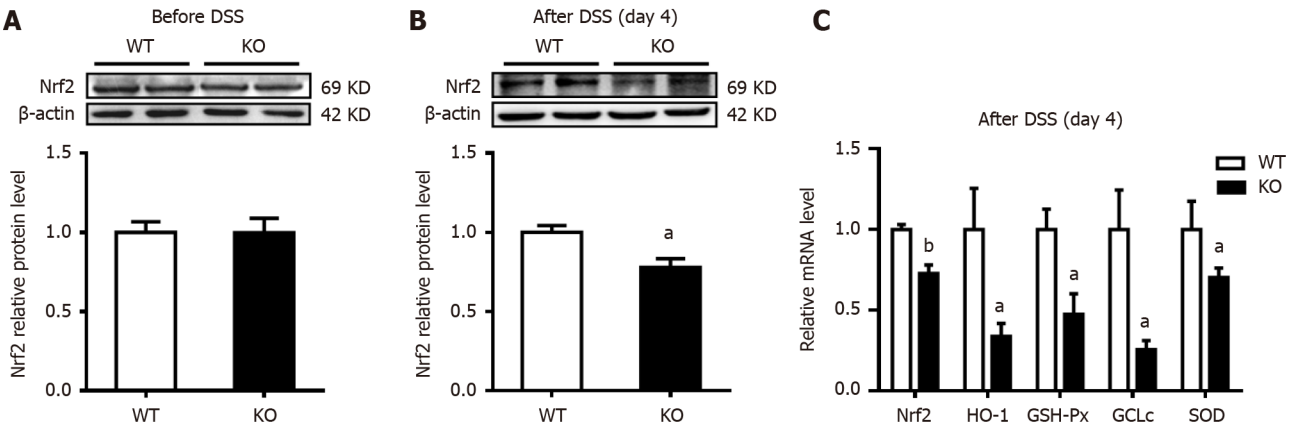

Figure 6 Changes in the expression of colonic nuclear factor erythroid 2-related factor 2 and antioxidant enzymes after dextran sulfate sodium induction. The mice were given normal drinking water before dextran sulfate sodium (DSS) treatment, and the mice were then given 3% DSS water for 4 d. A and B: Western blot analysis of nuclear factor erythroid 2-related factor 2 (Nrf2) was performed on homogenates of colonic mucosa tissues before and after DSS induction; C: Quantitative real-time reverse transcription-polymerase chain reaction was used to measure the mRNA levels of Nrf2 and its target antioxidant genes in colonic mucosa tissues. n = 4 per group. $^{a}P < 0.05$, $^{b}P < 0.01$ compared with wild-type (WT) mice. GCLc: Glutamate-cysteine ligase catalytic subunit; GSH-Px: Glutathione peroxidase; HO-1: Heme oxygenase-1; KO: Gene knockout; SOD: Superoxide.

alk-SMase deficiency developed more severe colitis than normal animals after DSS exposure. In this colitis model, we noticed significant changes in body weight and the DAI score on day 5 after DSS induction and only slight changes in all symptoms on day 4, indicating that intestinal epithelial damage did not occur on day 4. Therefore, it was reasonable to select the fourth day of DSS induction as the time point for follow-up experiments to observe the molecular changes induced by DSS in the intestine[27].

Previous studies have demonstrated the progressive downregulation of alk-SMase activity in patients with chronic UC and colorectal adenocarcinoma[18]. Intestinal alk-SMase has been shown to exert anti-inflammatory effects through the hydrolysis of SM and lyso-PC and inactivation of PAF[16,20,28,29]. However, the specific role of alk-SMase, which is a key enzyme involved in the hydrolysis of phospholipids in intestinal cell membranes, in intestinal barrier function and the underlying mechanism of its anti-inflammatory effect are poorly understood.

To assess damage to the intestinal mucosal barrier, we initially investigated changes in intestinal permeability in mice with DSS-induced colitis by measuring the concentration of FITC-D in the blood, which serves as a reliable indicator of an increase in permeability[30]. We observed a significant increase in FITC-D concentrations in the serum of all the mice following DSS induction, and KO mice exhibited higher levels of FITC-D than WT mice beginning on day 4. These findings suggest that KO mice experience more severe intestinal permeability during the inflammatory response than WT mice, indicating that alk-SMase deficiency exacerbates damage to the intestinal mucosal barrier in a DSS-induced colitis model.

The mechanical barrier of the intestine is crucial for preventing pathogen migration into the mucosa and subsequent inflammation; this barrier consists of TJs, adherens junctions, and desmosomes and plays a crucial role in maintaining the normal permeability of the intestinal mucosa[31]. Proteins such as occludin, claudins, and ZO-1, ZO-2, and ZO-3 are integral components of these junctions[32-34]. Clinical studies have demonstrated that patients with Crohn's disease exhibit decreased protein expression and redistribution of occludin, claudin-3, claudin-5, and claudin-8, while patients with UC exhibit decreased protein expression and redistribution of occludin, claudin-1, and claudin-4[33,34]. The physical and biochemical functions of the intestinal epithelium and its associated mucus layer are important not only for the colonization of beneficial bacteria but also for the maintenance of mucosal immune homeostasis[10].

To evaluate alterations in intestinal permeability, we assessed the expression of various proteins implicated in the integrity of the intestinal mucosal barrier. Our findings revealed that the deletion of alk-SMase in mice resulted in a significant reduction in the protein levels of ZO-1, occludin, claudin-3, and claudin-5 and in the mRNA level of MUC2 before and after DSS induction, indicating that the colonic mucosal barrier was unstable in KO mice that did not receive any inflammatory agents[35,36]. However, when stimulated with an inflammatory agent, the susceptibility of intestinal epithelial cells increased significantly, resulting in exacerbated intestinal barrier function damage in KO mice. Notably, these changes in protein expression were observed on day 4 of DSS treatment and preceded the onset of severe epithelial cell damage induced by DSS. Moreover, the levels of sIgA, an immune protein secreted by intestinal epithelial secretory cells[37], did not significantly change in mucosal tissue on day 4 after DSS induction but did significantly decrease on day 6. This observation suggested that intestinal secretory cells did not experience severe damage on the 4th d but did exhibit damage by the 6th d, which aligns with our initial hypothesis. These findings suggest that alk-SMase plays a critical role in maintaining mucosal barrier function by upregulating the expression of intestinal TJ proteins and mucin secretory molecules during the early stages of inflammation.

Furthermore, we performed electron microscopy to examine the ultrastructure of intestinal epithelial cells. Our observations revealed significant alterations in intercellular junctions, the inflammatory response, and organelles following inflammatory induction, and there were more pronounced changes in alk-SMase KO mice than in WT mice. Notably, alk-SMase-deficient intestinal epithelial cells exhibited substantial damage in the presence of the inflammatory

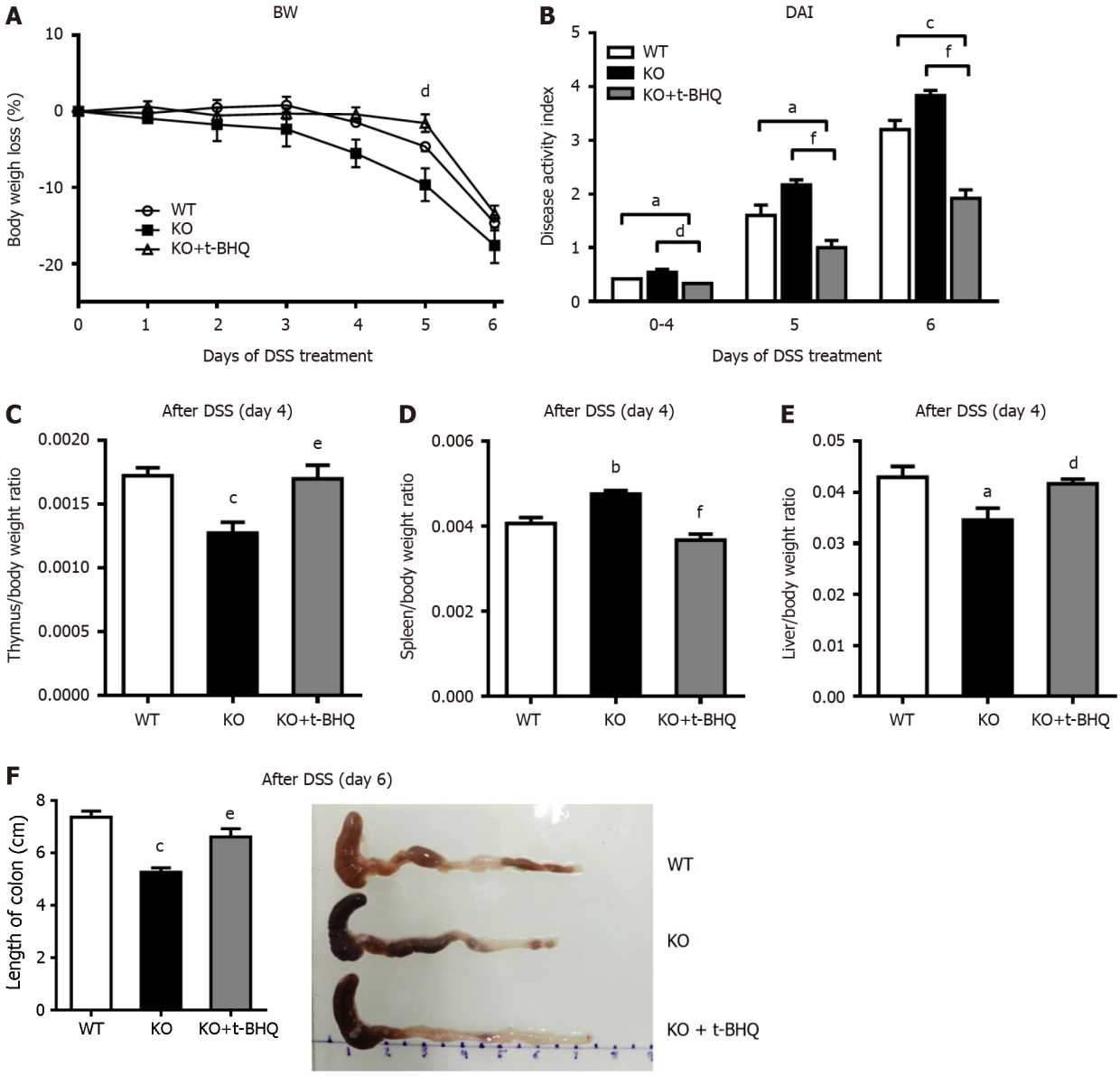

Figure 7 Changes in the incidence of experimental colitis after intraperitoneal injection of tertiary butylhydroquinone in mice. The mice were given 3% dextran sulfate sodium (DSS) drinking water for 6 d, and gene knockout (KO) mice in the tertiary butylhydroquinone (t-BHQ) group were intraperitoneally injected with 50 mg/kg t-BHQ every day. A: Body weight (BW) loss; B: The disease activity index (DAI), calculated according to BW loss, active state, stool consistency, and blood in the stool; C-E: On day 6 of DSS treatment, the mice were killed, the organs were removed and weighed, the ratios of organ weight to BW were calculated; F: The colon lengths were measured. n = 4 or 5 per group. $^{a}P < 0.05$, $^{b}P < 0.01$, $^{c}P < 0.005$, compared to wild-type (WT) mice. $^{d}P < 0.05$, $^{e}P < 0.01$, $^{f}P < 0.005$, compared to KO mice.

agent. These ultrastructural changes provide evidence of intestinal mucosal barrier damage that could lead to increased intestinal permeability. Additionally, during the ultrastructural examination, we observed common mitochondrial swelling in intestinal epithelial cells following DSS-induced inflammation, particularly in the context of alk-SMase deletion, indicating more pronounced mitochondrial degeneration. DSS-induced murine colitis has been previously reported to affect mitochondrial function, resulting in reduced intestinal barrier function and increased permeability[38-40].

To investigate whether alk-SMase exerts protective effects through the mitochondrial antioxidant pathway, we observed changes in the activity of several serum antioxidant enzymes. In general, mitochondria can be stimulated by cellular oxidative stress and produce antioxidants that play a key role in the anti-inflammatory response and in protecting against inflammatory agent invasion[41]. We observed changes in the activities of several serum antioxidant enzymes, such as GSH-Px and SOD, and the serum oxidative stress product MDA; we found that alk-SMase-deficient mice showed greater oxidative stress and decreased antioxidant capacity than WT mice after DSS induction. Several studies have reported the significant roles of SM, PC, and lyso-PC in maintaining intestinal mucosal barrier function and regulating permeability in UC[42-44]. Lipid peroxidation has been suggested to be a mechanism underlying sustained membrane permeability[45]. alk-SMase deficiency disrupts phospholipid metabolism and alters the levels of oxidized lipid molecules, which may contribute to changes in mucosal barrier function and the increase in permeability, thereby

influencing the progression of colon inflammation.

In the DSS-induced colitis model, intestinal inflammation regulates oxidative stress. Our study aimed to investigate the changes in oxidative stress molecules in intestinal mucosal tissue. Nrf2 is a transcription factor that binds to the promoters of downstream genes to upregulate expression and initiate the transcription of oxidative stress-related and anti-inflammatory genes[46,47]. In this study, we observed that alk-SMase regulated Nrf2 expression in colonic mucosal tissues during DSS-induced colitis. This regulation impacted the transcription levels of Nrf2 and its downstream genes, including HO-1, GSH-Px, GCLc, and SOD[48]. The downregulation of these antioxidant enzymes in the colonic mucosal tissues of alk-SMase-deficient mice confirmed the role of alk-SMase in regulating antioxidant capacity by decreasing Nrf2 levels in the DSS-induced colitis model.

The Nrf2 signaling pathway plays a crucial role in gastrointestinal tract function and is directly involved in the development of IBD. Drugs that modulate Nrf2 may be used to treat IBD[49]. Additionally, the previous study demonstrated that t-BHQ reduced intestinal epithelial cell injury and intestinal mucositis *via* activation of Nrf2[50]. To further confirm that alk-SMase regulates intestinal inflammation through the Nrf2 signaling pathway, alk-SMase KO mice with DSS-induced colitis were treated with t-BHQ, an activator of Nrf2[51]. In the present study, DSS inflammatory responses were effectively alleviated, and there were improvements in colonic length, body weight loss, stool bleeding, stool consistency, and disease signs. These results indicated that the downregulation of Nrf2 expression induced by alk-SMase deficiency was reversed.

Additionally, several studies have shown that Nrf2 can strengthen TJs in the intestinal epithelium[52,53]. Activation of the ERK/Nrf2/HO-1 signaling cascade reportedly enhanced the expression of occludin and ZO-1 proteins in the intestinal epithelial layer[54]. Furthermore, Nrf2 has been shown to bind to the promoter regions of certain claudins and increase their expression[55]. In our study, alk-SMase could maintain intestinal permeability, increase antioxidant capacity in colitis mice, and upregulate Nrf2. This effect may be one of the molecular mechanisms underlying the anti-inflammatory effect of alk-SMase. We propose that alk-SMase regulates intestinal mucosal barrier function and antioxidant capacity through the regulation of the Nrf2 signaling pathway. However, further research is needed to explore the relationship between these events and whether alk-SMase exerts anti-inflammatory effects through other pathways.

CONCLUSION

In conclusion, alk-SMase regulates the stability of the intestinal mucosal barrier and enhances antioxidant activity through the Nrf2 signaling pathway.

ARTICLE HIGHLIGHTS

Research background

Ulcerative colitis (UC) is a chronic inflammatory condition of the colon with unknown causes. Alkaline sphingomyelinase (alk-SMase), expressed in intestinal epithelial cells, shows anti-inflammatory effects, but its mechanism remains to be clarified.

Research motivation

This study was motivated by the need to understand the mechanism behind the anti-inflammatory effects of alk-SMase, particularly in relation to intestinal barrier function and oxidative stress in dextran sulfate sodium (DSS)-induced colitis.

Research objectives

The primary objective was to explore how alk-SMase impacts intestinal barrier function and manages oxidative stress, contributing to its anti-inflammatory role in DSS-induced colitis.

Research methods

Mice were given 3% DSS drinking water to induce colitis. The study assessed disease activity, intestinal permeability, bacterial translocation, and the ultrastructure of intestinal epithelial cells. Western blotting and quantitative real-time reverse transcription-polymerase chain reaction were employed to evaluate intestinal barrier proteins and mRNA, and serum oxidant and antioxidant levels were analyzed.

Research results

In gene knockout (KO) mice, inflammation and intestinal permeability were more severe compared to wild-type mice after DSS induction. There was a significant reduction in intestinal barrier proteins and an increase in serum malondialdehyde levels, indicating lower antioxidant capacity. Notably, the administration of the nuclear factor erythroid 2-related factor 2 (Nrf2) activator tertiary butylhydroquinone (t-BHQ) relieved colitis in KO mice.

Research conclusions

This study introduces the model that alk-SMase regulates intestinal barrier stability and antioxidant activity *via* the Nrf2

pathway, offering a new perspective on managing colitis. We employed a novel approach by using alk-SMase KO mice and treating them with t-BHQ to isolate and understand the specific effects of alk-SMase and Nrf2 in colitis.

Research perspectives

The findings underscore the potential of alk-SMase in maintaining intestinal barrier stability and increasing antioxidant capacity, offering insights into novel therapeutic approaches for colitis. Future research will delve into the mechanisms by which alk-SMase influences the Nrf2 pathway, further illuminating its therapeutic potential in colitis.

ACKNOWLEDGEMENTS

The authors would like to acknowledge the laboratory of Harbin Medical University for providing the laboratory space for part of the animal experiments.

FOOTNOTES

Co-first authors: Ye Tian and Xin Li.

Author contributions: Petersen JDD and Zhang P initiated the study; Tian Y, Li X, and Wang X contributed equally to this study; Li X and Wang X conducted the experiments; Tian Y wrote the manuscript; Pei ST, Pan HX, Cheng YQ, and Li YC conducted the preliminary data analysis; Zhang P contributed to the preliminary data analysis supervision; Cao WT reviewed and reanalyzed the data and confirmed the authenticity of the data. All of the authors discussed the results, commented on the manuscript, and approved the publication submission.

Supported by the Natural Science Foundation of Hainan Province, No. 823MS046; and the Talent Program of Hainan Medical University, No. XRC2022007.

Institutional animal care and use committee statement: This study was conducted in strict accordance with ethical guidelines for animal research. All experimental animals were housed in a controlled environment. Isoflurane was used for anesthesia prior to operations to minimize pain and discomfort. The experimental protocols involving animals were carefully designed to reduce suffering and were reviewed and approved by the Ethics Committee of Hainan Medical University (Approval No. HYLL-2022-128).

Conflict-of-interest statement: The authors report no relevant conflicts of interest for this article.

Data sharing statement: No additional data are available. The data for this study are available upon request to the corresponding author pending approval from Hainan Medical University.

ARRIVE guidelines statement: The authors have read the ARRIVE guidelines, and the manuscript was prepared and revised according to the ARRIVE guidelines.

Country/Territory of origin: China

ORCID number: Ping Zhang 0000-0002-0987-4949.

S-Editor: Wang JJ
L-Editor: Filipodia
P-Editor: Yuan YY

REFERENCES

1 **Nagao-Kitamoto H**, Kitamoto S, Kamada N. Inflammatory bowel disease and carcinogenesis. *Cancer Metastasis Rev* 2022; **41**: 301-316 [PMID: 35416564 DOI: 10.1007/s10555-022-10028-4]
2 **Du L**, Ha C. Epidemiology and Pathogenesis of Ulcerative Colitis. *Gastroenterol Clin North Am* 2020; **49**: 643-654 [PMID: 33121686 DOI: 10.1016/j.gtc.2020.07.005]
3 **Guo M**, Wang X. Pathological mechanism and targeted drugs of ulcerative colitis: A review. *Medicine (Baltimore)* 2023; **102**: e35020 [PMID: 37713856 DOI: 10.1097/MD.0000000000035020]
4 **Zhang Y**, Si X, Yang L, Wang H, Sun Y, Liu N. Association between intestinal microbiota and inflammatory bowel disease. *Animal Model Exp Med* 2022; **5**: 311-322 [PMID: 35808814 DOI: 10.1002/ame2.12255]
5 **Chen ML**, Sundrud MS. Cytokine Networks and T-Cell Subsets in Inflammatory Bowel Diseases. *Inflamm Bowel Dis* 2016; **22**: 1157-1167

[PMID: 26863267 DOI: 10.1097/MIB.0000000000000714]
6 **Fantini MC**, Guadagni I. From inflammation to colitis-associated colorectal cancer in inflammatory bowel disease: Pathogenesis and impact of current therapies. *Dig Liver Dis* 2021; **53**: 558-565 [PMID: 33541800 DOI: 10.1016/j.dld.2021.01.012]
7 **Grivennikov SI**. Inflammation and colorectal cancer: colitis-associated neoplasia. *Semin Immunopathol* 2013; **35**: 229-244 [PMID: 23161445 DOI: 10.1007/s00281-012-0352-6]
8 **Dey P**, Chaudhuri SR, Efferth T, Pal S. The intestinal 3M (microbiota, metabolism, metabolome) zeitgeist - from fundamentals to future challenges. *Free Radic Biol Med* 2021; **176**: 265-285 [PMID: 34610364 DOI: 10.1016/j.freeradbiomed.2021.09.026]
9 **Martínez Y**, Más D, Betancur C, Gebeyew K, Adebowale T, Hussain T, Lan W, Ding X. Role of the Phytochemical Compounds like Modulators in Gut Microbiota and Oxidative Stress. *Curr Pharm Des* 2020; **26**: 2642-2656 [PMID: 32410554 DOI: 10.2174/1381612826666200515132218]
10 **Stolfi C**, Maresca C, Monteleone G, Laudisi F. Implication of Intestinal Barrier Dysfunction in Gut Dysbiosis and Diseases. *Biomedicines* 2022; **10** [PMID: 35203499 DOI: 10.3390/biomedicines10020289]
11 **Wang K**, Ding Y, Xu C, Hao M, Li H, Ding L. Cldn-7 deficiency promotes experimental colitis and associated carcinogenesis by regulating intestinal epithelial integrity. *Oncoimmunology* 2021; **10**: 1923910 [PMID: 34026335 DOI: 10.1080/2162402X.2021.1923910]
12 **Barbara G**, Barbaro MR, Fuschi D, Palombo M, Falangone F, Cremon C, Marasco G, Stanghellini V. Inflammatory and Microbiota-Related Regulation of the Intestinal Epithelial Barrier. *Front Nutr* 2021; **8**: 718356 [PMID: 34589512 DOI: 10.3389/fnut.2021.718356]
13 **Okumura R**, Takeda K. Roles of intestinal epithelial cells in the maintenance of gut homeostasis. *Exp Mol Med* 2017; **49**: e338 [PMID: 28546564 DOI: 10.1038/emm.2017.20]
14 **Sharma A**, Rudra D. Emerging Functions of Regulatory T Cells in Tissue Homeostasis. *Front Immunol* 2018; **9**: 883 [PMID: 29887862 DOI: 10.3389/fimmu.2018.00883]
15 **Duan RD**. Alkaline sphingomyelinase: an old enzyme with novel implications. *Biochim Biophys Acta* 2006; **1761**: 281-291 [PMID: 16631405 DOI: 10.1016/j.bbalip.2006.03.007]
16 **Wu J**, Nilsson A, Jönsson BA, Stenstad H, Agace W, Cheng Y, Duan RD. Intestinal alkaline sphingomyelinase hydrolyses and inactivates platelet-activating factor by a phospholipase C activity. *Biochem J* 2006; **394**: 299-308 [PMID: 16255717 DOI: 10.1042/BJ20051121]
17 **Alyamani M**, Kadivar M, Erjefält J, Johansson-Lindbom B, Duan RD, Nilsson Å, Marsal J. Alkaline sphingomyelinase (NPP7) impacts the homeostasis of intestinal T lymphocyte populations. *Front Immunol* 2022; **13**: 1050625 [PMID: 36741374 DOI: 10.3389/fimmu.2022.1050625]
18 **Sjöqvist U**, Hertervig E, Nilsson A, Duan RD, Ost A, Tribukait B, Löfberg R. Chronic colitis is associated with a reduction of mucosal alkaline sphingomyelinase activity. *Inflamm Bowel Dis* 2002; **8**: 258-263 [PMID: 12131609 DOI: 10.1097/00054725-200207000-00004]
19 **Chen Y**, Zhang P, Xu SC, Yang L, Voss U, Ekblad E, Wu Y, Min Y, Hertervig E, Nilsson Å, Duan RD. Enhanced colonic tumorigenesis in alkaline sphingomyelinase (NPP7) knockout mice. *Mol Cancer Ther* 2015; **14**: 259-267 [PMID: 25381265 DOI: 10.1158/1535-7163.MCT-14-0468-T]
20 **Zhang P**, Chen Y, Zhang T, Zhu J, Zhao L, Li J, Wang G, Li Y, Xu S, Nilsson Å, Duan RD. Deficiency of alkaline SMase enhances dextran sulfate sodium-induced colitis in mice with upregulation of autotaxin. *J Lipid Res* 2018; **59**: 1841-1850 [PMID: 30087205 DOI: 10.1194/jlr.M084285]
21 **Andersson D**, Kotarsky K, Wu J, Agace W, Duan RD. Expression of alkaline sphingomyelinase in yeast cells and anti-inflammatory effects of the expressed enzyme in a rat colitis model. *Dig Dis Sci* 2009; **54**: 1440-1448 [PMID: 18989780 DOI: 10.1007/s10620-008-0509-2]
22 **Chassaing B**, Aitken JD, Malleshappa M, Vijay-Kumar M. Dextran sulfate sodium (DSS)-induced colitis in mice. *Curr Protoc Immunol* 2014; **104**: 15.25.1-15.25.14 [PMID: 24510619 DOI: 10.1002/0471142735.im1525s104]
23 **Zhang Y**, Cheng Y, Hansen GH, Niels-Christiansen LL, Koentgen F, Ohlsson L, Nilsson A, Duan RD. Crucial role of alkaline sphingomyelinase in sphingomyelin digestion: a study on enzyme knockout mice. *J Lipid Res* 2011; **52**: 771-781 [PMID: 21177474 DOI: 10.1194/jlr.M012880]
24 **Viennois E**, Chen F, Laroui H, Baker MT, Merlin D. Dextran sodium sulfate inhibits the activities of both polymerase and reverse transcriptase: lithium chloride purification, a rapid and efficient technique to purify RNA. *BMC Res Notes* 2013; **6**: 360 [PMID: 24010775 DOI: 10.1186/1756-0500-6-360]
25 **Yan F**, Wang L, Shi Y, Cao H, Liu L, Washington MK, Chaturvedi R, Israel DA, Wang B, Peek RM Jr, Wilson KT, Polk DB. Berberine promotes recovery of colitis and inhibits inflammatory responses in colonic macrophages and epithelial cells in DSS-treated mice. *Am J Physiol Gastrointest Liver Physiol* 2012; **302**: G504-G514 [PMID: 22173918 DOI: 10.1152/ajpgi.00312.2011]
26 **Bauer C**, Duewell P, Mayer C, Lehr HA, Fitzgerald KA, Dauer M, Tschopp J, Endres S, Latz E, Schnurr M. Colitis induced in mice with dextran sulfate sodium (DSS) is mediated by the NLRP3 inflammasome. *Gut* 2010; **59**: 1192-1199 [PMID: 20442201 DOI: 10.1136/gut.2009.197822]
27 **Cochran KE**, Lamson NG, Whitehead KA. Expanding the utility of the dextran sulfate sodium (DSS) mouse model to induce a clinically relevant loss of intestinal barrier function. *PeerJ* 2020; **8**: e8681 [PMID: 32195049 DOI: 10.7717/peerj.8681]
28 **Li Q**, Chen G, Zhu D, Zhang W, Qi S, Xue X, Wang K, Wu L. Effects of dietary phosphatidylcholine and sphingomyelin on DSS-induced colitis by regulating metabolism and gut microbiota in mice. *J Nutr Biochem* 2022; **105**: 109004 [PMID: 35351615 DOI: 10.1016/j.jnutbio.2022.109004]
29 **Yun CC**. Lysophosphatidic Acid and Autotaxin-associated Effects on the Initiation and Progression of Colorectal Cancer. *Cancers (Basel)* 2019; **11** [PMID: 31323936 DOI: 10.3390/cancers11070958]
30 **González-González M**, Díaz-Zepeda C, Eyzaguirre-Velásquez J, González-Arancibia C, Bravo JA, Julio-Pieper M. Investigating Gut Permeability in Animal Models of Disease. *Front Physiol* 2018; **9**: 1962 [PMID: 30697168 DOI: 10.3389/fphys.2018.01962]
31 **Nighot P**, Ma T. Endocytosis of Intestinal Tight Junction Proteins: In Time and Space. *Inflamm Bowel Dis* 2021; **27**: 283-290 [PMID: 32497180 DOI: 10.1093/ibd/izaa141]
32 **Landy J**, Ronde E, English N, Clark SK, Hart AL, Knight SC, Ciclitira PJ, Al-Hassi HO. Tight junctions in inflammatory bowel diseases and inflammatory bowel disease associated colorectal cancer. *World J Gastroenterol* 2016; **22**: 3117-3126 [PMID: 27003989 DOI: 10.3748/wjg.v22.i11.3117]
33 **Zeissig S**, Bürgel N, Günzel D, Richter J, Mankertz J, Wahnschaffe U, Kroesen AJ, Zeitz M, Fromm M, Schulzke JD. Changes in expression and distribution of claudin 2, 5 and 8 lead to discontinuous tight junctions and barrier dysfunction in active Crohn's disease. *Gut* 2007; **56**: 61-72 [PMID: 16822808 DOI: 10.1136/gut.2006.094375]
34 **Vetrano S**, Rescigno M, Cera MR, Correale C, Rumio C, Doni A, Fantini M, Sturm A, Borroni E, Repici A, Locati M, Malesci A, Dejana E,

Danese S. Unique role of junctional adhesion molecule-a in maintaining mucosal homeostasis in inflammatory bowel disease. *Gastroenterology* 2008; **135**: 173-184 [PMID: 18514073 DOI: 10.1053/j.gastro.2008.04.002]

35 **Liu Y**, Yu X, Zhao J, Zhang H, Zhai Q, Chen W. The role of MUC2 mucin in intestinal homeostasis and the impact of dietary components on MUC2 expression. *Int J Biol Macromol* 2020; **164**: 884-891 [PMID: 32707285 DOI: 10.1016/j.ijbiomac.2020.07.191]

36 **Ma TY**, Nighot P, Al-Sadi R. Tight junctions and the intestinal barrier. In: Physiology of the gastrointestinal tract (sixth edition). United States: Elsevier, 2018: 587-639

37 **Pietrzak B**, Tomela K, Olejnik-Schmidt A, Mackiewicz A, Schmidt M. Secretory IgA in Intestinal Mucosal Secretions as an Adaptive Barrier against Microbial Cells. *Int J Mol Sci* 2020; **21** [PMID: 33291586 DOI: 10.3390/ijms21239254]

38 **Wang A**, Keita ÅV, Phan V, McKay CM, Schoultz I, Lee J, Murphy MP, Fernando M, Ronaghan N, Balce D, Yates R, Dicay M, Beck PL, MacNaughton WK, Söderholm JD, McKay DM. Targeting mitochondria-derived reactive oxygen species to reduce epithelial barrier dysfunction and colitis. *Am J Pathol* 2014; **184**: 2516-2527 [PMID: 25034594 DOI: 10.1016/j.ajpath.2014.05.019]

39 **Amrouche-Mekkioui I**, Djerdjouri B. N-acetylcysteine improves redox status, mitochondrial dysfunction, mucin-depleted crypts and epithelial hyperplasia in dextran sulfate sodium-induced oxidative colitis in mice. *Eur J Pharmacol* 2012; **691**: 209-217 [PMID: 22732651 DOI: 10.1016/j.ejphar.2012.06.014]

40 **Goudie L**, Mancini NL, Shutt TE, Holloway GP, Mu C, Wang A, McKay DM, Shearer J. Impact of experimental colitis on mitochondrial bioenergetics in intestinal epithelial cells. *Sci Rep* 2022; **12**: 7453 [PMID: 35523978 DOI: 10.1038/s41598-022-11123-w]

41 **Chen Y**, Zhou Z, Min W. Mitochondria, Oxidative Stress and Innate Immunity. *Front Physiol* 2018; **9**: 1487 [PMID: 30405440 DOI: 10.3389/fphys.2018.01487]

42 **Schneider H**, Braun A, Füllekrug J, Stremmel W, Ehehalt R. Lipid based therapy for ulcerative colitis-modulation of intestinal mucus membrane phospholipids as a tool to influence inflammation. *Int J Mol Sci* 2010; **11**: 4149-4164 [PMID: 21152327 DOI: 10.3390/ijms11104149]

43 **Sugita M**, Fujie T, Yanagisawa K, Ohue M, Akiyama Y. Lipid Composition Is Critical for Accurate Membrane Permeability Prediction of Cyclic Peptides by Molecular Dynamics Simulations. *J Chem Inf Model* 2022; **62**: 4549-4560 [PMID: 36053061 DOI: 10.1021/acs.jcim.2c00931]

44 **Sukocheva OA**, Lukina E, McGowan E, Bishayee A. Sphingolipids as mediators of inflammation and novel therapeutic target in inflammatory bowel disease. *Adv Protein Chem Struct Biol* 2020; **120**: 123-158 [PMID: 32085881 DOI: 10.1016/bs.apcsb.2019.11.003]

45 **Wiczew D**, Szulc N, Tarek M. Molecular dynamics simulations of the effects of lipid oxidation on the permeability of cell membranes. *Bioelectrochemistry* 2021; **141**: 107869 [PMID: 34119820 DOI: 10.1016/j.bioelechem.2021.107869]

46 **He F**, Ru X, Wen T. NRF2, a Transcription Factor for Stress Response and Beyond. *Int J Mol Sci* 2020; **21** [PMID: 32640524 DOI: 10.3390/ijms21134777]

47 **Piechota-Polanczyk A**, Fichna J. Review article: the role of oxidative stress in pathogenesis and treatment of inflammatory bowel diseases. *Naunyn Schmiedebergs Arch Pharmacol* 2014; **387**: 605-620 [PMID: 24798211 DOI: 10.1007/s00210-014-0985-1]

48 **Audousset C**, McGovern T, Martin JG. Role of Nrf2 in Disease: Novel Molecular Mechanisms and Therapeutic Approaches - Pulmonary Disease/Asthma. *Front Physiol* 2021; **12**: 727806 [PMID: 34658913 DOI: 10.3389/fphys.2021.727806]

49 **Piotrowska M**, Swierczynski M, Fichna J, Piechota-Polanczyk A. The Nrf2 in the pathophysiology of the intestine: Molecular mechanisms and therapeutic implications for inflammatory bowel diseases. *Pharmacol Res* 2021; **163**: 105243 [PMID: 33080322 DOI: 10.1016/j.phrs.2020.105243]

50 **Deng S**, Wu D, Li L, Li J, Xu Y. TBHQ attenuates ferroptosis against 5-fluorouracil-induced intestinal epithelial cell injury and intestinal mucositis *via* activation of Nrf2. *Cell Mol Biol Lett* 2021; **26**: 48 [PMID: 34794379 DOI: 10.1186/s11658-021-00294-5]

51 **Bursley JK**, Rockwell CE. Nrf2-dependent and -independent effects of tBHQ in activated murine B cells. *Food Chem Toxicol* 2020; **145**: 111595 [PMID: 32702509 DOI: 10.1016/j.fct.2020.111595]

52 **Lau WL**, Liu SM, Pahlevan S, Yuan J, Khazaeli M, Ni Z, Chan JY, Vaziri ND. Role of Nrf2 dysfunction in uremia-associated intestinal inflammation and epithelial barrier disruption. *Dig Dis Sci* 2015; **60**: 1215-1222 [PMID: 25399330 DOI: 10.1007/s10620-014-3428-4]

53 **Lechuga S**, Ivanov AI. Disruption of the epithelial barrier during intestinal inflammation: Quest for new molecules and mechanisms. *Biochim Biophys Acta Mol Cell Res* 2017; **1864**: 1183-1194 [PMID: 28322932 DOI: 10.1016/j.bbamcr.2017.03.007]

54 **Liu Y**, Bao Z, Xu X, Chao H, Lin C, Li Z, Liu Y, Wang X, You Y, Liu N, Ji J. Extracellular Signal-Regulated Kinase/Nuclear Factor-Erythroid2-like2/Heme Oxygenase-1 Pathway-Mediated Mitophagy Alleviates Traumatic Brain Injury-Induced Intestinal Mucosa Damage and Epithelial Barrier Dysfunction. *J Neurotrauma* 2017; **34**: 2119-2131 [PMID: 28093052 DOI: 10.1089/neu.2016.4764]

55 **Fan X**, Staitieh BS, Jensen JS, Mould KJ, Greenberg JA, Joshi PC, Koval M, Guidot DM. Activating the Nrf2-mediated antioxidant response element restores barrier function in the alveolar epithelium of HIV-1 transgenic rats. *Am J Physiol Lung Cell Mol Physiol* 2013; **305**: L267-L277 [PMID: 23748533 DOI: 10.1152/ajplung.00288.2012]

World Journal of Gastroenterology

Submit a Manuscript: https://www.f6publishing.com

World J Gastroenterol 2024 March 14; 30(10): 1420-1430

DOI: 10.3748/wjg.v30.i10.1420

ISSN 1007-9327 (print) ISSN 2219-2840 (online)

ORIGINAL ARTICLE

Basic Study

Preliminary exploration of animal models of congenital choledochal cysts

Shu-Hao Zhang, Yue-Bin Zhang, Duo-Te Cai, Tao Pan, Ken Chen, Yi Jin, Wen-Juan Luo, Zong-Wei Huang, Qing-Jiang Chen, Zhi-Gang Gao

Specialty type: Gastroenterology and hepatology

Provenance and peer review: Unsolicited article; Externally peer reviewed.

Peer-review model: Single blind

Peer-review report's scientific quality classification

Grade A (Excellent): 0
Grade B (Very good): B, B
Grade C (Good): 0
Grade D (Fair): 0
Grade E (Poor): 0

P-Reviewer: Kordzaia D, Georgia; Mijwil MM, Iraq

Received: October 17, 2023
Peer-review started: October 17, 2023
First decision: January 15, 2024
Revised: January 17, 2024
Accepted: February 21, 2024
Article in press: February 21, 2024
Published online: March 14, 2024

Shu-Hao Zhang, Yue-Bin Zhang, Duo-Te Cai, Tao Pan, Ken Chen, Yi Jin, Wen-Juan Luo, Zong-Wei Huang, Qing-Jiang Chen, Zhi-Gang Gao, Department of General Surgery, Children's Hospital, Zhejiang University School of Medicine, Hangzhou 310000, Zhejiang Province, China

Corresponding author: Zhi-Gang Gao, PhD, Chief Doctor, Department of General Surgery, Children's Hospital, Zhejiang University School of Medicine, No. 3333 Binsheng Road, Binjiang District, Hangzhou 310000, Zhejiang Province, China. ebwk@zju.edu.cn

Abstract

BACKGROUND

Various animal models have been used to explore the pathogenesis of choledochal cysts (CCs), but with little convincing results. Current surgical techniques can achieve satisfactory outcomes for treatment of CCs. Consequently, recent studies have focused more on clinical issues rather than basic research. Therefore, we need appropriate animal models to further basic research.

AIM

To establish an appropriate animal model that may contribute to the investigation of the pathogenesis of CCs.

METHODS

Eighty-four specific pathogen-free female Sprague-Dawley rats were randomly allocated to a surgical group, sham surgical group, or control group. A rat model of CC was established by partial ligation of the bile duct. The reliability of the model was confirmed by measurements of serum biochemical indices, morphology of common bile ducts of the rats as well as molecular biology experiments in rat and human tissues.

RESULTS

Dilation classified as mild (diameter, ≥ 1 mm to < 3 mm), moderate (≥ 3 mm to < 10 mm), and severe (≥ 10 mm) was observed in 17, 17, and 2 rats in the surgical group, respectively, while no dilation was observed in the control and sham surgical groups. Serum levels of alanine aminotransferase, aspartate aminotransferase, total bilirubin, direct bilirubin, and total bile acids were significantly elevated in the surgical group as compared to the control group 7 d after surgery, while direct bilirubin, total bilirubin, and gamma-glutamyltransferase were

further increased 14 d after surgery. Most of the biochemical indices gradually decreased to normal ranges 28 d after surgery. The protein expression trend of signal transducer and activator of transcription 3 in rat model was consistent with the human CC tissues.

CONCLUSION
The model of partial ligation of the bile duct of juvenile rats could morphologically simulate the cystic or fusiform CC, which may contribute to investigating the pathogenesis of CC.

Key Words: Choledochal cyst; Animal model; Partial ligation; Cystic and fusiform dilation; Juvenile rats

Core Tip: Recent studies have focused more on clinical issues rather than etiology and pathogenesis of choledochal cyst (CC). In this study, our partial ligation of the bile duct of juvenile rats successfully simulated the pathological processes of recanalization after incomplete obstruction of the distal bile duct. The postoperative disease progression of this model was more consistent with the natural course of CC formation which may assist in further basic research on the pathogenesis of CC.

Citation: Zhang SH, Zhang YB, Cai DT, Pan T, Chen K, Jin Y, Luo WJ, Huang ZW, Chen QJ, Gao ZG. Preliminary exploration of animal models of congenital choledochal cysts. *World J Gastroenterol* 2024; 30(10): 1420-1430
URL: https://www.wjgnet.com/1007-9327/full/v30/i10/1420.htm
DOI: https://dx.doi.org/10.3748/wjg.v30.i10.1420

INTRODUCTION

Choledochal cyst (CC) is a congenital hepatic malformation characterized by cystic or fusiform dilation of the common bile duct either with or without dilation of the intrahepatic bile duct. The hypothesis of pancreaticobiliary maljunction (PBM) proposed by Babbit[1] in 1969 is the most likely cause of CC, emphasizing that pancreatic juice could cause segmental stricture, fibrosis, and thinning of the common bile duct. However, with the increased proportion of prenatal diagnosis of CCs, researchers have found that pancreatic acini are just beginning to appear, enzymes are immature during that time period, and there is no evidence of pancreatic secretion observed by electron microscopy[2]. Therefore, the role of fetal pancreatic juice in the formation of CCs remains controversial because the pancreas of newborns does not yet produce functional enzymes[3]. Accumulating evidence from clinical cases suggests that PBM cannot fully explain the pathogenesis of CCs.

Various animal models to simulate the disease process in humans have been used to investigate the pathogenesis of cystic and fusiform CCs. However, anastomosis of the pancreatic and biliary ducts, which allow pancreatic juice to enter the bile duct, only resulted in mild dilation of the common bile duct without cystic dilatation[4]. Moreover, even in large animal models, such as minipigs, no one was observed to have dilatation of the bile ducts[5]. In contrast, complete ligation of the lower segment of the common bile duct in neonatal lambs[6] and infant rats[7] can successfully create a model of cystic dilation, while in mature sheep, rats, dogs or rabbits, no cystic dilation was observed through the ligation of the lower segment of the common bile duct. However, it is not recognized as a conventional CC animal model because it does not conform to the mainstream hypothesis of PBM. Some researchers also constructed an animal model by combining anastomosis of the pancreatic and biliary ducts with ligation of the lower segment of the common bile duct. However, it is still unclear whether dilation of the common bile duct is caused solely by ligation of the lower segment or by the combination of both factors. Satisfactory outcomes achieved with current surgical techniques for CCs have led to a pause in basic research on the etiology of CCs, and recent studies have primarily focused on reporting large clinical series, improvements of surgical techniques and the management of postoperative complications[8]. Hence, appropriate animal models should be established to further basic research. In our study, our partial ligation of the bile duct of juvenile rats successfully simulated the pathological processes of recanalization after incomplete obstruction of the distal bile duct. The postoperative changing trends of biochemical indexes in rat model was similar to those observed in CCs, and the changing trend of signal transducer and activator of transcription 3 (STAT3) in the rat model was consistent with that observed in human CC tissues. Therefore, our study has established an animal model that may contribute to the investigation of the pathogenesis of CCs.

MATERIALS AND METHODS

Experimental animals and grouping

Specific pathogen-free female SD rats (n = 84; mean body weight, 200 g ± 10 g) were purchased from Sibeifu Biotech-

nology Co., Ltd. (Beijing, China) and housed in an animal care facility operated by Zhejiang Yingyang Pharmaceutical Co., Ltd., (Hangzhou, China) at a constant temperature of 22 °C ± 2 °C and humidity of 50%-60% under a 12-h light-dark cycle with total air exchange at 15-20 times/h.

The 84 rats were randomly allocated to one of 7 groups of 12 rats each. Rats in groups A, B, and C were dissected on days 7, 14, and 28 after partial ligation of the bile duct, respectively. Rats in group D were dissected on day 28 after sham surgery without bile duct ligation. Rats in groups E, F, and G were dissected after 7 d, 14 d, and 28 d of feeding, respectively.

Partial ligation surgery of the bile duct of infant rats

(1) Anesthesia: 2.5% pentobarbital sodium (0.25 mL/100 g) was injected into the abdominal cavity; (2) Positioning: After anesthesia, the rats were fixed with a supine position on the surgical table; (3) Skin preparation: The hair below the xiphoid process in the middle of the abdomen was removed with an electric shaver, exposing about 5 cm × 3 cm of skin, followed by iodine disinfection; (4) Skin incision: A midline longitudinal incision was made on the abdomen with surgical scissors, about 2 cm in length; (5) Bile duct isolation: Wet cotton swabs were used to separate the organs and locate the duodenum and pancreas, and then the bile duct was located with forceps; (6) Partial ligation: Place a 1 mL needle parallel to the bile duct and use 6-0 absorbable suture to ligate the bile duct and needle together at the lower segment of the bile duct. Then the needle was removed carefully after tightening the absorbable suture; and (7) Closure of the incision: After ligation, and the incision was intermittently sutured with 5-0 silk thread. Penicillin was administered intraperitoneally to prevent infection (0.3 mL, 400000 units/mL). Detailed surgical procedures were shown in Figure 1.

lncRNA sequencing analysis

An adequate amounts of human bile duct tissues were sent for lncRNA sequencing analysis. The pretreatment of tissue specimens, filtration of sequencing data, obtainment of clean reads, calculation of gene expression levels and differential expression analysis were performed by BGI Genomics CO., Ltd (seen in previous reported study[9]). To gain insights into the phenotypic changes, GO (http://www.geneontology.org/) and KEGG (https://www.kegg.jp/) enrichment analysis of annotated differentially expressed genes was performed using Phyper (https://en.wikipedia.org/wiki/Hypergeometric_distribution) based on the Hypergeometric test. The significant levels of terms and pathways were rigorously corrected using a *Q* value threshold of ≤ 0.05 by Bonferroni[10].

Biochemical indices in rat plasma

The rat blood samples were centrifuged at 3000-4000 rpm for 10 min at 4 °C and the plasma was frozen for further analysis of biochemical parameters, which included alanine aminotransferase (ALT), aspartate aminotransferase (AST), total bilirubin (TBIL), direct bilirubin (DBIL), gamma-glutamyltransferase (GGT), and total bile acids (TBA). Reagent kits from Ningbo Puruibo company were shown as follows: ALT kit (Lot: ALT01), AST kit (Lot: AST01), TBA kit (Lot: TBA01S), DBIL kit (Lot: DBI01), TBIL kit (Lot: TBI01), and GGT kit (Lot: GGT01).

Molecular biology detection of human and rat common bile duct tissues

RNA Isolation and quantitative reverse transcription-polymerase chain reaction: Total cellular RNA was extracted from CC patients' common bile ducts and rats' common bile ducts with TRIzol reagent (Invitrogen, cat. 15596026/15596018) and subjected to reverse transcription with PrimeScript RT reagent Kit (Takara, cat. RR037A) according to the manufacturers' instructions. The expressions of IL-6 and STAT3 were analyzed *via* quantitative reverse transcription-polymerase chain reaction (RT-qPCR) with a SYBR Premix EX Taq (Tli RNaseH plus, Takara, cat. RR420A) with primers listed in Table 1. For analysis, expression levels of the genes were normalized to the values of GAPDH. Analysis of relative gene expression data using real-time quantitative PCR was calculated with the 2-11Ct method[11].

Western blot: Tissue samples (50 mg) were washed with Tris-buffered saline to remove residual blood and ground into small fragments, which were lysed with radioimmunoprecipitation assay on ice for 30 min. After addition of protein inhibitors, the mixture was centrifuged at 13000 rpm for 10-15 min and the supernatant was collected. Then, 5 × loading buffer was added and the mixture was heated in a metal bath at 95 °C for 5 min to fully denature the proteins. Protein levels were determined against standards. Protein expression levels of STAT3 and phosphorylated (p)-STAT3 and were normalized to expression of glyceraldehyde 3-phosphate dehydrogenase.

Immunofluorescence histochemistry: The common bile duct sections were deparaffinized in three changes of xylene and two changes of 100% ethanol and subsequent gradation of 95%, 80%, and 70% alcohol for 3 min each. After being heat-induced epitope retrieval with a preheated epitope retrieval solution (pH 8.0, Enzo Life Sciences, Inc. United States), endogenous peroxidase was inactivated by incubation in 3% H_2O_2 for 20 min. Next, the sections were pre-incubated with 10% normal goat serum and then incubated overnight with primary antibodies: p-STAT3 (Abcam, ab76315). The next day, after washing, sections were incubated with Alexa Fluoro 488 Goat Anti-Rabbit IgG (Jackson, 111-545-144). At last, sections were counterstained with DAPI (Sigma-Aldrich). Slides were imaged using the Carl Zeiss Scope.A1.

Statistical analysis

Data were shown as the medians ± IQRs or mean ± SEM depending on data characteristics. Statistical analysis was performed with SPSS18.0 and Graphpad Prism 6. Statistical *P* values were analyzed by a two-tailed Student's *t*-test. *P* values < 0.05 were considered statistically significant.

Table 1 Primers of interleukin-6, signal transducer and activator of transcription 3, and GAPDH

Gene	Gene ID	Forward primers	Reverse primers
IL-6	3569	GGTGGGTGTGTCCTCATTCC	GGCATTGCATCCCTGAGTTG
STAT3	6774	GTGGGAAGAATCACGCCTTC	AGATCCTGCACTCTCTTCCG
GAPDH	2597	GAACGGGAAGCTCACTGG	GCCTGCTTCACCACCTTCT

IL: Interleukin; STAT3: Signal transducer and activator of transcription 3.

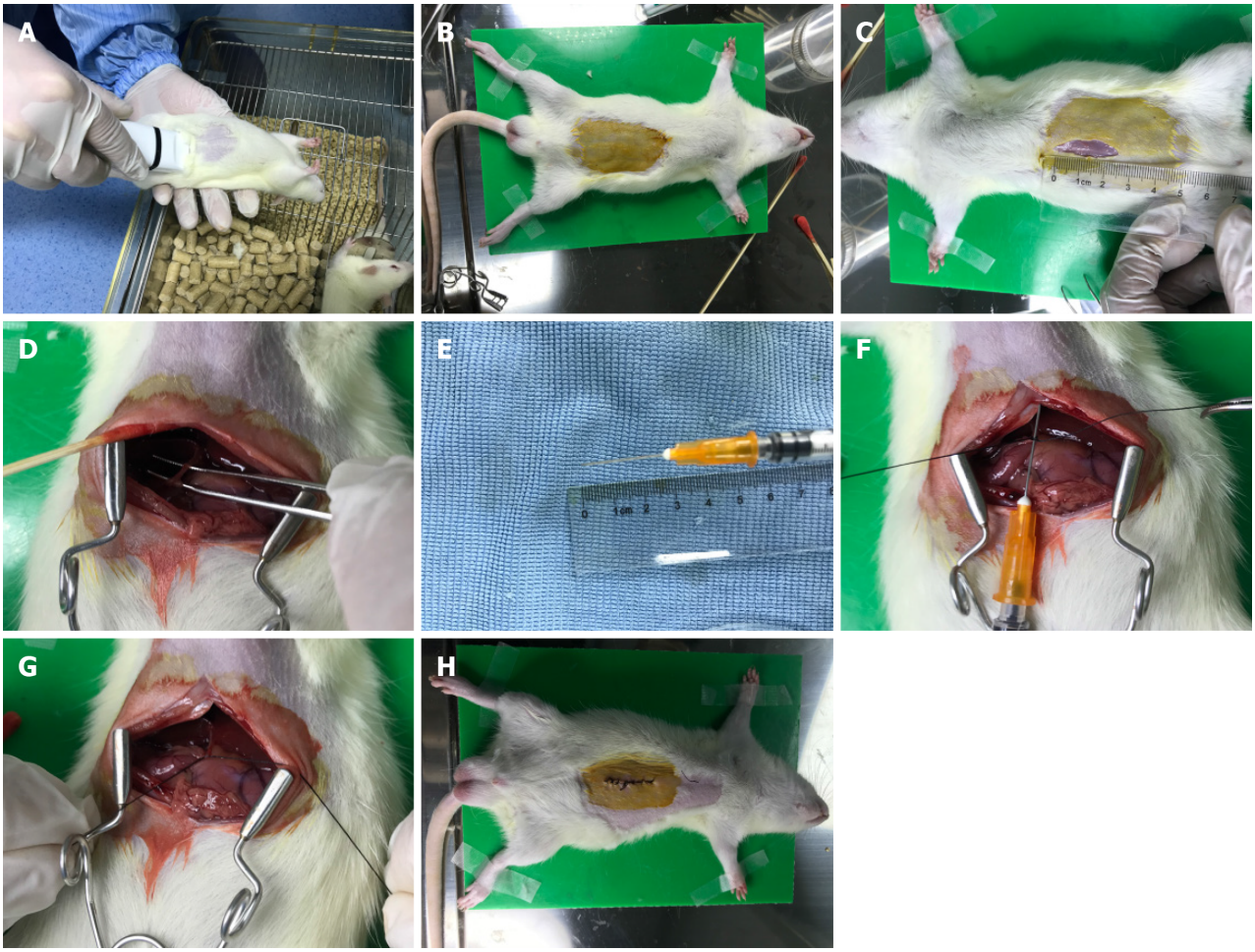

Figure 1 Surgical procedures of partial ligation of the bile duct of juvenile rats. A: Anesthesia: 2.5% pentobarbital sodium (0.25 mL/100 g) was injected into the abdominal cavity; B: Positioning: After anesthesia, the rats were fixed with a supine position; C: Skin preparation: The hair was removed to expose about 5 cm × 3 cm of skin, followed by iodine disinfection; D: Bile duct isolation: The bile duct was located with forceps; E and F: Partial ligation: Place a 1 mL needle parallel to the bile duct and use 6-0 absorbable suture to ligate the bile duct and needle; G: Remove: The needle was removed after partial ligation; H: Closure of the incision: After ligation, and the incision was intermittently sutured.

RESULTS

Rat models of CC

All 84 rats survived to the time of dissection. Rats in groups A-C showed varying degrees of dilation of the common bile ducts with slight damage to the liver, but no significant cholestasis or cirrhosis. Rats in group D developed slight adhesions around the surgical site and those in groups D-G showed no dilation of the common bile ducts. For normal rats, the diameter of the common bile duct is less than 1 mm. Based on measurements taken during dissection, dilation of the common bile duct was classified as none (< 1 mm), mild (≥ 1 mm to < 3 mm), moderate (≥ 3 mm to < 10 mm), and severe (≥ 10 mm). Mild to moderate dilation resembled fusiform CC, while severe dilation resembled cystic CC11 (Figure 2). Bile duct dilation for each group is summarized in Table 2.

Table 2 Numbers of various degrees of bile duct dilation in each group

Group	No dilation	Mild dilation	Moderate dilation	Severe dilation
	(φ < 1 mm)	(1 mm ≤ φ < 3 mm)	(3 mm ≤ φ < 10 mm)	(φ ≥ 10 mm)
A	0	10	2	0
B	0	5	7	0
C	0	2	8	2
D	11	1	0	0
E-G	36	0	0	0

φ: The maximum diameter of rat bile duct.

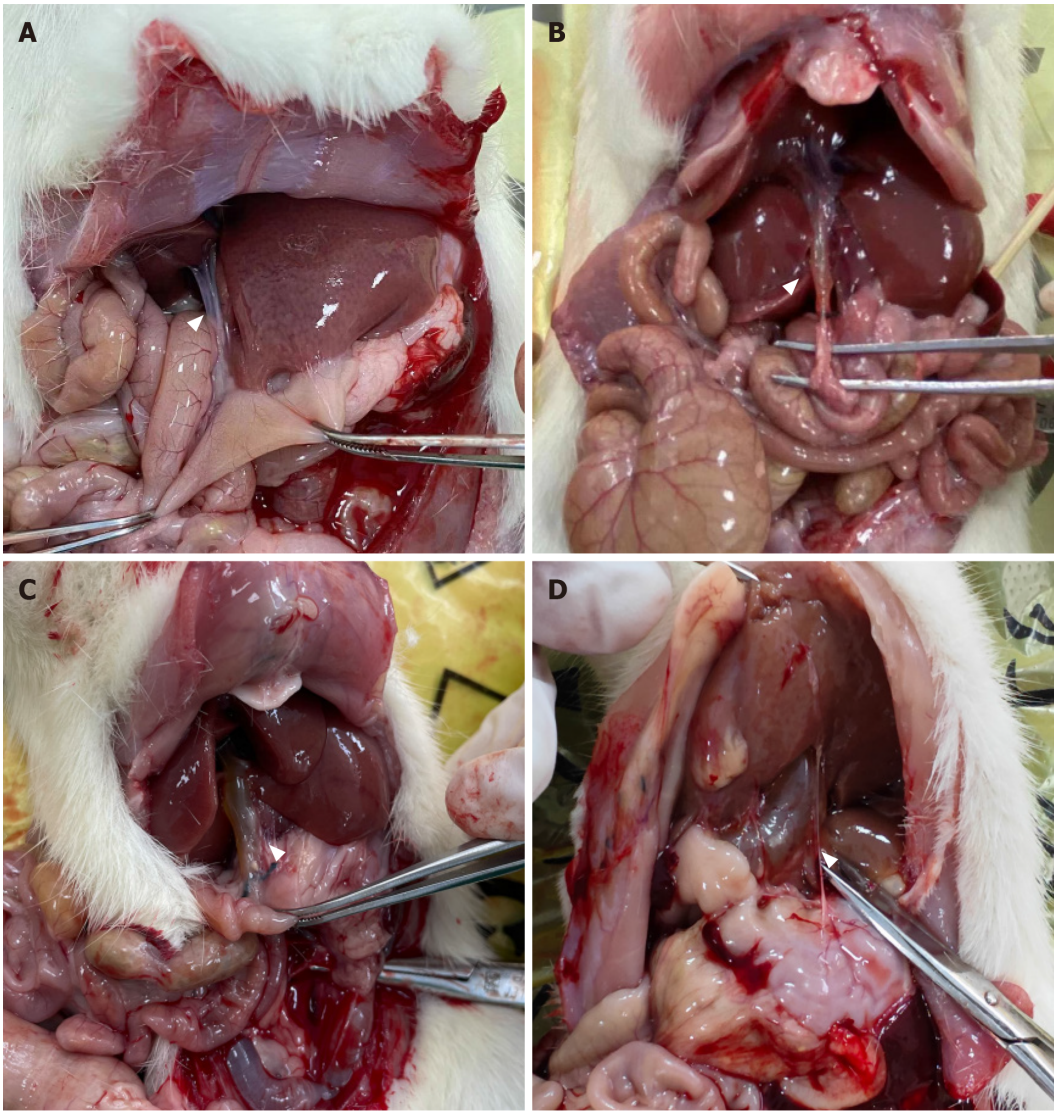

Figure 2 Representative pictures of dilated bile ducts. A: No dilation of the bile duct; B: Mild dilation of the bile duct; C: Moderate dilation of the bile duct; D: Severe dilation of the bile duct.

Identification of differentially expressed genes in human tissues

Of 103116 genes detected in the bile duct tissues between cystic and fusiform CCs, 993 were identified as differentially expressed genes (DEGs). Reference to the Kyoto Encyclopedia of Genes and Genomes (https://www.genome.jp/kegg/) revealed that 19 of the DEGs were enriched in the JAK-STAT signaling pathway (Figure 3). A protein-protein interaction network of the 19 DEGs in the JAK-STAT signaling pathway demonstrated that interleukin (IL)-6 had the highest node connectivity in the network, followed by the key factor STAT3 (Figure 3).

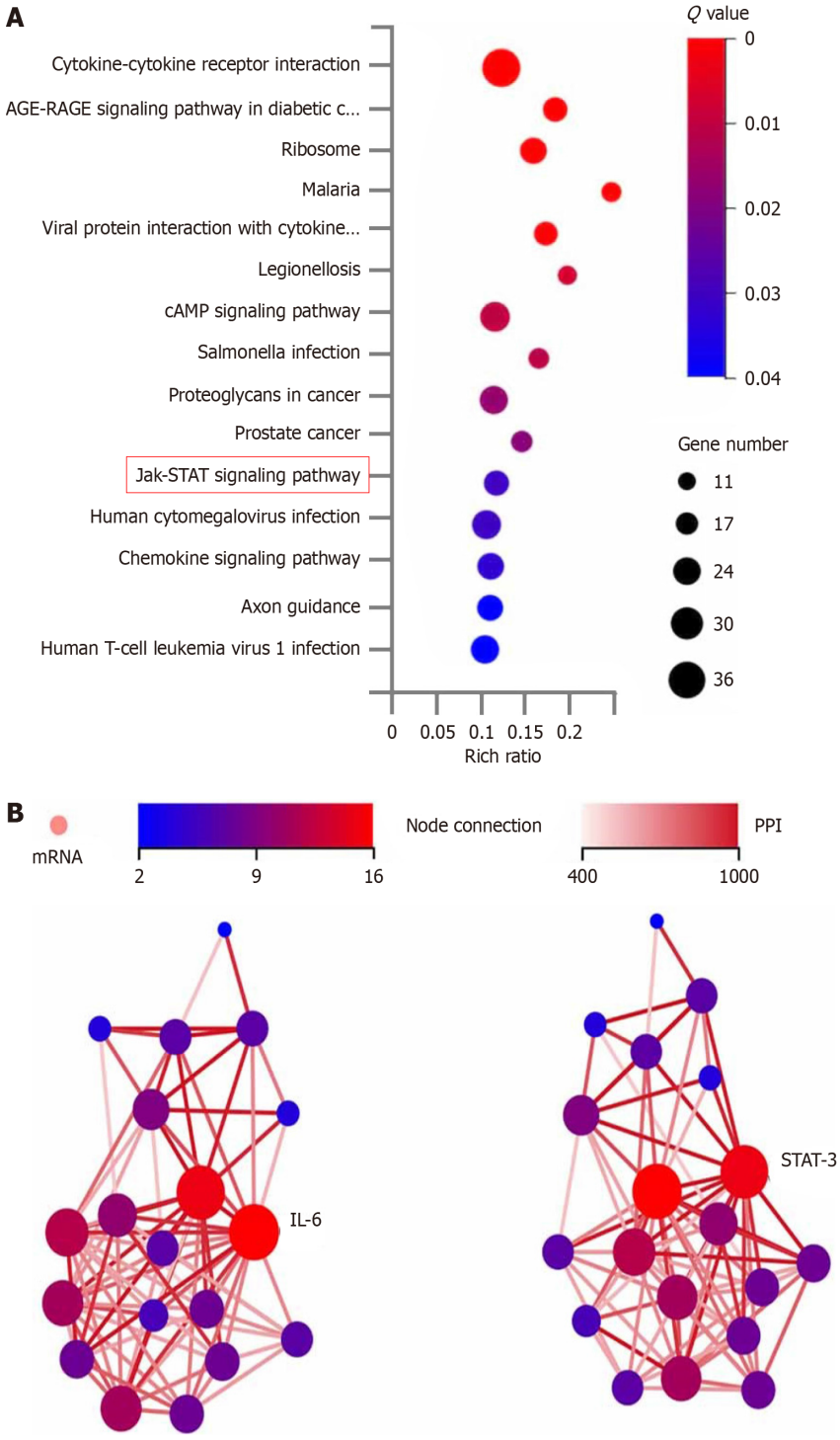

Figure 3 Analysis of differentially expressed genes in human tissues. A: Enrichment analysis of the differentially expressed genes (DEGs) by KEGG pathway; B: Protein interaction network analysis of the 19 DEGs in the JAK-STAT signaling pathway. IL: Interleukin; PPI: Protein interaction; STAT3: Signal transducer and activator of transcription 3.

Levels of biochemical indices in rats

The mean normal serum concentrations (ranges) of ALT, AST, TBIL, DBIL, GGT, and TBA for female SD rats (groups E-G) were 33.55 (24.50-39.10) U/L, 59.60 (38.95-75.35) U/L, 0.60 (0.40-0.70) μmol/L, 0.30 (0.20-0.40) μmol/L, 7.95 (7.30-8.40) μmol/L, and 17.45 (13.55-22.27) μmol/L, respectively. Serum ALT levels were significantly higher in group A than group E (P = 0.0145) and decreased to the normal range in group C. Serum AST levels were significantly higher in groups A and B than groups E and F (P = 0.0447 and 0.0204, respectively), and decreased to the normal range in group C. Serum TBIL levels were significantly higher in groups A and B than groups E and F (both, P < 0.0001), significantly higher in group B than group A (P < 0.0001), and decreased to the normal range in group C. Serum DBIL levels were significantly higher in groups A and B than groups E and F (both, P < 0.0001), significantly higher in group B than group A (P < 0.0001), and decreased to the normal range in group C. Serum GGT levels were significantly higher in group B than group F (P =

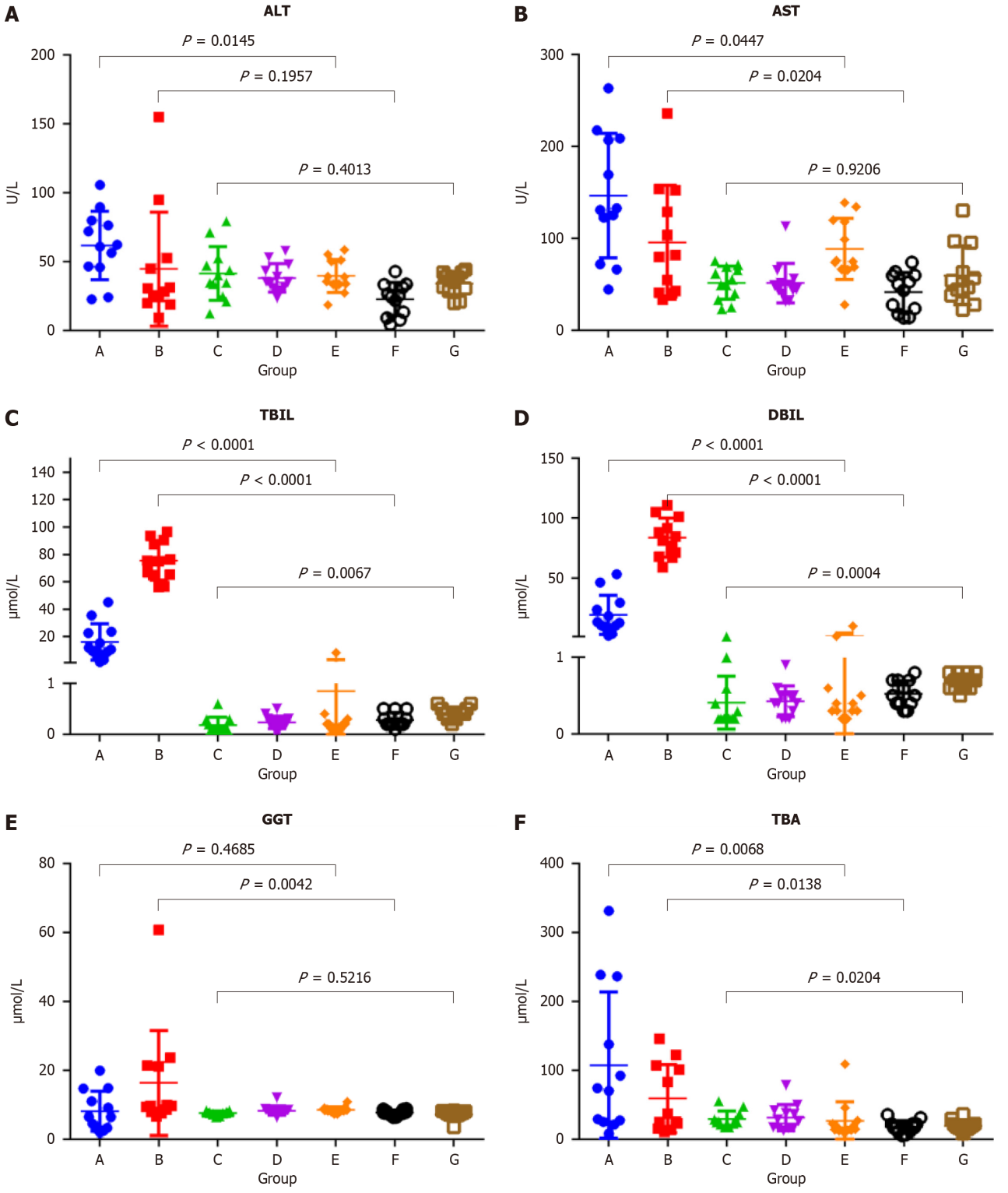

Figure 4 Comparison of biochemical indices levels in each group. A: Alanine aminotransferase; B: Aspartate aminotransferase; C: Total bilirubin; D: Direct bilirubin; E: Gamma-glutamyltransferase; F: Total bile acids. ALT: Alanine aminotransferase; AST: Aspartate aminotransferase; TBIL: Total bilirubin; DBIL: Direct bilirubin; GGT: Gamma-glutamyltransferase; TBA: Total bile acids.

0.0042) and decreased to the normal range in group C. Serum TBA levels gradually decreased in group A-C, but were slightly higher than the normal range ($P < 0.0204$) (Figure 4 and Table 3).

Western blot and immunofluorescence histochemical analyses for human and rats' tissues

The Western blot results of human bile duct tissues confirmed significant differences in the expression levels of p-STAT3 between cystic and fusiform CCs (Figure 4). Meanwhile, the Western blot results of the rat bile duct tissue (Figure 5A) showed upregulated expression of p-STAT3 on day 7 after partial ligation surgery, which further increased on day 14. However, p-STAT3 expression was significantly decreased on day 28. The expression level of p-STAT3 protein in group

Table 3 Biochemical indices of rats in each group

Biochemical indices	Group A	Group B	Group C	Group D	Group E	Group F	Group G
ALT (U/L)	61.55	29.30	37.40	35.20	37.15	24.80	35.90
	(45.95-78.90)	(20.85-50.68)	(27.13-51.25)	(30.65-46.60)	(33.53-50.68)	(10.13-32.70)	(29.03-41.27)
AST (U/L)	131.80	80.60	52.30	46.60	75.20	46.75	50.20
	(85.50-208.15)	(41.23-146.28)	(35.05-68.48)	(40.50-54.75)	(66.93-119.18)	(18.90-59.75)	(38.95-87.25)
TBIL (μmol/L)	12.90	82.90	0.20	0.40	0.35	0.50	0.70
	(9.48-27.85)	(68.45-98.70)	(0.20-0.55)	(0.23-0.50)	(0.30-0.58)	(0.40-0.70)	(0.60-0.80)
DBIL (μmol/L)	11.25	75.20	0.10	0.20	0.20	0.20	0.40
	(7.68-23.35)	(64.95-89.65)	(0.10-0.28)	(0.13-0.30)	(0.10-0.28)	(0.20-0.45)	(0.33-0.50)
GGT (μmol/L)	6.45	9.65	7.75	8.15	8.35	7.65	7.50
	(3.15-13.78)	(8.08-21.33)	(7.38-7.90)	(7.83-8.45)	(8.05-8.90)	(7.18-8.48)	(7.00-8.08)
TBA (μmol/L)	72.05	31.25	25.55	27.45	16.45	17.05	18.10
	(25.60-211.53)	(17.33-105.60)	(21.93-34.93)	(16.40-40.65)	(13.03-25.70)	(11.45-22.28)	(14.90-22.30)

ALT: Alanine aminotransferase; AST: Aspartate aminotransferase; TBIL: Total bilirubin; DBIL: Direct bilirubin; GGT: Gamma-glutamyltransferase; TBA: Total bile acids.

D-G were extremely low. And the expression level of STAT3 was significantly higher in groups A-D than groups E-G. Representative images of immunofluorescence staining of p-STAT3 in the bile duct tissues of groups B and F are shown in Figure 5B. Notably, p-STAT3 expression was significantly greater in the epithelial cells of group B as compared to group F, indicating potential involvement of the JAK-STAT signaling pathway in bile duct dilation after partial ligation.

DISCUSSION

Although the etiology of CC has been investigated for over a century, there is still a lack of appropriate animal models. In 1977, Spitz[6] reported an animal model of CC which involved distal ligation of the common bile duct in 2-d-old lambs. Subsequently, in 1979, Miyano *et al*[7] performed distal ligation of the common bile duct in 2-wk-old rats, thereby successfully establishing an animal model with dilated extrahepatic bile duct, while maintaining the normal intrahepatic bile duct. However, after the PBM hypothesis gained widespread recognition, subsequent animal models were mostly based on the anatomical structure of PBM. A dog model of PBM was initially constructed because of the similarity to the anatomical structures of the human pancreatic and bile ducts. Although anastomosis of the pancreatic and bile ducts causes abnormal anatomical structure and reflux of pancreatic juice, the refluxed pancreatic juice did not result in stenosis or typical cystic dilatation of the bile duct[12,13]. Improvements to the dog model have been attempted, such as partial ligation of the distal end of the common bile duct after pancreaticobiliary anastomosis[14]. However, it remains unclear whether dilation of the bile duct was caused by reflux of pancreatic juice, distal ligation, or both. In addition, most previous studies failed to provide an image of the model.

In our center, over 95% of CCs diagnosed prenatally are the cystic type and over 90% of cystic CCs were diagnosed in infants aged < 1 year. And several previous studies of CCs had reported the existence of distal stenosis of the bile duct[2,15]. Babbitt[1], who proposed the hypothesis of PBM, also claimed that distal stenosis played a key role in the pathogenesis of bile duct dilation. Based on previous animal models, we conclude that morphological mimicry of CCs requires the use of an infant animal and stenosis of the distal bile duct. Therefore, we established a juvenile rat model by partial ligation of the distal bile duct. In the present study, all 36 rats in groups A-C and all 12 in group D survived to the day of dissection. The bile ducts of rats in groups A-C exhibited various degrees of dilation, but not those of the rats in group D. Notably, all rats with severe bile duct dilation were in group C. Therefore, this model is relatively stable and repeatable.

In this study, the cystic and fusiform dilations of the bile duct in the partially ligated rat model were morphologically similar to the cystic or fusiform CCs. Further analysis of biochemical indices showed that the serum levels of ALT, AST, DBIL, TBIL, and TBA were significantly elevated at 7 d after surgery, indicating that partial ligation of the bile duct simulated the pathological process of bile stasis caused by biliary obstruction. Meanwhile, serum levels of DBIL, TBIL, and GGT increased to higher levels at 14 d after surgery, and most indices, with the exception of TBA, gradually decreased to normal ranges at 28 d after surgery. These findings indicate that partial ligation of the bile duct results in increasing intra-cystic pressure and dilation of the bile ducts until bile production and outflow reached a dynamic equilibrium. Then, the indices returned to normal or near-normal levels. During this process, the bile duct continued to dilate and eventually formed cystic or fusiform CCs. Hence, partial ligation was more consistent with the natural course of CC formation than complete ligation. Meanwhile, the reliability of the partial ligation rat model was further validated

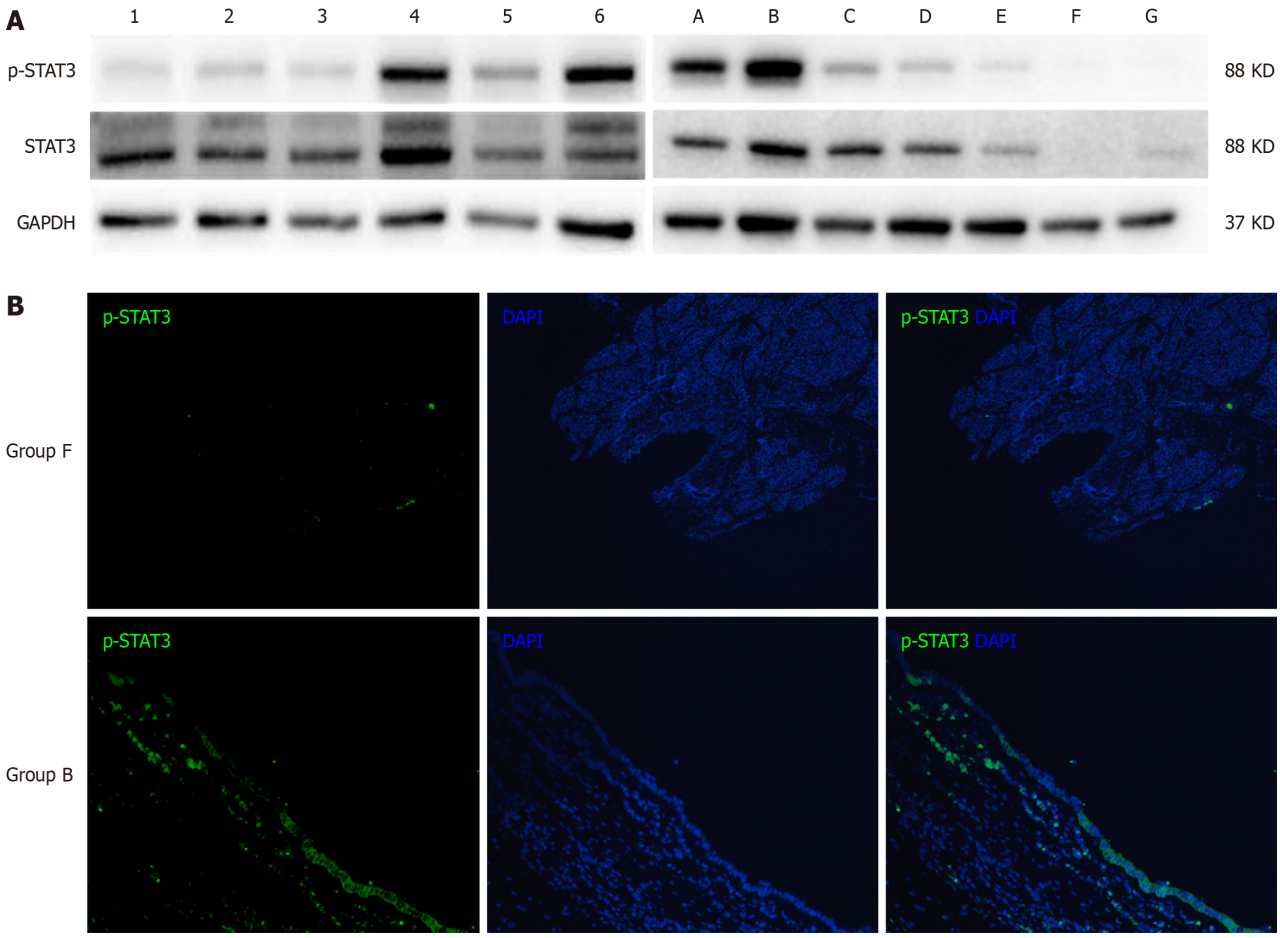

Figure 5 Western blot and immunofluorescence histochemical analyses for human and rats' tissues. A: The western blot results for human bile duct tissues were on the left, numbers 1, 2, and 3 represent fusiform choledochal cysts (CCs), while numbers 4, 5, and 6 represent cystic CCs. The western blot results for rat bile duct tissues were on the right, representative picture of each group (group A-group G) was shown; B: The representative picture of the expression of phosphorylated signal transducer and activator of transcription 3 protein in group B and group F. STAT3: Signal transducer and activator of transcription 3.

by comparison to the characteristics of the human bile duct. Notably, activation of the IL-6/JAK/STAT3 signaling pathway, which is involved in cell proliferation and differentiation[16], was significantly elevated in cystic CCs. Also, immunofluorescence staining showed that expression of p-STAT3 was significantly elevated in the subepithelial layer of the bile duct, which may cause accelerated cell proliferation in the bile duct and make it easier for the formation of cystic dilation. In the rat model, p-STAT3 expression was also increased after partial ligation and gradually decreased at 28 days after surgery but was still higher than normal rats, which was consistent with the results of biochemical indices.

CONCLUSION

In summary, our partial ligation of the bile duct in juvenile rats successfully morphologically simulated the cystic or fusiform human CCs. The postoperative disease progression was more consistent with the natural disease course of CC formation compared to complete ligation. Therefore, this stable and repeatable model can be utilized to investigate the pathogenesis of CC and further explore the causes of cystic and fusiform bile duct dilatations.

ARTICLE HIGHLIGHTS

Research background

Pancreaticobiliary maljunction (PBM) is the main hypothesis of choledochal cyst (CC). However, accumulating clinical evidence suggests that PBM cannot fully explain the pathogenesis of CC. Previously reported animal models, including models of anastomosis of the pancreatic and biliary ducts, models of complete ligation of the lower segment of the common bile duct, have been unable to adequately support basic researches on CCs.

Research motivation
Satisfactory outcomes achieved with current surgical techniques for CCs have led to a pause in basic research on the pathogenesis of CCs. Thus, we need appropriate animal models of CCs to further basic researches.

Research objectives
To establish a stable and repeatable animal model of CC based on partial ligation of the bile duct to investigate the pathogenesis of CCs.

Research methods
Specific pathogen-free female SD rats were randomly allocated to a surgical group (partial ligation of the bile duct), sham surgical group, or control group. The partial ligation of the bile duct was performed by ligating a 1 mL needle and the bile duct together, followed by the careful removal of the needle after tightening the absorbable suture. The reliability of the model was confirmed through measurements of serum biochemical indices, the morphology of common bile duct and molecular biology experiments in rat and human tissues.

Research results
All 84 rats survived to the time of dissection. Rats in the surgical group (groups A-C) showed varying degrees of dilation of the common bile ducts with slight damage to the liver and those in the sham surgical and control groups (groups D-G) showed no dilation of the common bile ducts. The changing trends of biochemical indexes indicated that the partially ligated bile ducts experienced a pathological process of recanalization after incomplete obstruction of the distal bile duct. And the reliability of the model was also confirmed by molecular biology experiments in rat and human tissues.

Research conclusions
The model of partial ligation of the bile duct of juvenile rats could morphologically simulate the cystic or fusiform CCs. This stable and repeatable model was more consistent with the natural disease course of CC formation than complete ligation which may assist in the basic researches of CCs.

Research perspectives
We hope our partial ligation of the bile duct of juvenile rats can promote the basic research of CCs and provide a reliable animal model for further research on the formation of cystic CCs or fusiform CCs.

FOOTNOTES

Author contributions: Zhang SH designed and performed the research and wrote the paper; Gao ZG, Zhang YB, and Cai DT designed the research and supervised the report; Chen K, Jin Y, Luo WJ, and Huang ZW designed the research and contributed to the analysis; Chen QJ and Pan T provided clinical advice and supervised the report.

Supported by the Key R&D Program of Zhejiang, No. 2023C03029; Health Science and Technology Plan of Zhejiang Province, No. 2022RC201; and Zhejiang Provincial Natural Science Foundation Project, No. LY20H030007.

Institutional review board statement: The study was reviewed and approved by the Ethics Committee of The Children's Hospital, Zhejiang University School of Medicine (approval No. 2022-IRB-108). Prior to inclusion in this study, written informed consent was obtained from all subjects.

Institutional animal care and use committee statement: The protocol of the animal study was approved by the Institutional Animal Care and Use Committee of Laboratory Animal Center of Zhejiang University (approval No. ZJU20230273).

Conflict-of-interest statement: The authors declare that they have no conflict of interest.

Data sharing statement: No additional data are available.

ARRIVE guidelines statement: The authors have read the ARRIVE guidelines, and the manuscript was prepared and revised according to the ARRIVE guidelines.

Country/Territory of origin: China

ORCID number: Shu-Hao Zhang 0000-0002-3124-9867; Zhi-Gang Gao 0009-0009-4020-7528.

S-Editor: Chen YL

L-Editor: A
P-Editor: Zheng XM

REFERENCES

1 **Babbitt DP**. [Congenital choledochal cysts: new etiological concept based on anomalous relationships of the common bile duct and pancreatic bulb]. *Ann Radiol (Paris)* 1969; **12**: 231-240 [PMID: 5401505]
2 **Greenholz SK**. Antenatal diagnosis of choledochal cyst at 15 weeks' gestation: etiologic implications and management. *J Pediatr Surg* 1990; **25**: 584 [PMID: 2352098 DOI: 10.1016/0022-3468(90)90672-v]
3 **Kolacek S**, Puntis JW, Lloyd DR, Brown GA, Booth IW. Ontogeny of pancreatic exocrine function. *Arch Dis Child* 1990; **65**: 178-181 [PMID: 2317062 DOI: 10.1136/adc.65.2.178]
4 **Ohkawa H**, Sawaguchi S, Yamazaki Y, Sakaniwa M, Ishikawa A. The production of anomalous pancreaticobiliary ductal union in canine models. *Z Kinderchir* 1981; **32**: 328-336 [PMID: 7282070 DOI: 10.1055/s-2008-1063280]
5 **Benhidjeb T**, Said S, Rudolph B, Siegmund E. Anomalous pancreatico-biliary junction--report of a new experimental model and review of the literature. *J Pediatr Surg* 1996; **31**: 1670-1674 [PMID: 8986984 DOI: 10.1016/s0022-3468(96)90045-7]
6 **Spitz L**. Experimental production of cystic dilatation of the common bile duct in neonatal lambs. *J Pediatr Surg* 1977; **12**: 39-42 [PMID: 833713 DOI: 10.1016/0022-3468(77)90293-7]
7 **Miyano T**, Suruga K, Suda K. Abnormal choledocho-pancreatico ductal junction related to the etiology of infantile obstructive jaundice diseases. *J Pediatr Surg* 1979; **14**: 16-26 [PMID: 423059 DOI: 10.1016/s0022-3468(79)80570-9]
8 **Friedmacher F**, Ford KE, Davenport M. Choledochal malformations: global research, scientific advances and key controversies. *Pediatr Surg Int* 2019; **35**: 273-282 [PMID: 30406431 DOI: 10.1007/s00383-018-4392-4]
9 **Huang J**, Qiu ZY, He J, Xu HS, Wang K, Du HY, Gao D, Zhao WN, Sun QG, Wang YS, Wen PZ, Li Q, Dong XO, Xie XZ, Jiang L, Wang HY, Liu YQ, Wan JM. Phytochrome B mediates dim-light-reduced insect resistance by promoting the ethylene pathway in rice. *Plant Physiol* 2023; **191**: 1272-1287 [PMID: 36437699 DOI: 10.1093/plphys/kiac518]
10 **Abdi H**. The Bonferonni and Šidák Corrections for Multiple Comparisons. encyclopedia of measurement & statistics. 2006. [cited 12 January 2023]. Available from: https://www.semanticscholar.org/paper/The-Bonferonni-and-%C5%A0id%C3%A1k-Corrections-for-Multiple-Abdi/8b4300f253644d49c778c037ee614b9cf42a908c
11 **Livak KJ**, Schmittgen TD. Analysis of relative gene expression data using real-time quantitative PCR and the 2(-Delta Delta C(T)) Method. *Methods* 2001; **25**: 402-408 [PMID: 11846609 DOI: 10.1006/meth.2001.1262]
12 **Diao M**, Li L, Cheng W. Congenital biliary dilatation may consist of 2 disease entities. *J Pediatr Surg* 2011; **46**: 1503-1509 [PMID: 21843715 DOI: 10.1016/j.jpedsurg.2010.12.022]
13 **Oguchi Y**. [Histopathological studies on congenital dilatation of the bile duct--with special reference to the regurgitation of pancreatic juice into the bile duct]. *Nihon Geka Gakkai Zasshi* 1986; **87**: 547-557 [PMID: 3713700]
14 **Qian D**, Jin BX. Experimental Study on the Etiology of Congenital Biliary Dilatation. *Chin J Pediatr Surg* 1990; **11**: 257-259 [DOI: 10.5223/pghn.2020.23.6.531]
15 **Tsang TM**, Tam PK, Chamberlain P. Obliteration of the distal bile duct in the development of congenital choledochal cyst. *J Pediatr Surg* 1994; **29**: 1582-1583 [PMID: 7877036 DOI: 10.1016/0022-3468(94)90224-0]
16 **Huang B**, Lang X, Li X. The role of IL-6/JAK2/STAT3 signaling pathway in cancers. *Front Oncol* 2022; **12**: 1023177 [PMID: 36591515 DOI: 10.3389/fonc.2022.1023177]

World Journal of Gastroenterology

Submit a Manuscript: https://www.f6publishing.com

World J Gastroenterol 2024 March 14; 30(10): 1431-1449

DOI: 10.3748/wjg.v30.i10.1431

ISSN 1007-9327 (print) ISSN 2219-2840 (online)

ORIGINAL ARTICLE

Basic Study

Serotonin receptor 2B induces visceral hyperalgesia in rat model and patients with diarrhea-predominant irritable bowel syndrome

Zheng-Yang Li, Yu-Qing Mao, Qian Hua, Yong-Hong Sun, Hai-Yan Wang, Xuan-Guang Ye, Jing-Xian Hu, Ya-Jie Wang, Miao Jiang

Specialty type: Gastroenterology and hepatology

Provenance and peer review: Unsolicited article; Externally peer reviewed.

Peer-review model: Single blind

Peer-review report's scientific quality classification

Grade A (Excellent): 0
Grade B (Very good): B
Grade C (Good): 0
Grade D (Fair): 0
Grade E (Poor): 0

P-Reviewer: Ghannam WM, Egypt

Received: November 27, 2023
Peer-review started: November 27, 2023
First decision: December 12, 2023
Revised: December 29, 2023
Accepted: February 6, 2024
Article in press: February 6, 2024
Published online: March 14, 2024

Zheng-Yang Li, Qian Hua, Hai-Yan Wang, Jing-Xian Hu, Ya-Jie Wang, Miao Jiang, Department of Gastroenterology, Jinshan Hospital of Fudan University, Shanghai 201508, China

Yu-Qing Mao, Department of Gastroenterology, Shanghai General Hospital, Shanghai Jiao Tong University School of Medicine, Shanghai 200080, China

Yong-Hong Sun, Department of Gastroenterology, Dalian Friendship Hospital, Dalian 116001, Liaoning Province, China

Xuan-Guang Ye, Department of Pathology, Jinshan Hospital of Fudan University, Shanghai 201508, China

Corresponding author: Miao Jiang, PhD, Researcher, Department of Gastroenterology, Jinshan Hospital of Fudan University, No. 1508 Longhand Road, Jinshan District, Shanghai 201508, China. jiangmiao_@fudan.edu.cn

Abstract

BACKGROUND

Serotonin receptor 2B (5-HT_{2B} receptor) plays a critical role in many chronic pain conditions. The possible involvement of the 5-HT_{2B} receptor in the altered gut sensation of irritable bowel syndrome with diarrhea (IBS-D) was investigated in the present study.

AIM

To investigate the possible involvement of 5-HT_{2B} receptor in the altered gut sensation in rat model and patients with IBS-D.

METHODS

Rectosigmoid biopsies were collected from 18 patients with IBS-D and 10 patients with irritable bowel syndrome with constipation who fulfilled the Rome IV criteria and 15 healthy controls. The expression level of the 5-HT_{2B} receptor in colon tissue was measured using an enzyme-linked immunosorbent assay and correlated with abdominal pain scores. The IBS-D rat model was induced by intracolonic instillation of acetic acid and wrap restraint. Alterations in visceral sensitivity and 5-HT_{2B} receptor and transient receptor potential vanilloid type 1 (TRPV1) expression were examined following 5-HT_{2B} receptor antagonist administration. Changes in visceral sensitivity after administration of the TRPV1 antago-

nist were recorded.

RESULTS

Here, we observed greater expression of the 5-HT_{2B} receptor in the colonic mucosa of patients with IBS-D than in that of controls, which was correlated with abdominal pain scores. Intracolonic instillation of acetic acid and wrap restraint induced obvious chronic visceral hypersensitivity and increased fecal weight and fecal water content. Exogenous 5-HT_{2B} receptor agonist administration increased visceral hypersensitivity, which was alleviated by successive administration of a TRPV1 antagonist. IBS-D rats receiving the 5-HT_{2B} receptor antagonist exhibited inhibited visceral hyperalgesia.

RESULTS

Moreover, the percentage of 5-HT_{2B} receptor-immunoreactive (IR) cells surrounded by TRPV1-positive cells (5-HT_{2B} receptor I^+) and total 5-HT_{2B} receptor IR cells (5-HT_{2B} receptor I_T) in IBS-D rats was significantly reduced by the administration of a 5-HT_{2B} receptor antagonist.

CONCLUSION

Our finding that increased expression of the 5-HT_{2B} receptor contributes to visceral hyperalgesia by inducing TRPV1 expression in IBS-D patients provides important insights into the potential mechanisms underlying IBS-D-associated visceral hyperalgesia.

Key Words: Diarrhea-predominant irritable bowel syndrome; Serotonin receptor 2B; Transient receptor potential vanilloid type-1; Visceral hypersensitivity; Abdominal pain

Core Tip: Higher expression of the serotonin receptor 2B (5-HT_{2B} receptor) was found in patients with irritable bowel syndrome with diarrhea (IBS-D) than in that of controls, which was correlated with abdominal pain scores. Exogenous 5-HT_{2B} receptor agonist administration increased visceral hypersensitivity, which was alleviated by successive administration of a transient receptor potential vanilloid type 1 (TRPV1) antagonist. IBS-D rats receiving the 5-HT_{2B} receptor antagonist exhibited inhibited visceral hyperalgesia. Hence, 5-HT_{2B} receptor-induced visceral hyperalgesia may be mediated by TRPV1 channels, and the analgesic effect of 5-HT_{2B} receptor antagonist could be used as a novel treatment for IBS-D.

Citation: Li ZY, Mao YQ, Hua Q, Sun YH, Wang HY, Ye XG, Hu JX, Wang YJ, Jiang M. Serotonin receptor 2B induces visceral hyperalgesia in rat model and patients with diarrhea-predominant irritable bowel syndrome. *World J Gastroenterol* 2024; 30(10): 1431-1449

URL: https://www.wjgnet.com/1007-9327/full/v30/i10/1431.htm

DOI: https://dx.doi.org/10.3748/wjg.v30.i10.1431

INTRODUCTION

Irritable bowel syndrome (IBS) is a chronic functional bowel disorder characterized by recurrent abdominal pain with altered bowel habits that affects approximately 15% of the population worldwide[1]. IBS significantly impacts the quality of life of patients. Although the pathogenesis of IBS is not completely understood, the role of abnormal visceral sensitivity in IBS has recently emerged[2,3]. 5-Hydroxytryptamine (5-HT) is known to play a key role in the physiological states of the gastrointestinal tract. Plasma 5-HT levels in IBS with diarrhea (IBS-D) patients were greater than those in healthy controls[4], suggesting a possible role of 5-HT in the pathogenesis of IBS-D.

The serotonin receptor 2 (5-HT_2 receptor) family comprises three subtypes: 5-HT_{2A}, 5-HT_{2B}, and 5-HT_{2c}. All 5-HT_2 receptors exhibit 46%-50% overall sequence identity, and all of these receptors preferentially bind to $G_{q/11}$ to increase inositol phosphates and intracellular calcium mobilization[5]. 5-HT_{2B} receptors are widely expressed throughout the gut, and experimental evidence suggests that the primary function of 5-HT_{2B} receptors is to mediate contractile responses to 5-HT through its action on smooth muscle[6]. The 5-HT_{2B} receptor is localized to both neurons of the myenteric nerve plexus and smooth muscle in the human colon. The 5-HT_{2B} receptor mediates 5-HT-evoked contraction of longitudinal smooth muscle[6]. These findings suggest that the 5-HT_{2B} receptor could play an important role in modulating colonic motility, which could affect sensory signaling in the gut. Other laboratories have shown that the 5-HT_{2B} receptor participates in the development of mechanical and formalin-induced hyperalgesia[7,8]. A 5-HT_{2B} receptor antagonist reduced 2,4,6-trinitrobenzene sulfonic acid (TNBS) and stress-induced visceral hyperalgesia in rats[9,10]. However, the role of the 5-HT_{2B} receptor in IBS-D patients and in acetic acid- and wrap restraint-induced IBS-D rat models was not investigated.

Transient receptor potential vanilloid type 1 (TRPV1) is a receptor that responds to heat, acidosis, capsaicin, and endovanilloids and is present on peripheral nerve endings, where its activation and signaling to the brain result in nociception[11]. Upregulation and/or sensitization of TRPV1 is considered an important mechanism of visceral hyperalgesia both in preclinical rat models and in patients with IBS[11,12]. The 5-HT_{2B} receptor mediates 5-HT-induced mechanical hyperalgesia by regulating TRPV1 function[13]. TRPV1 function is enhanced by 5-HT_{2B} receptor activation in mouse colon sensory neurons[14]. However, whether TRPV1 is involved in 5-HT_{2B} receptor-induced visceral hyperalgesia in IBS-D patients is unknown.

In this study, we demonstrated that 5-HT_{2B} receptor-induced visceral hyperalgesia in IBS-D patients occurs *via* the TRPV1 channel. 5-HT_{2B} receptor expression was increased in the colonic mucosa of IBS-D patients and correlated with abdominal pain scores. Administration of a 5-HT_{2B} receptor agonist significantly enhanced visceral sensitivity, and this increase was attenuated upon treatment with a TRPV1 antagonist. The number of 5-HT_{2B} receptor- and TRPV1-positive cells was greater in IBS-D rats than in control rats. Interestingly, a 5-HT_{2B} receptor antagonist not only alleviated visceral hypersensitivity but also decreased TRPV1 expression in IBS-D rats.

MATERIALS AND METHODS

Human subjects

A total of 15 healthy volunteers (9 women and 6 men; 51.1 ± 10.3 years), 10 patients with IBS with constipation (IBS-C) (6 women and 4 men; 51.0 ± 11.5 years), and 18 patients with IBS-D (10 women and 8 men; 51.4 ± 9.8 years) meeting the Rome IV criteria were consecutively enrolled[15]. Patients who underwent colonoscopy for polyps and cancer surveillance had negative results. Patients who were subjected to major abdominal surgery, who received nonsteroidal or other anti-inflammatory drugs, or who had organic diseases, including celiac disease, psychiatric disorders, or allergic diseases, were excluded. All participants had macroscopically normal bowel mucosa upon examination. In total, four biopsy specimens were obtained from each participant from the rectosigmoid junction to standardize the site of sampling. In all the patients, one biopsy sample was sent for hematoxylin and eosin (HE) histological analysis and immunohistochemical staining. One biopsy sample was subjected to tissue immunofluorescence. Another two biopsy samples were immediately placed into a prepared Eppendorf tube, frozen immediately on ice and stored at -80 °C for enzyme-linked immunosorbent assay (ELISA) analysis.

Informed consent statement

The use of human tissue samples and clinical data was approved by the ethics committee of Dalian Friendship Hospital. All donors were informed of the aim of the study and gave consent to donate their samples.

Symptom questionnaires

All patients and controls were asked to score abdominal pain over 2 wk using a previously described validated questionnaire[16] since recollection was poor beyond this limit. Shorter periods may not have appropriately reflected the usual clinical picture, and this timeframe has previously been shown to be a reliable predictor of average pain intensity [17]. The severity of abdominal pain was graded as 0-4 based on the influence on daily activities of patients: 0, absent; 1, mild (no influence on activity); 2, relevant (diverting from but not urgently necessitating modification of activity); 3, severe (influencing activity to a marked extent, consequently requiring modifications); and 4, extremely severe (precluding daily activity). The frequency of abdominal pain was graded as 0–4 according to the frequency of symptoms per week: 0, absent; 1, up to 1 day/week; 2, 2 or 3 days/week; 3, 4-6 days/week; and 4, daily.

Drugs and chemicals

The 5-HT_{2B} receptor agonist (BW723C86; Sigma–Aldrich, St. Louis, MO, United States) was diluted with saline. The 5-HT_{2B} receptor antagonist 2-amino-4-(4-fluoronaphth-1-yl)-6-isopropylpyridine (RS-127445; Tocris Bioscience, Ellisville, Missouri, United States) was dissolved in 20% dimethylsulfoxide in physiological saline. The TRPV1 antagonist *N*-(3-methoxyphenyl)-4-chlorocinnamide (SB366791; Sigma–Aldrich, St. Louis, MO, United States) was dissolved in 50% dimethylsulfoxide in physiological saline. A human anti-5-HT_{2B} receptor polyclonal antibody (MAB10322) was purchased from R&D Systems (Minneapolis, MN, United States). Mouse anti-5-HT_{2B} receptor (AB194333), anti-alpha smooth muscle actin (AB5694) and rabbit anti-TRPV1 polyclonal antibodies (AB10296) were purchased from Abcam (Cambridge, MA, United States). Rabbit anti-Ecadherin antibody (CST 3195) was purchased from Cell Biological Technology, Inc. (Boston, United States). The rabbit anti-protein-encoding gene product (PGP) 9.5 (14730-1-AP) polyclonal antibody, rabbit anti-pankeratin (26411-1-AP) polyclonal antibody, and mouse anti-TRPV1 polyclonal antibody (66983-1-Ig) were obtained from Proteintech Group, Inc. (Chicago, United States). A 5-HT_{2B} receptor ELISA kit was purchased from Jianglai Bio (Shanghai, China). A RNA polymerase chain reaction (PCR) kit was purchased from Takara Biotechnology (Dalian, China).

IBS-D model

Adult male Sprague-Dawley rats (180-200 g) were obtained from Shanghai SIPPR-BK Laboratory Animal Co., Ltd. (Shanghai, China). Animals were housed with *ad libitum* access to food and water in standard rodent cages at 23 °C in a temperature- and light-controlled room. IBS-D rats were established by intracolonic instillation of acetic acid and wrap restraint as described by Williams *et al*[18] and Chen *et al*[19], with slight modifications. In brief, on the first day, after an

overnight fast, the rats were anesthetized using ether, 1 mL of 4% acetic acid was instilled 8 cm proximal to the anus for 30 s, and then 1 mL of phosphate-buffered saline (PBS) was used to dilute the acetic acid and wash the colon. The rats were not subjected to any treatment for the following 3 d. From Days 5 to 18, the rats were subjected to wrap restraint stress for 2 wk (1 h per day).

Experimental protocol

The colorectal distension (CRD) test was carried out on Day 19 to evaluate visceral sensitivity, which was quantified using abdominal withdrawal reflex (AWR) scores. The threshold intensity of CRD was measured in rats on the same day, and the threshold intensity was determined as the pressure inducing the first abdominal contraction. Fecal weight and fecal water content were recorded on the same day. Rats that met the criteria for visceral hypersensitivity and had increased fecal weight and fecal water content were considered IBS-D rats.

The rats were divided into 6 groups, with 10 rats per group: (1) The normal control group included normal rats without any treatment; (2) In the BW723C86 group, normal control rats were injected intraperitoneally with BW723C86 (25 μg/kg/d, 100 μL/injection) daily for seven days; (3) In the BW723C86 + SB366791 group, normal control rats were injected intraperitoneally with SB366791 (10 mg/kg/d, 100 μL/injection) 30 min before BW723C86 was administered daily for seven days; (4) IBS-D rats without any treatment; (5) In the IBS-D + Vehicle group, IBS-D rats were injected intraperitoneally with 20% dimethylsulfoxide in physiological saline (100 μL/injection) daily for seven days; and (6) In the RS-127445 group, IBS-D rats were injected intraperitoneally with RS-127445 (10 mg/kg/d, 100 μL/injection) daily for seven days.

The doses and timings used in this study were chosen from previous studies[7,20]. At the end of the experiment, visceral sensitivity was evaluated by measuring the behavioral responses of the AWR to CRD in every animal group. The threshold intensity of CRD was measured in all the animal groups. Then, the animals were sacrificed, and distal colon tissue was collected. The colon was divided into 3 parts: One sample was used for ELISA analysis, and one sample was fixed in 4% paraformaldehyde for routine HE histological analysis, immunohistochemical staining and immunofluorescence. Under a stereomicroscope, another colon sample was gently peeled off, and the intestinal wall was peeled off into the mucosal layer and the intestinal muscle layer. Then, the tissue was stored at -80 °C for quantitative real-time reverse transcriptase polymerase chain reaction (RT-PCR). This study was approved by the Fudan University School of Medicine Animal Care and Use Committee and was performed in accordance with the guidelines of the International Association for the Study of Pain.

CRD test for visceral hyperalgesia

Briefly, rats were sedated with isoflurane for 1 min in a sealed cage connected to an animal anesthesia machine, and a flexible balloon guide wire (received as a gift from the Vascular Intervention Department of Jinshan Hospital of Fudan University) was then quickly inserted approximately 2.0 cm into the descending colon *via* the anus and firmly fixed with adhesive tape. The rats were placed in a restraint chamber that prevented them from escaping or turning around and allowed to adapt for 15 min. CRD was generated by slowly inflating the balloon to a constant pressure using a balloon vasodilation catheter to control inflation. The balloon was inflated to 15, 30, 45 and 60 mmHg for 20 s, followed by a resting interval of 5 min, and this process was repeated 3 times to achieve an accurate result. The responses of the animals to CRD were carefully observed until pain-related behaviors were observed. AWR scores were graded on a scale of 0–4 [21] (0, normal behavior; 2, contraction of abdominal muscles; 3, lifting of the abdominal wall; 4, body arching and lifting of pelvic structures). The final score was calculated from the mean scores of three data points.

Recordings of fecal weight and fecal water content

Fecal weight and fecal water content were recorded on Day 19 to evaluate the establishment of the IBS-D rat model. To measure the fecal weight and fecal water content, the feces expelled by each rat were collected and recorded after 3 h. The feces were weighed again after drying in an oven. Fecal water content = [wet fecal weight (g)-dried fecal weight (g)]/wet fecal weight (g) × 100%[19].

Histological examination of the colon

For histological experiments, distal colon tissue from each rat was fixed in 4% paraformaldehyde, embedded in paraffin, and cut into 4 μm sections. Sections were stained with HE and scored for histopathological structures by a pathologist.

ELISA

Mucosal samples and muscular samples were homogenized in a prepared ice-cold 100 nM Tris mixture containing protease inhibitors (Beyotime, Shanghai, China) supplemented with 1 mmol/L phenylmethanesulfonyl fluoride. The mucosal and muscular samples were centrifuged at 12000 × g for 15 min at 4 °C. The homogenates were centrifuged at low temperature for 20 min at 3000 rpm. The protein concentration in the supernatant was detected on a Nanodrop 2000 (Thermo Fisher Scientific, Waltham, MA, United States). The concentrations of the 5-HT_{2B} receptor in the supernatants were detected *via* ELISA using specific kits (Jianglai bio, Shanghai, China). The detection range for this assay was 2.5–40 ng/mL. Each sample was measured in duplicate. Reactivity was assessed at 450 nm.

Quantitative real-time RT-PCR

Total RNA was extracted from colon samples with TRIzol reagent (Tiangen Biotech, Beijing, China). SYBR Green quantitative RT-PCR was performed to determine the expression of the 5-HT_{2B} receptor and TRPV1 genes with a 7900HT Fast real-time PCR system (Applied Biosystems, Foster City, CA, United States) according to the instructions of the SYBR

Premix EX Taq Kit (Takara Biotechnology, Dalian, China). Control quantitative reactions were performed in the absence of cDNA template. β-Actin was used as the reference gene. The primer sequences are shown in Table 1.

Immunohistochemistry

Biopsy samples from participants and colon tissues from rats were fixed in 4% formalin, and 4 μm thick sections were used for immunohistological analyses. Following routine deparaffinization, rehydration and antigen retrieval, the sections were incubated with a rabbit anti-TRPV1 polyclonal antibody (1:300, AB1029) and mouse anti-5-HT_{2B} receptor (1:500, AB194333) overnight at 4 °C. Next, the sections were incubated at room temperature for 2 h with a horseradish peroxidase-conjugated secondary antibody (Jingmei Biological Engineering Co., Shenzhen, China). Visualization involved the use of diaminobenzidine as a chromogen. Subsequently, the slides were counterstained with hematoxylin and examined under a light microscope (Olympus, Tokyo, Japan).

Tissue immunofluorescence

Colonic tissue samples collected from rats and biopsy samples from participants were perfused with saline followed by fixative containing 4% paraformaldehyde. Sections of colonic tissues were incubated with a rabbit anti-TRPV1 polyclonal antibody (1:300, AB1029), mouse anti-5-HT_{2B} receptor (1:200, AB194333) or human anti-5-HT_{2B} receptor polyclonal antibody (1:200, MAB10322) overnight at 4 °C, followed by donkey anti-rabbit and anti-mouse secondary antibodies at a dilution of 1:200 (Sigma). Sections of colonic tissues from rats were costained with mouse anti-5-HT_{2B} receptor (1:100, AB194333), mouse anti-TRPV1 (1:200, Proteintech), rabbit anti-E-cadherin (1:400, CST 3195), rabbit anti-pankeratin (1:1500, Proteintech), anti-alpha smooth muscle actin (1:100, AB5694), and rabbit anti-PGP9.5 (1:1000, Proteintech) primary antibodies; FITC-conjugated goat-anti-rabbit-immunoglobulin G (IgG) antibody (1:200, Sigma); FITC-conjugated goat-anti-mouse-IgG antibody (1:200, Sigma); and FITC-conjugated goat-anti-guinea pig-IgG (1:200, Jackson ImmuoResearh). All the antibodies were diluted in PBS containing 1% BSA. The specimens were identified *via* a confocal microscope (Carl Zeiss AG, Jena, Germany). The digitized images were captured by using an automated acquisition system (TissueFAXS Plus, TissueGnostics GmbH, Austria). Then, 5-HT_{2B} receptor-immunoreactive (IR) cells surrounded by TRPV1-positive in one-third or more of the 5-HT_{2B} receptor-immunoreactive circumference were counted (5-HT_{2B} receptor I^+) and expressed as a percentage of total 5-HT_{2B} receptor IR cells (5-HT_{2B} receptor I_T) in the fields analyzed (5-HT_{2B} receptor I^+/5-HT_{2B} receptor I_T). The data for each group were collected from 10 slides. A t test for two proportions was used to test the level of significance.

Statistical analysis

Depending on the distribution of the variables, Student's *t*-test, Chi-square test, or Wilcoxon rank sum was used to test for differences in parameters between groups. Continuous variables are presented as arithmetic mean ± SD. Categorical variables are presented as numbers (percentages). Associations between two parameters were analyzed *via* Spearman's rank correlation. All statistical analyses were performed using R software (version 4.1.0) and GraphPad Prism (version 6.0). The statistical significance level was set at $P < 0.05$ (both sides).

RESULTS

Group characteristics

The clinical characteristics of the IBS-D patients, IBS-C patients and control subjects are described in Table 2. No significant differences in age or sex were evident among the three groups. A total of 18 patients with IBS-D were examined, and the mean scores of severity of abdominal symptoms were significantly greater in IBS-D patients than in controls ($P < 0.001$). The mean frequency of abdominal symptoms was significantly greater in IBS-D patients than in controls ($P < 0.001$). The mean scores of severity of abdominal symptoms in the IBS-C patients were significantly greater than that in the controls ($P < 0.001$). The mean frequency of abdominal symptoms in IBS-C patients was markedly greater than that in control patients ($P < 0.001$). We observed no significant differences between the IBS-D and IBS-C groups.

Measurement of the 5-HT_{2B} receptor in the intestinal mucosa

Compared with healthy controls, IBS-D patients exhibited significant upregulation of the 5-HT_{2B} receptor in the intestinal mucosa (IBS-D: 11.78 ± 1.67 ng/mg protein *vs* healthy controls: 5.22 ± 1.95 ng/mg protein, $P < 0.001$) (Figure 1A). Compared with healthy controls, IBS-C patients also exhibited slight upregulation of the 5-HT_{2B} receptor in the intestinal mucosa, but there was no significant difference between the IBS-C group and healthy controls (IBS-C: 6.08 ± 1.75 ng/mg protein vs. healthy controls: 5.22 ± 1.95 ng/mg protein, $P = 0.42$) (Figure 1A). Therefore, we selected the IBS-D group as our research group.

Correlation analysis

In patients with IBS-D, there was a significant correlation between mucosal 5-HT_{2B} receptor levels and both the severity and frequency of abdominal pain ($r = 0.71$, $P = 0.001$ and $r = 0.68$, $P = 0.001$, respectively) (Figure 1B and C); however, this correlation was not observed in the control group.

Immunohistochemistry findings

As shown in Figure 1D, the immunohistochemical data confirmed the abundant expression of the 5-HT_{2B} receptor in

Table 1 Gene primer sequences (5'-3')

Gene	Primer sequences (5'-3')	
ACTB	Forward	GGCTGTATTCCCCTCCATCG
	Reverse	CCAGTTGGTAACAATGCCATGT
5-HT2B receptor	Forward	AGAACCAGGGGAATACAG
	Reverse	GGGAAATGGCACAGAGA
TRPV1	Forward	TGAAGCCGTTGCTCAGAATAACTG
	Reverse	CTCAGGGTCTTTGAACTCGTT

5-HT_{2B} receptor: Serotonin receptor 2B; TRPV1: Transient receptor potential vanilloid type 1.

Table 2 Characteristics of the study subjects, *n* (%)

Clinical characteristics	Subjects (*n* = 43)			IBS subtype (*n* = 28)		
	IBS (*n* = 28)	Control (*n* = 15)	*P* value	IBS-D (*n* = 18)	IBS-C (*n* = 18)	*P* value
Age	51.2 (10.2)	51.1 (10.3)	0.96	51.4 (9.8)	51.0 (11.5)	0.93
Sex			0.86			
Male	12 (42.9)	6 (40.0)		8 (44.4)	4 (40.0)	1.00
Female	16 (51.7)	9 (60.0)		10 (55.6)	6 (60.0)	
Severity of abdominal pain			< 0.001			0.49
Absent (0)	0 (0.0)	8 (53.4)		/	/	
Mild (1)	10 (35.7)	7 (46.7)		7 (38.9)	3 (30.0)	
Relevant (2)	12 (42.9)	0 (0.0%)		8 (44.4)	4 (40.0)	
Severe (3)	6 (21.4)	0 (0.0)		3 (16.7)	3 (30.0)	
Frequency of abdominal pain			< 0.001			0.88
Absent (0)	0 (0.0)	9 (60.0)		/	/	
Up to 1 day/week (1)	9 (32.1)	6 (40.0)		6 (33.3)	3 (30.0)	
2 or 3 days/week (2)	14 (50.0)	0 (0.0)		9 (50.0)	5 (50.0)	
4-6 days/week (3)	4 (14.3)	0 (0.0)		2 (11.1)	2 (20.0)	
Daily (4)	1 (3.57)	0 (0.0)		1 (5.6)	0 (0.0)	

Depending on the distribution of the variables, Student's *t*-test, Chi-square test, or Wilcoxon rank sum was used to test for differences in parameters between groups. Continuous variables are presented as arithmetic mean ± SD. Categorical variables are presented as numbers (percentages). IBS: Irritable bowel syndrome; IBS-D: IBS with diarrhea; IBS-C: IBS with constipation.

human colonic mucosal epithelial cells. TRPV1 was also expressed in human colonic mucosal epithelial cells (Figure 1D). The 5-HT_{2B} receptor and TRPV1 were coexpressed in human colonic mucosal epithelial cells (Figure 1E).

The establishment of the IBS-D rat model

Visceral sensitivity was determined in animals on Day 19 by measuring the AWR scores in response to CRD. IBS-D rats had higher mean AWR scores at pressures of 30, 45 and 60 mmHg but not at 15 mmHg (Figure 2A). Compared with those in the normal control group, the threshold pressure in the IBS-D group also decreased (Figure 2B). Compared with that in the normal control group, the water content of the feces in the IBS-D group was significantly greater (Figure 2C). Additionally, the weight of the fecal pellets in the IBS-D group was greater than that in the normal control group (Figure 2D). HE-stained sections showed no obvious differences in histopathological structure between the IBS-D rats and normal control rats (Figure 2E). These results suggested that the IBS-D model was established successfully.

5-HT_{2B} receptor and TRPV1 expression was upregulated in the IBS-D group

We investigated the changes in 5-HT_{2B} receptor expression in the IBS-D rat group. A previous study showed that the 5-HT_{2B} receptor is located mainly in smooth muscle layers and the myenteric nerve plexus[6]. Our results showed that 5-

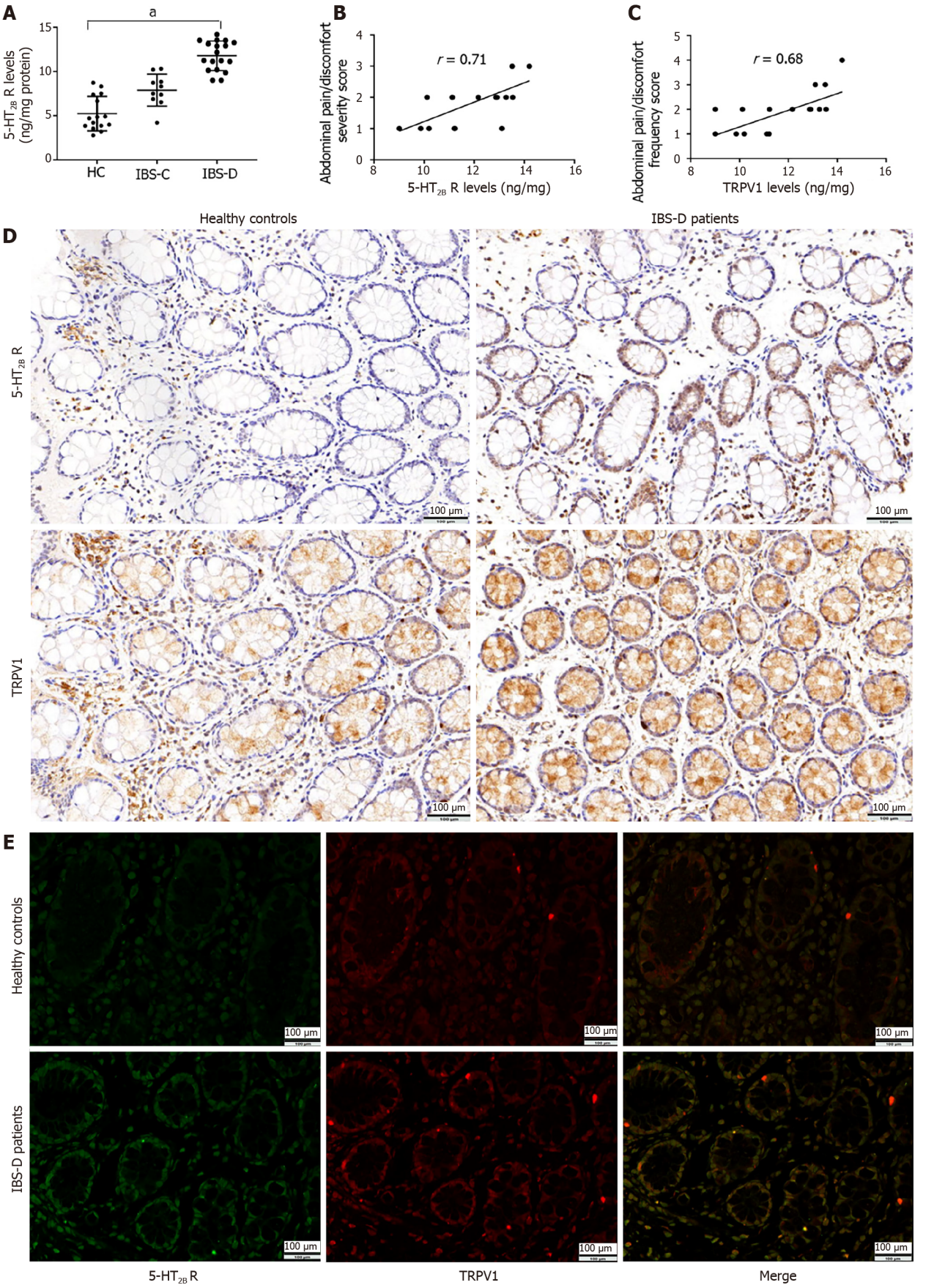

Figure 1 Irritable bowel syndrome with diarrhea patients presented increased serotonin receptor 2B and transient receptor potential vanilloid type 1 protein levels. A: Expression of the serotonin receptor 2B (5-HT$_{2B}$) receptor protein in colonic biopsies of patients with irritable bowel syndrome with diarrhea (IBS-D) (n = 18), patients with irritable bowel syndrome with constipation (n = 10), and control subjects (n = 15); B: Correlation between the severity of abdominal pain and the 5-HT$_{2B}$ receptor level in patients with IBS-D (Spearman correlation coefficient = 0.71, P = 0.001); C: Correlation between the frequency of

abdominal pain and the 5-HT$_{2B}$ receptor level in patients with IBS-D (Spearman correlation, r = 0.68; P = 0.001); D: Representative photomicrographs showing positive 5-HT$_{2B}$ receptor and transient receptor potential vanilloid type 1 (TRPV1) immunoreactivity in two serial sections of biopsy tissues from healthy controls and IBS-D patients. The magnification was 20 ×; E: Double-label immunofluorescence analysis of the 5-HT$_{2B}$ receptor (green) and TRPV1 (red) in the colonic mucosa of healthy controls and IBS-D patients. Merged image showing colocalization (yellow) of the 5-HT$_{2B}$ receptor and TRPV1 immunoreactivity. Magnification 20 ×. ^{a}P < 0.05. IBS-C: Irritable bowel syndrome with constipation; IBS-D: Irritable bowel syndrome with diarrhea; 5-HT$_{2B}$: Serotonin receptor 2B; HC: Healthy controls; TRPV1: Transient receptor potential vanilloid type 1.

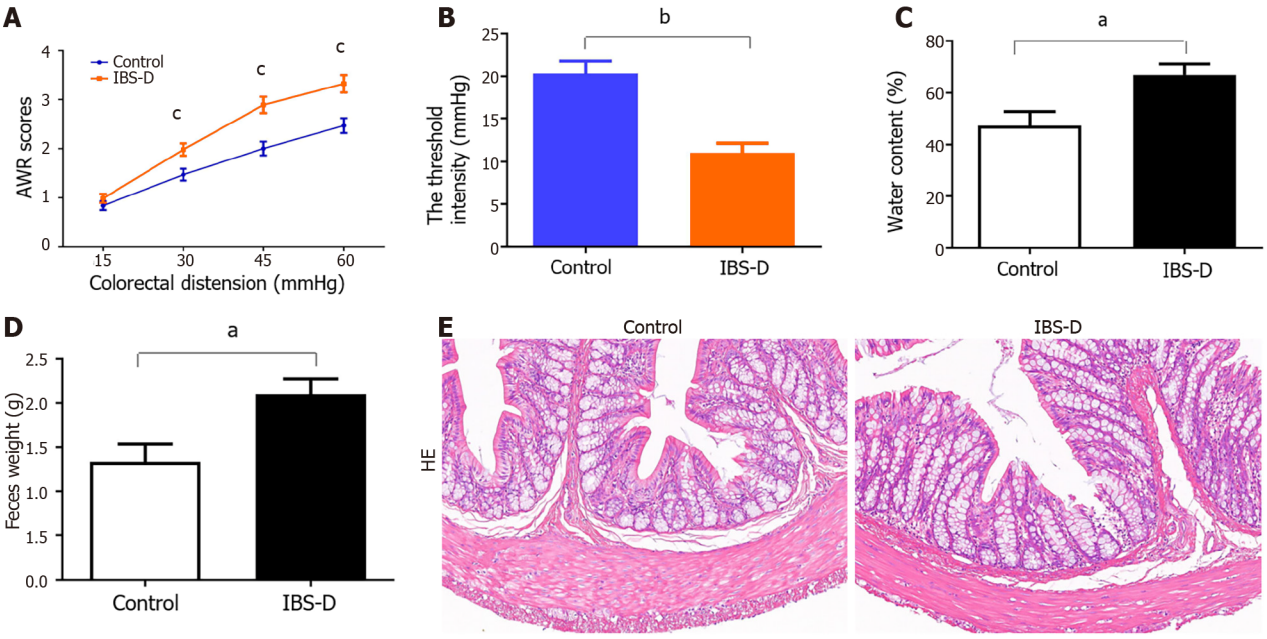

Figure 2 Validation of the establishment of an irritable bowel syndrome with diarrhea rat model. A: The irritable bowel syndrome with diarrhea (IBS-D) group had higher abdominal withdrawal reflex scores than did the normal control group, with colorectal distension pressures of 30, 45 and 60 mmHg but not 15 mmHg; B: The IBS-D group also had a decreased threshold pressure compared with that of the normal control group; C: The water content of the feces in the IBS-D group and normal control group; D: The weight of fecal pellets in the IBS-D group and normal control group; E: Inflammation evaluation of the colon in IBS-D rats and normal control rats using hematoxylin and eosin stain. No significant inflammation or abnormalities in structure were observed in IBS-D rats or normal control rats. Magnification 20 ×; ^{a}P < 0.05, ^{b}P < 0.01, ^{c}P < 0.001. IBS-D: Irritable bowel syndrome with diarrhea; HE: Hematoxylin and eosin; AWR: Abdominal withdrawal reflex.

HT$_{2B}$ receptor immunoreactivity not only localized to the smooth muscle layer and myenteric nerve plexus but also to the colonic mucosa layer (Figure 3A). Notably, the expression of the 5-HT$_{2B}$ receptor in the IBS-D group was greater than that in the normal control group. The intestinal tissue of the 5-HT$_{2B}$ receptor in the IBS-D group was significantly upregulated compared with that in the normal control group (Figure 3B and C). qRT-PCR revealed that the expression of 5-HT$_{2B}$ receptor mRNA in the IBS-D group was significantly greater than that in the normal control group (Figure 3D and E). Immunohistochemistry showed that TRPV1 was localized in the colonic mucosa layer, smooth muscle layer, and myenteric nerve plexus (Figure 3F). qRT-PCR revealed that the expression of TRPV1 mRNA in the IBS-D group was greater than that in the normal control group (Figure 3G and H). These results indicated that upregulated 5-HT$_{2B}$ receptor and TRPV1 expression were involved in the pathogenesis of IBS-D.

Involvement of the 5-HT$_{2B}$ receptor in visceral hyperalgesia in IBS-D patients

The 5-HT$_{2B}$ receptor was reported to participate in the pathophysiology of peripheral hyperalgesia[8]. The role of the 5-HT$_{2B}$ receptor in visceral hyperalgesia in IBS-D rats was investigated in our study. The 5-HT$_{2B}$ receptor antagonist RS-127445 was injected intraperitoneally into IBS-D rats. The results showed that, compared with vehicle, RS-127445 treatment induced a marked decrease in AWR and increased the threshold pressure (Figure 4A and B). Immunohistochemistry, qRT-PCR, and ELISA results demonstrated that 5-HT$_{2B}$ receptor protein and mRNA expression was downregulated in RS-127445-treated IBS-D rats (Figures 4C and 5A-D). Moreover, the 5-HT$_{2B}$ receptor agonist BW723C86 was injected intraperitoneally into healthy control rats once daily for 7 consecutive days. Interestingly, the results showed that the application of the 5-HT$_{2B}$ receptor agonist BW723C86 induced a marked increase in AWR scores and a decrease in threshold pressure in healthy rats compared with those in normal control rats (Figure 5E and F). These results demonstrated that the 5-HT$_{2B}$ receptor participated in the pathophysiology of visceral hyperalgesia in IBS-D rats.

5-HT$_{2B}$ receptor-induced visceral hyperalgesia was mediated via TRPV1

A previous study reported that a 5-HT$_{2B}$ receptor agonist induces mechanical hyperalgesia by regulating TRPV1 function [13]. In mouse colon sensory neurons, 5-HT$_{2B}$ receptor activation enhances TRPV1 function[14]. We hypothesized that 5-

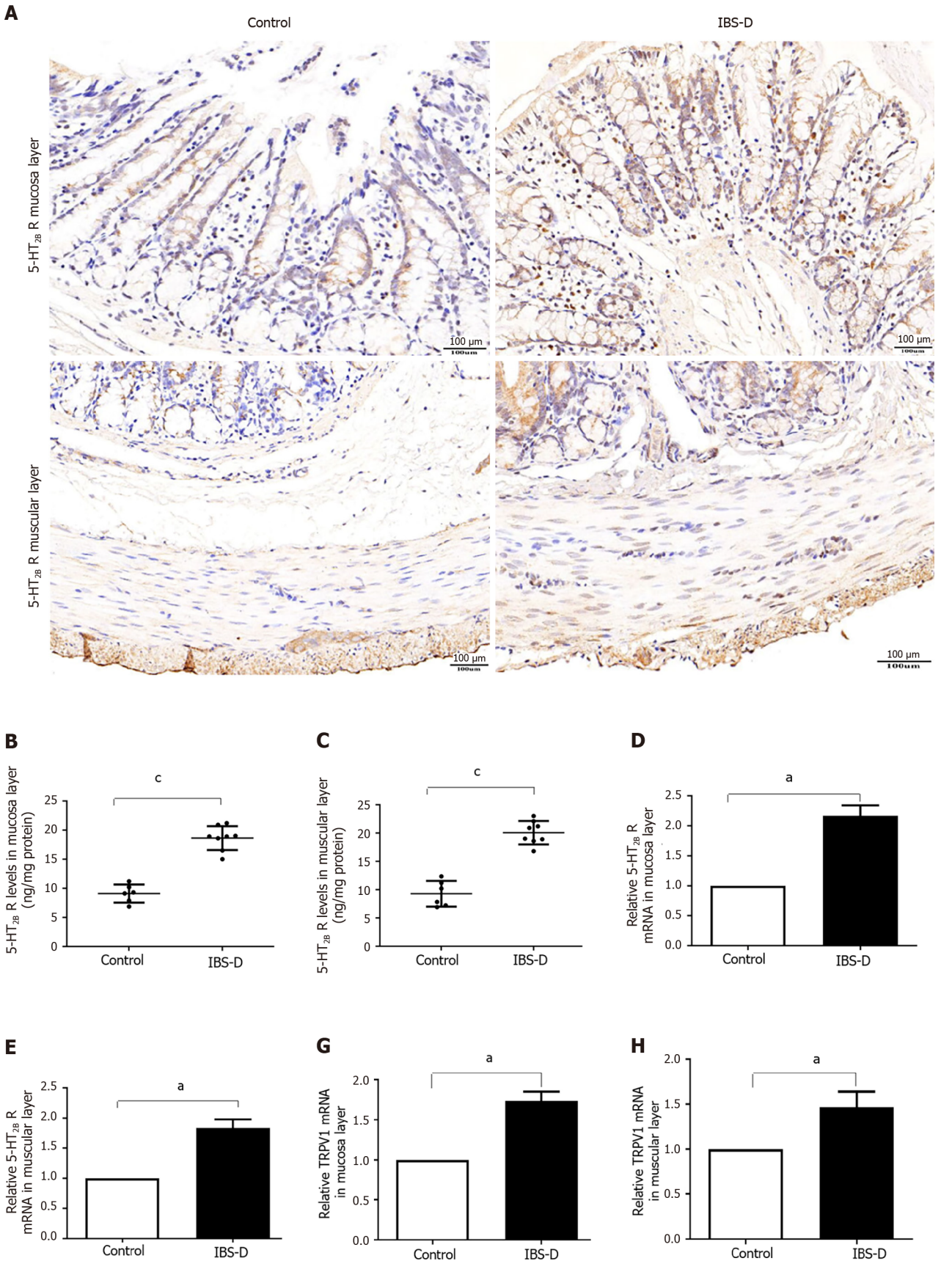
A
Control
IBS-D
5-HT2B R mucosa layer
5-HT2B R muscular layer
100 μm
B
5-HT2B R levels in mucosa layer (ng/mg protein)
C
5-HT2B R levels in muscular layer (ng/mg protein)
D
Relative 5-HT2B R mRNA in mucosa layer
E
Relative 5-HT2B R mRNA in muscular layer
G
Relative TRPV1 mRNA in mucosa layer
H
Relative TRPV1 mRNA in muscular layer
Control
IBS-D
a
c

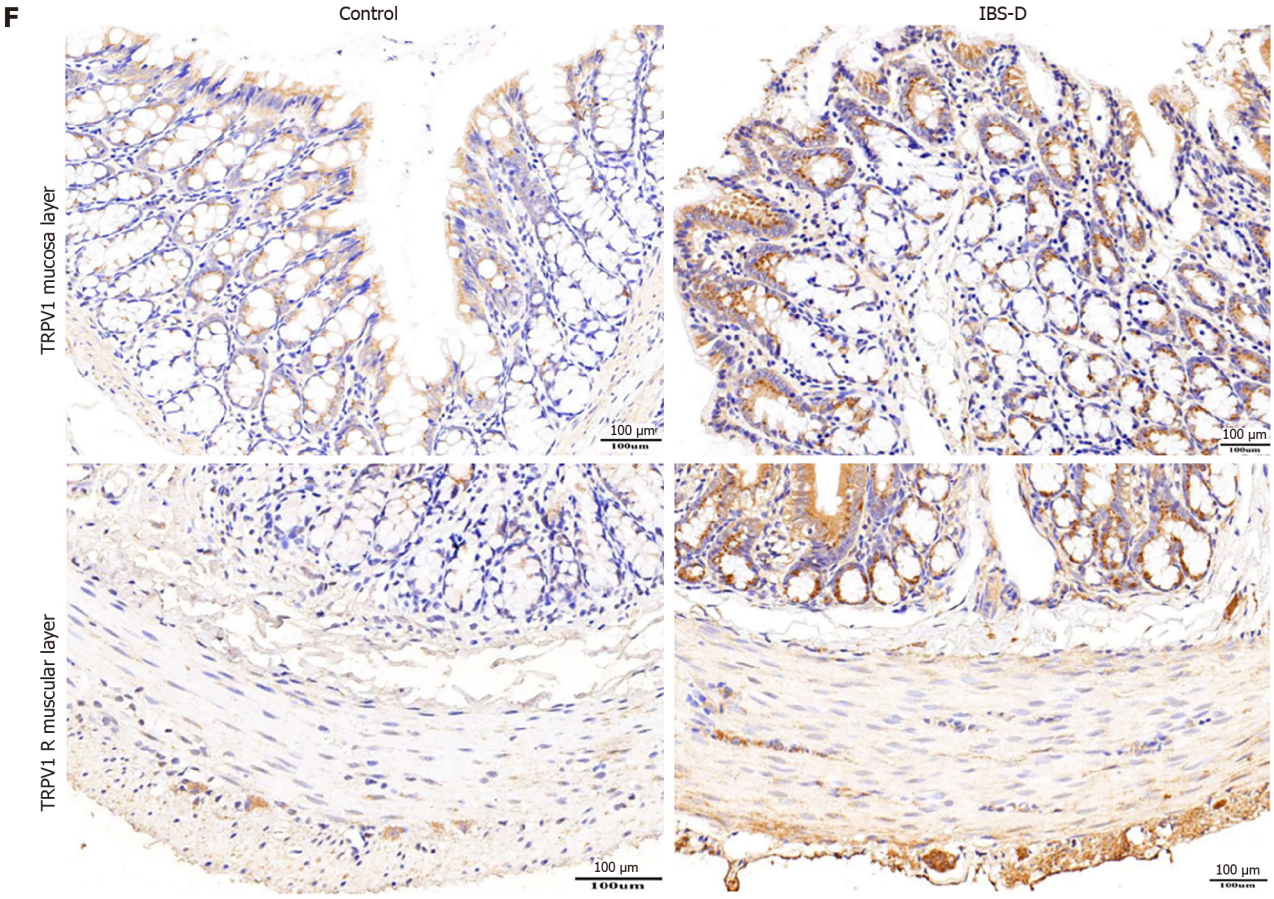

Figure 3 Increased serotonin receptor 2B and transient receptor potential vanilloid type 1 levels in the irritable bowel syndrome with diarrhea group. A: Immunohistochemical staining revealed the expression of the serotonin receptor 2B (5-HT$_{2B}$ receptor) in the colon tissue in irritable bowel syndrome with diarrhea (IBS-D) rats and normal control rats; Magnification 20 ×; B: Expression of 5-HT$_{2B}$ receptor protein in the colonic mucosa layer of the IBS-D group and normal control group; C: Expression of 5-HT$_{2B}$ receptor protein in the colonic muscular layer of the IBS-D group and normal control group; D: Levels of 5-HT$_{2B}$ receptor mRNA in the colonic mucosa layer from the IBS-D group and normal control group; E: Levels of 5-HT$_{2B}$ receptor mRNA in the colonic muscular layer from the IBS-D group and normal control group; F: Immunohistochemical staining showing the expression of transient receptor potential vanilloid type 1 (TRPV1) in the colon tissue in IBS-D rats and normal control rats. Magnification 20 ×; G: Levels of TRPV1 mRNA in the colonic mucosa layer from the IBS-D group and normal control group; H: Levels of TRPV1 mRNA in the colonic muscular layer from the IBS-D group and normal control group. $^{a}P < 0.05$, $^{c}P < 0.001$. IBS-D: Irritable bowel syndrome with diarrhea; 5-HT$_{2B}$: Serotonin receptor 2B; TRPV1: Transient receptor potential vanilloid type 1.

HT$_{2B}$ receptor-induced visceral hyperalgesia in IBS-D patients is mediated *via* the TRPV1 channel. First, we detected the coexpression of TRPV1 and the 5-HT$_{2B}$ receptor in colonic tissues. Immunofluorescence revealed that TRPV1 and the 5-HT$_{2B}$ receptor were coexpressed not only in smooth muscle layers and the myenteric nerve plexus but also in the colonic mucosa layer in humans and rats (Figures 1E, 6A and B). The percentage of 5-HT$_{2B}$ IR cells surrounded by TRPV1-positive cells (5-HT$_{2B}$ receptor I^{+}) and total 5-HT$_{2B}$ receptor IR cells (5-HT$_{2B}$ receptor I$_{T}$) in the IBS-D group was greater than that in the normal control group (Figure 6C and D).

Second, we aimed to identify in which layer the receptor of 5-HT$_{2B}$ and TRPV1 mediates visceral hyperalgesia in the IBS-D model. Then, 5-HT$_{2B}$ and TRPV1 were labeled with molecular markers of epithelial cells, peripheral nerve fibers and smooth muscle cells *via* immunofluorescence to determine the functions of these receptors in visceral pain sensation. Immunofluorescence staining demonstrated that 5-HT$_{2B}$ and TRPV1 were colocalized mainly in peripheral nerve fibers and colon epithelial cells (Figure 7). The 5-HT$_{2B}$ receptor and TRPV1 were not colocalized in smooth muscle cells. Visceral hypersensitivity is the most important pathophysiological alteration associated with visceral pain in IBS patients. The expression of 5-HT$_{2B}$ and TRPV1 in peripheral nerve fibers and the colonic mucosa layer may be involved in the gut sensation and visceral hyperalgesia observed in IBS-D patients.

Third, the TRPV1 antagonist SB366791 was administered to normal control rats 30 min before BW723C86, and the results showed that the BW723C86-induced visceral hyperalgesia was alleviated by SB366791 (Figure 5E and F).

Fourth, qRT-PCR and immunohistochemistry were used to detect the expression of TRPV1 in RS-127445-treated IBS-D rats. The results showed that injection of RS-127445 significantly decreased the expression of TRPV1 in the colonic tissues of IBS-D rats compared with those of control IBS-D rats (Figure 8).

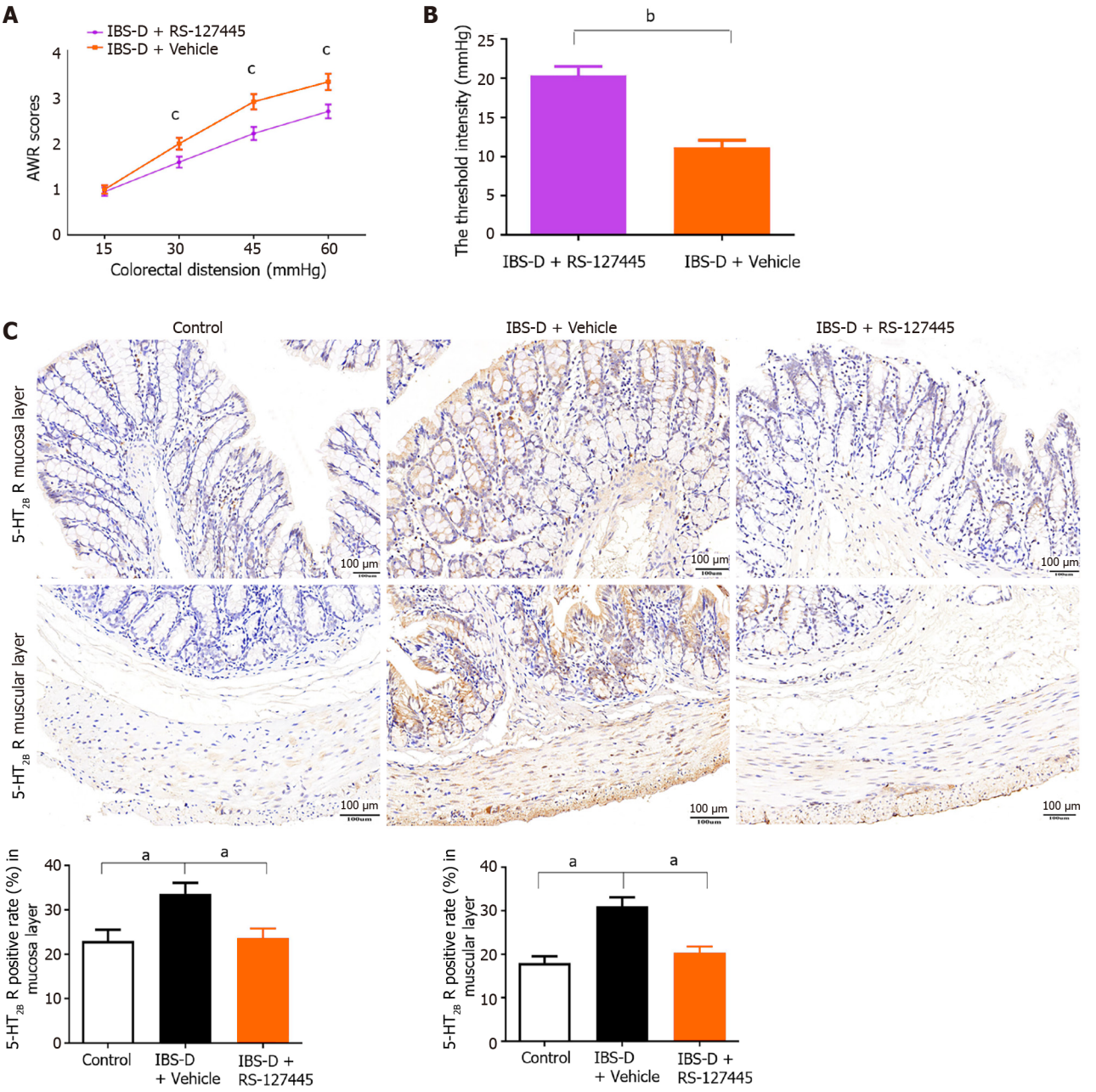

Figure 4 RS12-7445 decreased the visceral sensitivity and serotonin receptor 2B levels in irritable bowel syndrome with diarrhea rats. A: The irritable bowel syndrome with diarrhea (IBS-D) + Vehicle group had significantly greater abdominal withdrawal reflex scores than did the IBS-D + RS-127445 group with the same colorectal distension (CRD) pressure; B: The IBS-D + Vehicle group had significantly reduced threshold pressure than did the IBS-D + RS-127445 group with the same CRD pressure; C: Immunohistochemical staining showing the expression of the serotonin receptor 2B receptor in the colon mucosa layer and colon muscular layer of each group. Magnification 20 ×; $^{a}P < 0.05$, $^{b}P < 0.01$, $^{c}P < 0.001$. IBS-D: Irritable bowel syndrome with diarrhea; 5-HT$_{2B}$: Serotonin receptor 2B; AWR: Abdominal withdrawal reflex.

DISCUSSION

The 5-HT$_{2B}$ receptor has generated considerable interest in the research community owing to its critical role in the generation of hyperalgesic diseases. Previous studies have shown that peripheral and spinal 5-HT$_{2B}$ receptors have pronociceptive effects and participate in the development and maintenance of formalin-induced hyperalgesia[22]. The 5-HT$_{2B}$ receptor mediates 5-HT-induced mechanical hyperalgesia in mice[8]. Activation of the 5-HT$_{2B}$ receptor in meningeal nociception causes neurogenetic inflammation and the generation of migraine pain[23].

In the present study, we investigated the potential involvement of the 5-HT$_{2B}$ receptor in the visceral pain of IBS-D patients. Compared with those from control participants, colonic biopsies from patients with IBS-D revealed significant upregulation of the 5-HT$_{2B}$ receptor. Moreover, enhanced expression of the 5-HT$_{2B}$ receptor was positively correlated with the severity and frequency of abdominal pain symptoms. We instilled 1 mL of 4% acetic acid intracolonically and applied wrap restraint stress to induce an IBS-D rat model. Compared with normal control rats, this rat model showed visceral hypersensitivity and increased fecal weight and fecal water content, which was consistent with the clinical symptoms of

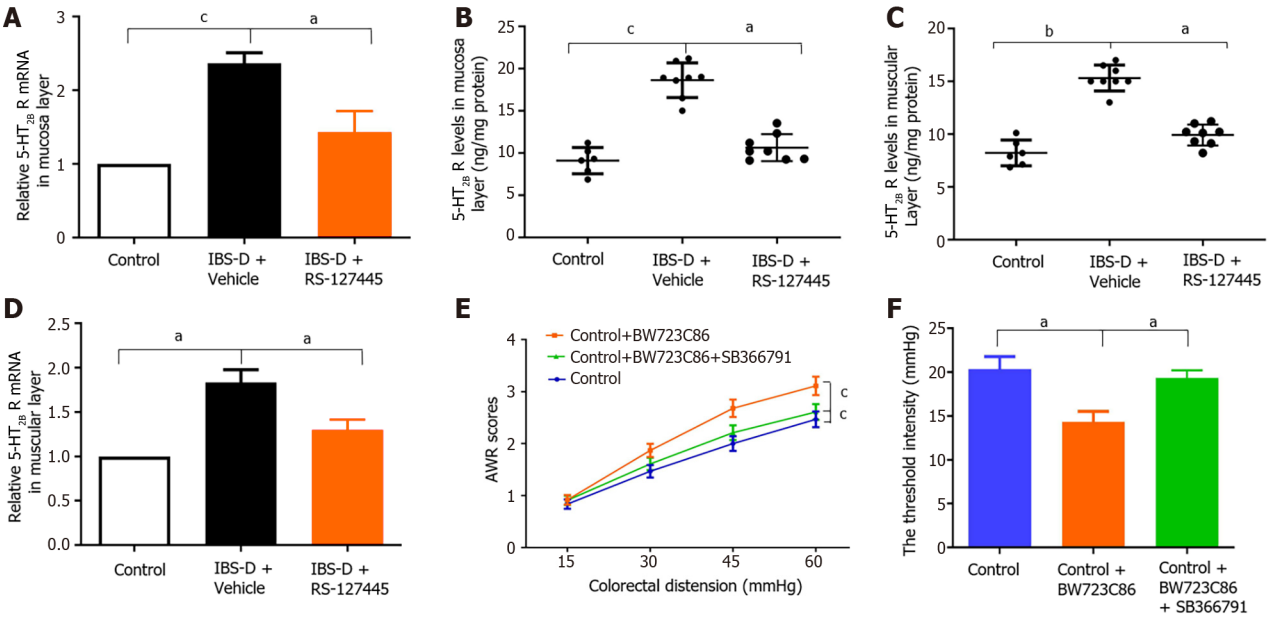

Figure 5 RS12-7445 decreased the serotonin receptor 2B levels in irritable bowel syndrome with diarrhea rats. Visceral sensitivity was detected by the colorectal distension. A: Serotonin receptor 2B (5-HT$_{2B}$ receptor) mRNA levels in the colonic mucosa layer were detected *via* quantitative reverse transcriptase polymerase chain reaction (qRT-PCR); B: Expression of the 5-HT$_{2B}$ receptor in colon mucosa tissues from each group was detected by ELISA; C: Expression of the 5-HT$_{2B}$ receptor in colon muscular tissues from each group was detected by ELISA; D: 5-HT$_{2B}$ receptor mRNA levels in the colonic muscular layer were detected *via* qRT-PCR; E: The Control + BW723C86 group had higher abdominal withdrawal reflex (AWR) scores than did the Control group, with colorectal distension (CRD) pressures of 30, 45 and 60 mmHg but not 15 mmHg. Similarly, the Control + BW723C86 group had increased AWR scores with the same CRD pressure compared with those of the Control + BW723C86 + SB366791 group; F: The Control + BW723C86 group had a decreased threshold pressure compared with that of the Control group. Similarly, the Control + BW723C86 group had reduced threshold pressure with the same CRD pressure compared with those of the Control + BW723C86 + SB366791 group. $^{a}P < 0.05$, $^{b}P < 0.01$, $^{c}P < 0.001$. IBS-D: Irritable bowel syndrome with diarrhea; 5-HT$_{2B}$: Serotonin receptor 2B; AWR: Abdominal withdrawal reflex.

IBS-D patients. Our findings showed that the 5-HT$_{2B}$ receptor was expressed not only in the colonic smooth muscle layers and myenteric nerve plexus but also in the colonic mucosa layer in rats. Increased expression of the 5-HT$_{2B}$ receptor in colon tissue was found in IBS-D rats compared with that in normal control rats. Previous studies demonstrated that the 5-HT$_{2B}$ receptor was expressed in smooth muscle layers and the myenteric nerve plexus of human and mouse intestines[6]. To our knowledge, this is the first study to explore the expression of the 5-HT$_{2B}$ receptor in the colon mucosa layer in IBS-D patients and rats. The upregulation of the 5-HT$_{2B}$ receptor in the colon mucosa layer may be involved in the gut sensation and visceral hyperalgesia of IBS-D patients.

Considering that visceral hypersensitivity is the most important pathophysiological alteration associated with visceral pain in IBS-D patients, we used a 5-HT$_{2B}$ receptor agonist (BW723C86). The administration of BW723C86 to normal control rats significantly increased visceral hypersensitivity. A 5-HT$_{2B}$ receptor antagonist (RS-127445) significantly decreased visceral hypersensitivity in IBS-D rats. In RS-127445-treated IBS-D rats, decreased mRNA expression of the 5-HT$_{2B}$ receptor was found in colon tissues. These results suggested the involvement of the 5-HT$_{2B}$ receptor in visceral hypersensitivity in rats. Our findings were consistent with previous work showing that RS-127445 inhibited visceral hyperalgesia in both TNBS-induced and stress-sensitive rat models of visceral hypersensitivity[9,10]. Tegaserod, which is effective at alleviating abdominal pain symptoms in IBS patients, is a potent 5-HT$_{2B}$ receptor antagonist[24]. Taken together, these data support the use of 5-HT$_{2B}$ receptor antagonists as novel treatments for visceral hyperalgesia in IBS-D patients.

Previous research has shown that 5-HT-induced excitatory effects in the human colon *in vitro* are mediated by the 5-HT$_{2B}$ receptor. RS-127445 inhibited 5-HT-induced excitatory effects[6]. Other research revealed that RS-127445 concentration-dependently reduced fecal output and peristaltic frequency in healthy mice[25]. A new study showed that the 5-HT$_{2B}$ receptor on interstitial cells of Cajal in diabetic mice was decreased and associated with constipation. Activation of the 5-HT$_{2B}$ receptor improved colonic motility and constipation in diabetic mice[20]. Taken together, these results indicated that 5-HT$_{2B}$ receptor activation was related to gut motility. Considering that the 5-HT$_{2B}$ receptor induces colonic motility, the upregulation of the 5-HT$_{2B}$ receptor may be related to the development of diarrhea in patients with IBS-D. Additionally, it is conceivable that the upregulation of the 5-HT$_{2B}$ receptor may be relevant to the visceral hyperalgesia that we observed in this study because disorders of muscle tone and colonic motility have been postulated to be related to visceral hyperalgesia.

The 5-HT$_{2B}$ antagonist RS-127445 effectively alleviated pain in the IBS-D model. However, it is not clear in which kind of cell these two receptors are located. It is also unclear in which layer of the colon the receptor of 5-HT$_{2B}$ and TRPV1 mediates visceral hyperalgesia in the IBS-D model. Because the same receptor plays different roles in different cells, 5-HT$_{2B}$ and TRPV1 were labeled with molecular markers of epithelial cells, peripheral nerve fibers and smooth muscle cells *via* immunofluorescence to determine the functions of these receptors in visceral pain sensation. The results demonstrated

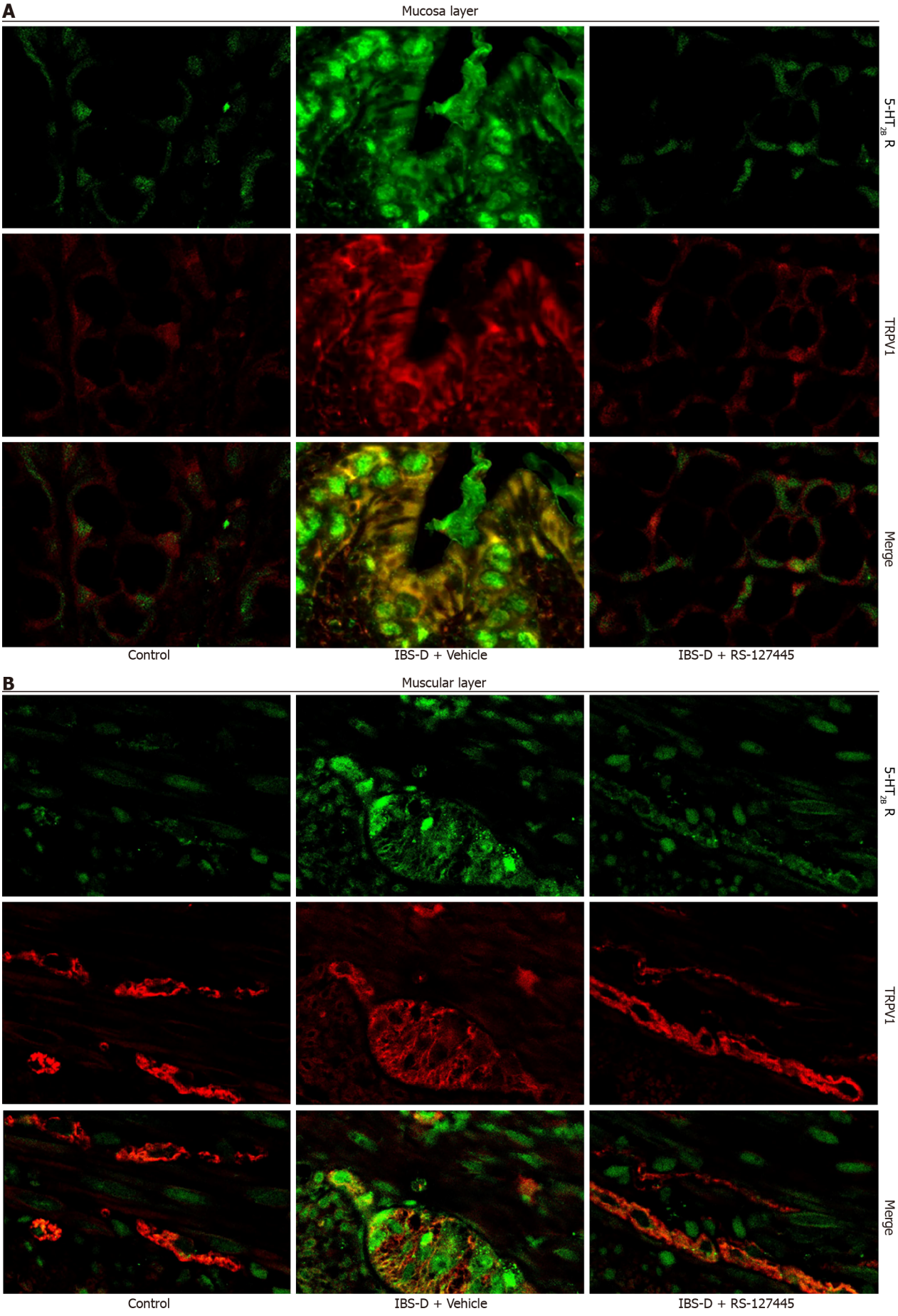
A
Mucosa layer
5-HT2B R
TRPV1
Merge
Control
IBS-D + Vehicle
IBS-D + RS-127445
B
Muscular layer
5-HT2B R
TRPV1
Merge
Control
IBS-D + Vehicle
IBS-D + RS-127445

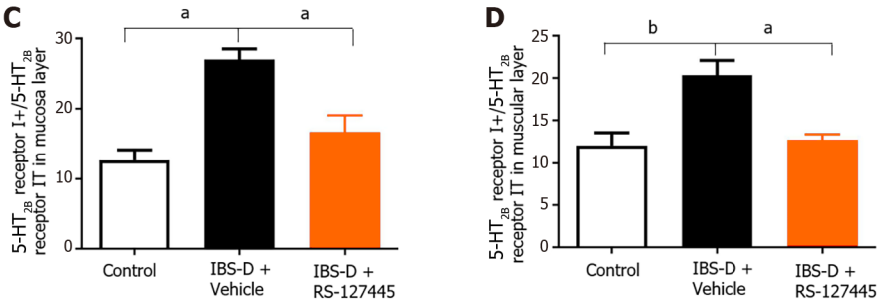

Figure 6 Double-label immunofluorescence analysis in the rat colon. A and B: Double-label immunofluorescence analysis of serotonin receptor 2B (5-HT$_{2B}$ receptor) (green) and transient receptor potential vanilloid type 1 (TRPV1) (red) in the colon mucosa layer (A) and muscular layer (B) in normal control rats, irritable bowel syndrome with diarrhea (IBS-D) + Vehilce rats and RS-127445-treated IBS-D rats. Merged image showing colocalization (yellow) of the 5-HT$_{2B}$ receptor and TRPV1 immunoreaction. Magnification 20 ×; C: The data are the percentages of 5-HT$_{2B}$ receptor I$^+$ cells in the colon mucosa layer among the total 5-HT$_{2B}$ receptor-immunoreactive (IR) cells in the colon mucosa layer (5-HT$_{2B}$ receptor I$_T$); D: The data are presented as the percentage of 5-HT$_{2B}$ receptor I$^+$ cells in the colon muscular layer relative to the total 5-HT$_{2B}$ IR cells in the colon muscular layer (5-HT$_{2B}$ receptor I$_T$). $^aP < 0.05$, $^bP < 0.01$. IBS-D: Irritable bowel syndrome with diarrhea; 5-HT$_{2B}$: Serotonin receptor 2B; TRPV1: Transient receptor potential vanilloid type 1.

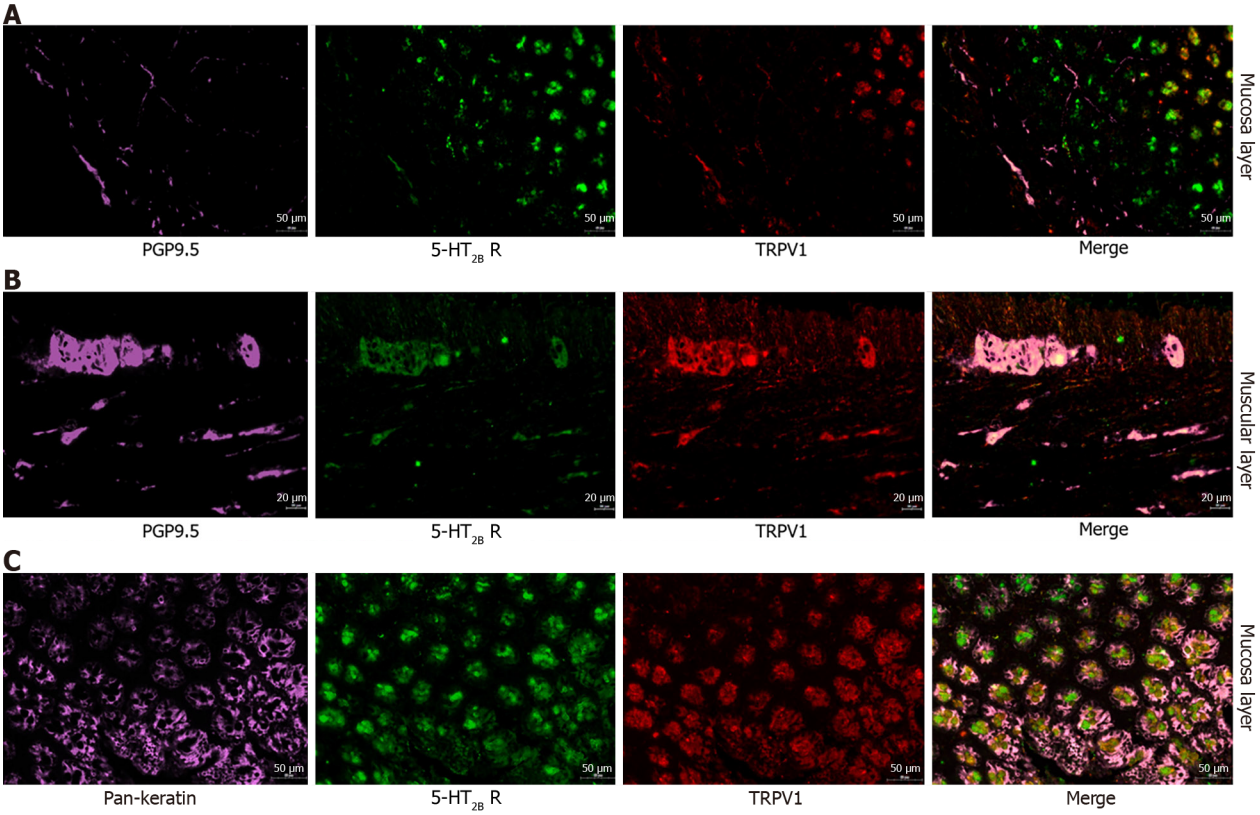

Figure 7 Immunofluorescence analysis of colon tissues costained with serotonin receptor 2B (green fluorescence), transient receptor potential vanilloid type 1 (red fluorescence), protein gene product 9.5 (purple fluorescence) and Pan-Keratin (purple fluorescence). A: Serotonin receptor 2B (5-HT$_{2B}$ receptor) receptor (green fluorescence), transient receptor potential vanilloid type 1 (TRPV1) (red fluorescence) and protein gene product 9.5 (PGP9.5) (purple fluorescence) in the rat colon mucosa layer. Merged image showing colocalization (pink) of the 5-HT$_{2B}$ receptor, TRPV1 receptor and PGP9.5 immunoreactivities in the rat colon mucosa layer; B: 5-HT$_{2B}$ receptor (green fluorescence), TRPV1 (red fluorescence) and PGP9.5 (purple fluorescence) in the rat colon muscular layer. Merged image showing colocalization (pink) of the 5-HT$_{2B}$ receptor, TRPV1 receptor and PGP9.5 immunoreactivities in the rat colon muscular layer; C: The 5-HT$_{2B}$ receptor (green fluorescence), TRPV1 (red fluorescence) and Pan-Keratin (purple fluorescence) in the rat colon mucosa layer. Merged image showing colocalization (pink) of the 5-HT$_{2B}$ receptor and TRPV1 and pankeratin immunoreactivities in the rat colon mucosa layer. Magnification 20 ×. PGP9.5: Protein gene product 9.5; 5-HT$_{2B}$: Serotonin receptor 2B; TRPV1: Transient receptor potential vanilloid type 1.

that 5-HT$_{2B}$ and TRPV1 were colocalized mainly in peripheral nerve fibers and colon epithelial cells. Visceral hypersensitivity is the most important pathophysiological alteration associated with visceral pain in IBS patients. The expression of 5-HT$_{2B}$ and TRPV1 in peripheral nerve fibers and the colonic mucosa layer may be involved in the gut sensation and visceral hyperalgesia observed in IBS-D patients.

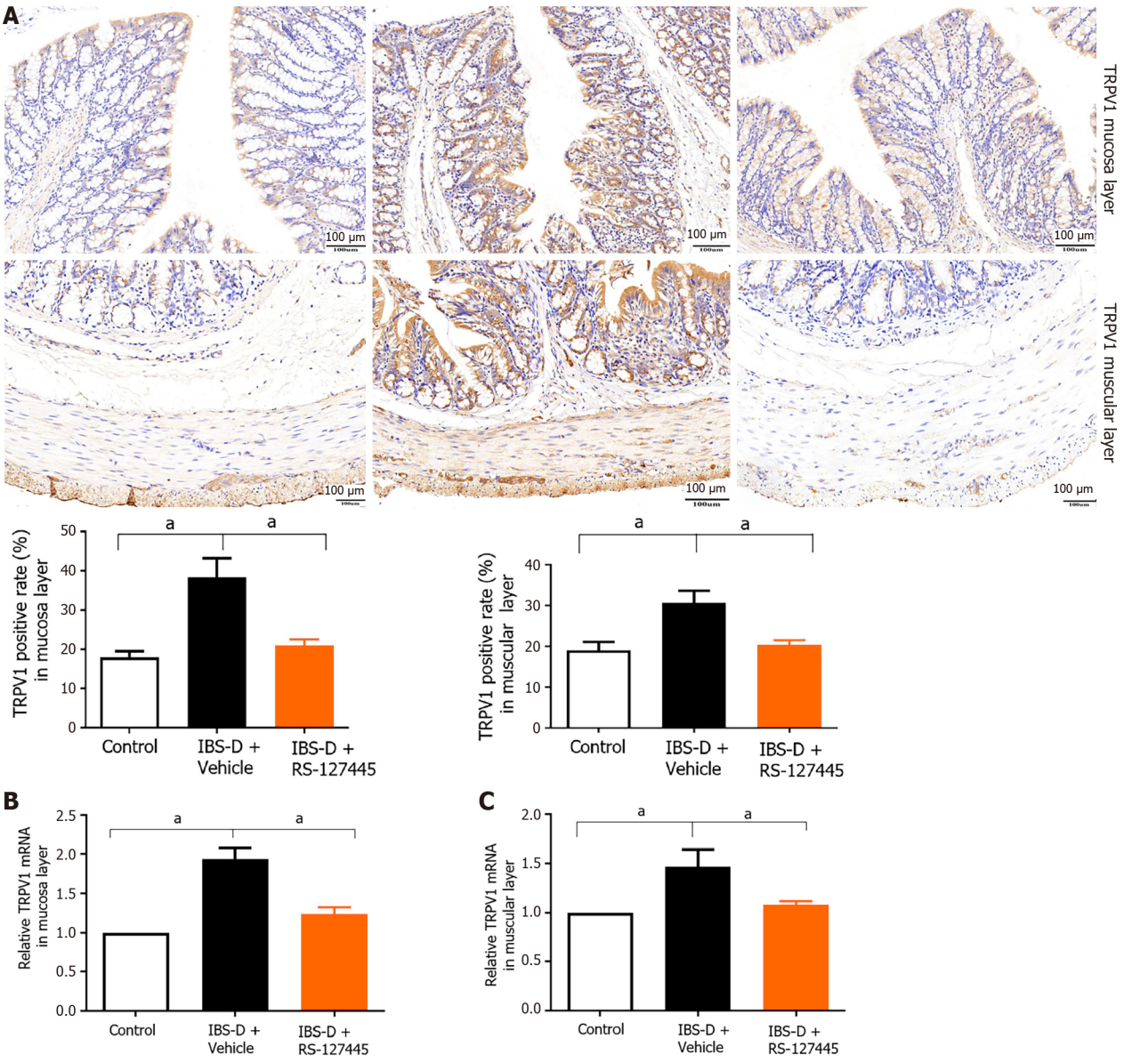

Figure 8 RS12-7445 decreased the transient receptor potential vanilloid type 1 levels in colon tissues in irritable bowel syndrome with diarrhea rats. A: Immunohistochemical staining showing the expression of transient receptor potential vanilloid type 1 (TRPV1) in the colon mucosa layer and colon muscular layer of each group. Magnification 20 ×; B: Levels of TRPV1 mRNA in colon mucosa layer tissues were measured by quantitative reverse transcriptase polymerase chain reaction (qRT-PCR); C: Levels of TRPV1 mRNA in colon muscular layer tissues were measured by qRT-PCR. $^{a}P < 0.05$. IBS-D: Irritable bowel syndrome with diarrhea; TRPV1: Transient receptor potential vanilloid type 1.

TRPV1 channels are critical contributors to normal and pathological pain and are likely to be activated by inflammatory products in IBS[26]. Upregulation and/or sensitization of TRPV1 is considered an important mechanism of visceral hyperalgesia both in preclinical rat models and in patients with IBS[27]. Our results indicated that TRPV1 was upregulated in IBS-D patients and rats, which was consistent with previous findings[27]. A previous report showed that TRPV1 activity is regulated by inflammatory mediators, including prostaglandins and bradykinin, likely through protein kinase C (PKC)- or cAMP-dependent protein kinase-mediated phosphorylation of the receptor. Generally, protein kinase-mediated phosphorylation of the TRPV1 receptor results in peripheral sensitization[28]. Data from a mouse model suggested that 5-HT$_{2B}$ receptor activation may enhance the responsiveness of the TRPV1 receptor to temperature and acid and thereby contribute to peripheral sensitization[14]. Serotonin signaling alterations in IBS may occur in part through TRPV1 sensitization[29].

A previous study demonstrated that the administration of antagonists of 5-HT$_{2B}$, PLCβ, PKCε, and TRPV1 inhibited 5-HT-induced mechanical hyperalgesia. In DRG neurons, 5-HT injection increased capsaicin- or 5-HT-induced calcium signals, which were regulated by the 5-HT$_{2B}$-PLCβ-PKCε pathway. The possible mechanism is as follows: Injection of 5-HT induces activation of 5-HT$_{2B}$-PLCβ-PKCε in the peripheral nociceptors, after which TRPV1 is relieved from PIP2 inhibition to produce peripheral sensitivity, which increases the number of neurons responding to 5-HT[13]. Thus, 5-HT$_{2B}$ mediates 5-HT-induced mechanical hyperalgesia by regulating TRPV1 function[13]. In mouse colon sensory neurons, 5-HT$_{2B}$ receptor activation enhances TRPV1 function[14]. Our present study demonstrated that 5-HT$_{2B}$ and TRPV1 are

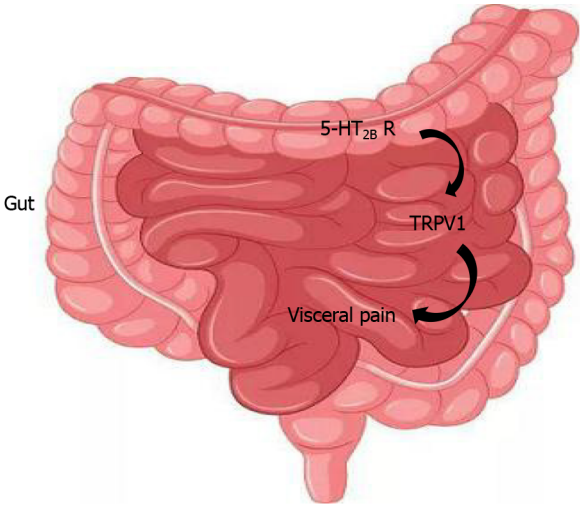

Figure 9 The visceral pain conduction pathway involves transient receptor potential vanilloid type 1. The expression of the serotonin receptor 2B (5-HT$_{2B}$) receptor and transient receptor potential vanilloid type 1 (TRPV1) increased in colon tissues from irritable bowel syndrome with diarrhea patients and rats. The administration of a 5-HT$_{2B}$ receptor agonist increased visceral pain, which was alleviated by successive administration of a TRPV1 antagonist. Treatment with a 5-HT$_{2B}$ receptor antagonist suppressed TRPV1. The sensation of pain is thus attenuated, and the pain threshold is increased. 5-HT$_{2B}$ receptor: Serotonin receptor 2B; TRPV1: Transient receptor potential vanilloid type 1.

located mainly in peripheral nerve fibers and that the number of 5-HT$_{2B}$ receptor- and TRPV1-positive cells was significantly greater in IBS-D rats than in normal control rats. The modulation of TRPV1 function by the 5-HT$_{2B}$ receptor may increase afferent input from the colon and provide a peripheral mechanism for the development of visceral pain symptoms in IBS-D patients. 5-HT$_{2B}$ receptor agonist-induced visceral hyperalgesia in normal rats was alleviated by a TRPV1 antagonist. RS-127445 not only inhibited visceral hyperalgesia but also decreased the expression of TRPV1. These results indicated that increased 5-HT$_{2B}$ receptor expression may participate in visceral hyperalgesia in IBS-D rats *via* TRPV1 channels. However, the exact underlying mechanism requires further research.

CONCLUSION

In conclusion, our present study showed that the 5-HT$_{2B}$ receptor may participate in visceral hyperalgesia in IBS-D patients. In addition, 5-HT$_{2B}$ receptor-induced visceral hyperalgesia may be mediated by TRPV1 channels (Figure 9). The analgesic effect of RS-127445 in IBS-D rats could be used as a novel treatment for IBS-D.

ARTICLE HIGHLIGHTS

Research background

Patients with irritable bowel syndrome with diarrhea (IBS-D) experience a significant reduction in their quality of life. While the exact pathogenesis of IBS-D remains incompletely understood, research indicates that serotonin receptor 2B (5-HT$_{2B}$ receptor) plays a critical role in many chronic pain conditions. The role of 5-HT$_{2B}$ receptor in the altered gut sensation of IBS-D was not investigated.

Research motivation

This study is to identify the role of 5-HT$_{2B}$ receptor in the altered gut sensation *via* transient receptor potential vanilloid type 1 (TRPV1) channels in rat model and patients with diarrhea-predominant IBS.

Research objectives

This study aims to elucidate the role of the 5-HT$_{2B}$ receptor in both IBS-D patients and rat models induced by acetic acid and wrap restraint. The findings are anticipated to offer novel insights into potential avenues for IBS-D treatment.

Research methods

Rectosigmoid biopsies were collected from IBS-D patients and healthy controls. The expression level of 5-HT$_{2B}$ receptor in colon tissue was measured and correlated with abdominal pain scores in IBS-D patients. The IBS-D rat model was induced by intracolonic instillation of acetic acid and wrap restraint. Alterations in visceral sensitivity, 5-HT$_{2B}$ receptor and TRPV1 expression were examined following 5-HT$_{2B}$ receptor antagonist administration. Changes in visceral sensitivity after the administration of the TRPV1 antagonist were recorded.

Research results

A higher expression of 5-HT_{2B} receptor was observed in the colonic mucosa of patients with IBS-D compared to controls, correlating with abdominal pain scores. The IBS-D rats was successfully established through intracolonic instillation of acetic acid and wrap restraint. Administration of the exogenous 5-HT_{2B} receptor agonist increased visceral hypersensitivity, which was subsequently alleviated by successive administration of TRPV1 antagonist. IBS-D rats receiving the 5-HT_{2B} receptor antagonist displayed inhibition of visceral hyperalgesia. Additionally, the percentage of 5-HT_{2B} receptor-immunoreactive (IR) cells surrounded by TRPV1-positive cells (5-HT_{2B} receptor I^+) and total 5-HT_{2B} receptor IR cells (5-HT_{2B} receptor I_T) in IBS-D rats significantly decreased with the administration of 5-HT_{2B} receptor antagonist.

Research conclusions

The increased expression of 5-HT_{2B} receptor contributing to visceral hyperalgesia through the induction of TRPV1 expression in IBS-D, providing important insights into the potential mechanisms underlying IBS-D-associated visceral hyperalgesia.

Research perspectives

The analgesic effect of RS-127445 in IBS-D rats suggests its potential as a novel treatment for IBS-D.

ACKNOWLEDGEMENTS

The authors would like to acknowledge Prof. Yuan-Yuan Ruan (School of Basic Medical Sciences, Fudan University, Shanghai, China), Prof. Wei-Wei Zheng (School of Public Health, Fudan University, Shanghai, China) and Prof. Qian-Li (School of Basic Medical Sciences, Fudan University, Shanghai, China) for skillful technical assistance.

FOOTNOTES

Co-corresponding authors: Ya-Jie Wang and Miao-Jiang.

Author contributions: Li ZY contributed to the research concept, animal surgery and behavioral studies, data analysis and interpretation, drafting of the manuscript; Mao YQ contributed to the animal surgery and behavioral studies; Hua Q contributed to the study supervision, participant enrollment, and supplementary experimental support; Sun YH contributed to the participant enrollment, analysis and technical and material support; Ye XG contributed to the acquisition of data, statistical analysis and technical support; Hu JX contributed to the study supervision, acquisition of data; Wang HY contributed to the acquisition of data, statistical analysis; Jiang M and Wang YJ contributed to the research concept, supervision of studies, critical revision of the manuscript.

Supported by The Health Commission of Jinshan District, Shanghai, China, No. JSKJ-KTMS-2019-01; The Youth Research Foundation of Jinshan Hospital of Fudan University, No. JYQN-JC-202101 and No. JYQN-JC-202216; and The Reserve Discipline Construction of Jinshan Hospital of Fudan University, No. HBXK-2021-2.

Institutional review board statement: The use of human tissue samples and clinical data was approved by the ethics committee of Dalian Friendship Hospital. All donors were informed of the aim of the study and gave consent to donate their samples.

Institutional animal care and use committee statement: This study was approved by the Fudan University School of Medicine Animal Care and Use Committee and was performed in accordance with the guidelines of the International Association for the Study of Pain.

Informed consent statement: All study participants or their legal guardian provided informed written consent about personal and medical data collection prior to study enrolment.

Conflict-of-interest statement: The authors declare that there are no conflicts of interest. Patient consent was obtained.

Data sharing statement: Technical appendix, statistical code, and dataset available from the corresponding author from the Department of Gastroenterology, Jinshan Hospital of Fudan University, Number 1508, Longhand Road, Jinshan District, Shanghai, 201508, People's Republic of China

ARRIVE guidelines statement: The authors have read the ARRIVE guidelines, and the manuscript was prepared and revised according to the ARRIVE guidelines.

Country/Territory of origin: China

ORCID number: Zheng-Yang Li 0000-0001-7894-6232; Ya-Jie Wang 0000-0002-2947-3229; Miao Jiang 0000-0002-7135-2498.

S-Editor: Fan JR
L-Editor: A
P-Editor: Yu HG

REFERENCES

1 **Lacy BE**, Pimentel M, Brenner DM, Chey WD, Keefer LA, Long MD, Moshiree B. ACG Clinical Guideline: Management of Irritable Bowel Syndrome. *Am J Gastroenterol* 2021; **116**: 17-44 [PMID: 33315591 DOI: 10.14309/ajg.0000000000001036]
2 **Lee YJ**, Park KS. Irritable bowel syndrome: emerging paradigm in pathophysiology. *World J Gastroenterol* 2014; **20**: 2456-2469 [PMID: 24627583 DOI: 10.3748/wjg.v20.i10.2456]
3 **Mamieva Z**, Poluektova E, Svistushkin V, Sobolev V, Shifrin O, Guarner F, Ivashkin V. Antibiotics, gut microbiota, and irritable bowel syndrome: What are the relations? *World J Gastroenterol* 2022; **28**: 1204-1219 [PMID: 35431513 DOI: 10.3748/wjg.v28.i12.1204]
4 **Cangemi DJ**, Lacy BE. Management of irritable bowel syndrome with diarrhea: a review of nonpharmacological and pharmacological interventions. *Therap Adv Gastroenterol* 2019; **12**: 1756284819878950 [PMID: 31632456 DOI: 10.1177/1756284819878950]
5 **Cussac D**, Boutet-Robinet E, Ailhaud MC, Newman-Tancredi A, Martel JC, Danty N, Rauly-Lestienne I. Agonist-directed trafficking of signalling at serotonin 5-HT2A, 5-HT2B and 5-HT2C-VSV receptors mediated Gq/11 activation and calcium mobilisation in CHO cells. *Eur J Pharmacol* 2008; **594**: 32-38 [PMID: 18703043 DOI: 10.1016/j.ejphar.2008.07.040]
6 **Borman RA**, Tilford NS, Harmer DW, Day N, Ellis ES, Sheldrick RL, Carey J, Coleman RA, Baxter GS. 5-HT(2B) receptors play a key role in mediating the excitatory effects of 5-HT in human colon in vitro. *Br J Pharmacol* 2002; **135**: 1144-1151 [PMID: 11877320 DOI: 10.1038/sj.bjp.0704571]
7 **Cervantes-Durán C**, Vidal-Cantú GC, Barragán-Iglesias P, Pineda-Farias JB, Bravo-Hernández M, Murbartián J, Granados-Soto V. Role of peripheral and spinal 5-HT2B receptors in formalin-induced nociception. *Pharmacol Biochem Behav* 2012; **102**: 30-35 [PMID: 22476011 DOI: 10.1016/j.pbb.2012.03.015]
8 **Lin SY**, Chang WJ, Lin CS, Huang CY, Wang HF, Sun WH. Serotonin receptor 5-HT2B mediates serotonin-induced mechanical hyperalgesia. *J Neurosci* 2011; **31**: 1410-1418 [PMID: 21273425 DOI: 10.1523/JNEUROSCI.4682-10.2011]
9 **Ohashi-Doi K**, Himaki D, Nagao K, Kawai M, Gale JD, Furness JB, Kurebayashi Y. A selective, high affinity 5-HT 2B receptor antagonist inhibits visceral hypersensitivity in rats. *Neurogastroenterol Motil* 2010; **22**: e69-e76 [PMID: 19740115 DOI: 10.1111/j.1365-2982.2009.01395.x]
10 **O'Mahony SM**, Bulmer DC, Coelho AM, Fitzgerald P, Bongiovanni C, Lee K, Winchester W, Dinan TG, Cryan JF. 5-HT(2B) receptors modulate visceral hypersensitivity in a stress-sensitive animal model of brain-gut axis dysfunction. *Neurogastroenterol Motil* 2010; **22**: 573-578, e124 [PMID: 20003079 DOI: 10.1111/j.1365-2982.2009.01432.x]
11 **Zhou Q**, Yang L, Larson S, Basra S, Merwat S, Tan A, Croce C, Verne GN. Decreased miR-199 augments visceral pain in patients with IBS through translational upregulation of TRPV1. *Gut* 2016; **65**: 797-805 [PMID: 25681400 DOI: 10.1136/gutjnl-2013-306464]
12 **Grover M**, Berumen A, Peters S, Wei T, Breen-Lyles M, Harmsen WS, Busciglio I, Burton D, Vazquez Roque M, DeVault KR, Camilleri M, Wallace M, Dasari S, Neumann H, Houghton LA. Intestinal chemosensitivity in irritable bowel syndrome associates with small intestinal TRPV channel expression. *Aliment Pharmacol Ther* 2021; **54**: 1179-1192 [PMID: 34472640 DOI: 10.1111/apt.16591]
13 **Su YS**, Chiu YY, Lin SY, Chen CC, Sun WH. Serotonin Receptor 2B Mediates Mechanical Hyperalgesia by Regulating Transient Receptor Potential Vanilloid 1. *J Mol Neurosci* 2016; **59**: 113-125 [PMID: 26635025 DOI: 10.1007/s12031-015-0693-4]
14 **Sugiuar T**, Bielefeldt K, Gebhart GF. TRPV1 function in mouse colon sensory neurons is enhanced by metabotropic 5-hydroxytryptamine receptor activation. *J Neurosci* 2004; **24**: 9521-9530 [PMID: 15509739 DOI: 10.1523/JNEUROSCI.2639-04.2004]
15 **Ford AC**, Lacy BE, Talley NJ. Irritable Bowel Syndrome. *N Engl J Med* 2017; **376**: 2566-2578 [PMID: 28657875 DOI: 10.1056/NEJMra1607547]
16 **Yu YB**, Zuo XL, Zhao QJ, Chen FX, Yang J, Dong YY, Wang P, Li YQ. Brain-derived neurotrophic factor contributes to abdominal pain in irritable bowel syndrome. *Gut* 2012; **61**: 685-694 [PMID: 21997550 DOI: 10.1136/gutjnl-2011-300265]
17 **Barbara G**, Stanghellini V, De Giorgio R, Cremon C, Cottrell GS, Santini D, Pasquinelli G, Morselli-Labate AM, Grady EF, Bunnett NW, Collins SM, Corinaldesi R. Activated mast cells in proximity to colonic nerves correlate with abdominal pain in irritable bowel syndrome. *Gastroenterology* 2004; **126**: 693-702 [PMID: 14988823 DOI: 10.1053/j.gastro.2003.11.055]
18 **Williams CL**, Villar RG, Peterson JM, Burks TF. Stress-induced changes in intestinal transit in the rat: a model for irritable bowel syndrome. *Gastroenterology* 1988; **94**: 611-621 [PMID: 2828144 DOI: 10.1016/0016-5085(88)90231-4]
19 **Chen Y**, Li Z, Yang Y, Lin L, Zhang H. Role of glucagon-like peptide-1 in the pathogenesis of experimental irritable bowel syndrome rat models. *Int J Mol Med* 2013; **31**: 607-613 [PMID: 23338623 DOI: 10.3892/ijmm.2013.1252]
20 **Jin B**, Ha SE, Wei L, Singh R, Zogg H, Clemmensen B, Heredia DJ, Gould TW, Sanders KM, Ro S. Colonic Motility Is Improved by the Activation of 5-HT(2B) Receptors on Interstitial Cells of Cajal in Diabetic Mice. *Gastroenterology* 2021; **161**: 608-622.e7 [PMID: 33895170 DOI: 10.1053/j.gastro.2021.04.040]
21 **Su Z**, Miao B, Xu MQ, Yang MJ, Fei SJ, Zhang JF. Protective effect of microinjection of glutamate into hypothalamus paraventricular nucleus on chronic visceral hypersensitivity in rats. *Brain Res* 2020; **1747**: 147048 [PMID: 32791142 DOI: 10.1016/j.brainres.2020.147048]
22 **Cervantes-Durán C**, Rocha-González HI, Granados-Soto V. Peripheral and spinal 5-HT receptors participate in the pronociceptive and antinociceptive effects of fluoxetine in rats. *Neuroscience* 2013; **252**: 396-409 [PMID: 23994595 DOI: 10.1016/j.neuroscience.2013.08.022]
23 **Segelcke D**, Messlinger K. Putative role of 5-HT(2B) receptors in migraine pathophysiology. *Cephalalgia* 2017; **37**: 365-371 [PMID: 27127104 DOI: 10.1177/0333102416646760]
24 **Beattie DT**, Smith JA, Marquess D, Vickery RG, Armstrong SR, Pulido-Rios T, McCullough JL, Sandlund C, Richardson C, Mai N, Humphrey PP. The 5-HT4 receptor agonist, tegaserod, is a potent 5-HT2B receptor antagonist *in vitro* and in vivo. *Br J Pharmacol* 2004; **143**: 549-560 [PMID: 15466450 DOI: 10.1038/sj.bjp.0705929]
25 **Bassil AK**, Taylor CM, Bolton VJ, Gray KM, Brown JD, Cutler L, Summerfield SG, Bruton G, Winchester WJ, Lee K, Sanger GJ. Inhibition of colonic motility and defecation by RS-127445 suggests an involvement of the 5-HT2B receptor in rodent large bowel physiology. *Br J*

Pharmacol 2009; **158**: 252-258 [PMID: 19371340 DOI: 10.1111/j.1476-5381.2009.00155.x]

26 **Iftinca M**, Defaye M, Altier C. TRPV1-Targeted Drugs in Development for Human Pain Conditions. *Drugs* 2021; **81**: 7-27 [PMID: 33165872 DOI: 10.1007/s40265-020-01429-2]

27 **Perna E**, Aguilera-Lizarraga J, Florens MV, Jain P, Theofanous SA, Hanning N, De Man JG, Berg M, De Winter B, Alpizar YA, Talavera K, Vanden Berghe P, Wouters M, Boeckxstaens G. Effect of resolvins on sensitisation of TRPV1 and visceral hypersensitivity in IBS. *Gut* 2021; **70**: 1275-1286 [PMID: 33023902 DOI: 10.1136/gutjnl-2020-321530]

28 **Premkumar LS**, Ahern GP. Induction of vanilloid receptor channel activity by protein kinase C. *Nature* 2000; **408**: 985-990 [PMID: 11140687 DOI: 10.1038/35050121]

29 **Atkinson W**, Lockhart S, Whorwell PJ, Keevil B, Houghton LA. Altered 5-hydroxytryptamine signaling in patients with constipation- and diarrhea-predominant irritable bowel syndrome. *Gastroenterology* 2006; **130**: 34-43 [PMID: 16401466 DOI: 10.1053/j.gastro.2005.09.031]

World Journal of Gastroenterology

Submit a Manuscript: https://www.f6publishing.com

World J Gastroenterol 2024 March 14; 30(10): 1450-1460

DOI: 10.3748/wjg.v30.i10.1450

ISSN 1007-9327 (print) ISSN 2219-2840 (online)

META-ANALYSIS

Shear-wave elastography to predict hepatocellular carcinoma after hepatitis C virus eradication: A systematic review and meta-analysis

Giorgio Esposto, Paolo Santini, Linda Galasso, Irene Mignini, Maria Elena Ainora, Antonio Gasbarrini, Maria Assunta Zocco

Specialty type: Gastroenterology and hepatology

Provenance and peer review: Invited article; Externally peer reviewed.

Peer-review model: Single blind

Peer-review report's scientific quality classification

Grade A (Excellent): 0
Grade B (Very good): 0
Grade C (Good): C
Grade D (Fair): 0
Grade E (Poor): 0

P-Reviewer: Wang ZX, China

Received: December 27, 2023
Peer-review started: December 27, 2023
First decision: January 5, 2024
Revised: January 13, 2024
Accepted: January 31, 2024
Article in press: January 31, 2024
Published online: March 14, 2024

Giorgio Esposto, Linda Galasso, Irene Mignini, Maria Elena Ainora, Maria Assunta Zocco, CEMAD Digestive Disease Center, Fondazione Policlinico Universitario "A. Gemelli" IRCCS, Catholic University of Rome, Rome 00168, Italy

Paolo Santini, Fondazione Policlinico Universitario Agostino Gemelli IRCCS, Fondazione Policlinico Universitario Agostino Gemelli IRCCS - Università Cattolica del Sacro Cuore, Rome 00168, Italy

Antonio Gasbarrini, Medicina Interna e Gastroenterologia, CEMAD Digestive Disease Center, Università Cattolica del Sacro Cuore, Fondazione Policlinico Universitario A Gemelli IRCCS, Rome 00168, Italy

Corresponding author: Maria Assunta Zocco, MD, PhD, Researcher, CEMAD Digestive Disease Center, Fondazione Policlinico Universitario "A. Gemelli" IRCCS, Catholic University of Rome, Largo gemelli 1, Rome 00168, Italy. mariaassunta.zocco@unicatt.it

Abstract

BACKGROUND

Direct-acting antiviral agents (DAAs) are highly effective treatment for chronic hepatitis C (CHC) with a significant rate of sustained virologic response (SVR). The achievement of SVR is crucial to prevent additional liver damage and slow down fibrosis progression. The assessment of fibrosis degree can be performed with transient elastography, magnetic resonance elastography or shear-wave elastography (SWE). Liver elastography could function as a predictor for hepatocellular carcinoma (HCC) in CHC patients treated with DAAs.

AIM

To explore the predictive value of SWE for HCC development after complete clearance of hepatitis C virus (HCV).

METHODS

A comprehensive literature search of clinical studies was performed to identify the ability of SWE to predict HCC occurrence after HCV clearance. In accordance with the study protocol, a qualitative and quantitative analysis of the evidence was planned.

RESULTS

At baseline and after 12 wk of follow-up, a trend was shown towards greater liver

stiffness (LS) in those who go on to develop HCC compared to those who do not [baseline LS standardized mean difference (SMD): 1.15, 95% confidence interval (95%CI): 020-2.50; LS SMD after 12 wk: 0.83, 95%CI: 0.33-1.98]. The absence of a statistically significant difference between the mean LS in those who developed HCC or not may be related to the inability to correct for confounding factors and the absence of raw source data. There was a statistically significant LS SMD at 24 wk of follow-up between patients who developed HCC *vs* not (0.64; 95%CI: 0.04-1.24).

CONCLUSION

SWE could be a promising tool for prediction of HCC occurrence in patients treated with DAAs. Further studies with larger cohorts and standardized timing of elastographic evaluation are needed to confirm these data.

Key Words: Shear-wave elastography; Hepatocellular carcinoma; Hepatitis C virus; Sustained virologic response

Core Tip: The role of shear wave-elastography (SWE) is still unclear in predicting hepatocellular carcinoma (HCC) after hepatitis C virus eradication. This is the first systematic review and meta-analysis that focuses on SWE as a predictor of HCC in sustained virologic response patients.

Citation: Esposto G, Santini P, Galasso L, Mignini I, Ainora ME, Gasbarrini A, Zocco MA. Shear-wave elastography to predict hepatocellular carcinoma after hepatitis C virus eradication: A systematic review and meta-analysis. *World J Gastroenterol* 2024; 30(10): 1450-1460

URL: https://www.wjgnet.com/1007-9327/full/v30/i10/1450.htm

DOI: https://dx.doi.org/10.3748/wjg.v30.i10.1450

INTRODUCTION

The hepatitis C virus (HCV) is an RNA virus that predominantly affects the liver, leading to both acute and chronic hepatitis. Its prolonged presence often leads to progressive liver damage, which can manifest as cirrhosis, decompensated liver disease, and hepatocellular carcinoma (HCC). In 2016, the World Health Organization aimed to eliminate HCV infection as a significant public health threat by 2030[1]. Despite notable advancements, an estimated 57 million individuals were still grappling with HCV infection in 2020, with an annual toll of 300000 HCV-related deaths[2].

Direct-acting antiviral agents (DAAs) have emerged as highly effective treatments for chronic hepatitis C (CHC)[3,4]. Numerous studies have highlighted the exceptional tolerability of these drugs, even among the most vulnerable patients, including those undergoing dialysis[5], awaiting liver transplantation[6], or affected by cardiac pathologies[7]. This tolerability has led to a significant increase in the number of treated patients achieving a sustained virologic response (SVR), which exceeds 90%[8] and represents a crucial benchmark for success in hepatitis C treatment. In fact, the primary objective of achieving SVR is the prevention of additional liver damage or complications associated with CHC infection.

However, despite positive data regarding DAA treatment response and improved outcomes, several cases of pharmacological resistance have been described[9], making HCV infection increasingly challenging and difficult to manage. Furthermore, emerging evidence suggests a persistent risk of HCC in CHC patients post-DAAs therapy, even after achieving SVR[10]. Therefore, in the effort to eradicate HCV and subsequently minimize its associated complications, there are countless studies focused on identifying high-risk patient profiles prone to post-SVR complications[11,12].

A recent study by Zou *et al*[13] demonstrated the ability to identify individuals who achieved SVR but remain susceptible to HCC. They developed a risk prediction model that includes liver function laboratory indices, which proved to be a pivotal step toward identification of patients at higher risk.

In addition, DAA therapy exerts an impact at the organic level, improving the degree of liver fibrosis and reducing key clinical scores such as Model for End-Stage Liver Disease, Child-Pugh-Turcotte (CPT) and Fibrosis-4 score[14,15].

For assessing the degree of hepatic fibrosis, liver stiffness (LS) measurement techniques have been implemented alongside clinical scores. Ultrasound (US) elastography[16] or magnetic resonance elastography (MRE)[17] are dependable alternatives to liver biopsy for evaluating fibrosis levels. These validated non-invasive methods play a crucial role in monitoring fibrosis regression and forecasting the risk of complications following DAA therapy[18].

In this context, various studies have aimed to understand how liver elastography could function as a predictor for HCC in CHC patients treated with DAAs, highlighting its role in assessing the risk of HCC[19-22]. These studies mainly employed Fibroscan®, and a recent meta-analysis[23] confirmed the capability of LS in predicting HCC onset in DAA-treated CHC patients.

Alongside Fibroscan® and MRE, shear-wave elastography (SWE) represents another novel technique used for evaluation of liver fibrosis. SWE holds several advantages over Fibroscan® as it allows the operator to vary depth and to select areas of liver parenchyma without vessels or structures that could interfere with the measurement. Additionally, while Fibroscan® requires dedicated machinery solely for measurements without offering a panoramic view of the liver,

SWE is performed using the same US device used for US B-mode imaging, providing a higher quality B-mode image compared to that obtained with Fibroscan®[24]. This could also influence operator variability, making SWE less exposed to it.

To the best of our knowledge, this represents the first systematic review and meta-analysis examining how SWE could serve as a predictor of HCC post-SVR.

MATERIALS AND METHODS

Research question

A systematic literature review was conducted to answer the following research question: "Can liver Shear Wave Elastography be used to predict risk of developing HCC after HCV eradication?"

Protocol registration

The study was performed according to the Preferred Reporting Items for Systematic reviews and Meta-Analyses[25,26] and synthetized with meta-analysis. The protocol for this systematic review was written and submitted to the International Register of Systematic Reviews (PROSPERO, ID: CRD42023491042) prior to the completion of the literature search.

Literature search strategy

The search was performed in the following electronic bibliographic databases: Medline (*via* PubMed), Embase (*via* Ovid), and Web of Science. To guarantee adequate sensitivity, the search strategy included terms strictly related to the diagnostic technique evaluated and the target population of patients affected by HCV who had undergone DAAs therapy and obtained SVR. Therefore, the three domains were combined regarding SVR, HCV and elasticity. The search string for each database can be found in Supplementary Table 1. The search was complemented by manual review of retrieved articles' references and of prior systematic reviews on this topic.

Selection criteria

According to the prognostic study design, studies were considered eligible if they met the following criteria: (1) Prospective and retrospective cohort studies; (2) written in English; (3) describing patients with HCV treated with DAAs who reached SVR; and (4) being evaluated with SWE after SVR. Moreover, meeting abstracts and oral or poster communications at scientific congresses were excluded. The results of the literature search were combined using EndNote™. Then, individual records were manually screened with title and abstract analysis by two independent reviewers (Esposto G and Galasso L). Any disagreement was settled by discussion. Records selected by manual screening were eligible for full-text analysis. Study selection, full-text analysis, and data extraction were performed by two reviewers (Esposto G and Galasso L). In the case of multiple records on a single study, the most recent published paper in which the outcomes of the review were reported in the most exhaustive and complete way was included.

Data extraction and data synthesis

The following data were collected: Author, location, publication year, study design, dates of study, origin of the study population, type of DAAs treatment, total number of patients, Fibrosis index (FI) measured *via* ultrasound SWE, and confounding factors reported in each study. In the case of ambiguity, the study investigators were contacted to provide clarification. Missing data were requested from study authors. In accordance with the study protocol, a qualitative analysis of the evidence was planned.

LS measured *via* SWE was reported as FI, *i.e.* the Young's modulus expressed in kPa. Where the original article expressed LS in terms of shear-wave velocity (Vs) expressed in m/s, a conversion formula was used. In fact, assuming an isotropic tissue density of 1 g/mL, shear-wave velocity can be converted into FI according to the following equation: $3 \times Vs\ (m/s)^2 = FI\ (kPa)$[27,28].

The quantitative synthesis of the data was performed through analysis of the Hedges' g standardized difference of the LS means in those who received a diagnosis of HCC *vs* those who did not develop this complication. Whenever the original work did not report the results in terms of mean and standard deviation, the relative median and interquartile range were converted according to the indications of the Cochrane Library[29]. Hence, standardized mean differences (SMDs) were meta-analyzed using a Random Effect model due the very high heterogeneity documented.

It was not possible to perform a quantitative synthesis of effect measures [*i.e.* hazard ratio (HR) or odds ratio] due to the absence of a predefined LS cut-off and the consequent non-comparability of the evidence reported by the individual studies.

Heterogeneity was assessed by τ^2 and I^2 statistics. The first accounts for the between-studies variance, while the latter represents the proportion of total variation across studies due to heterogeneity rather than chance.

Risk-of-bias assessment

Risk of bias of eligible studies was assessed with the Quality Assessment of Prognostic Accuracy Studies (QUAPAS) tool [30]. This assessment was performed by two independent authors (Santini P and Esposto G), and any disagreement between the two reviewers was settled by discussion with involvement of a third review author if necessary.

The number of studies was insufficient to allow a graphical assessment of publication bias by funnel plot or statistical assessment by Egger's test. However, all of the identified studies showed a statistically different LS by univariate or

multivariate analysis between patients who developed HCC and those who did not. Consequently, it cannot be excluded that this could reflect the presence of a certain degree of unmeasurable publication bias.

Outcomes

The primary outcome of this systematic review and meta-analysis is the development of HCC in HCV patients treated with DAAs who reached SVR. HCC was defined as an established radiological diagnosis with contrast-enhanced abdominal ultrasound, magnetic resonance imaging, or CT.

RESULTS

Study selection

Screening of three biomedical databases was conducted using the prespecified search methods on 21 November 2023, and a total of 10231 studies were found (Medline *via* PubMed: 1912; Embase: 4855; Web of Science: 3464). After duplicates were removed, 7313 records were screened for eligibility based on title and abstract. A total of 111 papers were considered eligible for full-text analysis. Exclusion occurred for 99 experimental studies: 87 studies evaluated the use of transient elastography, while 12 studies did not evaluate HCC development as an outcome. Moreover, we excluded seven previously published reviews according to the aforementioned inclusion criteria. Finally, five studies matched the pre-established eligibility requirements for the current systematic review and meta-analysis.

After a comprehensive risk-of-bias assessment, one original paper was excluded from quantitative synthesis due to an estimated high concern about applicability related to the systematic review and meta-analysis research question.

Figure 1 shows the PRISMA selection flow diagram that describes the study-selection process in detail.

Risk-of-bias assessment

Using the QUAPAS tool for QUAPAS[30], a structured examination of the risk of bias was conducted to assess the internal and external validity of each included study (Tables 1 and 2). It is important to emphasize that the risk-of-bias assessment does not judge the overall scientific quality of each included study; rather, it assesses each study in relation to the research questions of the current systematic review and meta-analysis.

Three studies were categorized as having an unknown risk of bias in the "Participants" domain because the enrollment strategy was not provided. Selection bias may have occurred because patients in these retrospective analyses are not specified to be consecutive or not[31-33]. In the same domain, one study was found to be at high risk of bias due to the exclusion of study subjects who had CPT stage C liver cirrhosis. The exclusion of these patients determines a selection of those who present lower HCC risk[34]. The "Index test" domain was judged to be at low risk of bias for all studies, although the question about the use of a prespecified threshold was ignored due to the absence of a validated LS cutoff predictive for the development of HCC. All studies were assessed as being at unclear risk of bias regarding the "Outcome" domain. In fact, no study has specified whether the subsequent screening for HCC was performed blind to the elastographic measurement of LS. One study was at high risk of bias in the "Flow and timing" and "Analysis" domains due to the lack of reporting of patients lost to follow-up and the lack of description of the statistical management of these subjects and censoring events[31].

The evaluation of concerns about applicability was found to be at high risk in the "Participants" domain in one study [31]. Hamada and colleagues described patients treated with both DAAs and interferon[31]. The impossibility of performing a sub-analysis of those who received therapy with DAAs determines an assessment of non-applicability of the results of this study to the research question of the present systematic review and meta-analysis. Consequently, this study was excluded from quantitative synthesis. A visual summary of distribution of Risk of Bias and Applicability Concerns across QUAPAS domains can be found in Supplementary Figures 1 and 2.

SWE to predict HCC after SVR: qualitative summary

The five studies considered eligible for qualitative synthesis had different study designs, inclusion and exclusion criteria, different baseline SWE evaluation and timing of elastographic evaluation after SVR (Table 3). A summary of the baseline characteristics of patients included in each study is available in Table 4. The number of study participants run from 196 to 525, for a total of 1458 patients. All of the included studies used SWE in the evaluation of LS. All five studies performed the first assessment of LS before treatment initiation[31-35], while only two evaluated LS at the End of Treatment (EOT) [32,33]. The successive SWE evaluations were conducted at 12 wk after EOT in three out of five studies[32,33,35] and at 24 wk after EOT in four out of five studies[31-34].

Hamada *et al*[31] included 196 patients treated with DAAs (n = 107) or interferon (n = 89). SVR was defined as negative search of HCV RNA at 24 wk after EOT. SWE was conducted with an Aixplorer® ultrasound system (SuperSonic Imagine S.A., Aix-en-Provence, France) to measure LS (kPa). The authors performed SWE before treatment initiation and at SVR 24 wk (SVR24). Median follow-up time after SVR was 26 [interquartile range (IQR): 5-109] mo, during which patients underwent regular liver screening for HCC every 3-4 mo. Eight patients developed HCC, and the median time to develop HCC from SVR was 28 (IQR: 6-46) mo. SWE results were 8.3 kPa (IQR: 3.4-36.2 kPa) at baseline and 5.9 kPa (IQR 2.7-31.3 kPa) at SVR24. Several factors were associated with HCC development, including SWE at SVR24. Multivariate analysis revealed that this association was independent and that the cut-off, determined by a receiver operator characteristics (ROC) analysis, was ≥ 11 kPa [relative risk= 28.71, HR: 28.71, 95% confidence interval (95%CI): 2.58-320.03; P = 0.006]. Patients with SWE values below this level had substantially lower risk of developing HCC during follow-up time.

Table 1 Risk of bias assessment according to Quality Assessment of Prognostic Accuracy Studies tool for quality assessment of prognostic accuracy studies

Ref.	Risk of bias				
	Participants	Index test	Outcome	Flow and timing	Analysis
Gyotoku *et al*[32], 2022	Unclear	Low	Unclear	Low	Low
Hamada *et al*[31], 2018	Unclear	Low	Unclear	High	Unclear
Kumada *et al*[35], 2022	Low	Low	Unclear	Low	Low
Masaoka *et al*[33], 2023	Unclear	Low	Unclear	Low	Low
Nicoletti *et al*[34], 2023	High	Low	Unclear	Low	Low

Table 2 Concerns about applicability according to Quality Assessment of Prognostic Accuracy Studies tool for quality assessment of prognostic accuracy studies

Ref.	Applicability concerns			
	Participants	Index test	Outcome	Flow and timing
Gyotoku *et al*[32], 2022	Low	Low	Low	Low
Hamada *et al*[31], 2018	High	Low	Low	Low
Kumada *et al*[35], 2022	Low	Low	Low	Low
Masaoka *et al*[33], 2023	Low	Low	Low	Low
Nicoletti *et al*[34], 2023	Low	Low	Low	Low

Table 3 Study characteristics of included publications

Ref.	Country	Study design	Patients, *n*	SWE evaluation	Follow-up time
Hamada *et al*[31], 2018	Japan	Retrospective	196	24 wk	26 (5-109) mo
Gyotoku *et al*[32], 2022	Japan	Retrospective	229	EOT, 12 and 24 wk	32.6 ± 19.5 mo
Kumada *et al*[35], 2022	Japan	Prospective	525	12 wk	5.0 (4.0-5.4) yr
Masaoka *et al*[33], 2023	Japan	Retrospective	279	EOT, 12 and 24 wk	33.8 (6-85) mo
Nicoletti *et al*[34], 2023	Italy	Prospective	229	24 wk	3.25 (0.5-4.7) yr

Continuous variables are described as mean ± standard deviation or median and interquartile range, when reported. EOT: End of treatment; SWE: Shear-wave elastography.

Table 4 Baseline patient characteristics in the included publications

Ref.	Age in yr	Sex as male/female	Fib4 score	HCC, *n*	Time to HCC in mo
Hamada *et al*[31], 2018	62 (29-89)	89/107	2.56 (0.39-12.13)	8	28 (6-46)
Gyotoku *et al*[32], 2022	66 (21-84)	93/136	3.49 (0.30-19.10)	8	21.3
Kumada *et al*[35], 2022	72 (65-79)	227/298	2.73 (1.90-4.23)	21	Not reported
Masaoka *et al*[33], 2023	66 (21-86)	118/161	3.41 (0.23-22.00)	12	33.8 (6-85)
Nicoletti *et al*[34], 2023	67 ± 11	136/93	5.77 ± 5.40	30	24 ± 14.5

Continuous variables are described as mean ± standard deviation or median and interquartile range, when reported. Fib4 score: Fibrosis-4; HCC: Hepatocellular carcinoma.

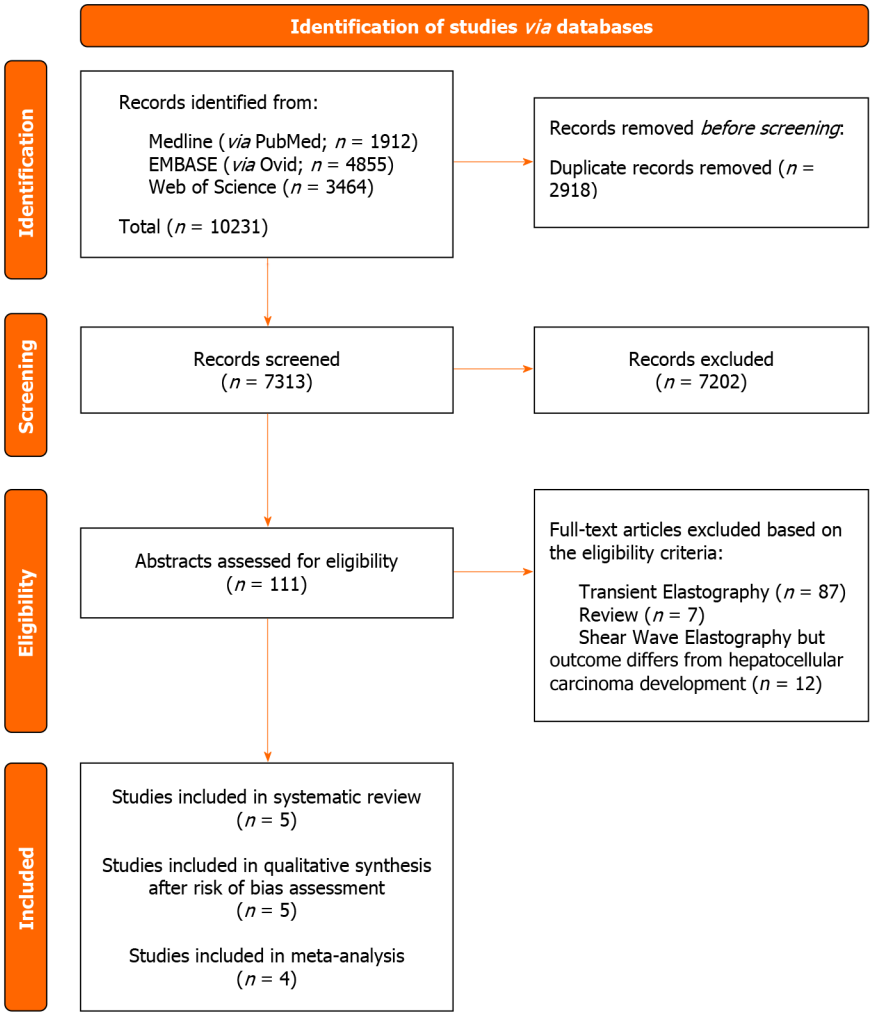

Figure 1 PRISMA study selection flow diagram.

Gyotoku *et al*[32] included 229 patients treated with DAAs. SVR was defined as negative search of HCV RNA at 12 wk after EOT. SWE was conducted with a LOGIQ E9 ultrasound system (GE Healthcare, Milwaukee, WI, United States) to measure shear wave velocity (Vs, m/s). All patients underwent SWE measurement before initiating treatment and later at EOT, 12 and 24 wk after EOT. During follow-up time, abdominal ultrasound was performed every 6 mo to screen for potential HCC. The mean observation time was 32.6 ± 19.5 mo, and HCC was diagnosed in eight patients with a mean time from EOT to HCC development of 21.3 mo. Patient characteristics were then grouped into those who developed HCC and those who did not. Vs values decreased during follow-up and were statistically higher in the HCC group than those in the non-HCC group at various stages of evaluation. At baseline, Vs was 1.86 ± 0.20 m/s in the HCC group compared to 1.58 ± 0.26 m/s in the non-HCC group (P = 0.004). Vs at EOT was 1.58 ± 0.26 m/s in the non-HCC group compared to 1.75 ± 0.22 m/s in the HCC group (P = 0.004). Vs at 12 wk follow-up was 1.49 ± 0.25 m/s compared to 1.66 ± 0.15 m/s in thee HCC group (P = 0.018). At 24 wk follow-up, Vs was 1.44 ± 0.24 m/s in the non-HCC group compared to 1.69 ± 0.121 m/s of HCC group (P = 0.031). ROC curve analysis revealed an area under the curve of 0.80 at baseline, 0.75 at EOT, 0.72 at 12 wk follow-up and 0.86 at 24 wk follow-up. A cut-off value with corresponding HR was not calculated.

In the study by Kumada *et al*[35], 525 patients treated with DAAs were enrolled. SVR was defined as undetectable HCV RNA at 12 wk after EOT. SWE was conducted with a LOGIQ S8 or E9 US system (GE Healthcare, Milwaukee, WI, United States) to measure LS (kPa). All patients underwent baseline measurement before initiating treatment and 12 wk after EOT. Patients were monitored for HCC every 6 mo for a median follow-up time of 5.01 (IQR: 3.97-5.41) years. In this period, HCC was diagnosed in 21 patients with a median time to HCC of 3.70 (IQR: 2.44-4.50) years. Median FI at baseline was 7.8 (IQR: 6.1-10.2) kPa in non-HCC group *vs* 15.7 (IQR: 11.7-19.1) kPa in HCC patients (P < 0.001). Median SWE at SVR12 was 6.8 (IQR: 5.6-8.6) kPa in non-HCC group *vs* 11.6 (IQR: 8.0-15.6) kPa in HCC patients (P < 0.001). ROC analysis identified a value of 11.7 kPa at baseline as the cut-off above which HCC risk increases (incidence of 3.3% and 8.9% at 2.5 years and 5 years *vs* 0.0% and 0.9% if FI < 11.7 kPa; P = 0.001).

Masaoka *et al*[33] included 279 patients treated with DAAs. SVR was defined as the absence of HCV RNA at 12 wk after EOT. SWE was conducted with a LOGIQ E9 ultrasound system (GE Healthcare, Milwaukee, WI, United States) to measure Vs (m/s). All patients underwent SWE measurement before initiating treatment and later at EOT, 12 and 24 wk after EOT. Abdominal ultrasound was performed every 6 mo after EOT for surveillance of HCC. The median observation time was 33.8 (IQR: 6-85) mo, and HCC was diagnosed in 12 patients. Based on age-male-albumin-bilirubin-platelets

Table 5 Predictive liver stiffness threshold for development of hepatocellular carcinoma after sustained virologic response and relative adjusted hazard ratio and area under the curve

Ref.	LS threshold in kPa	SWE timing	aHR (95%CI)	*P* value	AUC
Hamada *et al*[31], 2018	≥ 11.0	24 wk after EOT	28.71 (2.58-320.03)	0.006	0.93
Gyotoku *et al*[32], 2022	Not reported	24 wk after EOT	Not reported	Not reported	0.86
Kumada *et al*[35], 2022	11.7	Baseline	28.08 (5.53-132.60)	< 0.001	0.93
Masaoka *et al*[33], 2023	7.0	12 wk after EOT	Not reported	Not reported	Not reported
Nicoletti *et al*[34], 2023	ΔLS < 20%	Baseline and 48 wk after EOT	2.98 (1.01-8.11)	0.03	0.69

ΔLS = Baseline liver stiffness (LS) – LS at 48 wk. 95%CI: 95% Confidence interval; aHR: Adjusted hazard ratio; AUC: Area under the curve; EOT: End of treatment; FU: Follow-up; HCC: Hepatocellular carcinoma; SVR: Sustained virological response; SWE: Shear-wave elastography.

(aMAP) score, patients were divided into low, medium, and high-risk groups. Those in the medium and high-risk groups (aMAP scores ≥ 50, number of patients = 237) at 12 wk follow-up were further divided into HCC and non-HCC groups. In the non-HCC group, the median Vs was 1.45 (IQR: 0.95-2.14) m/s while it was 1.69 (IQR: 1.45-2.31) m/s (P = 0.0011) in the HCC group. Multiple regression analysis at 12 wk follow-up revealed a statistical difference in Vs (P = 0.030). Through ROC curve, the authors derived a cut-off value for Vs of 1.53 m/s for HCC development.

Nicoletti *et al*[34] enrolled 229 patients treated with DAAs. SVR was defined as negativity of HCV RNA at 12 wk after EOT. SWE was conducted with an Aixplorer® US system (Supersonic Imagine S.A., Aix-en-Provence, France) and LS was measured in kPa. Patients were evaluated within 3 mo before initiating therapy (baseline) and after 24 (T1) and 48 (T2) wk from EOT. Patients were then followed up for a median time of 3.25 years (IQR: 0.50-4.70) and HCC was diagnosed in 30 out of 229 patients, with a mean time to HCC of 24 ± 14.5 mo. LS decreased over time after treatment (EOT: 18.1 ± 6.6 kPa, T1: 13.6 ± 6.1 kPa, T2: 12.5 ± 6.1 kPa (P < 0.001) and was inversely correlated to HCC development. ROC curve analysis identified a decrease of at least 20% at 1-year follow-up as the optimal cut-off for risk of HCC (AUC: 0.690, sensitivity: 74%, specificity: 65%). Multivariate analysis confirmed that 1-year delta LS < 20% (HR: 2.98; 95%CI: 1.01-8.11; P = 0.03) was independently associated with HCC development. Hence, patients with a difference in LS less than 20% had higher risk for HCC at 1-year follow-up. This cut-off maintained its predictive capacity at 24, 48, 36 and 60 mo.

Table 5 shows the predictive LS threshold for developing HCC identified by each study and the related HR, when calculated.

SWE to predict HCC after SVR: Meta-analysis

The absence of a validated LS threshold predictive for HCC has determined a non-comparability of the effect measures reported by individual studies. Our quantitative synthesis then focused on the distribution of mean LS among those who did or did not develop HCC during follow-up. The SMD, calculated as Hedges' g SMD, at baseline and at 12 and 24 wk of follow-up is reported in Figure 2. Because of very high heterogeneity, SMDs were meta-analyzed using a Random Effect model.

At baseline and after 12 wk, standardizing the difference between LS means by the standard deviation of the measurement itself resulted in an SMD that was not statistically significant. The absence of a statistically significant difference between the mean LS in those who developed HCC or not may be related to an inability to correct for confounding factors in the absence of raw source data. Nonetheless, at these follow-up times, a trend was shown towards greater LS in those who will develop HCC compared to those who will not (baseline LS SMD: 1.15, 95%CI: 020-2.50; LS SMD after 12 wk: 0.83, 95%CI: 0.33-1.98). The LS measured at 24 wk showed a statistically significant SMD of 0.64 (95%CI: 0.04-1.24).

The measurement of LS in the two groups was burdened by very high heterogeneity at each of the follow-up times, as shown by the τ^2 and I^2 statistics, with a trend towards lower heterogeneity at 24 wk of follow-up.

DISCUSSION

In this meta-analysis, we included four out of five studies for a total of 1261 patients. The exclusion of Hamada *et al*[31] in 2018 from the quantitative synthesis is due to the heterogeneous population that included both patients treated with DAAs and interferon without the possibility to separate the data by treatment. The quantitative analysis of the remaining four studies showed a positive trend between higher LS values, measured in kPa, and risk of developing HCC, although statistical significance was not reached at EOT and 12 wk of follow-up, while LS at 24 wk showed a statically significant association with HCC development. The lack of statistical significance at EOT and 12 wk could be due to the small number of patients included and to the great heterogeneity among the studies, mainly in terms of included patients and timing of elastographic evaluation. However, it is possible that patients with higher LS at 24 wk after EOT have a percentage of liver fibrosis that cannot regress with antiviral treatment and therefore are at higher risk of HCC.

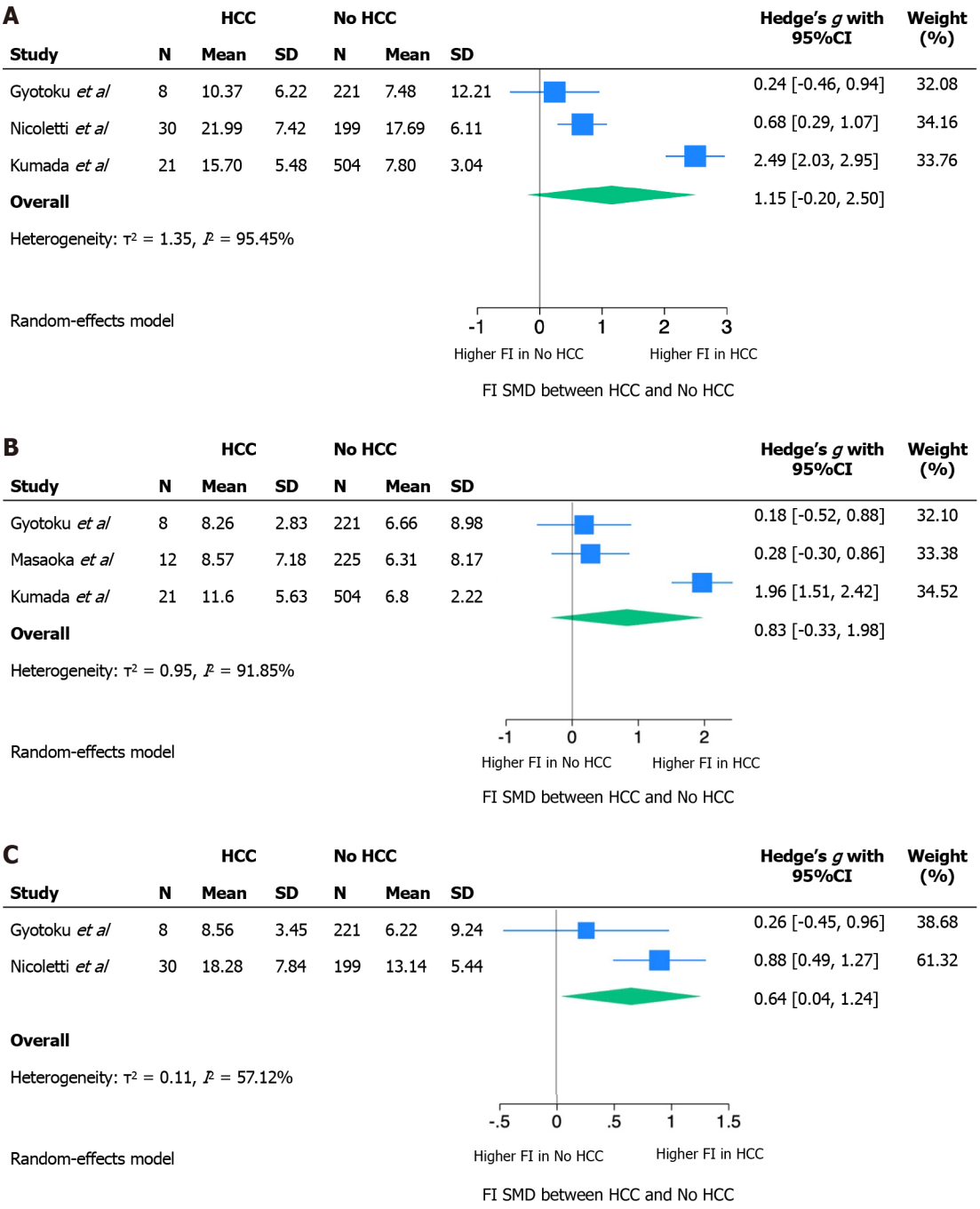

Figure 2 Standardized mean difference of liver stiffness. A: Standardized mean difference (SMD) of liver stiffness (LS) at baseline in patients who did or did not develop hepatocellular carcinoma (HCC) during follow-up; B: SMD of LS at 12 wk after sustained virological response (SVR) in patients who did or did not develop HCC during follow-up; C: SMD of LS at 24 wk after SVR in patients who did or did not develop HCC during follow-up. 95%CI: 95% Confidence interval.

Concerning the heterogeneity, only two out of four studies measured SWE at EOT[32,33], while the other two studies [34,35] considered the baseline values as those measured before starting antiviral treatment. SVR evaluation, intended as SWE measure at 12 wk after EOT, was performed in three out of four studies[32,33,35]. Three studies explored SWE values at 24 wk after EOT[32-34], but only two of them reported complete data for HCC and non-HCC groups[32,34]. The absence of complete data for Gyotoku *et al*[32] and Masaoka *et al*[33] could have influenced the quantitative analysis and the capability to reach statistical significance.

In terms of patient inclusion, Nicoletti *et al*[34] excluded patients with CPT stage C cirrhosis, possibly leading to an underestimation of HCC occurrence. These exclusion criteria are explained by the nature of the study that aimed to identify non-invasive parameters that could predict liver-related complications; hence patients with decompensated cirrhosis had to be excluded from the study population.

The major difference between mean LS from HCC and non-HCC groups was seen in the study of Kumada *et al*[35]. Apart from the higher number of subjects in the study, this could be explained by the design of the study itself. The authors followed up with patients with both SWE and MRE. Therefore, this could have led to an increased rate of detection of low-grade HCC.

These data are consistent with previous studies that focused mainly on TE. A recent meta-analysis by You *et al*[23] on a total of 3398 patients subjected to TE concluded that the pooled HR for HCC development between positive and negative LS results was 3.45 (95%CI: 1.63-7.19). This implies that a high LS is associated with higher HCC occurrence rate, as we found in our meta-analysis of SWE.

Our study has several limitations, starting from the small number of included studies and patients. These studies were heterogeneous in many aspects, including population, SVR definition, LS unit measure (m/s and kPa) and timing of LS measurement. Due to the absence of a validated LS threshold for HCC prediction, we could not compare the effect measures reported by individual studies nor derive a pooled HR for the intended outcome. Hence, we focused the quantitative synthesis on the distribution of mean LS among those who developed HCC and those who did not. Moreover, the comparison of LS between the two sets of patients was burdened by a significant heterogeneity at each of the follow-up times, as shown by the τ^2 and I^2 statistics, with a trend towards lower heterogeneity at 24 wk after EOT.

Despite the described limitations, SWE seems to be a promising tool for predicting HCC occurrence. To explore the presence of a statistically significant relationship between SWE measured LS and HCC occurrence, future studies need to be designed in a more homogenous way in order to be easily compared. SWE evaluation should be conducted prior to initiating treatment, at EOT, 12 and 24 wk after EOT, to derive the optimal follow-up point in which SWE has the higher predictive capability for HCC occurrence.

CONCLUSION

This meta-analysis highlights the potential value of SWE in routine US follow-up of SVR patients, for early identification of those at higher risk of developing HCC. SWE acquisition can be performed with the same ultrasound machine used for B-mode evaluation and it takes only a few minutes more than standard US. LS measure with Fibroscan® has already shown its value in routine follow-up of CHC patients. Because SWE could soon replace TE, further studies with larger cohorts and standardized timeline are needed to confirm its value in prediction of HCC after clearance of HCV.

ARTICLE HIGHLIGHTS

Research background

Direct-acting antiviral agents (DAAs) modified the natural history of chronic hepatitis C. However, despite the advancements in sustained virologic response (SVR), some patients remain at risk of developing hepatocellular carcinoma (HCC). In this context, liver stiffness (LS) measurement could serve as a predictor of HCC, allowing for the identification of patients at higher risk.

Research motivation

Identification of SVR patients at higher risk of HCC development could enhance follow-up timing and improve early diagnosis and overall prognosis.

Research objectives

The aim of this meta-analysis is to investigate shear-wave elastography (SWE) as a predictor of HCC occurrence after hepatitis C virus (HCV) clearance with DAAs.

Research methods

We conducted a systematic literature review and planned a qualitative and quantitative synthesis of the evidence through analysis of the Hedges' g standardized difference of the LS means in those who developed HCC and those who did not. The absence of a predefined LS cut-off prevented us from deriving the effect measures (*i.e.* hazard ratio or odds ratio).

Research results

LS at baseline and 12 wk follow-up showed a trend towards greater values in those who will develop HCC compared to those who will not [baseline LS standardized mean difference (SMD): 1.15, 95% confidence interval (95%CI): 020-2.50; LS SMD after 12 wk: 0.83, 95%CI: 0.33-1.98]. The standardized mean difference between LS in the two groups at 24 wk follow-up was statistically significant (0.64; 95%CI: 0.04-1.24).

Research conclusions

This study explored the ability of SWE to predict HCC after HCV eradication.

Research perspectives

LS, measured by SWE, looks a promising predictor of HCC occurrence in SVR patients. These results need to be further confirmed by larger cohorts.

FOOTNOTES

Author contributions: Zocco MA, Ainora ME, Gasbarrini A designed the research; Esposto G, Santini P, Galasso L, Mignini I performed the research; Esposto G, Santini P contributed analytical tools; Esposto G, Santini P analyzed the data; Esposto G, Santini P, Galasso L, Zocco MA wrote the paper.

Conflict-of-interest statement: All authors declare no conflicts-of-interest related to this article.

PRISMA 2009 Checklist statement: The authors have read the PRISMA 2009 Checklist, and the manuscript was prepared and revised according to the PRISMA 2009 Checklist.

Country/Territory of origin: Italy

ORCID number: Giorgio Esposto 0009-0007-8296-168X; Irene Mignini 0000-0002-8192-631X; Maria Elena Ainora 0000-0001-5847-1065; Antonio Gasbarrini 0000-0003-4863-6924; Maria Assunta Zocco 0000-0002-0814-9542.

S-Editor: Lin C
L-Editor: Filipodia
P-Editor: Yuan YY

REFERENCES

1 **Cui F**, Blach S, Manzengo Mingiedi C, Gonzalez MA, Sabry Alaama A, Mozalevskis A, Séguy N, Rewari BB, Chan PL, Le LV, Doherty M, Luhmann N, Easterbrook P, Dirac M, de Martel C, Nayagam S, Hallett TB, Vickerman P, Razavi H, Lesi O, Low-Beer D. Global reporting of progress towards elimination of hepatitis B and hepatitis C. *Lancet Gastroenterol Hepatol* 2023; **8**: 332-342 [PMID: 36764320 DOI: 10.1016/S2468-1253(22)00386-7]

2 **Martinello M**, Solomon SS, Terrault NA, Dore GJ. Hepatitis C. *Lancet* 2023; **402**: 1085-1096 [PMID: 37741678 DOI: 10.1016/S0140-6736(23)01320-X]

3 **Fehily SR**, Papaluca T, Thompson AJ. Long-Term Impact of Direct-Acting Antiviral Agent Therapy in HCV Cirrhosis: Critical Review. *Semin Liver Dis* 2019; **39**: 341-353 [PMID: 31041785 DOI: 10.1055/s-0039-1685538]

4 **Pugliese N**, Polverini D, Arcari I, De Nicola S, Colapietro F, Masetti C, Ormas M, Ceriani R, Lleo A, Aghemo A. Hepatitis C Virus Infection in the Elderly in the Era of Direct-Acting Antivirals: Evidence from Clinical Trials and Real Life. *Trop Med Infect Dis* 2023; **8** [PMID: 37999621 DOI: 10.3390/tropicalmed8110502]

5 **Toyoda H**, Kikuchi K. Management of dialysis patients with hepatitis C virus in the era of direct-acting antiviral therapy. *Ther Apher Dial* 2023; **27**: 831-838 [PMID: 37217295 DOI: 10.1111/1744-9987.14003]

6 **Pacheco LS**, Ventura PE, Kist R, Garcia VD, Meinerz G, Tovo CV, Cantisani GPC, Zanotelli ML, Mucenic M, Keitel E. Real-world effectiveness and safety of direct-acting antivirals for the treatment of hepatitis C virus in kidney and liver transplant recipients: experience of a large transplant center in Brazil. *Rev Inst Med Trop Sao Paulo* 2023; **65**: e59 [PMID: 38055377 DOI: 10.1590/S1678-9946202365059]

7 **Roguljic H**, Nincevic V, Bojanic K, Kuna L, Smolic R, Vcev A, Primorac D, Vceva A, Wu GY, Smolic M. Impact of DAA Treatment on Cardiovascular Disease Risk in Chronic HCV Infection: An Update. *Front Pharmacol* 2021; **12**: 678546 [PMID: 34045969 DOI: 10.3389/fphar.2021.678546]

8 **Zarębska-Michaluk D**, Brzdęk M, Jaroszewicz J, Tudrujek-Zdunek M, Lorenc B, Klapaczyński J, Mazur W, Kazek A, Sitko M, Berak H, Janocha-Litwin J, Dybowska D, Supronowicz Ł, Krygier R, Citko J, Piekarska A, Flisiak R. Best therapy for the easiest to treat hepatitis C virus genotype 1b-infected patients. *World J Gastroenterol* 2022; **28**: 6380-6396 [PMID: 36533109 DOI: 10.3748/wjg.v28.i45.6380]

9 **Izhari MA**. Molecular Mechanisms of Resistance to Direct-Acting Antiviral (DAA) Drugs for the Treatment of Hepatitis C Virus Infections. *Diagnostics (Basel)* 2023; **13** [PMID: 37835845 DOI: 10.3390/diagnostics13193102]

10 **Hsu CC**, Gopalakrishna H, Mironova M, Lee MH, Chen CJ, Yang HI, Wiese M, Chang KM, Wright EC, Abijo T, Feld JJ, Kaplan DE. Risk of Hepatocellular Carcinoma After Spontaneous Clearance of Hepatitis C Virus and in Noncirrhosis Chronic Hepatitis C Patients With Sustained Virological Response: A Systematic Review. *Clin Infect Dis* 2023; **77**: S245-S256 [PMID: 37579210 DOI: 10.1093/cid/ciad380]

11 **Toyoda H**, Kanneganti M, Melendez-Torres J, Parikh ND, Jalal PK, Piñero F, Mendizabal M, Ridruejo E, Cheinquer H, Casadei-Gardini A, Weinmann A, Peck-Radosavljevic M, Dufour JF, Radu P, Shiha G, Soliman R, Sarin SK, Kumar M, Wang JH, Tangkijvanich P, Sukeepaisarnjaroen W, Atsukawa M, Uojima H, Nozaki A, Nakamuta M, Takaguchi K, Hiraoka A, Abe H, Matsuura K, Watanabe T, Shimada N, Tsuji K, Ishikawa T, Mikami S, Itobayashi E, Singal AG, Johnson PJ. Regional Differences in Clinical Presentation and Prognosis of Patients With Post-Sustained Virologic Response Hepatocellular Carcinoma. *Clin Gastroenterol Hepatol* 2024; **22**: 72-80.e4 [PMID: 37442316 DOI: 10.1016/j.cgh.2023.06.026]

12 **Fraile-López M**, Alvarez-Navascués C, González-Diéguez ML, Cadahía V, Chiminazzo V, Castaño A, Varela M, Rodríguez M. Predictive models for hepatocellular carcinoma development after sustained virological response in advanced hepatitis C. *Gastroenterol Hepatol* 2023; **46**: 754-763 [PMID: 36716928 DOI: 10.1016/j.gastrohep.2023.01.008]

13 **Zou Y**, Yue M, Jia L, Wang Y, Chen H, Zhang A, Xia X, Liu W, Yu R, Yang S, Huang P. Accurate prediction of HCC risk after SVR in patients with hepatitis C cirrhosis based on longitudinal data. *BMC Cancer* 2023; **23**: 1147 [PMID: 38007418 DOI: 10.1186/s12885-023-11628-1]

14 **El-Sherif O**, Jiang ZG, Tapper EB, Huang KC, Zhong A, Osinusi A, Charlton M, Manns M, Afdhal NH, Mukamal K, McHutchison J,

Brainard DM, Terrault N, Curry MP. Baseline Factors Associated With Improvements in Decompensated Cirrhosis After Direct-Acting Antiviral Therapy for Hepatitis C Virus Infection. *Gastroenterology* 2018; **154**: 2111-2121.e8 [PMID: 29535028 DOI: 10.1053/j.gastro.2018.03.022]

15 **Thi Thu PN**, Hoang Van D, Ngo Thi Quynh M, Tran Thi N, Pham Minh K, Pham Van L. Metabolic, renal, and hematological changes in chronic hepatitis C patients achieving rapid virologic response after 12 weeks of direct-acting antiviral treatment: A prospective cohort study. *PLoS One* 2023; **18**: e0290235 [PMID: 37656689 DOI: 10.1371/journal.pone.0290235]

16 **Li Q**, Chen T, Shi N, Ye W, Yuan M, Shi Y. Quantitative evaluation of hepatic fibrosis by fibro Scan and Gd-EOB-DTPA-enhanced T1 mapping magnetic resonance imaging in chronic hepatitis B. *Abdom Radiol (NY)* 2022; **47**: 684-692 [PMID: 34825269 DOI: 10.1007/s00261-021-03300-8]

17 **Kumada T**, Toyoda H, Yasuda S, Sone Y, Ogawa S, Takeshima K, Tada T, Ito T, Sumida Y, Tanaka J. Prediction of Hepatocellular Carcinoma by Liver Stiffness Measurements Using Magnetic Resonance Elastography After Eradicating Hepatitis C Virus. *Clin Transl Gastroenterol* 2021; **12**: e00337 [PMID: 33888672 DOI: 10.14309/ctg.0000000000000337]

18 **Cerrito L**, Ainora ME, Nicoletti A, Garcovich M, Riccardi L, Pompili M, Gasbarrini A, Zocco MA. Elastography as a predictor of liver cirrhosis complications after hepatitis C virus eradication in the era of direct-acting antivirals. *World J Hepatol* 2021; **13**: 1663-1676 [PMID: 34904036 DOI: 10.4254/wjh.v13.i11.1663]

19 **Nakai M**, Yamamoto Y, Baba M, Suda G, Kubo A, Tokuchi Y, Kitagataya T, Yamada R, Shigesawa T, Suzuki K, Nakamura A, Sho T, Morikawa K, Ogawa K, Furuya K, Sakamoto N. Prediction of hepatocellular carcinoma using age and liver stiffness on transient elastography after hepatitis C virus eradication. *Sci Rep* 2022; **12**: 1449 [PMID: 35087141 DOI: 10.1038/s41598-022-05492-5]

20 **John BV**, Dang Y, Kaplan DE, Jou JH, Taddei TH, Spector SA, Martin P, Bastaich DR, Chao HH, Dahman B. Liver Stiffness Measurement and Risk Prediction of Hepatocellular Carcinoma After HCV Eradication in Veterans With Cirrhosis. *Clin Gastroenterol Hepatol* 2023 [PMID: 38061410 DOI: 10.1016/j.cgh.2023.11.020]

21 **Rodprasert N**, Hongboontry T, Cherdchoochart C, Chaiteerakij R. Association between Liver Stiffness and Liver-Related Events in HCV-Infected Patients after Successful Treatment with Direct-Acting Antivirals. *Medicina (Kaunas)* 2023; **59** [PMID: 36984603 DOI: 10.3390/medicina59030602]

22 **Cossiga V**, La Civita E, Bruzzese D, Guarino M, Fiorentino A, Sorrentino R, Pontillo G, Vallefuoco L, Brusa S, Montella E, Terracciano D, Morisco F, Portella G. Enhanced liver fibrosis score as a noninvasive biomarker in hepatitis C virus patients after direct-acting antiviral agents. *Front Pharmacol* 2022; **13**: 891398 [PMID: 36059971 DOI: 10.3389/fphar.2022.891398]

23 **You MW**, Kim KW, Shim JJ, Pyo J. Impact of liver-stiffness measurement on hepatocellular carcinoma development in chronic hepatitis C patients treated with direct-acting antivirals: A systematic review and time-to-event meta-analysis. *J Gastroenterol Hepatol* 2021; **36**: 601-608 [PMID: 32875681 DOI: 10.1111/jgh.15243]

24 **Osman AM**, El Shimy A, Abd El Aziz MM. 2D shear wave elastography (SWE) performance versus vibration-controlled transient elastography (VCTE/fibroscan) in the assessment of liver stiffness in chronic hepatitis. *Insights Imaging* 2020; **11**: 38 [PMID: 32152802 DOI: 10.1186/s13244-020-0839-y]

25 **Page MJ**, McKenzie JE, Bossuyt PM, Boutron I, Hoffmann TC, Mulrow CD, Shamseer L, Tetzlaff JM, Akl EA, Brennan SE, Chou R, Glanville J, Grimshaw JM, Hróbjartsson A, Lalu MM, Li T, Loder EW, Mayo-Wilson E, McDonald S, McGuinness LA, Stewart LA, Thomas J, Tricco AC, Welch VA, Whiting P, Moher D. The PRISMA 2020 statement: an updated guideline for reporting systematic reviews. *Syst Rev* 2021; **10**: 89 [PMID: 33781348 DOI: 10.1186/s13643-021-01626-4]

26 **McInnes MDF**, Moher D, Thombs BD, McGrath TA, Bossuyt PM; and the PRISMA-DTA Group, Clifford T, Cohen JF, Deeks JJ, Gatsonis C, Hooft L, Hunt HA, Hyde CJ, Korevaar DA, Leeflang MMG, Macaskill P, Reitsma JB, Rodin R, Rutjes AWS, Salameh JP, Stevens A, Takwoingi Y, Tonelli M, Weeks L, Whiting P, Willis BH. Preferred Reporting Items for a Systematic Review and Meta-analysis of Diagnostic Test Accuracy Studies: The PRISMA-DTA Statement. *JAMA* 2018; **319**: 388-396 [PMID: 29362800 DOI: 10.1001/jama.2017.19163]

27 **Palmeri ML**, Nightingale KR. Acoustic radiation force-based elasticity imaging methods. *Interface Focus* 2011; **1**: 553-564 [PMID: 22419986 DOI: 10.1098/rsfs.2011.0023]

28 **Lin LI**. A concordance correlation coefficient to evaluate reproducibility. *Biometrics* 1989; **45**: 255-268 [PMID: 2720055]

29 **Higgins JPT**, Li T, Deeks JJ. Choosing effect measures and computing estimates of effect. In: Higgins JPT, Thomas J, Chandler J, Cumpston M, Li T, Page MJ, Welch VA, editors. Cochrane Handbook for Systematic Reviews of Interventions. 2nd ed. Hoboken: Wiley, 2023 [DOI: 10.1002/9781119536604.ch6]

30 **Lee J**, Mulder F, Leeflang M, Wolff R, Whiting P, Bossuyt PM. QUAPAS: An Adaptation of the QUADAS-2 Tool to Assess Prognostic Accuracy Studies. *Ann Intern Med* 2022; **175**: 1010-1018 [PMID: 35696685 DOI: 10.7326/M22-0276]

31 **Hamada K**, Saitoh S, Nishino N, Fukushima D, Horikawa Y, Nishida S, Honda M. Shear wave elastography predicts hepatocellular carcinoma risk in hepatitis C patients after sustained virological response. *PLoS One* 2018; **13**: e0195173 [PMID: 29672518 DOI: 10.1371/journal.pone.0195173]

32 **Gyotoku Y**, Shirahashi R, Suda T, Tamano M. Role of liver stiffness measurements in patients who develop hepatocellular carcinoma after clearance of the hepatitis C virus. *J Med Ultrason (2001)* 2022; **49**: 253-259 [PMID: 35129720 DOI: 10.1007/s10396-021-01188-x]

33 **Masaoka R**, Gyotoku Y, Shirahashi R, Suda T, Tamano M. Combining the age-male-albumin-bilirubin-platelets score and shear wave elastography stratifies carcinogenic risk in hepatitis C patients after viral clearance. *World J Clin Cases* 2023; **11**: 5204-5214 [PMID: 37621583 DOI: 10.12998/wjcc.v11.i22.5204]

34 **Nicoletti A**, Ainora ME, Cintoni M, Garcovich M, Funaro B, Pecere S, De Siena M, Santopaolo F, Ponziani FR, Riccardi L, Grieco A, Pompili M, Gasbarrini A, Zocco MA. Dynamics of liver stiffness predicts complications in patients with HCV related cirrhosis treated with direct-acting antivirals. *Dig Liver Dis* 2023; **55**: 1472-1479 [PMID: 37142455 DOI: 10.1016/j.dld.2023.04.018]

35 **Kumada T**, Toyoda H, Yasuda S, Ogawa S, Gotoh T, Tada T, Ito T, Sumida Y, Tanaka J. Combined ultrasound and magnetic resonance elastography predict hepatocellular carcinoma after hepatitis C virus eradication. *Hepatol Res* 2022; **52**: 957-967 [PMID: 35841314 DOI: 10.1111/hepr.13814]

World Journal of Gastroenterology

Submit a Manuscript: https://www.f6publishing.com

World J Gastroenterol 2024 March 14; 30(10): 1461-1465

DOI: 10.3748/wjg.v30.i10.1461

ISSN 1007-9327 (print) ISSN 2219-2840 (online)

LETTER TO THE EDITOR

Current considerations on intraductal papillary neoplasms of the bile duct and pancreatic duct

Efstathios T Pavlidis, Ioannis N Galanis, Theodoros E Pavlidis

Specialty type: Gastroenterology and hepatology

Provenance and peer review: Unsolicited article; Externally peer reviewed.

Peer-review model: Single blind

Peer-review report's scientific quality classification

Grade A (Excellent): 0
Grade B (Very good): B
Grade C (Good): 0
Grade D (Fair): D
Grade E (Poor): 0

P-Reviewer: Mikulic D, Croatia

Received: January 2, 2024
Peer-review started: January 2, 2024
First decision: January 17, 2024
Revised: January 19, 2024
Accepted: February 26, 2024
Article in press: February 26, 2024
Published online: March 14, 2024

Efstathios T Pavlidis, Ioannis N Galanis, Theodoros E Pavlidis, 2nd Propedeutic Department of Surgery, Hippokration General Hospital, School of Medicine, Aristotle University of Thessaloniki, Thessaloniki 54642, Greece

Corresponding author: Theodoros E Pavlidis, Doctor, PhD, Emeritus Professor, Surgeon, 2nd Propedeutic Department of Surgery, Hippokration General Hospital, School of Medicine, Aristotle University of Thessaloniki, Konstantinoupoleos 49, Thessaloniki 54642, Greece. pavlidth@auth.gr

Abstract

Pancreatobiliary intraductal papillary neoplasms (IPNs) represent precursors of pancreatic cancer or bile duct cholangiocarcinoma that can be detected and treated. Despite advances in diagnostic methods, identifying these premalignant lesions is still challenging for treatment providers. Modern imaging, biomarkers and molecular tests for genomic alterations can be used for diagnosis and follow-up. Surgical intervention in combination with new chemotherapeutic agents is considered the optimal treatment for malignant cases. The balance between the risk of malignancy and any risk of resection guides management policy; therefore, treatment should be individualized based on a meticulous preoperative assessment of high-risk stigmata. IPN of the bile duct is more aggressive; thus, early diagnosis and surgery are crucial. The conservative management of low-risk pancreatic branch-duct lesions is safe and effective.

Key Words: Biliary tree diseases; Pancreatic cystic neoplasms; Biliary tract neoplasms; Extrahepatic cholangiocarcinoma; Pancreatic adenocarcinoma

Core Tip: The balance between overlooking a potential malignancy and the outcomes of a high-risk major operation should be accounted for in the decision-making process of the therapeutic plan. Despite the use of modern diagnostic modalities, overtreatment may occur in many patients; thus, the correct management of pancreatobiliary intraductal papillary neoplasms (IPNs) must be individualized. The proper management of pancreatobiliary IPNs is based on a precise preoperative diagnosis that correctly evaluates the defined high-risk stigmata and worrisome features.

Citation: Pavlidis ET, Galanis IN, Pavlidis TE. Current considerations on intraductal papillary neoplasms of the bile duct and pancreatic duct. *World J Gastroenterol* 2024; 30(10): 1461-1465
URL: https://www.wjgnet.com/1007-9327/full/v30/i10/1461.htm
DOI: https://dx.doi.org/10.3748/wjg.v30.i10.1461

TO THE EDITOR

We read the paper by Mocchegiani *et al*[1] with great interest, and we would like to congratulate the authors for their very nice work on intraductal papillary neoplasm of the bile duct (IPNB), which is an updated impressive approach. This neoplasm resembles the pancreatic intraductal papillary mucinous neoplasm (IPMN). Taking this opportunity, we will make some considerable comments on pancreatobiliary intraductal papillary neoplasms since both IPNB and pancreatic IPMN have a common genomic background, corresponding manifestations and several similarities; however, peculiarities and some differences exist in their biological behavior and subsequent management. IPMN was first described by Ohashi *et al*[2] in 1982 as a different entity from mucinous cystic neoplasms and cancer and is considered a premalignant lesion of pancreatic ductal adenocarcinoma[3]. However, IPNB is rare, less common than IPMN, and more aggressive since it can progress to cholangiocarcinoma[4]. Both IPNB and IPMN are characterized by intraductal overproduction of mucin and growth of the papillary epithelium, which results in similar imaging findings[4].

Panceatobiliary intraductal neoplasms include: (1) IPMN pancreatic, IPNB; (2) Intraductal oncocytic papillary neoplasm (IOPN); and (3) Intraductal tubulopapillary neoplasm[5].

IBNB, first described by Chen *et al*[6] in 2001, is a slow-growing precancerous lesion that evolves into carcinoma[1,7,8]. The other precursor lesion of invasive cholangiocarcinoma, an aggressive disease with poor outcomes, is biliary intraepithelial neoplasia[7,9]. The mucin produced may cause transient ductal obstruction manifested by recurrent episodes of acute cholangitis, obstructive jaundice and bile duct dilatation[8,10]. IPNB must be considered when a patient presents with such a clinical situation without common bile duct gallstones. Early diagnosis and proper management of this precancerous lesion are important for preventing a dismal disease course and improving long-term oncological outcomes [4].

IPNB has histopathological features and genetic substrates, *i.e.*, gene mutations, similar to those of pancreatic IPMN. IPNB and IPMN usually constitute distinct entities with separate development. However, rare cases of simultaneous coexistence or even metachronic tract occurrences after initial surgical resection, which are rarer, have been reported[11]. Additionally, metachronic development of another new lesion may occur after curative intervention, but the development of a new lesion in the bile duct is less common than that in the pancreatic remnant[12].

The involved mutations included mutations in the *Tp16, TP53, KRAS, GNAS*, *BRAF*, SMAD4, STK11 *CTNNB1, PIK3CA, RNF43*, *APC*, *CTNNB1*, *ZNRF3*, *CDKNZA, BRCA 1* and *BRCA 2* genes[1,13,14]. There is an association between *KRAS* and *GNAS* gene mutations in IPNNs and between the *PRKACA* and *PRKACB* genes in IOPNs, which influences oncocytic tumorigenesis and morphology and may lead to therapeutic targets[13].

IPNB represents 5%-15% of relatively rare bile duct neoplasms and is found mainly in East Asia, particularly in elderly individuals older than 67 years[8,10,14,15]. These tumors develop throughout the intrahepatic (type 1) and extrahepatic (type 2) biliary tree[8,14]. Type 2 tumors are more common than type 1 tumors and have a worse prognosis. Magnetic resonance imaging (MRI)-magnetic resonance cholangiopancreatography (MRCP) features may be valuable in distinguishing between the two types of lesions and evaluating the risk of malignancy[15]. These tumors may be adenomas, borderline neoplasias, in situ carcinomas with regular overgrowth, or tubular mucinous adenocarcinomas with irregular overgrowth[1]. High peritumoral and intratumoral budding may be prognostic factors for worse outcomes in patients with extrahepatic distal cholangiocarcinoma[16].

Extensive radical surgical resection is the management method of choice for surgically fit patients with IPNB. Depending on the location, hepatectomy, pancreatoduodenectomy or radical common bile duct resection can be performed[10].

A recent European multicenter study showed a median postoperative survival of 5.7 years and a 5-year overall survival of 63%[17]. In unfit patients, novel endoscopic resection[1], endoscopic radiofrequency ablation or photodynamic therapy can be performed[8]. High-risk imaging findings and strong indications for surgery included a mural nodule more than 12 mm in length and mural nodule enhancement[1]. They are shown in Figure 1[1,4].

Pancreatic IPMNs represent approximately 1% of all pancreatic neoplasms and usually cause recurrent episodes of acute pancreatitis, which can lead to pancreatic dysfunction but may also be asymptomatic. The biological behavior of these tumors ranges from benign to malignant according to the type. The majority of these tumors do not progress to invasive pancreatic carcinoma. There are three types of lesions: Main-duct (MD)-IPMNs, branch-duct (BD)-IPMNs and mixed IPMNs[3]. Both age and metabolic syndrome increase the occurrence of IPMNs[18]. Acute pancreatitis predicts malignancy and constitutes an indication for pancreatectomy[19]. High-risk stigmata and worrisome features may predict malignant transformation in clinical practice and determine management policy, as shown in Table 1[3,20].

Improvements in diagnostic modalities have led to a continual increase in the incidence of IPNB[6]. MRI is the main imaging tool used[4,8,15]. These lesions are intraductal masses accompanied by proximal dilatation and occasionally distal dilatation. The "thread sign" shown in MRCP corresponds to filling defects due to mucin hypersecretion[4].

The first-line modern imaging techniques include contrast-enhanced ultrasound (US), MRI-MRCP and multidetector helical computed tomography, followed by endoscopic US (EUS)[8,21,22]. Additionally, EUS may provide guided needle biopsy[21].

Table 1 High-risk stigmata and worrisome features of malignant pancreatic intraductal papillary mucinous neoplasms

High-risk stigmata	Worrisome features
Dilated main pancreatic duct ≥ 10 mm	Cyst size 3 ≥ cm
Enhanced solid mural nodule 5 ≥ mm	Thickened and enhanced cyst wall
Obstructive jaundice	Abrupt dilatation of the main pancreatic duct 5-9 mm
	Distal atrophy of the pancreas
	Lymph node involvement

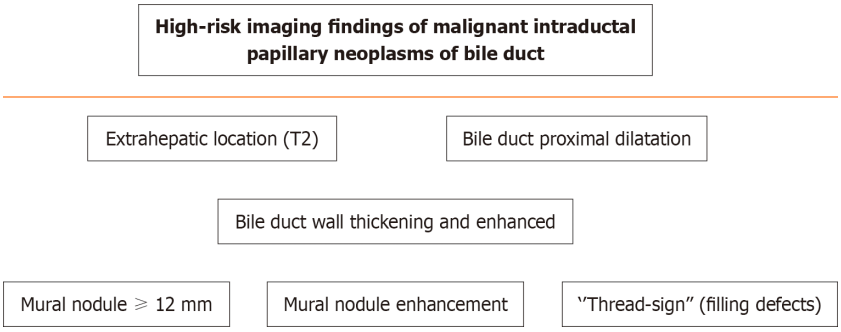

Figure 1 Scheme of Magnetic resonance imaging-cholangiopancreatography indications for malignant intraductal papillary neoplasm of the bile duct (bile duct).

Tumor metabolic activity was detected by positron emission tomography (PET) using ^{18}FDG-PET[8] or the novel ^{68}Ga-labeled fibroblast activation protein inhibitors-PET[23].

Peroral cholangioscopy[24] or pancreatoscopy[25] can directly visualize ducts to aid in diagnosing neoplastic lesions. Additionally, intraoperative pancreatoscopy[26] or even robotic pancreatectomy[27] can assist in determining the extent of pancreatectomy.

The serum elastase-1 concentration[28] and carbohydrate antigen 19-9 concentration or pancreatic juice cytology[29] may predict malignancy. Liquid biopsy may assist in determining malignancy by detecting cancer cells or molecular parts in the blood[30].

For the vast majority of MD-IPMNs and mixed IPMNs, surgery is needed. BD-IPMNs without high-risk stigmata have a low possibility of malignancy; thus, conservative management with long-term imaging surveillance is appropriate[31-34].

After curative resection, IPNB malignancies exhibit a better prognosis than original cholangiocarcinomas[8], and IPMNs exhibit a better prognosis than pancreatic ductal adenocarcinomas[35]; however, the recurrence rate is up to 27% for IPNB[15] and up to 43% for IPMN[36]. Thus, regular follow-up is mandatory for early recurrence detection and reoperation in the pancreatic remnant[37].

In conclusion, surgery is the cornerstone of management for patients at high risk for potential malignancies, particularly bile duct IPNB and pancreatic main duct IPMN. Long-term follow-up ensures early detection of recurrence. Conservative management and surveillance are indicated for patients with low-risk pancreatic branch duct IPMNs. However, management must be individualized to avoid overtreatment or overlooking a malignancy.

FOOTNOTES

Author contributions: Pavlidis TE designed research, contributed new analytic tools, analyzed data and review; Galanis IN analyzed data and review; Pavlidis ET performed research, analyzed data, review, and wrote the paper.

Conflict-of-interest statement: All the authors report no relevant conflicts of interest for this article.

Country/Territory of origin: Greece

ORCID number: Efstathios T Pavlidis 0000-0002-7282-8101; Ioannis N Galanis 0009-0001-4283-0788; Theodoros E Pavlidis 0000-0002-8141-1412.

S-Editor: Li L
L-Editor: A
P-Editor: Zheng XM

REFERENCES

1 **Mocchegiani F**, Vincenzi P, Conte G, Nicolini D, Rossi R, Cacciaguerra AB, Vivarelli M. Intraductal papillary neoplasm of the bile duct: The new frontier of biliary pathology. *World J Gastroenterol* 2023; **29**: 5361-5373 [PMID: 37900587 DOI: 10.3748/wjg.v29.i38.5361]
2 **Ohashi K**, Murakami Y, Murayama M, Takekoshi T, Ohta H, Ohashi I. Four cases of mucus secreting pancreatic cancer. *Prog Dig Endosc* 1982; **20**: 348-351
3 **Pavlidis ET**, Sapalidis KG, Pavlidis TE. Modern aspects of the management of pancreatic intraductal papillary mucinous neoplasms: a narrative review. *Rom J Morphol Embryol* 2022; **63**: 491-502 [PMID: 36588487 DOI: 10.47162/RJME.63.3.03]
4 **Kraus M**, Klang E, Soffer S, Inbar Y, Konen E, Sobeh T, Apter S. MRI features of intraductal papillary mucinous neoplasm of the bile ducts, "The myth about the cyst": A systematic review. *Eur J Radiol Open* 2023; **11**: 100515 [PMID: 37609049 DOI: 10.1016/j.ejro.2023.100515]
5 **Nakanuma Y**, Sato Y, Kakuda Y, Naito Y, Fukumura Y, Fukushima M, Minato H, Aishima S, Ohike N, Furukawa T. Interobserver agreement of pathologic classification and grading of tumoral intraductal pre-invasive neoplasms of the bile duct. *Ann Diagn Pathol* 2024; **69**: 152247 [PMID: 38128439 DOI: 10.1016/j.anndiagpath.2023.152247]
6 **Chen TC**, Nakanuma Y, Zen Y, Chen MF, Jan YY, Yeh TS, Chiu CT, Kuo TT, Kamiya J, Oda K, Hamaguchi M, Ohno Y, Hsieh LL, Nimura Y. Intraductal papillary neoplasia of the liver associated with hepatolithiasis. *Hepatology* 2001; **34**: 651-658 [PMID: 11584359 DOI: 10.1053/jhep.2001.28199]
7 **Nagashima D**, Esaki M, Nara S, Ban D, Takamoto T, Mizui T, Shimada K, Hiraoka N. Novel insights into the intraepithelial spread of extrahepatic cholangiocarcinoma: clinicopathological study of 382 cases on extrahepatic cholangiocarcinoma. *Front Oncol* 2023; **13**: 1216097 [PMID: 37664071 DOI: 10.3389/fonc.2023.1216097]
8 **Kim JR**, Jang KT, Jang JY. Intraductal papillary neoplasm of the bile duct: review of updated clinicopathological and imaging characteristics. *Br J Surg* 2023; **110**: 1229-1240 [PMID: 37463281 DOI: 10.1093/bjs/znad202]
9 **Nakanuma Y**, Sugino T, Kakuda Y, Nomura Y, Watanabe H, Terada T, Sato Y, Ohnishi Y, Fukumura Y. Pathological survey of precursor lesions in cholangiocarcinoma. *J Hepatobiliary Pancreat Sci* 2023; **30**: 893-903 [PMID: 36707055 DOI: 10.1002/jhbp.1308]
10 **Wu X**, Li B, Zheng C. Clinicopathologic characteristics and long-term prognosis of intraductal papillary neoplasm of the bile duct: a retrospective study. *Eur J Med Res* 2023; **28**: 132 [PMID: 36945047 DOI: 10.1186/s40001-023-01102-w]
11 **Xiao G**, Xia T, Mou YP, Zhou YC. Reoperation for heterochronic intraductal papillary mucinous neoplasm of the pancreas after bile duct neoplasm resection: A case report. *World J Gastrointest Surg* 2023; **15**: 1542-1548 [PMID: 37555129 DOI: 10.4240/wjgs.v15.i7.1542]
12 **Ito T**, Hisa T, Ito Y, Kudo A, Yamada T, Osera S, Tomori A, Fukushima H, Aoyagi D, Shiozawa S. Intraductal papillary neoplasm of the bile duct with metachronous development in the downstream bile duct after radical resection. *Clin J Gastroenterol* 2024; **17**: 155-163 [PMID: 37837506 DOI: 10.1007/s12328-023-01867-x]
13 **Itoh T**, Omori Y, Seino M, Hirose K, Date F, Ono Y, Mizukami Y, Aoki S, Ishida M, Mizuma M, Morikawa T, Higuchi R, Honda G, Okamura Y, Kinoshita K, Unno M, Furukawa T. Gene Rearrangement and Expression of PRKACA and PRKACB Govern Morphobiology of Pancreatobiliary Oncocytic Neoplasms. *Mod Pathol* 2024; **37**: 100358 [PMID: 37871652 DOI: 10.1016/j.modpat.2023.100358]
14 **Wu RS**, Liao WJ, Ma JS, Wang JK, Wu LQ, Hou P. Epidemiology and outcome of individuals with intraductal papillary neoplasms of the bile duct. *World J Gastrointest Oncol* 2023; **15**: 843-858 [PMID: 37275447 DOI: 10.4251/wjgo.v15.i5.843]
15 **Jeon SK**, Lee JM, Yoo J, Park S, Joo I, Yoon JH, Lee KB. Intraductal papillary neoplasm of the bile duct: diagnostic value of MRI features in differentiating pathologic subclassifications-type 1 *vs* type 2. *Eur Radiol* 2023 [PMID: 38114846 DOI: 10.1007/s00330-023-10491-9]
16 **Jun SY**, Hong SM, An S. Prognostic Significance of Intratumoral and Peritumoral Budding in Distal Extrahepatic Bile Duct Carcinoma. *Pathobiology* 2023 [PMID: 38113866 DOI: 10.1159/000535847]
17 **Lluvs N**, Serradilla-Martvn M, Achalandabaso M, Jehaes F, Dasari BVM, Mambrilla-Herrero S, Sparrelid E, Balakrishnan A, Hoogwater FJH, Amaral MJ, Andersson B, Berrevoet F, Doussot A, Lσpez-Lσpez V, Alsammani M, Detry O, Domingo-Del Pozo C, Machairas N, Pekli D, Alcαzar-Lσpez CF, Asbun H, Bjφrnsson B, Christophides T, Dvez-Caballero A, Francart D, Noel CB, Sousa-Silva D, Toledo-Martvnez E, Tzimas GN, Yaqub S, Cauchy F, Prieto-Calvo M, D'Souza MA, Spiers HVM, van den Heuvel MC, Charco R, Lesurtel M, Ramia JM. Intraductal papillary neoplasms of the bile duct: a European retrospective multicenter observational study (EUR-IPNB study). *Int J Surg* 2023; **109**: 760-771 [PMID: 36917142 DOI: 10.1097/JS9.0000000000000280]
18 **Tanaka S**, Tsujimae M, Masuda A, Inoue J, Inomata N, Uemura H, Kohashi S, Nagao K, Masuda S, Abe S, Gonda M, Yamakawa K, Ashina S, Nakano R, Tanaka T, Yamada Y, Sakai A, Kobayashi T, Shiomi H, Fujita K, Anami T, Fujita T, Watanabe A, Kodama Y. Metabolic Syndrome Accelerates the Age-Related Increase of Intraductal Papillary Mucinous Neoplasm of the Pancreas. *Pancreas* 2024; **53**: e9-e15 [PMID: 37890158 DOI: 10.1097/MPA.0000000000002267]
19 **Xu JH**, Ni CY, Zhuang YY, Li L, Lin Y, Xia ZS, Wu WR, Chen QK, Zhong W. Acute pancreatitis in intraductal papillary mucinous neoplasm: a single-center retrospective cohort study with systematic review and meta-analysis. *BMC Gastroenterol* 2023; **23**: 424 [PMID: 38041073 DOI: 10.1186/s12876-023-02972-4]
20 **Kazami Y**, Arita J, Nishioka Y, Kawaguchi Y, Ichida A, Ishizawa T, Akamatsu N, Kaneko J, Nakai Y, Koike K, Hasegawa K. Preoperative Predictive Features of Invasive Carcinoma Among Intraductal Papillary Mucinous Neoplasm of the Pancreas. *Pancreas* 2022; **51**: 642-648 [PMID: 35835103 DOI: 10.1097/MPA.0000000000002078]
21 **Conti Bellocchi MC**, Manfrin E, Brillo A, Bernardoni L, Lisotti A, Fusaroli P, Parisi A, Sina S, Facciorusso A, Gabbrielli A, Crinç SF. Rare Pancreatic/Peripancreatic Cystic Lesions Can Be Accurately Characterized by EUS with Through-the-Needle Biopsy-A Unique Pictorial Essay with Clinical and Histopathological Correlations. *Diagnostics (Basel)* 2023; **13** [PMID: 38132247 DOI: 10.3390/diagnostics13243663]
22 **Minelli C**, Balducci F, Cavalleri C, Milanetto AC, Ferrara F, Crimμ F, Quaia E, Vernuccio F. Intraductal papillary mucinous neoplasms of the pancreas: Uncommon imaging presentation, evolution and comparison of guidelines. *Eur J Radiol Open* 2023; **11**: 100531 [PMID: 37920680 DOI: 10.1016/j.ejro.2023.100531]

23 **Lang M**, Spektor AM, Hielscher T, Hoppner J, Glatting FM, Bicu F, Hackert T, Heger U, Pausch T, Gutjahr E, Rathke H, Giesel FL, Kratochwil C, Tjaden C, Haberkorn U, Rφhrich M. Static and Dynamic (68)Ga-FAPI PET/CT for the Detection of Malignant Transformation of Intraductal Papillary Mucinous Neoplasia of the Pancreas. *J Nucl Med* 2023; **64**: 244-251 [PMID: 35906094 DOI: 10.2967/jnumed.122.264361]

24 **Koiwai A**, Hirota M, Murakami K, Katayama T, Kin R, Endo K, Kogure T, Takasu A, Sakurai H, Kondo N, Takami K, Yamamoto K, Katayose Y, Satoh K. Direct peroral cholangioscopy with red dichromatic imaging 3 detected the perihilar margin of superficial papillary extension in a patient with intraductal papillary neoplasm of the bile duct. *DEN Open* 2023; **3**: e228 [PMID: 36998349 DOI: 10.1002/deo2.228]

25 **Sarita MAT**, Sakai A, Tsujimae M, Kobayashi T, Masuda A, Kanzawa M, Toyama H, Kodama Y. Use of Peroral Pancreatoscopy in the Diagnosis of Elusive Intraductal Papillary Mucinous Neoplasm With High-Grade Dysplasia. *ACG Case Rep J* 2023; **10**: e01165 [PMID: 37811365 DOI: 10.14309/crj.0000000000001165]

26 **Ciprani D**, Frampton A, Amar H, Oppong K, Pandanaboyana S, Aroori S. The role of intraoperative pancreatoscopy in the surgical management of intraductal papillary mucinous neoplasms of the pancreas: a systematic scoping review. *Surg Endosc* 2023; **37**: 9043-9051 [PMID: 37907657 DOI: 10.1007/s00464-023-10518-8]

27 **Fong ZV**, Zwart MJW, Gorris M, Voermans RP, van Wanrooij RLJ, Wielenga T, Del Chiaro M, Arnelo U, Daams F, Busch OR, Besselink MG. Intraoperative Pancreatoscopy During Robotic Pancreatoduodenectomy and Robotic Distal Pancreatectomy for Intraductal Papillary Mucinous Neoplasm with Involvement of the Main Pancreatic Duct. *Ann Surg Open* 2023; **4**: e283 [PMID: 37601466 DOI: 10.1097/AS9.0000000000000283]

28 **Mishima T**, Takano S, Takayashiki T, Kuboki S, Suzuki D, Sakai N, Hosokawa I, Konishi T, Nishino H, Nakada S, Kouchi Y, Kishimoto T, Ohtsuka M. Serum elastase-1 predicts malignancy in intraductal papillary mucinous neoplasm of the pancreas. *Pancreatology* 2024; **24**: 93-99 [PMID: 38102054 DOI: 10.1016/j.pan.2023.11.015]

29 **Nagayama R**, Ueki T, Shimizu Y, Hijioka S, Nakamura M, Kitano M, Hara K, Masamune A, Kin T, Hanada K, Koshita S, Yamada R, Takenaka M, Itoi T, Yanagisawa A, Otuka T, Hirono S, Kanno A, Ideno N, Kuwahara T, Shimizu A, Kamata K, Asai Y, Takeyama Y. Is preoperative pancreatic juice cytology useful for determining therapeutic strategies for patients with intraductal papillary mucinous neoplasm of the pancreas? *J Hepatobiliary Pancreat Sci* 2023 [PMID: 38084510 DOI: 10.1002/jhbp.1394]

30 **Kuvendjiska J**, Móller F, Bronsert P, Timme-Bronsert S, Fichtner-Feigl S, Kulemann B. Circulating Epithelial Cells in Patients with Intraductal Papillary Mucinous Neoplasm of the Pancreas. *Life (Basel)* 2023; **13** [PMID: 37511945 DOI: 10.3390/life13071570]

31 **Ferronato M**, Lizzio CE, Berardinelli D, Marini D, Elia E, Andreetto L, Trentini A, Potenza MC, Serra C, Mazzotta E, Ricci C, Casadei R, Migliori M. Abdominal ultrasound in the characterization of branch-duct intraductal papillary mucinous neoplasms: A new tool for surveillance of low-risk patients? *Dig Liver Dis* 2023 [PMID: 38042636 DOI: 10.1016/j.dld.2023.11.010]

32 **Hesse F**, Ritter J, Hapfelmeier A, Braren R, Phillip V. Comparison of Magnetic Resonance Imaging and Endoscopic Ultrasound in the Sizing of Intraductal Papillary Mucinous Neoplasia of the Pancreas. *Pancreas* 2023; **52**: e315-e320 [PMID: 37906550 DOI: 10.1097/MPA.0000000000002264]

33 **Lattimore CM**, Kane WJ, Subbarao S, Venitti C, Cramer CL, Turkheimer LM, Bauer TW, Turrentine FE, Zaydfudim VM. Long-term surveillance of branch-duct intraductal papillary mucinous neoplasms without worrisome or high-risk features. *J Surg Oncol* 2023; **128**: 1087-1094 [PMID: 37530526 DOI: 10.1002/jso.27414]

34 **Deng H**, Dou W, Pan Y. The Surveillance for Presumed BD-IPMN of the Pancreas. *Gastroenterology* 2023 [PMID: 37549750 DOI: 10.1053/j.gastro.2023.07.023]

35 **Holmberg M**, Linder S, Kordes M, Liljefors M, Ghorbani P, Lφhr JM, Sparrelid E. Impact of spatio-temporal recurrence pattern on overall survival for invasive intraductal papillary mucinous neoplasia - A comparison with pancreatic ductal adenocarcinoma. *Pancreatology* 2022; **22**: 598-607 [PMID: 35501218 DOI: 10.1016/j.pan.2022.04.007]

36 **Habib JR**, Kinny-Kφster B, Amini N, Shoucair S, Cameron JL, Thompson ED, Fishman EK, Hruban RH, Javed AA, He J, Wolfgang CL. Predictors, Patterns, and Timing of Recurrence Provide Insight into the Disease Biology of Invasive Carcinomas Arising in Association with Intraductal Papillary Mucinous Neoplasms. *J Gastrointest Surg* 2022; **26**: 2311-2320 [PMID: 35915375 DOI: 10.1007/s11605-022-05428-4]

37 **Fuji T**, Umeda Y, Takagi K, Yoshida R, Yoshida K, Yasui K, Matsumoto K, Kato H, Yagi T, Fujiwara T. Optimal surveillance of intraductal papillary mucinous neoplasms of the pancreas focusing on remnant pancreas recurrence after surgical resection. *BMC Cancer* 2022; **22**: 588 [PMID: 35643422 DOI: 10.1186/s12885-022-09650-w]

World Journal of Gastroenterology

Submit a Manuscript: https://www.f6publishing.com

World J Gastroenterol 2024 March 14; 30(10): 1466-1469

DOI: 10.3748/wjg.v30.i10.1466

ISSN 1007-9327 (print) ISSN 2219-2840 (online)

LETTER TO THE EDITOR

Are we ready to use new endoscopic scores for ulcerative colitis?

Rodrigo Quera, Paulina Núñez F

Specialty type: Gastroenterology and hepatology

Provenance and peer review: Unsolicited article; Externally peer reviewed.

Peer-review model: Single blind

Peer-review report's scientific quality classification

Grade A (Excellent): A
Grade B (Very good): 0
Grade C (Good): 0
Grade D (Fair): 0
Grade E (Poor): 0

P-Reviewer: Knudsen T, Denmark

Received: January 6, 2024
Peer-review started: January 6, 2024
First decision: January 16, 2024
Revised: January 23, 2024
Accepted: February 25, 2024
Article in press: February 25, 2024
Published online: March 14, 2024

Rodrigo Quera, Paulina Núñez F, Universidad de los Andes, Inflammatory Bowel Disease Program, Clinica Universidad de los Andes, Digestive Disease Center, Santiago 7600976, RM, Chile

Paulina Núñez F, Digestive Disease Center, Inflammatory Bowel Disease Program, Clínica Universidad de los Andes, Santiago 7620157, Chile

Paulina Núñez F, Department of Gastroenterology, Universidad de Chile-Hospital San Juan de Dios, Santiago 770123, Chile

Corresponding author: Paulina Núñez F, MD, Assistant Professor, Digestive Disease Center, Inflammatory Bowel Disease Program, Clínica Universidad de los Andes, 2501 Plaza Avenue, Santiago 7620157, Chile. pnunez@clinicauandes.cl

Abstract

For ulcerative colitis (UC), the variability in inflammatory activity along the colon poses a challenge in management. The focus on achieving endoscopic healing in UC is evident, where the UC Endoscopic Index of Severity and Mayo Endoscopic Subscore are commonly used for evaluation. However, these indices primarily consider the most severely affected region. Liu *et al* recent study validates the Toronto Inflammatory Bowel Disease Global Endoscopic Reporting (TIGER) score offering a comprehensive assessment of inflammatory activity across diverse segments of the colon and rectum and a reliable index correlating strongly with UC Endoscopic Index of Severity and moderately with Mayo Endoscopic Subscore (MES). Despite recommendation, certain aspects warrant further investigation. Fecal calprotectin, an intermediate target, correlates with TIGER and should be explored. Determining TIGER scores defining endoscopic remission and response, evaluating agreement with histological activity, and assessing inter-endoscopist agreement for TIGER require scrutiny. Exploring the correlation between TIGER and intestinal ultrasound, akin to MES, adds value.

Key Words: Ulcerative colitis; Sigmoidoscopy; Colonoscopy; Score index

Core Tip: For ulcerative colitis (UC), the degree of inflammatory activity can vary along the length of the colon, ranging from the rectum to the proximal colon. Currently, achieving endoscopic healing is a long-term goal in the management of UC, with the UC Endoscopic Index of Severity score and Mayo Endoscopic Subscore being the most suggested indices to evaluate this target. However, both scores only consider the most severely affected area in their final assessment. Recently, the Toronto Inflammatory Bowel Disease Global Endoscopic Reporting score has shown its usefulness in determining the extent and severity of inflammatory activity across various segments of the colon and rectum. Despite this, there is no consensus regarding the endoscopic method (total colonoscopy or sigmoidoscopy) for evaluating the achievement of endoscopic healing in UC patients.

Citation: Quera R, Núñez F P. Are we ready to use new endoscopic scores for ulcerative colitis? *World J Gastroenterol* 2024; 30(10): 1466-1469
URL: https://www.wjgnet.com/1007-9327/full/v30/i10/1466.htm
DOI: https://dx.doi.org/10.3748/wjg.v30.i10.1466

TO THE EDITOR

Early recognition of inflammatory activity, prompt intervention, along with tight monitoring constitute the cornerstones of the treat-to-target approach in ulcerative colitis (UC)[1,2]. Recently, the Therapeutic Goals Consensus in Inflammatory Bowel Disease (STRIDE-II) has highlighted that achieving mucosa healing in the rectum and colon is the long-term goal for patients with UC (Figure 1)[2]. Total colonoscopy provides comprehensive information about the extent and severity of inflammatory activity in patients with UC. This approach enhances the precision of UC management, whether conducted *via* colonoscopy or sigmoidoscopy[3]. With this in mind, we would like to extend our congratulations to Liu *et al*[4] for their article published last month in the *World Journal of Gastroenterology*. Their results confirm that the Toronto Inflammatory Bowel Disease Global Endoscopic Reporting (TIGER) score is a reliable and straightforward endoscopic index for UC patients to assess the overall endoscopic disease burden[4]. In a retrospective study involving 166 patients with UC, the authors demonstrated a strong correlation between the TIGER index and the UC Endoscopic Index of Severity (UCEIS) score (r = 0.721, P < 0.001) and a moderate correlation with the Mayo Endoscopic Subscore (MES) (r = 0.626, P < 0.001). UCEIS and MES are widely used indices in UC. Furthermore, a TIGER score ≥ 317 was identified as an independent risk factor for advanced treatment. This includes, the use of systemic corticosteroids, biologics, immunomodulators, thalidomide, and surgery. Nonetheless, there are certain aspects that warrant further investigation in subsequent studies.

To commence, fecal calprotectin is regarded as an intermediate target in UC[2]. While Liu *et al*[4] did not incorporate this biomarker in their research, other studies have established a correlation between fecal calprotectin levels and TIGER.

Secondly, it is important to determinate the TIGER scores that define endoscopic remission and endoscopic response. While the UCEIS score and MES 0 have been proposed as definitions for endoscopic remission, a decrease in UCEIS by ≥ 2 points or a decrease in Mayo endoscopic score by ≥ 1 grade is suggested for defining endoscopic response in UC[5].

Thirdly, exploring the agreement between the TIGER score and histological activity in UC is crucial. Previous studies have established correlations between the endoscopic scores (UCEIS score and MES) and histological indices[6,7].

Fourthly, it is essential to assess the agreement among endoscopists for the TIGER score. Studies have demonstrated adequate, though not perfect, correlation between different endoscopists when using MES or UCEIS in UC patients[8], but agreement among endoscopists for the TIGER score has not been conclusively demonstrated[9].

Finally, considering the potential of intestinal ultrasound as a tool for assessing inflammatory activity in UC patients, like MES[10], it would be valuable to explore whether there is a correlation between the TIGER score and the intestinal ultrasound index.

As previously mentioned, there is currently a lack of consensus regarding the preferred endoscopic method for evaluating the goal of endoscopic healing in UC patients. Some studies have suggested that sigmoidoscopy might be sufficient, given the highest inflammatory activity is typically observed in the distal colon[11,12]. However, this recommendation has not been universally confirmed, as some UC patients may exhibit higher inflammatory activity in the ascending colon. In such cases, total colonoscopy becomes the most appropriate endoscopic examination to assess inflammation in UC patients[13,14]. Although sigmoidoscopy is limited to evaluating inflammatory activity from the rectum to the descending colon, it is essential to recognize some benefits of this procedure. Sigmoidoscopy is safer, requires reduced preparation, has a lower cost, and takes less time to perform compared to a total colonoscopy. Moreover, some patients may find this procedure preferable.

Given the current lack of consensus and the need for confirmation through prospective multicenter studies, a personalized approach should be recommended for the evaluation of activity and severity of inflammatory activity in UC patients using the TIGER score. Total colonoscopy is likely the preferred method in scenarios where sigmoidoscopy results are inconsistent with clinical setting or biomarkers. This is particularly applicable in patients with UC and primary sclerosing cholangitis and during surveillance for the development of colorectal neoplasia.

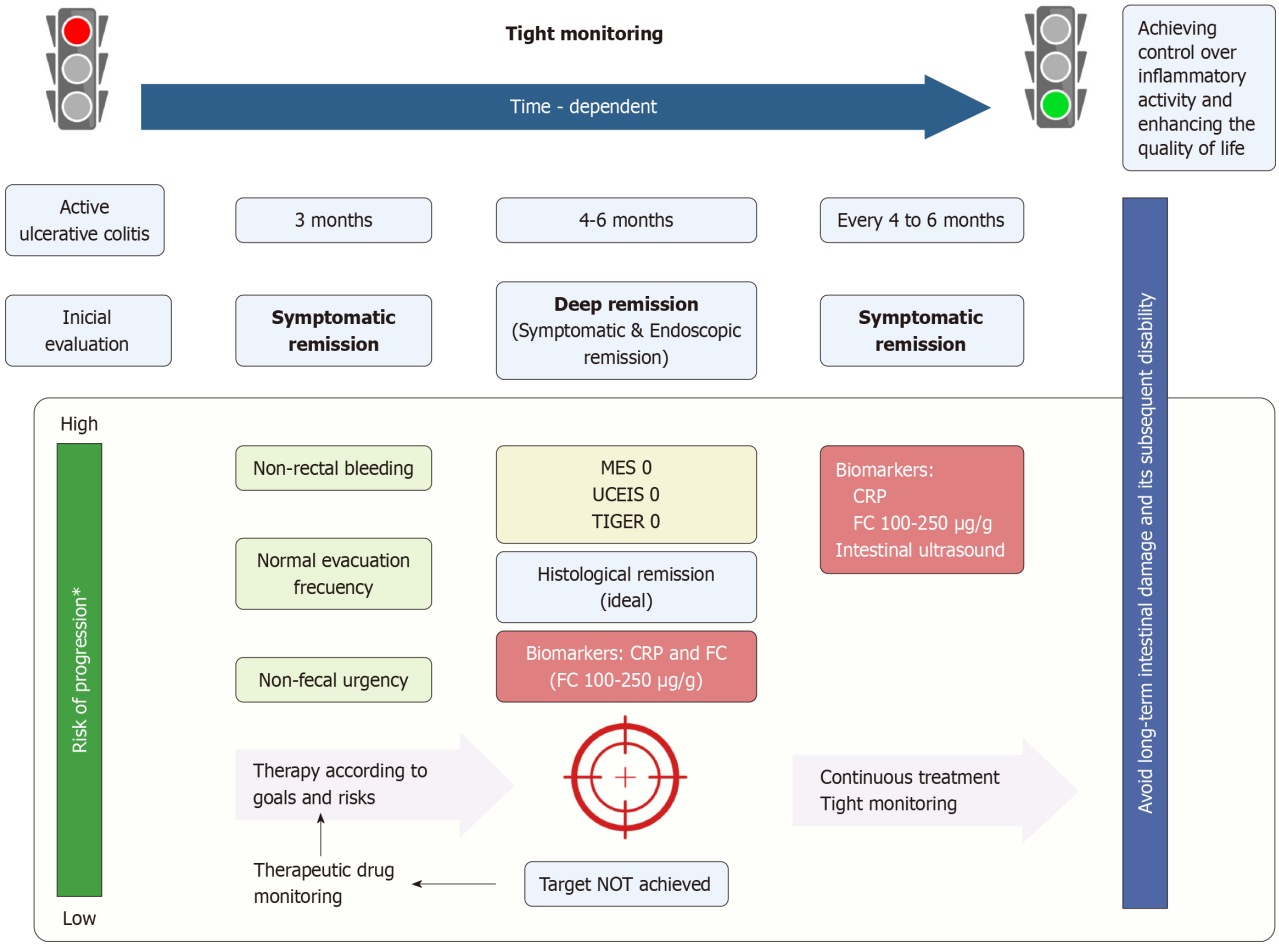

Figure 1 Treat-to-Target approach for ulcerative colitis. MES: Mayo Endoscopic Subscore; UCEIS: Ulcerative Colitis Endoscopic Index of Severity score; TIGER: Toronto Inflammatory Bowel Disease Global Endoscopic Reporting score; QoL: Quality of life; CRP: C-reactive protein; FC: Fecal calprotectin[15]. Citation: The authors have obtained the permission for figure using from the BioRender.com (Supplementary material)[16].

FOOTNOTES

Author contributions: Núñez F P and Quera R carried out the conception, made literature review; both authors wrote the letter, making critical revision and editing, and approved the final version.

Conflict-of-interest statement: The authors declare that they have no conflict of interest.

Country/Territory of origin: Chile

ORCID number: Rodrigo Quera 0000-0001-5854-0526; Paulina Núñez F 0000-0003-3727-1851.

S-Editor: Chen YL
L-Editor: A
P-Editor: Zheng XM

REFERENCES

1 **Nuñez F P**, Mahadevan U, Quera R, Bay C, Ibañez P. Treat-to-target approach in the management of inflammatory Bowel disease. *Gastroenterol Hepatol* 2021; **44**: 312-319 [PMID: 33070988 DOI: 10.1016/j.gastrohep.2020.06.032]

2 **Turner D**, Ricciuto A, Lewis A, D'Amico F, Dhaliwal J, Griffiths AM, Bettenworth D, Sandborn WJ, Sands BE, Reinisch W, Schölmerich J, Bemelman W, Danese S, Mary JY, Rubin D, Colombel JF, Peyrin-Biroulet L, Dotan I, Abreu MT, Dignass A; International Organization for the Study of IBD. STRIDE-II: An Update on the Selecting Therapeutic Targets in Inflammatory Bowel Disease (STRIDE) Initiative of the

International Organization for the Study of IBD (IOIBD): Determining Therapeutic Goals for Treat-to-Target strategies in IBD. *Gastroenterology* 2021; **160**: 1570-1583 [PMID: 33359090 DOI: 10.1053/j.gastro.2020.12.031]

3 **Zittan E**, Steinhart AH, Aran H, Milgrom R, Gralnek IM, Zelber-Sagi S, Silverberg MS. The Toronto IBD Global Endoscopic Reporting [TIGER] Score: A Single, Easy to Use Endoscopic Score for Both Crohn's Disease and Ulcerative Colitis Patients. *J Crohns Colitis* 2022; **16**: 544-553 [PMID: 34272937 DOI: 10.1093/ecco-jcc/jjab122]

4 **Liu XY**, Tian ZB, Zhang LJ, Liu AL, Zhang XF, Wu J, Ding XL. Clinical value of the Toronto inflammatory bowel disease global endoscopic reporting score in ulcerative colitis. *World J Gastroenterol* 2023; **29**: 6208-6221 [PMID: 38186862 DOI: 10.3748/wjg.v29.i48.6208]

5 **Vuitton L**, Peyrin-Biroulet L, Colombel JF, Pariente B, Pineton de Chambrun G, Walsh AJ, Panes J, Travis SP, Mary JY, Marteau P. Defining endoscopic response and remission in ulcerative colitis clinical trials: an international consensus. *Aliment Pharmacol Ther* 2017; **45**: 801-813 [PMID: 28112419 DOI: 10.1111/apt.13948]

6 **Fluxá D**, Simian D, Flores L, Ibáñez P, Lubascher J, Figueroa C, Kronberg U, Pizarro G, Castro M, Piottante A, Vial MT, Quera R. Clinical, endoscopic and histological correlation and measures of association in ulcerative colitis. *J Dig Dis* 2017; **18**: 634-641 [PMID: 28949435 DOI: 10.1111/1751-2980.12546]

7 **Irani NR**, Wang LM, Collins GS, Keshav S, Travis SPL. Correlation Between Endoscopic and Histological Activity in Ulcerative Colitis Using Validated Indices. *J Crohns Colitis* 2018; **12**: 1151-1157 [PMID: 29893824 DOI: 10.1093/ecco-jcc/jjy081]

8 **Belvis Jiménez M**, Hergueta-Delgado P, Gómez Rodríguez B, Maldonado Pérez B, Castro Laria L, Rodríguez-Téllez M, Morales Barroso ML, Galván Fernández MD, Guerra Veloz M, Jiménez García VA, Romero-Castro R, Benítez-Roladán A, Castro Márquez C, Aparcero López R, Garrido-Serrano A, Caunedo-Álvarez Á, Argüelles-Arias F. Comparison of the Mayo Endoscopy Score and the Ulcerative Colitis Endoscopy Index of Severity and the Ulcerative Colitis Colonoscopy Index of Severity. *Endosc Int Open* 2021; **9**: E130-E136 [PMID: 33532549 DOI: 10.1055/a-1313-6968]

9 **Belvis Jiménez M**, Hergueta-Delgado P, Gómez Rodríguez BJ, Maldonado Pérez B, Castro Laria L, Rodríguez-Téllez M, Morales Barroso ML, Galván Fernández MD, Guerra Veloz MF, Jiménez García VA, Romero Castro R, Benítez Roldán A, Castro Márquez C, Aparcero López R, Garrido Serrano A, Caunedo Álvarez Á, Argüelles Arias F. Index of the Mayo Endoscopy and Ulcerative Colitis Endoscopy Index of Severity: are they equally valid? *Rev Esp Enferm Dig* 2020; **112**: 821-825 [PMID: 33054301 DOI: 10.17235/reed.2020.6832/2019]

10 **Bots S**, Nylund K, Löwenberg M, Gecse K, D'Haens G. Intestinal Ultrasound to Assess Disease Activity in Ulcerative Colitis: Development of a novel UC-Ultrasound Index. *J Crohns Colitis* 2021; **15**: 1264-1271 [PMID: 33411887 DOI: 10.1093/ecco-jcc/jjab002]

11 **Colombel JF**, Ordás I, Ullman T, Rutgeerts P, Chai A, O'Byrne S, Lu TT, Panés J. Agreement Between Rectosigmoidoscopy and Colonoscopy Analyses of Disease Activity and Healing in Patients With Ulcerative Colitis. *Gastroenterology* 2016; **150**: 389-95.e3 [PMID: 26526713 DOI: 10.1053/j.gastro.2015.10.016]

12 **Park SB**, Kim SJ, Lee J, Lee YJ, Baek DH, Seo GS, Kim ES, Kim SW, Kim SY. Efficacy of sigmoidoscopy for evaluating disease activity in patients with ulcerative colitis. *BMC Gastroenterol* 2022; **22**: 83 [PMID: 35220941 DOI: 10.1186/s12876-022-02178-0]

13 **Kato J**, Kuriyama M, Hiraoka S, Yamamoto K. Is sigmoidoscopy sufficient for evaluating inflammatory status of ulcerative colitis patients? *J Gastroenterol Hepatol* 2011; **26**: 683-687 [PMID: 21054518 DOI: 10.1111/j.1440-1746.2010.06562.x]

14 **Jamil OK**, Shaw D, Deng Z, Dinardi N, Fillman N, Khanna S, Krugliak Cleveland N, Sakuraba A, Weber CR, Cohen RD, Dalal S, Jabri B, Rubin DT, Pekow J. Inflammation in the proximal colon is a risk factor for the development of colorectal neoplasia in inflammatory bowel disease patients with primary sclerosing cholangitis. *Therap Adv Gastroenterol* 2023; **16**: 17562848231184985 [PMID: 37692199 DOI: 10.1177/17562848231184985]

15 **Calderón P**, Núñez P, Nos P, Quera R. Personalized therapy in inflammatory bowel disease. *Gastroenterol Hepatol* 2023 [PMID: 38101615 DOI: 10.1016/j.gastrohep.2023.12.006]

16 **BioRender**. [cited 2 February 2024]. Available from: https://www.biorender.com/

Published by **Baishideng Publishing Group Inc**
7041 Koll Center Parkway, Suite 160, Pleasanton, CA 94566, USA
Telephone: +1-925-3991568
E-mail: office@baishideng.com
Help Desk: https://www.f6publishing.com/helpdesk
https://www.wjgnet.com